Materials Degradation and Failures Series

Biobased and Environmentally Benign Coatings

Edited by **Atul Tiwari, Anthony Galanis, and Mark D. Soucek**



Scrivener Publishing

WILEY

Contents

Cover

Half Title page

Title page

Copyright page

Preface

Chapter 1: Novel Biobased Polymers for Coating Applications

- 1.1 Introduction
- 1.2 Polymers Based on Plant Oils
- 1.3 Polymers Based on Cardanol
- 1.4 Polymers Based on Eugenol
- 1.5 Conclusion
- Acknowledgments
- Disclaimer
- References

Chapter 2: Deposition of Environmentally Compliant Cerium-Containing Coatings and Primers on Copper-Containing Aluminium Aircraft Alloys

- 2.1 Importance and Indispensability of the Corrosion-Protective Coating Layers
- 2.2 Introduction to the Cerium Conversion Primer Layers
- 2.3 Elaboration of Hybrid and Composite Upper and Finishing Coating Layers
- Acknowledgment
- References

Chapter 3: Ferrites as Non-Toxic Pigments for Eco-Friendly Corrosion Protection Coatings

- 3.1 Introduction
- 3.2 Crystalline Structure, Physicochemical Properties, and Inhibition Mechanism of Ferrites
- 3.3 Methods for the Preparation of Ferrites
- 3.4 Novel Types of Ferrite Pigments
- 3.5 Ferrite-Based Multifunctional Coatings
- 3.6 Conclusion
- Acknowledgement
- References

Chapter 4: Application of Edible Coatings on Fruits and Vegetables

- 4.1 Introduction
- 4.2 Coatings versus Films
- 4.3 Structural Matrix: Hydrocolloids and Lipids
- 4.4 Application of Hydrocolloids Coatings
- 4.5 Application of Lipid Coatings
- 4.6 Application of Composite Coatings
- 4.7 Addition of Active Compounds
- 4.8 Nanotechnology
- 4.9 Commercial Application of Edible Coatings
- 4.10 Problems Associated with Edible Coatings
- 4.11 Regulatory Status and Food Safety Issues
- 4.12 Conclusions
- References

Chapter 5: Development of Novel Biobased Epoxy Films with Aliphatic and Aromatic Amine Hardeners for the Partial Replacement of Bisphenol A in Primer Coatings

- 5.1 Introduction

5.2 Recent Advances on Vegetable Oils Chemistry
5.3 Control of the Epoxidation Reaction of Vegetable Oils
5.4 Spectroscopy Characterization of Epoxidized Linseed Oil Cured with Amine Hardeners
5.5 Thermal Properties of Epoxidized Linseed Oil Cured with Amine Hardeners
5.6 Swelling, Wettability and Morphology of New Epoxy Films
5.7 Mechanical Properties of Epoxidized Linseed Oil Cured with Amine Hardeners
5.8 Applications of Vegetable Oils in Coatings
5.9 Conclusions
Acknowledgments
References

Chapter 6: Silica-Based Sol–Gel Coatings: A Critical Perspective from a Practical Viewpoint

6.1 Introduction: Need for a Practical Perspective
6.2 A Green, Simple Technology
6.3 The Market
6.4 Conclusions
Acknowledgements
References

Chapter 7: Fatty Acid-Based Waterborne Coatings

7.1 Introduction
7.2 Fatty Acids as Raw Materials
7.3 Polymerization of Fatty Acid-Based Monomers in Aqueous Media
7.4 Incorporation of Fatty Acid Derivatives in Waterborne Coatings
7.5 Conclusion
References

Chapter 8: Environmentally Friendly Coatings

8.1 Waterborne Coatings
8.2 Seed Oil-Based Coatings
8.3 Conclusion
References

Chapter 9: Low-Temperature Aqueous Coatings for Solar Thermal Absorber Applications

9.1 Introduction
9.2 Samples Preparation
9.3 Structural and Morphological Investigations of α-Cr_2O_3 Monodispersed Meso-spherical Particles
9.4 Growth Mechanism
9.5 Potential Applications in Solar Absorbers
9.6 Conclusions
Acknowledgements
References

Chapter 10: Eco-Friendly Recycled Pharmaceutical Inhibitor/Waste Particle Containing Hybrid Coatings for Corrosion Protection

10.1 Introduction
10.2 Hybrid Coating Preparation
10.3 Hybrid Coatings Performance
10.4 Conclusions
Acknowledgment
References

Chapter 11: Chemical Interaction of Modified Zinc–Phosphate Green Pigment on Waterborne Coatings in Steel

11.1 Introduction

11.2 Cathodic Delamination of Coatings
11.3 Modified Zinc–Phosphate Pigment
11.4 Conclusions
Acknowledgement
References

Chapter 12: Development of Soybean Oil-Based Polyols and Their Applications in Urethane and Melamine-Cured Thermoset Coatings

12.1 Introduction
12.2 Experimental
12.3 Results and Discussion
12.4 Conclusion
Acknowledgements
References

Chapter 13: Powder Coatings from Recycled Polymers and Renewable Resources

13.1 Introduction
13.2 Powder Coating as a Green Approach to Coatings
13.3 The Use of Materials from Renewable Resources in Powder Coating Applications
13.4 The Use of Recycled Polymers for the Preparation of Coatings
13.5 Powder Coatings from the Combined Chemical Recycle of Polymers and the Use of Renewable Resources
13.6 Conclusions
References

Chapter 14: The Synthesis and Applications of Non-isocyanate Based Polyurethanes as Environmentally Friendly “Green” Coatings

14.1 Introduction to Isocyanate-based Polyurethane Chemistry

14.2 Synthesis of Isocyanates
14.3 Toxicological Properties of Isocyanates
14.4 Synthesis of Phosgene-free Precursors
14.5 Non-isocyanate-based Polyurethanes (NIPU)
14.6 Applications of Non-isocyanate Polyurethanes (NIPU)
14.7 Conclusions
Acknowledgements
References

Index

Biobased and Environmental Benign Coatings

Scrivener Publishing
100 Cummings Center, Suite 541J
Beverly, MA 01915-6106

Materials Degradation and Failure Series

Studies and investigations on materials failure are critical aspects of science and engineering. The failure analysis of existing materials and the development of new materials demands in-depth understanding of the concepts and principles involved in the deterioration of materials The *Material's Degradation and Failure* series encourages the publication of titles that are centered on understanding the failure in materials. Topics treating the kinetics and mechanism of degradation of materials is of particular interest. Similarly, characterization techniques that record macroscopic (e.g., tensile testing), microscopic (e.g., *in-situ* observation) and nanoscopic (e.g., nanoindentation) damages in materials will be of interest. Modeling studies that cover failure in materials will also be included in this series.

Series Editors: Atul Tiwari and Baldev Raj
Dr. Atul Tiwari, CChem
Director, R&D, Pantheon Chemicals
225 W. Deer Valley Road #4
Phoenix, AZ 85027 USA
Email: atulmrc@yahoo.com, atiwari@pantheonchemical.com

Dr. Baldev Raj, FTWAS, FNAE, FNA, FASc, FNASc
Director, National Institute of Advanced Studies
Indian Institute of Science Campus
Bangalore 560 012, India
Email: baldev.dr@gmail.com, baldev_dr@nias.iisc.ernet.in

Publishers at Scrivener
Martin Scrivener(martin@scrivenerpublishing.com)
Phillip Carmical (pcarmical@scrivenerpublishing.com)

Biobased and Environmental Benign Coatings

Edited by

Atul Tiwari, Anthony Galanis, and Mark D. Soucek



WILEY

Copyright © 2016 by Scrivener Publishing LLC. All rights reserved.

Co-published by John Wiley & Sons, Inc. Hoboken, New Jersey, and Scrivener Publishing LLC, Salem, Massachusetts.
Published simultaneously in Canada.

No part of this publication may be reproduced, stored in a retrieval system, or transmitted in any form or by any means, electronic, mechanical, photocopying, recording, scanning, or otherwise, except as permitted under Section 107 or 108 of the 1976 United States Copyright Act, without either the prior written permission of the Publisher, or authorization through payment of the appropriate per-copy fee to the Copyright Clearance Center, Inc., 222 Rosewood Drive, Danvers, MA 01923, (978) 750-8400, fax (978) 750-4470, or on the web at www.copyright.com. Requests to the Publisher for permission should be addressed to the Permissions Department, John Wiley & Sons, Inc., 111 River Street, Hoboken, NJ 07030, (201) 748-6011, fax (201) 748-6008, or online at http://www.wiley.com/go/permission.

Limit of Liability/Disclaimer of Warranty: While the publisher and author have used their best efforts in preparing this book, they make no representations or warranties with respect to the accuracy or completeness of the contents of this book and specifically disclaim any implied warranties of merchantability or fitness for a particular purpose. No warranty may be created or extended by sales representatives or written sales materials. The advice and strategies contained herein may not be suitable for your situation. You should consult with a professional where appropriate. Neither the publisher nor author shall be liable for any loss of profit or any other commercial damages, including but not limited to special, incidental, consequential, or other damages.

For general information on our other products and services or for technical support, please contact our Customer Care Department within the United States at (800) 762-2974, outside the United States at (317) 572-3993 or fax (317) 572-4002.

Wiley also publishes its books in a variety of electronic formats. Some content that appears in print may not be available in electronic formats. For more information about Wiley products, visit our web site at www.wiley.com.

For more information about Scrivener products please visit www.scrivenerpublishing.com.

Library of Congress Cataloging-in-Publication Data:
Names: Tiwari, Atul, editor. | Galanis, Anthony, editor. | Soucek, Mark D., editor.
Title: Biobased and environmental benign coatings / edited by Atul Tiwari, Anthony Galanis, and Mark D. Soucek.
Description: Salem, Massachusetts : Scrivener Publishing ; Hoboken, New Jersey : John Wiley & Sons, 2016. |
Includes bibliographical references and index.
Identifiers: LCCN 2015049858| ISBN 9781119184928 (cloth) |
ISBN 9781119185116 (Adobe PDF) |
ISBN 9781119185109 (epub)
Subjects: LCSH: Coatings. | Coatings--Environmental aspects.
Classification: LCC TA418.9.C57 B56 2016 | DDC 667/.9--dc23 LC record available at http://lccn.loc.gov/2015049858

ISBN 978-1-119-18492-8

Preface

An enormous volume of petrochemicals is being consumed in the preparation of coatings for a wide variety of applications. The ever-growing demand and competitive edge in industry has compelled scientists to develop new materials that are high performance and cost-effective. The global sale in the coating industry is estimated to be approximately $127 billion that includes areas such as industrial, architectural, decorative, protective, and energy related etc. An exceedingly large volume of petrochemicals used to manufacture coatings has led to severe environmental damage from volatile organic compounds that continuously outgas throughout the lifespan of the products.

Due to the vast amounts of chemical ingredients being used around human, plant, and other animal life forms, it becomes imperative that ingredients used in preparing such compounds are environmentally and human friendly. The biobased chemicals are increasingly being utilized in making new coatings; however, such formulations do not always meet the stringent properties demanded by industry compared with their synthetic counterparts. Inferior thermal and environmental stability along with the increased competitive cost often pose challenges on the reaction mechanistic routes adopted by scientists.

A major portion of such biobased ingredients is that these are derived from our live feedstocks and that poses additional burdens on the growers. Agricultural scientists are working tirelessly on devising new genetically engineered crops that can be used to create protective materials consumed by an exponentially expanding human population. For example, genetically modified soybean and linseed oils are the new ingredients for biobased coatings. Development of biobased coatings is in its infancy and toxicologists are concerned of possible negative implications on human health after prolong usage as the new genetically modified crops have not yet been tested for long term stability. It is a common misperception that cheapest is easiest to make although the reverse is true with coatings and paints. It is worth noting that more than sixty variable parameters need to be tested and verified on coatings before any product can achieve a commercial success.

New raw materials, relatively untested compositions, elevated cost and inferior properties compared to the petroleum-based competitors constantly pose immediate threats to utilization of new biobased or benign coating materials. An extended knowledge of chemical and physical science along with engineering technology is needed for such a demanding product development. Although numerous open and patented literatures are flooded with compounds that claim lucrative properties from relatively new formulas, it is crucial to educate students and researchers who are involved in such technological developments. This book is a collection of articles written on various process parameters involved in the development of complex environmental benign high performance coatings. The first few chapters of this book describe the state-of-the-art technologies presently available. The conversion of soybean oil to polyvinyl ether and use of cerium and ferrite compounds in coatings are described in these chapters. Similarly, there is a dedicated chapter on the use of coatings and films on fruits and vegetables. The next few chapters of this book are meant for the developers who will learn the new concepts helping those formulating innovative products for commercial success. For example, the use of biobased epoxy to replace bis-phenol A-based epoxy resin in coating is discussed in a separate chapter followed by a chapter on silica-based sol-gel coatings. The use of fatty acid for the manufacturing of waterborne coatings is also discussed. Finally, the book focuses on the various testing and evaluation parameters followed by new

conceptual methods. The utilization of pharmaceutical inhibitors or recycled polymers in coatings is reviewed in detail along with nonisocyanate cured polyurethane coatings.

We are confident that this book will be of interest to the readers from diverse backgrounds in chemistry, physics, biology, materials science, and chemical engineering. It can serve as a reference book for students and research scholars and as a unique guide for the industrial technologists.

Atul Tiwari
Anthony Galanis
Mark D. Soucek
USA,
February 9, 2016

Chapter 1

Novel Biobased Polymers for Coating Applications

Harjoyti Kalita[1,2], Deep Kalita[3], Samim Alam[3], Andrey Chernykh[1], Ihor Tarnavchyk[1,3], James Bahr[1], Satyabrata Samanta[1], Anurad Jayasooriyama[1], Shashi Fernando[1], Sermadurai Selvakumar[4], Dona Suranga Wickramaratne[1], Mukund Sibi[4], and Bret J. Chisholm[1,2,3*]

[1]*Center for Nanoscale Science and Engineering, North Dakota State University, Fargo, ND, USA*

[2]*Materials and Nanotechnology Program, North Dakota State University, Fargo, ND, USA*

[3]*Department of Coatings and Polymeric Materials, North Dakota State University, Fargo, ND, USA*

[4]*Department of Chemistry and Biochemistry, North Dakota State University, Fargo, ND, USA*

[*]*Corresponding author*: bret.chisholm@ndsu.edu

Abstract

Linear, soluble polymers were produced from unsaturated biobased compounds using a carbocationic polymerization process. The unsaturated biobased compounds that were first converted to vinyl ether monomers and subsequently polymerized were plant oil triglycerides, cardanol, and eugenol. As a result of the much higher reactivity of the vinyl ether group compared to the unsaturation derived from the biobased compounds and the ability to tailor the cationic polymerization process, polymerization was exclusively limited to vinyl ether groups. By preserving the unsaturation derived from the biobased compounds, the polymers could be cross-linked into insoluble coatings by autoxidation. In addition, the unsaturation can be converted to other functional groups, such as epoxy groups, which enable other cross-linking mechanisms. This document describes some of the polymers and coatings that have been produced with the technology.

Keywords: Plant oil, soybean oil, poly(vinyl ether), coating, autoxidation, biobased, cardanol, eugenol, cationic polymerization

1.1 Introduction

Prior to the ample supply of petrochemicals, coatings were largely derived from renewable resources such as plant oils, fats, plant proteins, polysaccharides, terpenes, and minerals [1]. As a result of the low cost and tremendous diversity of petrochemicals, development of new coating

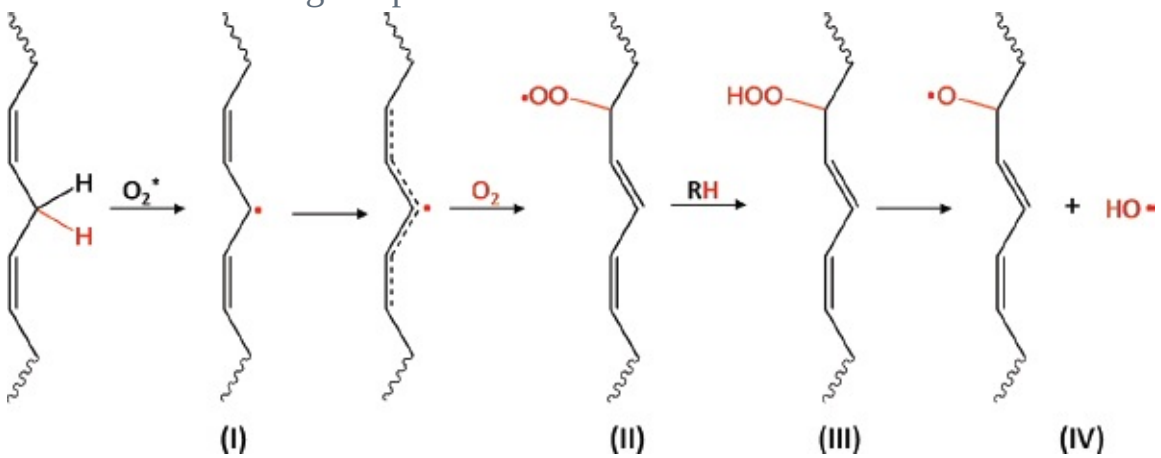
components based on renewable/biobased resources was largely abandoned. Due to concerns with the finite supply of fossil resources, geo-political events, the environment, and human health, the use of biobased materials in the coatings industry is making a resurgence.

In general, technology innovation within the coatings industry has been largely driven by regulations aimed at protecting both the environment and human health. These regulations have historically been focused on the reduction of the volatile organic compound (VOC) content of coatings. However, due to growing consumer demand for more environmentally friendly products, the chemical and materials industries have been placing more emphasis on the complete environmental impact of products. The total environmental impact of a product or material is typically assessed by conducting a life cycle analysis.

Of the coating resin technologies utilized today, alkyd resin technology uses a significant fraction of biobased materials. Alkyd resins were developed in the mid-1920s primarily as a means to reduce the drying time of coatings based on drying oils such as linseed oil, tung oil, walnut oil, perilla oil, and poppy seed oil [2]. Plant oil triglycerides are highly flexible molecules and, as a result, a significant degree of crosslinking is required for a drying oil-based coating to become dry to the touch. With the availability of petrochemicals, aromatic monomers, such as phthalic anhydride and isophthalic acid, were used to produce polyesters modified with fatty acid esters chains derived from a plant oil. The higher glass transition temperature (T_g) of these polyesters, referred to as alkyds, enabled films to become dry to the touch shortly after solvent evaporation from the film. Chemical resistance and film hardness were developed over time due to cross-linking by autoxidation.

The mechanism of the oxidative process, commonly referred to as autoxidation, is a free-radical process that possesses initiation, propagation, and termination steps [3–7]. As shown in Figure 1.1, initiation occurs by abstraction of a bis-allylic hydrogen by singlet oxygen to produce a carbon-centered radical (I). This radical is delocalized over the pentadiene structure and reacts with oxygen to produce the peroxy radical and conjugation in the fatty acid ester chain (II). The peroxy radical can participate in a number of reactions including hydrogen abstraction to produce the hydroperoxide (III). The hydroperoxide is thermally unstable and can undergo homolytic cleavage to produce an ether radical and a hydroxyl radical (IV). Cross-links are formed primarily by radical coupling reactions that result in a variety of cross-links including ether bonds, peroxide bonds, and carbon–carbon bonds.

Figure 1.1 A schematic illustrating the process of autoxidation.



The general classes of resins/polymers currently used in the coatings industry include epoxies, polyurethanes, alkyds, acrylics, polyesters, and amino resins. Of these, acrylic resins represent the highest volume resins used in the coatings industry. The utility of acrylic resins can be largely

attributed to the tremendous diversity in thermal and physiochemical properties that can be achieved through copolymerization. Most coating films derived from acrylic resins are thermoplastic and thus possess limited chemical and stain resistance. It has long been recognized that the incorporation of fatty acid ester chains into the pendent groups of acrylic resins would be a useful method for introducing cross-links into coating films to provide enhanced properties [8–13]. However, acrylate or methacrylate monomers possessing the linoleic and linolenic fatty acid ester pendent groups needed for effective oxidative cross-linking would be expected to be problematic due to the presence of the readily abstractable bis-allylic hydrogen atoms. These bis-allylic hydrogen atoms would be expected to lead to extensive chain transfer and perhaps gelation during the polymerization.

In the past few decades, tremendous progress has been made in the carbocationic polymerization of vinyl monomers [14]. Although carbocations are generally very reactive species, processes have been developed that enable very controlled polymerization. In fact, living carbocationic polymerization systems have been developed for a number of monomers including vinyl ethers [15], isobutylene [16], and styrene [17]. The controlled reactivity of the propagation step with these living polymerization systems is generally believed to be the result of a propagation step that involves an equilibrium between dormant and active species [18, 19]. A number of polymerization variables can be used to tailor the nature of a carbocationic polymerization including temperature, initiator composition, Lewis acid co-initiator composition, Lewis acid co-initiator concentration, addition of a Lewis base, Lewis base composition, Lewis base concentration, and solvent composition.

1.2 Polymers Based on Plant Oils

Using simple base-catalyzed transesterification of a vinyl ether alcohol with either a plant oil triglyceride or fatty alkyl ester, a novel vinyl ether monomer was produced [13]. Figure 1.2 shows the synthetic process using 2-(vinyloxy)ethanol as the vinyl ether alcohol and methyl soyate as the fatty alkyl ester. As illustrated in the figure, this monomer, 2-(vinyloxy)ethyl soyate (2-VOES), is a mixture based on the fatty acid ester composition of methyl soyate. As illustrated in Figure 1.3, the polymerization system developed for these plant oil-based vinyl ether monomers involves the use of the addition product of isobutyl vinyl ether and acetic acid as the initiator, ethylaluminum sesquichloride as the co-initiator, and toluene as the solvent. Using this system, a living polymerization was achieved [20].

Figure 1.2 The synthetic scheme used to produce a novel soybean oil-based vinyl ether monomer, i.e. 2-VOES.

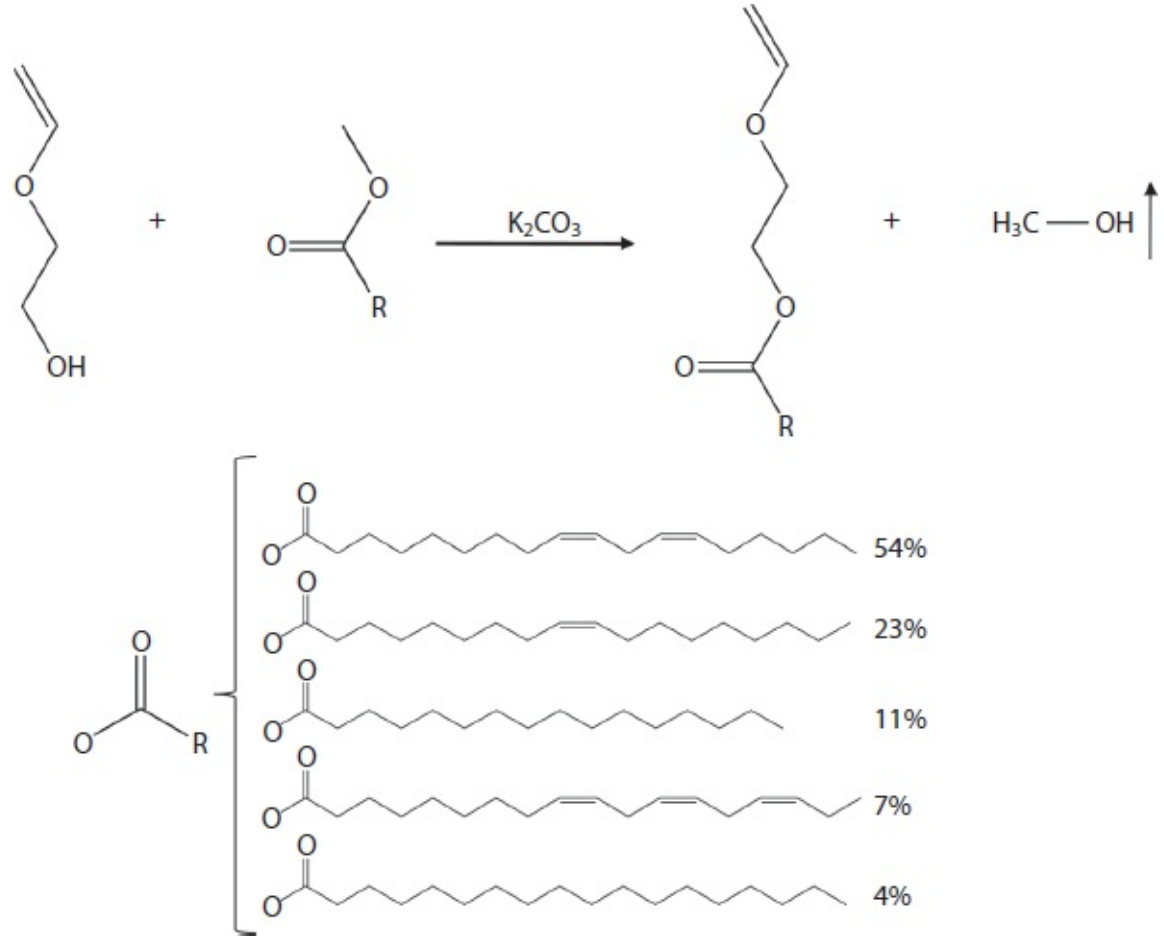
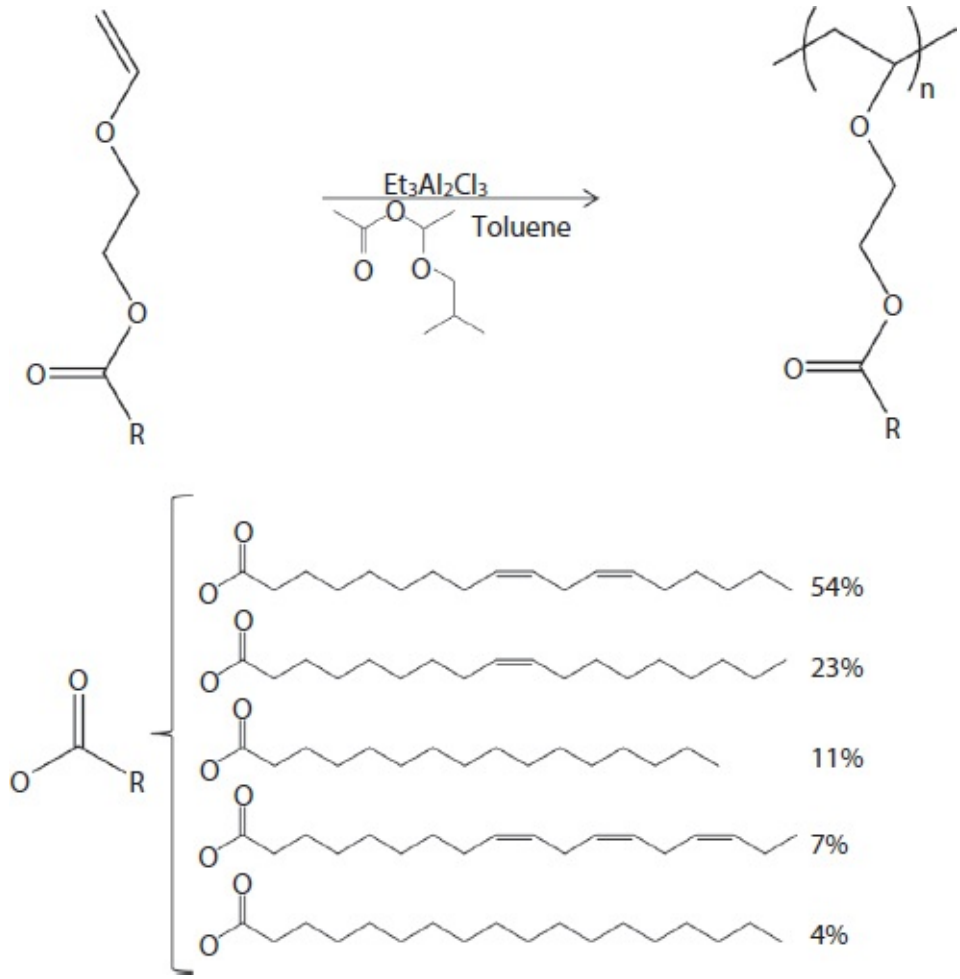


Figure 1.3 An illustration of the polymerization system utilized for the production of plant oil-based poly(vinyl ether)s.



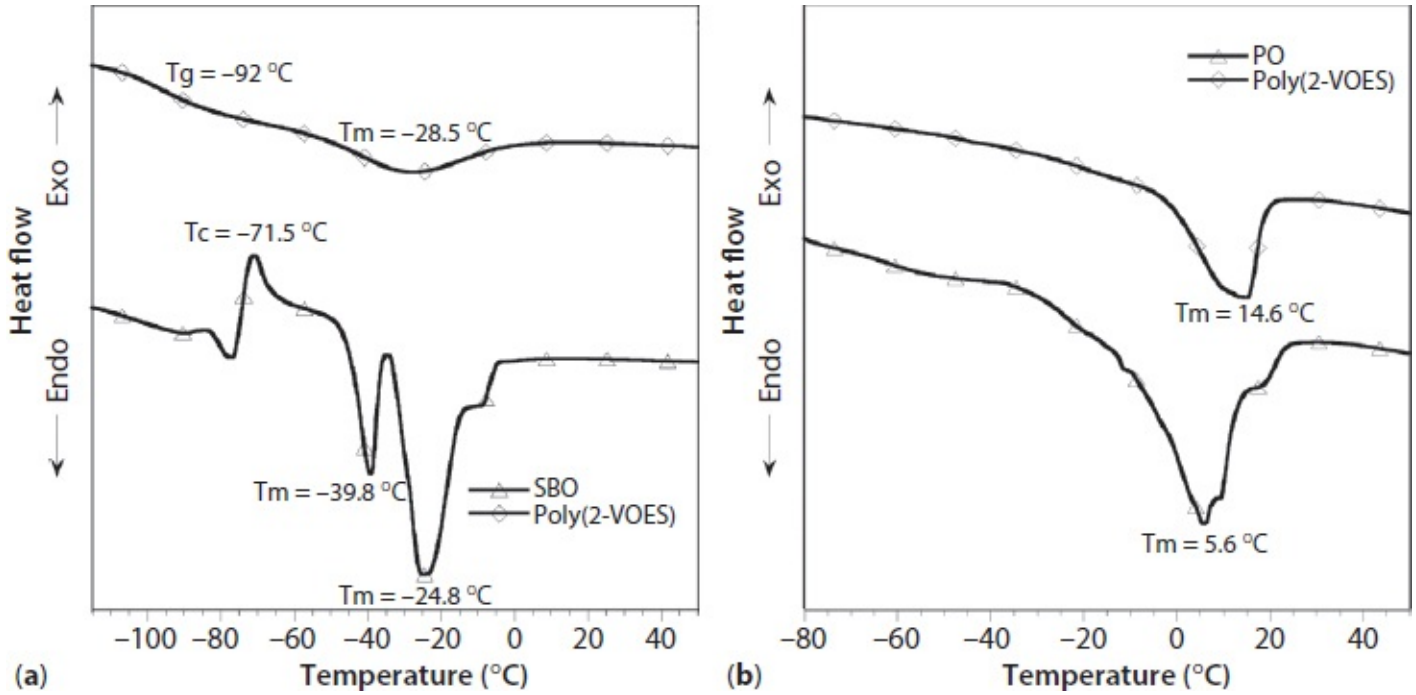
For most carbocationic polymerizations of a vinyl ether produced using a Lewis acid co-initiator,

such as ethylaluminum sesquichloride, an appropriate concentration of a Lewis base is needed to obtain a living polymerization. The mechanism of 'Lewis-base assisted living cationic polymerization' is believed to involve an equilibrium between dormant and active chain ends with the concentration of active chain ends being much lower than that of the dormant chain ends. The Lewis base is believed to reduce both the concentration of active chain ends and the reactivity of active chain ends. As described by Kanazawa *et al*. [18, 19, 21], the Lewis base: (1) complexes with the Lewis acid co-initiator resulting in the formation of monomeric Lewis acid species and an adjustment of acidity; (2) stabilizes active chains through direct interaction; and (3) stabilizes the counteranion generated upon initiation. For the polymerization of 2-VOES, it is believed that the ester group present in the monomer serves the role of a Lewis base additive typically utilized in a 'Lewis base-assisted' living carbocationic polymerization. The obtainment of a living polymerization enabled control of polymer molecule weight, narrow molecular weight distribution polymers, and the production of block copolymers [22].

1.2.1 Properties of Homopolymers and Their Surface Coatings

To date, plant oil-based poly(vinyl ether) homopolymers have been produced using soybean oil (SBO), hydrogenated SBO (HSBO), corn oil (CO), and palm oil (PO) as the parent plant oil. As expected, the thermal properties of these novel polymers varied as a function of the oil or fatty methyl ester used to produce the monomer. For example, polymers based on SBO and CO were amorphous liquids at room temperature, while the polymer based on HSBO was a waxy solid. The solid nature of the latter can be attributed to the high chain packing efficiency of the saturated fatty acid ester pendent chains. While the polymers based on SBO and CO were liquids at room temperature, side chain crystallization was observed using differential scanning calorimetry (DSC). For example, as shown in Figure 1.4a, the DSC for the SBO-based polymer, poly(2-VOES), displays a weak, broad endotherm with a peak maximum at –25 °C and a T_g at –92 °C [13, 22]. Compared to the parent oil, i.e. SBO, the heat of fusion for the SBO-based polymer was much lower indicating that the higher viscosity and polymeric nature of the latter significantly inhibited fatty acid ester chain crystallization. As shown in Figure 1.4b, the polymer based on PO, poly[2-(vinyloxy)ethyl palmitate] [poly(2-VOEP)], showed a melting temperature just below room temperature, which is consistent with the relative content of saturated fatty acid ester chains compared to the polymer based on SBO [23].

Figure 1.4 DSC thermograms for poly(2-VOES) and SBO (a) as well as poly(2-VOEP) and PO (b). Reproduced with permission from the American Coatings Association [13].



As a result of the polymeric nature of the plant oil-based polymers, the number of bis-allylic protons, allylic protons, and double bonds per molecule is much higher than that of the parent oil. As a result, the degree of autoxidation needed to produce a cross-linked network is significantly reduced compared to the parent oil. In fact, it was demonstrated that a coating produced by simply blending titanium dioxide with poly(2-VOES) became tack free in less than one-tenth the time required for an analogous coating based on linseed oil to become tack free [24]. Thus, by converting a semi-drying oil, such as SBO, to a polymer, drying properties can be achieved that are far superior to that of a drying oil. This feature of the plant oil-based polymer technology also translates to other curing chemistries. For example, the double bonds in poly(2-VOES) were converted to epoxide groups using peracetic acid and cross-linked networks produced using an anhydride curing agent. To illustrate the relative difference in the time required to reach the gel point for this network as compared to an analogous network based on epoxidized SBO (ESBO), rheological measurements were made as a function of time at 100 °C. For the epoxidized poly(2-VOES)/anhydride mixture, viscosity began to rise after just 20 min, while 2 h was required for the ESBO/anhydride mixture [22].

A similar trend was also observed for a comparison between polyurethane networks based on a polyol derived from poly(2-VOEP) to analogous networks based on a polyol derived from PO. Hydroxy groups were incorporated into poly(2-VOEP) and PO by first epoxidizing the double bonds in the materials and then ring-opening the epoxide groups with methanol [25]. In addition to providing a lower degree of functional group conversion to produce a cross-linked network, the molecular architecture of a plant oil-based polymer enables a significantly higher cross-link density compared to the triglyceride analog. This feature can be attributed to the methine carbon atoms present in the polymer backbone that function as additional cross-links in the network when the material is cured [22]. Further, cure shrinkage for cross-linked networks derived from a plant oil-based polymer would be expected to be lower than that for an a analogous network based on the parent triglyceride simply because of the molecular weight difference between the two materials.

Another attribute of the plant oil-based polymer technology is the ability to produce polymers that are essentially colorless. In general, plant oils possess some degree of color which is related to its composition. The common drying oil used in paints and coatings is linseed oil. As shown in Figure 1.5a, linseed oil is quite yellow in color. The yellowness of linseed is problematic for the production

of white and pale colored paints. Figure 1.5b shows a coating film produced by simply blending rutile titanium dioxide with linseed oil, casting the coating onto a substrate, and allowing the coating to cure at ambient conditions. As shown in Figure 1.5b, the cured coating is “off-white” due to the yellowness of the linseed oil. Since the vinyl ether monomers produced from a plant oil are significantly lower molecular weight, they can be vacuum distilled to remove color. It was found that the colorless vinyl ether monomer can be polymerized by cationic polymerization to produce a colorless polymer. Figure 1.6a provides an image of poly(2-VOES) produced from vacuum-distilled 2-VOES, while Figure 1.6b shows an image of a white paint produced from the poly(2-VOES) and rutile titanium dioxide in analogous fashion as that described for the linseed oil paint shown in Figure 1.5b. A comparison of Figure 1.6b to Figure 1.5b shows that the poly(2-VOES) derived from vacuum-distilled 2-VOES provides a white paint that does not possess the yellowness that is obtained when linseed oil is used as the binder.

Figure 1.5 Images showing the color of linseed oil (a) and a paint produced by blending linseed oil with rutile titanium dioxide (b).

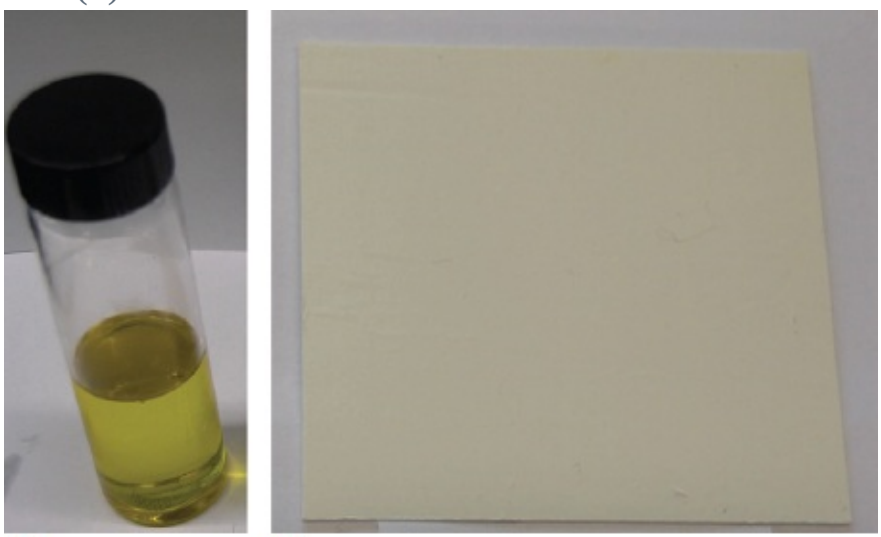
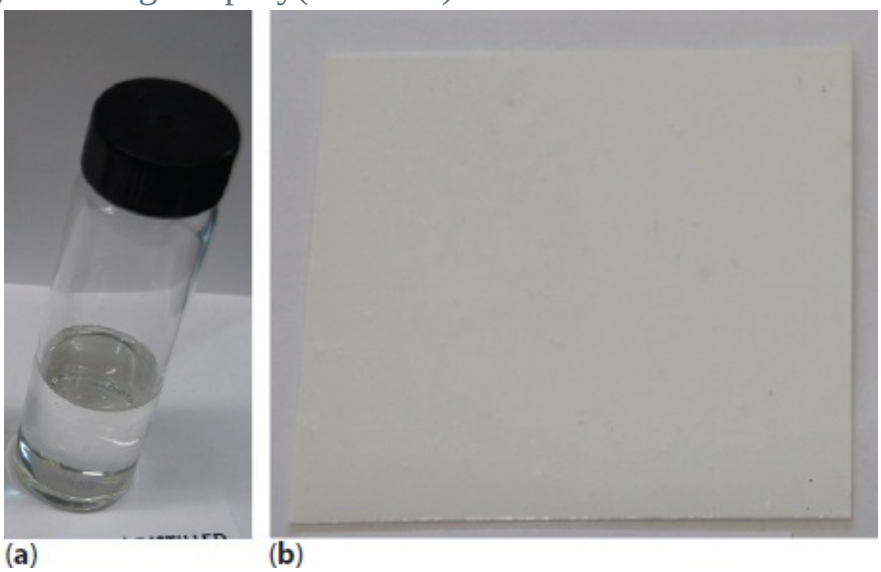


Figure 1.6 Images showing the color of poly(2-VOES) derived from vacuum-distilled 2-VOES (a) and a paint produced by blending the poly(2-VOES) with rutile titanium dioxide (b).



1.2.2 Properties of Copolymers and Their Surface Coatings

Probably, the most useful aspect of the plant oil-based polymer technology is the ability to widely tailor properties through copolymerization. This was demonstrated using a number of co-monomers including cyclohexyl vinyl ether (CHVE), menthol vinyl ether (MVE), and pentaethylene glycol ethyl vinyl ether (PEGEVE). Since homopolymers of the plant oil-based vinyl ethers possess a very low T_g, it was of interest to increase polymer T_g by copolymerization. As illustrated in Figure 1.7, both CHVE and MVE possess the cyclohexyl ring attached to the vinyl ether oxygen atom with MVE possessing a substituted ring. CHVE is commercially available, while MVE was synthesized in-house. MVE represents a potentially biobased monomer since menthol is a naturally occurring terpene that can be obtained from the peppermint plant, *Mentha x pipertia* (Lamiaceae) [26]. As expected, copolymerization of 2-VOES with these cycloaliphatic vinyl ether monomers enabled the formation of cross-linked films with increased T_g's compared to the control film based on the homopolymer of 2-VOES (i.e. poly(2-VOES)). Figure 1.8 shows the variation in T_g as a function of comonomer content for films cured at room temperature by autoxidation [27, 28].

Figure 1.7 Chemical structures for vinyl ether monomers that were copolymerized with 2-VOES.

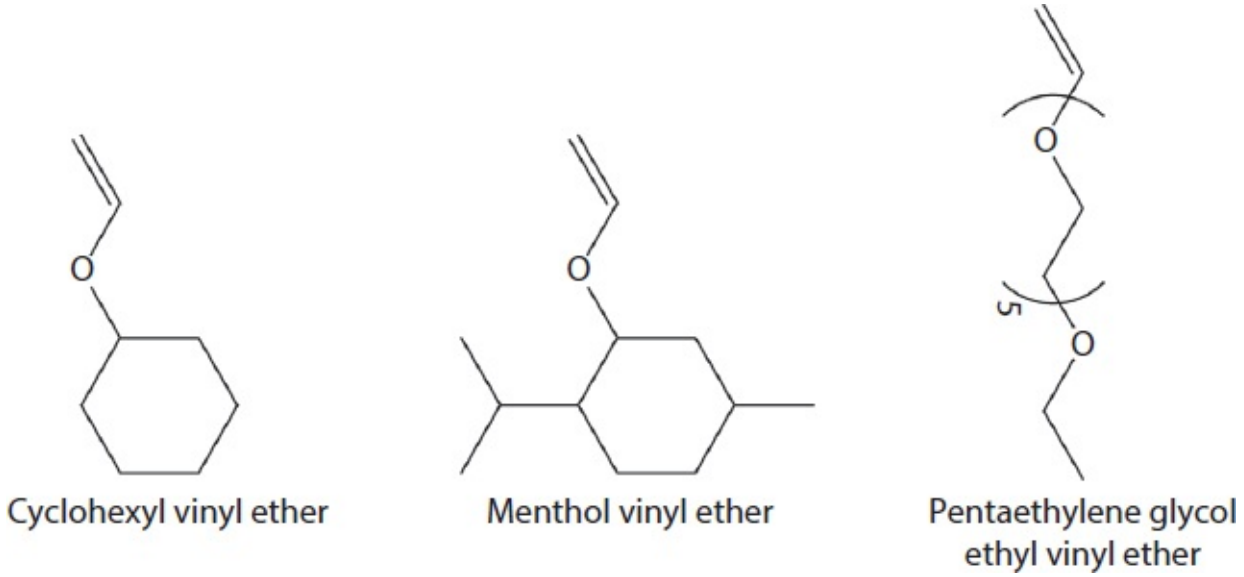
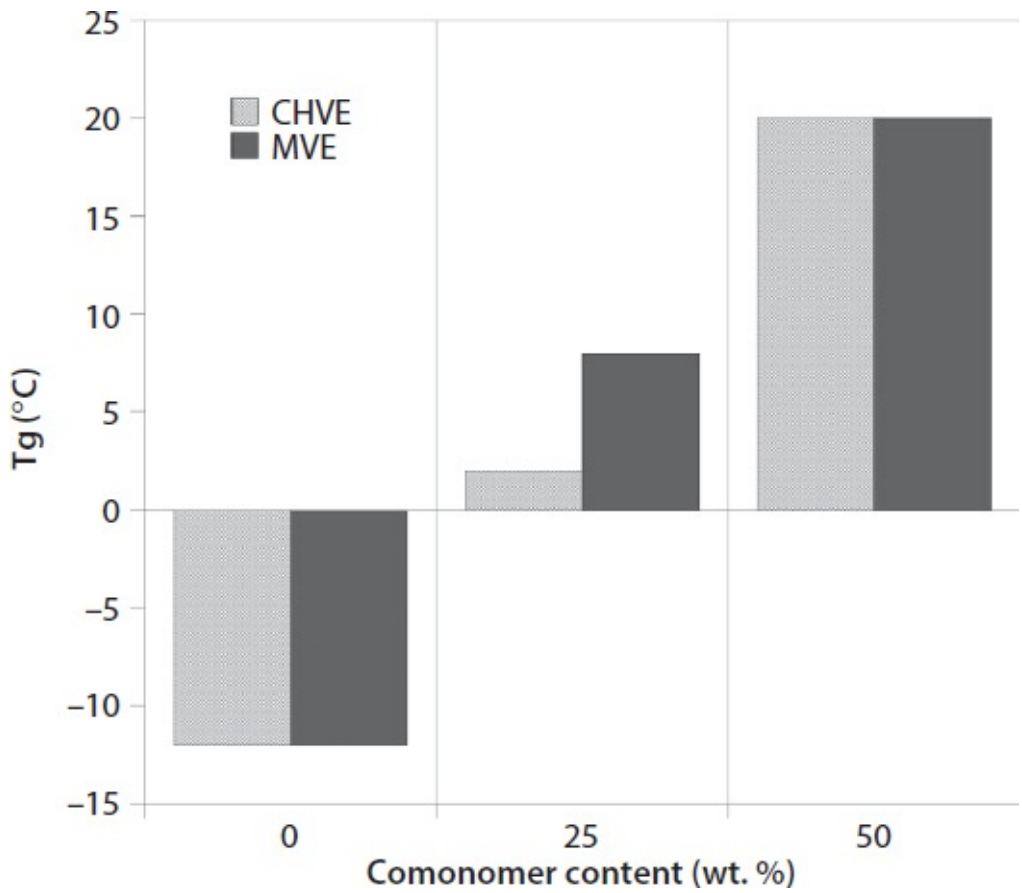
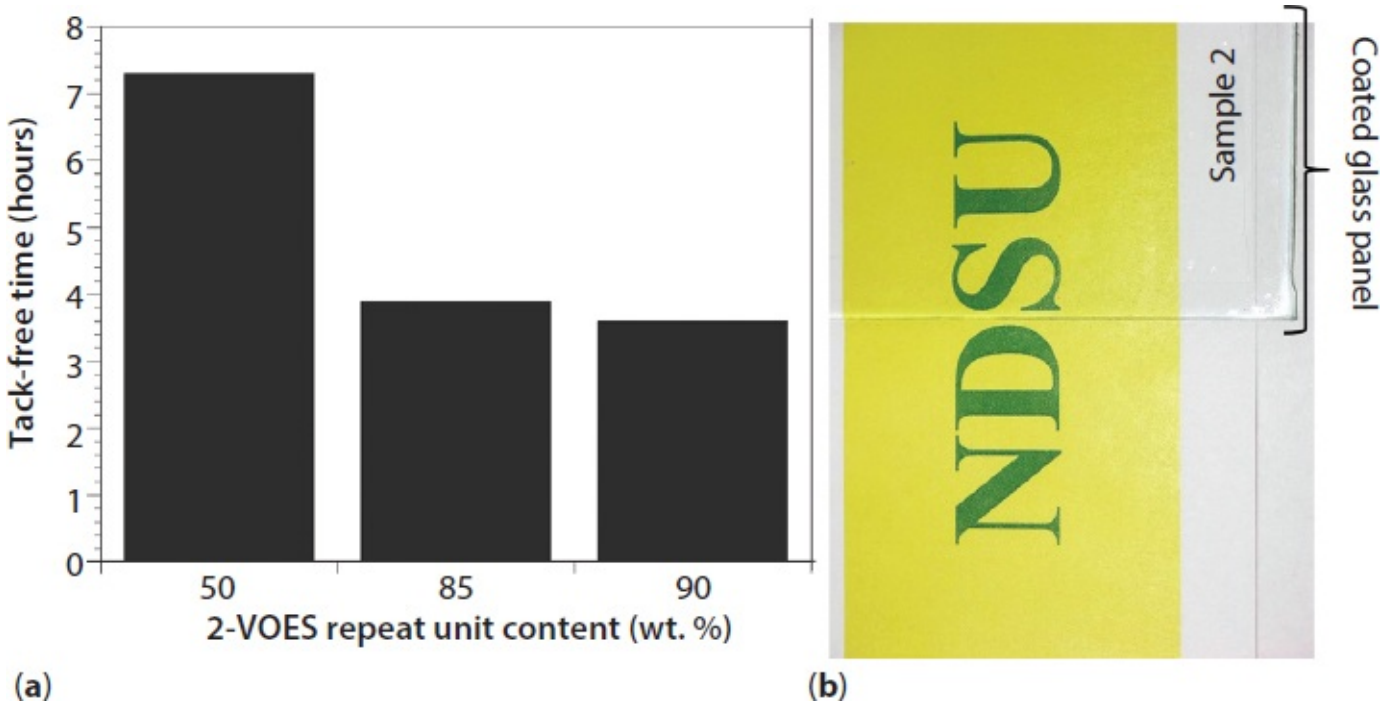


Figure 1.8 The variation in T_g with comonomer content for 2-VOES-based copolymer films cured at room temperature by autoxidation.



Copolymerization of 2-VOES with PEGEVE was utilized as a means to provide dispersability of the polymer in water without the need for surfactant. The amphiphilic copolymers produced were shown to be surface active as determined by measuring critical micelle concentration [29]. Three different copolymers were produced that varied with respect to PEGEVE repeat unit content. From these copolymers, aqueous dispersions were produced that also contained a water-based drier package. The solids content of the dispersions was 30 wt.% and all three copolymers gave stable dispersions. Figure 1.9a shows the variation in drying time with copolymer composition, while Figure 1.9b provides an image of a coating cast and cured at ambient conditions on a glass panel. As shown in Figure 1.9a, coatings cured relatively fast with the tack-free time decreasing with increasing 2-VOES repeat unit content. From Figure 1.9b, it can be seen that cured films had excellent optical clarity, which can be attributed to the lack of surfactant in the films.

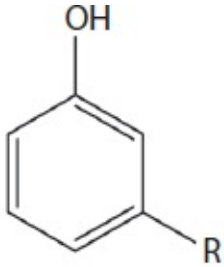
Figure 1.9 Tack-free time as a function of PEGEVE repeat unit content (a) and an image of a coated glass panel partially laid over the NDSU logo (b).



1.3 Polymers Based on Cardanol

Cardanol is derived from cashew nut liquid, which is a byproduct of cashew nut processing [30]. The primary component of cashew nut liquid is anacardic acid, which can be converted to cardanol by thermal decarboxylation. Cardanol is a mixture of four different *meta*-alkyl phenols that differ with respect to the degree of unsaturation in the alkyl side chain, as shown in Figure 1.10 [31]. As a result of the success obtained with the plant oil-based poly(vinyl ether)s described earlier, it was of interest to produce and characterize poly(vinyl ether)s containing cardanol units in the pendent chains of the repeat units. A novel vinyl ether monomer of cardanol, i.e. cardanol ethyl vinyl ether, was produced using the Williamson ether synthesis reaction shown in Figure 1.11. This monomer was successfully polymerized using the same polymerization system used for the production of the plant oil-based vinyl ethers. With this polymerization system, a soluble, tacky polymer was produced.

Figure 1.10 The chemical structure of cardanol.



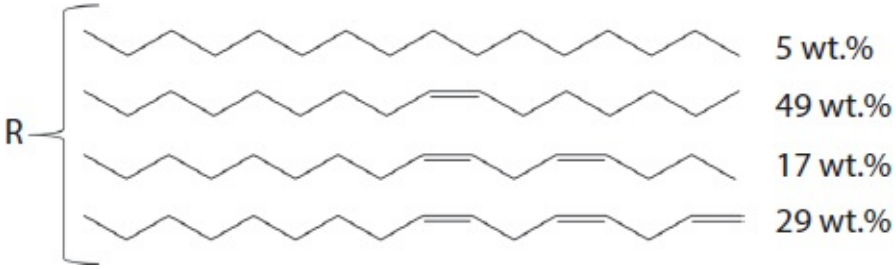
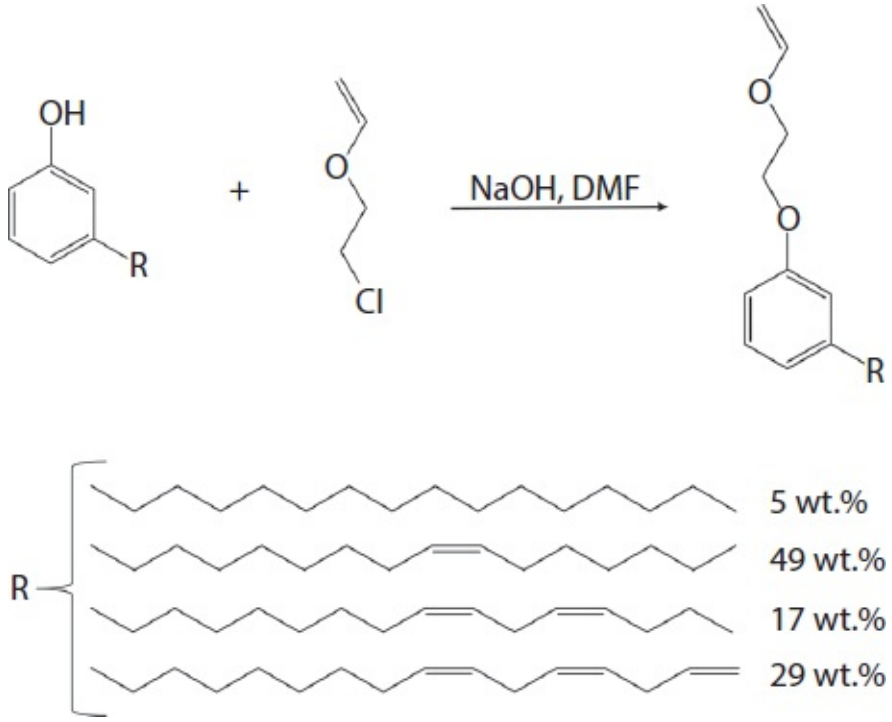


Figure 1.11 A schematic illustrating the synthesis of cardanol ethyl vinyl ether.



A solution of the polymer was combined with a drier package and films were cast on steel panels. Three different curing conditions were investigated. Curing at room temperature was done over a period of two weeks, while curing at 120 °C and 150 °C was done for 1 h. For elevated temperature curing, coated panels were placed into the oven shortly after the solvent had evaporated from the film. In addition to coated steel panels, free films specimens were prepared by casting films over Teflon™-laminated glass panels. Table 1.1 displays the properties of the coatings and free films prepared. In general, the coatings produced were relatively flexible and possessed sub-ambient T_g's. Although the coatings possessed sub-ambient T_g's, they exhibited good solvent resistance as expressed by the number methyl ethyl ketone (MEK) double rubs.

Table 1.1 Data obtained for cured films of poly(cardanol ethyl vinyl ether).

Curing temperature	23 °C	120 °C	150 °C
ASTM test			
König pendulum hardness (s) ASTM D4366	37 ± 1	38 ± 0	41 ± 1
Crosshatch adhesion ASTM D3359	3B ± 0	4B ± 0	4B ± 0
Conical mandrel bend test (% elongation) ASTM D522	>30%	>30%	>30%
Reverse impact (in lb) ASTM D2794	≥172	≥172	≥172
MEK double rubs ASTM D5402	120 ± 10	120 ± 7	150 ± 15
Tensile testing of free film specimens			
Young's modulus (MPa)	18.9 ± 1.3	20.9 ± 1.3	46.2±1.3
Elongation at break (%)	20.3 ± 1.1	19.0 ± 1.7	16.1 ± 0.8
Dynamic mechanical analysis of free films			
Storage modulus at 100 °C (MPa)	8.2	9.5	11.2
T_g from tan δ (°C)	5	11	13

1.4 Polymers Based on Eugenol

Eugenol is a major component of Ocimum, Cinnamon, and Clove oils [32]. Eugenol is primarily obtained from the clove buds of *Eugenia aromatic* and *Eugenia caryophyllata* belonging to the family Mytraceae indigenous to the Molluca Islands. It is also cultivated in other parts of Indonesia, Zanzibar, Madagascar, and Ceylon. Eugenol is also a potential product from the breakdown of lignin, and approximately 50 million tons of lignin is produced annually from the pulp and paper industries worldwide [33].

Analogous to the monomer based on cardanol, eugenol ethyl vinyl ether (EEVE) was produced from eugenol and 2-chloroethyl vinyl ether. This monomer was readily polymerized by cationic polymerization to produce a soluble polymer that was a viscose, tacky liquid at room temperature with a T_g of approximately 2 °C. Using proton nuclear magnetic resonance spectroscopy, preservation of the allyl group derived from eugenol was confirmed.

As illustrated in Figure 1.12, the methylene hydrogen atoms between the vinyl group and the phenyl group should be very labile to abstraction by singlet oxygen since the radical can be resonance stabilized by both the adjacent double bond and the phenyl ring. As a result, it was of interest to determine if poly(EEVE) could be cured into a cross-linked film by autoxidation. A poly(EEVE) sample with a number-average molecular weight of 17,900 g/mol was dissolved in toluene at 35 wt.%. To this solution, a drier package containing cobalt 2-ethylhexanoate, zirconium 2-ethylhexanoate, and zinc carboxylate was added. With this system, a cast film became dry-to-the-touch in 10 min. Coating specimens were produced using three different curing conditions, i.e. curing at

room temperature for 3 weeks, 120 °C for 1 h, and 150 °C for 1 h. In addition to films cast on steel substrates, free films were produced and used to determine film mechanical and viscoelastic properties. Table 1.2 shows the properties obtained for the coatings and films produced.

Figure 1.12 Illustration of resonance stabilization of a radical generated by hydrogen abstraction by singlet oxygen.

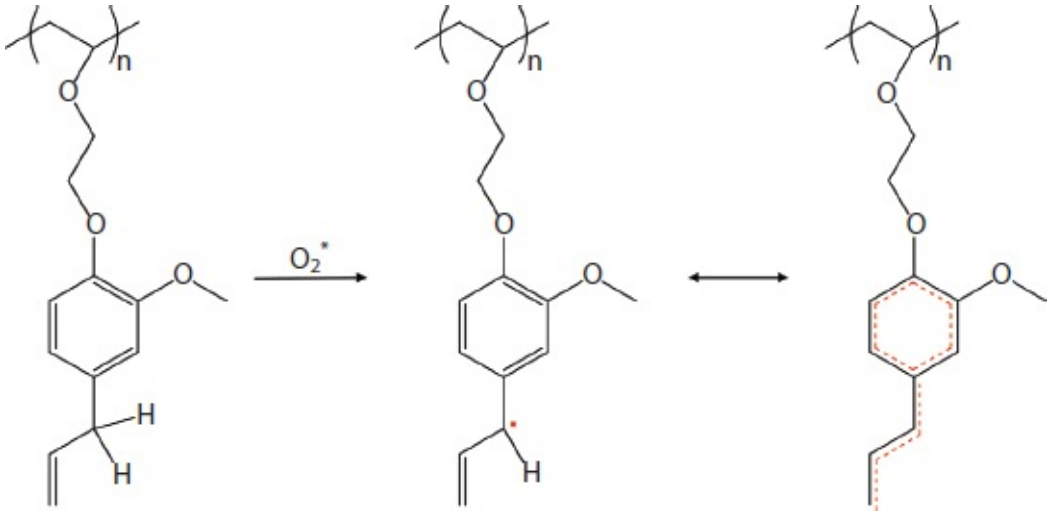


Table 1.2 Data obtained for cured films of poly(EEVE).

Curing temperature	23 °C	120 °C	150 °C
ASTM test			
Pencil hardness	F	2H	2H
König pendulum hardness (s) ASTM D4366	95.0 ± 1	75.6 ± 1.5	74.3 ± 1.5
Crosshatch adhesion ASTM D3359	5B ± 0	5B ± 0	5B ± 0
Conical mandrel bend test (% elongation) ASTM D522	>30%	>30%	>30%
Reverse impact (in lb) ASTM D2794	≥172	≥172	≥172
MEK double rubs ASTM D5402	413 ± 5.7	496 ± 30.0	500 ± 15.2
Tensile testing of free film specimens			
Young's modulus (MPa)	214 ± 21	394 ± 68	484 ± 63
Elongation at break (%)	44.8 ± 0.9	30.1 ± 0.45	35.5 ± 0.62
Dynamic mechanical analysis of free films			
Storage modulus at 100 °C (MPa)	1.98	4.23	7.13
T_g from tan δ (°C)	20	27	37

As shown in Figure 1.13, the presence of the vinyl groups in poly(EEVE) enables the production of polyepoxide resins by simple oxidation using, for example, *m*-chloroperoxybenzoic acid as the oxidant. An epoxidized version of poly(EEVE) was produced and cross-linked films generated using diethylenetriamine (DETA) as the cross-linking agent and a 1/1 epoxy/NH mole/mole ratio. For comparison purposes, cross-linked films of the diglycidyl ether of bisphenol-A (DGEBPA) were also produced using DETA. Figure 1.14 displays the viscoelastic properties of the network derived from

epoxidized poly(EEVE) and DETA. From the tangent delta data, a T_g of 130 °C was determined. It was very interesting to observe this high of a T_g considering the relatively high molecular mobility of the poly(vinyl ether) polymer backbone. Obviously the very high cross-link density derived from the high number of epoxy groups per polymer molecule enables such a high T_g.

Figure 1.13 The synthetic scheme used to produce an epoxidized version of poly(EEVE).

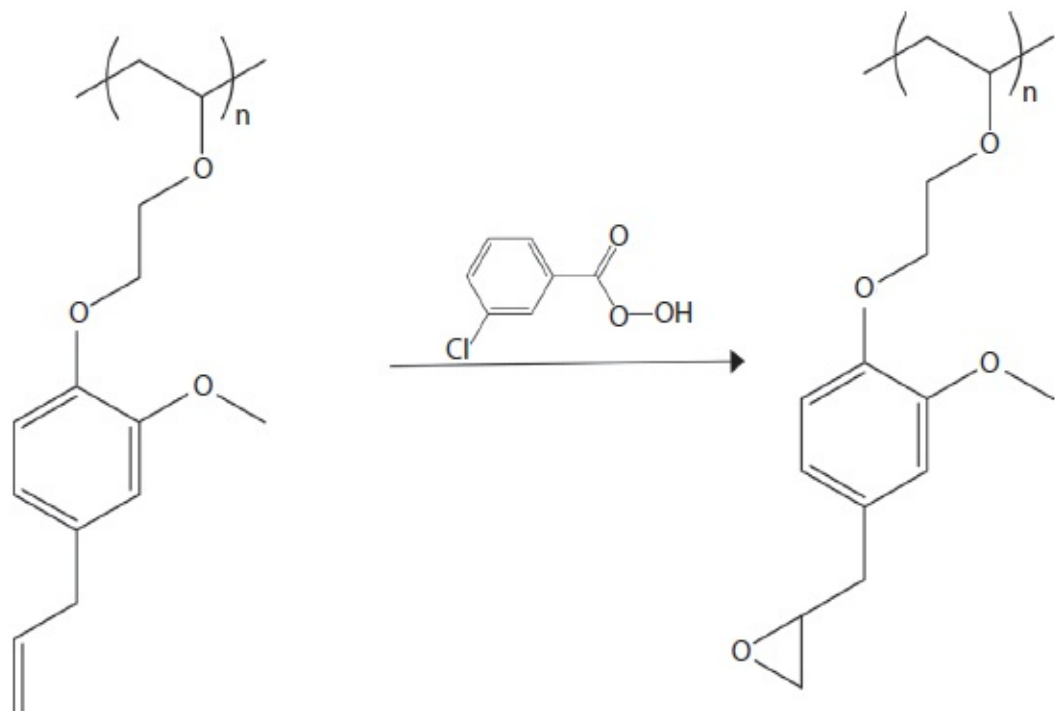


Figure 1.14 The viscoelastic properties of the network derived from epoxidized poly(EEVE) and DETA.

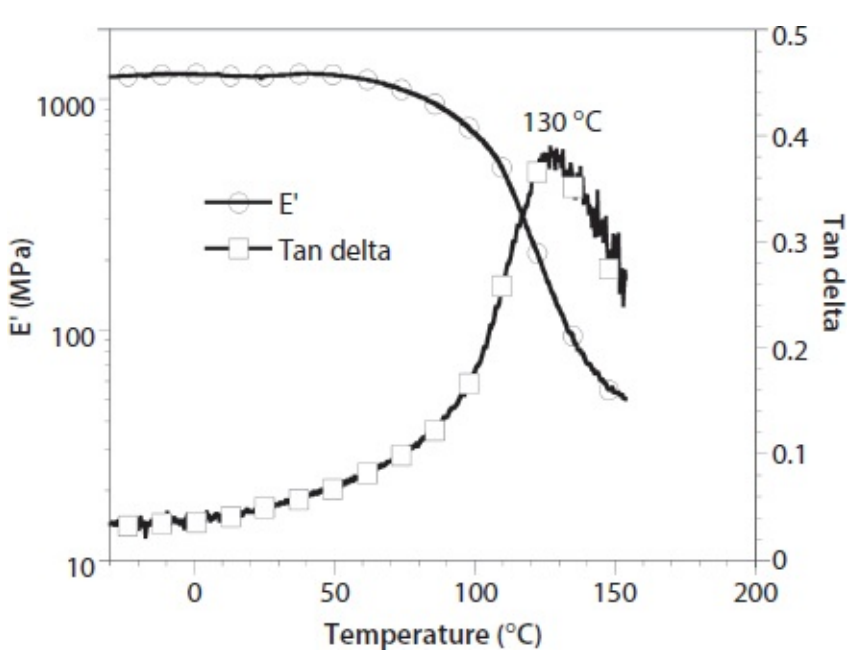


Table 1.3 provides a comparison of the properties of coatings cast and cured on steel substrates. As shown in the table, the hardness, flexibility, and adhesion of the coating based on epoxidized poly(EEVE) was similar to that of the analogous coating based on DGEBPA. The primary difference between these two coatings involved the chemical resistance and impact resistance. The chemical

resistance, as expressed using the MEK double rub test, was dramatically better for the coatings based on epoxidized poly(EEVE). After 1,000 MEK double rubs, no visible damage to the coating was observed. In contrast, the coating based on DGEBPA failed after 310 double rubs. With regard to impact resistance, the coating based on the epoxidized poly(EEVE) showed a lower impact resistance than the coating based on DGEBPA. The higher MEK resistance and lower impact resistance associated with the epoxidized poly(EEVE) are consistent with a higher cross-link density for this coating.

Table 1.3 Data obtained for coatings based on epoxidized poly(EEVE) and DGEBPA that were cast and cured on steel substrates.

Epoxy resin	DGEBPA	Epoxidized poly(EEVE)
König pendulum hardness (s) ASTM D4366	225 ± 2	205 ± 1
Crosshatch adhesion ASTM D3359	5B ± 0	5B ± 0
Conical mandrel bend test ASTM D522	>30% elong.	>30% elong.
Reverse impact (in lb) ASTM D2794	43	8
MEK double rubs ASTM D5402	310	>1,000

1.5 Conclusion

The results presented in this document demonstrate the utility of a carbocationic polymerization system for producing novel biobased polymers that retain the unsaturation derived from the biobased component. The high reactivity of the vinyl ether functional group and the appropriate choice of the polymerization system enabled linear polymers to be produced with relatively narrow molecular weight distributions. The ability to retain unsaturation from the biobased component enabled the production of cross-linked coatings using autoxidation. The high number of allylic hydrogens and double bonds per molecule associated with these unsaturated poly(vinyl ether)s results in relatively fast curing by autoxidation due to the gel point being reached at relatively low extents of reaction. Another important aspect of this polymer technology is the ability to utilize copolymerization to tailor polymer and coating properties. The unsaturation present in the polymer produced can also be easily converted to other functional groups, such as the epoxy group, to enable other cross-linking mechanisms.

Acknowledgments

The authors thank the Department of Energy (grant DE-FG36-08GO088160), United States Department of Agriculture/National Institute of Food and Agriculture (grant 2012-38202-19283), United Soybean Board, National Science Foundation (grants IIA-1330840, IIA-1355466, and IIP-1401801), and North Dakota Soybean Council for financial support.

Disclaimer

This report was prepared as an account of work sponsored by an agency of the US Government. Neither the US Government nor any agency thereof, nor any of their employees, makes any warranty,

express or implied, or assumes any legal liability or responsibility for the accuracy, completeness, or usefulness of any information, apparatus, product, or process disclosed, or represents that its use would not infringe privately owned rights. Reference herein to any specific commercial product, process, or service by trade name, trademark, manufacturer, or otherwise does not necessarily constitute or imply its endorsement, recommendation, or favoring by the US Government or any agency thereof. The views and opinions of authors expressed herein do not necessarily state or reflect those of the US Government or any agency thereof.

References

1. J.T.P. Derksen, F. Pertus Cuperus, and P. Kolster, Renewable resources in coatings technology: A review. *Progress in Organic Coatings*, 27, p. 45–53, 1996.

2. A. Hofland, Alkyd resins: From down and out to alive and kicking. *Progress in Organic Coatings*, 73(4), p. 274–282, 2012.

3. J. Mallegol, J.-L. Gardette, and J. Lemaire, Long-term behavior of oil-based varnishes and paints I. Spectroscopic analysis of curing drying oils. *Journal of the American Oil Chemists' Society*, 76, p. 967–976, 1999.

4. J. Mallegol, J. Lemaire, and J.-L. Gardette, Drier influence on the curing of linseed oil. *Progress in Organic Coatings*, 39, p. 107–113, 2000.

5. J. Mallegol, J.-L. Gardette, and J. Lemaire, Long-term behavior of oil-based varnishes and paints. Fate of hydroperoxides in drying oils. *Journal of the American Oil Chemists' Society*, 77, p. 249–255, 2000.

6. J. Mallegol, J.-L. Gardette, and J. Lemaire, Long-term behavior of oil-based varnishes and paints. Photo- and thermooxidation of cured linseed oil. *Journal of the American Oil Chemists' Society*, 77, p. 257–263, 2000.

7. M.D. Soucek, T. Khattab, and J. Wu, Review of autoxidation and driers. *Progress in Organic Coatings*, 73, p. 435–454, 2012.

8. S. Thames, *et al.*, New Monomers from Vegetable Oils, Specialty Monomers and Their Polymers. ACS *Symposium Series*, 755, p. 159–169, 2000.

9. E.H. Brister, W. Jarrett, and S.F. Thames, Castor-acrylated monomer 1H- and 13C-nuclear magnetic resonance spectral assignments. *Journal of Applied Polymer Science*, 82(8), p. 1850–1854, 2001.

10. C. Quintero, *et al.*, Miniemulsion polymerization of vegetable oil macromonomers. *Progress in Organic Coatings*, 57(3), p. 195–201, 2006.

11. C. Quintero, *et al.*, Reaction calorimetry as a tool to determine diffusion of vegetable oil macromonomers in emulsion polymerization. *Progress in Organic Coatings*, 57(3), p. 202–209, 2006.

12. G. Booth, D.E. Delatte, and S.F. Thames, Incorporation of drying oils into emulsion polymers for use in low-VOC architectural coatings. *Industrial Crops and Products*, 25(3), p. 257–265, 2007.

13. S. Alam and B. Chisholm, Coatings derived from novel, soybean oil-based polymers produced using carbocationic polymerization. *Journal of Coatings Technology and Research*, 8, p. 671–683, 2011.

14. S. Aoshima and S. Kanaoka, A Renaissance in Living Cationic Polymerization. *Chemical Reviews*,

109(11), p. 5245–5287, 2009.

15. M. Miyamoto, M. Sawamoto, and T. Higashimura, Living polymerization of isobutyl vinyl ether with hydrogen iodide/iodine initiating system. *Macromolecules*, 17(3), p. 265–268, 1984.

16. R.F. Storey, B.J. Chisholm, and L.B. Brister, Kinetic Study of the Living Cationic Polymerization of Isobutylene Using a Dicumyl Chloride/TiCl4/Pyridine Initiating System. *Macromolecules*, 28(12), p. 4055–4061, 1995.

17. T. Higashimura, y. ishihama, and M. sawamoto, Living cationic polymerization of styrene: new initiating systems based on added halide salts and the nature of the growing species. *Macromolecules*, 26(4), p. 744–751, 1993.

18. A. Kanazawa, S. Kanaoka, and S. Aoshima, Major Progress in Catalysts for Living Cationic Polymerization of Isobutyl Vinyl Ether: Effectiveness of a Variety of Conventional Metal Halides. *Macromolecules*, 42(12), p. 3965–3972, 2009.

19. S. Aoshima, *et al.*, New stage in living cationic polymerization: An array of effective Lewis acid catalysts and fast living polymerization in seconds. *Journal of Polymer Science Part A: Polymer Chemistry*, 45(10), p. 1801–1813, 2007.

20. A. Chernykh, *et al.*, Living carbocationic polymerization of a vinyl ether monomer derived from soybean oil, 2-(vinyloxy)ethyl soyate. *Green Chemistry*, 15(7), p. 1834–1838, 2013.

21. A. Kanazawa, S. Kanaoka, and S. Aoshima, Recent Progress in Living Cationic Polymerization of Vinyl Ethers. *Chemistry Letters*, 39(12), p. 1232–1237, 2010.

22. S. Alam, *et al.*, 2-(Vinyloxy)ethyl soyate as a versatile platform chemical for coatings: An overview. *European Journal of Lipid Science and Technology*, 116(1), p. 2–15, 2014.

23. D. Kalita, *et al.*, Novel high molecular weight polymers based on palm oil. *Journal of Oil Palm Research*, in press, 2015.

24. K. Harjoyti, *et al.*, Synthesis and Characterization of Novel Soybean Oil-Based Polymers and Their Application in Coatings Cured by Autoxidation, in *Soy-Based Chemicals and Materials* 2014, American Chemical Society. p. 371–390.

25. H. Kalita, *et al*., Novel high molecular weight polymers based on palm oil. *Journal of Oil Palm Research*, in press, 2015.

26. J.A. Farco and O. Grundmann, Menthol–pharmacology of an important naturally medicinal "cool." *Mini Review in Medicinal Chemistry*, 13, p. 124–131, 2013.

27. H. Kalita, *et al.*, Novel Biobased Poly(vinyl ether)s and Their Application as Alkyd-Type Surface Coatings. *Green Chemistry*, 16, p. 1974–1986, 2014.

28. H. Kalita, *et al.*, Novel alkyd-type coating resins produced using cationic polymerization. *Journal of Coatings Technology and Research*, submitted for publication, 2015.

29. S. Alam, *et al.*, Soy-Based Surface Active Copolymers As a Safer Replacement for Low Molecular Weight Surfactants. *ACS Sustainable Chemistry & Engineering*, 1(1), p. 19–22, 2012.

30. V.S. Balachandran, *et al.*, Recent advances in cardanol chemistry in a nutshell: from nut to nanomaterials. *Chemical Society Reviews*, 42, p. 427–438, 2013.

31. J.H.P. Tyman, *Synthetic and Natural Products*, Amsterdam: Elsevier, 2008.

32. G. Anuj and S. Sanjay, Eugenol: A potential phytochemical with multifaceted therapeutic activities. *Pharmacologyonline*, 2, p. 108–120, 2010.

33. P. Varanasi, *et al*., Survey of renewable chemicals produced from lignocellulosic biomass during ionic liquid pretreatment. *Biotechnology for Biofuels*, 6(1), p. 1–9, 2013.

Chapter 2

Deposition of Environmentally Compliant Cerium-Containing Coatings and Primers on Copper-Containing Aluminium Aircraft Alloys

Stephan V. Kozhukharov

University of Chemical Technology and Metallurgy, Sofia, Bulgaria

**Corresponding author,* stephko1980@abv.bg; stefko1980@abv.bg

Abstract

This chapter describes the basic concepts related to the application of cerium compounds as a main alternative to the already restricted approaches of the use of toxic and environmentally unacceptable compounds. The chapter begins with a brief description of the importance of aluminium alloys for the aircraft industry and the basic corrosion forms and damages typical for these alloys. Besides the indispensability of the coating procedures for providing long-term corrosion protection, the basic multilayered coatings systems are also discussed. Following this, the basic stages and factors of deposition of cerium conversion coatings (CeCCs) as primer coating layers are described. Subsequently, various methods that involve cerium compounds as active components in upper and finishing coating layers are proposed based on the literature analysis. Furthermore, some alternatives of the cerium compounds as environmentally friendly active coating ingredients, such as organic corrosion inhibitors, are also proposed. The chapter finishes with the recent and the most actual directions for further improvement of coatings. Finally, the development of dense, self-healing, sun-light-protected, hydrophobic coatings are described.

Keywords: Aircraft alloys, corrosion protection, cerium conversion coatings, technological aspects, hybrid and nanocomposite materials, corrosion inhibitors, multifunctionality

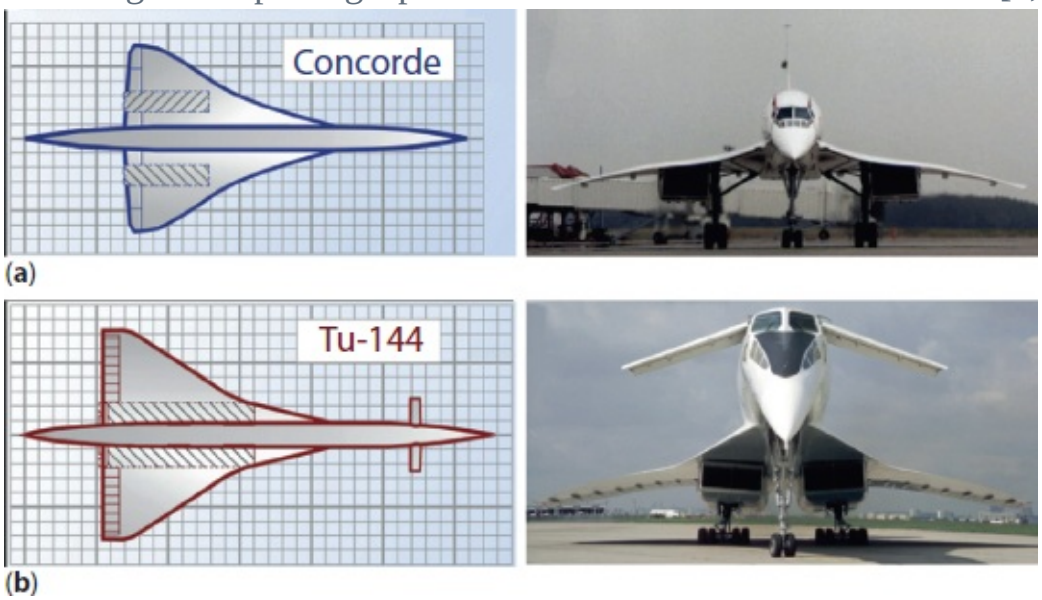
2.1 Importance and Indispensability of the Corrosion-Protective Coating Layers

2.1.1 Employment of Reliable Materials for the Aircraft Industry

The aircraft industry provides high-speed and long-distance transport options. However, the

reliability of this kind of transport services depends primarily on the ability for regular flights, regardless of the climatic conditions. During the flight, the external surface of airplanes is exposed to severe environmental conditions due to the sharp changes in temperature, caused by both the temperature difference between different altitudes and various local climatic zones the airplane passes through. Even in summer, the airplanes are exposed to low-temperature conditions at high altitude (e.g., the temperature at 10 000 m of altitude is about –70 °C, even at mid-summer). The high speeds of the modern flights lead to additional decrease in temperature, because of the resulting air flows that abrade (spoil) the airplane surface at about 850–900 km/h. Furthermore, since 1970s, following the inventions in the branch of the military aviation, promoted by the cold war, the commercial aircraft started to introduce models that enable flights even at ultrasonic speeds. The famous European commercial airplane “Concord” and its Russian analogue “Tu 144” are direct examples for ultrasonic commercial liners (Figure 2.1). As a result of these flight velocities, each flight is subject to sharp temperature changes in a wide range, usually from +40 °C to –70 °C. The endeavour for achievement of higher speeds of the flight will bring even sharper and more severe thermal shocks onto the fuselage during the flight.

Figure 2.1 Schematic images and photographs of commercial ultrasonic aircraft [1, 2].



These low temperature levels cause ice-heaping of the wings and propeller blades of the planes, leading to remarkable changes in their aerodynamics. These changes cause remarkable decrease in the efficiency, resulting in increase in the fuel spends, and might even endanger the safety of flight. Furthermore, the airplane travels through various local climate zones, with different humidity levels that form aerosols both in liquid (water drops) and solid (ice fogs) forms. Given the high speed of the flight, the abrading impact of these aerosols promotes scratching of the coating surface. Any rain water entrapment and/or water condense inside the scratches, combined with posterior volume expansion, causes disruption of the coating followed by crack proliferation. The already formed coating cracks favour localized forms of corrosion, such as filiform, pitting and crevice corrosion of the metallic body of the airplane. Each of these corrosion effects leads to stress corrosion cracking that seriously decreases the exploitation lifetime of the airplanes and can even be the reason for explosion-like splitting of the entire fuselage during flight.

Another important trend in the aviation sector is the elaboration of aircraft alternative to the airplanes. Indeed, the helicopters are among the most widely used aircraft. These have proved to enable transport service to destinations that appear to be impossible for any other kind of transport

(Figure 2.2).

Figure 2.2 Image of a commercial helicopter [3].

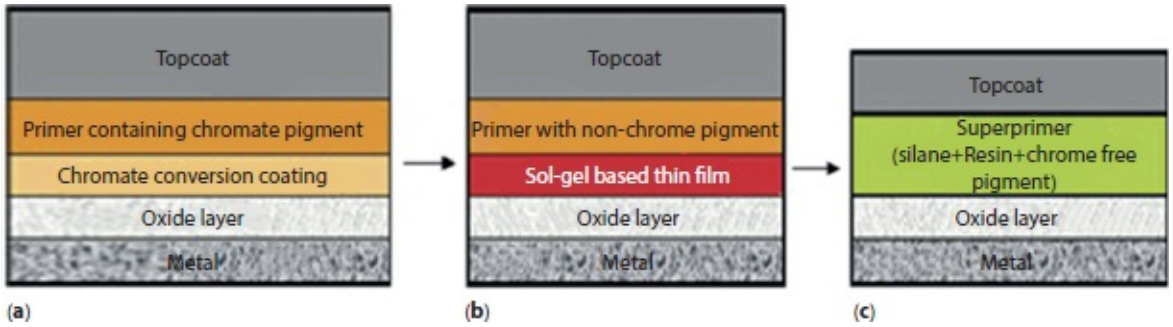


The most important feature of the helicopter transport branch is the indispensability of these devices in rescue missions in high mountains and other inaccessible regions. Nevertheless, among the most important problems related to the aircraft industry are the flight safety, reliability and the fuel spends, which besides the economic impact, provoke environmental contamination. Undoubtedly, this is one of the main roads for overcoming connected to improvement of the constructive materials and technologies.

Regardless of the employment of entire generations of new materials as carbon fibre composites in the transport and especially in the aircraft industry, the aluminium alloys still remain the basic constructive materials [4]. Especially, AA2024 and AA7075 alloys are objects of special attention, due to their remarkable mechanical strength [5], being the basic constructional material for commercial [6] and military [7, 8] aircraft. In the former case, the aluminium fuselages render “visibility” for the aircraft and airport radars, whereas in the military air transport, the Al frames shield the on-board navigation and communication equipment against exterior electromagnetic influence. Recently, the importance of these alloys increased, due to their capabilities to be employed in the automobile industry [9–12]. In addition, the aluminium alloys encountered application in the marine industry for production of sport boats and even ships [13–15], and the automotive industry [16, 17]. The main advantage of the aluminium alloys compared to the steels is that the former are much lighter (about 2.723 tonnes/m^3) than the latter (about 7.840 tonnes/m^3) [18]. Finally, the aluminium alloys are valuable for military naval building, rendering to the ships lower radar detection visibility [18], compared to the steel constructions. Nevertheless, the corrosion protection by coatings is indispensable for all kinds of aluminium details and equipment. The conventional coatings are always composed of multilayer systems, where each layer has its own function [19–21]. On the other hand, the environmental restrictions regarding the employment of chromium and other heavy metals in the European Community [22, 23] and the Unites States [24, 25] impose demands for elaboration of environmentally compliant coatings.

The elaboration of quick and efficient technological approaches for deposition of cerium conversion coatings (CeCCs) is an efficient response to all these challenges. These coatings should serve as primers for upper organic, hybrid or composite layers. The behaviour of these exterior coatings, especially their aptitude for cracking, blistering or/and partial detachment, is strongly dependent on the primer coating layers. In their review article, Balgude and Sabnis [21] have remarked the state-of-the-art and the ongoing future trends in the field of development of new multilayer systems for corrosion protection. These authors even schematically illustrated their vision about the ongoing trends regarding the elaboration of advanced multilayered anticorrosion coatings, as shown in Figure 2.3.

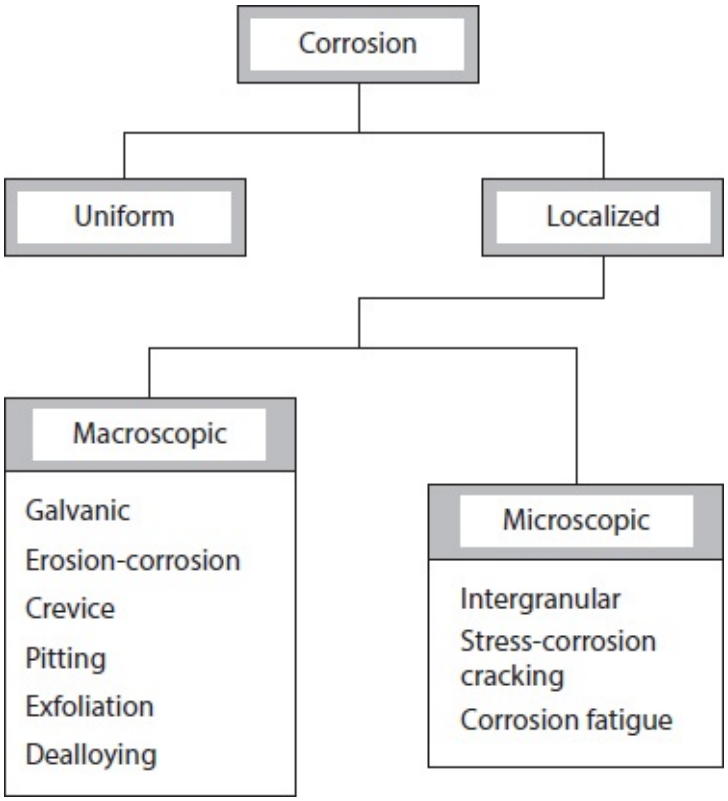
Figure 2.3 Schematic representation of (a) conventional chromate-based coating system, (b) newly developed sol–gel-based films and (c) environmentally friendly chrome-free super primer technology [21].



2.1.2 Corrosion Phenomena, Basic Definitions and Concepts

In the literature, there are various definitions about the corrosion processes. It could be considered as undesirable loss of properties of solid materials, as consequence of their interaction with their surrounding environment. These interactions, as nature and intensity, strongly depend on the nature (composition structure and properties) of the material, the environmental conditions (composition, pH, temperature, etc.) and also on the exposed surface area of the material. The importance of the last factor is originated from the heterogeneous character of the corrosion reactions, occurring between the solid metallic surface and the liquid or gaseous environment. According to Davis [26], the corrosion processes can be divided into several basic groups, as shown in Figure 2.4.

Figure 2.4 Basic classification of corrosion processes [26].



All these forms of corrosion attack proceed on the metallic surface, resulting in decrease of the efficient cross section of the respective metallic details. Combined with the presence of mechanical tensions, they lead to stress corrosion cracking, followed by complete constructional failure. The most famous case of such failure is the partial rupture of the fuselage during flight No. 243, in 1988 [27].

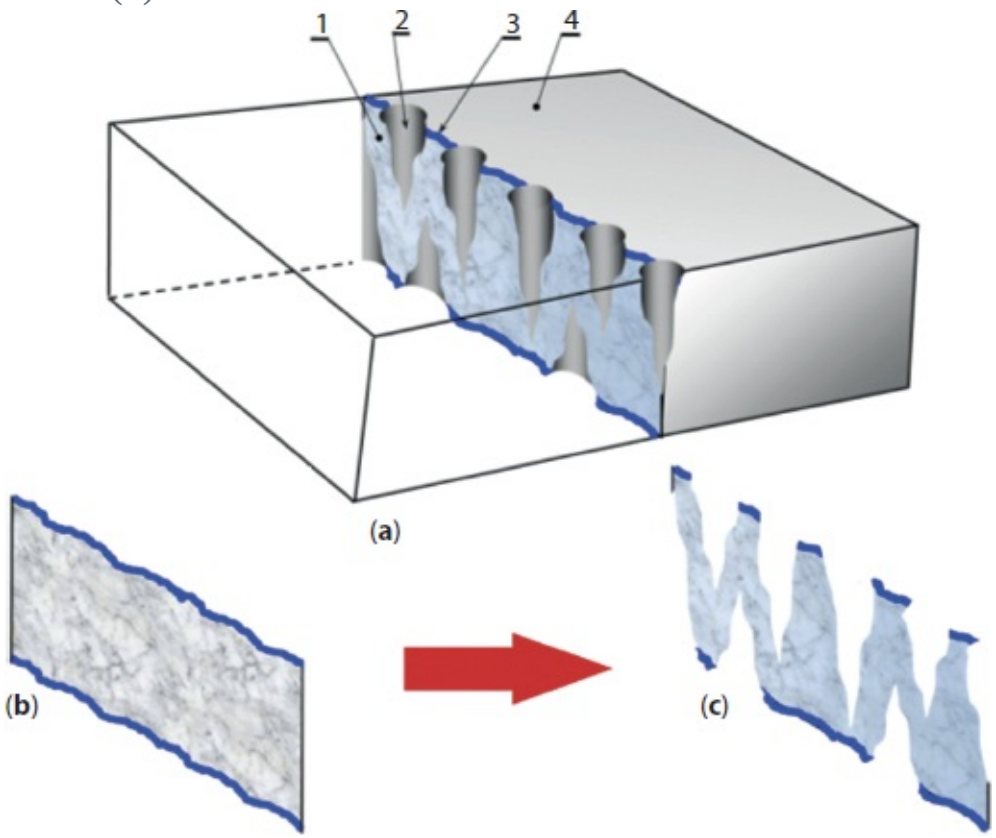
In general, the pure aluminium is well known to passivate by covering with superficial barrier oxide layer. Nevertheless, in the industrial practice, this metal is almost always in the form of alloys with elevated mechanical strength. The basic international nomenclature of the most widely used aluminium alloys is provided in Table 2.1. According to Ref. [28], the aluminium alloys are named "AA", with four-digit numbers, revealing their compositions and permitted levels of contamination. Additional numbering could indicate the method applied for metallurgical post-treatment. In these alloys, the alloying elements disrupt the completeness of this oxide layer, forming simultaneously galvanic coupling with the basic Al matrix. As consequence, the metallic alloys, in general, are strongly susceptible to accelerated electrochemical corrosion, unless they are not in the form of solid solutions. Indeed, Petrucci and Harwood [29] describe the electrochemical superficial corrosion processes on alloy surfaces as "undesirable voltaic cells".

Table 2.1 Nomenclature of the aluminium alloy according to Ref. [28].

Code of the aluminium alloy (AA)	Concentration of the main alloying element
AA1XXX	99.0% minimum;
AA2XXX	Copper (1.9% … 6.8%);
AA3XXX	Manganese (0.3% … 1.5%);
AA4XXX	Silicon (3.6% … 13.5%)
AA5XXX	Magnesium (0.5% … 5.5%);
AA6XXX	Magnesium and silicon (Mg 0.4% … 1.5%, Si 0.2% … 1.7%);
AA7XXX	Zinc (1% … 8.2%);
AA8XXX	Others

Thus, from the constructive point of view, the corrosion phenomena provoke decrease in the efficient cross section of the corresponding details, elevating the aptitude for appearance of stress corrosion cracking, followed by complete constructional failure. Figure 2.5 shows schematically the decrease in the efficient cross section by pitting corrosion.

Figure 2.5 Schematic illustration of efficient cross section decrease caused by localized corrosion: (a) 3D image of damaged metallic detail, and cross section before (b) and after (c) the corrosion attack. (1) Cross section, affected by corrosion, (2) corrosion pits, (3) superficial borders of the affected cross section and (4) metallic detail.



2.1.3 Brief Summary

The utilization of aluminium alloys is continuously increasing for elaboration and industrial production of various transport vehicles such as airplanes and their alternative aircraft, automobiles, boats and ships. Nevertheless, although the aluminium is a corrosion-resistant material with passivation aptitude, its alloys are prone to suffer localised corrosion attack. The localised corrosion causes decrease in the efficient cross-sectional area, resulting in remarkable loss of mechanical strength enabling stress corrosion cracking and subsequent constructional failure. This is the reason that makes coating and painting the metallic surfaces indispensable, which protects them from the aggressive action of surrounding environment. Moreover, the coating systems are always multilayered, and each layer has its own function. The reason for the use of multilayered systems is to achieve enhanced barrier properties and coating durability. Both these capabilities enable higher corrosion-protective ability of the resulting coating systems.

Since the corrosion phenomena proceed also during the preliminary superficial treatment and during the conversion coating deposition, these phenomena, together with the structural and compositional characteristics of AA2024 aircraft alloy, are described in the next paragraphs.

2.2 Introduction to the Cerium Conversion Primer Layers

2.2.1 Background and Basic Definitions

The specific function of the conversion coatings, in general, is to serve as primer layers that provide superior adhesion between the metallic substrate (i.e. the material of the fuselage) and the exterior protective paint layers. Following the definition of Arenas [30], it can be considered that the term “conversion coating” comprises each metal oxide layer deposited on a metallic surface, via whatever chemical or electrochemical process, that partially or completely substitutes the native superficial metal oxide.

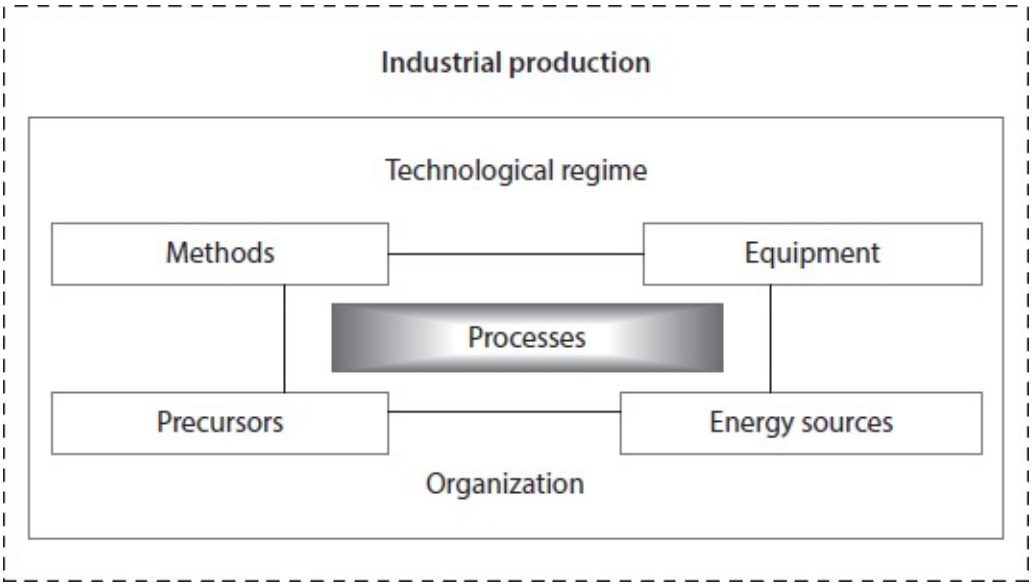
Obviously, the performance of the conversion coatings is entirely predetermined by the technology employed for their synthesis and deposition. In the scope of the material sciences, the term “technology” means the combination of all stages and processes that results in complete conversion of given raw or recycled materials and precursors into industrial product with desirable features.

The entire conjunction of all production stages and processes in their subsequence form the so-called “technological regime.” The maintenance of the technological regime enables us to choose the correct procedure for industrial production of a desired product with their predetermined features (characteristics) and predictable performance when used by the respective customer.

Therefore, the industrial production in general is based on the complete conversion to the final product and is carried out on the territory of the corresponding industrial production plants, supported by the necessary equipment. In order to maintain a regular industrial process, besides equipment and raw materials, energy sources are also necessary. Naturally in the industry, the energy sources are in various forms, but the most wide-spread forms are the thermal and electrical energies. The latter is applied in completely different types of devices for chemical conversion, mixing of the reactants, compression, vacuum, thermal heating and material transport connections among the corresponding apparatus.

Besides the equipment, raw and intermediated materials, and energy supply, the organization of the industrial process is another important factor that provides assurance of the regular production. The combination of the indispensable factors for the industrial production is represented in Figure 2.6.

Figure 2.6 Indispensable factors for any industrial process [31].



Hence, the technologist must know each process in each industrial stage to maintain the appropriate parameters of the processes composing the entire industrial technological process. Composition of the precursor mixtures, pH of the media, duration of the chemical conversion, rate of mixing and pressure are few examples of such parameters in the chemical industry.

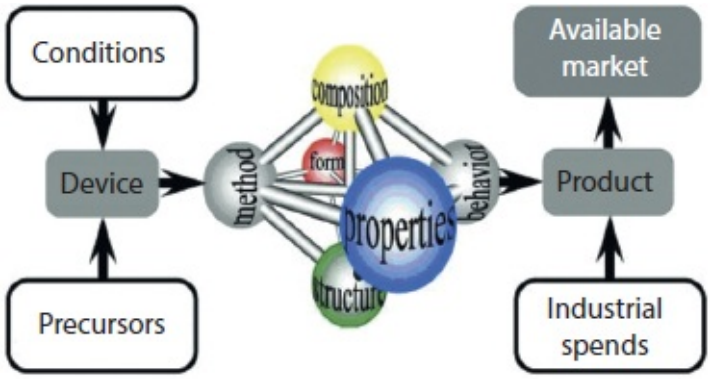
Besides maintaining adequate productivity of the available industrial installations, the industry also requires to maintain the parameters and conditions of the respective processes.

2.2.2 Deposition Methods

Another aspect of the industrial technologies is the elaboration of various methods. Especially in the case of coating, various deposition methods are developed such as spray deposition [32], spontaneous deposition by dip-coating [33–35], electrochemical deposition [36–39] and reactive magnetron sputtering [40].

The combination of the method applied and the conditions for the synthesis predetermines the quality of the product. The quality is the desired properties of the respective product, and it predetermines its performance in the real conditions of exploitation. On the other hand, the properties are always predetermined by the composition, structure and form of the respective product. These features are outcome of proper exploitation of precursors, conditions and the synthesis method, as shown in Figure 2.7 [41, 42].

Figure 2.7 Combination of the synthesis method, the characteristics and the performance of a given industrial product [41, 42].



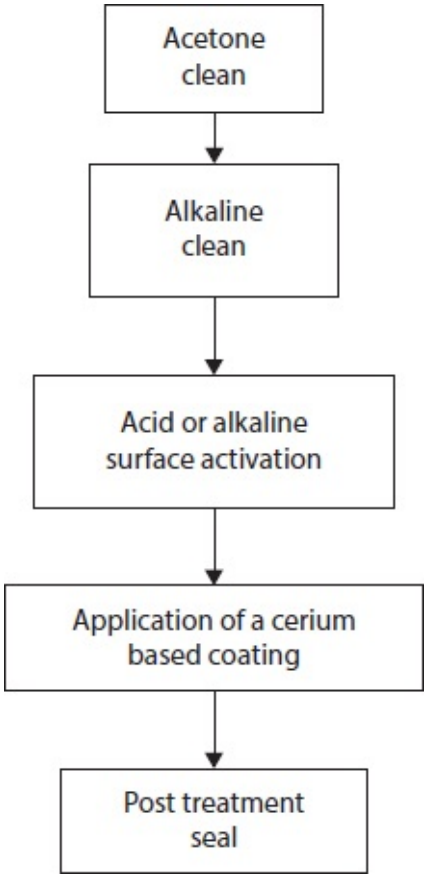
In the case of the CeCCs, they are deposited in the form of thin films on the respective metallic alloys. The most important properties of these coatings are its thickness, density, adhesion to the

substrate, scratch resistance and roughness. Since these coatings serve as primer layers, their colour is not so important. Moreover, the properties of the layer should be distributed uniformly on the entire metallic surface. That is the reason for the tremendous importance of the conditions of synthesis since they predetermine the structural and compositional equality on the entire coated surface. These features determine the entire performance of the coating, which can be summarized in barrier ability and durability. The perfectly deposited coatings play a role of a barrier between the stress from the surrounding environment and the protected metallic substrate. The conjunction of these properties predetermines the corrosion-protective ability of the respective coating.

2.2.3 Technical Stages of CeCC Deposition

Regardless of the method applied for deposition of CeCC on aluminium alloy substrate, there are three main stages for deposition of complete CeCC layer with satisfactory performance: (1) substrate preliminary treatment, (2) deposition of CeCC layer and (3) finishing sealing of the already deposited film. Figure 2.6 depicts the main procedures and steps of CeCC deposition, according to O'Keefe *et al*. [43], as shown in Figure 2.8.

Figure 2.8 Block scheme of the main procedures related to CeCC deposition [43].



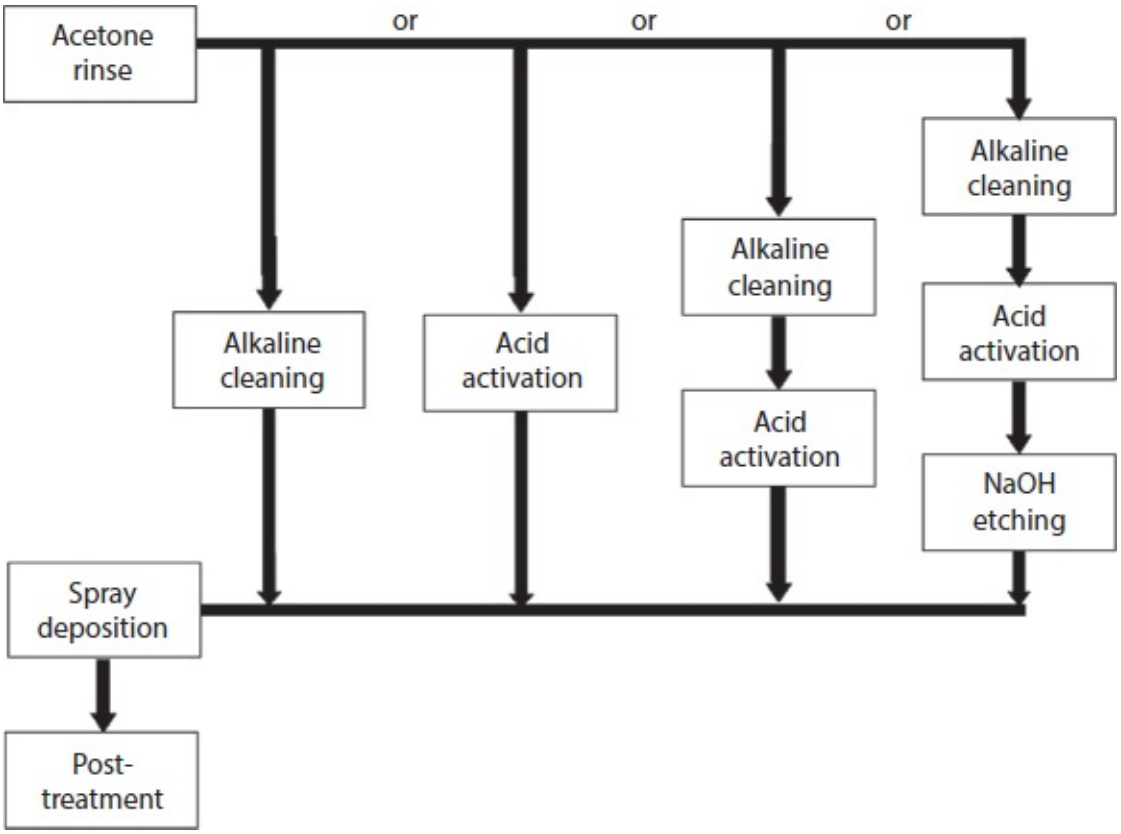
2.2.3.1 Preliminary Treatment Procedures

The metallic surface characteristics prior to coating deposition predetermine these of the interface with the primer coating, and consequently – the *adhesion* of the deposited layer. This property depends generally on the state of the metallic surface prior to deposition of the coating. Consequently, the most important factors that influence on the coating adhesion are the chemical composition of the metal substrate and the structure of the superficial oxide layer. Other important features of the metallic substrate are its roughness and superficial morphology. The larger number of edges and

peaks provides better adsorption ability of the metallic surface. Indeed, Hinton [44] mentions that the deposition relies on electrochemical interactions between the aluminium matrix and intermetallic inclusions that make up structural aluminium alloys. It is worth noting that the superficial composition could be modified by aggressive (alkaline or acidic) solutions. Generally, in the literature, it is preferred to apply the sequence of degreasing, desmutting and acidic activation [45, 46]. This sequence is preferred by the majority of the researchers, although in some cases only mechanical treatment has been applied prior to film deposition [47, 48]. Furthermore, various methods are available in the literature for preliminary chemical treatments [49–51]. Usually, the preliminary treatments are performed by commercial chemicals, as is described elsewhere [43]. However, the quality of the preliminary treatments depends on the compositions of the solutions used as well as on the conditions of the treatment (i.e. temperature and duration of exposure of the specimens). For this reason, Rivera *et al.* [52] have compared the properties of commercial solutions in different durations and temperatures. Finally, it should be mentioned that the procedures of preliminary treatment and the respective effects on the subsequent deposition are object of special investigations [53]. These authors concluded that only once deposited film after acidic activation excels 40-layered coating after alkaline etching.

Geng *et al.* [54] represent entire scheme of the diverse approaches for preliminary treatment as shown in Figure 2.9.

Figure 2.9 Schematic representation of various approaches of superficial treatment prior to coating deposition [54].



Prior to the preliminary treatments, the metallic substrate surfaces possess typical chemical composition, structure and roughness. These features are entirely predetermined by the technology applied for the metallurgical production of the metallic substrates. The chemical composition of the initial fusion predetermines composition of the obtained metal, whereas its structure is strongly influenced by the metallurgical thermal post-treatment procedures, such as forging, moulding and annealing. Namely, these procedures predetermine the phase formation inside the metallic sheet. The

roughness depends on other post-treatment procedures, like cold rolling, hot rolling, etc. Finally, each stage of the metallurgical production predetermines all the features of the produced alloys, such as the composition (during the fusion), the structure (thermal post-treatment) and the roughness (hot and cold rolling).

Particularly, the magnesium- and copper-containing aircraft alloys, such as AA2024-T3 [28] and its analogues ISO AlCu4Mg1 (regarding the International Organisation of Standardisation) [55, 56]; AA2024-T4, ASME SB211; as ISO – for European Community; GOST 172342-99 [57] for Russian federation; CSA CG42 (Canada), NF A-U4G1 (France); DIN AlCuMg2 (Germany); LY12 for China [58], etc., possess a wide variety of intermetallic particles with various compositions.

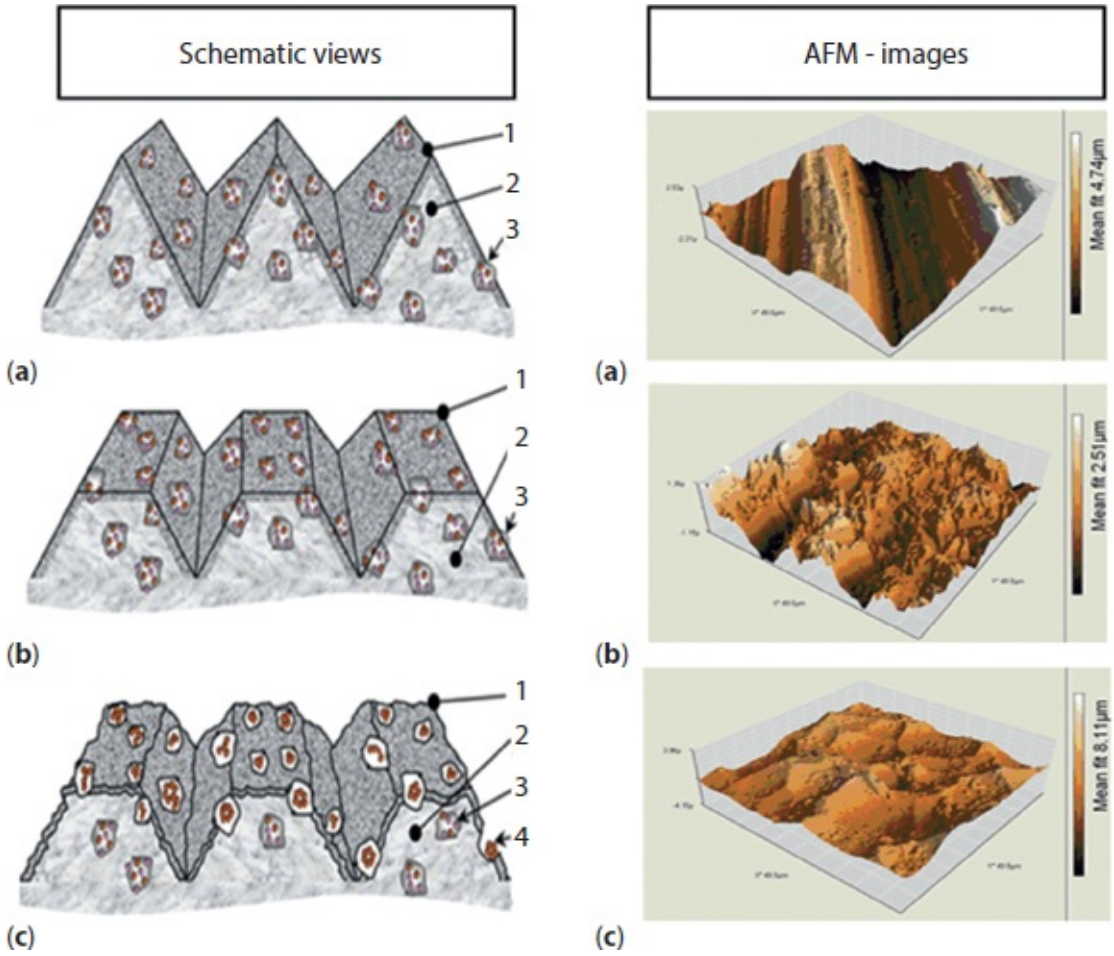
Various authors have performed detailed examinations on the exact compositional and structural features of these alloys. According to Yasakau *et al*. [59], the majority of them belong to the so-called "S-phase", composed of Al_2CuMg. Furthermore, the authors mention that these intermetallics cover almost 3% of the geometrical surface area of AA2024 alloy. The second type of intermetallics that occurs in the alloy's composition is Al_{16}(Cu, Fe, Mn) constituting 12% of all the precipitates. Minor concentrations of $Al_{20}Mn_3Cu_2$, $A_{l2}Cu$, $A_{l7}Cu_2Fe$ and $(Al, Cu)_6Mn$ are also present in the alloy.

Besides them, other intermetallics such as θ-phase, composed of Al_2Cu, are also described in the literature [59, 60]. Some authors mention that the decrease in the grain size of all the aluminium alloys results in decrement in the corrosion rate [61–64]. Furthermore, nine different phases with the basic composition of $(Al, Cu)_x(Fe, Mn)_ySi$ are described elsewhere [65].

Indeed, Rao and Rao [66] divide the intermetallics into bigger, coarse particles and fine precipitates. In the same paper, the authors mention that the larger coarse inclusions are the preferable locations of pitting nucleation, subsequent meta-stable pits appearance and further stable pitting growth. This process proceeds with coincident copper re-deposition, resulting in entire copper redistribution on the metallic surface.

Matter *et al*. [67] have developed a brief study regarding the influence of the superficial preliminary treatments and even chemical modifications on the behaviour of AA2024 plates in a model corrosive medium. Figure 2.10 reveals the apparently different morphologies obtained by the authors after the respective preliminary treatment procedures. The untreated surface possesses laminar shape, obtained during the rolling in the producer. After the mechanical polishing, the morphology has suffered remarkable conversion, and a large number of small pyramidal features appeared. The last one reveals wide zones occupied by craters. They are result of the aggressive chemical attack by the NaOH solution during the chemical etching. The surface, after the last approach, resembles the severe pitting corrosion features, typical for this group of alloys. That is why, the subsequent removal of the etching agents from the metallic surface by vigorous cleaning prior to further coating stages is of extreme importance.

Figure 2.10 Illustrations and AFM images of the various approaches of superficial treatment prior coating deposition [67]: (a) metallic surface of as-received specimen, (b) metallic surface after mechanical grinding and (c) metallic surface after mechanical and chemical preliminary treatments. (1) Superficial oxide layer, (2) aluminium matrix, (3) S-phase intermetallics and (4) copper remnants.



The authors have also established that the superficial treatments have a strong influence on the structure and the thickness of the native oxide layer. Usually, in the metallurgical industries, the metals undergo thermal post-treatments in order to achieve more equal distribution of the internal mechanical tensions. These treatments have impact on the surface oxide layer as well. The oxide layer is described to be composed of various Al–O compounds, for example, Al_2O_3, $Al(OH)_3$, and/or AlO(OH) [68–71]. Additionally, the oxide layer is rather a multilayered system, composed of a thin corundum layer below and a porous layer above, as is described elsewhere [72, 73]. Moreover, the authors mention the application of the Al-oxide layer for humidity sensors [72, 74–78], because of its ability for moisture uptake due to the presence of highly developed porosity.

Undoubtedly, the chemical preliminary treatment approach also has a great impact on both the superficial morphology and chemical composition of the metallic substrate and consequently on the adherence of the primer layers on it. This fact is well demonstrated by Ping *et al.* [53], who have performed research on various chemical preliminary treatments in alkaline or acidic solutions before deposition of CeCC through spray deposition. As the main result, the authors concluded that the surface preparation prior to the spray deposition had a significant effect on the thickness of the subsequent cerium-based conversion coating.

2.2.3.2 Deposition Process, Mechanisms and Factors

2.2.3.2.1 Mechanism

As mentioned in Paragraph 2.2.2, various methods for CeCC deposition are investigated until recently. The chemical nature of the CeCC deposition mechanism is based on several chemical reactions, as described by Aldykewicz [79]. This mechanism could conditionally be divided into three

basic stages:

- ***Formation of intermediated complex species*:**

(2.1) $2Ce^{3+}{}_{aq}. + H_2O_2 + 2OH^- \rightarrow Ce(OH)_2{}^{2+}{}_{aq}.$

- ***Reaction of the obtained complex ions with hydroxyl ions near the metallic surface*:**

(2.2) $Ce(OH)_2{}^{2+}{}_{aq}. + 2OH^- \rightarrow Ce(OH)_4 \rightarrow CeO_2 + 2H_2O$

- ***Subsequent conversion of the cerium hydroxides to the respective oxides*:**

(2.3) $Ce(OH)_4 \rightarrow CeO_2 + 2H_2O$

According to the authors, these reactions proceed accompanied by the following supplemental reactions:

- ***Direct interaction of the Ce^{3+} with the hydroxyl ions*:**

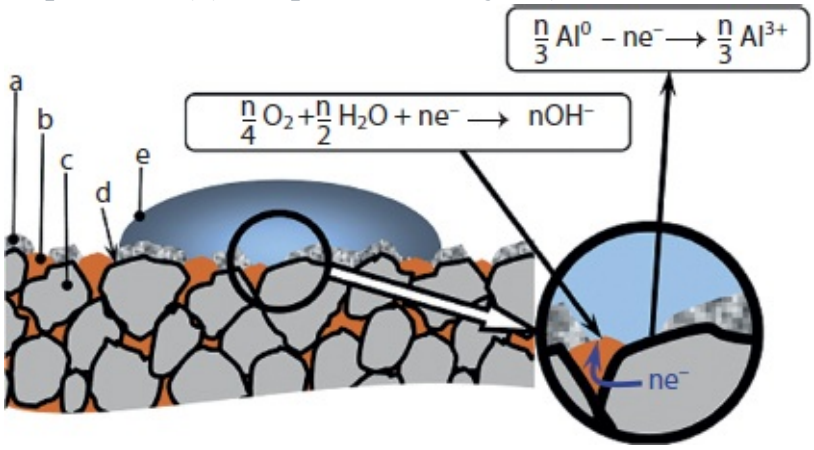
(2.4) $Ce^{3+} + 3OH^- \rightarrow Ce(OH)_3$

At spontaneous coating deposition, it is also possible to proceed further electrochemical oxidation of the generated $Ce(OH)_3$ on the electrodes' surface to CeO_2 (reaction 2.5)

(2.5) $Ce(OH)_3 \rightarrow CeO_2 + H_3O^+ + e^-$

Following this mechanism, it becomes clear that the OH^- ion content in the bulk solution has tremendous importance for the entire deposition process. Particularly, the AA2024 metallic surface suffers corrosion during the CeCC deposition process, and this process appears to be the main provider of hydroxyl ions, as shown in Figure 2.11.

Figure 2.11 Illustration of electrochemical corrosion of Al–Cu alloy: (a) superficial native oxide layer on the Al-anodic part, (b) copper inclusion, (c) area of the aluminium matrix, (d) superficial boundary of the aluminium part and (e) drop of electrolyte (water solution of NaCl) [80].



Thus, during the CeCC deposition from cerium salt solutions with hydrogen peroxide addition on Al–Cu alloys, they act as galvanic elements, where the copper inclusions play the role of cathodes where oxygen and peroxide reductions appear:

(2.6) $O_2 + 2H_2O + 4e^- \rightarrow 4OH^-$

(2.7) $2H_2O + 2e^- \rightarrow 2OH^-$

Whereas the rest of the aluminium alloy matrix behaves as an anode, suffering oxidation and dissolution:

(2.8) $Al \rightarrow Al^{3+} + 3e^-$

The aluminium ions in the solution react with a part of the hydroxyl ions on the metallic surface, resulting in the formation of polyoxohydroxy aluminium complexes, with Keggin structures [81], which hinder the further ingress of the species from the solution towards the metallic surface [82]. This is the reason for the presence of Al species inside the CeCCs.

The superficial oxide layer on the aluminium matrix is also important factor for the CeCC formation. Conde *et al.* [83] remark that the desired covering layer is obtained through chemisorption processes on the superficial oxide layer of the aluminium, which could briefly be described as follows:

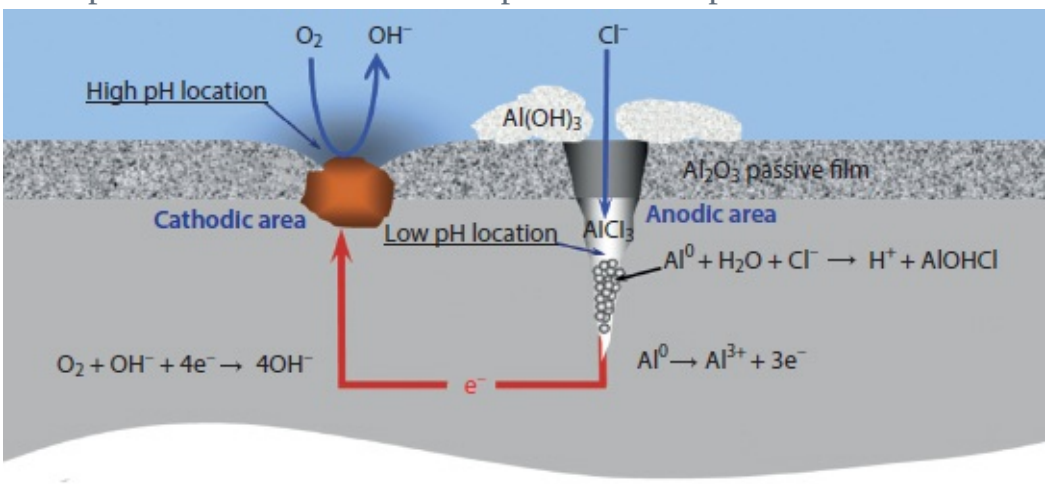
(2.9) $-Al-OH_2^+ \leftrightarrow -AlOH + H^+$

(2.10) $-Al-OH + Ce^{3+} \leftrightarrow [-Al-O....Ce(III)]^{2+} + 2H^+$

This supplemental heterogeneous process is crucial for the formation of adherent protective film instead of colloidal precipitates and sediments in the solution.

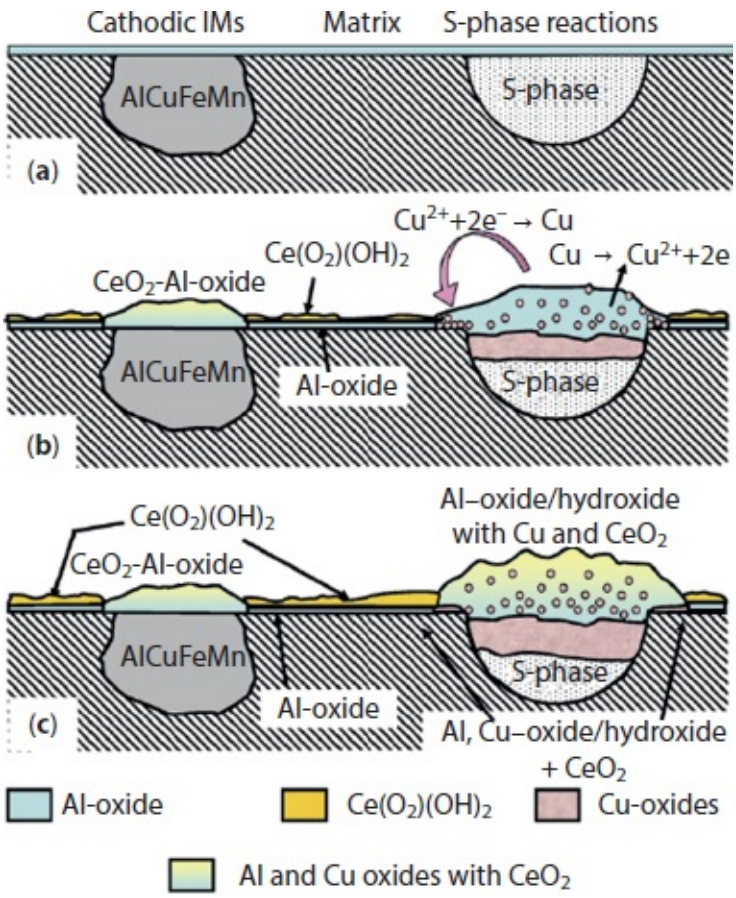
The structure of the oxide layer is irregular and composed of sub-layers of various aluminium oxides and hydroxides. The defects and irregularities in the superficial oxide layer also render their influence on the CeCC formation, being additional providers of Al^{3+} ions. Figure 2.12 represents the possibility for participation of Al-oxide layer defects in the pitting formation on Al–Cu alloy [84].

Figure 2.12 Schematic presentation of corrosion process of separated cathodic and anodic areas [84].



The mechanism described in the present section and presented by reactions from 2.1 to 2.9 is well illustrated in the literature [85]. As can be seen from Figure 2.13, intermetallic particles with various compositions could impart simultaneously in the deposition process, forming cathodic areas with different activities. The deposition process initiates on the areas surrounding the most active S-phase intermetallics and subsequently proliferates on the rest of less active cathodic zones. This mechanism of coating formation is named by Aldykiewicz [79] as “island growth mechanism”.

Figure 2.13 Model of precipitation of the Ce-based conversion coating: (a) surface prior to CeCC, (b) early stages of coating and (c) latter stages of coating [85].



Following the mechanism described earlier, it can be inferred that the CeCCs possess a variable composition, represented by the presence of various Ce and Al oxides hydroxides and oxy-hydroxides. Because of the presence of areas with varying pH, the coating composition varies on the metallic surface, being predetermined so by the metal surface morphology prior to coating deposition and by the conditions of CeCC deposition.

2.2.3.2.2 Factors

Metallic surface morphology and composition: As already mentioned in Paragraph 2.2.3.1, the preliminary treatments have a great importance for the metallic surface modification prior to CeCC deposition. They are necessary to prepare the metallic surface prior to film deposition. The basic purpose of these treatments is to provide clean surface with determined roughness and superficial chemical composition. This is the reason to apply various procedures for preliminary treatment.

Mechanical grinding: It is the simplest method for predetermination of the surface roughness before coating deposition. This approach is used by several authors [86, 87]. This process is industrially unattractive, and its application is usually avoided.

Degreasing: The metal alloys usually are protected by temporal hydrophobic coatings, so they have to be cleaned using organic solvents. Usually, this procedure is performed by rinsing in acetone, ether, alcohol or mixtures of them for several minutes.

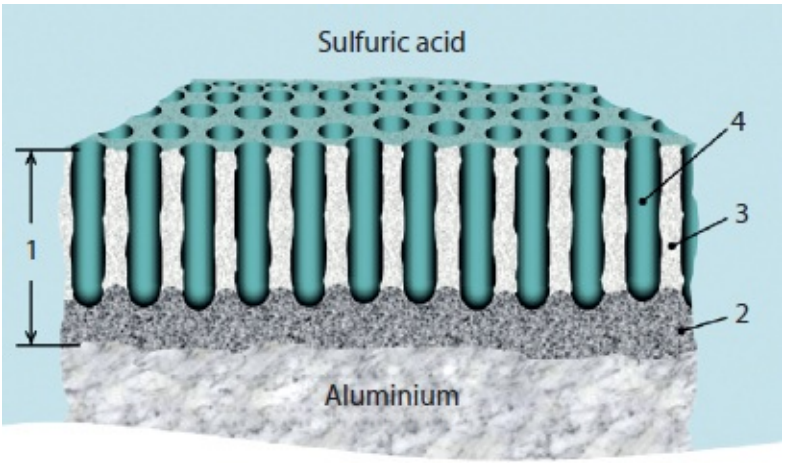
Alkaline cleaning (desmutting): It leads to entire removal of the superficial metallic layer, together with all its defects, because of the high solubility of aluminium in alkaline media. The application of this procedure can substitute the mechanical grinding. There are standard procedures, as described in Refs. [88, 89], but some authors prefer alternative methods. These methods vary with respect to the composition of the alkaline bath, the temperature and duration of the exposure.

Alkaline etching of AA6060 alloy in 100g/l NaOH solution, at 60 °C, for 50 s is proposed by Lunder *et al.* [90]. Decroly and Petitjean applied immersion of AA6082 plates in 50 g/l aqueous

NaOH solution for 3–10 min at room temperature [91]. Other authors preferred more soft conditions, namely immersion for 2 min in 0.5 M NaOH solution [92].

Acidic activation: This operation enables partial dissolution of the Al-oxide layer by diluted acids. In these conditions, as a result of the simultaneous growth and dissolving of the superficial film, it reaches a channel-pore structure. When positive electric current is simultaneously applied, the structure of the oxide layer achieves the morphology as shown in Figure 2.14.

Figure 2.14 Illustration of formation of porous oxide films on pure Al surface after anodization in acidic medium: (1) anodized aluminium oxide layer, (2) thin dense part of the layer, (3) thick porous part of the layer and (4) channel shape pores.



The purpose of this preliminary procedure is to obtain much more uniform deposition of CeCC. Generally, this procedure consists on immersion in diluted acids for relatively short period of time. Again, some authors preferred to apply standard procedures with commercial acidic solutions [81, 88, 89]. Other procedures are also found in the literature, such as treatment in 0.5 M acetic acid for 5 min [92], in 0.05 M $(NH_4)_4Ce(IV)(SO_4)_4 \cdot 2H_2O$, 0.5 M H_2SO_4 at 35°C for 10 min 0.05 M H_2SO_4 [93], or in a perchloric acid/ethanol mixture for 3 min [46]. Preliminary treatments including alkaline etching in Na_3PO_4 [94, 95] or activation in phosphoric acid [96] are also proposed.

Finally, a research work has been performed to compare the impacts of the acidic and alkaline treatments prior to spray deposition of CeCC coating from $CeCl_3$ solution [52]. As result, the authors report that the performance of only one time deposited coating after acidic treatment (in commercial cleaner) excels 40-layered coating after the alkaline procedure (for 5 min in 1 wt.% H_2SO_4 at 50 °C).

Deposition solution composition, influence of the additives: It comprises the composition of the chemical compound used as Ce precursor for deposition, the concentration and the Ce substance, presence of oxidants, pH of the solution, etc. During the investigations over the spontaneous and electrochemical CeCC deposition, it was established that the optimal concentration of Ce provider is about 0.03 ~ 0.05 mol/l of cerium ions content in the deposition solution [4, 35, 37, 38, 93]. The higher concentrations of the cerium provider result in accelerated precipitation of Ce oxides/hydroxides so that the resulting precipitates form superficial agglomerates, or sediments, instead of desirable uniform coating with satisfying adherence to the substrate.

Various studies have been performed on the additional compounds impact [35, 37, 78, 91–93]. As was mentioned in the previous paragraph, the hydrogen peroxide has a crucial importance as an additional OH^- provider on the CeCC deposition kinetics and the structure of the resulting coatings. Nevertheless, the excessively accelerated coating deposition does not lead to dense and uniform Ce primer layers. Undoubtedly, the H_2O_2 content has a direct relationship to pH of the solution. This

relationship is investigated in detail by Scholes *et al.* [93], who have established the presence of buffering effects during titration of H_2O_2 containing acidified 0.035 M $CeCl_3$ solutions by NaOH.

The authors attribute the presence of these buffering zones with the presence of $Ce(OH)_2^{2+}{}_{aq.}$ complexes which undergo decomposition at defined pH values (reactions 2.11 and 2.12) or with formation of non-soluble peroxo compounds (reaction 2.13).

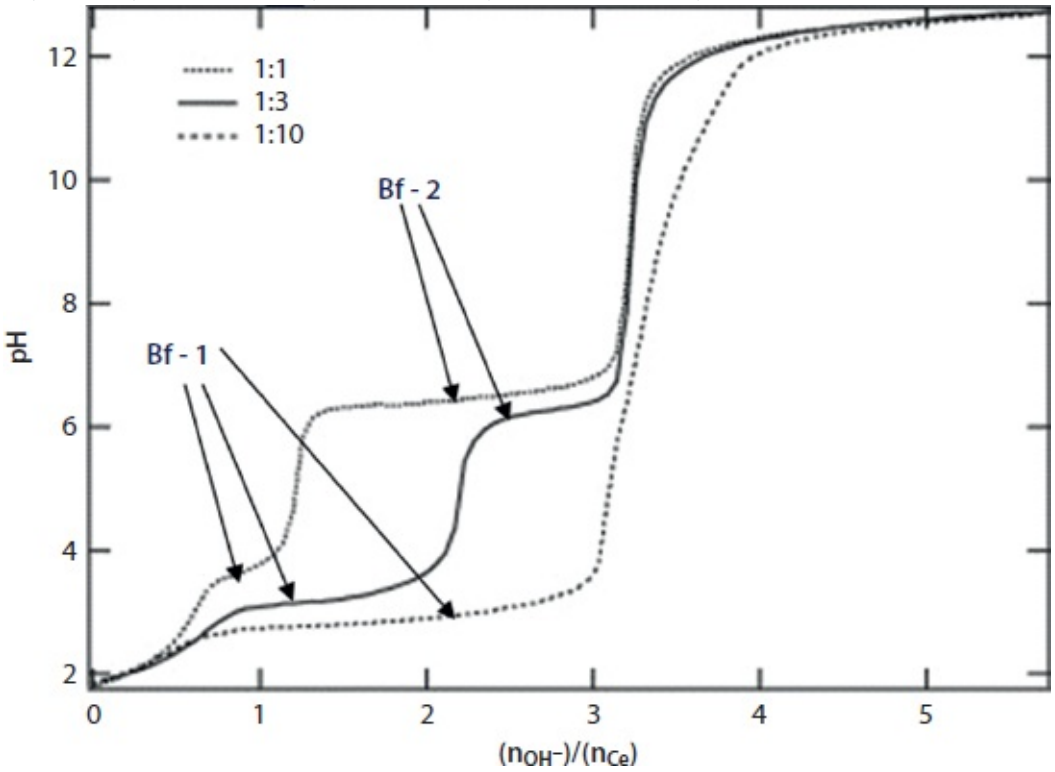
(2.11) $$Ce(H_2O_2)^{3+}{}_{aq.} + OH^- \rightarrow Ce(H_2O_2)^{2+}{}_{aq.} + H_2O$$

(2.12) $$Ce(H_2O_2)^{2+}{}_{aq.} + OH^- \rightarrow CeO_2^{+}{}_{aq.} + H_2O$$

(2.13) $$Ce(O_2)^{2+}{}_{aq.} + 2OH^- \rightarrow Ce(O_2)(OH)_{2aq.}$$

These buffering areas are shown in Figure 2.15.

Figure 2.15 Titration of acidified 0.035 M $CeCl_3$ solution with added H_2O_2 at Ce:H_2O_2 molar ratios of 1:1 (dotted curve), 1:3 (solid curve) and 1:10 (dashed curve) [93].



The authors have also established that the molar ratio between H_2O_2 and Ce content predetermines the colour of the obtained Ce oxide/hydroxide precipitates. This fact is undoubtedly related to their particle size, as is well known from the colloidal chemistry.

The possibility for direct addition of buffers to CeCC solutions is also investigated by Decrily and Petitjean [91]. In general, the use of buffers has a contradictive effect. By their use, any undesirable Ce-oxide/hydroxide precipitation can be avoided, indeed. However, the majority of buffering solutions contain organic compounds that are able to reduce the H_2O_2 and Ce(IV) compounds, deactivating them, altering the entire deposition mechanism.

Having in mind that the presence of copper is able to accelerate the CeCC deposition, forming additional cathodic areas for OH^- generation, Palomino *et al.* [92] have performed entire investigation on Al alloy 2024-T3 covered with Cu-rich smut. The authors have concluded that the presence of Cu cathodic particles uniformly deposited on the electrode surface favours the

homogeneous nucleation of the conversion layer, apparently reducing the role of intermetallics in the layer precipitation mechanism. Since the CeCC deposition proceeds simultaneously with the generation of Al^{3+} ions, from the Al matrix (see reaction 2.8), other authors have executed study on the impact of Al^{3+} ions, introduced into the deposition solution as $AlCl_3$ [97]. As a result, the authors have established appearance of buffering effect, originated from complex formation in the solution bulk, according to the following reaction:

(2.14) $$n\mathrm{Al(H_2O)^{3+}_6} + x\mathrm{OH^-} \rightarrow [n\mathrm{Al(OH)}_x]^{(3n-x)+}$$

In general, the majority of the authors prefer to use $CeCl_3$ as Ce provider, because the Cl^- ions penetrate across the Al-oxide layer on the metallic matrix creating elevation of the number of the anodic active locations (see Figures 2.11 and 2.12). This was the reason for the investigation of the impact of supplemental NaCl on the CeCC deposition process and the resulting coating layers [83].

Load per volume (LPV): Recently, a method for maintenance of relatively stable solution composition and pH, alternative to the introduction of buffers was proposed, as well [34]. This is done through exposing the smaller metallic surface to larger volumes of deposition solution, which enables to significantly decrease the impact of the auxiliary products on the physical–chemical properties of the deposition solution during the deposition process. As high is the LPV value, as low is the impact of the corrosion product heaping on the electrolyte composition and properties. In this sense, attention should always be paid to the volume of the deposition solution (*V*), corresponding to a unit of the metallic surface (S), because this factor entirely predetermines the concentration distribution of the deposition solution on the metallic surface, so the rate of its contamination by accompanying corrosion products in the solution (see Equation 2.15):

(2.15) $$\theta = V/S$$

Furthermore, the larger surface areas exposed to lower solution volumes predetermine drastic changes of the solution ingredient contents, enabling complete alteration of the deposition solution.

Temperature of deposition: According to the literature, the CeCC deposition is a kinetically controlled process, and thus the higher temperatures lead to acceleration of the coating deposition. Nevertheless, the most often used oxidant is H_2O_2, and the temperature should not be more than 50–60 °C because the higher temperatures could lead to decomposition of the peroxide and/or the additional acids in the solution. In addition, the excessively high deposition rates lead to formation of irregular porous agglomerates, instead of uniform, thin and dense layers. This is the reason for the necessity for determination of an optimal deposition temperature to obtain dense and uniform barrier layer within as short deposition time as possible, decreasing the energetic and time expense in the industrial practice.

Duration of the deposition process: There is an optimal duration of this process. Because it requires participation of Al from the substrate (see Equations 2.9 and 2.10), when enough dense coverage by the CeCC is already formed, it does not allow any further contact between the metallic surface and the deposition solution. After this moment, any further continuation of the deposition process leads neither to thickening nor to densification.

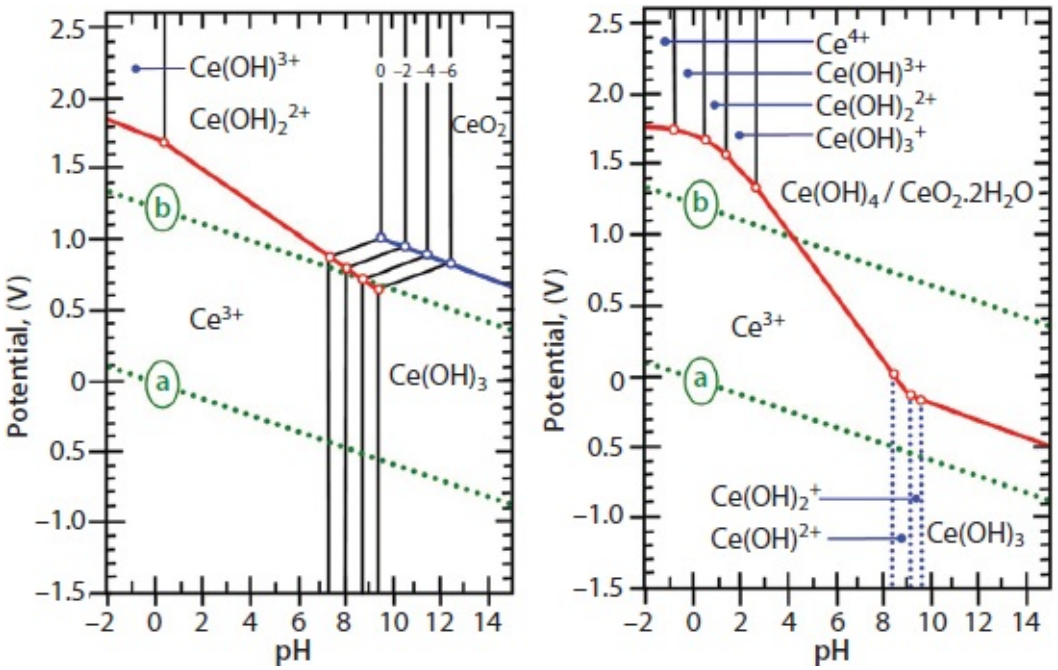
Number of multiple depositions: Usually, the number of repetition of the coating procedure leads to improvement of their performance. Additionally, it enables obtaining of multilayer systems with individual composition of each layer. However, in the case of conversion coatings, it is more reasonable to extend the deposition time, instead of applying multiple depositions, although the latter approach could lead to decrease of the cracks of the resulting coating. Otherwise, the deposition at

static conditions should predetermine irregularities as consequence of gas bubble fixation of the metallic surface and/or appearance of local areas with concentration variations. Alternative methods to decrease the formation of gas bubbles, as product of hydrogen evolution during deposition in acidic media, are the use of non-aqueous solutions, as is proposed in the literature [98, 99], or their hydrodynamic removal by stirring.

Impact of the applied electrical current or potential: Besides via spontaneous deposition, the CeCC could be deposited by electrochemical deposition. Unlike the classical electroplated coatings, the electrodeposited CeCC possesses a composition similar to the spontaneously deposited ones, instead to be composed of metallic cerium. No case of electrochemically deposited metallic cerium is found in the literature. The reason is that the conditions necessary for cerium film electroplating appear to be extremely aggressive for the majority of metallic substrates and even can cause electrolyte decomposition (electrolysis) accompanied by intensive gas emission due to hydrogen or oxygen evolution.

In general, prior to start any electrochemical CeCC synthesis, the investigator should use the corresponding Pourbaix diagrams [100–102], which render information for the thermodynamically possible cerium compounds, at given conjunction of pH and applied electric potential. These diagrams are very important for the electrochemistry and the respective electrochemical technology, so the phase diagrams for the metallurgy, the ceramic and glass technology. This is the reason for the continuous re-examinations of these diagrams in the case of CeCC electrochemical coating depositions (Figure 2.16).

Figure 2.16 The original E-pH diagram (on the left side) and the revised E-pH diagram (on the right side) [100–102].



The electrochemical CeCC deposition proceeds by electrochemical reactions, between ingredients of the liquid phase (electrolyte) and the solid phase (substrate), which in this case serves as working electrode (WE). In this case, it is necessary to know the working surface of the substrate because it predetermines the current density at given current applied to the electrode. The relationship between the kinetics of the electrochemical reactions and the current applied to the electrode is given directly by Faraday's equation [103]:

(2.16) $$m = \left(\frac{Q}{F}\right)\left(\frac{M}{z}\right)$$

where m is the mass of the substance exchanged between the electrode and the electrolyte (g), Q is the total electric charge passed through the substance (C), F = 96485 C mol^{-1} is the Faraday constant, M is the molar mass of the substance (g/mol) and z is the valency number of ions of the substance (electrons transferred per ion).

This equation cannot be used directly because the corresponding electrochemical reactions in the real electrochemical systems always proceed accompanied by auxiliary processes, which also consume electrical current.

Regardless of whether the CeCC is being deposited at galvanostatic [37, 38] or potentiostatic [104, 105] regime, the current density varies during the deposition because of the changes of the accessible metallic surface area, as consequence of (i) the CeCC deposition itself, (ii) electrochemical gas evolution or/and (iii) electrical double layer charging. Moreover, during the deposition, the pH values of the electrolyte also undergo changes due to the altering of its chemical composition.

In general, the application of electric current as a motive power for CeCC deposition results in much faster deposition, but the obtained coatings possess a large number of pores, defects and detached zones because of the coincident hydrogen gas evolution at too high current densities [37, 38, 105].

Furthermore, the aluminium-based alloys are prone to suffer cathodic dissolution phenomena [37, 38, 106–109]. Despite their name, these processes do not possess an electrochemical nature, but rather they appear to be a result of the hydroxyl ions generated by the oxygen reduction reaction. According to Mokaddem [108] and Olge [109], the aluminium cathodic dissolution proceeds through the following reactions:

(2.17) $$Al + 3OH^- \rightarrow Al(OH)_3 + 3e^-$$

(2.18) $$Al(OH)_3 + 3OH^- \rightarrow Al(OH)_4^-$$

Obviously, the Al–substrate dissolution disturbs the formation of uniform, dense conversion coating so that a special attention should be paid on the potential appearance of such Al–cathodic dissolution phenomena. Furthermore, the excessive OH^- anions in the surrounding liquid medium of the deposition solution can provoke undesirable precipitation of cerium hydroxides in the solution bulk instead of CeCC formation. Such case of coagulation of Ce(III) and/or Ce(IV) hydroxides in the solution bulk, followed by their precipitation on the metallic surface, instead of gradual CeCC growth, is described elsewhere [110].

2.2.3.3 Posterior Sealing Procedures

The post-treatment procedure could substantially improve the performance of the CeCC. The temperature and duration of the post-treatment have been the object of research in Ref. [111]. The authors have performed it by immersion of CeCC-coated AA 2024-T3 plates in 2.5 wt.% $NH_4H_2PO_4$ solution, for different times, 10, 30 and 120 s, and temperatures 55, 70 and 85 °C, respectively. They conclude that the best coating is obtained for at least 10 min at minimum 70 °C. Additionally, at room temperature, no changes have been observed. The authors explain the beneficial effect of the post-treatment through formation of supplemental hydrated $CePO_4$ that fills the cracks on the CeCC

coating, making it much denser. Other authors also propose phosphating procedure at pH 4.5 and 85 °C for a final sealing step [112]. Furthermore, similar methods are proposed by the work team of Fachikov for corrosion protection of zinc [113] and low carbon steel [114]. The treatment by phosphates is also a well-known preliminary treatment prior to deposition of various galvanic coatings [51].

2.2.4 Brief Summary

The main function of the primer layers in the multilayered coating systems is to improve the adherence of the upper layers to the metallic substrate. In this sense, the conversion coatings are in the form of metal oxides or/and hydroxides that partially or completely substitute the native superficial oxide layer of the metallic substrate. The CeCCs are among the basic pretenders for substitution of the chromium ones. Although a wide variety of approaches are employed for CeCC deposition, all these approaches are based on three main technical stages:

i. *Preliminary surface treatment*: This operation is necessary for surface roughness control and superficial chemical modification by controlled partial selective dissolution of some of the alloy's ingredients.

ii. *CeCC deposition itself*: It can be performed by different methods such as dip-coating, spray coating, electroplating and magnetron sputtering. Besides the method applied, the deposition conditions are of crucial importance for the coating morphology, composition and structure. The combination of these features completely predetermines the performance of this primer coating layer and consequently the adherence of the entire multilayered coating system.

iii. *CeCC sealing*: For further improvement of the CeCC primer and enhancement of the upper layers' adhesion, it undergoes subsequent sealing, usually in phosphate solutions.

After completion of the CeCC deposition, this primer layer should be covered by upper coatings, comprised of organic substances (polymers), to provide elasticity for reduction of the mechanical stresses, originated from the difference between the dilatation of the metallic substrate and the coating system itself. These subsequent coating layers should also correspond with the environmental restrictions related to the use of volatile organic compounds (VOCs) and to provide a possibility for active corrosion protection, besides their barrier capabilities. Some important aspects related to the recent trends in the elaboration of advanced upper layers are described in the next section.

2.3 Elaboration of Hybrid and Composite Upper and Finishing Coating Layers

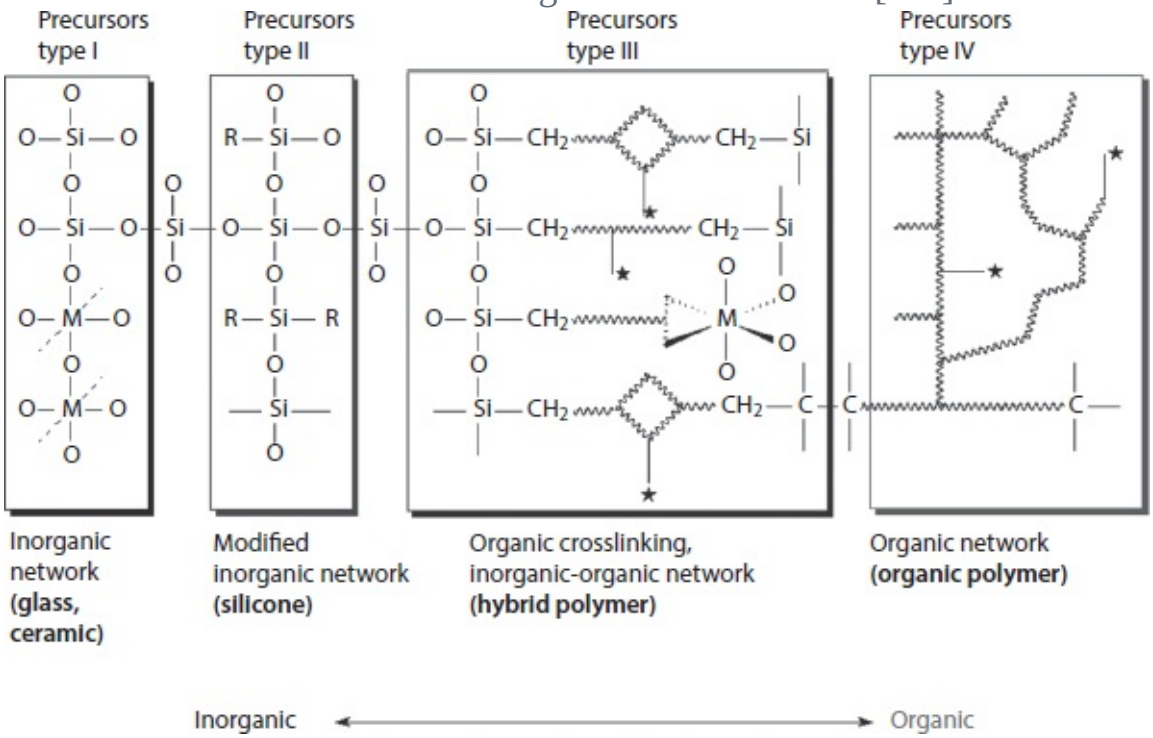
2.3.1 Advantages of the Hybrid Coatings Systems

The hybrid materials belong to the newest generations of materials are the object of research and development during the recent decades. The interest related to this group of materials origins from their ability to combine desirable properties (benefits) of both of organic and inorganic materials. The sol–gel methods enable easy synthesis of hybrid materials. Although the first publications on the sol–gel method of synthesis appear in the mid-nineteenth century [115], the interest to this group of

methods has progressively risen during the recent decades, since these methods enable preparation of entirely new generations of solids, which cannot be obtained by any other method.

Karl Heinz Haas and Klaus Rose [116] have divided the solid materials into four basic groups, according to their basic matrix: (1) purely inorganic networks (glass and ceramics), (2) organically modified inorganic networks (silicones), (3) organic crosslinking, inorganic–organic networks (hybrid polymers) and (4) purely organic polymers (plastics, resins, etc.). Their classification is illustrated in Figure 2.17.

Figure 2.17 Classification of the solids according to Heintz and Rose [116].

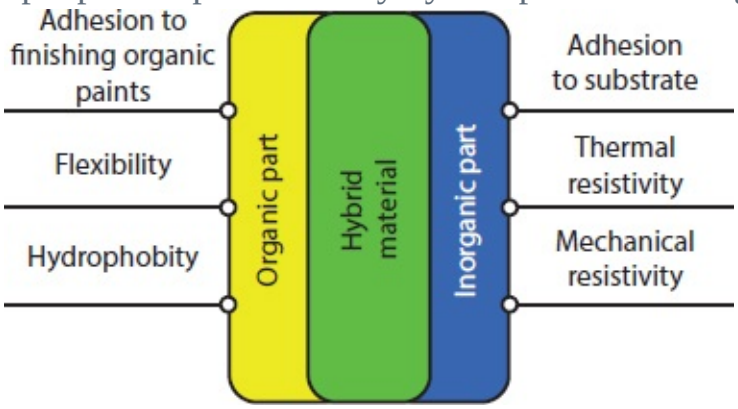


In that means, the benefits of the application of the hybrid materials as primer coatings have been emphasized by Zheludkevich [117]. He remarks that the hybrid primer coating combines the desirable properties of both the organic and inorganic moieties, and in that manner, it forms reliable and durable barrier layer with remarkable corrosion-protective ability.

Taking into account the aforementioned benefits of the hybrid primer coatings, it can be concluded that they belong to the so-called *"advanced materials"*.

Figure 2.18 clearly represents the combination of properties rendered by the hybrid primer coatings.

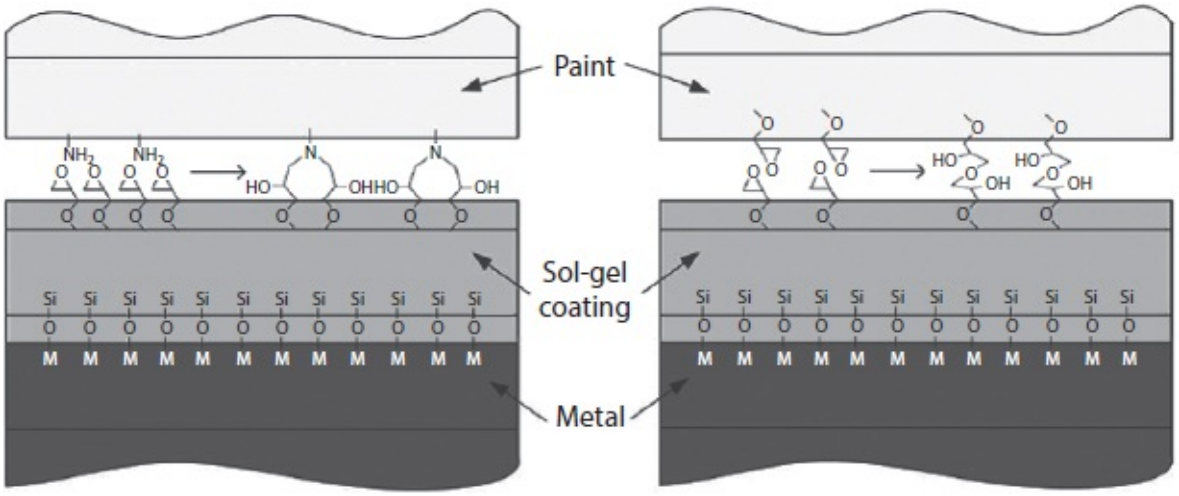
Figure 2.18 Combination of properties possessed by hybrid primer coatings.



Furthermore, in the same article, Zheludkevich represents schematic profile of hybrid primary

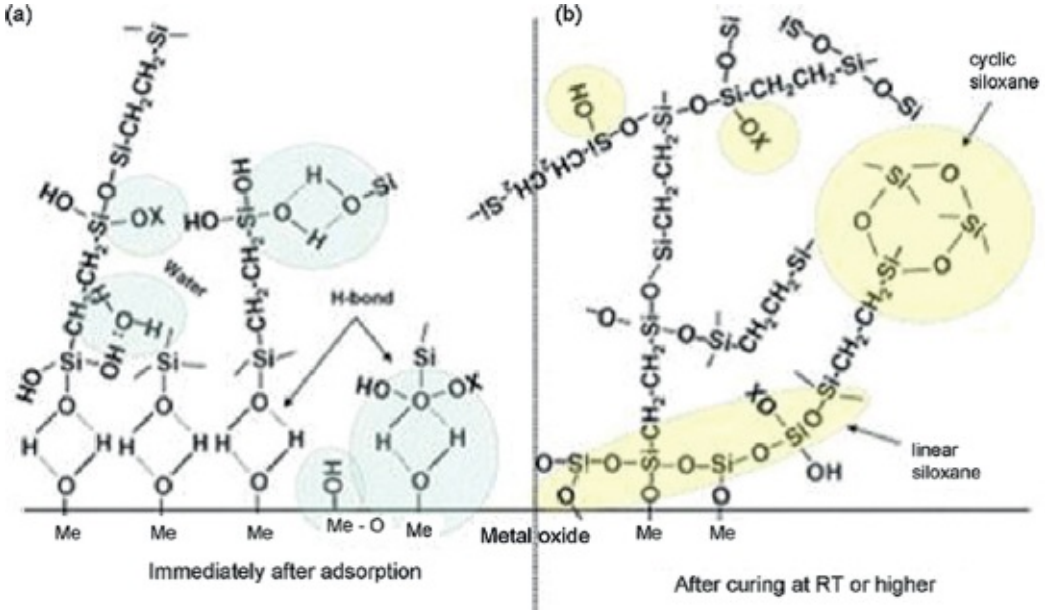
coating (or sol–gel coating), which is shown in Figure 2.19.

Figure 2.19 Schematic view of hybrid primer coating together with the layers above and below it [117].



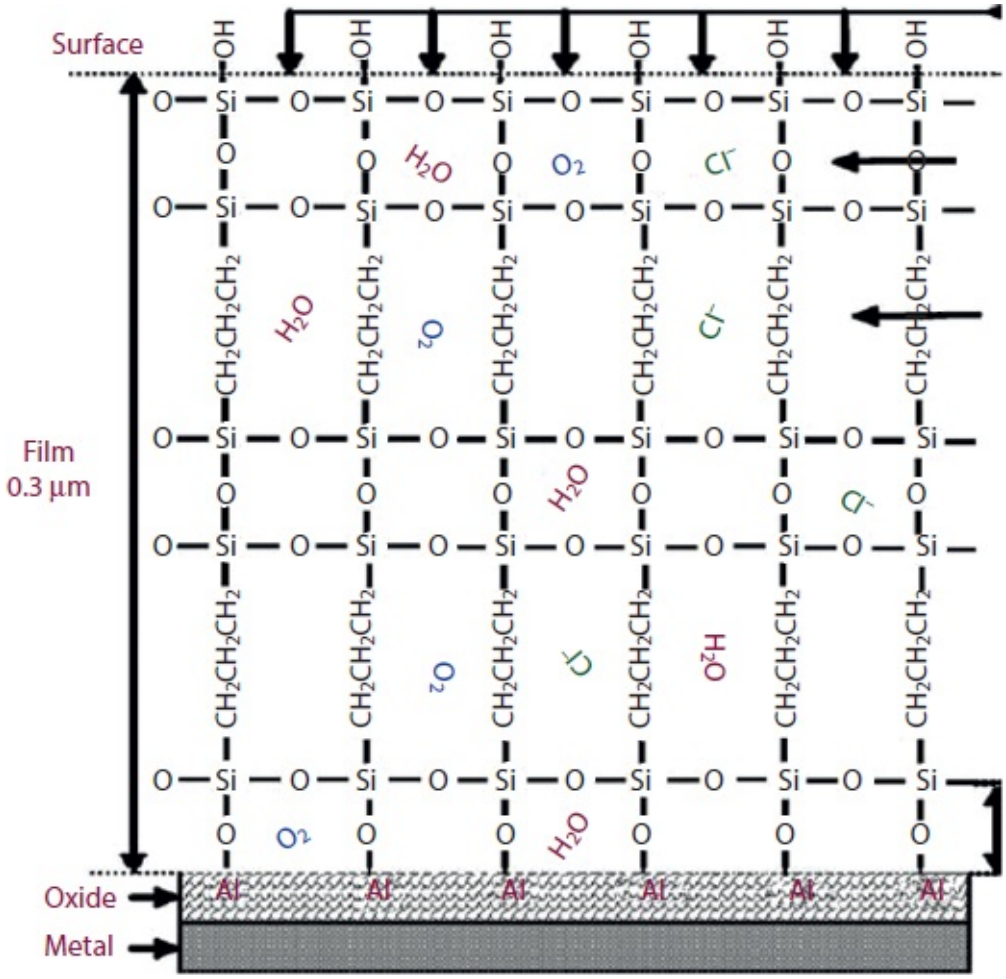
As composition and structure, the hybrid coatings can be described as relatively dense layers composed of hybrid polymers comprising organic and inorganic moieties bonded covalently among them. Figure 2.20 shows a simplified illustration of hybrid coating layer, according to Wang and Bierwagen [118].

Figure 2.20 Simplified schematic of bonding mechanism between silane molecules and metal surface hydroxide layer (a) before condensation: hydrogen-bonded interface; (b) after condensation: covalent-bonded interface [118].



Despite the apparent advantages provided by the hybrid coatings, they are susceptible to deterioration during their exploitation due to partial hydrolysis processes. In that means, Palavinel [119] has discovered that the hybrid materials reveal partial permeability for species originated from the corrosive medium. He has represented schematically a hybrid primer coating with inclusions of penetrated water molecules as well as various corrosive ions (Figure 2.21).

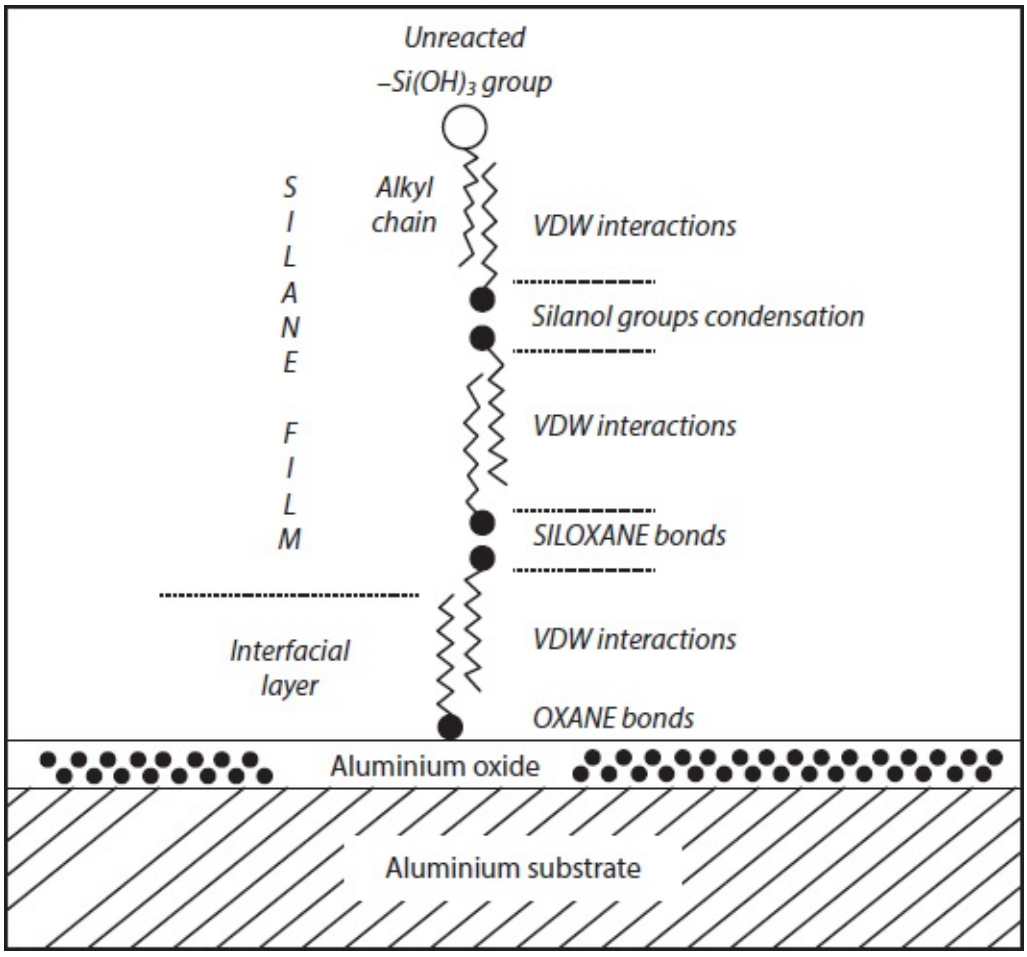
Figure 2.21 Schematic view of hybrid coating with inclusion of various corrosive ions and compounds [119].



This disadvantage could be significantly diminished by application of metal alkoxides with larger aliphatic chains. Frignani *et al.* [120] have done comparative assessment of primer coatings obtained from alkoxides with different aliphatic chains as follows: c *n*-propyl trimetoxisilane-C_3H_7-Si-$(OCH_3)_3$; *n*-octyl trimetoxisilane-C_8H_{17}-Si-$(OCH_3)_3$; *n*-octadecyl trimetoxisilane-$C_{18}H_{37}$-Si-$(OCH_3)_3$ and bis-trioximethyl-silil-ethane-$(CH_3O)_3$-Si-C_2H_7-Si-$(OCH_3)_3$. In conclusion, the authors have established that the larger aliphatic chains enhance the obtaining of thicker layers. These layers reveal the ability for self-assembling, and this kind of hybrid materials is also known as self-assembled monolayers (SAM). They have significantly a lower number and size of defects in their structures and thus enable more efficient protection through formation of dense barrier layers [121, 122]. Furthermore, a remarkable variety of possible metal–organic precursors are shown in several review papers [17, 20, 21, 123–126], which reveal that the basic interest is directed towards the organic derivatives of titanium, silicon and zirconium. However, whenever a new composition is developed, the recently accepted limitation directives for reducing the utilization of VOCs [127, 128] should be taken into account.

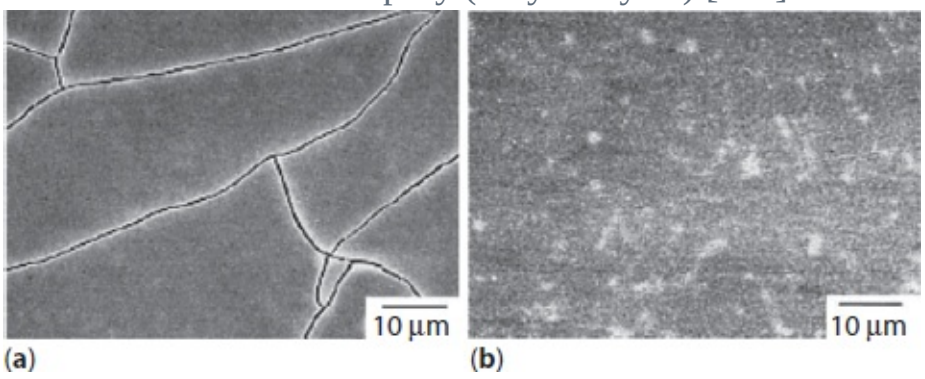
In addition, the SAM layers reveal additive self-recuperation ability due to the flexible nature of the large aliphatic chains [129–131]. Furthermore, the large aliphatic chains predetermine remarkably stronger van der Waals' intermolecular attraction interactions. The latter predetermine the formation of self-assembled dense barrier layers [132, 133] as shown in Figure 2.22.

Figure 2.22 Schematic view of self-assembled barrier protective film on aluminium surface [120].



The clear evidence for the reliability of the concepts described earlier is represented by the direct comparative observations via scanning electron microscopy (SEM) (Figure 2.23), as performed by Ono *et al.* [134].

Figure 2.23 SEM images of silica and silica-polymer hybrid films: (a) film composed of pure silica and (b) film composed of silica + 0.5 wt.% of poly (vinyl-butyral) [134].

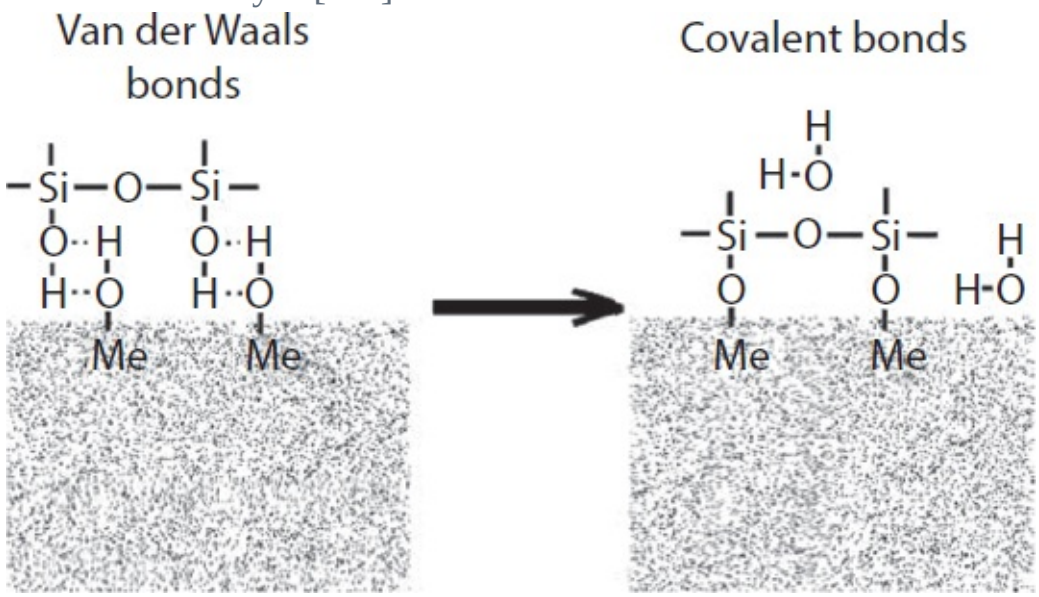


The authors [134] have clearly evinced that the hybrid coatings are superior to the inorganic coatings due to the flexibility of the hybrid matrix originated from the organic moiety represented in its composition. The organic moieties render elasticity, preventing the cracking in the coating structures, appeared as a result of dilatation coefficient difference of the metallic substrate and the coating layers. It is worth to mention the extreme potential danger that originates from the cracks formation in the coating. Each crack in the coating structure appears accelerator of local corrosion phenomena on the metallic surface beneath the coating rupture, even at the absence of liquid corrosive media. The rupture of coating promotes adsorption of air humidity, followed by enhanced capillary water condensation, as is described in the literature [135]. The condensation of water beneath the coating fracture leads to the stress corrosion cracking of the underlying metal by

providing the liquid medium for localized electrochemical corrosion processes as described in Equations (2.6–2.8) and also illustrated in Figures 2.11 and 2.12. The cracking phenomena are of so great importance that special sensor elements are proposed in the literature [136]. The expansion of the solid corrosion products heaped inside the cracks promotes mechanical tension of the coatings, leading to further creeping of the respective cracks. Similar detrimental effect could be provided by the expansion caused by freezing of the condensed or penetrated water during high-altitude flights. The flexible and elastic organic ingredients of the coating could efficiently suppress this effect.

On the other hand, the inorganic part of the hybrid material renders enhanced ability for adhesion to the metal substrate, by van der Waals' intermolecular interactions, which convert to covalent bonds between the natural oxide layer of the aluminium, and the partially hydrolysed metal alkoxides, represented in the corresponding sol–gel system. Figure 2.24 shows schematic representation of the transition of van der Waals' intermolecular interactions to covalent bonds during coating process of aluminium substrate by sol–gel system. Here, it should be mentioned that, according to the literature [117], the native oxide layer is consisted generally of boehmite γ-AlO(OH), with a thickness relatively equal to 5 nm. Thus, during the coating by sol–gel system, the alkoxides from the system interact with the oxide layer of the substrate.

Figure 2.24 Schematic representation of formation of covalent bonds between sol–gel-derived primer coating and metal oxide layer [117].



2.3.2 Technological Bases of the Sol–Gel Approach

Hybrid and inorganic gel products can be synthesized via hydrolysis/polymerization processes of metal alkoxides. This class of substances is composed of molecules that consisted on organic moieties, connected via chemical bonds with metal oxide groups, and they correspond to general formulae $(R–O)_nMe$, where "R" is the organic radicals, "Me" is the corresponding metal ion and "n" is the number of organic radicals, and correspond to the oxidation state of the metal ion. Here, it should be mentioned that there is a large diversity of different metal alkoxides. The name of given metal alkoxide depends on the metal as well as the chemical composition of the organic radicals connected with it. The most widely used alkoxides are tetraethoxysilane, also known as tetraethylorthosilicate (TEOS), and 3-Glycidoxypropyltrimethoxysilane (GPTMS).

Here, the sol–gel synthesis is based on hydrolysis/polymerization processes of the corresponding alkoxides in liquid medium, represented by alcohol–water mixtures, in the presence of acid. The last

one is initiator and catalyst of the hydrolysis process. The moieties activated via the hydrolysis react between themselves, obtaining a polymeric product, with enclosed and uniformly distributed liquid phase in its bulk (chemical gel) [41].

Besides the silicon, other metals could also be represented in the composition of the corresponding metal alkoxide. Samuneva *et al.* [137] applied light refractive coatings on glass, composed of TiO_2, by hydrolysis/polymerization of tetrabuthyloxititanate (TBOT) and subsequent calcination of the hybrid gel product.

The chemical reactions can be described as follows:

Hydrolysis:

(2.19) $$Ti(OC_4H_9)_4 + 4H_2O \rightarrow Ti(OH)_4 + 4C_4H_9OH$$

Tetrabuthyloxytitanate tetrahydroxititanate buthanol

Polymerization:

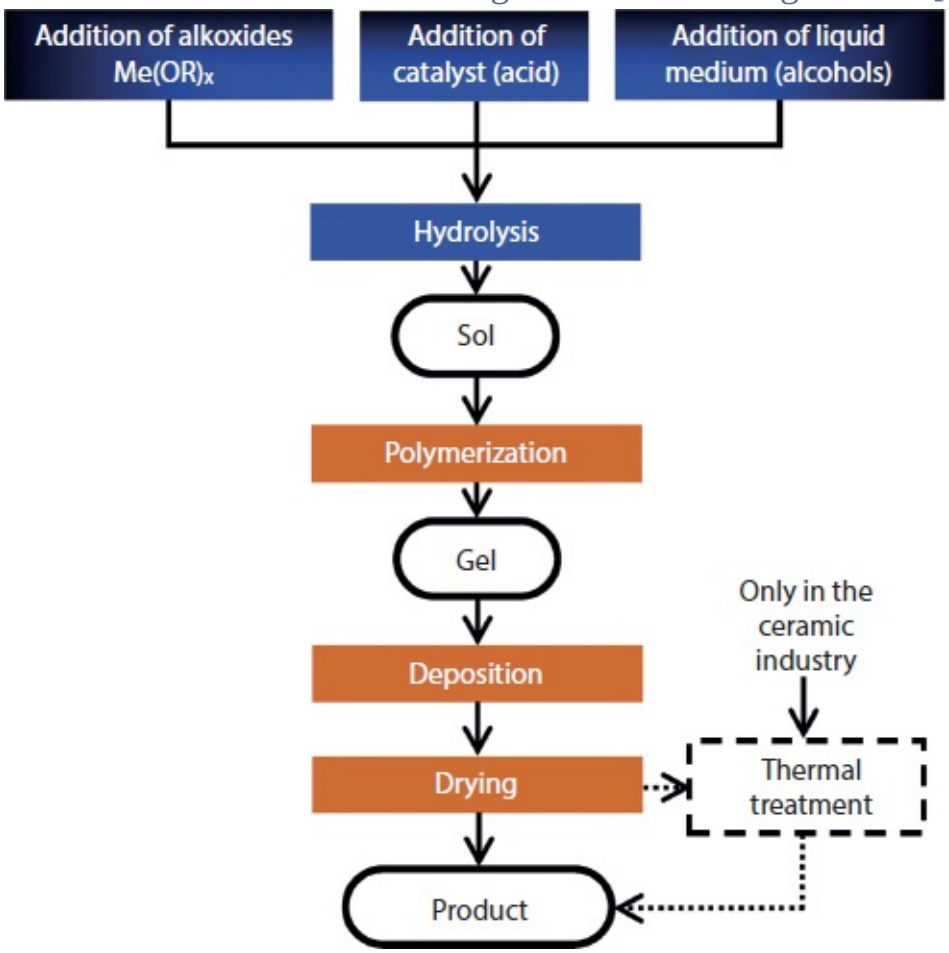
(2.20) $$nTi(OH)_4 \rightarrow (TiO_2)n + nH_2O$$

Titanate ceramics

Similar processes are involved in obtaining of hybrid primer coatings via sol–gel route.

The general scheme of the sequence of the technological processes related to the sol–gel route is presented in Figure 2.25.

Figure 2.25 General schematic view of the technologies based on sol–gel route [41].



Usually, the gel undergoes drying (annealing) to become a desired final product. If the desired product should be with completely inorganic composition, then the corresponding gel (as intermediated product) undergoes sintering process. At this posterior process, all of the organic bridging compounds combust or decompose so that only the inorganic part remains. Thus, it is clear

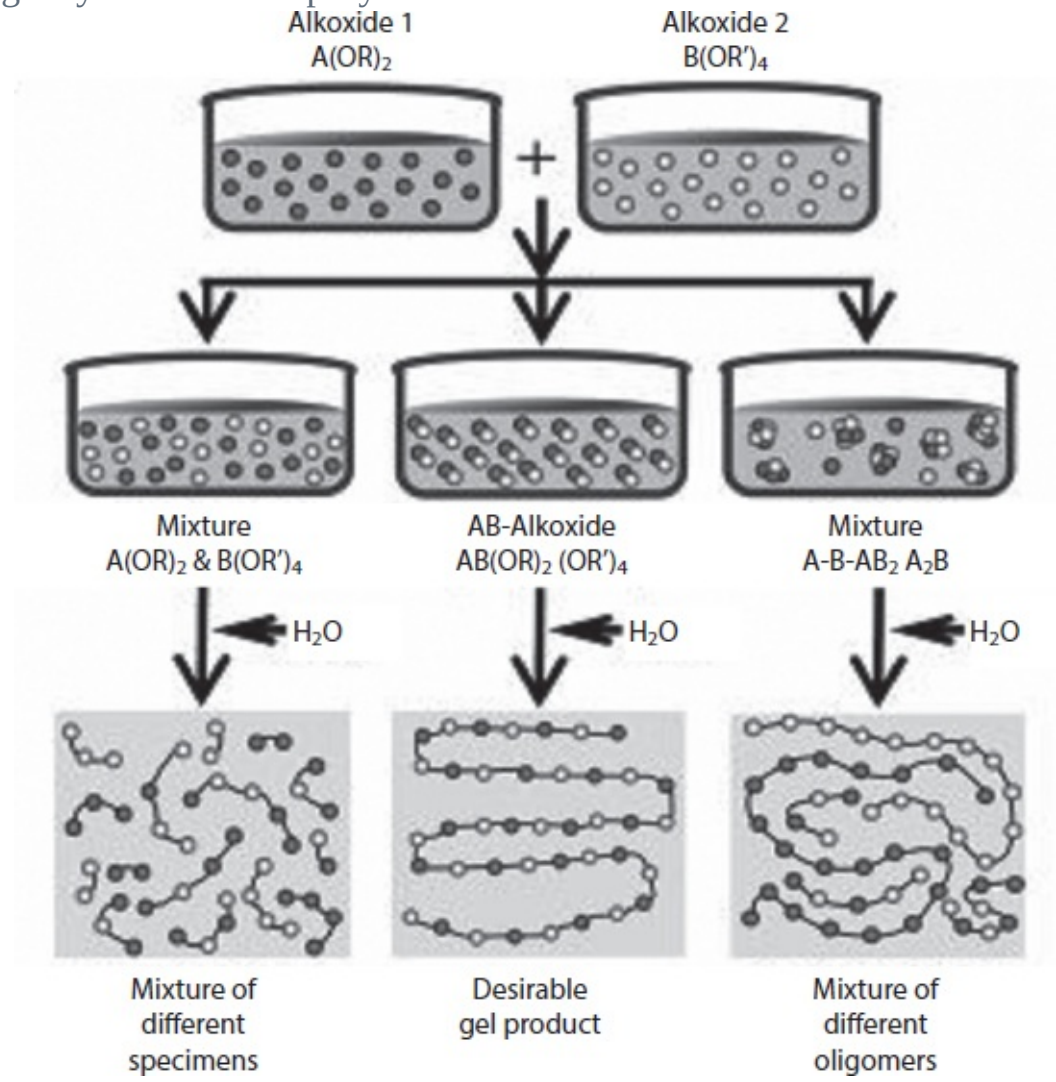
that there is narrow correlation between the structure and composition of the obtained products and the conjunction among composition of the precursors, the method and conditions applied for their synthesis.

Seven general factors predetermine the features and performance of the products obtained via sol–gel route [41]:

- Chemical composition of the liquid medium
- Chemical composition of the precursors (alkoxides)
- Molar factor (ratio between the alcohol as medium and the alkoxides as precursors)
- pH of the medium
- Presence of additives
- Temperature
- Pressure and chemical composition of the gaseous medium over the gelling system during the dry (annealing) process

When more than one alkoxide is represented in the sol–gel system, then the respective product can have more than one metallic element in its composition. This system is represented in Figure 2.26.

Figure 2.26 Sol–gel system with co-polymerization of two different metal alkoxides [41].



The correct performance of sol–gel process in case of two different metal alkoxides recommends information regarding hydrolysis ability of the respective alkoxides. The alkoxide with higher aptitude should be added to the system after the other. Since the hydrolysis/polymerization processes are indispensible for all sol-gel systems, based on metal alkoxide precursors, the pH is a key factor

for their correct execution. Its control is, however, difficult because these processes proceed simultaneously, and it is extremely difficult to control the rate of hydrolysis. Nevertheless, the hydrolysis rate at given pH can be estimated by measurement of the viscosity of the respective sol–gel system, since the use of pH meters should be avoided. The problem is that they use membrane electrochemical reference electrodes, which can be obstructed by the polymerizing sol–gel system. In order to avoid this inconvenience, the hydrolysis/polymerization systems should be submitted to measurement of their viscosity and its evolution within the time during the hydrolysis/polymerization process. At the initial period (immediately after addition of the acid), a slight decrement of the viscosity can be observed, when the hydrolysis process proceeds with higher rate than the polymerization. Otherwise, the polymerization process should proceed very slowly, being dependent on the hydrolysis. The reason for this dependence is that the polymerization process demands already hydrolyzed moieties as a precursor. Consequently, the hydrolysis process appears to be the limiting factor (bottle neck) for the entire gel formation process. The viscosity of the initial mixtures of alkoxides should be measured as a referent point (preliminarily heated to the respective temperature). Afterwards, the viscosity should be measured after introduction of the acid (as hydrolysis initiator) at the same temperature. The measurement of the viscosity variation for extended periods of time at different (constant) temperatures can serve as calibration curves and indicatives for the hydrolysis rate.

Finally, it should be mentioned that there is an optimal viscosity of the sol–gel system. If this system is deposited at its high viscosities, then thick films will be obtained. These films are susceptible to cracking and disruption during the final curing (e.g. annealing) of the already obtained coating. However, if the viscosity is too low, the obtained films will be very thin and will not possess remarkable barrier ability.

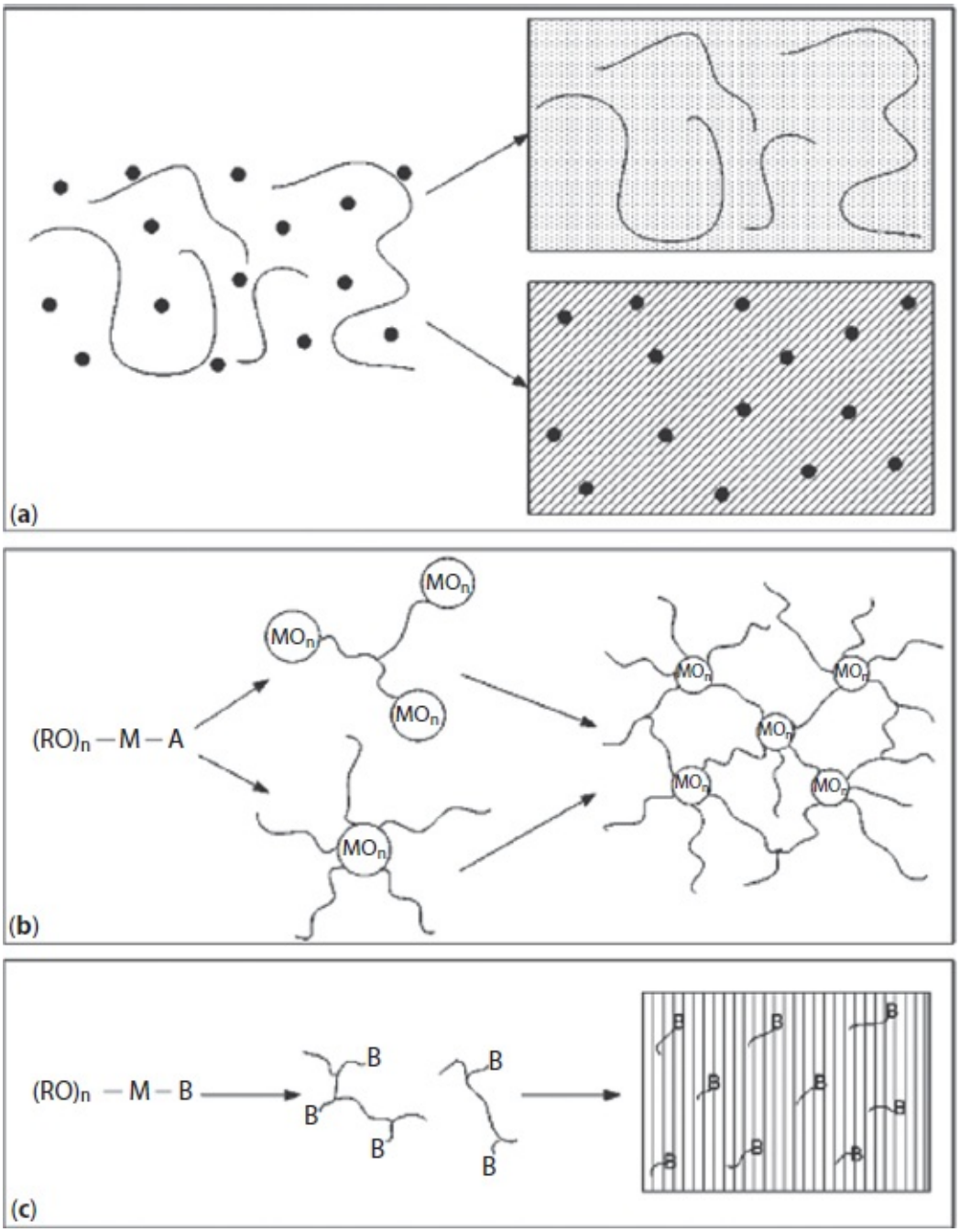
The hybrid coatings could be further improved by addition of powder or fibre-formed material as reinforcing phase and carriers of corrosion inhibitor.

2.3.3 Hybrid Nanocomposite Primer Coatings: Basic Concepts

As mentioned earlier, the hybrid nanocomposite coatings excel the hybrid ones due to the presence of reinforcing phase in the form of equally distributed nanoparticles in their structures [130, 131]. The presence of this reinforcing phase leads to increase in the thickness as well as suppression of the formation of disruptions in the primer coatings during the annealing process. Here, it should be mentioned that the diameter of the nanoparticles should be less than 300 nm.

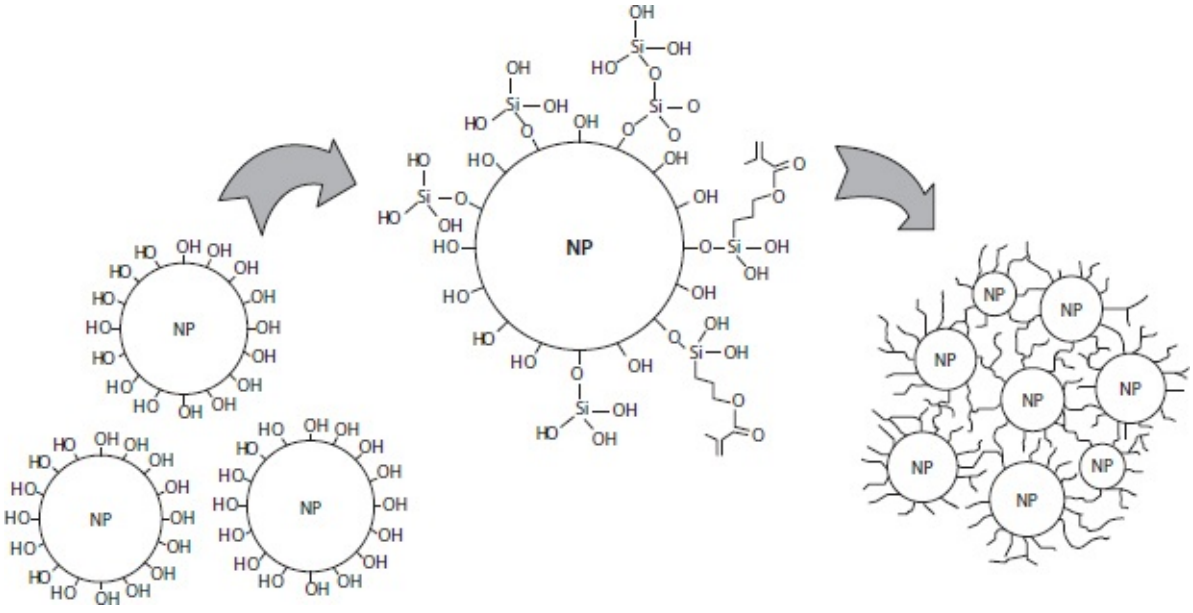
Further, the hybrid nanocomposite primer coatings could be classified into three basic groups, based on the interaction between the inorganic and the organic parts in the hybrid matrix [130], as follows: (1) with the absence of chemical bonds between them; (2) with the presence of chemical bonds between the inorganic and organic parts; (3) with presence of chemical bonds between the inorganic part and non-polymerizable organic moieties (Figure 2.27).

Figure 2.27 Various approaches for achievement of hybrid nanocomposite coating materials [130].



In the literature, there is an example for obtaining of hybrid nanocomposite primer coating by polymerization of hybrid matrix in colloidal liquid medium with dispersed SiO_2 [131], as illustrated in Figure 2.28. The authors describe their product as a hybrid nanocomposite primer coating with significantly stable structure, where the OH^- groups are adsorbed on the surface of the silica particles, and they interact with the partially hydrolysed TEOS, resulting in the formation of stable hybrid nanocomposite systems.

Figure 2.28 Schematic representation of nanoparticles inclusions during hydrolysis–polymerization processes of the matrix [131].

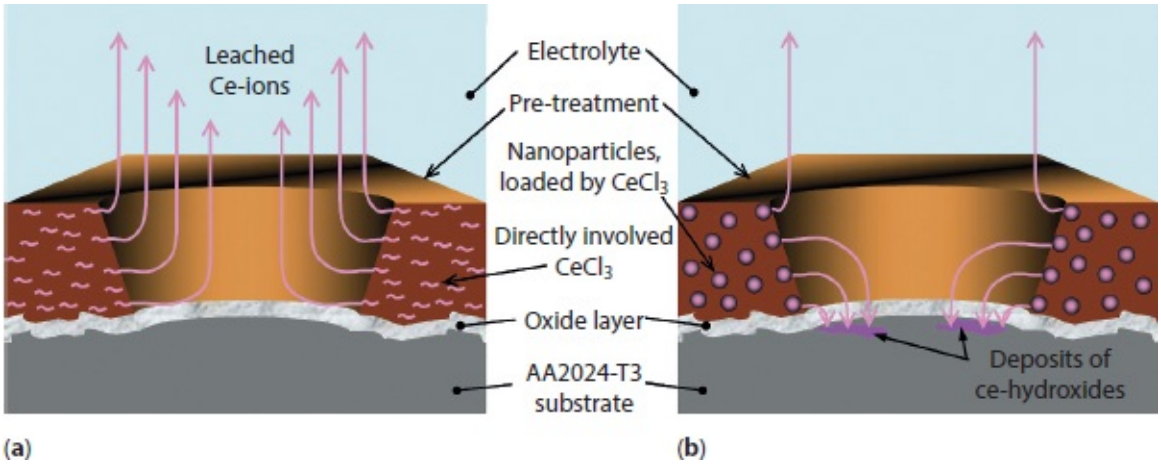


The basic problem related to the application of this kind of technologies is the agglomeration of the particles during the synthesis process. It can be avoided by addition of surfactants and detergents to the system, as shown in Figure 2.28.

Alternative approach for the synthesis of hybrid, nanocomposite primer coatings is via formation of nanoparticles into the sol–gel system, during its synthesis. This process of "*in situ*" synthesis of hybrid nanocomposite primer coatings is known as self-assembling of nanoparticles (SNAP) [138–140]. In this sense, an interesting approach is the use of graphenes or carbon nanotubes, as is proposed by Hammer *et al.* [141], because this relatively new generation of materials is an object of increasing interest for various applications [142–146].

If the nanoparticles are previously impregnated by corrosion inhibitor, then the former serve as inhibitor containers or reservoirs. Thus, the nanoparticles have a double role: as reinforcing phase for the hybrid matrix, and as carriers of inhibitor, which releases it gradually into the zones of the scratch, rupture or any other defect of the primer coating, as shown in Figure 2.29 [147].

Figure 2.29 Schematic representation of high (a) and low (b) rates of inhibitor leaching [147].



When inhibitors are gradually released, then the undesirable process of its leaching could be suppressed, and thus, higher efficiency of its inhibitive effect could be expected. This concept is well described by Zheludkevich *et al.* [117].

2.3.4 Corrosion Inhibitors as Self-Healing Coating Ingredients

2.3.4.1 Rare Earth Salts as Corrosion Inhibitors

As already described in the previous sections, the coating cracking is a result of either a difference between the dilatation coefficients of the metallic substrate and the coating layers, or a consequence of partial hydrolysis of the coating when contact with aqueous media. Namely the crack bottoms play the role of moisture containers accelerating local corrosion phenomena. Both these reasons impose the necessity for addition of corrosion inhibitor to the coating composition. Prior to add an inhibitor to a coating, it is necessary to evaluate its inhibition efficiency directly in a model corrosive medium.

Such preliminary investigations are necessary because the involvement of an inhibitor to a coating composition, during its preparation, can cause inactivation of both the inhibitor added and whatever coating ingredient. Indeed, the detrimental effect of direct $Ce(NO_3)_3$ inhibitor addition is already reported [148]. Similar detrimental effect is also observed after direct addition of various inorganic inhibitors to Zr and Si containing hybrid primer layer [134]. The authors have performed a comparative research on several inhibitors, such as $Na_2Cr_2O_7$, $Ce(NO_3)_3$, Na_2MoO_4 and $NaVO_3$ and concluded that all these compounds possess a detrimental effect on the barrier ability of the resulting coating system. In addition, the authors report that Na_2MoO_4 and $NaVO_3$ shows the strongest detrimental effects. According to the authors, these substances crystallize inside the coating, during its preparation. Afterwards, the NaCl containing aqueous corrosive media dissolve the already formed crystals in the coating structure, reaching by this manner easier Cl^- ingress to the substrate metallic surface.

Nevertheless, Suegama *et al.* [149] report even beneficial effect of Ce(IV) ions on the polymerization of *bis*-[triethoxysilyl]ethane (BTSE) film deposited on carbon steel. According to them, the protective properties of the Ce(IV) modified coating are a consequence of the formation of a more uniform and densely reticulated silane film, due to the accelerative role of Ce(IV) ions on the cross-linking of the silane layer.

This controversion between the above concepts imposes demands for additional elucidation of the corrosion inhibitors, not as coating ingredients, but rather in direct exposition of metallic specimens to model corrosive media. Various alternatives to the use of chromium compounds have been proposed in the worldwide literature. Among them, the lanthanides have proved to be really promising candidates. The action mechanism of these compounds is identical to that of CeCC formation. In brief, the lanthanide ions form insoluble hydroxides [150] and can be considered as “cathodic inhibitors”. Besides, these elements possess a low toxicity [151, 152]. Furthermore, lanthanides can be considered as economically competitive products [153], since some of these elements are relatively abundant in nature; for instance, cerium is as plentiful as copper [154], and their industrial production is continuously increasing [155]. Comparative research works on the inhibition efficiency of various lanthanide compounds are performed by various authors. Allachi *et al.* [156, 157] performed studies on the inhibitive activities of $Ce(NO_3)_3$, $La(NO_3)_3$, $Gd(NO_3)_3$ and $Tb(NO_3)_3$, on the corrosion of AA6060 alloy in chloride solutions. The activity of other inhibitors such as YCl_3, $LaCl_3$, $PrCl_3$ and $NdCl_3$ has been investigated against corrosion of AA7075 aluminium alloy [158]. $CeCl_3$, $LaCl_3$, $SmCl_3$ and their binary mixtures have been investigated as corrosion

inhibitors of AA5083 Al–Mg alloy [159–161] in aerated 3.5% NaCl aqueous solution, as well.

Since the corrosion phenomena possess generally electrochemical inherent nature, the electrochemical analytical techniques, such as the linear sweep or cyclic voltammetry, (i.e. LVA or CVA) and the electrochemical impedance spectroscopy (EIS) appear to be the most efficient classical techniques for inhibitor efficiency evaluation. These methods are indispensable for determination of the local corrosion rate and impact, because weight loss quantification is applicable only for uniform corrosion characterization. The experimental data for the former two groups of methods (i.e. LVA and CVA) are in the form of graphical presentations of the correlation between the potential and the current density, determined during the electrochemical measurements, performed on the basis of a referent electrode (RE) with a constant potential. These methods enable determination of the corrosion current density by comparison of its values obtained after measurements at both cases of inhibitor presence and absence in the model corrosive medium.

Thus, on the basis of electrochemical measurements, the inhibition efficiency η (%) of given inhibitor can be determined by the percentage relation between the corrosion currents, registered at the presence i^{inh}_{corr} (A/cm^2) and the absence i^{0}_{corr} (A/cm^2) of the investigated inhibitor:

$$\eta = \left(1 - \frac{i^{inh}_{corr}}{i^{0}_{corr}}\right) \times 100 \quad (2.21)$$

Alternatively, the inhibition efficiency can be calculated on the basis of the respective polarization resistances:

$$\eta = \left(1 - \frac{Rp^{0}_{corr}}{Rp^{inh}_{corr}}\right) \times 100 \quad (2.22)$$

where Rp^{0}_{corr} (Ω.cm^2) is the polarization resistance at the absence of inhibitor, and Rp^{inh}_{corr} (Ω.cm^2) is the polarization resistance determined at the presence of inhibitor.

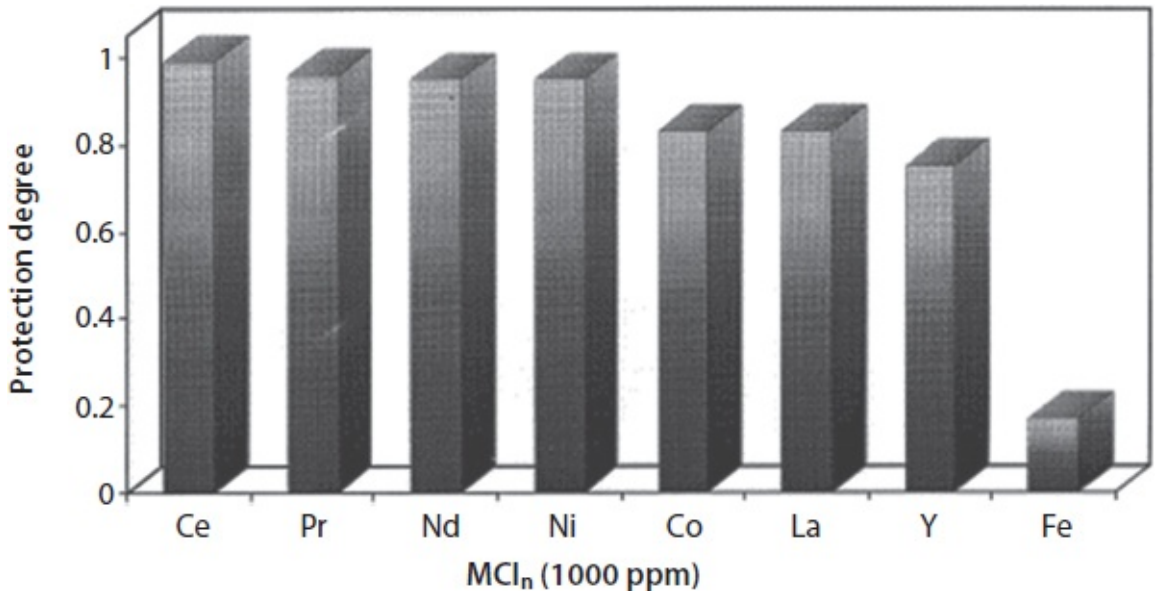
When the inhibition efficiency is being calculated on the basis of the aforementioned electrochemical measures, a serious attention should be paid on the conditions of the respective electrochemical measurements, since any excessive polarization of the investigated metallic substrates (which serve as working electrodes (WEs) during the electrochemical measurements) allows great deviations between the obtained results for the η values and the real inhibition efficiency of the investigated inhibitor. As a rule of thumb, the electrochemical polarization measurements (e.g. LVA or CVA) must be performed at the lowest possible potential deviations from the open circuit potential (OCP), which are able to give a smooth graphic data. The OCP value is namely the corrosion potential E_{corr} of the WE measured against a given RE (usually calomel or silver chloride electrode). If there is a notable difference between the OCP values before and after the electrochemical measurement, then the respective results can be considered as “suspicious”, since the WE has undergone a strong polarization during the measurement. The polarization (i.e. namely the deviation of the WE potential by external source of electricity) is driven by the electrochemical device (potentiostat or galvanostat) through a counter electrode (CE), and the OCP values can be obtained only when CE is switched off. The three electrodes RE, WE and CE are exposed to the inhibitor containing model corrosive medium, which serves as an electrolyte, in three electrode electrochemical cells. There are special rules for the cell design, described in ISO 16773-2:2007 (E). The most important requirements for the cell design are that the counter electrode should be

composed of noble metal, such as platinum, and the WE (i.e. the investigated metallic substrate) should have well-defined geometrical surface area and to be mounted in front of the RE. Using similar cell, when the galvanostat/potentiostat is equipped by frequency response analyser (FRA module), it becomes possible to perform electrochemical impedance spectroscopy. This method is based on the measurement of the electrical response to alternating current with gradually changing frequency. The corrosion inhibition efficiency could also be evaluated by this electrochemical analytical method. Nevertheless, the data obtained by this electrochemical method should be interpreted by an imaginable electric model, named "equivalent circuit", identical to that proposed by Zheludkevich *et al*. [148]. In this case, for calculation of the inhibitive efficiency, the charge transfer resistance R_{ct} values related to the electrochemical reactions on the interface between the WE and the respective corrosive medium should be used.

Nowadays, new alternative electrochemical methods for assessment of the corrosion rate and its inhibition, based on the mapping of the current or potential value fluctuations, on the metallic surface [162–166], or within the time [167, 168] are proposed. The former methods are based on scanning of the metallic surface by a reference electrode, whereas the latter are related to a statistical treatment of stochastic signal fluctuations. In general, when electrochemical measurement methods are applied for inhibitor characterization, another question arises, related to the repeatability of the obtained results, which is predetermined by the random distribution of the intermetallics on the metallic surface, and the impact of the preliminary surface treatment, as is established by Matter *et al*. [67].

Using electrochemical test methods, Bethencourt *et al*. [169] have evinced that the cerium chloride possesses the highest corrosion inhibitive ability for AA7075 among various metallic chlorides, added to 3.5%, NaCl, model corrosive medium, as demonstrated in Figure 2.30.

Figure 2.30 Degree of protection against uniform corrosion of alloy AA7075 in NaCl solutions provided by additions of 1000 ppm of different metallic chlorides [169].



Furthermore, the corrosion inhibition properties of this compound are assessed in various research works [59, 156, 159, 160, 167, 170, 171].

Machkova *et al*. [84] have performed comparative research on the corrosion-protective activity of cerium compounds with different anionic parts, added 0.01 M NaCl model corrosive medium on AA2024-T3. As a result, they have concluded that at low concentrations (i.e. 10^{-5} mol/l) all compounds possess identical protective ability, whereas at 10^{-2} mol/l, these compounds possess distinguishable inhibition efficiencies, combined with altering of the entire inhibition mechanism.

Thus, the compounds tested can be ordered in the following order, regarding their inhibition efficiency:

(2.23) $Ce(NO_3)_3 > (NH_4)_2Ce(NO_3)_5 > Ce_2(SO_4)_3 > CeCl_3$

In the same paper, the authors describe the reasons for the difference observed among the inhibition mechanisms related to the corresponding substances and its dependence on the respective anion. The authors explain the superior inhibitor performance of the nitrates, proposing dissolution of the oxide layer on the copper re-deposits (reaction 2.24):

(2.24) $3Cu_2O + 14H^+ + 2NO_3^- \rightarrow 6Cu^{2+} + 2NO + 7H_2O$

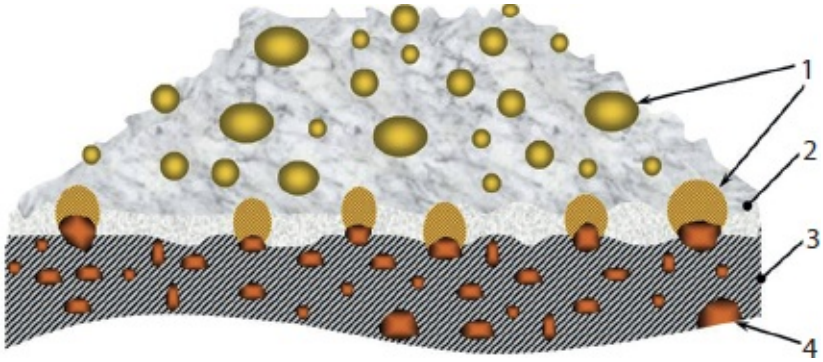
The inferior behaviour of the cerium chloride, on the other hand, is explained taking into account the aggressive action of the supplemental chlorine anions, originated from the dissolved $CeCl_3$, according to the following equation:

(2.25) $Al_2O_3 + 6H^+ + 6Cl^- \leftrightarrow AlCl_3 + 3H_2O$

The same author's work team has performed a study on the oxidation state of the cerium, comparing Ce(III) and Ce(IV) ammonium nitrates, concluding that the latter compound is able to enhance the corrosion attack at higher concentration. The cerium nitrate is examined as corrosion inhibitor for aluminium alloys by other authors, as well [172, 173].

In general terms, although the variations are caused by the inhibitor concentration, the anionic nature of the respective salt, the medium pH, the alloy's composition, etc., the mechanism of the corrosion inhibition by lanthanide salts proceeds by island-like deposition of cerium oxides/hydroxides, as is described by Aldykewicz [79], on the cathodic areas of the alloy, as described by Yasakau [59]. This mechanism is illustrated in Figure 2.31.

Figure 2.31 Visual model of aluminium alloy with inhibitor deposits on its surface: (1) inhibitor deposits, (2) surface oxide layer, (3) aluminium matrix and (4) intermetallic inclusions [80].



New direction in the scope of the cerium inhibitors is the introduction of cerium-containing organic substances, such as cerium salicylate ($Ce(Sal)_3$) [174], cerium acetylacetonate ($Ce(acac)_3$) [175] and cerium cinnamate [176], against the corrosion of different aluminium alloys. The basis of the general concept of cerium organic salts employment for corrosion protection is to achieve an effect of synergism between the cathodic inhibition, provided by the cerium ions and coincident blocking of the rest part of the metallic surface.

2.3.4.2 Organic Compounds as Corrosion Inhibitors

The alternative research branch of inhibitor characterization is to evaluate the capabilities of organic compounds to be used as efficient corrosion inhibitors. An example for such inhibitor is the 8-hydroxyquinoline (QH) and its derivatives [177, 178]. According to different authors [179–182], this

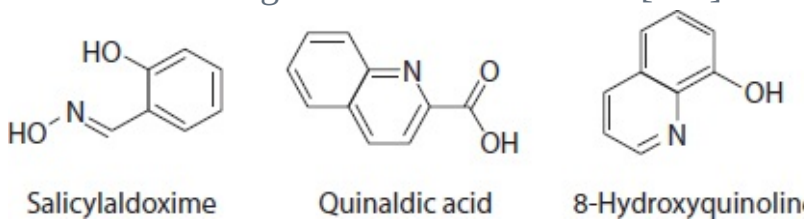
compound behaves as an efficient inhibitor. The inhibition mechanism, in this case, is based on the formation of low soluble chelate complexes with the copper and aluminium, according the following reactions:

(2.26) $$Cu^{2+} + 2(8\text{–}HQ) \rightarrow Cu(8\text{–}Q)_2 + 2H^+$$

(2.27) $$Al^{3+} + 3(8\text{–}HQ) \rightarrow Al(8\text{–}Q)_3 + 3H^+$$

Lamaka [182] has compared the inhibitive capability of this compound with other two substances, as shown in Figure 2.32.

Figure 2.32 Structural formulas of the organic inhibitors used in [182].



Salicylaldoxime Quinaldic acid 8-Hydroxyquinoline

Other authors have examined the corrosion inhibition capability of benzotriazole and tolyltriazole [183–185], evincing the possibility for the use of these compounds as corrosion inhibitors. The inhibition capabilities of QH and benzotriazole as additions to sol–gel coatings are examined, as well [186]. The inhibition efficiency of other triazole and thiazole derivatives on the corrosion inhibition of AA6061 [187] and AA2024 [188] is also tested.

Liu *et al*. [189] have proposed a kind of nontoxic compound pigment, composed of phosphate, molybdate, citrate and thiazole/imidazole derivatives on the fatigue crack growth rates of 7075-T76 aluminium alloy in 3.5% NaCl solution. A range of structurally related compounds [190] were tested for their capacity to inhibit corrosion on aluminium alloys AA2024-T3 and AA7075-T6 in 0.1 M NaCl solution. The corrosion-inhibitive properties of a wide variety of organic substances are tested such as sodium benzoate [191, 192], 1,4-naphthoquinone [193], 1,5-naphthalenediol [194], 2-amino-4,5-imidazoledicarbonitril (AID), 5-amino-4-imidazolecarboxamide, imidazole [195], sodium decanoate [196] and even some industrial dyes [197].

The amino acids are the basic composing components of all proteins, being among the most important constructive units of all the living organisms on earth. Recently, these important for the living nature substances are already examined as corrosion inhibitors, as well. Thus, nowadays the number of research works in the perspective field of examination of the corrosion inhibition ability, possessed by this class of biocompatible compounds, is continuously increasing. Examples for testing of l-glutamine, [198], tryptophan [199], glycine derivatives [200], etc. can be found in the literature. The corrosion-protective capabilities of some nutrition products such as vanillin [201], caffeine [202] and other natural products [203] are also investigated.

Nevertheless, the testing of natural products as potential corrosion inhibitors should be performed very attentively, because these substances could serve as nutritional source and convenient growth medium for alcaligenes or acidogenic microorganisms, causing the microbially influenced corrosion (MIC), which is well described in the literature [204–208]. Alternatively, antibiotics such as ampicillin and benzyl penicillin can be used as organic corrosion inhibitors, preventing simultaneously any MIC development, as is proposed by Fouda and El-Abbasy [209]. However, the application of such compounds should be done with respective environmental considerations. Indeed, the real danger, originated from the impact, caused by MIC on aircraft materials is already

demonstrated by Rosales and Iannuzzi [210].

Besides the aluminium alloys that serve as fuselage and frame structure material, the carbon and mild steels appear to be also very important materials, composing a great part of the on-board aircraft equipment. That is why, the inhibition efficiency of various organic compounds on the corrosion of carbon [211, 212] and mild steel [213–216] was assessed.

Furthermore, the correlation between the electronic structure and the inhibitive efficiency of various classes of unsaturated aliphatic, aromatic compounds, as well as nitrogen and sulphur containing derivatives is theoretically calculated by Lukovits *et al*. [217], on the basis of the energy contents of the highest occupied and the lowest unoccupied molecular orbitals. Since the corrosion inhibition by organic compounds is generally based on the occupation of the metallic surface and proceeds either by physical adsorption or by chemisorption, the theoretical investigations on these processes are related to determination of the adsorption isotherms, as is proposed by Popova *et al*. [218].

2.3.5 Technological Features of the Production of Hybrid Nanocomposite Primer Coatings

As it was mentioned above in the present text, and even illustrated by Figure 2.29, position b, the inhibitor could be involved into nanoparticles, prior its addition to the sol–gel system, during the synthesis of the respective hybrid primer coating. Hence, the nanoparticles have a double role, as reinforcing phase for the hybrid matrix as well as carriers of corrosion inhibitor.

Thus, the technology for the preparation of the corresponding hybrid nanocomposite primer coatings includes two intermediate stages:

- Formation of colloidal system, composed by solid phase represented by the nanoparticles, dispersed into a liquid medium consisted on solution of the inhibitor's lanthanide salt into liquid solvent.
- Gradual saturation of the obtained colloid by evaporation of the liquid solvent, in conditions of intensive perturbation in order to obtain a slurry system. For some cases, supplementary addition of detergents could be necessary to suppress undesirable agglomeration of the nanoparticles.
- Optional drying procedure to obtain dry powder material composed of hollow nanoparticle's agglomerates incorporated by corrosion-inhibitive substance. Finishing ball milling could be applied to diminish the size of the derivative clusters.

After all these procedures, the obtained slurry or powder (composed of nanoparticles with impregnated inhibitor) could be applied into the corresponding sol–gel system. The obtained conjugate deposits over the metal substrate. After the accomplishment of the hydrolysis–polymerization processes, the obtained polymer hybrid matrix encloses the clusters of nanoparticles together with the involved inhibitor inside.

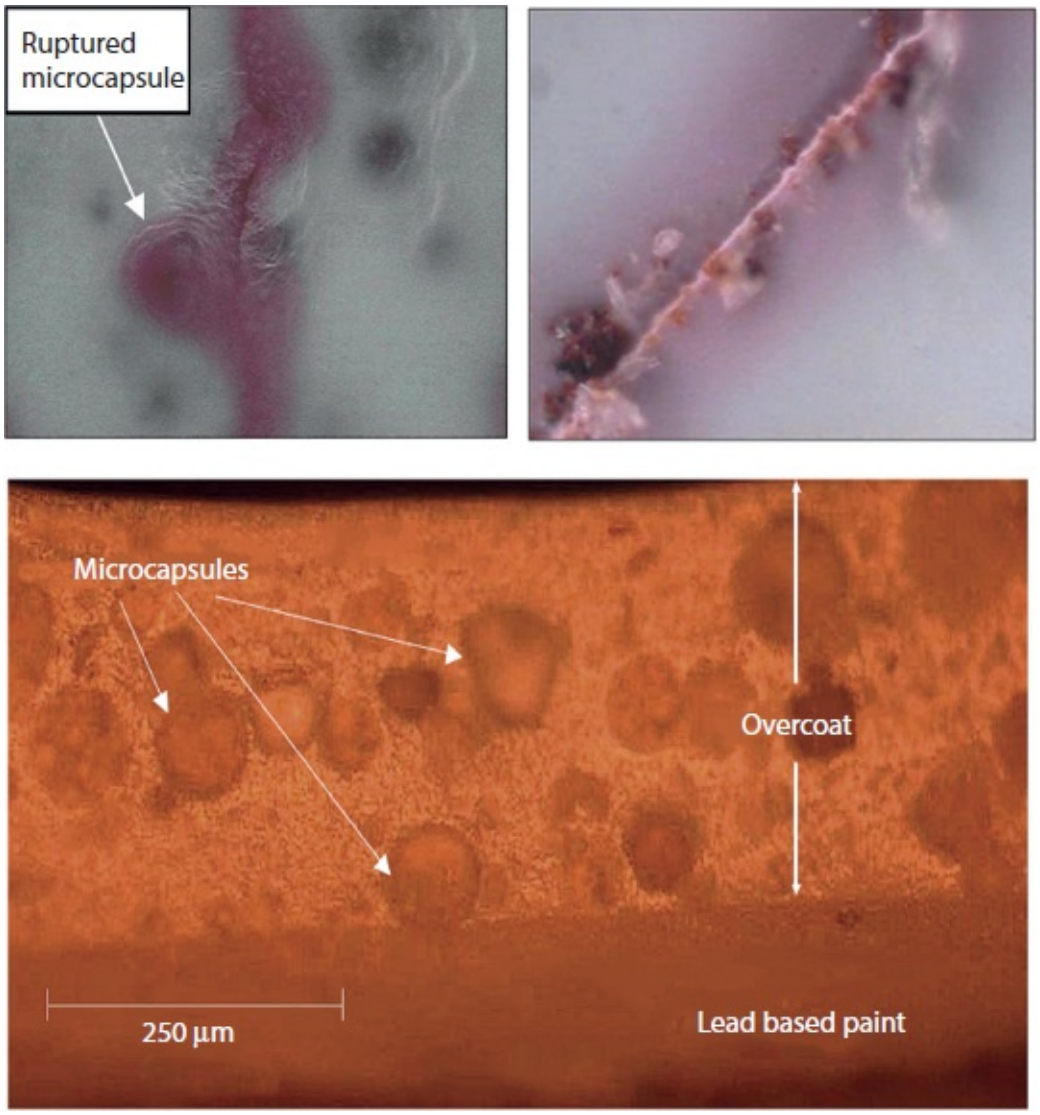
Examples for the synthesis of hybrid nanocomposite primer coatings could be found in the literature [129, 130, 175, 212, 219] and could also be the object of patents [221].

2.3.6 Alternatives for the Inhibitor Containing Self-Healing Coatings

2.3.6.1 Coatings with Recuperative Microcapsules

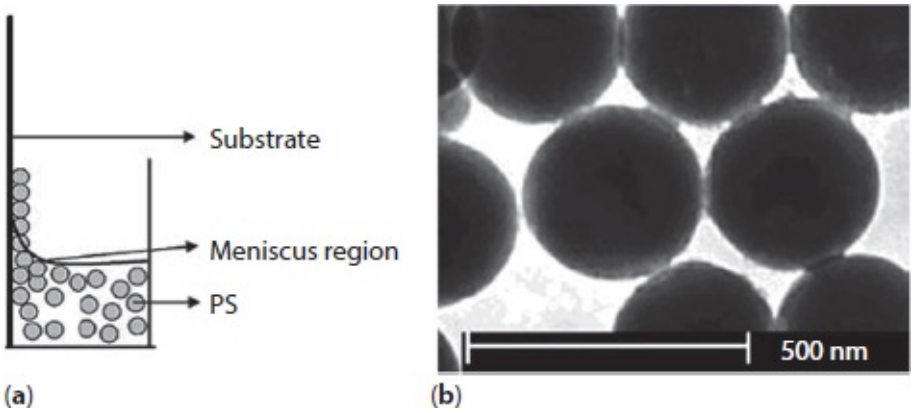
Stephenson and Kumar propose alternative approach for obtaining of coating materials with self-healing effect [222]. The principle of self-healing effect in their case is rather different. They enclose microcapsules into organic polymer. The microcapsules, in their case, contain no polymerized material. When the integrity of the microcapsules is corrupted due to mechanical scratch, the internal liquid content moves to the surface and fills the zone of scratch. Afterwards, when it is exposed to the environment, it polymerizes due to interaction with the air (Figure 2.33).

Figure 2.33 Photographic and refractive optical microscopy images of coatings with inclusions of microspheres with colorant after artificial defect [222].



This approach is achieved by incorporation of urea–formaldehyde microspheres into the composition of organic coating. For demonstration of this approach, the authors made photographs of the coating, as shown in Figure 2.34.

Figure 2.34 Schematic presentation of dip-coating procedure of deposition of coating with microspheres (a) and image of microsphere obtained by means of transmission electron microscopy (b) [223].



Liu *et al.* [223] have investigated the process of involvement of microspheres of polystyrene in hybrid matrix composed of poly-tetrabutyl ortotitanate $n[(C_4H_9O)_4Ti]$. Afterwards, they have dip-coated glass substrates. The pasting (deposition) of the coating on the glass surface during the withdrawing of the substrate is shown in Figure 2.35a. Figure 2.36 contains images of polystyrene microspheres, acquired via SEM.

Figure 2.35 SEM images of polystyrene microspheres with different image magnifications [223].

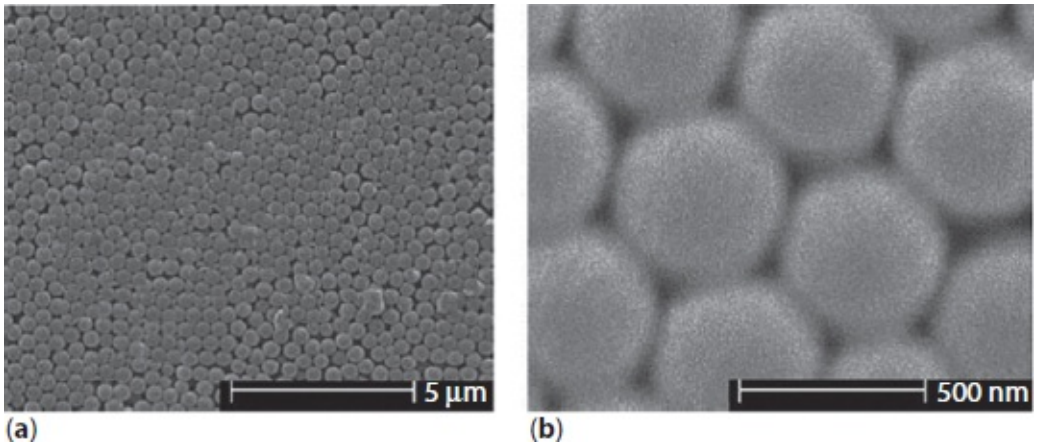
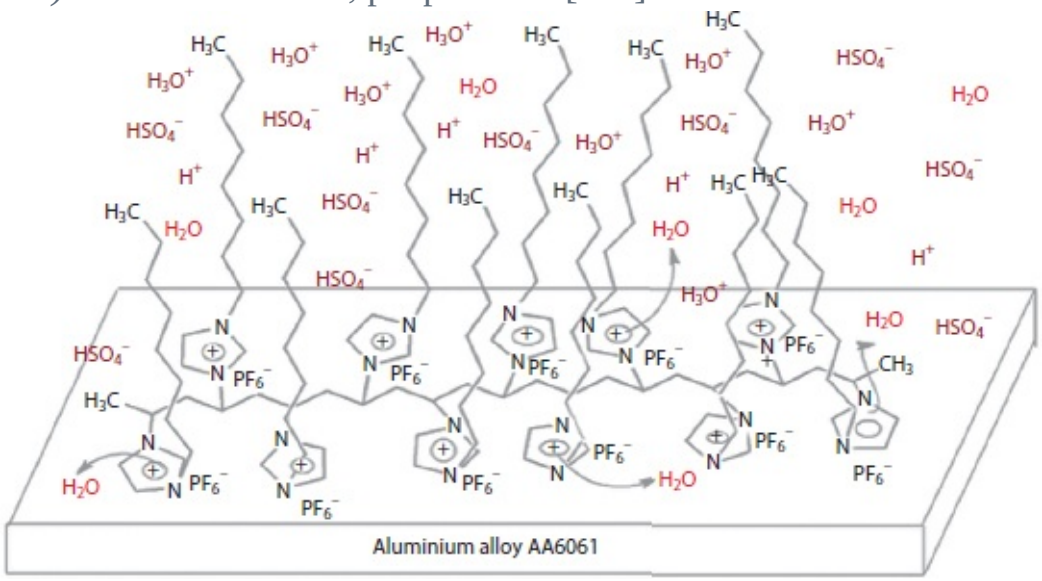


Figure 2.36 Schematic model of the corrosion protective action of *Poly(1-vinyl-3-alkyl-imidazolium Hexafluorophosphate)* towards AA 6061, proposed in [227].



The possible approaches, compositions and technologies for elaboration of self-repairing coatings with encapsulated polymerizing compounds are widely discussed in the literature [224] so that this group of coatings will not be submitted to detailed discussion in the present chapter.

2.3.6.2 Exterior Ice-Phobic and UV Protective Finishes

Another approach to avoid the localized corrosion phenomena after coating failure is to repel the collection of moisture and condensed water in the affected zones. In this case, an efficient way to achieve this effect is the use of hydrophobic coating materials. This approach enables to avoid the snow and ice heaping on the wings, which was the suspected reason for the aircraft crash on 7th of February 1958 in Munich, which killed most of the “Manchester United” football team [225].

Nowadays, the de-icing procedures, accepted as a common practice for the winter time exploitation in the commercial aircraft services, appears to be the main reason for inconveniences often related to schedule delays. In addition, these operations are economically expensive, due to the needs for de-icing solutions, staff and equipment. In this sense, the hybrid polyfluorinated hybrid coatings [226] appear to be rather attractive alternative, since these coating materials combine the hydrophobicity with the beneficial features of the hybrid materials, as discussed in the previous sections.

An interesting approach appears to be the proposed one by Arellanes-Lozada *et al.* [227]. These authors’ work team proposes poly(1-vinyl-3-alkyl-imidazolium hexafluorophosphate (Figure 2.36) as corrosion inhibitor for aluminium corrosion in acidic media. This polymer seems really interesting, since it is able to be used as an alternative hydrophobic coatings system, because it combines the beneficial effects of the presence of phosphate groups, long aliphatic chains and hydrophobic fluorine moieties.

Undoubtedly, the elaboration of durable and reliable ice-phobic coatings systems will be an object of increasing interest in the near future. Other possible compounds available for the development of ice-phobic coatings could be taken from the textile industry, as proposed elsewhere [228, 229].

Besides the difference between the dilatation coefficients of the metallic substrate and the hydrolytic activity of the water-based solutions, the sun radiation appears to be another factor of coating cracking, since the UV spectrum band of the sunlight causes destructive effects on various polymeric materials, as is described by Bubev *et al.* [230]. This problem could be suppressed, if the coatings contain UV absorbers. Both these obviously interesting directions will be the objects of continuously increasing interest in the further years and even decades.

Nevertheless, these topics are not related to the objectives of the present chapter.

2.3.7 Brief Summary

The new generation hybrid materials are able to combine the benefits of both organic and inorganic materials. The sol–gel technology has recently enabled the synthesis of various Ti, Si and Zr containing organic and hybrid polymeric protective films. However, when new composition is being developed, always the recently accepted limitation directives restricting the use of VOCs should be taken into account.

Despite their apparent advantages, the hybrid coatings are susceptible to deterioration during their exploitation due to water uptake. The durability of the hybrid coating can remarkably be improved by the use of self-assembled dense barrier layers and precursors with large aliphatic chains.

An alternative is to add fine-dispersed powder materials as reinforcing phase to the basic hybrid matrix. The coating materials obtained in this way form other class of materials known as “hybrid composites” or “hybrid nanocomposites”, depending on the size of the reinforcing phase particles.

Further protection can be achieved, when the reinforcing phase particles are preliminary loaded by environmentally compliant corrosion inhibitor. In this case, the reinforcing phase obtains additional

function of reservoir for gradual inhibitor release. For this purpose, the inhibitor properties should be investigated prior to the involvement of the respective inhibitor to the coating. Otherwise, detrimental effects of inhibitor inactivation and/or undesirable modification of coating ingredients are expectable. In this sense, the inhibition efficiency of various inorganic and organic compounds is elucidated. The lanthanides and particularly the cerium compounds have revealed the most promising results. However, the excessive Ce inhibitor content promotes even corrosion impact enhancement. These compounds act as cathodic inhibitors, and their inhibition mechanism is similar to that of the CeCC formation and growth (commented in the previous sections), whereas the organic compounds inhibit the corrosion through adsorption processes. Both the cerium ion oxidation state and the anionic moieties enable altering of the corrosion inhibition mechanism. Finally, the possible synergistic effects between the compositional parts of some Ce organic compounds such as cerium salicylate, acetylacetonate and cerium cinnamate have been examined.

Among the organic inhibitors, the amino acids are really interesting environmentally friendly corrosion inhibitors. However, their use may cause MIC. Thus, some antibiotics have shown corrosion-inhibitive activity as well, but these compounds could be environmentally unacceptable.

Another alternative for elaboration of durable and reliable coating systems is the encapsulation of active substances, which enable coating recuperation after mechanical damage.

Other directions for further extension of the coatings lifespan and enhancement of their protective abilities are the use of hydrophobic compositions and UV-light absorbers.

Acknowledgment

The author gratefully acknowledges the Bulgarian National Scientific Fund for the financial support through project BG NSFB T02-27.

References

1. http://www.ualberta.ca/~droles/aviation/concord3.html

2. https://www.google.bg/?gfe_rd=cr&ei=YSV3U7eIIenc8gfmloD4Bg#q=tu+144

3. https://www.google.bg/search, British_Airways_Helicopters_S-61_G-ATFM.jpg

4. A. Heinz, A. Haszler, C. Keidel, S. Moldenhauer, R. Benedictus, and W.S Miller, Recent development in aluminium alloys for aerospace applications, *Mater. Sci. Eng. A*, 280(1), 102–107, 2000.

5. E.A. Starke, Jr., and J.T. Staley, Application of Modern Aluminum Alloys to Aircraft, *Prog. Aerospace Sci.*, 32, 131–172, 1996.

6. AIRBUS A380, Airplane characteristics, Issue 30.03.05 (2005), www.content.airbusworld.com/SITES/Technical…/AC_A380.pdf3

7. W.E. Frazier, E.W. Lee, M.E. Donnellan, and J.J. Thompson, Advanced lightweight alloys for aerospace applications, *Journal of The Minerals, Metals & Materials Society*, 41, 22–26, 1989.

8. C. Giummarra, B. Thomas, and R.J. Rioja, New aluminum lithium alloys for aerospace applications, Proceedings of the Light Metals Technology Conference 2007, September 24–26, 2007, Saint-Saveur, Québec, (Canada).

9. K.M. Gatenby and S.A. Court, Aluminium–Magnesium Alloys for Automotive Applications – Design Considerations and Material Selection, IBEC '97 Proceedings, Stuttgart, Germany, 30 Sept.–2 Oct. p. 139, 1997.

10. P. Ostash, I.M. Andreiko, Yu.V. Holovatyuk, and O.I. Semenets, Effect of corrosive media on the fatigue life of degraded D16- and V95-type aluminum alloys, *Mater. Sci.*, 44, 672–682, 2008.

11. J.A. Rodríguez-Martínez, A. Rusinek, and A. Arias, Thermo-Viscoplastic behaviour of AA2024 aluminium sheets subjected to low velocity perforation at different temperatures, accessible via: http://earchivo.uc3m.es/bitstream/10016/11941/1/rodriguez_thermoT-WS2011ps.pdf

12. Y. Komatsu, New pretreatment and painting technology for all aluminum automotive body, paper no. 910787, SAE Technical Paper Series-International Congress/AIRP Meeting (Warrendale, PA: SAE International, 1991).

13. http://www.sbfships.com.au/

14. http://www.aluminiumleader.com/en/around/transport/ship

15. http://www.advancedrobotic.com/blog/cnc-routers/cost-savings-in-the-manufacture-of-aluminium-ships

16. G. Davies, "Materials for Automobile Bodies", 1st. ed. (2003) Linacre House, Jordan Hill, Oxford, p. 87–90.

17. A. Stankiewicz, I. Szczygieł, and B. Szczygieł, Self-healing coatings in anti-corrosion applications, *J. Mater. Sci.*, 48, 8041–8051, 2013.

18. D. Eyres, *"Ship construction"*, 6th ed. 2007, Linacre House, p. 50–52, ISBN 10:0-75-068070-913. http://nation.time.com/2011/07/05/u-s-navys-brand-new-aluminum-ship-foiled-by-seawater/

19. R.B. Figueira, C.J.R. Silva, and E.V. Pereira, Hybrid sol–gel coatings for corrosion protection of hot-dip galvanized steel in alkaline medium, *Surf. Coat. Technol.*, 265, 191–204, 2015.

20. S.A. Kulinich and A.S. Akhtar, On Conversion Coating Treatments to Replace Chromating for Al Alloys: Recent Developments and Possible Future Directions, *Russian Jour. Non-Ferrous Met.*, 53, 176–203, 2012.

21. D. Balgude and A. Sabnis, Sol–gel derived hybrid coatings as an environment friendly surface treatment for corrosion protection of metals and their alloys, *J. Sol-Gel Sci. Technol.*, DOI 10.1007/s10971-012-2838-z.

22. Directive 2004/107/EC of the European Parliament and of the Council of 15 December 2004 relating to arsenic, cadmium, mercury, nickel and polycyclic aromatic hydrocarbons in ambient air. Official Journal of the European Communities L 23, 26.1.2005, p. 3–16, Special edition in Bulgarian: Chapter 15 Volume 21, p. 124–137.

23. EU Directive 2002/95/EC "Restriction of Hazardous Substances in Electrical and Electronic Equipment" (RoHS directive 2002), www.broadcom.com/docs/ и www.chem.agilent.com/

24. U.S. Department of Health and Human Services, Public Health Service, Agency of Toxic Substances and Disease Registry (2008) Toxicological profile for Chromium, www.atsdr.cdc.gov/toxprofiles/tp7.pdf.

25. U.S. Environmental Protection Agency Washington, DC, August (1998) Toxicological review of hexavalent chromium. http://www.epa.gov/iris/toxreviews/0144tr.pdf

26. J. Davis, ASM International. "*Corrosion: Understanding the Basics*" American Technical

Publishers Ltd, Materials Park, Ohio, p. 6–10, 2000.

27. D. Miller, Corrosion Control on Aging Aircraft: What Is Being Done? *Materials Performance*, 29, pp. 10–11, 1990.

28. F. M. Mazzolani *"Aluminium alloy structures"* E& FN SPON ed. Second edition pp. 5–25, 1985.

29. R. Petrucci and W. Harwood, *"General Chemistry. Principles and modern applications"*, 7th ed. Prentice Hall, S.R.L. Iberia, p. 747, 1990. ISBN 84-8322-043-1.

30. M.A. Arenas, J.J. de Damborenea, Generación de capas de conversión con elementos de tierras raras sobre acero galvanizado Rev. Metal, Extra Volume, p. 433, 2005.

31. *"High temperature methods for synthesis of nanoparticle and nanostructures"* lecture course-Stephan Kozhukharov, UCTM– Sofia, 2014.

32. Vaidehi Chandrahasya Dongre, *Spontaneous Spray Deposition of Cerium Oxide Conversion Coatings on 7075-T6 Aluminum Alloy*, Ed.: University of Missouri-Rolla, USA, 2004.

33. B.F. Rivera, B.Y. Johnson, M.O'Keefe, and W.G. Farenholz, Deposition and characterization of cerium oxide conversion coatings on aluminum alloy 7075-T6, *Surf. Coat. Technol.*, 176, 349–356, 2004.

34. S. Kozhukharov, O.F. Acuña, M.S. Machkova, and V. Kozhukharov, Influence of buffering on the spontaneous deposition of cerium conversion coatings for corrosion protection of AA2024-T3 aluminum alloy, *J. Appl. Electrochem.*, 44, 1093–1105, 2014. http://link.springer.com/article/10.1007/s10800-014-0718-7

35. D.S. Rodrìguez, S. Kozhukharov, M. Machkova, and V. Kozhukharov, Influence of the deposition conditions on the properties of D16 AM clad alloy, dip-coated in Ce-containing baths, *Bul. Chem. Commun.* 45, Spec. issue-A, pp. 24–32, 2013. http://www.bcc.bas.bg/BCC_Volumes/Volume_45_Special_A_2013/BCC-45-SE-A-24-32.pdf

36. B. Jegdic, L. Zivkovic, J. Popic, J. Bajat, V. Miškovic-Stankovic, Electrochemical methods for corrosion testing of Ce-based coatings prepared on AA6060 alloy by the dip immersion method, *J. Serb. Chem. Soc.*, 78, 997–1011, 2013.

37. J.A. Ayuso, S. Kozhukharov, M. Machkova, and V. Kozhukharov, Electrodeposition of cerium conversion coatings for corrosion protection of D16 AM clad alloy, *Bul. Chem. Commun.*, 45, Spec. Issue-A, 33–40, 2013.

38. S. Kozhukharov, J.A.P. Ayuso, D.S. Rodrìguez, O.F. Acuña, M. Machkova, and V. Kozhukharov, Optimization of the basic parameters of cathodic deposition of Ce-conversion coatings on D16 AM clad alloy, *J. Chem. Technol. Metall.*, 48, 296–307, 2013. http://www.uctm.edu/journal/j2013-3/11-Stefan_Kojukharov-296-307.pdf

39. J. Creus, F. Brezault, C. Rebere, and M. Gadouleau, Synthesis and characterisation of thin cerium oxide coatings elaborated by cathodic electrolytic deposition on steel substrate, *Surf. Coat. Technol.*, 200, 4636–4645, 2006.

40. S. Ershov, M.E. Druart, M. Poelman, D. Cossement, R. Snyders, and M.-G. Olivier, Deposition of cerium oxide thin films by reactive magnetron sputtering for the development of corrosion protective coatings, *Corros. Sci.*, 75, 158–168, 2013.

41. S. Kozhukharov, Relationship between the conditions of preparation by the sol-gel route and the properties of the obtained products, *J. Univ. Chem. Technol. Met.*, 44, 143–150, 2009.

42. S. Kozhukharov and S. Tchaoushev, Perspectives for development and industrial application of

spray pyrolysis method, Annual Proceedings “Angel Kanchev” University of Rousse (Bulgaria) 50, 9.1, pp. 46–50, 2011. accessible via: http://conf.uni-ruse.bg/bg/docs/cp11/9.1/9.1-7.pdf

43. M.J. O’Keefe, S. Geng, and S. Joshi, Cerium-Based Conversion Coatings as Alternatives to Hex Chrome, *Metalfinishing*, 25–28, 2007.

44. B.R.W. Hinton, *J. Alloys Compounds*, 18, p. 15, 1992.

45. W.G. Fahrenholtz, M.J. O’Keefe, H. Zhou, and J.T. Grant, Characterization of cerium-based conversion coatings for corrosion protection of aluminum alloys, *Surf. Coat. Technol.*, 155, 208–213, 2002.

46. B.F. Rivera, B.Y. Johnson, M.J. O’Keefe, and W.G. Fahrenholtz, Deposition and characterization of cerium oxide conversion coatings on aluminum alloy 7075-T6, *Surf. Coat. Technol.*, 176, 349–356, 2004.

47. D. Zhao, J. Sun, L. Zhang, Y. Tan, and J. Li, Corrosion behavior of rare earth cerium based conversion coating on aluminum alloy, *Journal of Rare Earths*, 28, 371–374, 2010.

48. I. Aziz, Z. Qi, and X. Min, Corrosion Inhibition of SiCp/5A06 Aluminum Metal Matrix Composite by Cerium Conversion Treatment, *Chinese Journal of Aeronautics*, 22, 670–676, 2009.

49. B. Pentchev and S. Detchev, *Manual of Galvano-techniques,”* Technika” Gov. Ed., Sofia 1982.

50. L.Y. Kadaner, *Manual of Galvanostegy*, “Technika” Gov. Ed., Kiev, 1976.

51. I. Gadzhov *“Manual for Galvanotechniques” Sofia*, p. 87, 2008.

52. B.F. Rivera, B.Y. Johnson, M.J. O’Keefe, and W.G. Fahrenholtz, Deposition and characterization of cerium oxide conversion coatings on aluminum alloy 7075-T6, *Surf. Coat. Technol.*, 176, 349–356, 2004.

53. W. Pinc, S. Geng, M. O’Keefe, W. Fahrenholtz, and T. O’Keefe, Effects of acid and alkaline based surface preparations on spray deposited cerium based conversion coatings on Al 2024-T3. *Appl. Surf. Sci.*, 255, 4061–4065, 2009.

54. S. Geng, S. Joshi, W. Pinc, W.G. Fahrenholtz, M.J. O’Keefe, T.J. O’Keefe, and P. Yu, Influence of processing parameters oncerium based conversion coatings, Proceed “TRI–Service–2007” - corrosion conference: Accessible via: https://www.corrdefense.org/Technical%20Papers/Influence%20of%20Processing%20Parameters%20Conversion%20Coatings.pdf

55. http://www.iso.org/iso/home.html

56. http://asm.matweb.com/search/SpecificMaterial.asp?bassnum=MA2024T4

57. http://www.splav.kharkov.com/en/e_mat_start.php?name_id=1438

58. http://www.alu.com.cn/enCompany/ShowPro_3367_dflc.html

59. K.A. Yasakau, M.L. Zheludkevich, S.V. Lamaka and M.G. S, Ferreira, Mechanism of Corrosion Inhibition of AA2024 by Rare-Earth Compounds, *J. Phys. Chem. B*, 110, 5515–5528, 2006.

60. G. Brunner, N.Birbilis, K.D. Ralston, and S. Virtanen, Impact of ultrafine-grained microstructure on the corrosion of aluminium alloy AA2024, *Corros. Sci.*, 57, 209–214, 2012.

61. K.D. Ralston, D. Fabijanic, and N. Birbilis, Effect of grain size on corrosion of high purity aluminium, *Electrochim. Acta*, 56, 1729–1736, 2011.

62. E. Kus, Z. Lee, S. Nutt, and F. Mansfeld, A comparison of the behavior of nanocrystalline and conventional Al 5083 samples, *Corrosion*, 62, 152–161, 2006.

63. E. Sikora, X.J. Wei, and B.A. Shaw, Corrosion behavior of nanocrystalline buld Al– Mg–based alloys, *Corrosion*, 60, 387–398, 2006.

64. T.C. Tsai and T.H. Chuang, Role of grain size on the stress corrosion cracking of 7475 aluminum alloys, *Mater. Sci. Eng.*, A 225, pp. 135–144, 1997.

65. A.E. Hughes, C. MacRae, N. Wilson, A. Torpy, H.T. Muster, and A.M. Glenn, Sheet AA2024-T3: a new investigation of microstructure and composition, *Surf. Int. Anal.*, 42, 334–338, 2010.

66. K. Srinivasa Rao and K. Prasad Rao, Pitting corrosion of heat-tratable aluminium alloys and welds: a review, *Trans. Indian Inst. Met.*, 57(6), 593–610 2004.

67. E. Matter and S. Kozhukharov, Correlation between preliminary pretreatments and the behaviour of AA2024 – aluminium alloy in 3.5% NaCl model corrosive medium, Annual proceedings of "Angel Kanchev" University of Ruse (Bulgaria), 49, pp. 14–19, 2010. access via: http://conf.uni-ruse.bg/bg/docs/cp10/9.1/9.1-2.pdf

68. D. Zhao, J. Sun, L. Zhang, Y. Tan, and J. Li, Corrosion behavior of rare earth cerium based conversion coating on aluminum alloy, *Journal of Rare Earths*, 28, 371–374, 2010.

69. J. van den Brand, W. G. Sloof, H. Terryn, J. H. W. de Wit, Correlation between hydroxyl fraction and O/Al atomic ratio as determined from XPS spectra of aluminium oxide layers, *Surf. Interface An.* 36(1), 81–88, 2004.

70. C.M. Rangel, T.L. Paiva, and P.P. Daluz, Anticorrosion treatments for aluminum and aluminum alloys, *Proceeds. "European Symposium on Corrosion Inhibitor"*, 29(9), 507, 2000.

71. M. Bethencourt, F.J. Botana, and M.J. Cano, High protective, environmental friendly and short-time developed conversion coat- ings for aluminum alloys. *Appl. Surf. Sci.*, 189(1/2), 162–173, 2002.

72. Z. Nenova, S. Ivanov, and T. Nenov, *Sensors in industrial automation*, Ed. EKS-PRES (Gabrovo), 95, 2011.

73. C. Girginov and S. Kozhukharov, Surface of Alumina Films after Prolonged Breakdownsin Galvanostatic Anodization, *Internat. Jour. Electrochem.*, ID 126726, p. 5, 2012.

74. C.K. Chung, O.K. Khor, C.J. Syu, and S.W. Chen, Effect of oxalic acid concentration on the magnetically enhanced capacitance and resistance of AAO humidity sensor, *Sens. Actuators, B Chemical*, 210, 69–74, 2015.

75. H. Tsuchiya, S. Berger, J.M. Macak, A.G. Munoz, and P. Schmuki, A new route for the formation of self-organized anodic porous alumina in neutral electrolytes, *Electrochem. Commun.*, 9, 545–550, 2007.

76. N. Yamazoe, Humidity sensors: Principles and applications, 10, 379–398, 1986.

77. L. Yao, M. Zheng, H. Li, L. Ma, and W. Shen, High-performance humidity sensors based on high-field anodized porous alumina films, *Nanotechnology*, 22, 379–501, 2011. (1pp), doi:10.1088/0957-4484/22/37/379501.

78. E.C. Dickey, O.K. Varghese, K.G. Ong, D. Gong, M. Paulose, and C.A. Grimes, Room temperature ammonia and humidity sensing using highly ordered nanoporous alumina films, *Sensors*, 2, 91–110, 2002.

79. A.J. Aldykiewicz, A.J. Davenport, and H.S. Isaacs, Studies of the Formation of Cerium-Rich Protective Films Using X-Ray Absorption Near-Edge Spectroscopy and Rotating Disk Electrode Methods. *J. Electrochem. Soc.*, 143, 147–154, 1996.

80. J.E. Pernas, S. Kozhukharov, A.A Salve, E. Matter, and M. Machkova, Influence of the oxidation state of Ce-ions on the inhibition of AA2024 Alloy corrosion in a model corrosive medium, *J. Univ. Chem. Technol. Met.* 47, 311–318, 2012.

81. S. Kozhukharov, V. Kozhukharov, M. Wittmar, M. Schem, M. Aslan, H.Caparrotti, and M.Veith, Protective abilities of nanocomposite pre-treatments containing Al_2O_3 nanoparticles loaded by $CeCl_3$, *Prog. Org. Coat.* 71, 198–205, 2011.

82. A.A. Salve, S. Kozhukharov, J.E. Pernas, E. Matter, and M. Machkova, Comparative research on hybrid nano-composite protective primary coatings for AA2024 aircraft alloy, *J. Univ. Chem. Technol. Met.* 47, 319–326, 2012.

83. A. Conde, M.A. Arenas, A. de Frutos, and J. de Damborenea, Effective corrosion protection of 8090 alloy by cerium conversion coatings, *Electrochim. Acta*, 53, 7760–7768, 2008.

84. M. Machkova, E.A. Matter, S. Kozhukharov, and V. Kozhukharov, Effect of the anionic part of various Ce(III) salts on the corrosion inhibition efficiency of AA2024 aluminium alloy, *Corros. Sci.*, 69, 396–405, 2013.

85. D. Lau, A.M. Glenn, A.E. Hughes, F.H. Scholes, T.H. Muster, and S.G. Hardin, Factors influencing the deposition of Ce-based conversion coatings, Part II: The role of localised reactions, *Surf. Coat. Technol.*, 203, 2937–2945, 2009.

86. D. Zhao, J. Sun, L. Zhang, Y. Tan, and J. Li, Corrosion behavior of rare earth cerium based conversion coating on aluminum alloy, *Journal of Rare Earths*, 28, 371–374, 2010.

87. E.A. Matter, S. Kozhukharov, M. Machkova, and V. Kozhukharov, Electrochemical studies on the corrosion inhibition of AA2024 aluminium alloy by rare earth ammonium nitrates in 3.5 % NaCl solutions, Proc. 9th Eur. Symp. Electrochem. Engineering, Chania, (Greece), 2011, P2. 05.

88. S. Kozhukharov, V. Kozhukharov, M. Schem, M. Aslan, M. Wittmar, A. Wittmar, and M. Veith, Protective ability of hybrid nano-composite coatings with cerium sulphate as inhibitor against corrosion of AA2024 aluminium alloy, *Prog. Org. Coat.*, 73, 95–103, 2012.

89. G. Tsaneva, V. Kozhukharov, S. Kozhukharov, M. Ivanova, J. Gerwann, M. Schem, and T. Schmidt, Functional nanocomposite coatings for corrosion protection of aluminium alloy and steel, *J. Univ. Chem. Technol. Met.*, 43(2), 231–238, 2008.

90. O. Lunder, J.C. Walmsley, P. Mack, and K. Nisancioglu, Formation and characterisation of a chromate conversion coating on AA6060 aluminium, *Corros. Sci.*, 47, 1604–1624, 2005.

91. A. Decroly, and J.P. Petitjean, Study of the deposition of cerium oxide by conversion on to aluminium alloys, *Surf. Coat. Technol.*, 194, 1–9, 2005.

92. L.E.M. Palomino, I.V. Aoki, and H.G. de Melo, Microstructural and electrochemical characterization of Ce conversion layers formed on Al alloy 2024-T3 covered with Cu-rich smut, *Electrochim. Acta*, 51, 5943–5953, 2006.

93. F.H. Scholes, C. Soste, A.E. Hughes, S.G. Hardin, and P.R. Curtis, The role of hydrogen peroxide in the deposition of cerium-based conversion coatings, *Appl. Surf. Sci.*, 253, 1770–1780, 2006.

94. E.A. Matter, S.V. Kozhukharov, and M.S. Machkova, Effect of preliminary treatment on the superficial morphology and the corrosion behaviour of AA2024 aluminum alloy, *Bul. Chem. Commun.*, 43(1), 23–30, 2011.

95. E.A. Matter, S. Kozhukharov, M. Machkova, and V. Kozhukharov, Reproducibility of the corrosion parameters for aa2024-t3 aluminium alloy in chloride solution after different preliminary treatment

procedures, *J. Chem. Technol. Metall.*, 50(1), 52–64, 2015.

96. C. Girginov and S. Kozhukharov, Impact of the preliminary surface treatment of aluminum on its electrochemical behaviour, Ann. Proceed. of "Anguel Kanchev" University of Rousse 52(10.1), 29–32, 2013. Access via: http://conf.uni-ruse.bg/bg/docs/cp13/10.1/10.1-5.pdf

97. A.E. Hughes, F.H. Scholes, A.M. Glenn, D. Lau, T.H. Muster, and S.G. Hardin, *Surf. Coat. Technol*., 203, 2927–2936, 2009.

98. D. Guergova, E. Stoyanova, D. Stoychev, I. Avramova, G. Atanasova, and P. Stefanov, Corrosion stability of stainless steel, modified electrochemically with Ce_2O_3 – CeO_2 films, in 3.5% NaCl media, *Bul. Chem. Commun.*, 43(1), 150–157, 2011.

99. E. Stoyanova, D. Guergova, D. Stoychev, I. Avramova, and P. Stefanov, Passivity of OC404 steel modified electrochemically with CeO_2–Ce_2O_3 layers in sulfuric acid media, *Electrochim. Acta,* 55, 1725–1732, 2010.

100. B.R.W. Hinton, D.R. Arnott, and N.E. Ryan, *Materials Forum*, 9(3), 162–173, 1986.

101. P. Yu, S.A. Hayes, T.J. O'Keefe, M. OKeefe, and J.O. Stoffer, The phase stability of cerium species in aqueous systems: II. the Ce(III/IV)-H_2O–H_2O_2/O_2 systems. equilibrium considerations and Pourbaix diagram calculations, *J. Electrochem. Soc.*, 153, C74-C79, 2006.

102. P. Yu and T.J. O'Keefe, The phase stability of cerium species in aqueous systems - III. The Ce(III/IV)-H_2O-H_2O_2/O^{-2} systems dimeric Ce(IV) species, *J. Electrochem. Soc.*, 153, C80-C85, 2006.

103. Ehl, Rosemary Gene and A. Ihde, Faraday's Electrochemical Laws and the Determination of Equivalent Weights. *Journal of Chemical Education* 31(5): 226–232, 1954. Bibcode:1954JChEd..31..226E. doi:10.1021/ed031p226.

104. Lj.S. Zivkovic, J.S. Popic, B.V. Jegdic, Z. Dohcevic-Mitrovuic, J.B. Bajat, and V.B. Miskovic-Stankovic, Corrosion study of ceria coatings on AA6060 aluminium alloy obtained by cathoduic electrodeposition: Effect of deposition potential, *Surf. Coat. Technol*. 240, 327–335, 2014.

105. T. Gil, S. Kozhukharov, and C. Girginov, Deposition of cerium conversion coatings on AA2024-T3 aircraft alloy at fixed potentials, Annual proceedings of "Angel Kanchev" University of Ruse (Bulgaria), 53, 9–13, 2014. Access via: http://conf.uni-ruse.bg/bg/docs/cp14/10.1/10.1-1.pdf

106. M.D. Tkalenko, On the Anomalous Cathodic Dissolution of Aluminum in Connection with Concentration Changes Near the Electrode, *Protection of Metals*, 37(4), 301–304, 2001.

107. T. Picard, G. Cathalifaud-Feuillade, M. Mazet, and C. Vandensteendam, Cathodic dissolution in the electrocoagulation process using aluminium electrodes, *J. Environ. Monit.*, 2(1), 77–80, 2000.

108. M. Mokaddem, P. Volovitch, F. Rechou, R. Oltra, and K. Ogle, The anodic and cathodic dissolution of Al and Al–Cu–Mg alloy, *Electrochim. Acta,* 55, 3779–3786, 2010.

109. K. Ogle, M. Serdechnova, M. Mokaddem, and P. Volovitch, *Electrochim. Acta*, 56, 1711, 2011.

110. E. Matter, S. Kozhukharov, and M. Machkova, SEM & EDS determination of the impact of inhibitor containing corrosive media over the AA2024 superficial morphology, Ann. Proceed. "Anguel Kanchev" University of Rousse, 50, 9.1, 60–64, 2011. access via: http://conf.uni-ruse.bg/bg/docs/cp11/9.1/9.1-10.pdf

111. D.K. Heller, W.G. Fahrenholtz, and M.J. O'Keefe, The effect of post-treatment time and temperature on cerium-based conversion coatings on Al 2024-T3, *Corros. Sci.*, 52, 360–368, 2010.

112. CHEN Dong-chu, LI Wen-fang, GONG Wei-hui, WU Gui-xiang, and WU Jian-feng,

Microstructure and formation mechanism of Ce-based chemical conversion coating on 6063 Al alloy, *Trans. Nonferrous Met. Soc.*, (China) 19, 592–600, 2009.

113. D.I. Ivanova, Phosphating of zinc surfaces in zinc-calcium solutions, *Bul. Chem. Commun.*, 43, 54–59, 2011.

114. Y. Tumbaleva, D. Ivanova, and L. Fachikov, Effect of the P_2O_5:NO_3 – ratio on the zinc phosphate coating formation, *J. Univ. Chem. Technol. Met.*, 46, 357–362, 2011.

115. Y. Dimitriev, Y. Ivanova, and R. Iordanova, History of sol-gel science and technology (review), *J. Univ. Chem. Technol. Metall.*, 43(2), 181–192, 2008.

116. K.-H. Haas, and K. Rose, Hybrid inorganic/organic polymers with nanoscale building blocks: precursors, processing, properties and applications, *Rev. Adv. Mater. Sci*., 5, 47–52, 2003.

117. M.L. Zheludkevich, I.M. Salvado, and M.G. Ferreira, Sol-gel coatings for corrosion protection of metals, *J. Mater. Chem.*, 15(48), 5099–5111, 2005.

118. D. Wang, G.P. Bierwagen, Sol-gel coatings on metals for corrosion protection, *Prog. Org. Coat.*, 64, pp. 327–338, 2009.

119. V. Palavinel, Y. Huang, and W. van Ooij, Effects of addition of corrosion inhibitors to silane films on the performance of AA2024-T3 in 0.5 M NaCl solutioin, *Prog. Org. Coat.*, 53, 153–168, 2005.

120. A. Frignani, F. Zucchi, G. Trabanelly, and V. Grassi, Protective action towards aluminium corrosion by silanes with long aliphatic chain, *Corros. Sci.*, 48, 2258–2273, 2006.

121. P. Laibinis, G. Whitesides, D. Allara, Y-T. Tao, A. Parkin, and R. Nuzzo, Comparison of the structures and wetting properties of self-assembled monolayers of n-alkanethiols on the coinage metal surfaces, copper, silver, and gold, *J. Am. Chem. Soc.*, 113, 7152–7167, 1991.

122. J. Malzbender and G. de With, Measuring mechanical properties of coatings: a methodology applied to nano-particle-filled sol–gel coatings on glass, *Adv. Eng. Mater.*, 4, 296–302, 2002.

123. R.B. Figueira, C.J.R. Silva, and E.V. Pereira, Organic–inorganic hybrid sol–gel coatings for metal corrosion protection: a review of recent progress, *J. Coat. Technol. Res.*, 12, 1–35, 2015.

124. T. Materne, F. de Buyl, and G. Witucki, *Organosilane Technology in Coating Applications: Review and Perspectives*, Dow Corning S.A. (Belgium), accessible via: http://www.dowcorning.com/content/publishedlit/26-1402-01.pdf

125. K. Joncoux-Chabrol, J.-P. Bonino, M Gressier, M.-J. Menu, and N. Pébère, Improvement of barrier properties of a hybrid sol-gel coating by incorporation of synthetic talc-like phyllosilicates for corrosion protection of a carbon steel, *Surf. Coat. Technol.*, 206, 2884–2891, 2012.

126. M. Abdolah-Zadeh, S. van der Zwaag, and S.J. Garcia, Routes to extrinsic and intrinsic self-healing corrosion protective sol-gel coatings: a review, *Self-Healing Mater,* 1–18, 2013. DOI: 10.2478/shm-2013-0001.

127. Directive 2001/81/EC on national emission ceilings for certain atmospheric pollutants, Official Journal of the European Communities, L 1309/22, 27-11-2001.

128. Council Directive on the limitation of emissions of VOC due to the use of organic solvents in certain activities and installations, *Official Journal of the European Communities,* L 85/1, 29–3, 1999.

129. F. Zamborini and R. Crooks, Corrosion Passivation of Gold by n-Alkanethiol Self-Assembled Monolayers: Effect of Chain Length and End Group, *Langmuir,* 14, 3279–3286, 1998.

130. M. Zheludkevich, R. Serra, M. Montemor and M. Ferreira., Oxide nanoparticle reservoirs for storage and prolonged release of the corrosion inhibitors, *Electrochem. Commun*., 7, 836, 2005.

131. N. Rosero-Navarro, S. Pellice, Y. Castro, M. Aparicio and A. Durán, Improved corrosion resistance of AA2024 alloys through hybrid organic-inorganic sol–gel coatings produced from sols with controlled polymerisation, *Surf. Coat. Technol*., 203, 1897–1903, 2009.

132. G. Jennings, T. Yong, J. Munro, and P. Laibinis, *Jour. Am. Chem. Soc.*, 125, 2950, 2003.

133. Y. Ma, C. Yang, S. Chen, L. Jiao, X. Huang, G. Li and L. Luo, *Electrochim. Acta*, 48, 4277, 2003.

134. S. Ono, H. Tsuge, Y. Nishi, S. Hirano, and J. Sol-Gel, *Sci. Technol.*, 29, 147, 2004.

135. S. Kozhukharov, Z. Nenova, T. Nenov, N. Nedev, and M. Machkova, Humidity sensing elements based on cerium doped titania-silica thin films prepared via a sol–gel method, *Sensors and Actuators B: Chemical*, 210, 676–684, 2015.

136. A. Trinchi, T.H. Muster, I.S. Cole, J.B. Dunlop, and S.J. Collocott, Embedded magnetic nanoparticle sensors for monitoring primer failure beneath paint, *Sensors and Actuators B: Chemical*, 210, 446–452, 2015.

137. B. Samuneva, V. Kozhukharov, Ch. Trapalis, and R. Kranold, Sol-gel processing of titanium-containing thin coatings. Part I Preparation and structure, *J. Mater. Sci.*, 28, 2353–2360, 1993.

138. N. Voevodin, J. Kurdziel and R. Mantz, Corrosion protection for aerospace aluminum alloys by Modified Self-assembled NAno-Phase (MNSNAP) sol-gel, *Surf. Coat. Technol.*, 201, 1080–1084, 2006.

139. N. Voevodin, N. Grebash, W. Soto, F. Arnold and M. Donley, Potentiodynamic evaluation of Sol-Gel Coatings with inorganic inhibitors, *Surf. Coat. Tech.*, 140, pp. 24–28, 2001.

140. A. Vregdenhil, V. Balbyshev, and M. Donley, Nanostructured silicon sol-gel surface treatments for AA2024-T3 protection, *J. Coat. Technol.*, 73, 35–43, 2001.

141. P. Hammer, F.C. dos Santos, B.M. Cerrutti, S.H. Pulcinelli, and C.V. Santil, Carbon nanotube-reinforced siloxane-PMMA hybrid coatings with high corrosion resistance, *Prog. Org. Coat.*, 76, 601–608, 2013.

142. L. Hu, D.S. Hecht, and G. Grüner, Carbon Nanotube Thin Films: Fabrication, Properties, and Applications, *Chem. Rev.*, 110, 5790–5844, 2010.

143. B. Safadi, R. Andrews, and E.A. Grulke, Multiwalled carbon nanotube polymer composites: Synthesis and characterization of thin films, *J. Appl. Polym. Sci.*, 84, 2660–2669, 2002.

144. L. Xiao, Z. Chen, C. Feng, L. Liu, Z-Q. Bai, Y. Wang, L. Qian, Y. Zhang, Q. Li, K. Jiang, and S. Fan, Flexible, Stretchable, Transparent Carbon Nanotube Thin Film Loudspeakers, *Nano Lett*, 8, 4539–4545, 2008.

145. B.E. Kilbride1, J.N. Coleman1, J. Fraysse, P. Fournet, M. Cadek, A. Drury, S. Hutzler, S. Roth, and W.J. Blau, Experimental observation of scaling laws for alternating current and direct current conductivity in polymer-carbon nanotube composite thin films, *J. Appl. Phys.*, 92, 4024, 2002.

146. B.B. Parekh, G. Fanchini, G. Eda, and M. Chhowalla, Improved conductivity of transparent single-wall carbon nanotube thin films via stable postdeposition functionalization, *Appl. Phys. Lett.*, 90, 121913, 2007.

147. E. Matter, S. Kozhukharov, M. Machkova, and V. Kozhukharov, Influence of the interactions between the corrosion inhibitor and nanocontainers over the corrosion protective capability of hybrid

nanocomposite pre-treatments, Annual proceed. Rousse University 48, pp. 19–23, 2009. Accessible via: http://conf.uni-ruse.bg/bg/docs/cp09/9/9-3.pdf

148. M.L. Zheludkevich R. Serra, M.F. Montemor, K.A. Yasakau I.M. Miranda Salvado, and M.G.S. Ferreira, Nanostructured sol-gel coatings doped with cerium nitrate as pretreatments for AA2024-T3 Corrosion protection performance, *Electrochim Acta*, 51, 208–217, 2005.

149. P. Suegama, H. de Melo, A. Benedetti, and I. Aoki, Influence of cerium (IV) ions on the mechanism of organosilane polymerization and on the improvement of its barrier properties, *Electrochim Acta*, 54, 2655–2662, 2009.

150. N.N. Greenwood and A. Earnshaw, *Chemistry of the Elements*, Pergamon Press, Oxford, England, 1437, 1984.

151. T.J. Haley, *J. Pharm. Sci.*, 54, 633, 1965.

152. Registry of toxic effects of chemical substances in, DHHS-NIOSH, 103, 1986.

153. P.J. Falconnet, The rare earth industry: a world of rapid change, *J. Alloys Comp.*, 192, 114–117, 1993.

154. G.K.Muecke and P. Möller, The Not-So-Rare Earths., *Sci. Amer.*, 258, 72, 1988.

155. U.S. Geological Survey, Mineral commodity summaries, in: *U.S.Geological Survey*, 198, 2011.

156. H. Allachi, F. Chaouket, and K. Draoui, Corrosion inhibition of AA6060 aluminium alloy by lanthanide salts in chloride solution, *J. Alloys Comp.*, 475, 300–303, 2009.

157. H. Allachi, F. Chaouket, and K. Draoui, Protection against corrosion in marine environments of AA6060 aluminium alloy by cerium chlorides, *J. Alloys and Comp.*, 491, 223–229, 2010.

158. B.R.W. Hinton, D.R. Arnott, and N.E. Ryan, *Mater. Forum*, 9, 16, 1986.

159. A. Aballe, M. Bethencourt, F.J. Botana, and M. Marcos, $CeCl_3$ and $LaCl_3$ binary solutions as environment-friendly corrosion inhibitors of AA5083 Al–Mg alloy in NaCl solutions, *J. Alloys Comp.*, 323–324, 855–858, 2001.

160. M.A. Arenas, M. Bethencourt, F.J. Botana, J. de Damborenea, and M. Marcos, Inhibition of 5083 aluminium alloy and galvanised steel by lanthanide salts, *Corros. Sci.*, 43, 157–170, 2001.

161. M. Bethencourt, F.J. Botana, M.A. Cauqui, M. Marcos, J.A. Pérez, and J.M. Pintado, Ibero-Americano Corros. *Protec.*, 1, 321, 1995.

162. H.N. McMurray, S.R. Magill, and B.D. Jeffs, Scanning Reference Electrode Techniques Tool for Investigating Localised Corrosion Phenomena in Galvanised Steels, *Iron and Steelmaking*, 23, 183–188, 1996.

163. S. Kallip, A.C. Bastos, M.L. Zheludkevich, and M.G.S. Ferreira, A multi-electrode cell for high-throughput SVET screening of corrosion inhibitors, *Corros. Sci.*, 52, 3146–3149, 2010.

164. R. Akid, Localised Corrosion: A New Evaluation Approach, *Materials World*, 3, 522–525, 1995.

165. S.J. Garcia-Vergara, P. Skeldon, G.E. Thompson, G. Williams, and H.N. McMurray, Enrichment of Alloying Elements in Aluminum: A Scanning Kelvin Probe Approach, *J. Electrochem. Soc.*, 159(9), C428-C433, 2012.

166. F. Anderatta, M-E. Druant, E. Marin, D. Cossement, M-G. Olivier, and L. Fedrizzi, Volta potential of clad AA2024 aluminium after exposure to $CeCl_3$ solution, *Corros. Sci.*, 86, 189–201, 2014.

167. A. Aballe, M. Bethencourt, F.J. Botana, M. Marcos, and R.M. Osuna, Electrochemical noise

applied to the study of the inhibition effect of $CeCl_3$ on the corrosion behaviour of Al–Mg alloy AA5083 in seawater, *Electrochim. Acta*, 47, 1415–1422, 2002.

168. J. Kearns, J. Scully, P. Roberge, D. Reichert, and J. Dawson, Electrochemical noise measurement for corrosion applications, ASTM publ. PCN 04-01270-27, PA – USA, 1996.

169. M. Bethencourt, F.J. Botana, J.J. Calvino, M. Marcos, and M.A. Rodriguez-Chacon, Lanthanide compounds as environmentally-friendly corrosion inhibitors of aluminium alloys: A review, *Corros. Sci.*, 40, 1803–1819, 1998.

170. B. Davó and J.J. de Damborenea, Use of rare earth salts as electrochemical corrosion inhibitors for an Al-Li-Cu (8090) alloy in 3.56% NaCl, *Electrochim. Acta*, 49, 4957–4965, 2004.

171. S.J. García, T.H. Muster, Ö. Özkanat, N. Sherman, A.E. Hughes, H. Terryn, J.H.W. de Wit, and J.M.C. Mol, The influence of pH on corrosion inhibitor selection for 2024-T3 aluminium alloy assessed by high-throughput multielectrode and potentiodynamic testing, *Electrochim. Acta*, 55, 2457–2465, 2010.

172. A.C. Balaskas, M. Curioni, and G.E. Thompson, Evaluation of Inhibitor Performance by Electrochemical Methods: Comparative Study of Nitrate Salts on AA 2024-T3, *J. Electrochem. Soc.* 161(9), C389–C394, 2014.

173. N.C. Rosero-Navarro, M. Curioni, R. Bingham, A. Durán, M. Aparicio, R.A. Cottis, and G.E. Thompson, Electrochemical techniques for practical evaluation of corrosion inhibitor effectiveness. Performance of cerium nitrate as corrosion inhibitor for AA2024T3 alloy, *Corros. Sci.*, 52, 3356–3366, 2010.

174. E. Hughes, D. Ho, M. Forsyth, and B.R.W. Hinton, Rare earth inhibited systems, in: *Tri-Service Corrosion Conference* Nov. 14–18, Orlando, FL, 1–10, 2005.

175. M. Schem, T. Schmidt, H. Caparrotti, M. Wittmar, and M. Veith, Corrosion inhibiting cerium compounds for chromium-free corrosion protective coatings on AA 2024, in: *Eurocorr*, Freiburg, Germany, 2007.

176. H. Shi, E.-H. Han, and F. Liu, Corrosion protection of aluminium alloy 2024-T3 in 0.05 M NaCl by cerium cinnamate, *Corros. Sci.*, 53, 2374–2384, 2011.

177. S.-m. Li, H.-r. Zhang, and J.-h. Liu, Corrosion behavior of aluminum alloy 2024-T3 by 8-hydroxy-quinoline and its derivative in 3.5% chloride solution, *Transactions of Nonferrous Metals Society of China*, 17, 318–325, 2007.

178. S.-m. Li, H.-r. Zhang, and J.-h. Liu, Preparation and performance of fluorescent sensing coating for monitoring corrosion of Al alloy 2024, *Transactions of Nonferrous Metals Society of China*, *16*, *Supplement*, 1, s159–s164, 2006.

179. K.Yasakau, M. Zheludkevich, and O. Karavali, Influence of inhibitor addition on the corrosion protection performance of sol – gel coatings on AA2024, *Progress in Organic Coatings*, 63, 352–361, 2008.

180. G. Cicileo, B. Rosales, F. Varela, and J.Vilche, *Corros. Sci*. 40, 1915–1921, 1998.

181. I. Devol and E. Bardez, *J. Colloid Interface Sci.*, 200, 241, 1998.

182. S. Lamaka, M. Zheludkevich, K.Yasakau, M. Montemor, and M. Ferreira, High effective organic corrosion inhibitors for 2024 aluminium alloy, *Electrochim. Acta*, 52, 7231–724, 2007.

183. A.N. Önal and A.A. Aksüt, Corrosion inhibition of aluminium alloys by tolyltriazole in chloride

solutions, *Anti-Corrosion Methods and Materials*, 47, 339–349, 2000.

184. R. Parkhill, E. Knobbe and M.Donley, *Prog. Org. Coat.*, 41, pp. 261–269, 2001.

185. V. Palanivel, Y. Huang, and W.J. van Ooij, Effects of addition of corrosion inhibitors to silane films on the performance of AA2024-T3 in a 0.5 M NaCl solution, *Prog. Org. Coat.*, 53, 153–168, 2005.

186. K.A. Yasakau, M.L. Zheludkevich, O.V. Karavai, and M.G.S. Ferreira, Influence of inhibitor addition on the corrosion protection performance of sol–gel coatings on AA2024, *Prog. Org. Coat.*, 63, 352–361, 2008.

187. P. Kumari, J. Nayak, and A. Shetty, 3-Methyl-4-amino-5-mercapto-1,2,4-triazole as corrosion inhibitor for 6061 Al alloy in 0.5 M sodium hydroxide solution, *J. Coat. Technol. Res*, 8, 685–695, 2011.

188. M.L. Zheludkevich, K.A. Yasakau, S.K. Poznyak, and M.G.S. Ferreira, Triazole and thiazole derivatives as corrosion inhibitors for AA2024 aluminium alloy, *Corros. Sci.*, 47, 3368–3383, 2005.

189. X.F. Liu, S.J. Huang, and H.C. Gu, Crack growth behaviour of high strength aluminium alloy in 3.5%NaCl solution with corrosion inhibiting pigments, *International Journal of Fatigue*, 24, 803–809, 2002.

190. T.G. Harvey, S.G. Hardin, A.E. Hughes, T.H. Muster, P.A. White, T.A. Markley, P.A. Corrigan, J. Mardel, S.J. Garcia, J.M.C. Mol, and A.M. Glenn, *The effect of inhibitor structure on the corrosion of AA2024 and AA7075*, Corros. Sci., 53, 2184–2190, 2011.

191. R. Rosliza, W.B. Wan Nik, and H.B. Senin, The effect of inhibitor on the corrosion of aluminum alloys in acidic solutions, *Mater. Chem. Phys.*, 107, 281–288, 2008.

192. R. Rosliza, H.B. Senin, and W.B.W. Nik, Electrochemical properties and corrosion inhibition of AA6061 in tropical seawater, *Colloids and Surfaces A: Physicochemical and Engineering Aspects*, 312, 185–189, 2008.

193. E.M. Sherif, and S.-M. Park, Effects of 1,4-naphthoquinone on aluminum corrosion in 0.50 M sodium chloride solutions, *Electrochim. Acta*, 51, 1313–1321, 2006.

194. E.M. Sherif, and S.-M. Park, Effects of 1,5-Naphthalenediol on Aluminum Corrosion as a Corrosion Inhibitor in 0.50 M NaCl, *J. Electrochem. Soc.*, 152, B205–B211, 2005.

195. K. Khaled and M. Amin, Electrochemical and molecular dynamics simulation studies on the corrosion inhibition of aluminum in molar hydrochloric acid using some imidazole derivatives, *J. Appl. Electrochem.*, 39, 2553–2568, 2009.

196. G. Boisier, N. Portail, and N. Pébère, Corrosion inhibition of 2024 aluminium alloy by sodium decanoate, *Electrochim. Acta*, 55, 6182–6189, 2010.

197. L.H. Madkour, R.M. Isaa, and I.M. El-Ghrabawy, Kinetics of substitited bis- and mono-azo dyes as corrosion inhibitors for aluminium in hydrochloric acid and hydroxide solutions, *J. Chem. Res.*, 408–409, 1701–1726, 1999.

198. H. Ashassi-Sorkhabi, and E. Asghari, Electrochemical corrosion behavior of Al7075 rotating disc electrode in neutral solution containing l-glutamine as a green inhibitor, *J. Appl. Electrochem.*, 40, 631–637, 2010.

199. X. Li, B. Xiang, X.-l. Zuo, Q. Wang, and Z.-d. Wei, Inhibition of Tryptophan on AA 2024 in Chloride-Containing Solutions, *Jour. Mater. Eng. Perform.*, 20, 265–270, 2011.

200. A. Mohammed, A newly synthesized glycine derivative to control uniform and pitting corrosion processes of Al induced by SCN– anions – Chemical, electrochemical and morphological studies, *Corros. Sci.*, 52, 3243–3257, 2010.

201. R. Rosliza, A. Nora'aini, and W. Wan Nik, Study on the effect of vanillin on the corrosion inhibition of aluminum alloy, *J. Appl. Electrochem*, 40, 833–840, 2010.

202. R. Sabino, D. Azambuja, and R. Gonçalves, Electrochemical behavior of aluminum alloy AA2024 in aqueous solutions in the presence of caffeine, *J. Solid State Electrochem.*, 14, 1255–1260, 2010.

203. P.B. Raja and M.G. Sethuraman, Natural products as corrosion inhibitor for metals in corrosive media—A review, *Mater. Lett*, 62, 113–116, 2008.

204. X. Shi, N. Xie, and J. Gong, Recent Progress in the Research on Microbially Influenced Corrosion: A Bird's Eye View through the Engineering Lens, *Recent Patents on Corrosion Science*, 1, 118–131, 2011.

205. M.A. Alsaleh, General Characterization of Microbially Influenced Corrosion (MIC) Realted Microorganisms in Crude Oil, *NACE Internat-2012*, ISBN: 01267 2012 CP.

206. H.A. Videla and W.G. Characklis, Biofouling and microbially influenced corrosion, *International Biodeterioration & Biodegradation*, 29, 195–212, 1992.

207. A. Mollica, Biofilm and corrosion on active-passive alloys in seawater, *International Biodeterioration & Biodegradation*, 29, 213–229, 1992.

208. S.C. Dexter and S.-H Lin, Effect of marine biofilms on cathodic protection, *International Biodeterioration & Biodegradation*, 29, 231–249, 1992.

209. I.A.S. Fouda and H.M. El-Abbasy, Inhibitive Action of Ampicillin and Benzyl Penicillin Drugs for Corrosion of Type 304 Stainless Steel in 1.0 M HCl Solution, *Corrosion*, 68(1), 015002-1-015002-9, 2012.

210. B. Rosales and M. Iannuzzi, Aluminium AA2024 T351 aeronautical alloy. Part 1. Microbial influenced corrosion analysis, *Mater. Sci. Eng.* A, 472, 15–25, 2008.

211. A.M. Al-Sabagh, N.M. Nasser, A.A. Farag, M.A. Migahed, A.M.F. Eissa, and T. Mahmoud Structure effect of some amine derivatives on corrosion inhibition efficiency for carbon steel in acidic media using electrochemical and Quantum Theory Methods, *Egyptian Journal of Petroleum*, 22, 101–116, 2013.

212. A.M. Al-Sabagh, N.Gh. Kandil, O. Ramadan, N.M. Amer, R. Mansour, and E.A. Khamis, Novel cationic surfactants from fatty acids and their corrosion inhibition efficiency for carbon steel pipelines in 1 M HCl, *Egyptian Journal of Petroleum*, 20, 47–57, 2011.

213. F. Bentiss, M. Outirite, M. Traisnel, H. Vezin, M. Lagrenée, B. Hammouti, S.S. Al-Deyab, and C. Jamant, Improvement of Corrosion Resistance of Carbon Steel in Hydrochloric Acid Medium by 3,6-bis(3-Pyridyl)Pyridazine, *J. Electrochem. Sci.*, 7, 1699–1723, 2012.

214. F. Bentiss, M. Traisnel, and M. Lagrenee, The substituted 1,3,4-oxadiazoles: a new class of corrosion inhibitors of mild steel in acidic media, *Corros. Sci.*, 42, 127–146, 2000.

215. F. Bentiss, M. Lagrenee, M. Traisnel, and J.C. Hornez, Corrosion Inhibition of Mild Steel in 1 M Hydrochloric Acid by 2,5-Bis(2-Aminophenyl)-1,3,4- Oxadiazole, *Corrosion*, 55, 968–976, 1999.

216. A. Popova, E. Sokolova, S. Raicheva, and M. Christov, AC and DC study of the temperature effect on mild steel corrosion in acid media in the presence of benzimidazole derivatives, *Corros. Sci.*, 45,

33–58, 2003.

217. I. Lukovits, E. Kálmán, and F. Zucchi, Corrosion Inhibitors—Correlation between Electronic Structure and Efficiency, *Corrosion*, 57, 3–8, 2001.

218. A. Popova, M. Christov, S. Raicheva, and E. Sokolova, Adsorption and inhibitive properties of benzimidazole derivatives in acid mild steel corrosion, *Corros. Sci*., 46, 1333–1350, 2004.

219. V. Kozhukharov, S. Kozhukharov, G. Tsaneva, J. Gerwann, M. Schem, T. Schmidt, and M. Veith, Investigation on the corrosion protection ability of nanocomposite hybrid coatings, *Impedance Contributions,* Online 5, P-1–P2-16, 2007. accessible via: http://accessimpedance.iusi.bas.bg

220. V. Kozhukharov, G. Tsaneva, S. Kozhukharov, J. Gerwann, M. Schem, T. Schmidt, and M. Veith, Corrosion protection properties of nanocomposite hybrid coatings with zirconia and ceria, *Bul. Chem.Commun.*, 78, 23–29, 2007.

221. G. Jonschker, S. Langenfeld, and H. Schmidt, Method for protecting a metallic substrate against corrosion, US Patent No. 6,403,164 (2002).

222. L. Stephenson, and A. Kumar, Technology Demonstration of Self-Healing Coatings for In-Place Management of Lead-Based Paint Hazards, US Army Corporation of Engineers-Engineer Research and Development Center; December 2003, pages 5–6.

223. Z. Liu, Z. Jin, X. Liu, Y. Fu and G. Liu, Fabrication of orderd TiO2 porous Thin Film by Sol-Dipping PS Template Method, *J. Sol-Gel Sci. Technol*. 38, 73–78, 2006.

224. A. Tiwari, L. Hihara, and J. Rawlins, Eds. Intelligent Coatings for Corrosion Control, *Butterworth Heinemann*, ISBN: 978-0-12-411467-8, 2014.

225. Accessible via: http://www.theguardian.com/media/from-the-archive-blog/2011/may/28/munich-manchester-united-busby-1958

226. R. Suriano, V. Oldani, and C.L. Bianci, AFM. Nanomechanical properties and durability of new hybrid polyfluorinated sol-gel coatings, *Surf. Coat. Technol.*, 264, 87–96, 2015.

227. P. Arellanes-Lozada, O. Olivares-Xometl, D. Guzmán-Lucero, N.V. Likhanova, M.A. Domínguez-Aguilar, I.V. Lijanova, and E. Arce-Estrada, The Inhibition of Aluminum Corrosion in Sulfuric Acid by Poly(1-vinyl-3-alkyl-imidazolium Hexafluorophosphate), *Materials*, 7(8), 5711–5734, 2014.

228. C. Pereira, C. Alves, A. Monteiro, C. Magén, A.M. Pereira, A. Ibarra, M.R. Ibarra, P. B. Tavares, J.P. Araújo, G. Blanco, J.M. Pintado, A.P. Carvalho, J. Pires, M.F.R. Pereira, and C. Freire, Designing Novel Hybrid Materials by One-Pot Co-condensation: From Hydrophobic Mesoporous Silica Nanoparticles to Superamphiphobic Cotton Textiles, *ACS Appl. Mater. Interfaces*, 3(7), 2289–2299, 2011.

229. B. García, J. Saiz-Poseu, R. Gras-Charles, J. Hernando, R. Alibés, F. Novio, J. Sedó, F Busqué, and D. Ruiz-Molina, Mussel-inspired hydrophobic coatings for water-repellent textiles and oil removal, *ACS Appl Mater Interfaces*, 6, 17616–17625, 2014.

230. E. Bubev, V. Bozhilov, S. Kozhukharov, M. Machkova, and V. Kozhukharov, Flexible UV-absorbing films-deposition and charaterization, *Journal of International Scientific Publications: Materials, Methods and Technologies*, 8, ISSN 1314–7269; (Online), Published at: http://www.scientific-publications.net

Chapter 3

Ferrites as Non-Toxic Pigments for Eco-Friendly Corrosion Protection Coatings

D.O. Grigoriev[1]*, T. Vakhitov[2], and S.N. Stepin[2]

[1]*Department of Interfaces, Max-Planck Institute of Colloids and Interfaces, Potsdam, Germany*

[2]*Kazan National Research Technological University, Kazan, Republic of Tatarstan, Russia*

**Corresponding author*: dmitry.grigoriev@mpikg.mpg.de

Abstract

Contemporary challenges in the field of corrosion protection coatings are connected with the necessity to reduce the use of toxic and environmentally hazardous components in these systems. Application of ferrites as anticorrosive pigments of low toxicity could answer this problem in eco-friendly way. Current activities in this research field are focused on the proper choice of initial components and techniques used for ferrites syntheses and therefore on the methods leading to ferrites with broadly diversified compositions. It enables, together with the adjusting the shape and size of pigment particles, the significant enhancement of corrosion protection performance of coatings on the ferrites basis. Since very recently, a new research area connected with the preparation of ferrite pigments with core–shell morphology is intensively developing. In these pigments, ferrites can be utilized in both core and shell of pigment particles. In the latter case, the low-priced fillers are used as core materials allowing the significant price reduction for the final product. The works investigating the utilization of industrial wastes for the synthesis of ferrite pigments, which can simultaneously solve the problem of materials recycling, serve the same purpose. Additional important factors making the use of ferrite pigments even more promising are, along with their properties to combat corrosion, their thermal and light stability as well as the ability to absorb efficiently the microwave radiation. These features may impart the multifunctionality to the protective coatings containing ferrites.

Keywords: Corrosion protection, steels, paints, environmentally benign coatings, non-toxic anticorrosive pigments, synthesis techniques, mechanisms of action, core–shell pigment, nanomaterials, multifunctional protective coatings, magnetic properties

3.1 Introduction

Global industrial progress leads simultaneously to several side effects such, for example, as continuously increasing impact of technogenic pollutants on the environment. As a consequence, the corrosivity of ambient media including atmosphere, aquatic environment, and soil rises

correspondingly. This, in turn, causes a clamant need for the further improvement of metal corrosion protection, especially protection of steel, which remains till now a main engineering and constructional material. One of the most efficient and economically sound methods widely used for the corrosion protection is painting the metal substrate, including the application of corrosion-inhibiting primers. Mechanisms of protective effect of these primers may be very variable, but practically always their protection performance is determined by properties of anticorrosive pigments included in the coating formulation. The highest efficiency of corrosion protection performance demonstrated till recently the primers on the basis of chromate pigments [1, 2]. However, they are currently almost completely banned because of high toxicity and environmental hazards [3]. Thus, development of novel environmentally friendly alternative solutions for the highly efficient anticorrosive paintworks is nowadays a high-priority task in many industry branches.

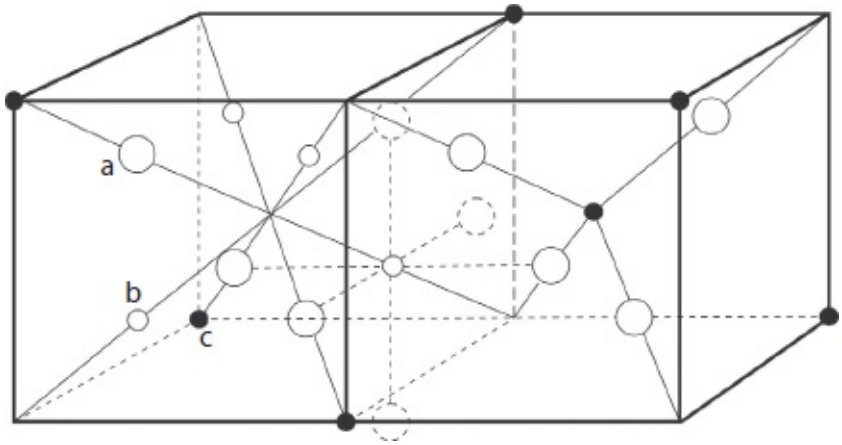
One of the solutions of this problem could be the use of practically non-toxic metal ferrites as corrosion combating pigments in the coating formulations aimed at corrosion protection [4–6].

3.2 Crystalline Structure, Physicochemical Properties, and Inhibition Mechanism of Ferrites

Ferrites are crystalline compounds possessing spinel structure (Figure 3.1), which can be considered as mixed oxides of general composition $MO \times Fe_2O_3$ or as salts of the ferrous acid with formula MFe_2O_4, where M denotes a cation of salt-forming divalent metals like Zn^{2+}, Ni^{2+}, Co^{2+}, $Mn^{2}+$, Cu^{2+}, etc. [7]. Main ferrite properties are determined by the characteristics of their crystal lattice.

Figure 3.1 Schematic representation of a spinel structure unit cell: (a) oxygen ions, (b) metallic cation on octahedral position, and (c) metallic cation on tetrahedral position.

Adopted from Ref. [4].

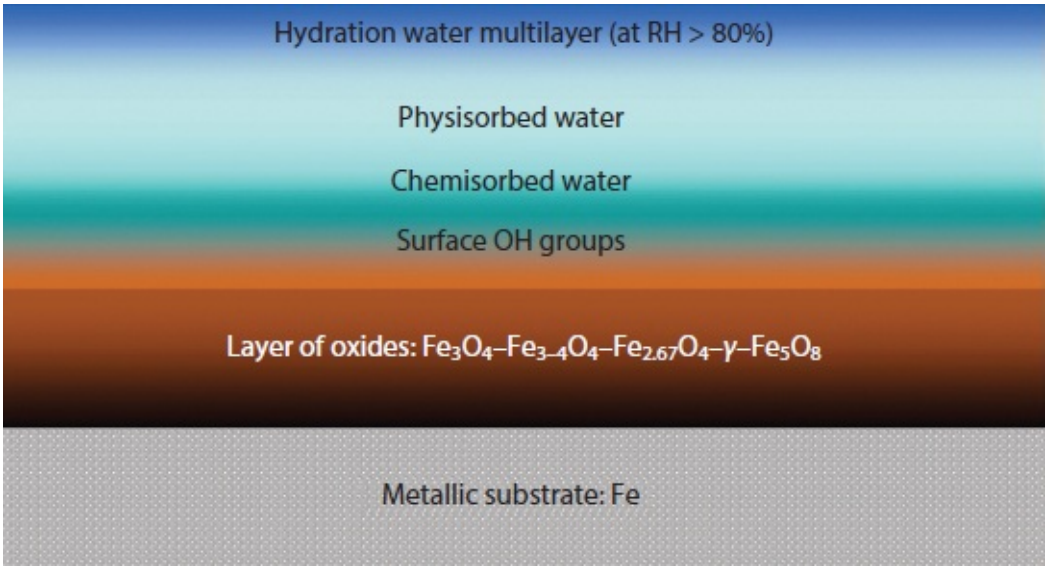


After discovering the ability of ferrites to inhibit the corrosion of steel, active investigations focused on the mechanism of their anticorrosive effect and on the possibilities of further enhancement of the latter were started. Ferrite pigments of the first generation were single-cation ferrites with predominantly Zn, Ca, and Mg used as salt-forming metals. Later, the double- and multi-cation ferrites were synthesized in order to enhance their protective performance [8]. Ferrites are basic substances since they could formally be considered as salts of a week (ferrous) acid and strong

bases. Passivating effect of ferrites is related to the high pH value of an aqueous medium adjacent to pigments caused by their hydrolysis [9].

Iron and iron alloys undergo in the air atmosphere the oxidation process leading to the formation of the oxide layer on the substrate surface that is shown schematically in Figure 3.2 [10]. At the natural conditions, the thickness of the oxide layer amounts to approximately 5 nm. In case of plain steel, the gradient of the steel oxidation degree and related to these changes in the stoichiometric composition are observed. Fe_2O_3 on the surface of bulk metal is followed firstly by unstable $Fe_{2.67}O_4$ and then by γ-Fe_2O_3, that can be denoted in the presence of the chemisorbed water as HFe_5O_8. If the relative humidity (RH) attains the level over 80% RH, the physisorption of water on the oxide layer is ascertained which finally lead to the formation of hydration multilayer with the properties of bulk water.

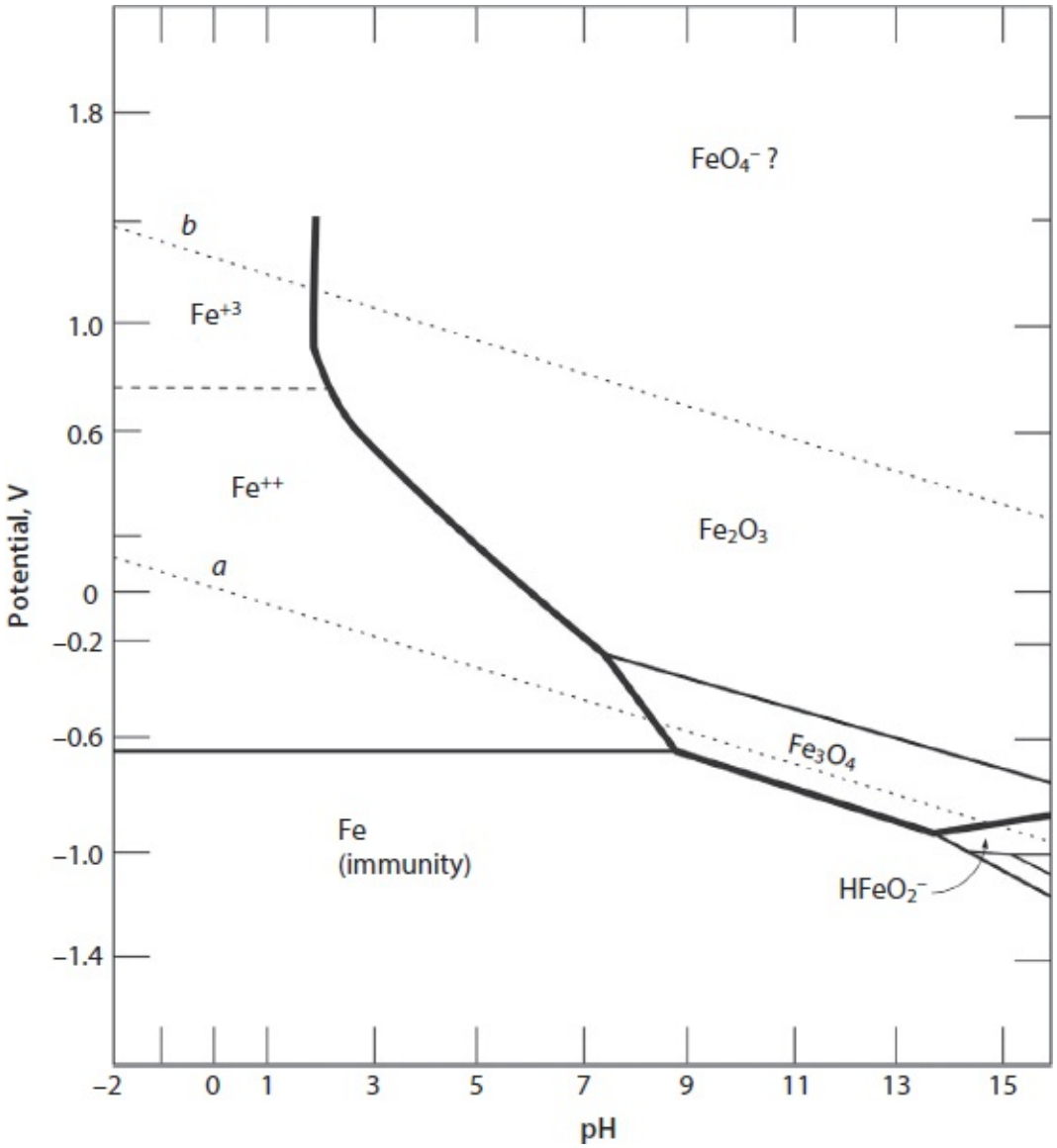
Figure 3.2 Schematic structure of the oxide hydrate layer on the carbon steel surface according to Ref. [10]. More details are given in the corresponding paragraph.



Corrosion stability of steel depends largely on stability of the iron oxide surface layer which, in turn, is determined by the pH value of the medium contacting the steel surface [11]. Effect of pH on the corrosion process could be visually presented by means of the Pourbaix diagram for the corresponding metal. This diagram for iron is well known (Figure 3.3) and relates the potential of iron to pH values in the surrounding medium.

Figure 3.3 The Pourbaix diagram for the iron–water system at 25 °C with only Fe, Fe_3O_4, and Fe_2O_3 as solid phases.

Adopted from Ref. [11].



Lines a and b delimitate the domain of the thermodynamic water stability. Outside this domain, the following reactions take place:

(3.1) $2H_2O - 4e^- \rightarrow O_2 + 4H^+$ (above Line b)

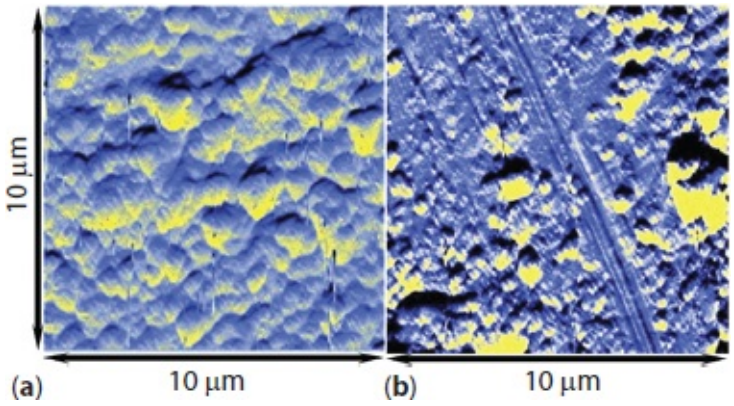
(3.2) $2H_2O + 2e^- \rightarrow OH^- + H_2\uparrow$ (below Line a)

According to this figure, the stability domain for the layer of surface oxides and, therefore, for the passivity of iron becomes more and more extended with the pH increase.

Indeed, the corrosion protection efficiency correlates with the pH value of aqueous ferrite extract: In case of calcium ferrite with pH between 12.5 and 13.0 protection efficiency attains the value of 99.3%; for the magnesium ferrite (pH 10.5–11.0), the protection efficiency becomes moderate value of 73.1%, and for ferrite of zinc (pH between 6.7 and 7.0), it drops till only 33.3% [9]. Mechanism of the anticorrosive effect of ferrites was clearly demonstrated in Ref. [12] in the following experiment using atomic force microscopy (AFM) technique (Figure 3.4). The AFM image of the cathodic site on the periphery of the droplet of aqueous ferrite extract deposited on the steel surface showed the precipitate coverage (Figure 3.4a). On the contrary, the substrate surface in the middle part of the droplet (anodic area) remained almost free of sediment (Figure 3.4b).

Figure 3.4 Images of the surface of steel after 1 h exposure of ferrite extract droplet: (a) close to the three-phase contact line (cathodic area) and (b) in the central part of droplet (anodic area).

Adopted from Ref. [12].



This phenomenon can be explained taking into account the set of reactions proceeding in different parts of droplet. Cathodic reaction in the area close to the droplet edge lead to the formation of OH^- ions:

(3.3) $O_2 + 2H_2O + 4e^- \rightarrow 4OH^-$

These ions react with the metal cations of corresponding ferrite compound and iron cations diffusing from the middle part of extract droplet where the anodic reaction takes place:

(3.4) $4Fe - 8e^- \rightarrow 4Fe^{2+}$

As a result, hardly soluble mixed hydroxides are formed

(3.5) $yM^{2+} + (3-y)Fe^{2+} + 6OH^- \rightarrow M_yFe_{3-y}(OH)_6$

falling as tight deposit which hinders the transfer of species participating in cathodic process. Thus, the inhibition of corrosion is achieved.

It is worth noting that the nature of the binder agent in the coating can influence the pH value in the medium adjacent the surface of the painted steel substrate. In particular, a noticeable decrease of pH was observed for the water upon its diffusion through the coating film on the basis of the alkyd oligomers widely used as binders [13]. This effect is connected with the presence of free acids in the polymeric coating matrix as well as with the formation of water-soluble acidic products of binder degradation during the coating curing. Incorporation of ferrite pigments possessing alkaline properties in the coating composition facilitates the reduction of acidity in the aqueous medium penetrating toward substrate through the coating. Acidic water-soluble components of binder are neutralized by the alkaline saponification.

For example, pH values of aqueous extracts of filled pentaphtol coatings with the pigment volume fraction of 0.35 amount to 5.6 and 5.4 for calcium and zinc ferrite, correspondingly [14]. Due to acidity decrease in the aqueous solution reaching the surface of the steel substrate, the increase of polarization of the cathodic reaction and, as a consequence, enhancement of the electrochemical potential of steel and the corrosion mitigation are observed.

It was also ascertained in several studies [13, 14] that the products of saponification of acidic components can also improve the protective performance of coatings owing to the adsorption passivation of the surface of the painted steel and enhancement of coating barrier characteristics due to sealing its defects and pores. It is noteworthy that abovementioned values of pH for extracts of ferrite-filled alkyd coatings are exactly in the range corresponding to the maximal inhibitive performance of metallic soaps [13, 14].

As an additional confirmation of two possible mechanisms of the ferrites anticorrosive effect (increase of pH in the corrosive medium adjacent the metal surface and adsorption inhibiting by

saponified coating components), one can consider the results reported in Ref. [15]. Therein, the corresponding dual protective action was demonstrated for the coatings based on neutral epoxy or acidic alkyd-acrylic binders [15].

Depending on the nature of salt-forming metal and binder, the optimal degree of coating filling by ferrites may be very different: Strontium ferrite in coatings with epoxy binders reveals the maximal corrosion protection performance at the ratio binder/pigment 4:1. On the other hand, magnesium ferrite shows the best performance in both epoxy-based and linseed oil-based coatings if this ratio amounts to 4:2 [16, 17].

3.3 Methods for the Preparation of Ferrites

3.3.1 Ceramic Method

The most common way of preparing ferrite pigments is so-called “ceramic” technique, utilizing the high-temperature solid-phase reaction proceeding upon calcination of a mixture of dispersed initial components, usually iron oxides and compounds of salt-forming metal [4]. As a rule, carbonates are used as a second reactant since their thermal decomposition provides the corresponding metal oxides possessing the increased chemical activity. Moreover, the usage of carbonates allows avoiding the contamination of a final product, as, for example, in the case of chlorides or nitrates application.

Reactions proceeding at the preparation of several widely used single- and double-cation ferrite pigments by the “ceramic” technique are considered in Ref. [18].

As was already mentioned above, one of the most important properties of ferrites contributing to their protective effect is the basic pH of aqueous ferrite extracts typical for commonly used ferrites like calcium, magnesium, and zinc ferrite. Thus, to achieve the pH level essential for the efficient corrosion protection, ferrite should contain a portion of water-soluble ingredients providing upon their dissolution appropriate basicity of the surrounding medium. On the other hand, the amount of water-soluble substances should not exceed a certain limits, above which the barrier properties of the coating with embedded ferrites can be deteriorated. Table 3.2 correlates these technical parameters (content of water-soluble substances and pH of the corresponding aqueous extract) of some ferrite compounds with the corrosion protection performance of coatings containing these ferrites [4].

Table 3.1 High-temperature solid-phase reactions proceeding upon synthesis of several conventional single- and double-cation ferrites (after Ref. [18]).

Reaction	**Temperature**
Synthesis of zinc ferrite	
Stage 1: $2FeO(OH) + Fe_2O_3 \rightarrow H_2O$	320–400 °C
Stage 2: $Fe_2O_3 + ZnO \rightarrow ZnFe_2O_4$	700–900 °C
Totally: $FeO(OH) + ZnO \rightarrow ZnFe_2O_4 + H_2O$	
Synthesis of magnesium ferrite	
Stage 1: $2FeO(OH) \rightarrow Fe_2O_3 + H_2O$	320–400 °C
Stage 2: $MgCO_3 \rightarrow MgO + CO_2$	800–900 °C
Stage 3: $MgO + Fe_2O_3 \rightarrow MgFe_2O_4$	950–1050 °C
Totally: $2FeO(OH) + MgCO_3 \rightarrow MgFe_2O_4 + CO_2 + H_2O$	

Synthesis of double-cation ferrite $Ca_{0.2}Zn_{0.8}Fe_2O_4$	
Stage 1: $2FeO(OH) \rightarrow Fe_2O_3 + H_2O$	320–400 °C
Stage 2: $CaCO_3 \rightarrow CaO + CO_2$	900–920 °C
Stage 3: $0.2CaO + 0.8ZnO + Fe_2O_3 \rightarrow Ca_{0.2}Zn_{0.8}Fe_2O_4$	950–1050 °C
Totally: $2FeO(OH) + 0.8ZnO + 0.2CaCO_3 \rightarrow Ca_{02}Zn_{08}Fe_2O_4 + H_2O + 0.2\ CO_2$	

Table 3.2 Interrelation between chemico-technical characteristics and anticorrosive efficiency for some ferrite pigments. Adopted from Ref. [4].

Ferrite pigment	pH of the aqueous extract	Content of water-soluble substances, wt.%	Corrosion damage of substrate after 800 h of salt spray test (ASTM D 7654-92), %	
			Alkyd coating	Acrylate coating
$ZnFe_2O_4$	10.7	0.1001	0.1	3
$Mg_{0.2}Zn_{0.8}Fe_2O_4$	10.4	0.1256	0.03	1
$Mg\ Fe_2O_4$	10.0	0.1193	0.3	10
$Ca_{0.2}Mg_{0.8}Fe_2O_4$	10.6	0.1392	0.3	10
$CaFe_2O_4$	10.3	0.1819	1	16
$Ca_{0.2}Zn_{0.8}Fe_2O_4$	10.3	0.2016	3	10

Corrosion protection performance of new magnesium ferrite pigments MF_1, MF_2, and MF_4 synthesized at molar ratios $MgO:Fe_2O_3$ of 1:1, 2:1, and 4:1, respectively, was compared [15, 19] with the performance of widely used low-toxic zinc–aluminum polyphosphate hydrate (ZP) and commercial zinc ferrite ZF. Two types of water-base film-forming systems: short-oil acryl-modified alkyd resin and cold-curing epoxy resin with the concentrations of anticorrosive pigments 15 and 25 vol.% with respect to the total pigment content were studied. Titanium dioxide, Mg–Al–silicate and yellow iron oxide were utilized as additional pigment components in the case of an epoxy coating, whereas for the acryl-modified alkyd coating ferric oxide, zinc oxide, talc, and silica were used for this purpose. Relation of the pigment volume concentration to its critical volume concentration (PVC/CPVC ratio) was kept constant at 0.5 for both investigated coating formulations.

The cool-rolled mild steel panels were coated by both types of coatings yielding finally the uniform layers with a dry thickness of 20 ± 5 μm. Then, the coated panels were subjected to a series of corrosion tests. In particular, the corresponding test results after 672 h of condensed water test are given in Table 3.3.

Table 3.3 Degrees of rusting after 672 h of condensed water test according to ASTM D4585-92. The scale for rust: 10 = no rusting or less than 0.01% of surface rusted. Adopted from Ref. [15].

Pigment	Content in a coating, vol%	Epoxy coatings	Acryl-modified alkyd coatings
ZP	15	7	9
	25	6	
ZF	15	8	9
	25	7	
MF_1	15	8	9
	25	7	
MF_2	15	6	9
	25	4	
MF_4	15	8	9
	25	5	

Enhanced corrosion protection performance observed in Ref. [15] for alkyd coatings could be explained by reaction between magnesium ferrite pigments and the acidic binders resulting in the formation of saponification products with subsequent passivation of the substrate. Another interesting phenomenon reported in this work is the finding (see Table 3.3) that the lower content of magnesium ferrite pigment in the formulations with a neutral binder such as an epoxy resins lead to the higher efficiency of corrosion protection. Inverse proportionality between the anticorrosive effect of the magnesium ferrite and its concentration in coatings was recently confirmed also by Abd El-Ghaffar *et al*. [20].

In order to impart to ferrites in addition to their anticorrosive effect also ability to improve the barrier properties of coatings, the method for the synthesis of platelet-shaped ferrite pigments denoted as “micaceous zinc ferrite” was developed [21]. The proposed technique is based on the oxidative thermal treatment of molten initial salts without washing out the product to be prepared [21].

The shape of particles of different iron oxides (hematite, goethite, magnetite, and specularite) employed for the synthesis of zinc ferrite in “ceramic” way can affect the shape of the product particles [22]. The latter being combined with various coating formulations – solvent-based epoxy ester, water-based epoxy, and water-based styrene-acrylic – determine in turn the protective properties of corresponding coatings. The best protective performances have been found for the following binder/ferrite pigment combinations: epoxy ester + needle-shaped zinc ferrite (prepared from goethite), epoxy + isomeric zinc ferrite (magnetite), and styrene-acrylic + platelet-shaped zinc ferrite (specularite).

3.3.2 Ceramic Method with Utilizing Industrial Wastes

In order to reduce the production costs of ferrites prepared by the ceramic technique and to solve simultaneously ecological problems related to the environmental pollutions, several attempts were made for using industrial wastes containing iron oxides as initial raw materials for ferrite synthesis [23–27].

In particular, a simple and economic method for the preparation of calcium ferrite was developed [23] on the basis of galvanic sludge obtained after chemical treatment of galvanic wastewater. Galvanic sludge was initially mixed with lime, then this mixture was dried and finally calcined at temperature ranging from 650 °C to 800 °C. Investigation of the protective performance of the

synthesized calcium ferrite was carried out by electrochemical methods in the aqueous NaCl medium containing its extract. The obtained results showed its superior corrosion protection ability over such toxic pigments as lead silicochromate or strontium chromate giving the possibility to replace them by calcium ferrite in water-borne primers for electrophoretic applications.

Other way for the synthesis of calcium ferrite utilizes as initial raw material the waste of foundry – aspiration dust, consisting predominantly of iron oxides [24, 25]. Second main component used in this version of "ceramic" technique is calcium hydroxide formed as a by-product of the acetylene production from calcium carbide. It was established that the maximum anticorrosive efficiency demonstrates pigment obtained at a molar ratio in the initial mixture Fe:Ca = 1:0.4 and calcination temperature and duration of calcination of 850 °C and 4.5 h, respectively.

Even easier the mixture of magnesium ferrite and widely used conventional filler of various anticorrosive paints and varnishes, calcium carbonate, can be obtained by the calcinations of the aspiration dust and cheap natural mineral dolomite which is a double carbonate of calcium and magnesium: $CaMg(CO_3)_2$ [26, 27]. In this case, the synthesis of ferrite pigment proceeds at a temperature of 630 °C and lasts for 4.5 h.

Tests of the corrosion resistance clearly demonstrated (Figure 3.5) that alkyd coating containing the ferrite pigment described above has in the salt spray chamber the same stability as coatings with embedded toxic pigment zinc tetraoxychromate (zinc yellow).

Figure 3.5 Panels of cold-rolled steel coated with alkyd primers containing magnesium ferrite pigment (left) and zinc yellow (right) after 240 h neutral salt spray (NSS) test.



Another convincing example of high corrosion protection efficiency of ferrites is given below in the paragraph 4 devoted to advanced forms of ferrite pigments.

3.3.3 Other Methods of Ferrites Preparation

Attempts to decrease the calcination temperature of the initial reactants at the syntheses of ferrites as well as to reduce the size of resulting ferrite particles induce the dynamic development of other (non-ceramic) techniques of their preparation [28–36].

The mechanochemical approach was applied for the synthesis of zinc ferrite [28] using the wet-

milling of metallic iron and zinc micropowders in the distilled water. After 22 h at 350 rpm in a planetary ball mill, the precursor powder was obtained. This precursor was then calcined at 700 °C at ambient conditions in a porcelain crucible for 1 h and milled again for 2–20 h. Finally, the nanopowder of zinc ferrite with an average particle size from 38.2 to 19.4 nm (for 2 and 20 h, respectively) was obtained.

So-called co-precipitation method is also frequently used for the synthesis of nanodimensional ferrite particles [29–31]. Typically, the stoichiometric amounts of aqueous solutions of iron salt and salt(s) of ferrite-forming metal were mixed together and then precipitated out by the increase of pH upon gradual addition of aqueous NaOH solution. The following annealing of the precipitate at the precisely controlled temperature enabled the size control of resulting $MgFe_2O_4$ nanoparticles ranging between 6 and 18 nm [29]. Sufficiently larger particles of strontium hexaferrite $SrFe_{12}O_{19}$ with the sizes between 30 and 80 nm were obtained by means co-precipitation method from citrate precursor [30]. Initially, salts of strontium and iron serving as sources of these elements were transformed to the mixture of the corresponding citrates with the Fe:Sr ratio, which was close to the required molecular formula of $SrFe_{12}O_{19}$. The latter was dehydrated and water-free precursors were annealed at 550 °C to form the crystalline strontium hexaferrite $SrFe_{12}O_{19}$. The final particle size was established at the further high temperature treatment at 800 °C showing its gradually decrease from 55 to 26 nm upon decreasing Fe:Sr ratio. In similar manner, magnesium and calcium ferrites were synthesized by co-precipitation method starting from the corresponding oxalates as raw materials [31]. Upon following heat treatment, oxalate mixtures decompose to oxides and then form calcium or magnesium ferrite pigments.

Novel promising sol–gel method was employed for the preparation of magnesium ferrite pigments with very fine particles [32]. For this purpose, either magnesium and iron oxides or magnesium and iron oxalates are homogeneously distributed in the concentrated acrylic acid solution (sol stage). Then, the gelation stage at 50 °C and action of ammonium persulfate as initiator was occurred. Finally, the dried gel was annealed at different temperatures between 400 °C and 1000 °C yielding polydisperse magnesium ferrite particles with the average size from 0.5 to 5 μm and from 0.1 to 1 μm for oxide and oxalate pathways, respectively. In the same work, magnesium and iron chlorides were utilized as starting materials but for the gelation in the urea formaldehyde resin. In this case, the resulting magnesium ferrite particles showed a bimodal size distribution with the maxima at 0.5 and 5 μm. Interesting modification of sol–gel route for the synthesis of nanodimensional nickel ferrite particles with sucrose as a chelating agent was recently developed by Souza *et al.* [33]. Herein, the aqueous solutions of sucrose, nickel and iron (III) nitrates were mixed together keeping the stoichiometric ratio Ni:Fe = 1:2 and then homogenized by the heating of the mixture to 60 °C. After drying, the resulting gel was annealed in the air at 300 °C, 600 °C, and 750 °C and annealing rates of 5, 10, und 12.5 °C/min giving the fine nanoparticles of nickel ferrite. Noteworthy that the particle size was in all cases equal (11 nm) and was influenced neither by annealing temperature nor by annealing rates.

A low-temperature synthesis of nanoscale zinc and nickel ferrites with narrow granulometric composition was proposed in Ref. [34]. This technique combines the advantages of the citrate precursor method where citric acid is used as chelating agent and glycine–nitrate type of combustion technique. Freshly prepared zinc nitrate (from nitric acid and zinc powder), nickel nitrate, iron (III) nitrate, citric acid, and glycine were mixed together as aqueous solutions. Amounts of citric acid and glycine were taken, which enable the complexation of cations and complete combustion of nitrates,

2.67 and 4.45 moles per one mole of the future ferrite, respectively. The resultant homogeneous solution was firstly boiled for 1.5 h and then dried forming viscous gel which was further dehydrated for 6–10 h at 110 °C. Controlled autocatalytic combustion of this gel was carried out at a low temperature of approximately 175 °C and was accompanied by strong gas emission. Finely, very small $Ni_{0.5}$ $Zn_{0.5}Fe_2O_4$ particles with the average size of 2.5 nm and narrow size distribution were obtained. Similar technique was employed to prepare zinc ferrite, nickel ferrite, and mixed zinc–nickel ferrite with general formula $(Zn_{1-x}Ni_x)Fe_2O_4$ (with x = 0, 0.5 and 1) [35]. The powders of the corresponding metal nitrates, zinc, nickel and iron (III), were mixed with urea as fuel. This mixture was then subjected to heating up to 480 °C until it self-ignited, producing nanodimensional ferrite particles. The combustion temperatures for the single-cation ferrites were lower than for the mixed double-cation zinc–nickel ferrite, whereas the particle size decreased continuously from zinc to nickel ferrite ranging between 29 and 11 nm.

Another novel method of synthesis of ceramic oxides and, inter alia, ferrites is the microwave-assisted hydrothermal route [36]. Using advantages of both microwave heating and hydrothermal treatment, nanodimensional magnesium ferrite, was synthesized under mild microwave hydrothermal (MH) conditions. To do this, aqueous solutions of the magnesium and iron (III) nitrates, in the stoichiometric 1:2 molar ratio, were placed in a reaction vessel, and the pH value in this medium was attained by KOH to be above 10. The MH reaction was performed under mild conditions of temperature 150 °C, pressure 344.7 kPa and reaction time of 25 min. After the finishing of treatment, the slurry-like product was several times washed with distilled water and dried overnight at 80 °C. The resulting $MgFe_2O_4$ particles were narrow distributed with an average size around 2.3 nm according to the transmission electron microscopy (TEM) data.

3.4 Novel Types of Ferrite Pigments

A new stage in the development of advanced types of ferrite pigments is related to the preparation of pigment particles where ferrite shell is formed around a particle made of economical filler or extender materials serving as a core of the resulting ferrite pigment particle. This structure of novel ferrite pigments not only allows an essential decrease of ferrite production costs but also enables, in some particular cases, the synergistic combination of anticorrosive effect of ferrites with the advantages of core material. The preparation of this novel type of ferrite pigments called also “kernel” pigments is, as a rule, based on the combustion process.

Amorphous silica nanoflakes with the surface inclusion of zinc–nickel double-cation ferrite were obtained by novel sol–gel auto-combustion method [37, 38]. An initial nitrate–citrate–silica gel was prepared on the basis of aqueous solutions of the corresponding metal nitrates and citric acid by addition of the nanodimensional silica powder (Aerosil 200; <100 nm). After thorough mixing of this composition which ensures the homogeneous distribution of components, the gel was dried under vacuum conditions at 100 °C to remove any traces of water. Being ignited, this dry gel burnt in a self-propagating combustion manner until yielding a loose powder composed of NiZn ferrite dispersed in silica powder. The effect of pH on the size of resulting $Ni_{0.5}Zn_{0.5}Fe_2O_4$ particles was observed: The increase in pH from 3 to 7 led to the particle growth from 13 to 25 nm. Increasing the pH is a consequence of a citrate/nitrate ratio decrease, which resulted in increase in decomposition rate and particle size.

Wastes of optical industry were utilized for the preparation of core–shell pigments [39] with the core made of glass microgranules and ferrite shell. Deposition of nickel and copper ferrites on the surface of microgranules led to the highly porous shell structure with enhanced sorption properties and high adhesion ability at interaction with the paint and varnish binders.

Core–shell ferrite pigments prepared by depositing a surface layer of ferrite on a bulk of cheap extender pigment kaolin were described in Ref. [40]. Initially, kaolinite (calcined kaolin) particles were impregnated in nitrate solutions of Zn, Mg, Ca, and Fe that were combined to synthesize single, double, and triple ferrites. To achieve the homogeneous distribution of the ferrite precursors on kaolin surface, these mixtures were stirred for 1 h, then dried at 300 °C and ground. After calcination at 1000 °C, kaolin particles with ferrites chemically bonded to their surface with a general metal ratio 2X:6Fe were obtained.

The obtained core-shell ferrite/kaolin pigments were incorporated in the medium oil alkyd resin paint formulations in amounts corresponding to 50 and 75 wt.% of the total pigment content. Cold-rolled steel specimens were then coated by these formulations, dried, cross-scribed and subjected to an immersion test in a 3.5 wt.% salt solution for 28 days. After this time, such parameters related to the corrosion development as thread-like filament propagation under the coating (filiform); degree of rusting and degree of blistering were evaluated.

Corrosion protection properties of all coatings containing the new core–shell ferrite pigments showed much better inhibition properties with respect to paint films containing only kaolin. Figure 3.6 demonstrates, for example, a comparative photograph of specimens coated with standard medium oil alkyd resin containing only kaolin versus different core–shell ferrite pigments with always the same concentration of kaolin or ferrite of 75 wt.% related to the total pigment content.

Figure 3.6 Corrosion development after 28 days of immersion test in 3.5 wt.% NaCl solution: upper row – standard medium oil alkyd resin with kaolin pigment; middle row, from left to right – with Zn ferrite + kaolin, with Mg ferrite + kaolin; with Ca ferrite + kaolin; lower row, from left to right – with Zn-Mg ferrite + kaolin; with Mg-Ca ferrite + kaolin; with Zn-Ca ferrite + kaolin; with Zn-Mg-Ca ferrite + kaolin. Content of ferrite was always 75 wt.% of total pigment amount. Adopted from Ref. [40].



One can easily see the superior corrosion protection properties of the coatings with ferrites in contrast to the standard. Moreover, qualitative appearance of coatings with double- and triple-cation core–shell ferrite pigments reveals the best anticorrosive efficiency. Interestingly that the same coatings containing common ferrite pigments showed lower corrosion protection performance than novel core–shell ferrite pigments confirming the synergistic protective effect of both ferrite shell and kaolin core of latter.

Anticorrosion efficiency of lamellar single- and double-cation ferrites of the Zn, Ca, and Mg and core–shell ferrites of the same shell composition with core consisted of the nonisometric muscovite particles was compared for the alkyd coatings applied onto steel panels [41]. The coated panels containing 10 vol.% of ferrite were subjected to salt spray and water condensation tests, for 600 and 800 h, respectively. However, the lamellar ferrites showed, in general, better corrosion protection efficiency than the core–shell ferrites, double-cation ferrite pigments with the composition $Mg_{0.2}Zn_{0.8}Fe_2O_4$ – of both the lamellar and core–shell type – were most effective against corrosion.

Core–shell ferrite pigments with the inverse structure, i.e. with ferrite core enveloped in an organic shell made of polyaniline (PANI) were recently synthesized [42] and compared with the same unmodified ferrites for the protection efficiency. For this purpose, zinc ferrite, nickel ferrite, and double-cation zinc–nickel ferrite were incorporated both in the unmodified state and PANI-coated state in a conventional acrylic primer, which was then used for the coating of carbon steel panels by two layer coating system with the epoxy topcoat. For the evaluation of anticorrosive performance of these coatings they underwent salt spray test for 400 and 800 h. The final results revealed that the especially strong protective ability possess PANI-modified ferrites even compared with pristine ferrites or coatings doped only with PANI indicating clearly the presence of a synergistic effect of both components on the corrosion protection performance. The best protection efficiency was showed by coatings containing PANI-modified zinc–nickel ferrites where only very little traces of

corrosion were observed even after 800 hours of testing.

3.5 Ferrite-Based Multifunctional Coatings

It is necessary to stress here that ferrites have along with the properties enabling their efficient use in the corrosion protection also several other valuable characteristics imparting to these pigments a real polyfunctionality. For example, zinc–nickel ferrites with general formula $Ni_xZn_{(1-x)}Fe_2O_4$, (where x = 0, 0.2, 0.4, 0.6, 0.8, and 1.0) showed not only excellent anticorrosive efficiency due to inhibition of the cathodic reaction by sediment deposition in an alkaline medium caused by pigments and reaction but can also function as a microwave radiation shield [12]. A significant reduction of electromagnetic radiation was experimentally established for 2-mm-thick epoxy coatings containing 10 vol.% NiZn ferrites. The highest microwaves reflection loss was found in the frequency range from 10 to 12 GHz and was amounted to 8–16 dB. Ferrites, due their highly stable spinel structure, maintain their physicochemical characteristics even upon long-term exposition to elevated temperatures in the range from 50 °C to 700 °C [43]. This excellent resistance of ferrites against influence of high temperatures together with their anticorrosive properties makes them very promising materials for the heat-resistant corrosion protection coatings. Anticorrosive organic coatings aimed at the application in temperature range from 200 °C to 500 °C were prepared [43] on the basis of a methyl phenyl silicone resin binder and addition of 10 vol.% of various single- and double-cation ferrites. The coated samples were initially subjected to 10 h thermal shock (200–500 °C) and then underwent the accelerated corrosion tests in a condensation chamber with condensing SO_2-containing water vapor at 38 ± 2 °C for 300 h. Outstandingly better results for the corrosion protection performance after heat treatments were ascertained for ferrite pigments which were superior even against zinc chromate. Among ferrites, the highest anticorrosion efficiency was shown by the double-cation pigments containing zinc and magnesium.

The core–shell ferrite pigment with the scaly form of particles made of synthetic mica cores and zinc ferrite $ZnFe_2O_4$ shells was used as a pearlescent pigment with an enhanced environmental and weathering stability [44]. The lamellar shape of these core–shell ferrite particles not only enabled very stable optical properties (no changes in optical appearance) of coatings but also contributed to the additional improvement its barrier properties allowing therefore a two-fold effect on their corrosion protection performance.

3.6 Conclusion

Ferrites as quite rare simultaneously highly efficient and low-toxic anticorrosive pigments have sufficient and yet not completely exhausted applicative potential. Most promising current trends in the development of ferrites as pigments aimed at corrosion protection are synthesis of ferrites with novel more efficient combinations of metal cations (multi-cation ferrites) and preparation of core–shell ferrite pigments with various nature and shapes of core particles. Moreover, some other unique properties of ferrites such as microwave absorbability, high thermal and light stability, etc. enable on their basis the development of new multifunctional protective coatings.

Acknowledgement

D. Grigoriev acknowledges the financial support from the project 03 EFCBB028 “SigmA” in the framework of “EXIST Transfer of Research” program of the Federal Ministry of Economics and Energy (BMWi), Germany.

References

1. J. Sinko, *Prog. Organic Coatings,* Vol. 42, pp. 267–282, 2001.

2. M.W. Kendig and R.G. Buchheit, *Corrosion,* Vol. 59, pp. 379–400, 2003.

3. Directive 2000/53/EC of the European Parliament and of the council of 18 September 2000 on end-of life vehicles, *Official J. Eur. Comm.,* Vol. L269, pp. 34–42, 2000; Accessible online at http://eur-lex.europa.eu/resource.html?uri=cellar:02fa83cf-bf28-4afc-8f9f-eb201bd61813.0005.02/DOC_1&format=PDF, last successful access on 31st May 2015.

4. A. Kalendová and J. Brodinova, *Anti-Corrosion Methods and Materials,* Vol. 50, pp. 352–363, 2003.

5. A. Kalendová, J. Šňupártek, and P. Kalenda, *Dyes and Pigments,* Vol. 30, pp. 129–140, 1996.

6. A. Kalendová, D. Veselý, and P. Kalenda, *Pigment & Resin technology,* Vol. 35, pp. 83–94, 2006.

7. M. Svoboda, Properties of zinc and calcium ferrites as anticorrosion pigments, *Protection of Metals,* Vol. 24, pp. 31–33, 1988.

8. D. Veselý and M. Ulbrich, *Transfer inovácií,* Vol. 20, pp. 60–65, 2011.

9. A. Kalendová, *Progress in organic coatings,* Vol. 38, pp. 199–206, 2000.

10. M.R. Ziganshina, Anticorrosive properties of synthetic manganese based pigments and development of primers containing these, PhD Thesis, Kazan State Technological University, Kazan, Russia, 2002 (in Russian).

11. H.H. Uhlig and R.W. Revie, *Corrosion and corrosion control: An introduction to corrosion science and engineering,* 4th Ed., Hoboken New Jersey, John Wiley & Sons, 2008.

12. A. Miszczyk and K. Darowicki, *Anti-Corrosion Methods and Materials,* Vol. 58, pp. 13–21, 2011.

13. M. Svoboda, *Farbe und Lack,* Vol. 96, pp. 506–508, 1980 (in German).

14. A. Miszczyk and J. Bordzitowski, *Ochr. Koroz.,* Vol. 33, pp. 213–215, 1990 (in Polish).

15. H.S. Emira and F.F. Abdel-Mohsen, *Pigment & Resin technology,* Vol. 32, pp. 259–265, 2003.

16. I. Sekine, and T. Kato, *Journal of the Oil and Colour Chemist’s Association,* Vol. 70, pp. 256–267, 1987.

17. I. Sekine, T. Kato, and H. Suda, Corrosion Protective Property of Ferrite Paint Films, *Corrosion Engineering (Boshoku Gijutsu),* Vol. 36, pp. 487–491, 1987.

18. A. Kalendová and D. Veselý, *Anti-Corrosion Methods and Materials,* Vol. 54, pp. 3–15, 2007.

19. H.S. Emira, F.F. Abdel-Mohsen, S.B. Hana, T. Schauer, and H. Greisiger, *European Coatings Journal,* Vol. 11, pp. 22–24, 2002.

20. M.A. Abd El-Ghaffar, N.M. Ahmed, and E.A. Youssef, *Journal of Coatings Technology Research,* Vol. 7, pp. 703–713, 2010.

21. H.S. Emira, *Pigment and Resin Technology,* Vol. 34, pp. 132–138, 2005.

22. M. Ulbrich and A. Kalendová, *Physics Procedia*, Vol. 44, pp. 247–255, 2013.

23. O.V. Ladygina, V.M. Makarov, E.A. Indejkin, and N.A. Tarhunov, *Lakokrasochnye materialy i ih primenenie*, Vol. 40, pp. 26–28, 32, 2000 (in Russian).

24. V.I. Usmanov, A.V. Vahin, A.P. Svetlakov, and S.N. Stepin, *Lakokrasochnye materialy i ih primenenie*, Vol. 48, pp. 40–42, 2008 (in Russian).

25. V.I. Usmanov, A.V. Vahin, A.P. Svetlakov, and S.N. Stepin, Method of Preparing anticorrosion pigment, Russian Patent 2391365, assigned to KNRTU, June 6, 2008.

26. M.I. Safiullin and S.N. Stepin, *Himicheskaja tehnologija*, Vol. 13, pp. 385–389, 2012.

27. S.N. Stepin, I.R. Sagbiev, A.H. Gatijatullin, A.V. Vahin, and M.I. Safiullin, Method of Producing anticorrosion pigment, Russian Patent 2505571, assigned to "NPP "PigBi", July 20, 2012.

28. O. Sadan, K. Burak, C.M. Mutlu, and F. Tezer, *Mater. Sci. and Eng.* B., Vol. 121, pp. 278–281, 2005.

29. Q. Chen and Z.J. Zhang, *J. Appl. Phys. Lett.*, Vol. 73, pp. 3156, 1998.

30. A. Vijayalakshimi and N.S. Gajbhiye, *J. Appl. Phys.*, Vol. 83, pp. 400–406, 1998.

31. S.B. Hana, F.F. Abdel-Mohsen, and H.S. Emira, *InterCeram: International Ceramic Review*, Vol. 54, pp. 106–110, 2005.

32. F.F. Abdel-Mohsen, and H.S. Emira, *Pigment & Resin Technology*, Vol. 34, pp. 312–320, 2005.

33. E.A. Souza, J.G.S. Duque, L. Kubota, and C.T. Meneses, *J. Phys. and Chem. Solids*, Vol. 68, pp. 594–599, 2007.

34. V. Seema, S.D. Pradhan, P. Renu, S.R. Sainkar, and P.A. Joy, *J. Amer. Ceram. Soc.*, Vol. 88, pp. 2597–2599. 2005.

35. A.C.F.M. Costa, A.M.D. Leite, H.S. Ferreira, R.H.G.A. Kiminami, S. Cava, and L. Gama L, *J. Eur. Ceram. Soc.*, Vol. 28, pp. 2033–2037, 2008.

36. S. Verma, P.A. Joy, Y.B. Khollam, H.S. Potdar, and S.B. Deshpande, *Mater. Lett.*, Vol. 58, pp. 1092–1095, 2004.

37. K.H. Wu, C.H. Yu, Y.C. Chang, and D.N. Horng, *J. Solid State Chem.*, Vol. 177, pp. 4119–4125, 2004.

38. K.H. Wu, Y.C. Chang, G.P. Wang, *J. Magn. Magn. Mater.*, Vol. 269, pp. 150–155, 2004.

39. E.V. Shinkareva, V.D. Koshevar, Yu.G. Zonov, *Glass and Ceramics*, Vol. 65, pp. 52–55, 2008.

40. N.M. Ahmed, and M.M. Selim, *Pigment and Resin Technology*, Vol. 39, pp. 101–111, 2010.

41. D. Veselý, P. Němec, and A. Kalendová, *Phys. Status Solidi C8.*, Vol. 8, pp. 2665–2668, 2011.

42. V. Mittal, A.U. Chaudhry, and M.I. Khan, *J. Dispersion Sci. Technol.*, Vol. 33, pp. 1452–1457, 2012.

43. A. Kalendová, *Pigment & Resin Technology*, Vol. 29, pp. 164–172, 2000.

44. P. Cao, C. Lavallee, S. Jones, and D. Cacace, Synthetic mica based pearlescent pigments containing ferrites, US Patent 7470318, assigned to BASF Corporation, December 30, 2008.

Chapter 4

Application of Edible Coatings on Fruits and Vegetables

R.K. Dhall

Department of Vegetable Science, Punjab Agricultural University, Ludhiana, Punjab, India

**Corresponding author*: rajinderkumar@pau.edu

Abstract

Fruits and vegetables are susceptible to spoilage during the postharvest life due to rich nutrient substance, high water content, its own metabolism and microbial infection. The preservation of fruits and vegetables plays a significant role in maintaining their quality, extending the supply period and improving their economic benefits. Edible coatings can form a barrier between the fruit and surroundings, and this semi-permeable barrier has the capacity to modify fruit internal atmospheres, prevent water immigration, reduce mechanical injury to fruit during the transport and storage process as well as lower the risks of microbial contamination. As an effective preservation technology, the properties of edible coatings and films along with its application on fresh fruits and vegetables have been widely studied. In this chapter, in the first part I critically reviewed the effect of application of hydrocolloids, lipids and composite coatings on maintaining the quality of fruits and vegetables, after that I have a focus on the effect of second-generation coating material (bioactive compounds) on human health, especially due to the application of new microencapsulation or nanoencapsulation techniques. Moreover, I also tried to discuss the problem associated with edible coatings and films and their regulatory status and food safety issues.

Keywords: Antimicrobial, antioxidant, edible coatings, food safety, nanotechnology, nutraceutical

4.1 Introduction

Fruits and vegetables remain as living tissue until they are consumed fresh, cooked or processed. As soon as the fruit or vegetable is harvested, there is increase in the respiration rate of these living tissues, resulting in metabolic loss which ultimately takes the fruit or vegetable to a gradual maturation and eventual senescence. In fresh-cut fruits and vegetables, the wounding of tissues leads to texture breakdown, development of off-flavour and brown discoloration on the cut surface. Controlled respiration of these living tissues would improve storability and extend the shelf life of fresh and fresh-cut produce. Several techniques like controlled atmosphere (CA) storage and modified atmosphere packaging (MAP) have been used in fruits and vegetables to minimize quality changes and quantity losses during storage. Edible coatings can provide an alternative to CA storage

and MAP as these coatings modifies and control the internal atmosphere of the individual fruit or vegetable. Edible coatings may extend the shelf life of fresh and fresh-cut produce by regulating the transfer of moisture, oxygen and carbon dioxide; by retaining the aroma and taste compounds in a food system, and by improving the mechanical handling property of foodstuff [1, 2]. Edible coatings may also be used to improve structural integrity of frozen fruits and vegetables and preventing moisture absorption and oxidation of freeze-dried fruits or vegetables [3–5]. In addition, edible coatings can carry active ingredients such as anti-browning agents, colorants, antioxidants, antimicrobials, nutrients, flavours and spices to further enhance food stability, quality, functionality and safety [6–8]. Besides, edible coatings may replace plastic packaging to some extent by natural and biodegradable substances and their use could lead to reduction in overall packaging requirements and waste disposal problems.

Fruits or vegetables are usually coated by dipping in or by spraying with a range of edible materials, so that a semi-permeable membrane is formed on fruit surface [9]. The use of edible coating on fruits and vegetables is conditioned by the fulfilment of various characteristics such as cost, availability, functional attributes, mechanical properties (flexibility, tension), optical properties (brightness and opacity), the barrier effect against flow of gases, structural resistance to water and microorganisms and sensory acceptability. These characteristics are influenced by parameters such as the kind of material implemented as structural matrix (composition, molecular weight), the conditions under which coatings are preformed (type of solvent, pH, components concentration and temperature) and the type and concentration of additives (plasticizers, antimicrobials, antioxidants or emulsifiers) [10, 11].

4.2 Coatings versus Films

An edible coating is a thin layer of edible material formed as a coating on the surface of food product, while an edible film is a preformed stand-alone thin layer of edible material, which once formed can be placed on or between food components [12]. The main difference between them is that the edible coating are applied in liquid form on the food, usually by immersing the product in a solution-generating substance formed by the structural matrix (carbohydrate, protein, lipid or multi-component mixture), and edible film are first moulded as solid sheets, which are then applied as a wrapping on the food product. The main use of edible films is to test the structures of the material used for its barrier, mechanical, solubility and other properties. In this chapter, I use terminology edible coatings or edible films, this should be treated as same.

4.3 Structural Matrix: Hydrocolloids and Lipids

There is a very wide range of compounds that can be used in the formulation of edible coatings or films and their choice depends mainly on the target application. According to their components, edible films and coatings can be divided into three categories: hydrocolloids, lipids and composites. Hydrocolloids include proteins and polysaccharides. Lipids include waxes, resins, triglycerides (natural lipids) and fatty acids. Composites contain both hydrocolloid and lipids [13]. Several other

compounds such as plasticizers and emulsifiers can be added to edible coatings when lipids and hydrocolloids are combined. The purpose of adding plasticizers in film forming material is to decrease the intermolecular forces between polymer chains, which results in greater film flexibility, elongation, toughness and permeability. Plasticizers used for edible coatings include glycerol, sorbitol, sucrose, propylene glycol, polyethylene glycol, fatty acids and monoglycerides. Emulsifiers or surfactants are surface-active agents that are used to improve the stability of the emulsion, ensure good surface wetting, spreading, and adhesion of the coating to the food surface. Common emulsifiers used for coatings are fatty acids, ethylene glycol monostearate, glycerol monostearate, esters of fatty acids, lecithin, sucrose ester and sorbitan monostearate or polysorbates (tweens). In addition, food additives include antioxidants, colorants, flavouring agents and antimicrobial compounds which can also be added to edible coatings [14, 15].

4.4 Application of Hydrocolloids Coatings

Proteins and polysaccharides generally have a good barrier to oxygen at low relative humidity due to their tightly packed hydrogen-bonded network structure but have a poor moisture barrier due to their hydrophilic nature [16]. Therefore, hydrophobic compounds are generally added to make edible coatings. Proteins used to make edible coatings include corn zein, wheat gluten, soy protein, whey protein, casein, collagen/gelatin, pea protein, rice bran protein, cottonseed protein, peanut protein and keratin [3, 17]. Polysaccharides used in edible film formation include starch and starch derivatives, cellulose derivatives, alginate, carrageenan, pectin, pullulan, chitosan and various gums [17].

Zein-based coatings have been applied to fresh and dried fruits, often as a substitute for shellac coatings. Compared to shellac coatings, zein coatings are favourable for gloss and other quality characteristics on apples [18–20]. Zein coatings were able to maintain the firmness and colour of broccoli head [21]. The application of zein coating delayed colour change, weight loss and maintained firmness of tomato during storage [22, 23]. Carlin *et al.* [24] reported that zein coatings provide a continuous and stable coating with satisfactory sensory properties, and also reduce the growth *of Listeria monocytogenes* on cooked sweet corn. Caseinate and whey protein-based coatings have been applied on frozen peas and peanuts to provide a barrier to oxygen and moisture transfer for extending their shelf life [25]. Caseinate and whey protein isolate coatings were reported to delay the browning of apple and potato slices [26]. Lafortune *et al.* [27] reported that caseinate and whey protein coatings along with MAP protected carrots against dehydration and retained their firmness during storage. Soy protein coatings generally exhibit poor moisture resistance and water vapour barrier properties but were able to preserve freshness of apple slices [28] and to retard the senescence process of kiwifruit [29]. Eswaranandam *et al.* [30] applied soy protein coating containing malic or lactic acid on whole apple with the purpose to study its effect on the sensory quality of the fruit and observed that incorporation of organic acids to films did not adversely affect the sensory properties of coated apples after cold storage. The anti-microbial and anti-oxidant effects of protein based coatings are discussed in detail in sections 4.7.1 and 4.7.2 of this chapter.

Carboxy methyl cellulose (CMC) is by far the most important cellulose derivative for food applications [31]. Edible coatings made of CMC, methyl cellulose (MC), hydroxy propyl cellulose (HPC) and hydroxy propyl methyl cellulose (HPMC) have been applied to some fruits and vegetables for providing barriers to oxygen, oil or moisture transfer [32, 33] and for improving batter adhesion [34]. CMC is most used coatings which helped to maintain the original firmness and crispness of

apples, berries, peaches, celery, lettuce and carrots [35], preserved important flavour components of some fresh fruits and vegetables [36], and reduced oxygen uptake without increasing carbon dioxide level in the internal environment of coated apples and pears by simulating a CA environment [37–39]. Ribeiro *et al.* [40] studied the effect of polysaccharide-based edible coatings (starch, carrageenan and chitosan) on the shelf life of strawberry and observed minimum weight loss in strawberry by using carrageenan and chitosan-based edible coatings with added calcium chloride and lower microbial growth rate in strawberries coated with chitosan and calcium chloride. The anti-microbial and anti-oxidant effects of cellulose based coatings are discussed in detail in sections 4.7.1 and 4.7.2 of this chapter.

Chitosan, which is mainly obtained from de-acetylation of crustacean chitin, has been one of the most promising coating materials for fresh produce because of its excellent film-forming property, broad antimicrobial activity, and compatibility with other substances, such as vitamins, minerals, and antimicrobial agents [41–44]. Application of chitosan induces the production of plant defence enzymes such as chitinase. Chitosan-based coatings were reported to protect highly perishable fruits like strawberries, raspberries, mango, and grapes from fungal decay [45–49]. Reuck *et al.* [50] found that the combination of chitosan (1.0 g L^{-1}) + MAP was effective in preventing decay, browning and retaining the pericarp colour in the cultivar McLean's Red compared with single MAP. Shao *et al.* [51] revealed that apples (cv. Gala) fruits treated with heat [38 °C] + chitosan showed the lowest respiration rate, ethylene evolution, malondialdehyde and membrane leakage, and the highest firmness and consumer acceptance among the treatments. At the same time, this combined treatment could inhibit the loss of green colour, titratable acidity and weight loss compared with heat treatment alone. Chien *et al.* [45] reported the effectiveness of chitosan coating for extending shelf life and prolonging quality of sliced mango fruit. The application of chitosan coating delayed changes in contents of anthocyanin, flavonoid, and total phenolics, reduced weight loss and browning of litchi fruit and improved its storability [52]. Chitosan also reduced decay and improved appearance of carrots [53, 54]. The anti-microbial and anti-oxidant effects of chitosan based coatings are discussed in detail in sections 4.7.1 and 4.7.2 of this chapter.

Carrageenan, extracted from several red seaweeds, is a complex mixture of several polysaccharides, is another potential coating material for fruits and vegetables. Carrageenan-based coatings have been applied to fresh apples for reducing moisture loss, oxidation or disintegration of the apples [55]. Vina *et al.* [56] studies the effect of maize starch edible coating with glycerol (as a plasticizer) on Brussels sprouts. The buds were treated with the solution, stored in polystyrene trays and covered with polyvinyl chloride (PVC) film, preserving the quality parameters regarding different factors such as weight loss, firmness, surface colour of the food, commercial acceptability and nutritional quality.

4.5 Application of Lipid Coatings

Lipids due to their hydrophobic nature, are used in edible films coatings to provide a barrier to moisture. In addition, they are often used to provide gloss to food surfaces. However, lipids are not polymers, they form films or coatings with poor mechanical properties. Lipids used for the preparation of lipid-based edible films or coatings include neutral lipids, fatty acids, waxes (beeswax, candelilla wax, carnauba wax, rice bran wax) and resins (shellac, wood rosin). Most fatty acids derived from vegetable oils are considered GRAS (generally recognized as safety) and have been

suggested as substitutes for the petroleum-based mineral oils used in the preparation of edible coatings [57].

Waxes (carnauba wax, beeswax, paraffin wax and others) have been commercially used for coating fresh fruits and vegetables since the 1930s with the purpose to reduce moisture loss and surface abrasion during fruit handling [58], and controlling internal gas composition of the fruits [59]. In general, wax coatings are substantially more resistant to moisture transport than other lipid or non-lipid coatings [60, 61]. Wax coatings are commercially applied to citrus, apples, mature green tomatoes, rutabagas, cucumbers and other vegetables such as asparagus, carrots, radish, turnip, brinjal, knol khol, okra, parsnip, pepper, potato, sweet potato and squash, where high gloss and shine surface are desired [18, 19, 62–66]. McGuire and Hagenmaier [67] applied shellac coating to grapefruit and oranges over a CMC layer and observed that a shellac formulation at pH 9.0 with 5.2% ethanol was more toxic to the coliform bacteria *Enterobacter aerogenes* and *Escherichia coli* than a formulation at pH 7.25 with 12% ethanol.

4.6 Application of Composite Coatings

A composite coating may consist of lipids and hydrocolloids combined to form a bilayer or a stable emulsion. In bi-layer composite coatings, the lipid forms a second layer over the polysaccharide or protein layer. In emulsion composite coatings, the lipid is dispersed and entrapped in the supporting matrix of protein or polysaccharide [68, 69]. In some recent studies, the production of edible and biodegradable coatings by combining various polysaccharides, proteins and lipids is considered with the aim of taking advantage of the properties of each compound and the synergy between them. The mechanical and barrier properties of these films not only depend on the material used in the polymer matrix, but also on their compatibility [70]. The optimization of composition of edible coatings is in one of the most important steps to consider while film formation and it must be formulated according to the properties of the fruits and vegetables to which they have to be applied [11]. Thus, it is very important to characterize and test different coating solutions on fresh and fresh-cut produce, since both have different quality attributes to be maintained during the storage period [71]. Selecting a coating material with appropriate permeability for various gases is critical in modifying the internal environment of fresh produce for its preservation. In addition, storage temperature and relatively humidity is also critical in modifying the internal environment of fresh produce since coating permeability and produce respiration are affected by these parameters.

Composite coating formulation can be tailor made to suit to the needs of a specific commodity or farm produce. Recently, many researchers have extensively explored the development of composite films using lipid and HPMC, MC and lipid, MC and fatty acid, corn zein, MC and fatty acid, whey isolate and lipids, casein and lipids, gelatin and soluble starch, hydroxypropyl starch and gelatin, corn zein and corn starch, gelatin and fatty acid, soy protein isolate and gelatin, soy protein isolate and polylacetic acid [72–81].

Composite coatings with soy or zein protein with amylose ester or fatty acids provided an effective moisture barrier on carrot and fresh-cut apple slices [82]. Wheat gluten with lipid (beeswax, stearic acid and palmitic acid)-based bilayer coatings significantly retained firmness and reduced weight loss of fresh strawberries [83]. Chitosan–lauric acid composite coatings prevented fresh-cut apple slices from browning and water loss [84]. A casein-lipid emulsion coating formed a tight matrix that binds to the cut apple surfaces and protects apple slices from moisture loss and oxidative browning [85]. A

sodium caseinate/stearic acid emulsion coating reduced white blush and respiration rate of peeled carrots [86]. Calcium caseinate acetylated monoglyceride emulsion coating reduced water loss of apples, celery sticks, and zucchini as a result of increased water vapour resistance of the emulsion coatings [87–88]. HPMC–lipid composite coatings consisting of beeswax or shellac significantly reduced texture loss and internal breakdown of plums [89]. Composite coatings prepared from whey protein concentrate as the hydrophilic phase and beeswax or carnauba wax as the lipid phase exerted an anti-browning effect on fresh-cut apples [69, 89, 90]. Locust bean gum, shellac and beeswax coatings prolonged the storability of the cherries by reducing moisture loss [91]. An emulsion coating with CMC as the hydrophilic phase and paraffin wax, beeswax, or soybean oil as the hydrophobic phase also extended shelf life and reduced weight loss of apples, peaches and pears [92, 93].

Chitosan-based composite coatings significantly retarded colour development, reduced weight loss and respiration rate, maintained firmness and reduced titratable acidity of coated fruits (mango, banana, capsicum) compared to uncoated controls [94, 95]. Maqbool *et al*. [96] applied Arabic gum + chitosan edible coating on fresh banana fruits and observed that composite edible coating formed by 10% Arabic gum and 1% chitosan coating showed a synergistic behaviour that allowed maintaining sensory quality and microbiological parameters, without phytotoxic effects on bananas stored for 33 days. Strawberry fruits coated with 1% chitosan + 0.5% calcium gluconate maintain shelf life for one week at 10 °C and 70 ± 5% RH without any fungal decay and observed that addition of calcium to the chitosan solution increased the firmness and nutrients of the fruit [97]. Composite coating with 1% chitosan and 1% phytic acid could decrease the weight loss and malondialdehyde (MDA) content of fresh-cut lotus root, postpone browning, restrain the activities of peroxidase (POD), polyphenol oxidase (PPO) and phenylalanine ammonia-lyase (PAL), and maintain the content of vitamin C and polyphenol at relatively high level [98]. The combination of 1-MCP and chitosan coating could effectively extend the storage life and maintain the quality of Indian jujube fruit at room temperature storage [99]. Ozone water treatment (concentration of 4.2 mg m^{-3}) and a composite coating made of polyvinyl alcohol (1%), chitosan (1%), lithium chloride (0.5%), glacial acetic acid (2.5%) and sodium benzoate (0.05%) inhibits respiration, chlorophyll breakdown and PPO activity [100].

4.7 Addition of Active Compounds

Nowadays, edible coatings have different applications, and their use is expected to be expanded with the development of active coating compounds. These second generations of coating materials include chemicals, enzymes or microorganisms that prevent, for example, microbial growth or lipids oxidation in coated food products. In this sense essential oils, in combination with structural polymers, can be a promising source since different scientists showed the evidence of their effectiveness as antimicrobial and antioxidant compounds [101, 102]. Coatings of second generation may contain nutrients or other bioactive compounds that have a positive effect on health, especially due to the application of new microencapsulation or nanoencapsulation techniques. In this way, coating materials would act as carriers of these bioactive compounds to be transported to target sites such as the intestine without losing its activity, being within a matrix during its passage through the gastrointestinal tract [103].

4.7.1 Antimicrobial Coatings

Edible coatings with antimicrobial properties have evolved the concept of active packaging, being developed to reduce, inhibit or stop the growth of microorganisms on food surface [104]. As antimicrobial agents comprises of natural or synthetic compounds with known and minimal toxicological effects on mammals and the environment. Natural antimicrobial agents include chitosan, polypeptides and essential oils from fruits, vegetable and spices. It has been proved that essential oils of angelica, anise, carrot, cardamom, coriander, mint, vanillin, cinnamon, cloves, coriander, dill weed, fennel, garlic, nutmeg, oregano, parsley, rosemary, sage, or thymol have antimicrobial properties [105]. Synthetic antimicrobial agents are mostly organic acids which include acetic, benzoic, citric, fumaric, lactic, malic, propionic, sorbic, succinic, and tartaric acid. Potassium sorbate, sodium benzoate and benzoic acid are three organic acid salts more widely used as antimicrobial food additives. Additionally, hydrophobic compounds such as tea tree essential oil in HPMC-based films have also been used [106]. Antimicrobials used for the formulation of edible coatings must be classified as food-grade additives or compounds generally recognized as safe (GRAS) by the relevant regulations. In most fresh or fresh-cut products, microbial contamination is found maximum on their surface. Therefore in such cases, the incorporation of antimicrobial additives in edible films or coatings is very important as these additives can migrate selectively and gradually from the wrapping compounds to the surface of the food [107].

Starch-based coatings containing potassium sorbate were applied on the surface of fresh strawberries for reducing microbial growth and extending its storage life [108]. In addition, chitosan coatings containing potassium sorbate increased antifungal activity against the growth of *Cladosporium* and *Rhizopus* on fresh strawberries [49]. Lysozyme was incorporated into chitosan coatings for enhancing the antimicrobial activity of chitosan against *E. coli* and *Streptococcus faecalis* [109]. A new patented edible film comprising organic acids, protein, and glycerol (for example, 0.9% glycerol, 10% soy protein and 2.6% malic acid) can inhibit pathogen growth including *Listeria monocytogens*, *Salmonella gaminara* and *E. coli* 0157:H7. Such film also provides a method for coating comestible products with edible films without masking the colour but increasing the shelf life [110].

Chitosan has the ability to slow the growth of certain microorganisms that are deleterious in fruit postharvest such as *Fusarium* spp., *Colletotrichum musae* and *Lasiodiplodia theobromae* in banana [96, 111]. Chitosan treated longan fruit had reduced firmness loss, titratable acidity, total soluble solids, decay, respiration rates and polyphenol oxidase activity associated with peel discoloration compared to control fruits [112]. Chitosan increased vitamin C content, reduced ethylene production and delayed ripening in peach fruit as indicated by the high content of titratable acidity [113]. Moreover, El Ghaouth *et al.* [114] reported that the chitosan coatings (1–2%) reduced the deterioration in tomato caused by *Botrytis cinerea.* The application of chitosan significant reduces postharvest penicillium decay and delay of fruit senescence during cold storage of different citrus fruits [115]. The application of chitosan to apples at 0.25 to 2.0% concentration significantly induced resistance to postharvest blue mould, caused by the fungus *Penicillium expansum* [116]. The application of 2.0% chitosan to gala apples considerably reduced the severity of blue and grey mould [117]. The application of chitosan to peaches artificially inoculated with *Monilinia fructicola* significantly reduced the incidence of brown rot and delayed disease development as compared to control fruit. Moreover, chitosantreated peaches were firmer and had higher titratable acidity and vitamin C content than control peaches [113]. In tomatoes, chitosan coatings greatly reduced

postharvest black rot caused by the pathogen *Alternaria alternata* [118]. The application of chitosan significantly controlled tomato grey and blue moulds, caused by *B. cinerea* and *P. expansum*, respectively [119]. Han *et al.* [120, 121] reported that chitosan coatings on fresh strawberries and red raspberries extended their shelf life by decreasing weight loss and delaying changes in colour, titratable acidity, and pH during cold storage. The addition of oleic acid to chitosan coating not only enhanced the chitosan antimicrobial activity but also improved water vapour resistance of coated produce [122]. The chitosan-based coatings reduced the incidence of anthracnose (caused by *Colletotrichum gloeosporioides*) by about 40% in papaya [123]. Chitosan coatings containing natamycin were also effective in controlling decay of "Hami" melons caused by natural infections of *A. alternata* and *Fusarium semitectum.* Sangsuwan *et al.* [124] evaluated the inhibitory effect of chitosan/methyl cellulose stand-alone films, with and without vanillin, against *E. coli* and *Saccharomyces cerevisiae* on wrapped fresh-cut cantaloupe and pineapple and reported that both films inhibited the growth of *E. coli* and *S. cerevisiae* on fresh-cut cantaloupe, the film with vanillin being more effective. However, the application of the antimicrobial film reduced the ascorbic acid content in pineapple, remaining only 10% of its original content after storage. In general, the quality attributes of coated fresh-cut cantaloupe and pineapple were reported as acceptable in this study. This coating also improved the quality properties of coated fruit [125].

HPMC-based coatings containing 0.4% sorbic acid enhanced the inactivation of *Salmonella montevideo* on tomato fruit surface. However, these coatings caused a chalky appearance of the fruit surface, limiting its potential for commercial application [126]. Raybaudi-Massilia *et al.* [127] indicated that the addition of cinnamon, clove or lemongrass oils at 0.7% (v/v) or their active compounds (citral, cinnamaldehyde and eugenol) at 0.5% (v/v) into an alginate-based coating increased their antimicrobial effect, reduced the population of *E. coli* O157:H7 by more than 4 log CFU/g and extended the microbiological shelf life of Fuji apples for at least 30 days. However, they observed that lemongrass and citral acted faster against *E. coli* O157:H7 at day 0 than the other compounds, suggesting that both essential oils entered into the bacteria more easily (higher rate of diffusion), causing irreversible damage and cell death. Seydim and Sarykus [128] developed whey protein-based antimicrobial coatings by adding oregano, rosemary and garlic essential oils; Rojas-Grau *et al.* [129] used apple puree and high methoxyl pectin combined with oregano, lemon grass, or cinnamon oil at different concentrations. However, these coatings showed their efficacy in-vitro against a wide spectrum of microorganisms but they were not tested in real food systems and, as a result, there is a lack of available information about their possible impact on the aroma and flavour of the coated products [15].

Ozone is a strong antimicrobial agent with high reactivity, penetrability and spontaneous decomposition to a non-toxic product [130]. Several researchers have shown that treatment with ozone appears to have a beneficial effect in extending the storage life of fresh non-cut commodities such as broccoli, cucumber, apples, grapes, oranges, pears, raspberries and strawberries by reducing microbial populations and by oxidation of ethylene [130, 131]. The use of ozonated water has been applied to fresh-cut vegetables for sanitation purposes reducing microbial populations and extending the shelf life of some of these products [132]. However, scarce information is currently available about inactivation of food borne pathogens. Ozone has been declared in many countries to have potential use for food processing and declared in the USA as GRAS [133]. When compared to chlorine, ozone has a greater effect against certain microorganisms leaving no residues. However, a higher corrosiveness and initial capital cost for generator are the main disadvantages compared to the use of chlorine [134].

4.7.2 Antioxidant Coatings

Antioxidants are added to edible coatings to protect fruits and vegetables against oxidative rancidity, degradation, and discoloration. The sensory aspects are very important to ensure the success of new edible coatings and colour is one of the most important parameter that must be maintained during different postharvest operations. The colour change is usually caused by the enzyme polyphenol oxidase (PPO), which in presence of oxygen, converts phenolic compounds into dark-coloured pigments [135]. Some researchers have proved the effectiveness of edible coatings on the control of browning and polyphenol oxidase activity. Application of antioxidant treatments as dipping after peeling and/or cutting is the most common way to control browning of fresh-cut fruits [136–142]. Ascorbic acid (l-ascorbic acid) and its various neutral salts and other derivatives have been GRAS. The carrageenan-based coatings in combination with ascorbic acid resulted in positive sensory results and reduction of microbial levels on minimally processed apple slices [55].

Lettuce can undergo changes in colour due to different biochemical processes, mainly chlorophyll degradation and browning appearance in the case of the lettuce which is the limiting factor for marketability of fresh-cut lettuce [143–145]. Carrots effected by environmental and postharvest stresses can synthesize phenolic compounds along with wound barriers such as lignin [146–148] and lignin formation increases whiteness in carrots and the activation of certain enzymes after the processing can lead to degradation of antioxidants [149, 150].

Perez-Gago *et al*. [90] reported a substantial reduction in browning of fresh-cut apples when whey protein concentrate beeswax coating containing ascorbic acid, cysteine or 4-hexylresorcinol was used. Brancoli and Barbosa-Canovas [151] decreased surface discoloration of apple slices with maltodextrin and MC coatings including ascorbic acid. Baldwin *et al*. [1] found that CMC-based coating with antioxidants, including ascorbic acid, reduced browning and retarded water loss of cut apple. The coating with a mixture of apple puree, pectin and vegetable oils containing ascorbic acid and citric acid delayed browning of fresh-cut apples [12]. Olivas *et al*. [152] preserved surface browning of fresh-cut pear wedges by using a MC-based coating containing ascorbic acid and citric acid. Similar results were obtained by Lee *et al*. [55], who studied the effect of carrageenan and whey protein concentrate edible coatings in combination with anti-browning agents on fresh-cut apple slices and observed that the incorporation of ascorbic, citric and oxalic acids was advantageous in maintaining colour during two weeks. The incorporation of *N*-acetyl cysteine and glutathione into gellan, alginate or pectin formulations helped to control enzymatic browning of fresh-cut pears during two weeks of storage [71]. Ponce *et al*. [153] applied chitosan films enriched with olive and rosemary oleoresins on pumpkin slices, which showed a clear antioxidant effect by slowing the action of PPO and peroxidase (POD) within five days of storage. Chitosan coatings were also used by Eissa [154], who found that they delayed discoloration associated with reduced enzyme activity of PPO and other enzymes, and had a good effect on colour characteristics of fresh-cut mushroom during storage at 4 °C. Hui-Min *et al*. [155] studied the effects of three different edible coatings (carrageenan, CMC and sodium alginate) and their combinations on browning of fresh-cut peach during storage at 5 °C and observed that sodium alginate coating and the various composite combinations increased peach colour and reduced browning due to inhibition of PPO activity.

4.7.3 Texture Enhances

Fruits and vegetables that remain firm, crunchy texture are highly desirable because consumers

associate these characters with freshness. Textural changes in fruits and vegetables are related to certain enzymatic and non-enzymatic processes. The most common way of controlling softening phenomena in fruits and vegetables is by treatments with calcium salts and mostly calcium chloride ($CaCl_2$) is used as dip treatment in the range of 0.1–1.0% [142, 156, 157]. Calcium ions interact with pectin polymers to form a cross-linked network that increases mechanical strength, thus delaying senescence and controlling physiological disorders in fruits and vegetables [158]. Calcium lactate has been used as a firming agent for fruit such as cantaloupes, strawberry and others [159, 160]. It has been reported to be a good alternative to $CaCl_2$ because it avoids bitterness or off-flavours associated with this salt [160]. Hernandez-Munoz *et al.* [161] observed that the addition of calcium gluconate to the chitosan (1%) coating formulation increased the firmness of strawberries during refrigerated storage. Han *et al*. [139, 140] observed that a chitosan-based coating containing 5% calcium (Gluconal CAL) increased the firmness of frozen-thawed raspberries by approximately 25% in comparison to uncoated fruits.

Rojas-Grau *et al.* [162] observed that apple wedges coated with alginate and gellan edible coatings cross linked with calcium salts outstandingly maintained their initial firmness during refrigerated storage. Similar results were obtained by Oms-Oliu *et al.* [163] on fresh-cut melon coated with different calcium-cross-linked polysaccharide-based edible coatings (alginate, gellan and pectin). Lee *et al.* [55] indicated that incorporating 1% of calcium chloride within the whey protein concentrate coating formulation helped to maintain firmness of fresh-cut apple pieces. Some workers have reported that dip treatment of apple slices with $CaCl_2$ solution have no or slight effect on the preservation of texture. Olivas *et al.* [164] maintained firmness of fresh-cut “Gala” apples practically constant using alginate edible coatings. Optimal concentration of $CaCl_2$ treatments in minimally processed melon was found to be 2.5% [165]. Agar *et al.* [137] could not observe significant differences between 1 and 2% $CaCl_2$ treatments in kiwifruit slices.

4.7.4 Nutraceutical Coatings

Several researchers have incorporated minerals, vitamins and fatty acids into edible film and coating formulations to enhance the nutritional value of some fruits and vegetables. Tapia *et al*. [166] reported that the addition of ascorbic acid (1% w/v) to the alginate and gellan-based edible coatings preserve the natural ascorbic acid content in fresh-cut papaya throughout its storage. Han [15] reported that chitosan-based coatings have capability to hold high concentrations of calcium or vitamin E and therefore significantly increased their content in fresh and frozen strawberries and red raspberries. Similarly, Hernandez-Munoz *et al.* [167] observed that chitosan-coated strawberries retained more calcium gluconate than strawberries dipped into calcium solutions. Han *et al*. [121] improved the nutritional and physicochemical quality of strawberries and raspberries by means of chitosan-based coatings enriched with calcium and vitamin E.

Xanthan gum coating was utilized to contain a high concentration of calcium and vitamin E for not only preventing moisture loss and surface whitening, but also significantly increasing the calcium and vitamin E contents of the carrots [168]. The development of chitosan coatings containing high concentrations of calcium, zinc or vitamin E also provided alternative ways to fortify fresh fruits and vegetables that otherwise could not be accomplished with common processing approaches [43].

4.8 Nanotechnology

Nowadays nanotechnology is applied in many research areas. A nanoparticle is an ultrafine particle of nanometre size, which is able to form nanobiocomposite films when it is combined with natural polymers. Some of the applications associated with nanotechnology include improved taste, colour, flavour, texture and consistency of foodstuffs, increased absorption and bioavailability of food or food ingredients (nutrients), and the development of new food packaging materials with improved mechanical, barrier and antimicrobial properties [169]. Traditionally, mineral fillers such as clay, silica and talc have been incorporated in film preparation in order to reduce its cost or to improve its performance to some extent [170]. Both proteins [171] and polysaccharides [172, 173] have given rise to films in combination with nanoclay particles. However, other nanoparticles such as tripolyphosphate-chitosan [174], microcrystalline cellulose [175] and silicon dioxide [176] have also been added to biopolymers to obtain films.

4.9 Commercial Application of Edible Coatings

Nowadays, many commercial edible coatings for use on fresh and fresh-cut fruits and vegetables are available in market to reduce weight loss, physiological disorders, and maintain produce quality. Most of them are assigned to maintain the quality of citrus and apples and, to a lesser extent, mangoes, papayas, pomegranates, avocados, or tomatoes [164]. Several commercial products available in the market for postharvest use, such as Biosave *(Pseudomonas syringae)* registered in the USA and “Shemer” *(Metschnikowia fructicola)* registered in Israel [177]. Pro-long, TAL-Prolong (Courtaulds Group, London), Semperfresh (AgriCoat Industries Ltd., Berkshire, UK), and Natural Shine 9000 (Pace International, Seattle, USA) are commercially available composite coating formulations based on CMC [178]. They contain sucrose fatty acid ester, sodium salt of CMC and emulsifier. Available in powder or granular form, their aqueous solution (0.5–2% concentration) is used to extend shelf life of many fruits. Coating of TAL-Prolong (1%) on mangoes showed delayed ripening with an extended shelf life. Nature-Seal (Eco-science Product System Division, Orlando, FL), is another cellulose-based edible coating formulation used for delayed ripening of tomatoes and mangoes. Nature-Seal has also been used (in combination with antimicrobials, plasticizers, antioxidants, etc.) to coat fresh-cut apples and potatoes. The coating significantly reduced weight loss of apples and potatoes more than those treated with water solutions and was not objectionable in taste during several weeks of storage [1]. The coating has also been used to effectively reduce the discoloration of mini-peeled carrots without affecting microbial and chemical quality [179]. A commercial fruit coating, Nutri-Save (Nova Chem, Halifax, Canada), was developed to serve as both film former and natural preservative and to create a modified atmosphere for whole apples and pears to reduce respiration rate and desiccation of these commodities [180]. Nutri-save reduces the respiration rate, weight loss and microbial decay in fresh cut pears and apples [136]. Table 4.1 shows some of the formulations that have already been applied to fresh fruits and vegetables [181]. Nowadays, there is a new generation of edible coatings that is being applied to fresh-cut fruits and vegetables. Some examples of the application of these coatings on fresh-cut fruits and vegetables are shown in Table 4.2.

Table 4.1 Applications of edible coatings to fresh fruits and vegetables.

Coating material	Composition	Fruit/vegetable	Effect of coating	Ref.
Semperfresh™	Sucrose esters with high proportion of short chain unsaturated fatty acid esters, sodium salts of CMC and mixed mono and diglycerides	Zucchini	Reduced water loss and internal CO_2 of zucchini fruit	[88]
		Cucumber, Summer squash	$O_2/H_2O/CO_2$ barrier	[182]
		Apple	Reduced colour changes, retained acid, increased shelf life and maintained quality	[183]
		Tomato	-------do------	[184]
		Banana	Decreased ethylene production and delayed chlorophyll loss	[178]
		Quince	$O_2/H_2O/CO_2$ barrier	[185]
Prolong™	Sucrose polyester of fatty acid esters, sodium CMC and mono and diglycerides	Mango	Retard ripening, reduce weight loss and chlorophyll loss	[186]
		Pear	Retention of firmness, green skin colour and titrable acidity	[187]
Tal-Prolong™	Sucrose fatty acid esters, sodium salt of CMC and mono and diglycerides	Mango	Delayed ripening with extended shelf life	[178]
Nature-seal™	Cellulose-based edible coating	Tomato	Delayed ripening	[184]
		Pomegranate	------	[187]
		Carrot	Retard discolouration and carotene loss and is a barrier for O_2 diffusion	[188]
Chitosan	Chitosan	Citrus	$O_2/H_2O/CO_2$ barrier	[189]
		Raspberry	H_2O barrier; Ca^{2+}, Vit. E carrier	[120]
	Chitosan; HPMC	Raspberry	H_2O barrier; carrier (antimicrobial)	[49]
	Chitosan and Tween 80	Strawberry, Cucumber, Bell pepper	Antimicrobial coatings	[46, 190]
		Apple, Pear, Plum, Peach	Act as gas barrier	[191, 192]

Coating material	Composition	Fruit/vegetable	Effect of coating	Ref.
Chitosan	Chitosan and Tween 80	Litchi	Reduce weight loss and browning, improve storability	[47]
		Carrot	Reduce decay and improve appearance	[53, 54]
		Tomato	Reduce respiration rate, ethylene production and increase titrable acidity	[114]
		Pear	Reduce ethylene production and delay ripening as indicated by high content of titrable acidity	[113]
Polysaccharide-lipid	Maltodextrin, CMC, propylene glycol, fatty acid esters, sodium benzoate	Mango		[193]
	MC, PEG, stearic acid, citric acid, ascorbic acid	Apricot		[194]
	Paraffin wax, beeswax, soybean oil; CMC from sugar beet pulp; emulgin PE, oleic acid and sodium oleate	Peach, Pear, Mandarin		[92, 195]
Carrageenan	Carrageenan, glycerol and Tween 80	Strawberry	–	[40]
Protein-Polysaccharide	CMC, WPI, Caseinates and Glycerol	Strawberry	–	[196]
Starch	Starch and glycerol	Strawberry	–	[197]
Soy protein	Soy protein, glycerol, malic acid, lactic acid	Apple		30
Zein	Corn zein protein	Tomato	Delayed colour change, loss of firmness and weight and extend shelf life	[22, 23]
	Corn zein protein and propylene glycol	Apple	–	[19]
	Corn zein protein	Mango	$O_2/H_2O/CO_2$ barrier	[198]

Nutri-save™	N,O carboxyl methyl chitosan	Apple, Pear, Pomegranate, Bread fruit, Cherry	Increases its shelf life	[94, 95, 199, 200]
Brilloshine	Sucrose esters and wax (shine)	Apple, Avocado, Melons, Citrus	Protect, increase shine and extend shelf life	[201]
Nu-coatFlo, Ban-seel	Sucrose eaters of fatty acids and sodium salt of CMC	Apple, Banana, Cucumber, Guava, Melon, Pear, Plum	Protect, increase shine and extend shelf life	[201]
Crisp Coat 868	Starch	Strawberry	–	[40]
Food Coat	Composite polysaccharides	Strawberry	–	[187]
Agri Coat	Composite polysaccharides	Avocado, Pear, Pomegranate	–	[187]
Citrashine	Sucrose ester and wax	Mandarin	Increase shine and extend shelf life	[202]
Casein	Calcium caseinate	Sweet pepper	Effective gas barrier to internal O_2 and CO_2, inhibit colour change and reduce decay	[203]
	Sodium caseinate and stearic acid	Carrot	Reduce moisture loss	[204]
Cellulose	MC and glycerol	Carrot	Extend storage life, result more carotene than control	[53]
		Strawberry, Avocado	–	[33]
FreshSeal™	Polyvinyl alcohol, starch and surfactant	Fruits	Extend shelf life	[187, 205]

Table 4.2 Application of edible coatings to fresh-cut fruits and vegetables.

Coating material	Functional ingredient	Fruit/vegetable	Effect	Ref.
Starch	Potassium sorbate, Citric acid	Strawberry	Antimicrobial effect, Inhibited the growth of mesophilic aerobes, mould and yeast counts.	[206]
Alginate	Cinnamon, Clove, Lemongrass, Cinnamaldehyde, Eugenol, Citral	Apple	Antimicrobial effect, Inhibited native microbiota during 30 days and reduced >4 log CFU/g of *E. coli* O157:H7 in the first week of storage.	[207]
	Malic acid, Palmarosa, Cinnamon, Lemongrass	Melon	Antimicrobial effect, Inhibited the microbial growth and reduced up to 3.1 log CFU/g after 30 days of storage.	[127]
Alginate, apple puree	Lemongrass, Oregano, Vanillin	Apple	Antimicrobial effect, Reduced native psychrophilic aerobes, moulds and yeast. Lemongrass (1.0–1.5%) and oregano (0.5%) reduced >4 log CFU/g of inoculated *Listeria innocua*.	[208]
Methylcellulose	Chitosan	Melon	Antimicrobial effect, Reduced the growth of mesophilic aerobes, psychrotrophs, yeast and moulds and maintained the growth of *E. coli*, *Staphylococcus aureus*, *Salmonella* sp. <10 CFU/g.	[209]
Chitosan	Chitosan	Water chestnut	O_2 barrier	[210]
Chitosan	Chitosan	Lettuce	O_2/H_2O barrier	[211]
Whey protein, Carrageenan	Ascorbic acid (1.0%), Citric acid (1.0%), Oxalic acid (0.05%)	Apple	Antioxidant effect, Maintained the original colour during storage without changes in sensory properties.	[55]
Whey protein, beeswax	Ascorbic acid (0.5–1.0%), Cysteine (0.1–0.5%), 4-Hexylresorcinol (0.005–0.02%)	Apple	Antioxidant effect, Reduced surface browning. 4-Hexylresorcinol showed the least effectiveness at reducing browning.	[90]
Corn zein protein	–	Apple	$O_2/H_2O/CO_2$ barrier, gloss.	[19]
Methylcellulose Maltodextrin	Ascorbic acid	Apple	Antioxidant effect, Reduced surface discoloration.	[151]

Methylcellulose	Ascorbic acid	Pear	Antioxidant effect, Prolonged shelf life by retarding browning.	[152]
CMC, Soy protein	Ascorbic acid	Apple	Antioxidant effect, Delayed browning more effectively when was applied in an edible coating than in an aqueous solution.	[1]
Pectin, apple puree	Ascorbic acid, Citric acid	Apple	Antioxidant effect, Preserved colour for 12 days at 5 °C.	[12]
Alginate, gellan	*N*-acetyl cysteine, Glutathione	Apple	Antioxidant effect, Prevented surface discoloration.	[208]
Alginate, gellan	*N*-acetyl cysteine	Apple	Antioxidant effect, Maintained the original colour by 2 weeks of storage.	[162]
Alginate, gellan	*N*-acetyl cysteine, Glutathione	Pear	Antioxidant effect, Prevented browning for 2 weeks.	[71]
Alginate, gellan	Calcium chloride	Apple	Texture enhancement, Maintained firmness by 2 weeks.	[162]
Alginate, gellan, pectin	Calcium chloride	Melon	Texture enhancement, Helped to maintain fruit firmness during 15 days.	[163]
Alginate	Calcium chloride	Apple	Texture enhancement, Maintained firmness during storage.	[164]
Alginate	Calcium lactate	Melon	Texture enhancement, Maintained firmness in coated samples.	[127]
Alginate	Calcium lactate	Apple	Texture enhancement, Maintain the texture for more than 30 days.	[207]
Alginate	Calcium chloride	Pineapple	Texture enhancement, Helped to retain internal liquids.	[212]
Whey protein	Calcium chloride	Apple	Texture enhancement, Inhibited the loss of firmness.	[55]
Chitosan	Calcium gluconate	Strawberry	Texture enhancement, Did not improve the firmness retention.	[161]
Chitosan	Calcium gluconate	Raspberry	Texture enhancement, Helped to maintain textural quality.	[120]
Chitosan	Calcium gluconate, vitamin E	Strawberry, Raspberry	Nutraceutical effect, Increased the content of these nutrients in both fruits.	[121]
Chitosan	Calcium gluconate	Strawberry	Increased nutritional value of the strawberries.	[161]
Alginate	Ascorbic acid	Papaya	Preserved the natural ascorbic acid content of the fruit.	[166]
Alginate, gellan	*Bifidobacterium lactis*	Apple, papaya	Maintained values of *B. lactis* >106 CFU/g by 10 days during storage.	[213]

4.10 Problems Associated with Edible Coatings

Success of edible coatings on fruits and vegetables mainly depends on selecting films or coatings that can give a desirable internal gas composition that is appropriate for a specific product. Shewfelt *et al*. [214] stated that colour change, firmness loss, ethanol fermentation, decay ratio and weight loss of edible film-coated fruits are important quality parameters for some products and these parameters must be monitored throughout the storage period.

Thick coating on fruits and vegetables surface becomes an undesirable barrier between the external and internal atmosphere and restricts exchange of respiratory gases (CO_2 and O_2) causing accumulation of high levels of ethanol and development of off-flavours [114, 179, 215, 216]. Therefore, it is necessary to adjust the thickness of the coating according to the variety, storage conditions and marketing temperature. Park *et al*. [23] reported that tomatoes coated with 2.6 mm zein film produced alcohol and off-flavours internally which is due to low oxygen and high carbon dioxide concentration. Smith *et al*. [217] summarized that use of coatings resulted in physiological disorders like core flush, flesh breakdown, accumulation of ethanol and alcoholic off-flavour in deciduous fruits which is due to modification of internal atmosphere. Waxes and shellac tend to restrict the gas exchange of O_2 and CO_2 between atmosphere and fruit to the extent that the internal O_2 level becomes too low to support aerobic respiration, resulting in high levels of internal ethanol, acetaldehyde and internal CO_2 [62, 218]. Smith and Stow [219] reported that application of sucrose fatty acid ester coating on apples (cv. Cox's Orange Pippin) resulted in reduction of fruit firmness, yellowing and weight loss, but also increased core flush incidence. Ben-Yehoshua [220] reported that the coatings having poor water vapour barrier properties could result in weight or moisture loss of the product, but it could prevent water vapour condensation, which could be a potential source of microbial spoilage in fruit and vegetable packaging. Films that have good gas barrier properties could cause anaerobic respiration and interferes with normal ripening [38]. Therefore, it is clear that the control of gas permeability should be a priority in the development of edible coatings [221].

Edible coatings are usually consumed with the coated products. Therefore, the incorporation of compounds such as antimicrobials, antioxidants and nutraceuticals should not affect consumer acceptance. Some authors have indicated that the incorporation of antimicrobial agents into edible coatings could impart undesirable sensorial modifications in foods, especially when essential oils are used [222]. Oms-Oliu *et al*. [71] summarized that the coating of fresh-cut melon with gellan gum increased the phenolic compounds during storage which further affect the sensory properties such as odour, colour and flavour. Rojas-Grau *et al*. [162] observed the synthesis of ethanol and acetaldehyde in apple slices coated with alginate and gellan gum after two weeks of storage which decreased its sensory quality especially fruit flavours. Sometimes the incorporation of certain anti-browning agents into edible coatings can yield an unpleasant odour, particularly when high concentrations of sulphur-containing compounds such as *N*-acetyl cysteine and glutathione are used as dipping agents [129, 223, 224]. The addition of nutraceutical compounds to edible coatings may impart bitter taste, astringent or off-flavour [225] that can lead to rejection of the product by consumers [226].

Many edible coatings are made from ingredients that could cause allergic reactions. Within these allergens, milk, soybeans, fish, peanuts, nuts and wheat are the most important. Therefore, the presence of a coating with a known allergen on a food must be also clearly labelled [227].

4.11 Regulatory Status and Food Safety Issues

According to the European Directive [228, 229], and USA regulations [133], edible coatings are those coatings that are formed from food products, food ingredients, food additives, food contact substances or food packaging materials. To maintain edibility, all film-forming components as well as any functional additives in the film-forming materials, should be food-grade, non-toxic and all process facilities should meet high standards of hygiene [10, 15, 230, 231]. According to the US Code of Federal Regulations, the amount of edible coating ingredients used must be only that which is necessary to accomplish the intended effect, and the ingredients have to be GRAS and be listed in the above-mentioned Code.

In the regulation of most countries, chemical substances added as antimicrobials are regarded as food additives if the primary purpose of the substances is shelf life extension. However, each country has its own regulations defining a list of approved additives [228, 232]. For instance, according to US regulations, organic acids including acetic, lactic, citric, malic, propionic, tartaric and their salts are GRAS for miscellaneous and general purpose usage [233]. On the other hand, many essential oils are used widely in the food, health and personal care industries and are also classified as GRAS substances or permitted as food additives. According to European Directive 1995 [228], the ingredients that can be incorporated into the formulations of edible coating include Arabic and karaya gum, pectins, shellac, bees wax, candelilla wax, and carnauba wax. This Directive was modified in 1998 [229] by introducing new ingredients such as lecithin, polysorbates, fatty acids, and fatty acid salts. On the other hand, additives used by US Food and Drug Administration (FDA) for coating fresh fruits and vegetables includes morpholine, polydextrose, sorbitan monostearate, sucrose fatty acid esters, cocoa butter and castor oil [133]. In India, as per the PFA section ZZZ (23) of Rule 42 (2006) which states that “The fresh fruits and vegetables may be coated with bees wax or carnauba wax under proper label declaration.” However, some consumers have concerns about their use. Vegetarians and others who avoid animal products may worry that fruits and vegetables contain animal-based waxes, such as oleic acid. Some people fear that the edible coating and films traps pesticides, making the fruit or vegetable unsafe to eat. If consumers want to avoid edible coated fruits and vegetables, FDA regulations that took effect in 1994 may help them to identify the appropriate products for them. These regulations require produce packers or grocers to provide information about the presence of coatings on fresh fruits and vegetables. The information will say that the product is (a) coated with food-grade animal-based wax or (b) coated with food-grade vegetable-, petroleum-, beeswax-, and/or shellac-based wax or resin to maintain freshness. FDA will also allow the statement “No wax or resin coating” on fresh fruits and vegetables that do not contain any coating. There are many safety concerns about nanomaterials, as their size may allow them to penetrate into cells and eventually remain in the human organism. So, the need for accurate information on the effects of nanomaterials on human health following chronic exposure is imperative before any nanostructured food packaging is available for commercialization.

4.12 Conclusions

Edible films and coatings applied to fresh, minimally processed and processed fruits and vegetables are effective in extending their shelf life, maintaining their microbiological, sensory and nutritional quality. Some formulations have been specifically tested on their ability to inhibit polyphenol oxidase

activity and delay browning reactions. In addition, edible coatings are able to transport substances that bring some benefits not only for food itself but also for the consumer, through the encapsulation of bioactive compounds, developing new products with nutraceutical or functional effect. Their use in highly perishable products such as horticultural ones, is based on some particular properties such as cost, availability, functional attributes, mechanical properties (flexibility, tension), optical properties (brightness and opacity), the barrier effect against gases flow, structural resistance to water and microorganisms and sensory acceptability. In some cases, edible coatings were not successful. The success of edible coatings on fresh fruits and vegetables totally depends on the control of internal gas composition. Basic information on film-coating formulation, properties, methods of application to fruit or vegetable surface and demonstration of effectiveness are lacking. Tremendous research is required in the area of applications of edible coatings on fresh and fresh-cut fruits and vegetables.

References

1. E.A. Baldwin, M.O. Nisperos-Carriedo, X. Chen, and R.D. Hagenmaier, Improving storage life of cut apple and potato with edible coating. *Postharvest Biology and Technology,* 9, 151–163, 1996.

2. H.J. Park, Development of advanced edible coatings for fruits. *Trends in Food Science and Technology,* 10, 254–260, 1999.

3. E.A. Baldwin and R.A. Baker, Use of proteins in edible coatings for whole and minimally processed fruits and vegetables. In: Gennadios A, editor. *Protein based films and coatings*. Boca Raton, Fla., CRC Press, pp. 501–515, 2002.

4. G.I. Olivas and G.V. Barbosa-Canovas, Edible coatings for fresh-cut fruits. *Critical Reviews in Food Science and Nutrition*, 45, 657–670, 2005.

5. H.J. Park, Edible coatings for fruit. In: Jongen W, editor. *Fruit and vegetable processing.* Boca Raton, Fla., CRC Press LLC, 2005.

6. J.M. Krochta and C. DeMulder-Johnston, Edible and biodegradable polymerfilms, challenges and opportunities. *Food Technology,* 51, 61–74, 1997.

7. F. Debeaufort, J.A. Quezada-Gallo, and A. Voilley, Edible films and coatings, tomorrow packaging, a review. *Critical Reviews in Food Science and Nutrition,* 38, 299–313, 1998.

8. S. Min and J.M. Krochta, Antimicrobial films and coatings for fresh fruit and vegetables. In: W. Jongen, editor. *Improving the safety of fresh fruit and vegetables.* New CRC York, Press, pp. 455–492, 2005.

9. A.K. Thompson, Postharvest treatments. In, *Fruit and vegetables.* Ames, Iowa, Blackwell Publishing Ltd., pp. 47–52, 2003.

10. S. Guilbert, N. Gontard, and L.G.M. Gorris, Prolongation of the shelf-life of perishable food products using biodegradable films and coatings. *LWT-Food Science and Technology,* 29, 10–17, 1996.

11. M.A. Rojas-Grau, R. Soliva-Fortuny, and O. Martin-Belloso, Edible coatings to incorporate active ingredients to fresh-cut fruits-a review. *Trends in Food Science and Technology,* 20, 438–447, 2009.

12. T.H. McHugh and E. Senesi, Apple wraps-A novel method to improve the quality and extend the shelf life of fresh-cut apples. *Journal of Food Science,* 65, 480–485, 2000.

13. E.A. Baldwin, J.K. Burns, W. Kazokas, J.K. Brecht, R.D. Hagenmaier, R.J. Bender, and E. Pesis,

Effect of two edible coatings with different permeability characterristics on mango Mangifera indica L. ripening during storage. *Postharvest Biology and Technology*, 17, 215–226, 1999.

14. D.S. Cha and M.S. Chinnan, Bipolymer-based antimicrobial packaging-A review. *Critical Reviews in Food Science and Nutrition*, 44, 223–237, 2004.

15. J.H. Han, Protein-based edible films and coatings carrying antimicrobial agents. In: Gennadios A, editor. *Protein-based films and coatings.* Boca Raton, Fla., CRC Press, pp 485–499, 2002.

16. T.H. McHugh and J.M. Krochta, Water-vapor permeability properties of edible whey protein-lipid emulsion films. *Journal of the American Oil Chemists Society*, 71, 307–312, 1994.

17. J.H. Han and A. Gennadios, Edible films and coatings- A review. In: *Innovations in Food Packaging*, J.H. Han, Ed., Elsevier Academic Press, Amsterdam, pp. 239–262, 2005.

18. J. Bai, E.A. Baldwin, and R.H. Hagenmaier, Alternatives to shellac coatings provide comparable gloss, internal gas modification, and quality for 'Delicious' apple fruit. *HortScience*, 37, 559–563, 2002.

19. J. Bai, V. Alleyne, R.D. Hagenmaier, J.P. Mattheis, and E.A. Baldwin, Formulation of zein coatings for apples (*Malus domestica* Borkh). *Postharvest Biology and Technology*, 28, 259–268, 2003.

20. J. Bai, R.D. Hagenmaier, and E.A. Baldwin, Coating selection for 'Delicious' and other apples. *Postharvest Biology and Technology*, 28, 381–390, 2003.

21. A.M. Rakotonirainy, Q. Wang, and G.W. Padua, Evaluation of zein films as modified atmosphere packaging for fresh broccoli. *Journal of Food Science*, 66, 1108–1111, 2001.

22. H.J. Park, M.S. Chinnan, and R.L. Shewfelt, Edible coating effects on storage life and quality of tomatoes. *Journal of Food Science*, 59, 568–570, 1994.

23. H.J. Park, M.S. Chinnan, and R.L. Shewfelt, Edible corn-zein film coating to extend storage life of tomatoes. *Journal of Food Processing and Preservation*, 18, 317–331, 1994.

24. F. Carlin, N. Gontard, M. Reich, and C. Nguyen, Utilization of zein coating and sorbic acid to reduce *Listeria monocytogenes* growth on cooked sweet corn. *Journal of Food Science*, 66, 1385–1389, 2001.

25. H. Chen, Functional properties and applications of edible films made of milk proteins. *Journal of Dairy Science*, 78, 2563–2583, 1995.

26. Le C. Tien, C. Vachon, M.A. Mateescu, and M. Lacroix, Milk protein coatings prevent oxidative browning of apples and potatoes. *Journal of Food Science*, 66, 512–516, 2001.

27. R. Lafortune, S. Caillet, and M. Lacroix, Combined effects of coating, modified atmosphere packaging, and gamma irradiation on quality maintenance of ready-to-use carrots *(Daucus carota)*. *Journal of Food Protection*, 68, 353–359, 2005.

28. B. Kinzel, Protein-rich edible coatings for food. *Agricultural Research*, 40, 20–21, 1992.

29. S. Xu, X. Chen, and D.W. Sun, Preservation of kiwifruit coated with an edible film at ambient temperature. *Journal of Food Engineering*, 50, 211–216, 2001.

30. S. Eswaranandam, N.S. Hettiarachchy, and J.F. Meullenet, Effect of malic and lactic acid incorporated soy protein coatings on the sensory attributes of whole apple and fresh-cut cantaloupe. *Journal of Food Science*, 71, 307–313, 2006.

31. G.R. Sanderson, Polysaccharides in foods. Food Technology, 35, 50–57, 1981.

32. K.L. Krumel, T.A. Lindsay, Nonionic cellulose ethers. *Food Technology*, 30, 36–38, 40, 43, 1976.

33. N. Maftoonazad and H.S. Ramaswamy, Postharvest shelf-life extension of avocados using methylcellulose edible coating. *LWT-Food Science and Technology,* 38, 617–624, 2005.

34. M.A. Meyers, Functionality of hydrocolloids in batter coating system. In: Kulp K, Loewe R, editors. Batters and breadings in food processing. *St. Paul, Minn., American Assn. of Cereal Chemists.*, pp. 117–141, 1990.

35. D.F. Mason, Fruit preservation process. U.S., patent 3, 472, 662, 1969.

36. M.O. Nisperos-Carriedo, and E.A. Baldwin, Edible coatings for fresh fruits and vegetables. In: *Subtropical technology conference proceedings,* Lake Alfred, Fla., 18 October 1990.

37. N.H. Banks, Internal atmosphere modification in Pro-long coated apples. *Acta Horticulture,* 157, 105, 1985.

38. M. Meheriuk and L.O. Lau, Effect of two polymeric coatings on fruit quality of Barlett and Anjou pears. *Journal of the American Society for Horticultural Science,* 113, 226–227, 1988.

39. C.R. Santerre, T.F. Leach, and J.N. Cash, The influence of the sucrose polyester, Sempfresh on the storage of Michigan grown 'McIntosh' and 'Golden Delicious' apples. *Journal of Food Processing and Preservation,* 13, 293–305, 1989.

40. C. Ribeiro, A.A. Vicente, J.A. Teixeira, and C. Miranda, Optimization of edible coating composition to retard strawberry fruit senescence. *Postharvest Biology and Technology,* 44, 63–70, 2007.

41. Q. Li, E.T. Dunn, E.W. Grandmaison, and M.F.A. Goosen, Applications and properties of chitosan. *Journal of Bioactive and Compatible Polymers,* 7, 370–397, 1992.

42. F. Shahidi, J.K.V. Arachchi, and Y. Jeon, Food applications of chitin and chitosans. *Trends in Food Science and Technology,* 10, 37–51, 1999.

43. S.I. Park and Y. Zhao, Incorporation of a high concentration of mineral or vitamin into chitosan-based films. *Journal of Agricultural and Food Chemistry,* 52, 1933–1939, 2004.

44. F. Devlieghere, A. Vermeulen, and J. Debevere, Chitosan: Antimicrobial activity, interactions with food components and applicability as a coating on fruit and vegetables. *Food Microbiology,* 21, 703–714, 2004.

45. P.J. Chien, F. Sheu, and F.H. Yang, Effects of edible chitosan coating on quality and shelf life of sliced mango fruit. *Journal of Food Engineering,* 78, 225–229, 2007.

46. El A. Ghaouth, J. Arul, R. Ponnampalam, and M. Boulet, Chitosan coating effect on storability and quality of fresh strawberries. *Journal of Food Science,* 12, 1618–1632, 1991.

47. D. Zhang and P.C. Quantick, Antifungal effects of chitosan coating on fresh strawberries and raspberries during storage. *The Journal of Horticultural Science and Biotechnology,* 73, 763–767, 1998.

48. G. Romanazzi, F. Nigro, A. Ippolito, D.D. Venere, and M. Salerno, Effects of pre- and postharvest chitosan treatments to control storage grey mold of table grapes. *Journal of Food Science,* 67, 1862–1867, 2002.

49. S. Park, S.D. Stan, M.A. Daeschel, and Y. Zhao, Antifungal coatings on fresh strawberries *(Fragaria ananassa)* to control mold growth during cold storage. *Journal of Food Science,* 70, 202–207, 2005.

50. K.D. Reuck, D. Sivakumar, and L. Korsten, Effect of integrated application of chitosan coating and

modified atmosphere packaging on overall quality retention in litchi cultivars. *Journal of the Science of Food and Agriculture*, 89, 915–920, 2009.

51. X.F. Shao, K. Tu, S. Tu, and J.A. Tu, Combination of Heat Treatment and Chitosan Coating Delays Ripening and Reduces Decay in "Gala" Apple Fruit. *Journal of Food Quality*, 35, 83–92, 2012.

52. D. Zhang and P.C. Quantic. Effects of chitosan coating on enzymatic browning and decay during postharvest storage of litchi (*Litchi Chinensis* Sonn.) fruit. *Postharvest Biology and Technology*, 12, 195–202, 1997.

53. P. Li and M.M. Barth, Impact of edible coatings on nutritional and physiological changes in lightly processed carrots. *Postharvest Biology and Technology*, 14, 51–60, 1998.

54. L.H. Cheah, B.B.C. Page, and R. Shepherd, Chitosan coating for inhibition of sclerotinia rot of carrots. *New Zealand Journal of Crop and Horticulture Science*, 25, 89–92, 1997.

55. J.Y. Lee, H.J. Park, C.Y. Lee, and W.Y. Choi, Extending shelf-life of minimally processed apples with edible coatings and anti-browning agents. *LWT-Food Science and Technology*, 36, 323–329, 2003.

56. S.Z. Vina, A. Mudridge, M.A. Garcia, R.M. Ferreyra, M.N. Martino, A.R. Chaves, and N.E. Zaritzky, Effects of polyvinylchloride and edible starch coatings on quality aspects of refrigerated Brussels sprouts. *Food Chemistry*, 103, 701–709, 2007.

57. E.A. Baldwin, M.O. Nisperos-Carriedo, R.D. Hagenmaier, and R.A. Baker, Use of lipids in coatings for food products. *Food Technology*, 51, 56–62, 1997.

58. J.F. Lawrence and J.R. Iyengar, Determination of paraffin wax and mineral oil on fresh fruits and vegetables by high temperature gas chromatography. *Journal of Food Science*, 5, 119–129, 1983.

59. J.J. Kester and O.R. Fennema, Edible films and coatings, a review. *Food Technology*, 40, 47–59, 1986.

60. G.G. Watters and J.E. Brekke, Stabilized raisins for dry cereal products. *Food Technology*, 15, 236–238, 1961.

61. H.J. Kaplan, Washing, waxing, and color adding. In: W.F. Wardowdki, S. Nagy, W. Grierson, editors. *Fresh citrus fruit*. Westport, Conn., AVI Publishing Co., pp. 379, 1986.

62. V. Alleyne and R. Hagenmaier, Candelilla-shellac, an alternative formulation for coating apples. *HortScience*, 35, 691–693, 2000.

63. R.D. Hagenmaier, Evaluation of a polyethylene–candelilla coating for 'Valencia' oranges. *Postharvest Biology and Technology*, 19, 147–154, 2000.

64. W.F. Da-Mota, L.C.C. Salomao, P.R. Cecon, and F.L. Finger, Waxes and plastic film in relation to the shelf life of yellow passion fruit. *Scientia Agricola*, 60, 51–57, 2003.

65. E. Fallika, Y. Shaloma, S. Alkalai-Tuviaa, O. Larkovb, E. Brandeisb, and U. Ravidb, External, internal and sensory traits in Galia-type melon treated with different waxes. *Postharvest Biology and Technology*, 36, 69–75, 2005.

66. R. Porat, B. Weiss, L. Cohena, A. Dausa, and A. Biton, Effects of polyethylene wax content and composition on taste, quality, and emission of off-flavor volatiles in 'Mor' mandarins. *Postharvest Biology and Technology*, 38, 262–268, 2005.

67. R. McGuire and R. Hagenmaier, Shellac formulation to reduce epiphytic survival of coliform bacteria on citrus fruit postharvest. *Journal of Food Protection*, 64, 1756–1760, 2001.

68. T.H. Shellhammer and J.M. Krochta, Whey protein emulsion film performance as affected by lipid

type and amount. *Journal of Food Science*, 62, 390–394, 1997.

69. M.B. Perez-Gago, M. Serra, M. Alonso, M. Mateos, del M.A. Rio, Effect of whey protein- and hydroxypropyl methylcellulose-based edible composite coatings on color change of fresh-cut apples. *Postharvest Biology and Technology*, 36, 77–85, 2005.

70. M. Altenhofen, A.C. Krause, and T. Guenter, Alginate and pectin composite films cross-linked with Ca^{+2} ions, effect of the plasticizer concentration. *Carbohydrate Polymers*, 77, 736–742, 2009.

71. G. Oms-Oliu, R. Soliva-Fortuny, and O. Martin-Belloso, Using polysaccharide-based coatings to enhance quality and antioxidant properties of fresh-cut melon. *LWT- Food Science and Technology*, 41, 1862–1870, 2008.

72. R.D. Hagenmaier and P.E. Shaw, Moisture permeability of edible films made with fatty acid and (hydroxypropyl) methyl cellulose. *Journal of Agricultural and Food Chemistry*, 38, 1799–1803, 1990.

73. I.K. Greener and O. Fennema, Barrier properties and surface characteristics of edible, bilayer films. *Journal of Food Science*, 54, 1393–1399, 1989.

74. V. Sapru and T.P. Labuza, Dispersed phase concentration effect on water vapor permeability in composite methyl cellulose-stearic acid edible films. *Journal of Food Processing and Preservation*, 18, 359–368, 1994.

75. T.H. McHugh, J.F. Aujard, and J.M. Krochta, Plasticized whey protein edible films, water vapor permeability properties *Journal of Food Science*, 59, 416–419, 1994.

76. R.J. Avena-Bustillos and J.M. Krochta, Water vapor permeability of caseinate-based films as affected by pH, calcium cross linking, and lipid content. *Journal of Food Science*, 58, 904–907, 1993.

77. I. Arvanitoyannis, A. Nakayama, and S. Aiba, Edible films made from hydroxypropyl starch and gelatin and plasticized by polyols and water. *Carbohydrate Polymers*, 36, 105–119, 1998.

78. S.Y. Ryu, J.W. Rhim, H.J. Roh, and S.S. Kim, Preparation and physical properties of zeincoated high-amylose corn starch film. *LWT-Food Science and Technology*, 35, 680–686, 2002.

79. L.C. Bertana, P.S. Tanada-Palmua, A.C. Sianib, and C.R.F. Grosso, Effect of fatty acids and 'Brazilian elemi' on composite films based on gelatin. *Food Hydrocolloids*, 19, 73–82, 2005.

80. N. Cao, Y. Fua, and Y. He, Preparation and physical properties of soy protein isolate and gelatin composite films. *LWT-Food Science and Technology*, 35, 680–686, 2002.

81. J.W. Rhim, J.H. Lee, and K.W. Perry, Mechanical and barrier properties of biodegradable soy protein isolate-based films coated with polylactic acid. *LWT-Food Science and Technology*, 40, 232–238, 2007.

82. L.G. Williams, Process for coating low moisture fruits. U.S., patent 3, 406, 078, 1968.

83. P.S. Tanada-Palmu and C.R.F. Grosso, Effect of edible wheat gluten-based films and coatings on refrigerated strawberry *(Fragaria ananassa)* quality. *Postharvest Biology and Technology*, 36, 199–208, 2005.

84. E. Pennisi, Sealed in (plastic) edible film. Sci. News, 141, 12, 1992.

85. J.M. Krochta, J.S. Hudson, W.M. Camirand, and A.E. Pavlath, Edible films for lightly processed fruits and vegetables. *American Society of Agricultural Engineers*, 88, 6523, 1988.

86. R.J. Avena-Bustillos, L.A. Cisneros-Zevallos, J.M. Krochta, and M.E. Saltveit, Application of casein-lipid edible film emulsions to reduce white blush on minimally processed carrots. *Postharvest Biology and Technology*, 4, 319–329, 1994.

87. R.J. Avena-Bustillos, J.M. Krochta, and M.E. Saltveit, Water vapor resistance of Red Delicious apples and celery sticks coated with edible caseinate-acetylated monoglyceride films. *Journal of Food Science,* 62, 351–354, 1997.

88. R.J. Avena-Bustillos, J.M. Krochta, M.E. Saltveit, R.J. Rojas-Villegas, and J.A. Sauceda-Perez, Optimization of edible coating formulations on zucchini to reduce water loss. *Journal of Food Engineering*, 21, 197–214, 1994.

89. M.B. Perez-Gago, C. Rojas, del M.A. Rio, Effect of hydroxypropyl methylcellulose-lipid edible composite coatings on plum (cv. Autumn giant) quality during storage. *Journal of Food Science*, 68, 879–883, 2003.

90. M.B. Perez-Gago, M. Serra, del M.A. Rio, Color change of fresh-cut apples coated with whey protein concentrate-based edible coatings. *Postharvest Biology and Technology*, 39, 84–92, 2006.

91. C. Rojas-Argudo, M.B. Perez-Gago, del M.A. Rio, Postharvest quality of coated cherries cv. 'Burlat' as affected by coating composition and solids content. *Food Science and Technology International*, 11, 417–424, 2005.

92. H. Togrul and N. Arslan, Extending shelf-life of peach and pear by using CMC from sugar beet pulp cellulose as a hydrophilic polymer in emulsions. *Food Hydrocolloids,* 18, 215–226, 2004.

93. H. Togrul and N. Arslan, Carboxymethyl cellulose from sugar beet pulp cellulose as a hydrophilic polymer in coating of apples. *Journal of Food Science and Technology*, 42, 139–144, 2005.

94. F.S. Kittur, N. Saroja, S. Habibunnisa, and R.N. Tharanathan, Polysaccharide based composite coating formulations for shelf life extension of fresh banana and mango. *European Food Research and Technology,* 213, 306–311, 2001.

95. P.C. Srinivasa, B. Revathy, M.N. Ramesh, Harish K.V. Prashanth, and R.N. Tharanathan, Storage studies of mango packed using biodegradable chitosan films. *Storage Technology,* 215, 504–508, 2002.

96. M. Maqbool, A. Ali, S. Ramachandran, D.R. Smith, and P.G. Alderson, Control of postharvest anthracnose of banana using a new edible composite coating. *Crop Protection,* 29, 1136–1141, 2010.

97. P.H. Munoz, E. Almenar, V.D. Valle, D. Velez, and R. Gavar, Effect of chitosan coating combined with postharvest calcium treatment on strawberry *(Fragaria ananassa)* quality during refrigerated storage. *Journal of Food Chemistry,* 110, 428–435, 2008.

98. Y.W. Yu, H. Li, D. Jinhua, and Y.Z. Ren, Study of Natural Film with Chitosan Combining Phytic Acids on Preservation of Fresh-cutting Lotus Root. *Journal of Chinese Institute Food Science and Technology*, 12, 131–136, 2012.

99. Q.P. Zhong and W.S. Xia, Effect of 1-methylcyclopropene and/or chitosan coating treatments on storage life and quality maintenance of Indian jujube fruit. *LWT-Food Science and Technology,* 40, 404–411, 2007.

100. M. Zhang, G. Xiao, G. Luo, J. Peng, and V.M. Salokhe, Effect of coating treatments on the extension of the shelf-life of minimally processed cucumber. *International Agrophysics*, 18, 97–102, 2004.

101. L. Atares, J. Bonilla, and A. Chiralt, Characterization of sodium caseinate-based edible films incorporated with cinnamon or ginger essential oils. *Journal of Food Engineering*, 100, 678–687, 2010.

102. L. Sanchez-Gonzalez, C. Gonzalez-Martinez, A. Chiralt, and M. Chafer, Physical and

antimicrobial properties of chitosan-tea tree essential oil composite films. *Journal of Food Engineering*, 98, 443–452, 2010.

103. H. Korhonen, Technology options for new nutritional concepts. *International Journal of Dairy Technology*, 55, 79–88, 2005.

104. P. Appendini and J.H. Hotchkiss, Review of antimicrobial food packaging. *Innovative Food Science and Emerging Technologies*, 3, 113–126, 2002.

105. A. Cagri, Z. Ustunol, and E.T. Ryser, Antimicrobial edible films and coatings. *Journal of Food Protection*, 67, 833–848, 2004.

106. L. Sanchez-Gonzalez, M. Vargas, C. Gonzalez-Martinez, A. Chiralt, and M. Chafer, Characterization of edible films based on hydroxypropylmethylcellulose and tea tree Essentials oil. *Food Hydrocolloids*, 23, 2102–2109, 2009.

107. B. Ouattara, R. Simard, G. Piette, A. Begin, and R.A. Holley, Inhibition of surface spoilage bacteria in processed meats by application of antimicrobial films prepared with chitosan. *International Journal of Food Microbiology*, 62, 139–148, 2000.

108. M.A. Garcia, M.N. Martino, and N.E. Zaritzky, Starch-based coatings, effect on refrigerated strawberry *(Fragaria ananassa)* quality. *Journal of the Science of Food and Agriculture*, 76, 411–420, 1998.

109. S.I. Park, M.A. Daeschel, and Y. Zhao, Functional properties of antimicrobial lysozymechitosan composite films. *Journal of Food Science*, 69, 215–221, 2004.

110. N.S. Hettiarachchy and E. Satchithanandam, Inventors; The Board of Trustees for the Univ. of Arkansas, assignee. 2007 Jan 1. *Organic acids incorporated edible antimicrobial films.* U.S. 2007, patent 7, 160, 580.

111. Kyu W.N. Kyu, P. Jitareerat, S. Kanlayanarat, and S. Sangchote, Effects of cinnamon extract, chitosan coating, hot water treatment and their combinations on crown rot disease and quality of banana fruit. *Postharvest Biology and Technology*, 45, 333–340, 2007.

112. Y. Jiang and Y. Li, Effect of chitosan coating on postharvest life and quality and longan fruit. *Food Chemistry*, 73, 39–143, 2001.

113. H. Li and T. Yu, Effect of chitosan on incidence of brown rot, quality and physiological attributes of postharvest peach fruit. *Journal of the Science of Food and Agriculture*, 81, 269–274, 2000.

114. El A. Ghaouth, R. Ponnampalam, F. Castaigne, and J. Arul, Chitosan coating to extend the storage life of tomatoes. *HortScience*, 27, 1016–1018, 1992.

115. P.J. Chien and C.C. Chou, Antifungal activity of chitosan and its application to control post-harvest quality and fungal rotting of Tankan citrus fruit *(Citrus tankan* Hayata). *Journal of the Science of Food and Agriculture*, 86, 1964–1969, 2006.

116. De G. Capdeville, C.L. Wilson, S.V. Beer, and J.R. Aist, Alternative disease control agents induce resistance to blue mold in harvested “Red Delicious” apple fruit. *Phytopathology*, 92, 900–908, 2002.

117. T. Wu, S. Zivanovic, F.A. Draughon, W.S. Conway, and C.E. Sams, Physicochemical properties and bioactivity of fungal chitin and chitosan. *Journal of Agricultural and Food Chemistry*, 53, 3888–3894, 2005.

118. M.V.B. Reddy, P. Angers, F. Castaigne, and J. Arul, Chitosan effects on blackmold rot and pathogenic factors produced by *Alternaria alternata* in postharvest tomatoes. *Journal of the American Society for Horticultural Science*, 125, 742–747, 2000.

119. J. Liu, S. Tian, X. Meng, and Y. Xu, Effects of chitosan on control of postharvest diseases and physiological responses of tomato fruit. *Postharvest Biology and Technology,* 44, 300–306, 2007.

120. C. Han, C. Lederer, M. McDaniel, and Y. Zhao, Sensory evaluation of fresh strawberries (*Fragaria ananassa*) coated with chitosan-based edible coatings. *Journal of Food Science*, 70, 172–178, 2004.

121. C. Han, Y Zhao, S.W. Leonard, and M.G. Traber, Edible coatings to improve storability and enhance nutritional value of fresh and frozen strawberries *(Fragaria ananassa)* and raspberries *(Rubus ideaus). Postharvest Biology and Technology,* 33, 67–78, 2004.

122. M. Vargas, A. Albors, A. Chiralt, and C. GonzalezMartinez, Quality of cold-stored strawberries as affected by chitosan-oleic acid edible coatings. *Postharvest Biology and Technology*, 41, 164–171, 2006.

123. S. Bautista-Banos, M. Hernandez-Lopez, E. Bosquez-Molina, and C.L. Wilson, Effect of chitosan and plant extracts on growth of Colletotrichum gloeosporoides, anthracnose levels and quality of papaya fruit. *Crop Protection,* 22, 1087–1092, 2003.

124. J. Sangsuwan, N. Rattanapanone, and P. Rachtanapun, Effect of chitosan/methyl cellulose films on microbial and quality characteristics of fresh-cut cantaloupe and pineapple. *Postharvest Biology and Technology*, 49, 403–410, 2008.

125. F. Cong, Y. Zhang, and W. Dong, Use of surface coatings with natamycin to improve the storability of Hami melon at ambient temperature. *Postharvest Biology and Technology*, 46, 71–75, 2007.

126. R. Zhuang, L.R. Beuchat, M.S. Chinnan, R.L. Shewfelt, and Y.W. Huang, Inactivation of Salmonella montevideoon tomatoes by applying cellulose-based films. *Journal of Food Protection,* 59, 808–812, 1996.

127. R.M. Raybaudi-Massilia, J. Mosqueda-Melgar, and O. Martin-Belloso, Edible alginate-based coating as carrier of antimicrobials to improve shelf-life and safety of fresh-cut melon. *International Journal of Food Microbiology*, 121, 313–327, 2008.

128. A.C. Seydim and G. Sarikus, Antimicrobial activity of whey protein based edible films incorporated with oregano, rosemary and garlic essential oils. *Food Research International*, 39, 639–644, 2006.

129. M.A. Rojas-Grau, R.J. Avena-Bustillos, M. Friedman, P.R. Henika, O. Martin-Belloso, and T.H. McHugh, Mechanical, barrier, and antimicrobial properties of apple puree edible films containing plant essential oils. *Journal of Agricultural and Food Chemistry*, 54, 9262–9267, 2006.

130. J.G. Kim, A.E. Yousef, and G.W. Chism, Applications of ozone for enhancing the microbiological safety and quality of foods, a review. *Journal of Food Protection,* 62, 1071–1087, 1999.

131. L.R. Beuchat, B.V. Nail, B.B. Adler, and M.R.S. Clavero, Efficacy of spray application of chlorine in killing pathogenic bacteria on raw apples, tomatoes, and lettuce. *Journal of Food Protection,* 61, 1305–1311, 1998.

132. D. Beltran, M.V. Selma, J.A. Tudela, and M.I. Gil, Effect of different sanitizers on microbial and sensory quality of fresh-cut potato strips stored under modified atmosphere or vacuum packaging. *Postharvest Biology and Technology,* 37, 37–46, 2005.

133. Food and Drug Administration (FDA). CFR Title 21, Foods and CFR Drugs, Part 172, Food

additives permitted for direct addition to food for human CFR consumption, Subpart C, Coatings, films and related substances. Silver MD. Spring, 2012, http//www.accessdata.fda.gov/scripts/cdrh/cfdocs/cfCFR/CFRSearch.cfm

134. J.L. Smilanick, C. Crisosto, and F. Mlikota, Postharvest use of ozone on fresh fruit. *Perishables Handling*, 99, 10–14, 1999.

135. J. Zawistowski, C.G. Biliaderis, and N.A.M. Eskin, Polyphenol oxidases. In D.S. Robinson, and N.A.M. Eskin (Eds.), *Oxidative enzymes in foods*, London: Elsevier, pp. 217–273, 1991.

136. E.A. Baldwin, M.O. Nisperos-Carriedo, P.E. Show, and J.K. Burns, Effect of Coatings and Prolonged Storage Conditions on Fresh Orange Flavor Volatiles, Degrees Brix, and Ascorbic Acid Levels. *Journal of Agricultural and Food Chemistry*, 43, 1321–1331, 1995.

137. I.T. Agar, R. Massantini, B. Hess-Pierce, and A.A. Kader, Postharvest CO_2 and ethylene production and quality maintenance of fresh-cut kiwifruit slices. *Journal of Food Science*, 64, 433–440, 1999.

138. J.G. Buta, H.E. Moline, D.W. Spaulding, and C.Y. Wang, Extending storage life of fresh-cut apples using natural products and their derivatives. *Journal of Agricultural and Food Chemistry*, 47, 1–6, 1999.

139. L. Dorantes-Alvarez, L. Parada-Dorantes, A. Ortiz-Moreno, T. Santiago-Pineda, A. Chiralt-Boix, and G. Barbosa-Canovas, Effect of anti-browning compounds on the quality of minimally processed avocados. *Food Science and Technology International*, 4, 107–113, 1998.

140. J.R. Gorny, B. Hess-Pierce, and A.A. Kader, Quality changes in fresh-cut peach and nectarine slices as affected by cultivar storage atmosphere and chemical treatments. *Journal of Food Science*, 64, 429–432, 1999.

141. R.C. Soliva-Fortuny, N. Grigelmo-Miguel, I. Odriozola-Serrano, S. Gorinstein, and O.Martin-Belloso, Browning evaluation of ready-to-eat apples as affected by modified atmosphere packaging. *Journal of Agricultural and Food Chemistry*, 49, 3685–3690, 2001.

142. R.C. Soliva-Fortuny, N. Grigelmo-Miguel, I. Hernando, M.A. Lluch, and O. Martin-Belloso, Effect of minimal processing on the textural and structural properties of fresh-cut pears. *Journal of Agricultural and Food Chemistry*, 82, 1682–1688, 2002.

143. H.R. Bolin and C.C. Huxsoll, Effect of preparation procedures and storage parameters on quality retention of salad-cut lettuce. *Journal of Food Science*, 56, 60–67, 1991.

144. R. Couture, M.I. Cantwell, D. Ke, and M.E. Saltveit, Physiological attributes and storage life of minimally processed lettuce. *HortScience*, 28, 723–725, 1993.

145. G. Lopez-Galvez, M.E. Saltveit, and M.I. Cantwell, The visual quality of minimally processed lettuce stored in air or controlled atmospheres with emphasis on romaine and iceberg types. *Postharvest Biology and Technology*, 8, 179–190, 1996.

146. I. Babic, M.J. Amiot, C. Nguyen, and S. Aubert, Changes in phenolic content in fresh ready-to-use shredded carrots during storage. *Journal of Food Science*, 58, 351–356, 1993.

147. L.R. Howard, L.E. Griffin, and Y. Lee, Steam treatment of minimally processed carrot sticks to control surface discoloration. *Journal of Food Science*, 59, 356–358, 1994.

148. S.T. Talcott, and L.R. Howard, Chemical and sensory quality of processed carrot puree as influenced by stress-induced phenolic compounds. *Journal of Agricultural and Food Chemistry*, 47, 1362–1366, 1999.

149. L.R. Howard and T. Dewi, Minimal processing and edible coating effects on composition and sensory quality of mini-peeled carrots. *Journal of Food Science,* 61, 643–645, 1996.

150. L.R. Howard and L.E. Griffin, Lignin formation and surface discoloration of minimally processed carrot sticks. *Journal of Food Science,* 58, 1065–1067, 1993.

151. N. Brancoli and G.V. Barbosa-Canovas, Quality changes during refrigerated storage of packaged apple slices treated with polysaccharide films. In: G.V. Barbosa-Canovas and G.W. Gould (Eds.), *Innovations in food processing.* Pennsylvania, Technomic Publishing Co., 2000, pp. 243–254.

152. G.I. Olivas, J.J. Rodriguez, and G.V. Barbosa-Canovas, Edible coatings composed of methylcellulose, steric acid, and additives to preserve quality of pear wedges. *Journal of Food Processing and Preservation,* 27, 299–320, 2003.

153. A.G. Ponce, S.I. Roura, del C.E. Valle, and M.R. Moreira, Antimicrobial and antioxidant activities of edible coatings enriched with natural plant extracts, *in vitro* and *in vivo* studies. *Postharvest Biology and Technology,* 49, 294–300, 2008.

154. H.A.A. Eissa, Effect of chitosan coating on shelf-life and quality of fresh-cut mushroom. *Polish Journal of Food and Nutrition Sciences,* 58, 95–105, 2008.

155. J. Hui-Min, H. To, L. Li-Ping, and Z. Hai-Ying, Effects of edible coatings on browning of fresh-cut peach fruits. *Transactions of the Chinese Society of Agricultural Engineering,* 25, 282–286, 2009.

156. J.M. Garcia, S. Herrera, and A. Morilla, Effects of postharvest dips in calcium chloride on strawberry. *Journal of Agricultural and Food Chemistry,* 44, 30–33, 1996.

157. R.C. Soliva-Fortuny, M.A. Lluch, A. Quiles, N. Grigelmo-Miguel, and O. Martin-Belloso, Evaluation of textural properties and microstructure during storage of minimally processed apples. *Journal of Food Science,* 68, 312–317, 2003.

158. B.W. Poovaiah, Role of calcium in prolonging storage life of fruits and vegetables. *Food Technology,* 40, 86–89, 1986.

159. G.L. Main, J.R. Morris, and E.J. Wehunt, Effect of preprocessing treatment on the firmness and quality characteristics of whole and sliced strawberries after freezing and thermal processing. *Journal of Food Science,* 51, 391–394, 1986.

160. I. Luna-Guzman, D.M. Barrett, Comparison of calcium chloride and calcium lactate effectiveness in maintaining shelf stability and quality of fresh-cut cantaloupe. *Postharvest Biology and Technology,* 19, 61–72, 2000.

161. P. Hernandez-Munoz, E. Almenar, V.D. Valle, D. Velez, and R. Gavara, Effect of chitosan coating combined with postharvest calcium treatment on strawberry quality during refrigerated storage. *Food Chemistry,* 110, 428–435, 2008.

162. M.A. Rojas-Grau, M.S. Tapia, and O. Martin-Belloso, Using polysaccharide-based edible coatings to maintain quality of fresh cut Fuji apples. *LWT-Food Science and Technology,* 41, 139–147, 2008.

163. G. Oms-Oliu, R. Soliva-Fortuny, and O. Martin-Belloso, Edible coatings with antibrowning agents to maintain sensory quality and antioxidant properties of fresh-cut pears. *Postharvest Biology and Technology,* 50, 87–94, 2008.

164. G.I. Olivas, D.S. Mattinson, and G.V. Barbosa-Canovas, Alginate coatings for preservation of minimally processed 'Gala' apples. *Postharvest Biology and Technology,* 45, 89–96, 2007.

165. I. Luna-Guzman, M. Cantwell, and D.M. Barrett, Fresh-cut cantaloupe, effects of $CaCl_2$ dips and heat treatments on firmness and metabolic activity. *Postharvest Biology and Technology,* 17, 201–213, 1999.

166. M.S. Tapia, M.A. Rojas-Grau, A. Carmona, F.J. Rodriguez, R. Soliva-Fortuny, and O. Martin-Belloso, Use of alginate and gellan-based coatings for improving barrier, texture and nutritional properties of fresh-cut papaya. *Food Hydrocolloids,* 22, 1493–1503, 2008.

167. P. Hernandez-Munoz, E. Almenar, M.J. Ocio, and R. Gavara, Effect of calcium dips and chitosan coatings on postharvest life of strawberries *(Fragaria ananassa). Postharvest Biology and Technology*, 39, 247–253, 2006.

168. Y. Mei, Y. Zhao, J. Yang, H.C. Furr, Using edible coating to enhance nutritional and sensory qualities of baby carrots. *Journal of Food Science,* 67, 1964–1968, 2002.

169. D. Restuccia, U.G. Spizzirri, O.I. Parisi, G. Cirillo, M. Curcio, F. Iemma, F. Puoci, G. Vinci, and N. Picci, New EU regulation aspects and global market of active and intelligent packaging for food industry applications. *Food Control,* 21, 1425–1435, 2010.

170. J.W. Rhim, P.K.W. Ng, Natural biopolymer-based nanocomposite films for packaging applications. *Critical Reviews in Food Science and Nutrition,* 47, 411–433, 2007.

171. R. Shotornvit, J. Rhim, S. Hong, Effect of nano-clay type on the physical and antimicrobial properties of whey protein isolate/ clay composite films. *Journal of Food Engineering,* 91, 468–473, 2009.

172. A. Casariego, B.W.S. Souza, M.A. Cerqueira, J.A. Teixeira, L. Cruz, R. Diaz, and A.A. Vicente, Chitosan/clay films properties as affected by biopolymer and clay micro/nanoparticles' concentrations. *Food Hydrocolloids*, 23, 1895–1902, 2009.

173. X. Tang, S. Alavi, and T.J. Herald, Effect of plasticizers on the structure and properties of starch-clay nanocomposite films. *Carbohydrate Polymers*, 74, 552–558, 2008.

174. De M.R. Moura, F.A. Aouada, R.J. Avena-Bustillos, T.H. McHugh, J.M. Krochta, and L.H.C. Mattoso, Improved barrier and mechanical properties of novel hydroxypropyl methylcellulose edible films with chitosan/tripolyphosphate nanoparticles. *Journal of Food Engineering*, 92, 448–453, 2009.

175. C. Bilbao-Sainz, R.J. Avena-Bustillos, D.F. Wood, T.G. Williams, and T.H. McHugh, Composite edible films based on hydroxypropyl methylcellulose reinforced with microcrystalline cellulose nanoparticles. *Journal of Agricultural and Food Chemistry*, 58, 3753–3760, 2010.

176. H. Tang, H. Xiong, S. Tang, and P. Zou, A starch-based biodegradable film modified by nano silicon dioxide. *Journal of Applied Polymer Science,* 113, 34–40, 2009.

177. S. Droby, M. Wisniewski, D. Macarisin, and C. Wilson, Twenty years of postharvest biocontrol research, is it time for a new paradigm? *Postharvest Biology and Technology,* 52, 137–145, 2009.

178. M.O. Nisperos-Carriedo, E.A. Baldwin, and P.E. Shaw, Development of an edible coating for extending postharvest life of selected fruits and vegetables. Florida State Horticultural Society, 104, 122–125, 1992.

179. L.R. Howard, T. Dewi, Sensory, microbiological and chemical quality of mini-peeled carrots as affected by edible coating treatment. Journal of Food Science, 60, 142–144, 1995.

180. C.M. Elson, E.R. Hayes, Development of the differentially permeable fruit coating Nutri-Save® for the modified atmosphere storage of fruit. In: Proceedings of the 4th National Controlled

Atmosphere Research Conference, Controlled Atmosphere for Storage and Transport of Perishable Agricultural Commodities, Raleigh, North Carolina, 1985, pp. 248–262.

181. R.K. Dhall, Advances in edible coatings for fresh fruits and vegetables-Review. *Critical Reviews in Food Science and Nutrition*, 53, 435–450, 2013.

182. K. Kaynas and I.S. Ozelkok, Effect of Semperfresh on postharvest behavior of cucumber (*Cucumis sativus* L.) and summer squash (*Cucurbita pepo* L.) fruits. *Acta Horticulturae,* 492, 213–220, 1999.

183. S.R. Drake, J.K. Fellman, and J.W. Nelson, Postharvest use of sucrose polyesters for extending the shelf-life of stored 'Golden Delicious' apples. *Journal of Food Science,* 52, 685–690, 1987.

184. O.E. Tasdelen and L. Bayindirli, Controlled atmosphere storage and edible coating effects on storage life and quality of tomatoes. *Journal of Food Processing and Preservation*, 22, 303–320, 1998.

185. S. Yurdugul, Preservation of quinces by the combination of an edible coating material, Semperfresh, ascorbic acid and cold storage. *European Food Research and Technology*, 220, 579–586, 2005.

186. R. Dhalla and W. Hanson, Effect of permeable coating on the storage life of fruits. II. Pro-Long treatments of mangoes (*Mangifera indica* L. cv. Julie). *International Journal of Food Science and Technology,* 23, 107–112, 1988.

187. J.N. Farber, L.J. Harris, M.E. Parish, L.R. Beuchat, T.V. Suslow, J.R. Gorney, E.H. Garrett, and F.F. Busta, Microbiological safety of controlled and modified atmosphere packaging of fresh and fresh-cut produce. *Comprehensive Reviews in Food Science and Food Safety,* 2, 142–160, 2003.

188. X.H. Chen, C.A. Campbell, L.A. Grant, P. Li, and M. Barth, Effect of nature seal® on maintaining carotene in fresh-cut carrots. *Proceedings of the Florida State Horticultural Society*, 109, 258–259, 1996.

189. F. Fornes, V. Almela, M. Abad, and M. Agusti, Low concentration of chitosan coating reduce water spot incidence and delay peel pigmentation of clementine mandarin fruit. *Journal of the Science of Food and Agriculture,* 85, 1105–1112, 2005.

190. El A. Ghaouth, J. Arul, and R. Ponnampalam, Use of chitosan coating to reduce water loss and maintain quality of cucumber and bell pepper fruits. *Journal of Food Processing and Preservation,* 15, 359–368, 1991.

191. C.M. Elson, E.R. Hayes, and P.K. Lidster, Development of the differentially permeable fruit coating 'Nutri-Save' for the modified atmosphere storage of fruit. In: M. Blankenship, editor. *Controlled atmosphere for storage and transport of perishable agricultural commodities.* N.C. Raleigh, North Carolina State Univ., pp. 248, 1985.

192. D.H. Davies, C.M. Elson, E.R. Hayes, N,O-carboxymethyl chitosan, a new water soluble chitin derivative. In: *Chitin and Chitosan, Source, Chemistry, Biochemistry, Physical Properties, and Application*, G. Skjak-Braek, T. Anthosen, and P. Sandford, Eds., Elsevier Applied Science, New York. 1989, pp. 467–472.

193. R. Diaz-Sobac, A.V. Luna, C.I. Beristain, de la J. Cruz, and H.S. Garcia, Emulsion coating to extend postharvest life of mango (*Mangifera indica* cv. Manila). *Journal of Food Processing and Preservation,* 20, 191–202, 1996.

194. E. Ayranci and S. Tunc, The effect of edible coatings on water and vitamin C loss of apricots (*Armeniaca vulgaris* Lam.) and green peppers (*Capsicum annuum* L.). *Food Chemistry,* 87, 339–342,

2004.

195. H. Togrul and N. Arslan, Carboxymethyl cellulose from sugar beet pulp cellulose as a hydrophilic polymer in coating of mandarin. *Journal of Food Engineering*, 62, 271–279, 2004.

196. C. Vachon, D'G. Aprano, M. Lacroix, and M. Letendre, Effect of edible coating process and irradiation treatment of strawberry (*Fragaria* spp.) on storage-keeping quality. *Journal of Food Science*, 68, 608–612, 2003.

197. M.A. Garcia, M.N. Martino, and N.E. Zaritzky, Plasticized starch-based coatings to improve strawberry (*Fragaria ananassa*) quality and stability. *Journal of Agricultural and Food Chemistry*, 46, 3758–3767, 1998.

198. T.T. Hoa, M.N. Ducamp, M. Lebrun, and E.A. Baldwin, Effect of different coating treatments on the quality of mango fruit. *Journal of Food Quality*, 25, 471–468, 2002.

199. D.B. Worrell, C.M.S. Carrington, and D.J. Huber, The use of low temperature and coatings to maintain storage quality of breadfruit *(Artocarpus altilis)*. *Postharvest Biology and Technology*, 25, 33–40, 2002.

200. O.L. Lau and M. Meheriuk, The effect of edible coatings on storage quality of mcintosh, delicious and spartan apples. *Canadian Journal of Plant Science*, 74, 847–852, 1994.

201. E.A. Baldwin, Edible coatings for fresh fruits and vegetables- Past, present, and future. In: J.M. Krochta, E.A. Baldwin, and M.O. Nisperos-Carriedo, Eds. *Edible coatings and films to improve food quality*. Lancaster, Technomic Publishing Company, Inc., pp. 25–64, 1994.

202. M. Ahmad and I. Khan, Effects of waxing and cellophane lining on chemical quality indices of citrus fruits. *Plant Foods for Human Nutrition*, 37, 47–57, 1987.

203. S. Lerdthanangkul and J.M. Krochta, Edible coating effects on post harvest quality of green bell peppers. *Journal of Food Science*, 61, 176–179, 1996.

204. J.M. Krochta, R.J. Avena-Bustillos, L.A. Cisneros-Zevallos, and M.E. Saltveit, Optimization of edible coatings on minimally processed carrots using response surface methodology. *Transactions of the American Society of Agricultural Engineering*, 36, 801–805, 1993.

205. R. Posey, E.C. Culbertson, and J.C. Westermeier, Clear barrier coating and coated film. U.S. 2005, Patent, 6, 911, 255 B2.

206. M.A. Garcia, M.N. Martino, and N.E. Zaritzky, Composite starch-based coatings applied to strawberries (Fragaria ananassa). *Nahrung Food*, 45, 267–272, 2001.

207. R.M. Raybaudi-Massilia, M.A. Rojas-Grau, J. Mosqueda-Melgar, and O. Martin-Belloso, Comparative study on essential oils incorporated into an alginate-based edible coating to assure the safety and quality of fresh-cut Fuji apples. Journal of Food Protection, 71, 1150–1161, 2008.

208. M.A. Rojas-Grau, R.M. Raybaudi-Massilia, R.C. Soliva-Fortuny, R.J. Avena-Bustillos, T.H. McHugh, and O. Martin-Belloso, Apple puree alginate edible coating as carrier of antimicrobial agents to prolong shelf-life of fresh-cut apples. *Postharvest Biology and Technology*, 45, 254–264, 2007.

209. W. Krasaekoopt and J. Mabumrung, Microbiological evaluation of edible coated fresh-cut cantaloupe. *Kasetsart Journal of Natural Science*, 42, 552–557, 2008.

210. L.T. Pen and Y.M. Jiang, Effects of chitosan coating on shelf life and quality of fresh-cut Chinese water chestnut. *Lebens Wissen Technology*, 36, 359–364, 2003.

211. S.L. Tay and C.O. Perera, Effect of 1-methylcyclopropene treatment and edible coatings on the quality of minimally processed lettuce. *Journal of Food Science,* 69, 131–135, 2004.

212. M. Montero-Calderon, M.A. Rojas-Grau, and O. Martin-Belloso, Effect of packaging conditions on quality and shelf-life of fresh-cut pineapple *(Ananas comosus). Postharvest Biology and Technology,* 50, 182–189, 2008.

213. M.S. Tapia, M.A. Rojas-Grau, F.J. Rodriguez, J. Ramirez, A. Carmona, and O. Martin-Belloso, Alginate- and gellanbased edible films for probiotic coatings on fresh-cut fruits. *Journal of Food Science,* 72, 190–196, 2007.

214. R.L. Shewfelt, S.E. Prussia, A.V.A. Resurreccion, W.C. Hurst, and D.T. Campbell, Quality changes of vine-ripened tomatoes within the postharvest handling system. *Journal of Food Science*, 52, 661–672, 1987.

215. W.R. Miller, D.L. Spalding, L.A. Risse, Decay firmness and color development of Florida bell peppers dipped in chlorine and imazalil and film wrapped. *Proceedings of the Florida State Horticultural Society*, 96, 347–350, 1983.

216. L. Cisneros-Zevallos and J.M. Krochta, Dependence of coating thickness on viscosity of coating solution applied to fruits and vegetables by dipping method. *Journal of Food Science*, 68, 503–510, 2003.

217. S.M. Smith, J. Geeson, and J. Stow, Production of modified atmospheres in deciduous fruits by the use of films and coatings. *HortScience,* 22, 772–776, 1987.

218. P.D. Petracek, H. Dou, and S. Pao, Influence of applied waxes on postharvest physiological behavior and pitting of white grapefruit. *Postharvest Biology and Technology,* 14, 99–106, 1998.

219. S.M. Smith and J.R. Stow, The potential of a sucrose ester coating material for improving the storage and shelf-life qualities of cox's orange pippin apples. *Annals of Applied Biology,* 104, 383–391, 1984.

220. S. Ben-Yehoshua, Individual seal-packaging of fruit and vegetables in plastic film-A new postharvest technique. *HortScience,* 20, 32–37, 1985.

221. D.F. Parra, C.C. Tadini, P. Ponce, and A.B. Lugao, Mechanical properties and water vapor transmission in some blends of cassava starch edible films. *Carbohydrate Polymers,* 58, 475–481, 2004.

222. S. Burt, Essential oils, their antibacterial properties and potential applications in A foods, review. *International Journal of Food Microbiology*, 94, 223–253, 2004.

223. N.F. Iyidogan and A. Bayindirli, Effect of L-cysteine, kojic acid and 4-hexylresorcinol combination on inhibition of enzymatic browning in Amasya apple juice. *Journal of Food Engineering*, 62, 299–304, 2004.

224. F.C. Richard, P.M. Goupy, and J.J. Nicolas, Cysteine as an inhibitor of enzymatic browning. 2. Kinetic studies. *Journal of Agricultural and Food Chemistry,* 40, 2108–2114, 1992.

225. A. Drewnowski and C. Gomez-Carneros, Bitter taste, phytonutrients and the A consumer, review. *American Journal of Clinical Nutrition,* 72, 1424–1435, 2000.

226. K. LeClair, Breaking the sensory barrier for functional foods. *Food Product Design,* 7, 59–63, 2000.

227. L.R. Franssen and J.M. Krochta, Edible coatings containing natural antimicrobials for processed foods. In: Natural Antimicrobials for Minimal Processing of Foods, S. Roller, Ed., CRC Press, Boca

FL. Raton, 2003, pp. 250–262.

228. ED-European Parliament and Council Directive N 95/2/EC. On food additive other than colors and sweeteners. 1995, Available from http,//ec.europa.eu/food/fs/sfp/addit flavor/flav11 en.pdf.

229. ED-European Parliament and Council Directive N 98/72/EC. On food additive other than colors and sweeteners. 1998, Available from http,//ec.europa.eu/food/fs/sfp/addit flavor/flav11 en.pdf.

230. S. Guilbert and N. Gontard, Edible and biodegradable food packaging. In: *Foods and Packaging Materials - Chemical Interactions,* P. Ackermann, M. Jagerstad and T. Ohlsson, (Eds.), The Royal Society of Chemistry, Cambridge, England, pp. 159–168, 1995.

231. A. Nussinovitch, Water Soluble Polymer Applications in Foods. Blackwell Science, Oxford, UK, 2003.

232. USDA-U.S. Food and Drug Administration. Food additive status list. 2006, Available from http://www.cfsan.fda.gov/dms/opa-appa.html. Accessed September 25, 2008.

233. S. Doores, Organic acids. In: Antimicrobials in Food, P.M. Davidson, and A.L. Branen, Eds., Marcel Dekker, Inc., New York, pp. 95–136, 1993.

Chapter 5

Development of Novel Biobased Epoxy Films with Aliphatic and Aromatic Amine Hardeners for the Partial Replacement of Bisphenol A in Primer Coatings

Rafael S. Peres[1,2], Carlos A. Ferreira[1], Carlos Alemán[2,3*], and Elaine Armelin[2,3*]

[1]*Departamento de Engenharia de Materiais, PPGEM, Universidade Federal do Rio Grande do Sul, Porto Alegre (RS), Brazil*

[2]*Departament d'Enginyeria Química, ETSEIB, Universitat Politècnica de Catalunya (UPC), Barcelona, Spain*

[3]*Center for Research in Nano-Engineering (CRnE), Universitat Politècnica de Catalunya (UPC), Barcelona, Spain*

[*]*Corresponding author*: carlos.aleman@upc.edu

Abstract

New insights into epoxidized linseed oil (ELO) reaction with several amine hardeners for partial replacement of diglycidyl ether of bisphenol A (DGEBA) in coatings formulations are discussed. Thermosets formed by ELO and a variety of hardeners have been examined using ^{1}H and ^{13}C nuclear magnetic resonance (NMR), Fourier transform infrared spectroscopy (FTIR), differential scanning calorimetry (DSC), thermogravimetric analysis (TGA), and scanning electron microscope (SEM) techniques. In addition, the mechanical properties, wettability, and swelling of the resulting films have been evaluated. Good properties of ELO cured with diamines, as hexamethylene diamine and *p*-phenylenediamine, were obtained. Both thermosets offer good impermeability to water, which is higher than that of the commercial epoxy resin, fabricated using DGEBA and polyaminoamide, and an excellent thermal stability. The mechanical behavior is also better than the brittle and rigid films obtained from DGEBA-based resins, films exhibiting the elastic-like behavior of rubber materials. This chapter offers new and promising perspectives in the use of vegetable oils for coatings formulations.

Keywords: Thermosetting plastics, vegetable oils, epoxy resin, amine hardener, coatings

5.1 Introduction

Currently, the challenge for manufacturers, which are subject to the interest of consumer by using sustainable materials of biological origin, is to offer materials that not only provide environmental and health benefits but also comply with demanding technical requirements. A clear example of the growing interest in eco-materials is the current use of bio thermoplastic polyurethane (Bio TPU) in the automotive industry [1, 2]. According to Ford Motors Company, all vehicles presently manufactured by this company in North America use soy oil-based foams in the seat cushions, backs and head restraints [3]. However, renewable TPU technology is not a 100% replacement of petroleum-based products. According to industry analysts, soybean oil (SO)-based polyurethane (PU) has a bio-based content between 5% and 60% for flexible and rigid foams to accomplish with the technical requirements of the products.

Bisphenol A (BPA), an organic molecule considered toxic in several sectors and subject of controversy nowadays, is produced in large quantities for use primarily in the production of polycarbonate plastics and epoxy resins. Its adverse effects, supposedly caused in humans, are leading research community and manufacturers efforts to develop alternatives for the partial or total replacement of this compound [4–8]. Numerous items made with BPA, including packaging for food, and both coatings and linings for tins, intensify the concern about health problems [9, 10]. Increase of cancer risk and fetal problems, associated to the exposure of BPA introduced as plasticizer or monomer for polymer fabrication [11, 12], led some countries strictly forbidden BPA use in baby bottles.

The high cost of the petroleum-based products and environmental impact problems also contribute to replace diglycidyl ether of BPA (DGEBA) from coatings formulations by renewable materials [13]. Within this scenario, vegetable oils (VOs) are emerging as promising alternatives for the development of coatings originated from renewable sources [14–21]. Several plants as linseed, castor, soybean, and others can provide oils with singular characteristics, depending of its chemical composition. VOs mainly consist of triglycerides, which can be formed by unsaturated or saturated fatty acids [2]. The number of unsaturations or double bonds determines the reactivity and application of the oil [18]. Linseed oil (LO) is well known in the paint industry due its large number of double bonds, which react with the oxygen in air facilitating the formation of films [22]. This oil is essentially formed by mono-, di-, and tri-unsaturated acids (oleic, linoleic, and linolenic, respectively) and saturated acids (palmitic and stearic) [23, 24], high levels of di- and tri-unsaturated esters favoring the mentioned polymerization reactions upon exposure to air.

Many modifications in the chemical composition of VOs have been proposed in the literature to obtain several types of polymers as was reviewed [2, 18]. Epoxies, polyesters, polyurethanes, and polyamides are some examples of the polymers prepared with VOs [13–20]. Güner *et al.* [25] studied the reactions of different diisocyanates with polyols derived from LO and sunflower oil. The characteristics of the formed films were dependent on the amount and nature of the diisocyanates. Chemical modifications of the castor oil (CO) have been made to produce aminoundecanoic acid, which is a well-known material to produce nylon-11 [26, 27]. On the other hand, in a pioneering work, Warth *et al.* [28] used several modified oils, such as soybean, linseed, and rape seed oils to prepare polyesters networks mixed with DGEBA.

Epoxidation of VOs is an important process used to obtain several kinds of polymers. The epoxidation reaction occurs in the double bonds of the unsaturated oils through the oxidation process

in the presence of peracids [18, 29]. Many works involving the epoxidation process of different VOs and catalysts are reported in the literature [30–37]. Cai *et al.* [30] used peroxyacetic acid (PAA) with sulfuric acid as catalyst in the epoxidation process of the soybean, corn, and sunflower oils. The own authors reported the temperature and reaction time dependence of the epoxidation process. Becchi *et al.* [31] proposed the epoxidation of CO to form hybrid films from inorganic precursors. The procedure of oxirane conversion was based in the use of hydrogen peroxide, acetic and sulfuric acids. The same reagents were used by Goud *et al.* [32] in the epoxidation of mahua oil. The most common procedure in the industry uses peracetic acid with strong acid as catalyst [30, 37]. However, if the reaction is not properly controlled, parallel reactions as oxirane ring opening can occur. Some researchers introduced the use of lipases as catalyst in the epoxidation of VOs [13, 37–39]. This procedure decreases the risk of oxirane ring opening, increasing the efficiency in the conversion of the double bonds. Nevertheless, the high cost of lipases as well as their storage temperature becomes unfavorable factors for this procedure, especially at industrial scale.

The aim of the present book chapter is to evaluate the recent advances and applications of VO in coatings. Another objective will be the study of the curing process among epoxidized linseed oil (ELO) and several amine hardeners to obtain stable and impermeable epoxy films for applications in solvent-borne primer coatings. ELO was chosen as representative epoxidized oil. The main long-term objective is to encourage the use of several epoxidized VOs for a replacement and partial reduction of BPA in the paint market, decreasing the environmental impact and possible health problems caused by this molecule. Within such framework, it is important to keep in mind that DGEBA was used as a model compound to demonstrate the feasibility of ELO crosslinking processes. On the other hand, the amine hardener plays an important role in the curing process, six different aliphatic and aromatic amines are being considered in this work. More specifically, the following series of amines has been evaluated: hexamethylenediamine, *p*-phenylenediamine, *N*,*N*′-bis-(1-methylheptyl)-1,4-phenylenediamine, *N*,*N*′-bis-(2-(phenyl-henyl-hydrazono)-ethylidene)-benzene-1,4-diamine, a commercial hardener Crayamid® 115 (from Cray Valley Co.), and polyhexamethylene biguanide. Polyhexamethylene biguanide hydrochloride is a water-soluble polymeric cationic antibacterial agent (commercially available as Vantocil™, Cosmocil™, and Lavasept™) that has been widely used in industry and hospital buildings. The influence of the molecular architecture, curing conditions, and formulations on thermal, mechanical, and morphological properties of ELO-amine hardeners have been examined and discussed. In addition, new trends in VO application to coatings formulations have been presented.

5.2 Recent Advances on Vegetable Oils Chemistry

In the past few years, chemical modifications of VOs have been mainly focused in the formulation of inorganic–organic hybrid materials. The primary goal is to combine the best properties of the inorganic phase with the best properties of the organic phase. In many cases, properties of the resulting new materials have exhibited surprising improvements. Among VOs, CO, and SO are the most studied. Martinelli and co-workers [40] have investigated the chemical reaction between epoxydized castor oil (ECO) and alkoxysilane, like 3-aminopropyltriethoxysilane (APTES) or tetraethoxysilane (TEOS), to obtain impermeable films for corrosion protection. Similar work has

been published with SO and vinyl trimethoxysilane (VTMS) to obtain SO-polydimethysiloxane interpenetrating polymer networks [41]. Allaudim *et al.* [42] recently reported one synthetic route for the modification of CO with 3-glycidoxypropyltrimethoxysilane (GPTMS), the film swelling properties of the resulting material being better than those of the unmodified oil. Nalawade *et al.* [43] published a work related to the functionalization of SO with fluorine, siloxane and allyl ether molecules via Diels–Alder cycloaddition reactions. These functionalized SOs acted as reactive diluents by reducing the viscosity of the long oil alkyd formulation by up to 86%. This represented an important reduction or partial substitution of volatile organic compounds (VOCs) in coatings processing by using reactive diluents derived from renewable materials.

Although transesterification [44] and amidation [45] allow for the incorporation of several functionalities to VOs based on the choice of alcohol or amine, the absence of hydroxyl groups in the fatty acid chains (unless CO is used) results in long fatty acid chains acting as elastic, unreactive chains. The recent development of thiol-ene click reactions offers promising routes for the preparation of polyols for polyurethane technology. A recent review has been published by Lligadas *et al.* [46].

Several routes have been proposed for the preparation of green polyols [47–49] for further applications in coatings technology. For example, green polyols were synthesized from ESO and CO fatty acids (COFA), by ring-opening reaction promoted with 1,8-diazabicyclo[5.4.0]-undec-7-ene (DBU) or pyridine, as catalyst, and in the absence of solvent. The main goal was the reduction of both the temperature and time required by the reaction between the epoxy from ELO and carboxylic groups from COFA [47, 50], which is usually conducted at high temperatures (approximately 170 °C) and with long cycle times (approximately 8 h) [47, 50].

Other works are devoted to the conversion of VOs to fatty acids for the achievement of water soluble PU dispersions [51, 52]. Ding and Matharu [53] recently reported a review with the transformation of VO fatty acids in potential starting materials for biobased curing agents.

Interesting challenges on VO technology are related to the incorporation of nanoparticles (NPs), nanotubes (NTs), or nanowires (NWs) of metallic and ceramic compounds to VO-based polymers. For example, Ganji *et al.* [54] prepared gold NPs and NWs with CO–polyethylene glycol-based PU to fabricate porous composite scaffolds for biomedical application. The own authors obtained higher cross-link density and cell adhesion and proliferation with CO-polyethylenglycol (PEG)-PU containing 50 ppm gold nanotube/nanowire than with pure PU. Karak and co-workers [55] developed new nanocomposites with CO-based hyperbranched PU and graphene oxide NPs. The nanocomposite demonstrated extensive enhancement in mechanical properties after the incorporation of a small amount of graphene oxide.

The inclusion of conductive nanomaterials in VO-based polymers was also explored. An interesting work has been described by Gharibi *et al.* [56], who synthesized new poly(urethane-*co*-pyrrole)s derived from CO as anticorrosion coatings for stainless steel with promising results. Karak and co-workers [44] also developed nanocomposites with polyaniline nanofibers added to CO, which was converted in a hyperbranched polyesteramide by transamidation reaction with diethanol amide. The new polymer was applied as a bio-based antistatic material. Gurunathan *et al.* [57] modified CO with isophorone diisocyanate for the production of blends of CO-based PU with polylactic acid (PLA). The resulting films showed very good mechanical properties with elastic deformation promoted by PLA matrix. Applications of chemically modified VOs will be briefly discussed later.

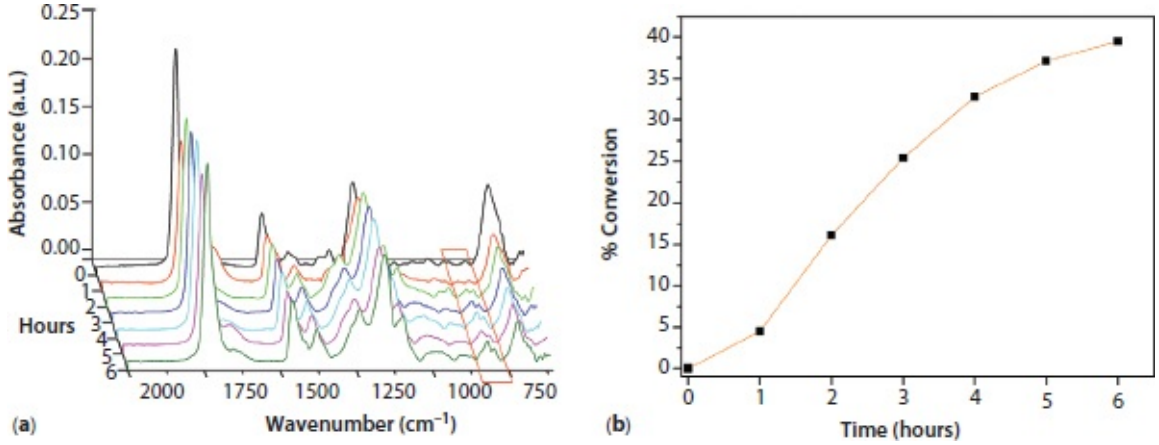
5.3 Control of the Epoxidation Reaction of Vegetable Oils

Epoxidized oils and derivatives are epoxidized fatty acid esters from naturally occurring long chain fatty acid sources. Several approaches have been described for the process of epoxidation, employing either PAA, enzymes, hydrogen peroxide, acid ion exchange resin, metal catalyst or others [58]. Taking as example the epoxidation of SO by PAA, generated *in situ*, described in the literature [30], proved that kinetic rate of epoxidation conversion depends on the VO nature. The epoxidation reaction is an important step which must be carefully controlled, due to its exothermic reaction and oxirane ring opening probability. Therefore, overheating must be avoided and oxirane ring formation must be followed by chemical or analytical analyses.

Here, we will describe the epoxidation reaction of LO and its characterization. The synthesis of ELO was adapted from the literature [30, 31], which can be used for a detailed information about the experimental procedure of synthesis. In order to monitor the epoxidation conversion of the LO, a small amount of reaction product is taken out every hour from the round-bottom flask and a Fourier transform infrared spectroscopy (FTIR) spectrum in absorbance mode is recorded. The area corresponding to the epoxy group at 827 cm^{-1} peak is compared with the analytical standard ELO (Sigma-Aldrich, CAS Number 8016-11-3), with known epoxidation ratio (~9%) to calculate the epoxidation conversion [30]. All areas are normalized to the 1700 cm^{-1} area, corresponding to the ester before the conversion calculation. This procedure was used to estimate the ideal reaction time for epoxy formation.

The temporal evolution of FTIR spectrum associated to the epoxidation reaction of the LO is shown in Figure 5.1. The band highlighted in Figure 5.1a is 827 cm^{-1}, corresponding to epoxy group formation. Epoxy band becomes more intense with increasing reaction time. Figure 5.1b shows the epoxidation conversion of the double bonds into oxirane ring with the reaction time. After 5 hours of the reaction, the conversion reaches an almost constant value. In this work the value used for the reaction time was 6 hours since opening of oxirane ring can occur with higher times, reducing the efficiency of the process.

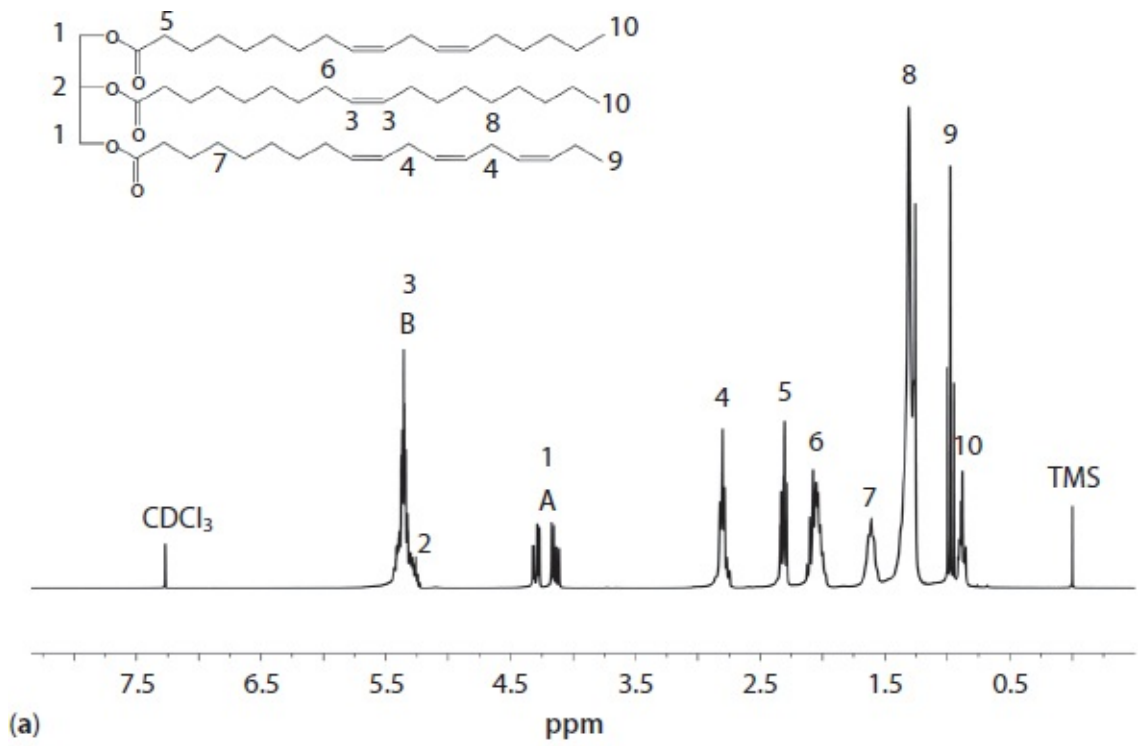
Figure 5.1 (a) FTIR of evolution of LO epoxidation reaction with time. (b) Percentage of LO epoxidation reaction conversion versus time, obtained from 827 cm^{-1} band.



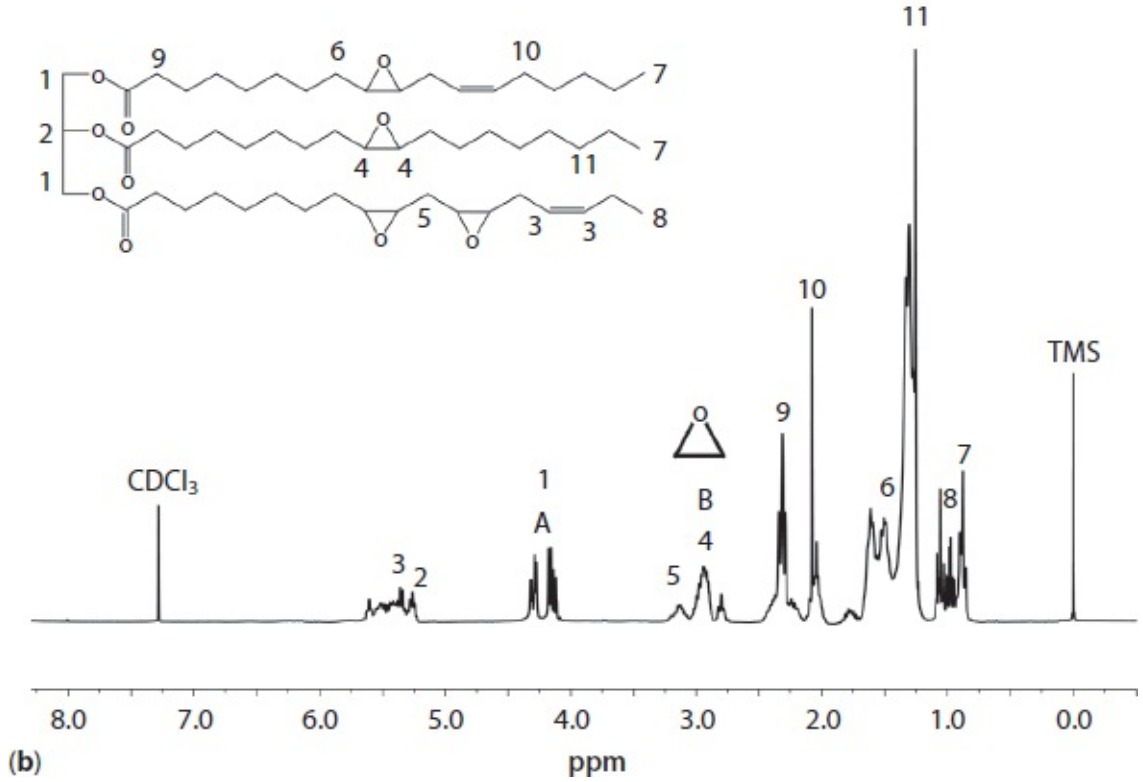
To corroborate the FTIR analyses, the conversion of the double bonds to oxirane rings was also verified by the ^{1}H and ^{13}C nuclear magnetic resonance (NMR) measurements after ELO purification. In this case, the epoxy number was used as parameter to calculate the degree of conversion. Figure 5.2

shows the ^{1}H NMR spectra, labeling of hydrogen atoms in the corresponding molecular structures being included for identification [13, 16, 59, 60]. Integrations of the proton signals arising from methylene beside ester units (–COO–CH_2–) enabled to determine the number of unsaturated groups (–CH=CH–) in the LO samples (Figure 5.2a), whereas the epoxy content in ELO samples was obtained by comparing the integrations of methylene ester (4–4.4 ppm, 2*H*) and epoxy ring (2.7–3.3 ppm, 2H) (Figure 2b). In ELO sample, the resonances from unsaturated groups (5.3–5.6 ppm) do not disappear, confirming the partial epoxidation of LO. The ^{13}C NMR showed in the Figure 5.2c, corroborates the expected chemical structure of ELO [60, 61]. New resonances appear in the ELO spectrum in 59–56 ppm region (Figure 5.2d), which have been attributed to epoxy ring, compared to LO samples (Figure 5.2c). Thus, the ^{1}H NMR, ^{13}C NMR, and FTIR analyses confirm the epoxidation of the LO samples promoted by PAA.

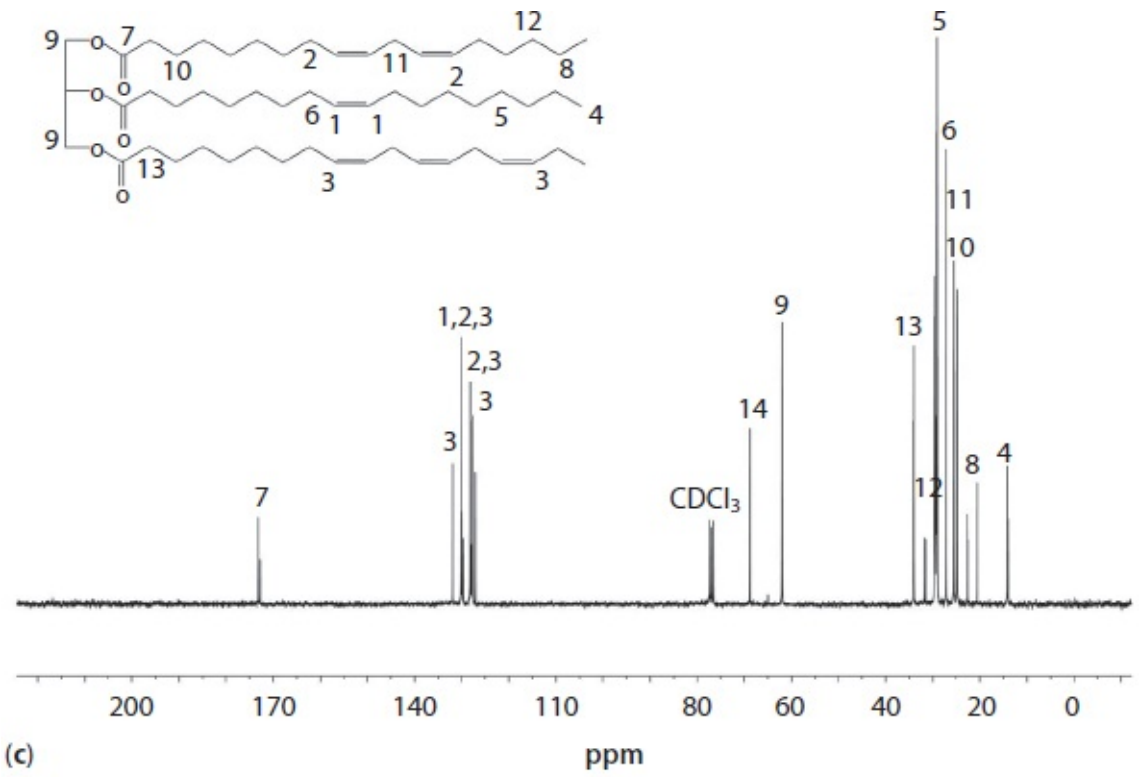
Figure 5.2 (a) and (b) ^{1}H NMR of the LO and ELO, respectively; (c) and (d) ^{13}C NMR of the LO and ELO, respectively.


1
2
1
5
10
6
10
3 3
8
7
4
4
9
3
B
2
1
A
CDCl3
4
5
6
7
8
9
10
TMS
7.5
6.5
5.5
4.5
3.5
2.5
1.5
0.5
ppm

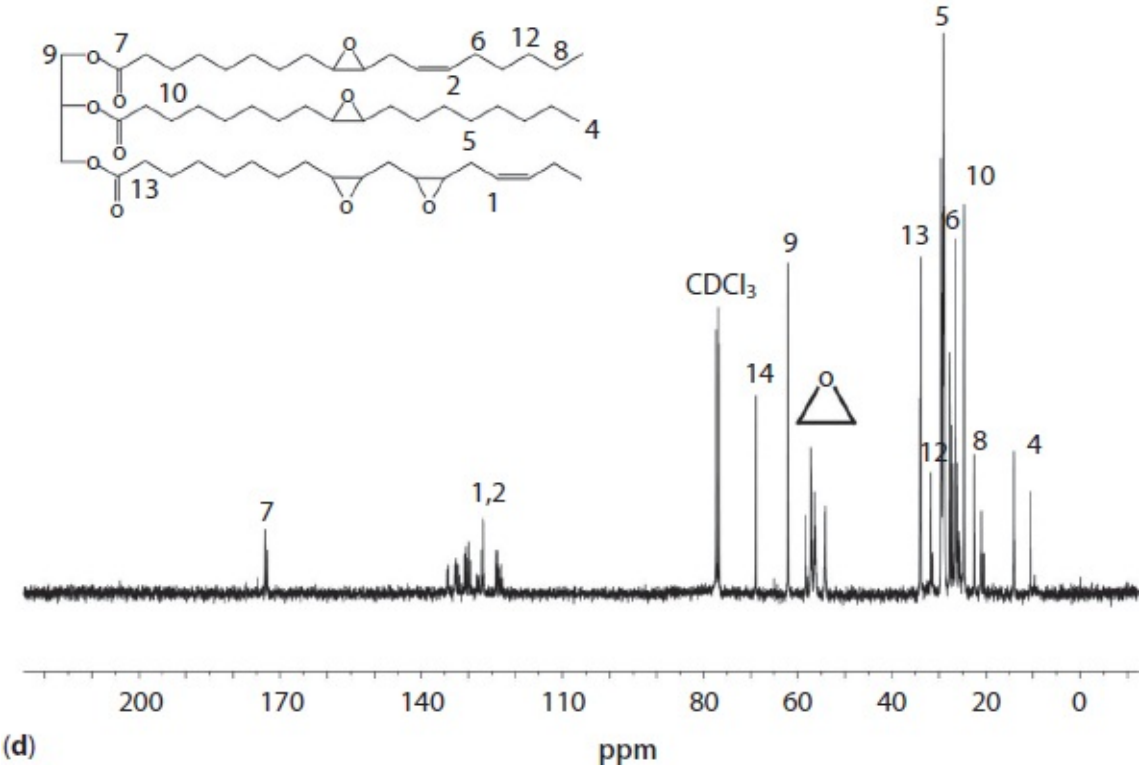
(a)


1
2
1
9
6
10
7
7
4 4
11
5
3 3
8
11
10
TMS
9
7
CDCl3
1
A
B
4
6
8
3
2
5
8.0
7.0
6.0
5.0
4.0
3.0
2.0
1.0
0.0
ppm

(b)



(c)



(d)

The percentage of the epoxidation conversion in ELO was also calculated derived from the ^{1}H NMR spectra for comparison with that of the FTIR method. The number of double bonds per molecule of triglyceride was calculated according to [16]:

$$C = \frac{C}{\text{trigly.mol.}} = \frac{\left[\left(B - A/4\right)/2\right]}{A/4} \quad (5.1)$$

where *A* and *B* are the areas showed in Figure 5.2a. The calculated number of double bonds per

molecule of LO was 6.48. The number of epoxy groups per molecule of triglyceride was determined according to [60]:

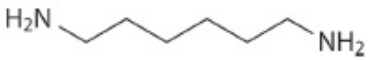
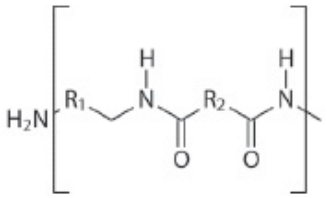
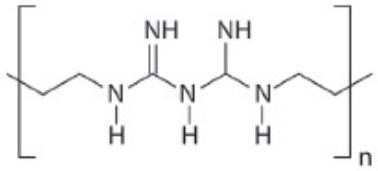
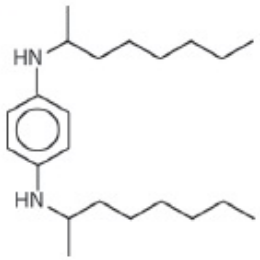
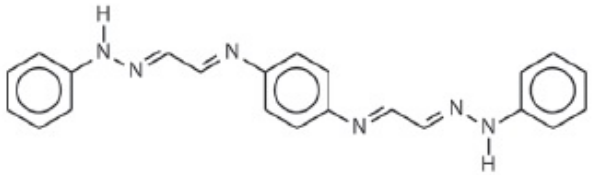
$$\frac{\text{Epoxy group}}{\text{trigly. mol.}} = \frac{B/2}{A/4} \quad (5.2)$$

where *A* and *B* correspond to the areas displayed in the Figure 5.2b. The calculated number of epoxy groups per molecule of ELO was 2.93. Comparison of this value with that of standard ELO (6.9) provides an efficiency of ~42% while the efficiency derived from the FTIR method was ~40%.

5.4 Spectroscopy Characterization of Epoxidized Linseed Oil Cured with Amine Hardeners

Epoxies can be cured with suitable curing agents, like amines, amides, acids and anhydrides, to yield cured polymer with desirable characteristics [14, 62]. Mechanical, thermal and impermeability properties of thermosetting materials used in coatings formulations strongly depend on the curing agent nature and cross-link interaction. Among chemical hardeners, the most important curing agents used for DGEBA are polyamines, polyaminoamides, and anhydrides. In the present study, several amine hardeners were explored for their compatibility and cross-linking performance with ELO. Thus, the freshly synthesized ELO was cured with six different hardeners, which are described in Table 5.1. The weight percentage ratio (epoxy/hardener) for each sample, as well as the conditions used, like temperature and time of film formation, are also included in the table.

Table 5.1 Chemical composition of the hardener and preparation conditions for the films of the epoxy-based coatings studied in the present work.

Hardener		Films		
Hardener	**Hardener name (Abbrev.)**	**Epoxy:Hardener mix ratio[a]**	**Abbrev.**	**Cure temperature/time**
	Hexamethylenediamine (HMDA)	85:15	ELO-HMDA	150 °C/15 h
	*p*-Phenylenediamine (PDA)	85:15	ELO-PDA	150 °C/15 h
	Amino polyamide (Crayamid 115) (C115)	50:50	ELO-C115	150 °C/15 h
	Polyhexamethylene biguanide (PHMB)	75:25	ELO-PHMB	150 °C/15 h
	*N,N'*-bis-(1-methylheptyl)-1,4-phenylenediamine (BMPDA)	60:40	ELO-BMPDA	150 °C/15 h[b] 170 °C/2 h[c]
	*N,N'*-bis-(2-(phenyl-henyl-hydrazono)-ethylidene)-benzene-1,4-diamine (BPPDA)	65:35	ELO-BPPDA	150 °C/15 h

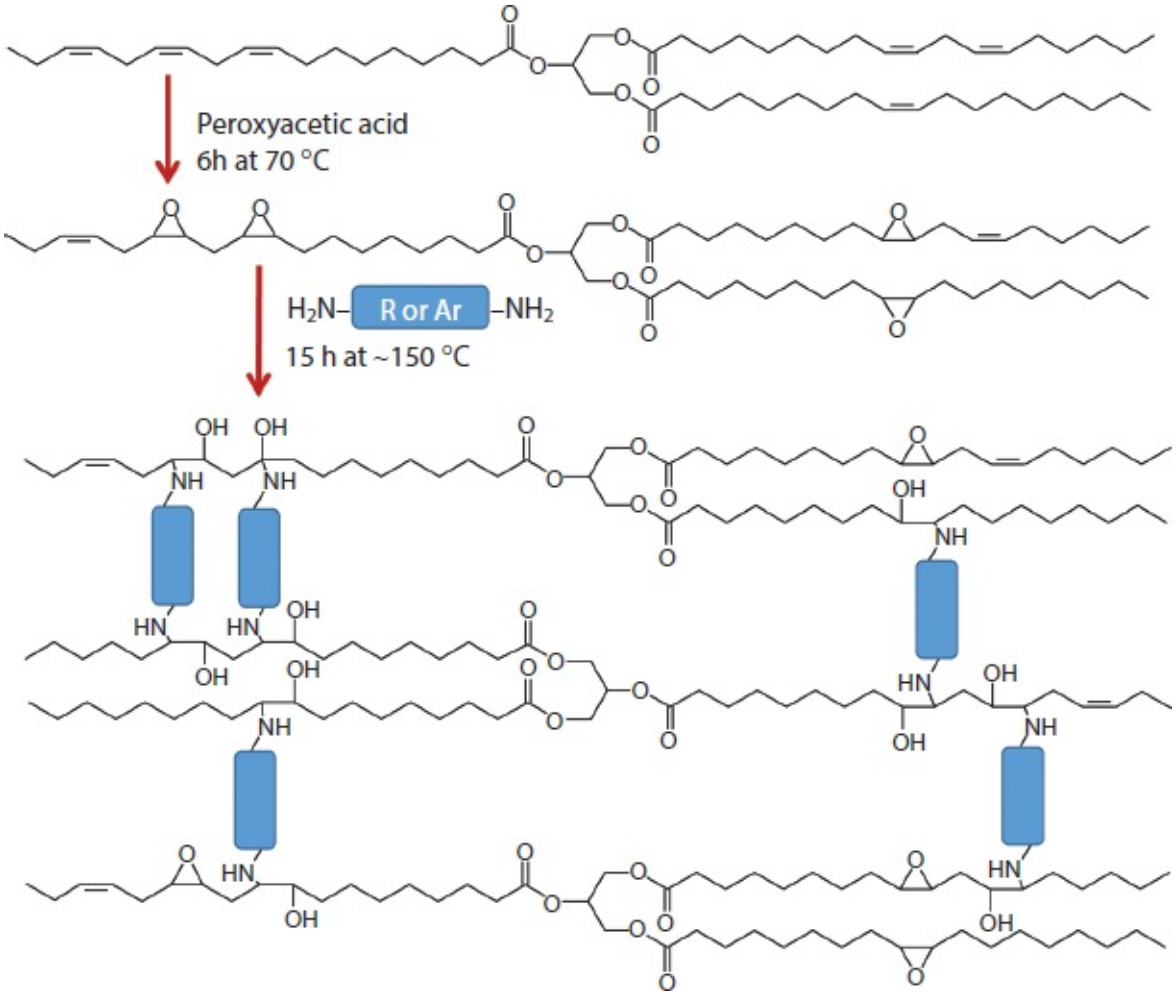
[a] Epoxy:amine mixing ratio based on solid resin weight mass.
[b] First curing stage.
[c] Second curing stage.

The ratio of epoxy/hardener was based on the stoichiometric ratio between the amine hydrogen equivalent weight (AHEW) of each amine component and the epoxide equivalent weight (EEW) of ELO [63, 64]:

$$\text{Stoichiometric relation} = (\text{AHEW} \times 100)/\text{EEW} \quad (5.3)$$

The epoxy number calculated for ELO is 2.93 epoxy groups per triglyceride molecule while the EEW obtained for ELO is 298 g/eq. In the stoichiometric relation displayed in Eq. (5.3), an excess of 10% weight of amine was used for each sample, which allowed us to ensure that the effectiveness of the cross-linking reaction. A summary of the synthesis has been shown in Scheme 5.1.

Scheme 5.1 Schematic view of LO epoxidation and cross-link reaction between ELO and aliphatic or aromatic amine hardeners.



All epoxy/hardener mixtures, with exception of PHMB that was solubilized in ethanol 96% before mixing with ELO, were homogenized without solvent addition. Variation on the procedure of mixing PHMB with ELO was necessary due to the insolubility of the solid hardener in the oil. After homogenization of the epoxy/hardener mixture, samples were placed on Teflon® discs and subsequently put in an oven for cure. All films were dried under vacuum for 3 days before characterization.

After the curing process, the samples were analyzed by FTIR to examine chemical modifications. The physical appearance of the resulting polymer films obtained is depicted in the Figure 5.3. ELO-HMDA shows good film formation properties, being more flexible than stiff and presenting elastomeric behavior. On the other hand, the aromatic hardener (PDA) enhances the stiffness of the thermoset but not the brittleness. ELO-C115 thermoset also exhibits good film formation (i.e. similar to the former ones), with elastic behavior, whereas DGEBA-C115 epoxy films based on BPA, which is

rigid and brittle, show the opposite behavior. Nevertheless, the bactericide, aromatic aliphatic and highly aromatic hardeners (PHMB, BMPDA, and BPPDA, respectively), do not exhibit good film formation, being very brittle or extremely gummy. This is a clear indication of deficiencies in the cross-link process. ELO-containing samples usually present dark color compared to the conventional DGEBA epoxy derivatives, which are mostly transparent (Figure 5.3g).

Figure 5.3 Optical photographs of (a) ELO-HMDA, (b) ELO-PDA, (c) ELO-C115, (d) ELO-PHMB, (e) ELO-BMPDA, (f) ELO-BPPDA, and (g) DGEBA-C115 cured films.

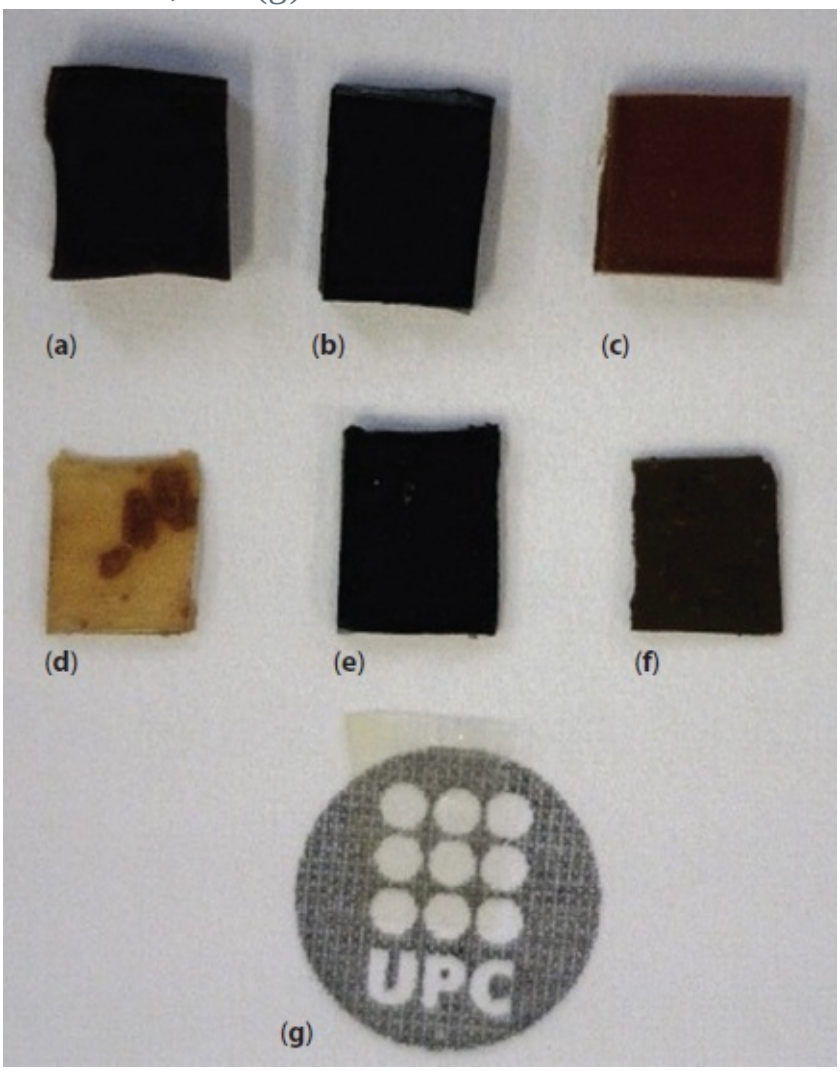
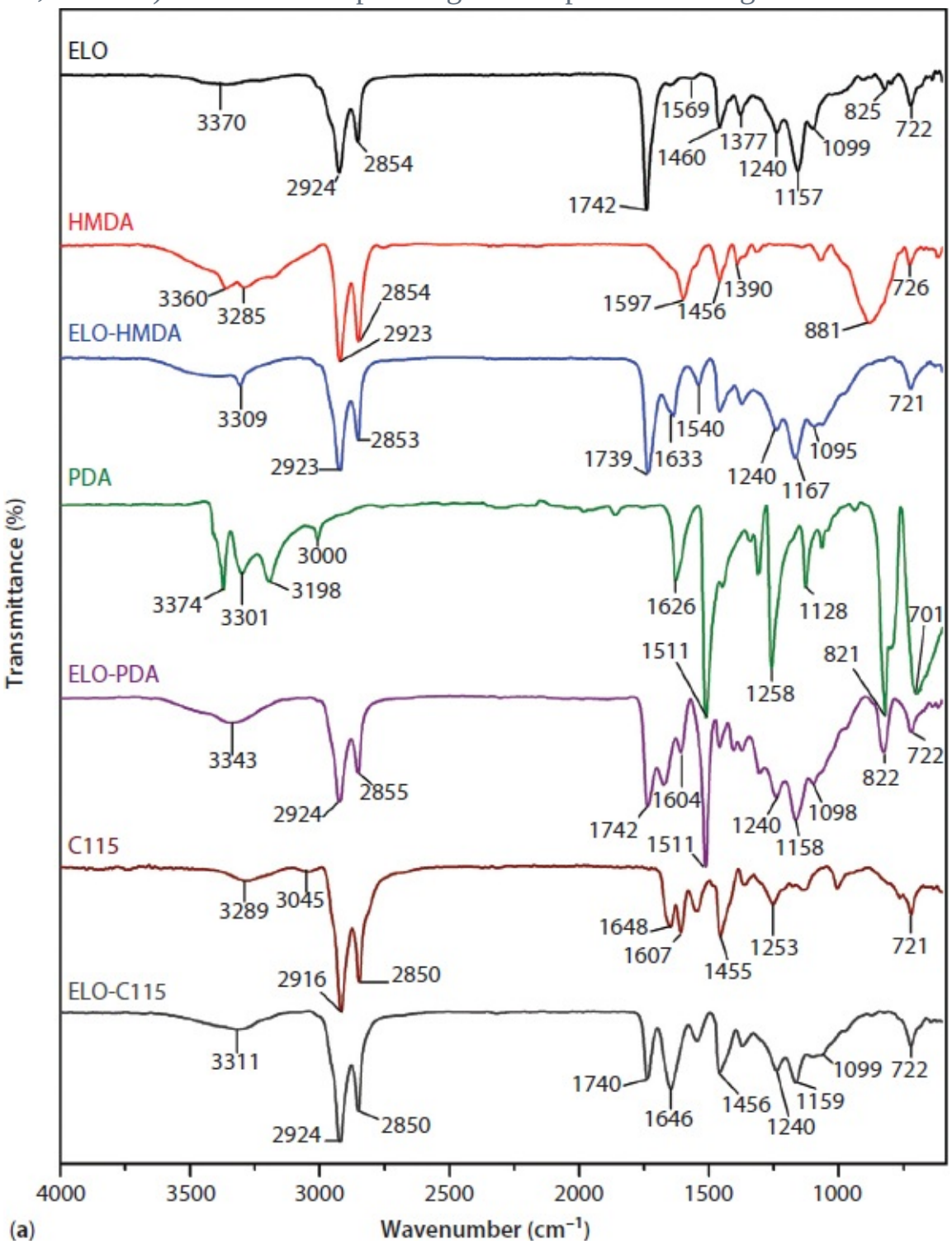
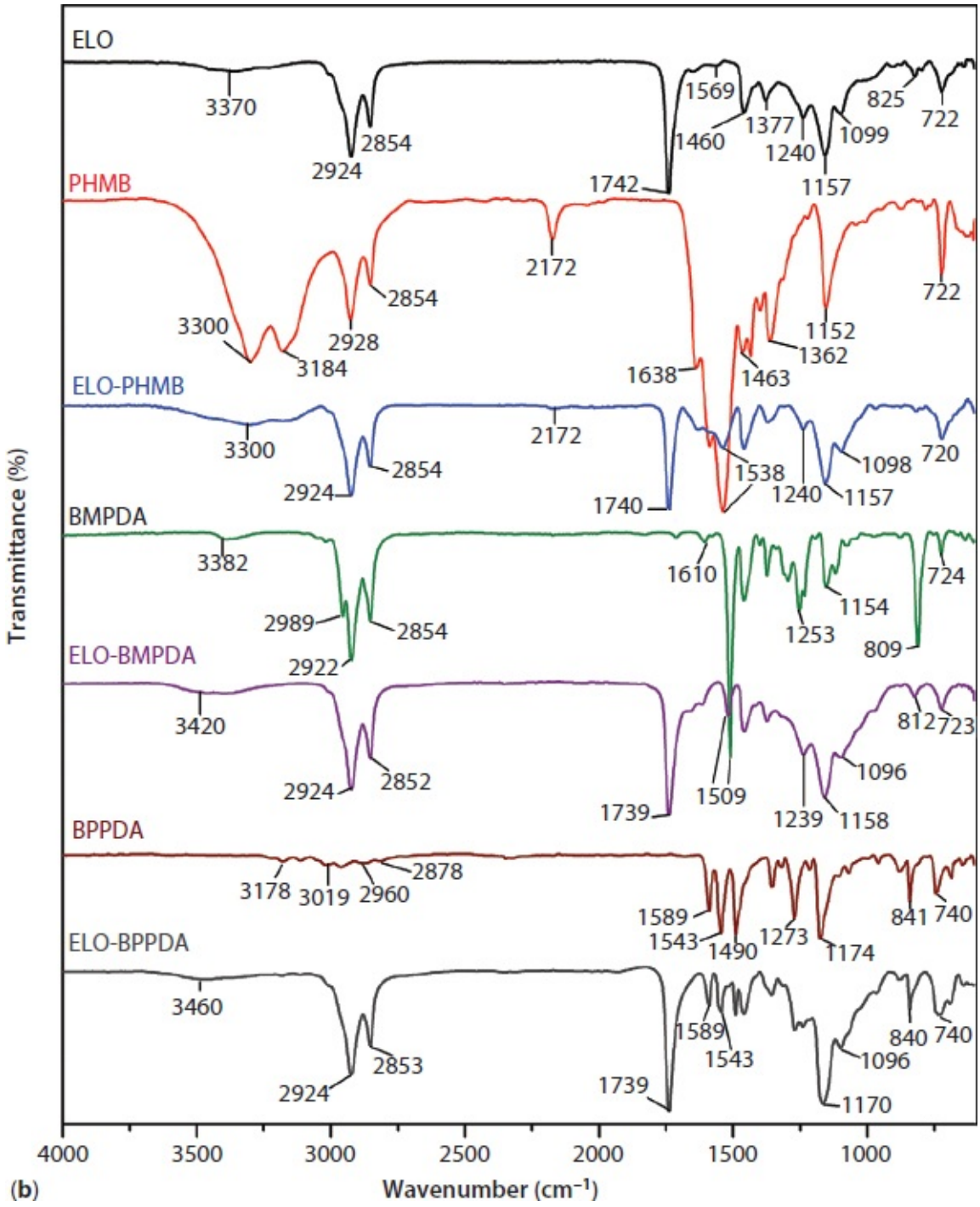


Figure 5.4a shows the FTIR spectra of ELO-HMDA, ELO-PDA and ELO-C115 as well as those of the individual hardeners and the ELO resin, whereas Figure 5.4b represents the FTIR spectra of ELO-PHMB, ELO-BMPDA, and ELO-BPPDA and their respective curing agents. The characteristics peaks for ELO were identified according to the literature [25, 30, 60] and corresponding to: low intensity peak at 3370 cm^{-1} due to the O–H stretching group derived from the oxirane opening in the epoxidation process; 2924 cm^{-1} (asymmetric stretching of CH_2), 2854 cm^{-1} (symmetric stretching of CH_2), 1742 cm^{-1} (asymmetric stretching of C=O), 1569 cm^{-1} (C=C residual, also observed at ~3010 cm^{-1} as CH=CH stretching mode), 1460 cm^{-1} (CH_2 scissors), 1377 cm^{-1} (CH_3 bending), 1240 cm^{-1} (asymmetric stretching of ester, C-O), 1157 cm^{-1} (asymmetric stretching of ester, C–O–C), 1099 cm^{-1} (symmetric stretching of ester, C–O), and 722 cm^{-1} ($-(CH_2)_n-$, rocking mode). The oxirane groups are being detected as the doublet at 800 and 826 cm^{-1}.

Figure 5.4 (a) FTIR spectra of the ELO epoxy resin, the hardeners (HMDA, PDA, C115) and the corresponding bi-component coatings; and (b) FTIR spectra of the ELO epoxy resin, the hardeners (PHMB, BMPDA, BPPDA) and the corresponding bi-component coatings.





Comparison of the FTIR spectra recorded for the HMDA monomer and the ELO-HMDA cured film (Figure 5.4a) confirms that the reaction between the amine and the epoxy groups was complete. The disappearance of the asymmetric and symmetric bands at around 3400–3100 cm^{-1} from N–H (doublet from primary amines), the disappearance of absorption band from the in-plane bending of R-NH_2 at 1597 cm^{-1} and also–CH_2-NH_2 from methylene out-of-plane bending (strong and broad band at 881 cm^{-1}), combined with the disappearance of the oxirane band from ELO (825 cm^{-1}), are clear evidences of the effective cross-linking between epoxy VO and the aliphatic hardener. Furthermore, the appearance of a new band at 3309 cm^{-1} corresponding to N-H bond from secondary amine in the ELO-HMDA spectrum is appreciated. The presence of two new peaks at 1633 cm^{-1} (R–NH inside the epoxy) and 1540 cm^{-1} (R–NH–R) corroborate the reaction between epoxy and diamine. Other absorption bands showed in the ELO-HMDA spectrum are related to the methylene polymeric chain and ester groups.

On the other hand, ELO-PDA spectrum is slightly different from that of ELO-HMDA due to the

presence of aromatic groups (3000 cm^{-1}, C–H stretching; 1626 cm^{-1}, C=C; 1511 cm^{-1}, Ar–NH_2; 1258 and 821 cm^{-1}, C–H out-of-plane bending; 701 cm^{-1}, phenyl primary amine). Moreover, the peak at 821 cm^{-1} of the ELO-PDA spectrum (Figure 5.4a), which corresponds to the aromatic C–H bond of PDA, overlaps with the epoxy band of ELO at 825 cm^{-1}. This fact makes unfeasible the analysis of oxirane group disappearance for cross-links evaluation. In spite of this, other absorption bands can be used for the appreciation of the cross-link. For example, the conversion of the three well-defined bands associated to the primary amine bonds (3374 cm^{-1}, asymmetric N–H stretching; 3301 cm^{-1}, N–H hydrogen bond; 3198 cm^{-1}, symmetric N–H stretching) into a broad absorption at 3600–3200 cm^{-1} in the ELO-PDA spectrum is an important evidence of the amine reaction. Furthermore, the broad and strong peak at 701 cm^{-1}, which corresponds to the phenyl amine group of PDA, is not present in the ELO-PDA FTIR spectrum. Moreover, a new peak appears at 1604 cm^{-1}, which has been associated to secondary amine. Thus, the overall of FTIR analyses confirms the reaction between PDA and ELO.

The main absorption bands from Crayamid 115 (C115), which is a polyaminoamide, correspond to: 3289 cm^{-1}, secondary N–H stretching (Amide A, hydrogen bond); 3045 cm^{-1}, N–H stretching (Amide B); 1648 cm^{-1}, C=O stretching (Amide I); 1607 cm^{-1}, N–H in-plane bending (Amide II); 1455 cm^{-1}, CH_2 stretching; 1253 cm^{-1}, N–H bending and C–N stretching (Amide III); and ~721 cm^{-1} as a doublet due to the $–(CH_2)_n–$ rock vibration of polymers with $n > 4$. Comparison of the absorption bands from monomers and cured film evidences the elimination of the epoxy absorption band at 825 cm^{-1}. Additionally, the appearance of the 3311 cm^{-1} band from O–H stretching indicates that the cross-linking was complete.

Figure 5.4b displays the other hardeners used as curing agents for ELO. PHMB is an important bactericide with characteristic bands at 3300 and 2172 cm^{-1} arising from the guanidine and $C=N^+H$ immonium groups, respectively, which are corroborated by several additional broad bands from 1650 to 1300 cm^{-1} associated to N–C and N–H vibrations. Like films shown in Figure 5.4a, no sign of the absorption bands associated to the epoxy groups (i.e. at about 820 cm^{-1}) is shown by ELO-PHMB after thermal curing. Unlike epoxy films shown earlier, ELO-BMPDA and ELO-BPPDA still maintain N–H groups without react, as is evidenced by the presence of a strong and sharp band at 1509 and 1589 cm^{-1} (in BMPDA and BPPDA, respectively). As occurred for ELO-PDA, the peak associated to the aromatic C–H bond of PDA at 809 cm^{-1} is almost overlapping the epoxy band of ELO at 825 cm^{-1}. However, the appearance of high intensity N–H bands led us to conclude that these films are not well cured, even after additional thermal treatment applied for ELO-BMPDA at 170 °C for 2 h (Table 5.1).

5.5 Thermal Properties of Epoxidized Linseed Oil Cured with Amine Hardeners

Thermal properties of cured samples were evaluated with differential scanning calorimetry (DSC) and thermogravimetric analysis (TGA) techniques. According to the thermograms (Figure 5.5a) obtained in a second heating scan, after eliminating the thermal history, all polymers are amorphous and the glass transitions temperatures (T_g) varied with the hardener composition (Table 5.2). Comparison of aliphatic and aromatic hardeners with the same number of carbons (ELO-HMDA and

ELO-PDA) indicates that the latter one gives the highest T_g value (above 0 °C), conferring more rigidity to the thermosetting chain than the former one, as expected [65]. A high value of T_g can also indicate a high cross-link density [42], which means that HMDA, PDA, and C115 amine hardeners provide good chemical reaction with ELO. However, other aromatic amines, BMPDA (with rigid and flexible parts) and BPPDA (with three benzene rings) (Figure 5.5a), showed not only significantly lower T_g values (–39 °C and –54 °C, respectively) but also an endothermic transition probably associated to unreacted segments of the epoxy network. This fact suggests an incomplete reaction or low reactivity of BMPDA and BPPDA with the epoxy. Since these hardeners have aromatic structures, we would expect higher T_g values for them compared to ELO-HMDA. Similarly, poor thermal behavior was also observed for ELO-PHMB films. The low reactivity of the PHMB bactericide, when used as hardener, provides a low T_g value (i.e. close to –55 °C), also followed by an endothermic transition similar to those BMPDA and BPPDA hardeners. Indeed, a second T_g appeared at ~80 °C, which has been attributed to the PHMB unreacted monomer. Therefore, ELO-PHMB thermosets present a clear degree of phase separation compared to the other hardeners. Boquillon and Fringant [14] reported several T_g values for the cure process of ELO with different anhydrides in the presence of catalysts. The obtained T_g values, which depended on the hardener and catalysts amount, were greater than room temperature (i.e. close to 100 °C).

Figure 5.5 (a) DSC, (b) TGA, and (c) DTG curves of ELO-HMDA, ELO-PDA, ELO-C115, ELO-PHMB, ELO-BMPDA, and ELO-BPPDA samples compared to a conventional DGEBA-C115 epoxy films.

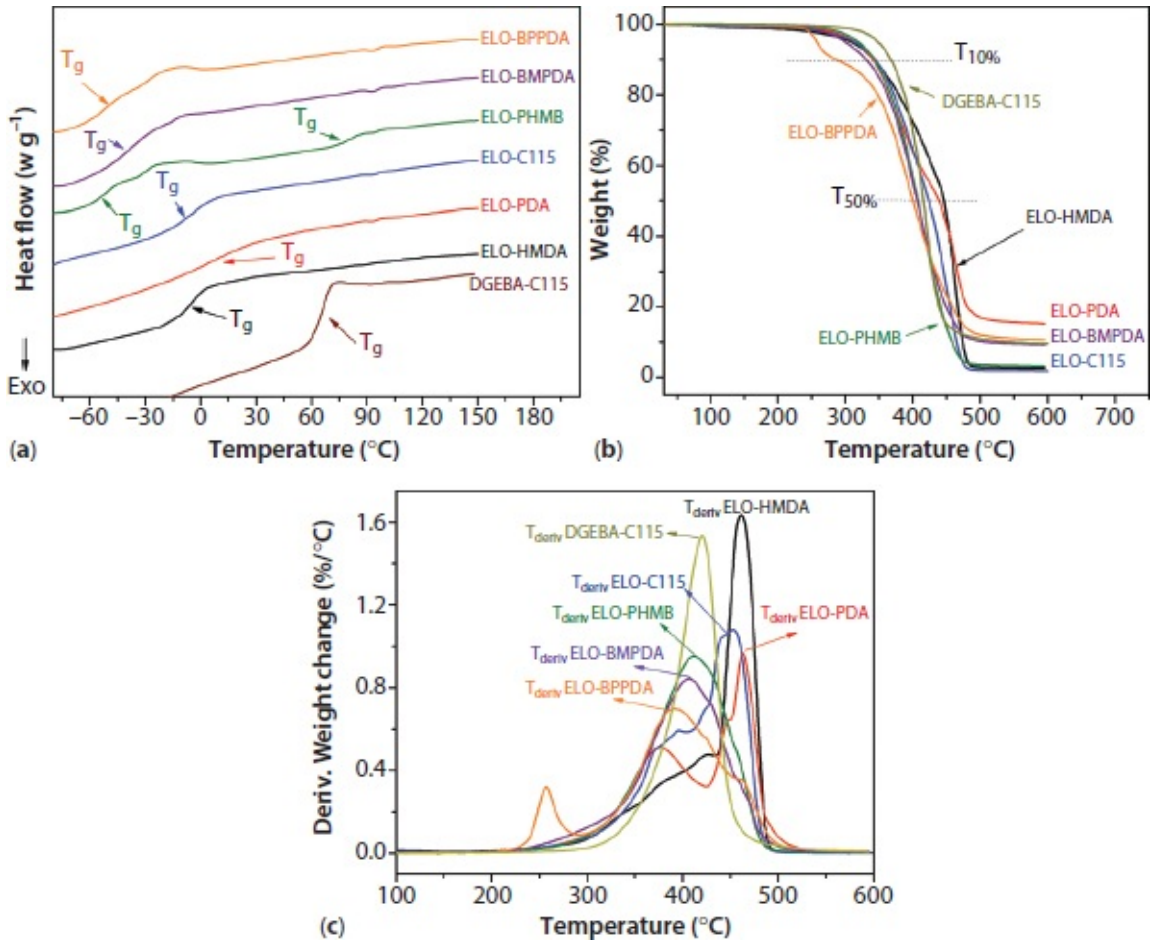


Table 5.2 Thermal properties of ELO-based epoxy resins cured with several amine hardeners.

Sample	T_g (°C)	$T_{10\%}$ (°C)	$T_{50\%}$ (°C)	T_{onset} (°C)	[a]Char yield (%)
ELO-HMDA	–5	342	447	485	2.6
ELO-PDA	7	341	439	376/464	15.2
ELO-C115	–6	344	424	396/453	1.9
ELO-PHMB	–55/79	343	407	411	3.2
ELO-BMPDA	–39	330	406	407	9.3
ELO-BPPDA	–52	286	400	257 / 391	10.5
DGEBA-C115	78	367	415	421	9.5

[a] Residue at 600 °C in nitrogen atmosphere.

The thermal behaviors of ELO-C115 with that of DGEBA-C115 evidence the plastic behavior of ELO as compared to that of DGEBA. DGEBA-C115 is brittle and rigid at room temperature and shows a T_g close to 80 °C similar to other epoxy bi-component resins [66]; whereas ELO-C115 is almost elastic and flexible at room temperature. Therefore, the chemical composition of both epoxy and hardeners has influenced the T_g values. In any case, it is possible to obtain ELO formulations with T_g values higher than room temperature replacing the amine hardener by anhydride hardeners (i.e. changing the hardener nature).

The thermal stability of the ELO-hardener films was analyzed by thermogravimetry in nitrogen atmosphere and compared to that of DGEBA-C115. TGA analyses of ELO-based epoxy (Figure 5.5b) showed several decomposition behaviors depending on the hardener composition. The decomposition was measured using three different temperatures: $T_{10\%}$, that corresponds to the temperature at which 10% in weight of sample is decomposed; T_{50}% that refers to the temperature required for decomposition of 50% in weight of sample; and T_{onset}, which is the temperature taken from the derivative thermogravimetric curve (DTG). These three decomposition temperatures are given in Table 5.2.

The highest stability was found for ELO-HMDA, ELO-PDA and ELO-C115 compositions (T_{onset} = 485 °C, 464 °C, and 453 °C, respectively) (Figure 5.5c). Indeed, the T_{onset} values of such three systems are higher than that of DGEBA-C115 cured films at 120 °C (T_{onset} = 421°C), even though the $T_{10\%}$ values of the formers are slightly lower than that of the latter. These results allowed us conclude that ELO does not influence negatively the thermal stability of the epoxy films. As it was expected, the char yield at 600 °C was higher for samples cured with aromatic hardeners (PDA, BMPDA, and BPPDA) than for the samples cured with non-aromatic hardeners (HMDA, PHMB, and C115) [67].

5.6 Swelling, Wettability and Morphology of New Epoxy Films

Polymers strongly permeable to water are not suitable for protecting coating applications. High water uptake is intrinsically related to acceleration of corrosion processes in metal surfaces when a polymeric barrier coating is applied as primer for metal protection. As the oil-based epoxies studied in this work have been prepared for protecting coating applications, water uptake and water contact

angle (WCA) are important properties to take into account. Table 5.3 presents WCA and water uptake results.

Table 5.3 WCA and water uptake of ELO-based epoxy resins with several amine hardeners.

Sample	Water drop	WCA (°)	Water uptake (%)
ELO-HMDA		107	0.75
ELO-PDA		103	0.99
ELO-C115		93	1.54
ELO-PHMB		72/100	1.28
ELO-BMPDA		91	1.62
ELO-BPPDA		76	4.16
DGEBA-C115		92	1.56

The WCA values obtained for all samples are close to 100° with the only exception of ELO-BPPDA and ELO-PHMB, which show higher surface hydrophilicity with the WCA = 76° and 72°, respectively. Analyses on ELO-PHMB were performed in two zones. The clear zone (see Figure 5.3d) corresponds to the lowest WCA value listed in Table 5.3, while the highest WCA is associated to the brown area. This behavior is consistent with the DSC results, which reflected two T_g's due to the presence of phaseseparation between the unreacted PHMB on the ELO resin.

According to Table 5.3, most of the films show low wettability or good hydrophobicity compared to other VO hybrid films previously reported. Allauddin *et al*. [42] described similar studies for PU/alkoxysilane CO films. The low contact angles and moderate swelling values, which varied from 74° to 82° and from 0.85% to 0.35% (both from high to low ECO concentrations), respectively, suggested that CO is hygroscopic. Therefore, decreasing in CO concentration on the hybrid material leads to an increasing hydrophobicity and decreasing water uptake.

Swelling measurements on cured films can be used to observe water resistance and hydrophobicity. Values higher than 1% suggest that the density of cross-links in such films is not high enough to hinder the swelling promoted by water-soluble oil segments present in ELO. Therefore, we conclude that cross-links in ELO-C115 and ELO-BMPDA are insufficient while ELO-PHMB is not well cross-linked provoking phase separation.

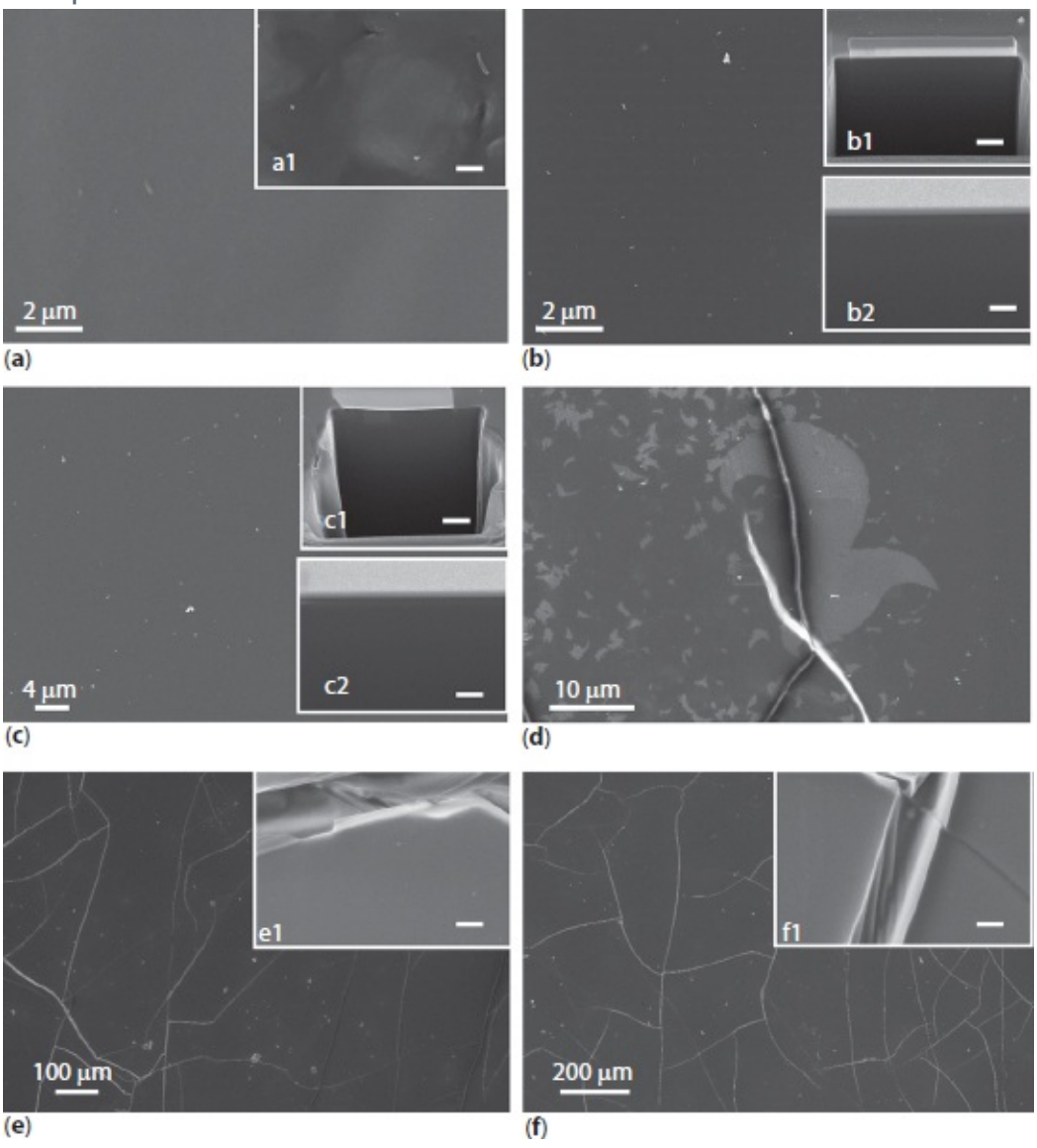
The lower water uptake values were obtained for ELO-HMDA (0.75%) and ELO-PDA (0.99%), which represent a low permeability of the films and suggest a material with high cross-linked density. This behavior is in agreement with the WCA values, which are the higher (107° and 103°, respectively). The highest water uptake value corresponds to ELO-BPPDA sample (4.16%), which shows the lowest WCA value. This high swelling ability and hydrophilicity is supported by the FTIR

spectrum of ELO-BPPDA (Figure 5.4b), which shows incomplete or absent reactions of epoxy with amine. The variability of WCA and water uptake values can be associated not only to the different chemical structures of the curing agents but also to their ability to cross-link with ELO.

Comparison of WCA and water uptake of ELO-C115 with DGEBA-C115 reveals similar values. DGEBA-C115 usually has a good barrier coating behavior when used as a primer, hindering water penetration. Accordingly, ELO-C115 should also act as a barrier protection since its impermeability properties are similar to those of the commercial epoxy coating.

The morphology of the samples was analyzed by SEM, micrographs being displayed in Figure 5.6. The aim of this study is to examine the porosity, brittleness, and phase separation of cured films to compare with the afore-discussed thermal analyses and swelling parameters. Films prepared using HMDA, PDA, and C115 hardeners present outer and inner smooth morphologies. No fissure was observed in these samples, which is consistent with the plasticized behavior observed before and after careful drying process. Insets in Figure 5.6b and c, which show the cross sections of the films after cut with the focused ion beam accessory, evidence the compact structures of these thermosets, as is reflected by the lack of pores and their highly homogenous aspect, even inside the films.

Figure 5.6 SEM micrographs of: (a) ELO-HMDA, (b) ELO-PDA, (c) ELO-C115, (d) ELO-PHMB, (e) ELO-BMPDA, and (f) ELO-BPPDA. The inset micrographs in (b) and (c) shows a cross section made after platinum deposition with FIB probe. Inset scale bars: a1 = 100 nm, b1 and c1 = 1 µm, b2 and c2 = 100 nm, e1 and f1 = 1 µm.



On the other hand, the components of ELO-PHMB do not present good compatibility, which is evidenced by se non-homogenous morphology with two polymeric phases (dark and white zones in Figure 5.6d). Micrographs show not only the large dimensions of the segregated phases, which are larger than 10 μm but also the existence of cracks. The morphology of ELO-PHMB is in agreement with the DSC results, which showed two different T_g's that were associated with two different phases (i.e. one formed by ELO unreacted resin and the other by PHMB homopolymer). The phase separation observed in ELO-PHMB samples has been attributed to compatibility problems in the mixture of ELO and PHMB components.

Thermosets with BMPDA and BPPDA curing agents show multiple surface cracks (Figure 5.6e and f). These cracks are extremely large and, in some cases, cut the whole surface of the film crossing from one end to the other, which causes a significant degree of weakness. These results support the fact ELO-BMPDA and ELO-BPPDA samples are not well cured, giving an insufficient cross-link density and provoking high water uptake values (see Table 5.3). Although good hydrophobicity should be obtained by analyzing the surface out of the cracked zones, micro-fissures (not observed by eyes) are present in the whole film inducing high water absorption in the swelling experiments.

To conclude, PHMB, BMPDA and BPPDA amines do not behave as good hardeners when they are used as curing agents with ELO resins, which have been attributed to their low reactivity compared to HMDA, PDA or C115 amines.

5.7 Mechanical Properties of Epoxidized Linseed Oil Cured with Amine Hardeners

Several physico-mechanical tests, like impact resistance, scratch hardness, gloss, and adhesion, are usually carried out to evaluate the mechanical behavior of epoxy films. As mentioned earlier, ELO-PHMB, ELO-BMPDA and ELO-BPPDA films were very brittle, breaking up only with a simple handling, due to the poor reactivity of their hardeners. Thus, ELO-HMDA, ELO-PDA and ELO-C115 were the only samples with good film formation and mechanical integrity to be used as coating. Here, we performed stress-strain test to analyze the mechanical resistance of the new bio-based films. The stress-strain curves of ELO-HMDA, ELO-PDA, and ELO-C115 samples are represented in Figure 5.7, the mechanical behavior offered by a conventional epoxy resin, used as reference of an epoxy without VO (DGEBA-C115), is being included for comparison. The parameters derived from stress-strain curves are listed in Table 5.4.

Figure 5.7 Stress–strain curves of ELO-HMDA, ELO-PDA, and ELO-C115 cured films. Inset: DGEBA-C115 for comparison. Stretch speed: 0.8 mm/min in all cases.

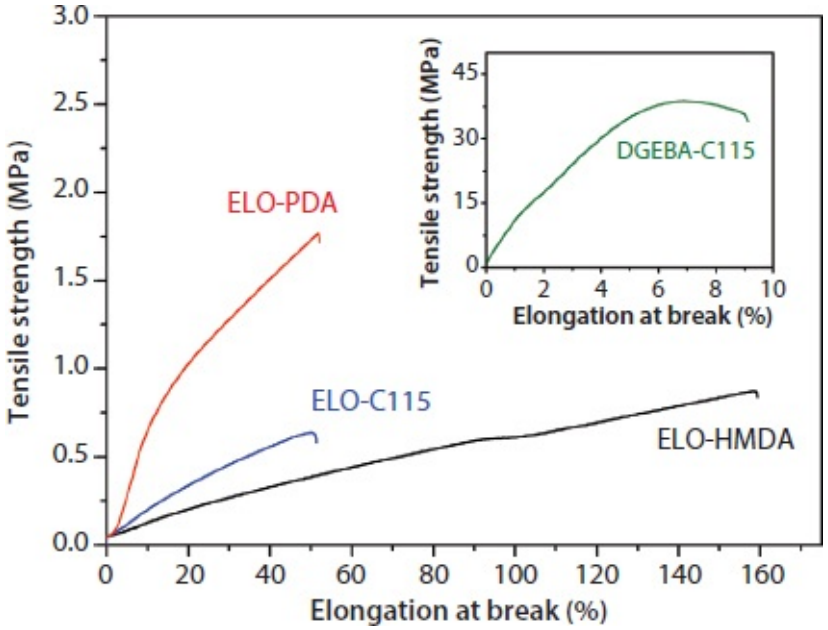


Table 5.4 Tensile parameters obtained from stress-strain curves.

Samples	[a]E (MPa) Mean ± S.D.*	[b]σ_{max} (MPa) Mean ± S.D.*	[c]$\varepsilon_{\sigma max}$ (%) Mean ± S.D.*
ELO-HMDA	0.91 ± 0.04	0.89 ± 0.10	161 ± 3
ELO-PDA	4.71 ± 0.10	1.86 ± 0.20	56 ± 4
ELO-C115	1.35 ± 0.10	0.63 ± 0.10	53 ± 3
DGEBA-C115	825 ± 95.0	39.0 ± 3.20	9 ± 1

* Standard Deviation;
[a] is Young's modulus;
[b] is the maximum tensile strength;
[c] Elongation at maximum tensile strength.

Clearly, the mechanical behavior of examined samples shows a great variability. Results from the tensile test show that all samples prepared with ELO epoxy resin have reduced mechanical properties in comparison with those of the unmodified epoxy resin. Comparison of the mechanical parameters (*e.g.* like tensile strength, elongation at break, scratch hardness, gloss and impact resistance) of different VO-modified epoxies allowed to conclude that resin actuates as a plasticizer, independent on the hardener nature [68, 69]. The decrease of tensile strength and increase of elongation at break of the thermosets with the increase of ELO content has been attributed to the decrease of cross-link density in the polymeric structure as supported by other analysis.

The three ELO-hardener films studied in this section present a high elongation at break and very low tensile strength values. In contrast, DGEBA-C115 exhibits high tensile strength but low elongation at break (Figure 5.7, inset). The elastic modulus E, which is closely related to the bonding forces of atoms in the material, is a measure for stiffness. According to Table 5.4, the ELO-PDA shows the highest *E* value (4.71 MPa), indicating that the aromatic amine used as curing agent increases the rigidity of the epoxy with respect to the epoxy cured with aliphatic amine (ELO-HMDA, 0.91 MPa). According to Mayr *et al.* [65] and Urbaczewski *et al.* [70], cross-links derived from aliphatic amines are more flexible than those obtained using aromatic amines. Consistently, the ELO-HMDA sample has the lowest *E* value and tensile strength. The maximum tensile strength (σ_{max}) also varies with the nature of the hardener. Aromatic amines make the polymer more rigid, the σ_{max} of ELO-PDA (1.86 MPa) being higher than those of ELO-HMDA (0.89 MPa) and ELO-C115 (0.63 MPa).

The high elongation value ($\varepsilon_{\sigma\ max}$)of ELO-HMDA (161%) indicates a behavior similar to that elastomeric materials, as for example styrene butadiene rubber (SBR), ethylene–propylene rubber (EPR), and silicone rubber.

5.8 Applications of Vegetable Oils in Coatings

Despite VOs have been used in paints and coatings for decades, several innovative applications have been recently reported in the literature, especially in self-healing coatings, organic–inorganic hybrid coatings and mainly PU coatings. The self-healing technology proposes an interesting way to improve the anticorrosion properties of coatings, representing an important innovation step in the paints formulation [71].

Thanawala *et al.* [72] developed a self-healing coating with anticorrosion properties using encapsulated LO in epoxy matrix. Behzadnasab *et al.* [73] studied the influence of the amount and size of LO microcapsules in the mechanical properties of coating films. Both works used urea-formaldehyde as capsules, epoxy resin as coating matrix and LO as healer. Oleic acid and triazole derivatives encapsulated in PU microcapsules shows an excellent self-healing property [74]. Es-haghi *et al.* [75] used LO encapsulated in silane-modified ethyl cellulose with potential compatibility with coating matrixes. Chaudhari *et al.* described the utilization of *Azadirachta indica juss* (neem oil) in the preparation of conventional and self-healing coatings [76–79]. Neem seed oil contains three saturated fatty acids, including palmitic (11.90%), stearic (29.96%), and arachidic (2.94%) acids. It also contains two unsaturated fatty acids viz. oleic (50.04%) and linoleic (5.15%) acids. The main advantage found in the use of neem oil was the fast dryness to touch, good gloss, pencil hardness, adhesion, and impact properties of produced PU films. They concluded that neem oil-based resins have excellent potential for use in the formulation of surface coating binders due to the employment of room temperature for cure. Therefore, their work represented an important advance to overcome the main problems related to VO compounds (i.e. the prolonged curing times, multi-step cure schedules at very high temperatures for complete cross-linking). Başẗurk *et al.* [80] developed hybrid organic–inorganic flame retardant coating using acrylated ESO and TEOS. Better thermal stability and amelioration in the mechanical properties of the films was obtained with increasing sol-gel content. Thus, today research emphasis is being laid on the modification of VOs to introduce novel properties, improved performance coupled with environment benefits. Allauddin *et al.* [42] also reported an improvement in the mechanical properties of hybrid films formed with a hydrolysable silane CO. Fu *et al.* [81] prepared alkoxysilane CO for obtaining hybrid PU/siloxane films. An increase in the hydrophobicity of the surface was observed when the silane network is present.

Nevertheless, most of publications devoted to study organic-inorganic hybrid coatings employing VOs are in the preliminary stage yet. Thus, these works only describe the preparation and physico-chemical characterization of cured solid films. Scarce works have been devoted to the application of the new materials. One of the few works found in this direction is that reported by Martinelli and co-workers [40]. Such authors prepared hybrid films from ECO and two different silanes and performed salt-spray tests to evaluate the protective action of new films against corrosion of aluminum substrate.

PU technology is the main area where VOs are being extensively applied, as mentioned earlier. For example, Rajput *et al.* [82–84] formulated PU coatings with oleic acid for wood finishing purposes. Palm oil-, soy oil- and sunflower oil-derivate PU coating were compared in a work developed by Ling *et al.* [85]. Waterborne PU from CO was developed by Fu *et al.* [86]. Cottonseed oil was

chemically modified to fatty polyesteramide and polyetheramide for the fabrication of polyesteramide and poly(ether-urethane) amide coatings, showing very good chemical resistance [87, 88]. Yildirim *et al.* [89] modified partial glycerides of sunflower oil with benzoxazine to develop a transparent coating with excellent adhesion in wood and steel. Bakhshi *et al.* [90] established a PU coating with bactericidal properties from the modification of SO with quaternary ammonium salts. The excellent biocompatibility and mechanical properties make this formulation an interesting product for biomedical purposes. Wasekar *et al.* [91] proposed the formulation of a CO-derivate coating with good dielectric properties. Saravari *et al.* [92] used a mixture of castor and jatropha oil in the preparation of a urethane alkyd coating with excellent flexibility together with acid and water resistance.

Some works regarding the use of VO-based eco-friendly epoxy coatings are found in the literature. Ahmad and co-workers are among the pioneers in the employment of VOs in epoxy anticorrosive coatings [93–96]. Coatings of oil epoxy curing agent combinations prepared from VO and adhered to metal surfaces, were subjected to physico-mechanical and anticorrosive tests in various corrosive media (water, saline water, acid, and alkali) [93].

More recently, Webster and co-workers have reported several chemical structure modifications of VOs for the preparation of epoxy thermoset coatings [6, 97–99]. A new 100% bio-based thermosetting coating system was developed from epoxidized sucrose soyate cross-linked with blocked bio-based dicarboxylic acids. These systems showed good adhesion to metal substrates and performed well under chemical and physical stress. Additionally, they found that the hardness of the coating system was dependent on the chain length of the diacid used, making it tunable [99].

5.9 Conclusions

The synthesis of ELO and its curing process using six different hardeners have been discussed. FTIR, ^{1}H NMR, and ^{13}C NMR are versatile tools to confirm the epoxidation reaction of the LO through the PAA method. On the other hand, FTIR is usually used to evaluate the effective reaction between the oxirane ring and the amine groups. However, DSC is considered the main tool, which allows verify the cross-linking degree between ELO and amine hardeners. DSC analyses have evidenced that HMDA, PDA, and C115 exhibit high reactivity with ELO, whereas PHMB, BMPDA, and BPPDA diamines have low reactivity or unreacted. On the other hand, despite some films do not present any crack or fissures in the optical microscope, SEM have shown that ELO-PHMB has two different phases. Moreover, films obtained from ELO-HMDA, ELO-PDA, and ELO-C115 presents a compact structure, without porosity, show better thermal stability and higher T_g values than the other samples. Particularly, ELO-C115 exhibit higher hydrophilicity and water uptake than ELO-HMDA and ELO-PDA hardeners. Therefore, these results lead us to conclude that HMDA and PDA hardeners provide the best cross-link density with ELO. The other amines failed in one or more characteristics.

Alam and co-workers [100] recently affirmed that “with persistent and extensive research efforts, VO coatings may compete well with their petro-based counterparts in performance and applications and may establish themselves as *greener* precursors to environment friendly coatings, in future”. Thus, ELO and other VO derivatives can be considered as promising substitutes of DGEBA for the formation of impermeable epoxy films to be used as solvent-borne primer coatings. In this way, a decrease in the environmental impact and healthy problems caused by BPA in the coatings industry can be achieved in a near future.

Acknowledgments

This work has been supported by MICINN and FEDER funds (MAT2012-34498). The authors thank the Brazilian government agencies CNPq (process 140077/2011-1) and CAPES (process BEX 13736124) for the financial support of Mr R.S. Peres (UFRGS). The authors would like to acknowledge Dr A. Martínez de Illarduya for his support and useful discussions in NMR analysis and Dr L. Franco for her support with the thermal analysis.

References

1. Z.S. Petrovic, Polyurethanes from vegetable oils. *Polymer Reviews,* 48(1), p. 109–155, 2008.

2. Y. Xia and R.C. Larock, Vegetable oil-based polymeric materials: synthesis, properties, and applications. *Green Chemistry,* 12(11), p. 1893–1909, 2010.

3. De D. Guzmán, *ACC CPI: PU players going green.* 2012; Available from: http://www.icis.com/Articles/2012/09/21/9597480/acc-cpi-pu-players-going-green.html.

4. A.M. Nelson, and T.E. Long, A perspective on emerging polymer technologies for bisphenol-A replacement. *Polymer International*, 61(10), p. 1485–1491, 2012.

5. C. Zhang, *et al.,* Soy-castor oil based polyols prepared using a solvent-free and catalyst-free method and polyurethanes therefrom. *Green Chemistry,* 15(6), p. 1477–1484, 2013.

6. T.J. Nelson, T.P. Galhenage, and D.C. Webster, Catalyzed crosslinking of highly functional biobased epoxy resins. *Journal of Coatings Technology and Research*, 10(5), p. 589–600, 2013.

7. X. Pan, P. Sengupta, and D.C. Webster, High biobased content epoxy-anhydride thermosets from epoxidized sucrose esters of Fatty acids. *Biomacromolecules*, 12(6), p. 2416–28, 2011.

8. X. Pan, P. Sengupta, and D.C. Webster, Novel biobased epoxy compounds: epoxidized sucrose esters of fatty acids. *Green Chemistry,* 13(4), p. 965–975, 2011.

9. C.A. Staples, *et al.,* A review of the environmental fate, effects, and exposures of bisphenol A. *Chemosphere*, 36(10), p. 2149–2173, 1998.

10. J. Kang, -H., F. Kondo, and Y. Katayama, Human exposure to bisphenol A. *Toxicology,* 2006. 226(2–3), p. 79–89.

11. B. Borrell, Toxicology: The big test for bisphenol A. *Nature*, 464(7292), p. 1122–1124, 2010.

12. S.M. Ho, *et al.*, Developmental exposure to estradiol and bisphenol A increases susceptibility to prostate carcinogenesis and epigenetically regulates phosphodiesterase type 4 variant 4. *Cancer Research*, 66(11), p. 5624–5632, 2006.

13. A.R. Mahendran, *et al.,* Synthesis and Characterization of a Bio-Based Resin from Linseed Oil. *Macromolecular Symposia*, 311(1), p. 18–27, 2012.

14. N. Boquillon, and C. Fringant, Polymer networks derived from curing of epoxidised linseed oil: influence of different catalysts and anhydride hardeners. *Polymer*, 41(24), p. 8603–8613, 2000.

15. O'R.D. Brien, *Fats and Oils: Formulating and Processing for Applications.* 2010, Boca Raton, USA: CRC Press.

16. D.D. Andjelkovic, *et al.,* Novel thermosets prepared by cationic copolymerization of various vegetable oils - synthesis and their structure-property relationships. *Polymer,* 46(23), p. 9674–9685,

2005.

17. G. Lligadas, *et al.*, Bionanocomposites from renewable resources: Epoxidized linseed oil-polyhedral oligomeric silsesquioxanes hybrid materials. *Biomacromolecules*, 7(12), p. 3521–3526, 2006.

18. F.S. Guner, Y. Yagci, and A.T. Erciyes, Polymers from triglyceride oils. *Progress in Polymer Science*, 31(7), p. 633–670, 2006.

19. F.I. Altuna, *et al.*, Copolymers based on epoxidized soy bean oil and diglycidyl ether of bisphenol a: Relation between morphology and fracture behavior. *Polymer Engineering and Science*, 54(3), p. 569–578, 2014.

20. X. Pan, T.J. Nelson, and D.C. Webster, Novel biobased dual-cure coating system. *Progress in Organic Coatings*, 73(4), p. 344–354, 2012.

21. X. Pan, and D.C. Webster, Impact of Structure and Functionality of Core Polyol in Highly Functional Biobased Epoxy Resins. *Macromol Rapid Commun*, 2011.

22. M. Lazzari, and O. Chiantore, Drying and oxidative degradation of linseed oil. *Polymer Degradation and Stability*, 65(2), p. 303–313, 1999.

23. Juita, *et al.*, Low temperature oxidation of linseed oil: a review. *Fire Science Reviews*, 1(1), p. 1–36, 2012.

24. F.D. Gunstone, *Fatty Acid and Lipid Chemistry*. 1996, New York, USA: Chapman & Hall.

25. F.S. Guner, *et al.*, Study of film properties of some urethane oils. *Journal of Coatings Technology*, 74(929), p. 55–59, 2002.

26. D.S. Ogunniyi, Castor oil: vital industrial raw material. *Bioresource Technology*, 97(9), p. 1086–1091, 2006.

27. F.C. Naughton, Production, Chemistry, and Commercial Applications of Various Chemicals from Castor-Oil. *Journal of the American Oil Chemists Society*, 51(3), p. 65–71, 1974.

28. H. Warth, *et al.*, Polyester networks based upon epoxidized and maleinated natural oils. *Angewandte Makromolekulare Chemie*, 249, p. 79–92, 1997.

29. F. Shahidi, *Bailey's Industrial Oil and Fat Products*. Hoboken, USA: John Wiley & Sons, Inc., 2005.

30. C. Cai, *et al.*, Studies on the kinetics of *in situ* epoxidation of vegetable oils. *European Journal of Lipid Science and Technology*, 110(4), p. 341–346, 2008.

31. D.M. Becchi, *et al.*, Organic-Inorganic Coatings Based on Epoxidised Castor Oil/APTES/TEOS. *Journal of the American Oil Chemists Society*, 88(1), p. 101–109, 2011.

32. V.V. Goud, A.V. Patwardhan, and N.C. Pradhan, Studies on the epoxidation of mahua oil (Madhumica indica) by hydrogen peroxide. *Bioresource Technology*, 97(12), p. 1365–1371.

33. V.V. Goud, *et al.*, Epoxidation of Jatropha (Jatropha curcas) oil by peroxyacids. *Asia-Pacific Journal of Chemical Engineering*, 5(2), p. 346–354, 2010.

34. S. Dinda, *et al.*, Epoxidation of cottonseed oil by catalysed by liquid aqueous hydrogen peroxide inorganic acids. *Bioresource Technology*, 99(9), p. 3737–3744, 2008.

35. P. Jiang, *et al.*, Novel Two-Phase Catalysis with Organometallic Compounds for Epoxidation of Vegetable Oils by Hydrogen Peroxide. *Journal of the American Oil Chemists Society*, 87(1), p. 83–91, 2010.

36. Z.S. Petrovic, *et al.*, Epoxidation of soybean oil in toluene with peroxoacetic and peroxoformic acids - kinetics and side reactions. *European Journal of Lipid Science and Technology*, 104(5), p. 293–299, 2002.

37. T. Vlcek, and Z.S. Petrovic, Optimization of the Chemoenzymatic Epoxidation of Soybean Oil. *Journal of the American Oil Chemists Society*, 73(3), p. 247–252, 2006.

38. G.J. Piazza, T.A. Foglia, and A. Nunez, Optimizing reaction parameters for the enzymatic synthesis of epoxidized oleic acid with oat seed peroxygenase. *Journal of the American Oil Chemists Society*, 78(6), p. 589–592, 2001.

39. M.R.G. Klaas, and S. Warwel, Lipase-catalyzed preparation of peroxy acids and their use for epoxidation. *Journal of Molecular Catalysis a-Chemical*, 117(1–3), p. 311–319, 1997.

40. D.M. Bechi, *et al*., Organic-inorganic coatings based on epoxidized castor oil with APTES/TIP and TEOS/TIP. *Progress in Organic Coatings*, 76(4), p. 736–742, 2013.

41. S. Dewasthale, *et al.*, Interpenetrating polymer networks derived from silylated soybean oil and polydimethylsiloxane. *Journal of Applied Polymer Science*, 130(4), p. 2479–2486, 2013.

42. S. Allauddin, R. Narayan, and K.V.S.N. Raju, Synthesis and Properties of Alkoxysilane Castor Oil and Their Polyurethane/Urea-Silica Hybrid Coating Films. *Acs Sustainable Chemistry & Engineering*, 1(8), p. 910–918, 2013.

43. P.P. Nalawade, *et al*., Modified Soybean Oil as a Reactive Diluent: Synthesis and Characterization. *Journal of Polymer Science Part a-Polymer Chemistry*, 52(21), p. 3045–3059, 2014.

44. S. Pramanik, *et al.*, Castor Oil Based Hyperbranched Poly(ester amide)/Polyaniline Nanofiber Nanocomposites as Antistatic Materials. *Industrial & Engineering Chemistry Research*, 52(16), p. 5700–5707, 2013.

45. D. Delatte, *et al.*, Synthesis and Characterization of a Soybean Oil- Based Macromonomer. *Journal of Applied Polymer Science*, 131(10), 2014.

46. G. Lligadas, *et al.*, Monomers and polymers from plant oils via click chemistry reactions. *Journal of Polymer Science Part A: Polymer Chemistry*, 51(10), p. 2111–2124, 2013.

47. C. Zhang, *et al.*, Polyurethanes from Solvent-Free Vegetable Oil-Based Polyols. *Acs Sustainable Chemistry & Engineering*, 2(10), p. 2465–2476, 2014.

48. S. Rengasamy, and V. Mannari, Hydrophobic and Oil-Resistant Coatings Based on Advanced Green Polyurethane Dispersions. *Journal of Applied Polymer Science*, 130(6), p. 3874–3884, 2013.

49. L.C. Bailosky, *et al.*, Synthesis of polyether polyols with epoxidized soy bean oil. *Progress in Organic Coatings*, 76(12), p. 1712–1719, 2013.

50. C. Zhang, R. Ding, and M.R. Kessler, Reduction of Epoxidized Vegetable Oils: A Novel Method to Prepare Bio-Based Polyols for Polyurethanes. *Macromolecular Rapid Communications*, 35(11), p. 1068–1074, 2014.

51. T.F. Garrison, *et al.*, Thermo-Mechanical and Antibacterial Properties of Soybean Oil-Based Cationic Polyurethane Coatings: Effects of Amine Ratio and Degree of Crosslinking. *Macromolecular Materials and Engineering*, 299(9), p. 1042–1051, 2014.

52. C.-W. Chang and K.-T. Lu, Linseed-oil-based waterborne UV/air dual-cured wood coatings. *Progress in Organic Coatings*, 76(7–8), p. 1024–1031, 2013.

53. C. Ding, and A.S. Matharu, Recent Developments on Biobased Curing Agents: A Review of Their

Preparation and Use. *Acs Sustainable Chemistry & Engineering*, 2(10), p. 2217–2236, 2014.

54. Y. Ganji, *et al.*, Synthesis and characterization of gold nanotube/nanowire-polyurethane composite based on castor oil and polyethylene glycol. *Materials Science & Engineering C-Materials for Biological Applications*, 42, p. 341–349, 2014.

55. S. Thakur, S. Barua, and N. Karak, Self-healable castor oil based tough smart hyperbranched polyurethane nanocomposite with antimicrobial attributes. *Rsc Advances*, 5(3), p. 2167–2176, 2015.

56. R. Gharibi, M. Yousefi, and H. Yeganeh, Synthesis, characterization and assessment of poly(urethane-co-pyrrole)s derived from castor oil as anticorrosion coatings for stainless steel. *Progress in Organic Coatings*, 76(10), p. 1454–1464, 2013.

57. T. Gurunathan, S. Mohanty, and S.K. Nayak, Preparation and performance evaluation of castor oil-based polyurethane prepolymer/polylactide blends. *Journal of Materials Science*, 49(23), p. 8016–8030, 2014.

58. Tayde S., P.M., Bhagt S.L., Renge V.C., Epoxidation of Vegetable Oils: A Review. *International Journal of Advanced Engineering Technology*, II(IV), p. 491–501, 2011.

59. A. Solladie-Cavallo, *et al.*, Linseed oil and mixture with maleic anhydride: H-1 and C-13 NMR. *Journal of the American Oil Chemists Society*, 80(4), p. 311–314, 2003.

60. M. Stemmelen, *et al*., A Fully Biobased Epoxy Resin from Vegetable Oils: From the Synthesis of the Precursors by Thiol-ene Reaction to the Study of the Final Material. *Journal of Polymer Science Part a-Polymer Chemistry*, 49(11), p. 2434–2444, 2011.

61. F.D. Gunstone, The study of natural epoxy oils and epoxidized vegetable-oils by c-13 nuclear-magnetic-resonance spectroscopy. *Journal of the American Oil Chemists Society*, 70(11), p. 1139–1144, 1993.

62. S. Ahmad, *et al.*, Development of amine–acid cured Annona squamosa oil epoxy anticorrosive polymeric coatings. *Progress in Organic Coatings*, 55(3), p. 268–275, 2006.

63. B.P.U. Müller, *Coatings Formulation. Part II: Solvent-Borne Paints*, in *Coatings Formulation*, B.P.U. Müller, Editor. Vincentz Network: Hanover, Germany. p. 112–123, 2006.

64. E.G. Karayannidou, D.S. Achilias, and I.D. Sideridou, Cure kinetics of epoxy-amine resins used in the restoration of works of art from glass or ceramic. *European Polymer Journal*, 42(12), p. 3311–3323, 2006.

65. A.E. Mayr, W.D. Cook, and G.H. Edward, Yielding behaviour in model epoxy thermosets - I. Effect of strain rate and composition. *Polymer*, 39(16), p. 3719–3724, 1998.

66. M. Marti, *et al.*, Novel Epoxy Coating Based on DMSO as a Green Solvent, Reducing Drastically the Volatile Organic Compound Content and Using Conducting Polymers As a Nontoxic Anticorrosive Pigment. *Acs Sustainable Chemistry & Engineering*, 1(12), p. 1609–1618, 2013.

67. S.H. Cheng, *et al.*, Novel aromatic poly(amine-imide)s bearing a pendent triphenylamine group: Synthesis, thermal, photophysical, electrochemical, and electrochromic characteristics. *Macromolecules*, 38(2), p. 307–316, 2005.

68. A. Sarwono, Z. Man, and M.A. Bustam, Blending of Epoxidised Palm Oil with Epoxy Resin: The Effect on Morphology, Thermal and Mechanical Properties. *Journal of Polymers and the Environment*, 20(2), p. 540–549, 2012.

69. S. Pramanik, *et al.*, Bio-degradable vegetable oil based hyperbranched poly(ester amide) as an advanced surface coating material. *Progress in Organic Coatings*, 76(4), p. 689–697, 2013.

70. E. Urbaczewskiespuche, *et al.*, Influence of chain flexibility and cross-link density on mechanical-properties of epoxy amine networks. *Polymer Engineering and Science*, 31(22), p. 1572–1580, 1991.

71. A.S.H. Makhhouf, *Handbook of Smart Coating for Materials Protection*, in *Handbook of Smart Coating for Materials Protection*. Woodhead Publishing Ltd.: UK. Cambridge, 2014.

72. K. Thanawala, *et al.*, Development of Self-Healing Coatings Based on Linseed Oil as Autonomous Repairing Agent for Corrosion Resistance. *Materials*, 7(11), p. 7324–7338, 2014.

73. M. Behzadnasab, *et al., Preparation and characterization of linseed oil-filled urea-formaldehyde microcapsules and their effect on mechanical properties of an epoxy-based coating. Colloids and Surfaces a-Physicochemical and Engineering Aspects*, 457, p. 16–26, 2014.

74. E. Koh, *et al*., Microencapsulation of the triazole derivative for self-healing anticorrosion coatings. *New Journal of Chemistry*, 38(9), p. 4409–4419, 2014.

75. H. Es-haghi, *et al.*, Preparation and characterization of pre-silane modified ethyl cellulose-based microcapsules containing linseed oil. *Colloids and Surfaces a-Physicochemical and Engineering Aspects*, 447, p. 71–80, 2014.

76. A.B. Chaudhari, *et al*., Synthesis, characterization and application of Azadirachta indica juss (neem oil) fatty amides (AIJFA) based polyurethanes coatings: A renewable novel approach. *Progress in Organic Coatings*, 76(12), p. 1779–1785, 2013.

77. A. Chaudhari, *et al*., Development of eco-friendly polyurethane coatings based on neem oil polyetheramide. *Industrial Crops and Products*, 50, p. 550–556, 2013.

78. A.B. Chaudhari, *et al.*, Polyurethane Prepared from Neem Oil Polyesteramides for Self-Healing Anticorrosive Coatings. *Industrial & Engineering Chemistry Research*, 52(30), p. 10189–10197, 2013.

79. A. Chaudhari, *et al.*, Development of anticorrosive two pack polyurethane coatings based on modified fatty amide of Azadirachta indica Juss oil cured at room temperature - a sustainable resource. *Rsc Advances*, 4(34), p. 17866–17872, 2014.

80. E. Basturk, T. Inan, and A. Gungor, Flame retardant UV-curable acrylated epoxidized soybean oil based organic-inorganic hybrid coating. *Progress in Organic Coatings*, 76(6), p. 985–992, 2013.

81. C. Fu, *et al.*, Properties of alkoxysilane castor oil synthesized via thiol-ene and its polyurethane/siloxane hybrid coating films. *Progress in Organic Coatings*, 77(8), p. 1241–1248, 2014.

82. S.D. Rajput, P.P. Mahulikar, and V.V. Gite, Biobased dimer fatty acid containing two pack polyurethane for wood finished coatings. *Progress in Organic Coatings*, 77(1), p. 38–46, 2014.

83. S.D. Rajput, *et al.*, Renewable Source Based Non-biodegradable Polyurethane Coatings from Polyesteramide Prepared in One-Pot Using Oleic Acid. *Journal of the American Oil Chemists Society*, 91(6), p. 1055–1063, 2014.

84. S.D. Rajput, *et al.*, Fatty acids based transparent polyurethane films and coatings. *Progress in Organic Coatings*, 77(9), p. 1360–1368, 2014.

85. J.S. Ling, *et al.*, Novel poly(alkyd-urethane)s from vegetable oils: Synthesis and properties. *Industrial Crops and Products*, 52, p. 74–84, 2014.

86. C. Fu, *et al.*, A fully bio-based waterborne polyurethane dispersion from vegetable oils: From synthesis of precursors by thiol-ene reaction to study of final material. *Progress in Organic Coatings*, 77(1), p. 53–60, 2014.

87. P.D. Meshram, *et al.*, Synthesis and characterization of modified cottonseed oil based

polyesteramide for coating applications. *Progress in Organic Coatings,* 76(9), p. 1144–1150, 2013.

88. P.D. Meshram, *et al.*, High performance moisture cured poly(ether-urethane) amide coatings based on renewable resource (cottonseed oil). *Journal of Coatings Technology and Research*, 10(3), p. 331–338, 2013.

89. C. Yildirim, A.T. Erciyes, and Y. Yagci, Thermally curable benzoxazine-modified vegetable oil as a coating material. *Journal of Coatings Technology and Research*, 10(4), p. 559–569, 2013.

90. H. Bakhshi, *et al*., Synthesis and characterization of antibacterial polyurethane coatings from quaternary ammonium salts functionalized soybean oil based polyols. *Materials Science & Engineering C-Materials for Biological Applications,* 33(1), p. 153–164, 2013.

91. P.A. Wasekar and S.T. Mhaske, Dielectric Coating of Castor-Oil-Based Polyurethane Modified with Leucoemeralidine Polyaniline. *International Journal of Polymeric Materials and Polymeric Biomaterials,* 62(4), p. 231–235, 2013.

92. O. Saravari and S. Praditvatanakit, Preparation and properties of urethane alkyd based on a castor oil/jatropha oil mixture. *Progress in Organic Coatings*, 76(4), p. 698–704, 2013.

93. S. Ahmad, F. Naqvi, E. Sharmin, and K.L. Verma, Development of amine–acid cured Annona squamosa oil epoxy anticorrosive polymeric coatings. *Progress in Organic Coatings*, 55, p. 268–275, 2006.

94. S. Ahmad, *et al.,* Studies on epoxy-butylated melamine formaldehyde-based anticorrosive coatings from a sustainable resource. *Progress in Organic Coatings*, 56(2–3), p. 207–213, 2006.

95. S. Ahmad, S.M. Ashraf, and M. Alam, Studies on melamine modified polyesteramide as anticorrosive coatings from linseed oil: A sustainable resource. *Journal of Macromolecular Science Part a-Pure and Applied Chemistry,* 2006. 43(4–5), p. 773–783.

96. E. Sharmin, *et al.*, Linseed amide diol/DGEBA epoxy blends for coating applications: Preparation, characterization, ageing studies and coating properties. *Progress in Organic Coatings,* 67(2), p. 170–179, 2010.

97. T.J. Nelson, *et al*., Highly functional biobased polyols and their use in melamine-formaldehyde coatings. *Journal of Coatings Technology and Research*, 10(6), p. 757–767, 2013.

98. T.J. Nelson, and D.C. Webster, Monomer-grafted sucrose ester resins. *Journal of Coatings Technology and Research,* 10(4), p. 515–525, 2013.

99. C.S. Kovash, Jr., *et al.,* Thermoset Coatings from Epoxidized Sucrose Soyate and Blocked, Bio-Based Dicarboxylic Acids. *Chemsuschem,* 7(8), p. 2289–2294, 2014.

100. M. Alam, *et al.*, Vegetable oil based eco-friendly coating materials: A review article. *Arabian Journal of Chemistry,* 7(4), p. 469–479, 2014.

Chapter 6

Silica-Based Sol–Gel Coatings: A Critical Perspective from a Practical Viewpoint

Rosaria Ciriminna[1], Alexandra Fidalgo[2], Giovanni Palmisano[3], Laura M. Ilharco[2], and Mario Pagliaro[1]*

[1]*Istituto per lo Studio dei Materiali Nanostrutturati, CNR, Palermo, Italy*

[2]*Centro de Química-Física Molecular and IN-Institute of Nanoscience and Nanotechnology, Instituto Superior Técnico, Complexo I, Lisboa, Portugal*

[3]*Institute Center for Water and Environment (iWater), Masdar Institute of Science and Technology, Abu Dhabi, United Arab Emirates*

**Corresponding author*: mario.pagliaro@cnr.it

Abstract

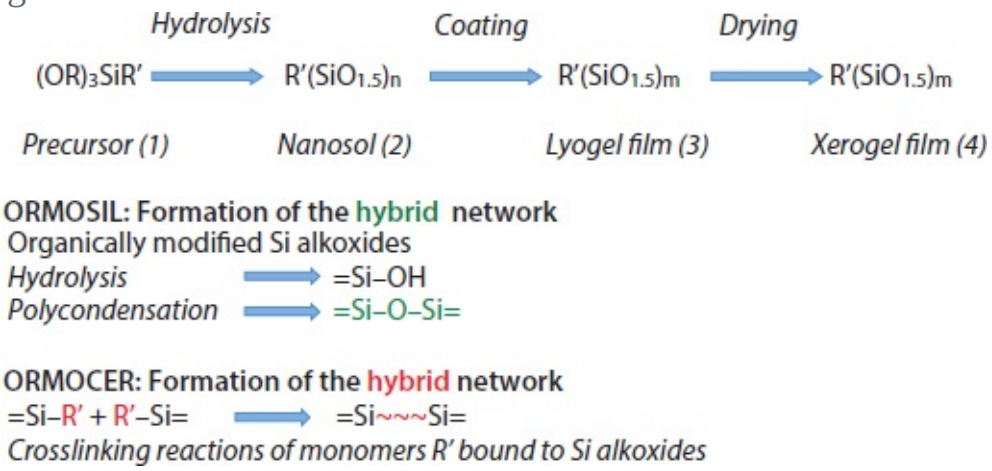
A critical overview of silica-based functional sol–gel coatings offers useful insight to evaluate the large-scale potential of this economically viable technology in the global coatings market. Current utilization of these truly advanced functional materials lies largely behind their applicative potential. Is it realistic to think that these multifunctional coatings may shortly replace conventional polymer-based alternatives at a significant extent?

Keywords: Sol–gel coatings, silica coatings, sol–gel, hybrid coatings

6.1 Introduction: *Need for a Practical Perspective*

Organosilica functional coatings obtained by the versatile sol–gel process are a well-established chemical technology with applications of great environmental and economic impact, ranging from anticorrosive to antifouling paints entirely devoid of harmful effects [1]. The principles behind this remarkable field of nanochemistry are thoroughly discussed in recent book chapters [2] and exaustive studies [3]. Here, we briefly remind the reader that said hybrid coatings are obtained under very mild conditions in liquid phase, either via the hydrolytic polycondensation of silicon alkoxides of general formula $Si(OR)_4$ and $R'_nSi(OR)_{4-n}$, affording an organically modified silicate (ORMOSIL), or via a complementary approach in which R' reacts with itself or with additional components, yielding an ORMOCER (organically modified ceramic) nanocomposite (Scheme 6.1).

Scheme 6.1 General schemes for the preparation of sol–gel ORMOSIL *(top)* and ORMOCER *(bottom)* nanocoatings.



In each case, the hybrid organic–inorganic coating lacks interface imperfections and its properties, intermediate between those of polymers and glasses, can deliver specific and unique requirements, not affordable by organic polymers and glasses alone.

The use of hybrid silica coating formulation, for example using tetraethoxysilane (TEOS) as an inorganic network precursor and methyl triethoxysilane (MTES) to create the organic network, reduces residual stresses of the layer, enhances the coating's flexibility and increases the thickness of the crack-free coating [1].

Furthermore, the incorporation of nanoparticles or nanocontainers into the sol–gel coating may lead to multifunctional protection coatings, especially for protection of metal substrates from corrosion [4]. The inherent stability and flexibility of the siloxane (Si–O–Si) bond, indeed, ensures the formation of a three dimensional network of –Si–O–Si– linkages, which helps to retard the penetration of corrosive medium through the coating (passivation of the substrate) [5].

Finally, contrary to other coating methods, such as chemical vapor deposition, which require the use of dedicated plants and deposition processes, sol–gel silica coatings are simply deposited using techniques as simple as spraying, dip- or spin-coating, or even electrochemical [6] (a most important route to develop sol–gel sensors).

Minami, whose team in Japan developed MTES formulations mixed with fine oxide powders to protect the steel heating panels of microwave ovens [7], in 2013 published an account on advanced sol–gel coatings for practical applications [8].

This chapter, thus, does neither review subsequent advances nor it comprehensively addresses successful sol–gel nanocoatings, but it rather offers a critical perspective on these multifunctional coatings, written from a practical viewpoint. For example, in 2009 we were writing that:

> "Overall, these features allow for a convenient replacement of older industrial coating technologies with new, affordable sol-gel methods that often are conducted employing aqueous formulations. Silica-based hybrid coatings will soon become ubiquitous nanomaterials with a multiplicity of applications in everyday life" [1].

Perhaps the recent subsequent introduction of biocide-free antifouling coatings, based on organically modified hybrid xerogels, to prevent the adhesion of fouling organisms on vessels and boats [9] is enough to show the relevance of the above arguments. Yet, almost a decade later, it is useful and instructive to review the situation of sol–gel nanocoatings in the context of the huge coatings industry.

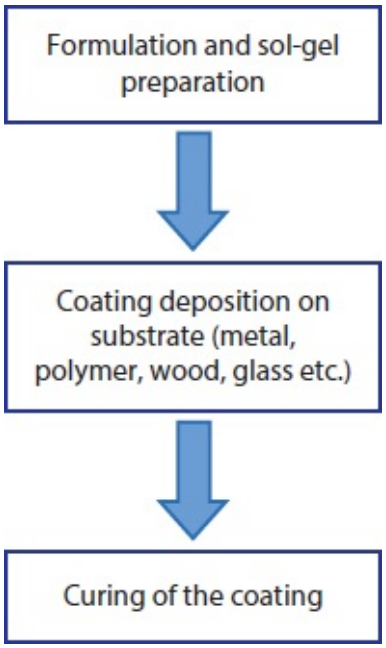
6.2 A Green, Simple Technology

The hydrolysis of silanes affords the release of plentiful alcohol (in normal silanes, more than 50% of their weight), which can be readily distilled yielding waterborne VOC-free sol–gel coating formulations that today are widely (and increasingly) used to combat corrosion, friction, stick and fouling, due to a number of *unique* advantages like room temperature synthesis, chemical inertness, high oxidation and abrasion resistance, excellent thermal stability, and little or none health hazard [10].

In the early 2000s, sol–gel coatings made of silanes formulated in water or in non-toxic alcohols were firstly used (at Boeing) to protect aircraft fuselage, thereby replacing at least a fraction of the highly toxic Cr(VI) present in the chromates conventionally used, and drastically reducing the amount of volatile organic compounds (VOCs) present in traditional formulations [11]. Since then, numerous companies, both large and small (including, for example, *Nanogate* and *Evonik*), have started to commercialize silane-based anti-stick, scratch-proof, anti-mist and anti-corrosion coatings based on sol–gel inorganic–organic nanochemistry technology.

The sol–gel coating fabrication procedure is general (Scheme 6.2). The hydrolysis of silanes is followed by alcohol removal and then by addition of fillers and one or more functional species (pigment, anti-microbial, fragrance, UV absorber, photocatalyst, etc.) according to the required application. This functionalization step uniquely allows creating coatings for unprecedented large range of applications.

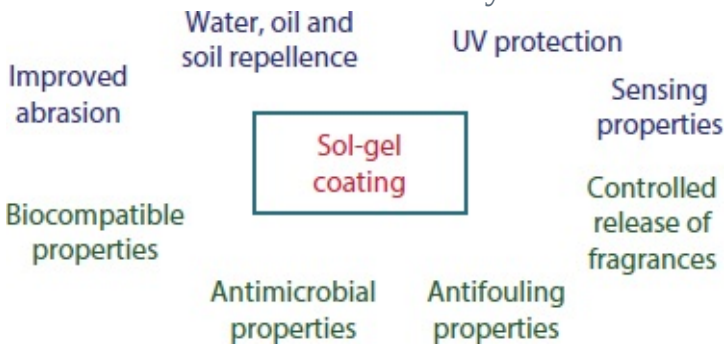
Scheme 6.2 The sol–gel coating fabrication procedure (adapted from Ref. [1], with kind permission).



The coating formulation is generally a transparent, low-viscosity, solvent-free stable liquid, with a shelf life of several months. The liquid coating can be applied on single side or both sides of a substrate via spray, dip or other coating application method, after which the coating is cured either by simple drying under atmospheric conditions, by mild heat treatment, or by UV light or ammonia curing, depending on the coating.

The functional sol–gel coating thus provides a material's interface with new, enhanced physical, chemical, mechanical, optical, electrical or biological properties (Scheme 6.3).

Scheme 6.3 Selected properties of surface functionalized by a modified sol–gel nanocoating.



Schmidt [12] Minami [8], Böttcher [13], Ferreira [14], Bright and Detty [15], Akid [16], Barbé [17] and their coworkers are among the scientists who largely contributed to major advances in the field.

Figueira *et al*. recently published a comprehensive review of recent progress (2001–2013) only in the field of sol–gel silica-based anti-corrosion coatings [18]. The number of research papers published in the field of "hybrid + sol–gel" materials between 1990 and 2013, they found, exceeds 21,000, with the number of publications in 2013 being about 45 times the number of those published in 1990.

The team concluded that these organic–inorganic sol–gel coatings show "high potential for the production of multilayer coating systems which are promising environmentally friendly candidates for replacement of the chromate-based pretreatments due to a synergistic effect of good barrier properties and effective 'self-healing' action" [18].

6.3 The Market

In 2014, a reputed market research company reported that the total global market for sol–gel products, valued at $1.7 billion in 2014, was expected to grow to $2.5 billion in 2019, at an annual growth rate approaching 8% from 2014 to 2019 [19]. Much of this growth, we argue here, will be due to the adoption of sol–gel silica coatings across many industries. Indeed, another market study [10] almost concomitantly concluded that "ever more manufacturers are turning to sol–gel coating technologies to further enhance current commercial products or add completely new properties to existing technology" [10]. Properties that can be achieved with sol–gel nanocoatings, continues said report, include the following:

- Hydrophobic surfaces
- Anti-fingerprinting
- Oleophobic surfaces
- Anti-microbial surfaces
- Easy to clean surfaces
- Protective transparent coatings
- Corrosion resistance
- Low friction
- Chemical resistance
- Anti-static surfaces
- Conducting/semi-conducting surfaces
- Extreme mechanical wear resistant properties
- UV protection

Among these, in general, easy-to-clean, anti-fingerprint and anti-bacteria sol–gel nanocoatings were the most required until 2011 (Table 6.1).

Table 6.1 Estimated easy-to-clean, anti-fingerprint and anti-bacteria sol–gel nanocoating market size (data of Future Markets, Inc.; reproduced from Ref. [20], with kind permission).

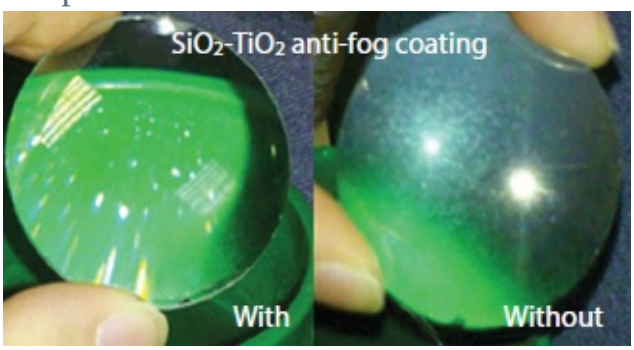
Application	Revenue (2014), million USD
Automotive	60.1
Consumer electronics	23.6
Construction	73.7
Sanitary	172.5
Food (anti-bacteria)	40.1
Medical (anti-bacteria)	134.4
Anti-bacteria (others)	197.8

Unlike conventional surface protection methodology with polymers, the sol–gel silica-based coatings are intrinsically multifunctional, so that additional features such as chemical resistance, anti-static, scratch resistance or ease of cleaning can be achieved according to customer requirements. End user markets are practically unlimited, including construction (pipes, facades, bridges), automotive (paint surface treatments, metal parts, metal structures, windows, mirrors and lamps, plastic hoods), marine (large vessels and recreational boats), sanitary, oil and gas (pipes), energy (wind power structures and blades, glass surfaces on solar panels), consumer electronics (displays and plastic and metal parts) and food and beverage packaging.

Opportunities abound in almost any traditional segment (application) of the broad coatings market. For example, anti-fog technology has a very large market potential, with industrial applications potentially including cars and cameras. However, the high cost of the existing anti-fog technologies has hampered their large-scale applications.

As a result, most digital cameras with price less than $1,000 do not carry this anti-fog effect. A simple alternative based on a single layer anti-fog and self-cleaning coating formed by superhydrophilic SiO_2–TiO_2 nanostructures developed by Singapore's scientists can be used to produce high-performing coatings at lower cost (Figure 6.1) [21].

Figure 6.1 Performance of sol–gel anti-mist, anti-fog silica–titania coating developed in Singapore. Manufacturing is ready for scale-up.

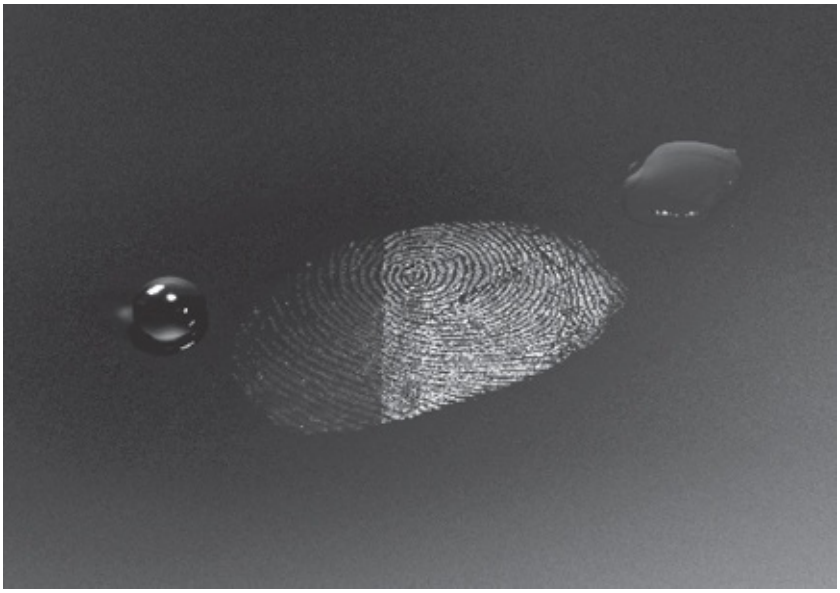


The coating is prepared by sol–gel dip/spin coating technique on glass substrates. The performance is superior to typical TiO_2 films, which rapidly lose their superhydrophilic properties, within hours of being isolated from a UV source; and is superior to SiO_2 films which are easily contaminated by organic compounds.

Another most recent example is a permanent anti-reflective *and* oleophobic coating for use on

cover glasses for touch displays to protect them against fingerprints (Figure 6.2).

Figure 6.2 Multifunctional coating for public touch displays
(reproduced from Ref. [22], with permission).



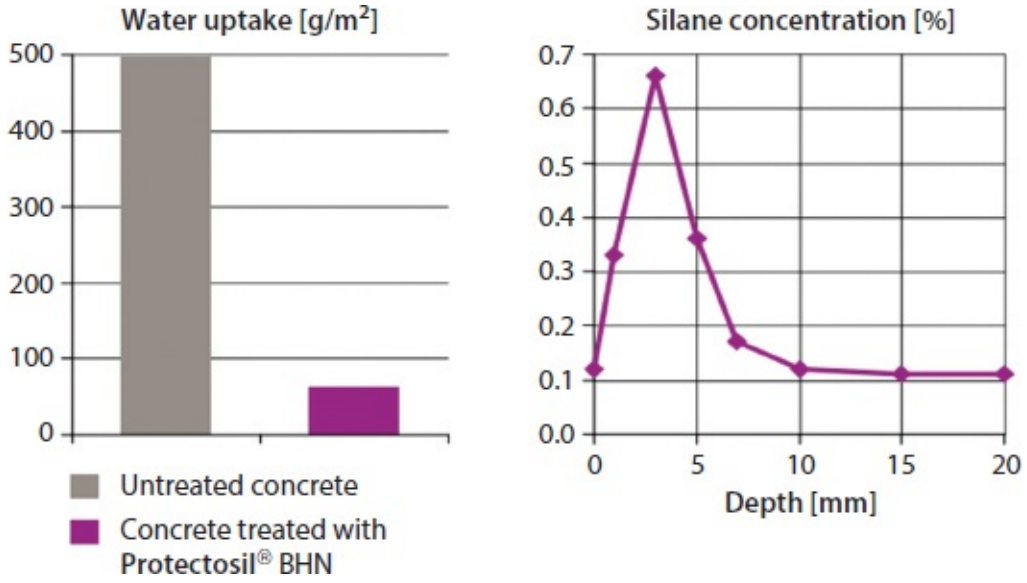
Such interactive displays today are ubiquitous and include educational drawing boards, kiosk systems in public places, devices in marine and medical technology, and many other examples. Resisting the burden of being touched many times by users, the multifunctional *Daro* coating is also anti-reflective, offering increased contrast in bright environments [22].

Another successful line of organosilanes water-based sol–gel products is the *Dynasylan* series of sol–gel coatings marketed for over a decade by *Evonik*. These coating formulations are comprised of stable, water-soluble silanol-containing organosilica sols obtained removing (by distillation) the alcohol released during the hydrolysis of the silanes [23]. A quick look to the areas of their fields of application claimed by the company renders the impressive market potential of these coatings [24]:

- Adhesives and sealants
- Building protection
- Coatings and metal treatment
- Fillers and pigments
- Glass fibers and mineral/glass wool insulation
- Plastics
- Special applications

Focusing onto building protection only, the company offers a series of hydrophobic silane formulations capable to protect concrete structures from the ingress of moisture and dissolved contaminants via capillary suction into the pores (where water and chlorides cause corrosion of reinforcing steel, salt burst or freeze-thaw damage). Figure 6.3, for example, shows the results of the treatment of the concrete joints of the 6.6-km-long Storebelt West Bridge in Denmark.

Figure 6.3 Treatment of the concrete joints of the Storebelt West Bridge in Denmark with *Protectosil BHN* affords significant reduction in water penetration due also to deep penetration of the sol–gel coating into the substrate
(reproduced from Ref. [25], with kind permission).



A reduction of water penetration of about 87%, when compared to untreated concrete, and a high penetration depth explain the long lasting protection offered by this sol–gel water-repellent coating, which also maintains the substrate's water vapor permeability.

The liquid coating *(Protectosil BHN)*, comprised of isobutyl triethoxysilane partly hydrolyzed, is indeed capable to protect highly alkaline substrates such as concrete for long periods of time. The isobutyl groups are stable against UV-induced degradation and provide hydrophobicity, while the ethoxide groups of the silane react with the hydroxyl groups at the concrete's surface providing excellent adhesion of the coating. Overall, this ensures prolonged durability of the protected structure in a challenging environment particularly susceptible to corrosion.

Many other advanced applications of functional sol–gel coatings exist, ranging from the functionalisation of textiles explored and commercialized by Boettcher, Mahltig and co-workers in Germany [26], affording functional textiles with improved properties (enhanced comfort, easy care, health and hygiene, protection against mechanical, thermal, chemical and biological attacks, water, oil and soil repellency and with antimicrobial and anti-allergic properties); as well as the sol–gel silica coatings used for making non-stick cookware (the *Thermolon* sol–gel coating replacing polytetrafluoroethylene coating, allowing for faster cooking at lower temperature, with no release of toxic fumes even when overheated beyond 450 °C) [27].

What is relevant here is that organosilica hybrids, in the form of water-based formulations abating the VOC content of traditional coating paints, are rapidly emerging as an innovative coating technology offering the versatility of organic polymers, along with the strength and durability typical of inorganic coatings; offering, in addition to the usual physical and chemical protection, a whole set of new functional properties to the coated substrate.

The multibillion dollars industry, which historically has relied upon organic polymers, in principle might be largely affected by the introduction of the sol–gel silica hybrid coatings nanochemistry technology on large scale.

A closer look at the coatings market reveals that coatings' manufacturers include some of the world's largest chemical companies *(Akzo Nobel, PPG, Sherwin-Williams, BASF, Valspar, Nippon Paint)*, whose revenues exceeded 120 billion USD only in 2013 (growing at a 5% annual rate) [28]. These companies supply customers across a wide range of sectors including automotive, consumer electronics, aviation, shipping and leisure craft, sports equipment, construction, furniture, and food and beverage. Beyond decorative coatings, the most advanced class of paints is comprised of so-called "performance coatings" (industrial and car finishes, marine and packaging coatings). These

companies use well-established manufacturing technologies that provide them with low (<10%) fixed costs as a percentage of revenue [29]. Under these conditions, changing existing manufacturing processes and product technologies may not be convenient.

On the other hand, we have recently explained elsewhere [30] that the historical barriers to commercialization of many innovative sol–gel products are now over. The cost of silanes has dropped and continues to diminish, while many successful sol–gel products and sol–gel coatings have been successfully commercialized.

It is the new companies specializing in sol–gel coatings that will likely continue to supply innovative coating formulations for a wide variety of applications, until customers will start to replace older technologies with the new hybrid silica-based coatings.

According to this argument, all the sol–gel nanocoatings suppliers identified by two innovation economists in 2007 [31] were just-established small- and medium-size companies (Table 6.2). One of them, *Nanogate*, originally a spin-off of the Leibniz Institut für neue Materialien in Germany, where the team led by Schmidt had developed the ORMOCER since the early 1980s, today is a public company with over 550 employees, and current turnover exceeding EUR 68 million, expected to reach EUR 80 million in 2015 [32].

Table 6.2 Selected sol–gel nanocoatings brought to the market as of 2007 (reproduced from Ref. [31], with kind permission).

Coating property	Application	User/producer
Scratch resistant	Synthetic glasses Driver's license Plexiglas lenses Centrifuges	Rupp & Hubrach Bundesdruckerei Berlin Schweizer Optik Surface Contacts
Anti-adherence	Medical tools Carpets	Nanosol Nanogate
Anti-bacterial	Hearing aid Medical probes	Audio Service Nanosol, Surface Contacts

When this turning point is reached, the largest suppliers of traditional, polymer-based coatings will also expand their technology portfolio and turn to sol–gel science and technology to manufacture their main "performance" (i.e. functional) coatings. It is somehow revealing, in this respect, to learn that industry-sponsored websites [33] already exist that try to reverse the first market losses in the non-stick coating market, supporting the cause of traditional products.

6.4 Conclusions

Thirty-five years after the pioneering work of Schmidt with ORMOCERs, hybrid silica sol–gel coatings easily obtained by depositing a thin layer (few tens of microns) of the liquid coating over substrates of practically any composition and shape are no longer a niche technology pursued by start-up companies, but rather a well-known nanochemistry technology, used across many industries worldwide to protect *and* to provide new properties to existing products.

Transparent sol–gel silica coatings are truly advanced functional materials whose utilization, however, is still largely beyond their full applicative potential. For example, following their introduction to the market in 2010, today approximately 1 billion people across the world use a tablet. It would be enough to ask them if they are satisfied with the fingerprint left on the display after a

single utilization cycle, to understand how obsolete are the coatings used (or, perhaps, *not* used) by the tablet manufacturers.

As mentioned above, a long lasting sol–gel coating for tablet and glass displays in general has been launched by late 2014. Similar arguments hold for anti-fog and anti-mist coatings that continue to *not* be applied by glass makers on the glass they supply to car, truck and train manufacturers.

Sol–gel coatings based on now well-mastered nanochemistry of the sol–gel process are the long-awaited, economically viable solution to these and related unmet customer requirements. The silane price has dropped, and sol–gel coatings became economically viable. Customers using silica and organosilica coatings in place of conventional polymeric materials, furthermore, provide their products with a dramatically improved sustainability profile. This study provides a critical overview of sol–gel silica nanocoatings in the context of the coatings industry and market.

Acknowledgements

We thank our friends and co-workers in the field of sol–gel coatings, David Avnir, Hebrew University of Jerusalem; Eric Le Bourhis, University of Poitiers; Frank V. Bright and Michael R. Detty, University of New York at Buffalo; Pietro Selvaggio and Sebastiano Tusa, Soprintendenza del Mare della Sicilia; and DavideTranchida, now at the University of Siegen. Their cooperation has been as fruitful as personally rewarding. Prolonged correspondence of one of us (M.P.) with Professor Horst Böttcher, GMBU eV Dresden, has inspired many arguments of the present study.

References

1. M. Pagliaro, R. Ciriminna, and G. Palmisano, *Journal of Materials Chemistry,* Vol. 19, pp. 3116–3126, 2009.

2. A. Julio López and J. Rams, Reinforced Sol–Gel Silica Coatings in D. Levy and M. Zayat, eds., *The Sol-Gel Handbook,* Wiley-VCH, Chapter 42, 2015.

3. D. Wang and G.P. Bierwagen, *Progress in Organic Coatings,* Vol. 64, pp. 327–338, 2009.

4. G. Kordas and E.K. Efthimiadou, Self-Healing Coatings for Corrosion Protection of Metals, in *The Sol-Gel Handbook,* D. Levy and M. Zayat, eds., Wiley-VCH, Chapter 47, 2015.

5. T. Materne, F. de Buyl, and G.L. Witucki, Organosilane Technology in Coating Applications: Review and Perspectives, *9th Congresso Internacional de Tintas - ABRAFATI 2005,* September 14–16, 2005, Sao Paulo, Brazil.

6. L. Liu and D. Mandler, Sol–Gel Coatings by Electrochemical Deposition in D. Levy and M. Zayat, eds., *The Sol-Gel Handbook,* Wiley-VCH, Chapter 3, 2015.

7. K. Izumi, T. Shimizu, and T. Minami, *Journal of the Ceramic Society of Japan,* Vol. 108, pp. 937–940, 2000.

8. T. Minami, *Journal of Sol-Gel Science and Technology,* Vol. 65, pp. 4–11, 2013.

9. M.R. Detty, R. Ciriminna, F.V. Bright, and M. Pagliaro, *Accounts of Chemical Research,* Vol. 47, pp. 678–687, 2014.

10. Future Markets, *The World Market for Sol-Gel Nanocoatings*, London, 2014.

11. Y. Huang, H. Zheng, C.J. Yang, Q. Wei, W. van Ooij, V. Palanivel, and J. Osborne, Non-VOC Water-Based Sol-Gel/Silane-Based Corrosion Protection Coating, *Surface Engineering Coatings and Heat Treatments 2002:Proceedings of the 1st ASM International Surface Engineering and the 13th IFHTSE Congress (ASM International),* Vol. 1, pp. 115–121, 2003.

12. M. Mennig, G. Jonschker, and H.K. Schmidt, *SPIE Proceedings,* Vol. 1758, pp. 125–134, 1992.

13. H. Böttcher, K.-H. Kallies, H. Haufe, and J. Seidel, *Advanced Materials,* Vol. 11, pp. 138–141, 1999.

14. M.L. Zheludkevich, I. Miranda Salvado, and M.G.S. Ferreira, *Journal of Materials Chemistry,* Vol. 15, pp. 5099–5111, 2005.

15. Y. Tang, J.A. Finlay, G.L. Kowalke, A.E. Meyer, F.V. Bright, M.E. Callow, J.A. Callow, D.E. Wendt, and M.R. Detty, *Biofouling* Vol. 21, pp. 59–71, 2005.

16. H. Wang, R. Akid, and M. Gobara, *Corrosion Science* Vol. 52, pp. 2565–2570, 2010.

17. E. Campazzi, M. Villatte, C. Druez, S. Senani, and C. Barbé, Alternatives to Chromate Systems for Corrosion Protection in Aerospace: Study of "Green"-Inhibitor Loaded Spheres in Model Sol-Gel Coatings, *9th Coatings Science International 2013,* June 24–28, 2013, Noordwijk, The Netherlands.

18. R.B. Figueira, C.J.R. Silva, and E.V. Pereira, *Journal of Coatings Technology and Research,* Vol. 12, pp. 1–35, 2015.

19. Sol-Gel Processing of Ceramics and Glass, BCC Research, Wellesley, MA, 2014.

20. Z. Xiao, "Easy-to-clean and antimicrobial coatings: Development and Perspectives in Aesthetic Applications", Singapore Institute of Manufacturing Technology, 19 August 2014.

21. Sol-Gel Coating with Persistent Anti-Fog and Self-Cleaning Properties, Intellectual Property Intermediary, Singapore, 2015.

22. Schott to offer its multifunctional Daro coating for touch displays on Conturan glass, Schott, Mainz, November 7, 2014.

23. J.R. Steinmetz and B.C. Arkles, Method for preparation of stable water-borne silane compositions, EP 675 128 B1, assigned to Sivento, March 31, 1994.

24. Dynasylan - the brand for functional silanes, http://www.dynasylan.com, May 2015.

25. Protectosil. Innovative building protection, Evonik, http://www.protectosil.com/product/protectosil/Documents/Protectosil-building-protection-case-studies-EN.pdf, 13 January 2012.

26. B. Mahltig and T. Textor, *Nanosols and Textiles,* World Scientific Publishing Company, 2008.

27. C. H. Phillips, Thermolon Mineral Coatings, Thermolon, Seoul, 2010.

28. Global Market Study on Paints and Coatings: Industrial Paints and Coatings to Witness Highest Growth by 2020, Persistence Market Research, New York, NY, 2013.

29. Meet Akzo Nobel, Akzo Nobel, February 2010.

30. R. Ciriminna, A. Fidalgo, F. Béland, V. Pandarus, L.M. Ilharco, and M. Pagliaro, *Chemical Reviews,* Vol. 113, pp. 6592–6620, 2013.

31. H. van Lente, and J. van Til, *International Journal of Foresight and Innovation Policy,* Vol. 3, pp. 121–138, 2007.

32. Nanogate plans to increase sales to over EUR 80 million - Preliminary figures for 2014 exceeded, Nanogate, Gottelborg, 23 April 2015.

33. Sol-Gel Ceramic Coatings, The Product Knowledge Network, http://www.productknowledge.com/SolGel-how-does-it-work.html, 2015.

Chapter 7

Fatty Acid-Based Waterborne Coatings

Mónica Moreno[1], Monika Goikoetxea[2], and María J. Barandiaran[1]*

[1]*POLYMAT, University of the Basque Country UPV/EHU, Joxe Mari Korta Zentroa, Donostia-San Sebastián, Spain*

[2]*CIC nanoGUNEConsolider, Donostia-San Sebastián, Spain*

**Corresponding author*: mariaje.barandiaran@ehu.es

Abstract

Creating new coatings with lower environmental impact is one of the most important challenges of industry nowadays. Waterborne dispersed polymers are the green alternative to solvent-based systems. The replacement of petroleum-based monomers by renewable resources is the other green approach. This chapter describes the use of fatty acid-based monomers to synthesize novel waterborne polymeric materials for coatings applications. Different approaches to produce fatty acid monomers able to undergo free radical polymerization are presented. Their synthesis via emulsion and miniemulsion polymerization is assessed, and the importance of preserving the double bonds of the alkyl chain is highlighted. Finally, some examples of their incorporation into waterborne paints are discussed.

Keywords: Waterborne coatings, fatty acids, renewable resources, (mini)emulsion polymerization

7.1 Introduction

The increasing environmental regulations limiting the use of volatile organic compounds (VOCs) [1, 2] had led to a global trend in developing waterborne coatings as an alternative to traditional solvent-based systems. Thus, emulsion polymerization came to scene, and nowadays it is a widespread technique to produce waterborne coatings at industrial level. Indeed, many companies offer waterborne coatings equivalent to solvent-borne ones but having lower levels of VOCs. Furthermore, waterborne coatings include additional advantages over solvent-borne coatings such as faster drying times, less smell and easier cleaning up [3, 4].

The most important polymers for emulsion coatings are copolymers of vinyl acetate with acrylate esters, acrylate–methacrylate, styrene–acrylate and styrene–butadiene copolymers [5]. However, the current approach to producing these carbon-based chemicals is non-sustainable as the feedstock needs millions of years to form. A transition from non-renewable to renewable carbon resources seems imperative because increasing demands for a finite resource cannot be sustainable. The progressive decline of fossil resources, and the variability in oil prices that also depends on geopolitical factors,

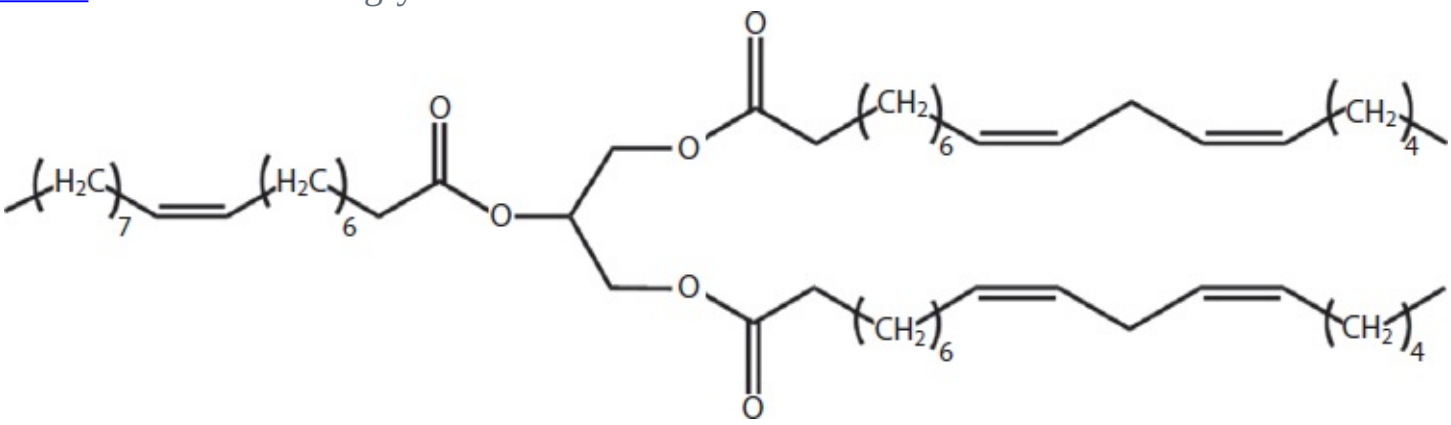
together with the environmental concerns, has promoted an intense search for alternatives based on renewable resource monomers for the production of polymers.

In this regard, the scientific and industrial community is performing extensive search of biobased monomers for the production of polymers capable of mimicking the properties of the petroleum-based counterpart. This is well reflected in the large number of books [6–10] and articles [11–27] that have reviewed the topic of polymers from renewable resources.

The use of vegetable oils as a source of materials dates back to the beginning of civilization when they were used for soaps and coating applications. In the past decades, the industrial interest in vegetable oils and fats has increased in such a way that today's applications have broadened to surfactants [28], lubricants [29], adhesives [30], paints and coatings [31, 32] or biodiesel [33, 34]. This interest has boosted the worldwide production of vegetable oils, which was around 125 Mt in 2005, and it raised to 176 Mt in 2014 [35]. From this amount, 15% was used for the chemical industry [36].

Vegetable oils are triglyceride esters of fatty acids and their general structure is shown in Figure 7.1. This genuine chemical structure including different amount, position and type of unsaturations enable them to undergo a wide variety of chemical transformations producing polymeric materials with versatile applications. Thus, the oxidative capacity of fatty acids carbon–carbon double bonds has traditionally been used during the curing process of alkyd resins to improve the mechanical properties and chemical resistance of the final polymers [19, 37–40]. Furthermore, they are easy available with relative low cost, have low toxicity and are biodegradable [41, 42]. All the above, had promoted research in the field of waterborne coatings based on renewable oil resources [43] such as waterborne alkyds [44, 45] alkyd-acrylic hybrids [46, 47], alkyd-acrylic blends [48, 49] and oil-modified polyurethane dispersions [50].

Figure 7.1 Sunflower oil triglyceride structure.



However, the fatty acid composition of any oil may change from crop to crop because climatic changes such as humidity and temperature, as well as soil type and growing location. This can represent an important drawback to the polymer industry because of the lack of reproducibility of the manufacturing products.

Fatty acids, which account for the 95% of the total weight of the vegetable oils, are available in their pure form as platform chemicals for polymer synthesis. In this chapter, the potential modification of fatty acids to produce polymers via free radical emulsion polymerization will be presented. The importance of preserving the double bonds during the modification in order to broaden the range of polymer characteristics and to improve their final properties will be discussed. Finally, some examples of their application as binders in waterborne coatings will be given.

7.2 Fatty Acids as Raw Materials

Fatty acids are the primary components of vegetable oils and important raw materials in the chemical industry. In fact, fatty acids are one of the main raw materials for the production of alkyd resins, which have been the dominant binder in most commercial solvent-borne coatings [51]. Alkyd resins are produced from esterification of polyhydroxy alcohols with polybasic acids and fatty acids [32].

As essential elements, fatty acids can be obtained biosynthetically in the organism from acetyl coenzyme A and malonyl coenzyme A precursors and by action of several enzymes [52]. Industrially, several physical and chemical methods for fatty acid production have been developed [53]. Few decades ago, the chemical hydrolysis at high temperature and pressure and the physical refining by means of distillation under high temperature and vacuum [54] was the technique most commonly used. However, since these processes involve high energy consumption, the enzyme-catalyzed hydrolysis of vegetable oils such as sunflower, olive, palm or soybean oil into their basic components fatty acids and glycerol is regarded nowadays as an effective method to obtaining fatty acids at mild conditions [55, 56].

The most common plant-based fatty acids from vegetable oils are palmitic, palmitoleic, stearic, oleic, linoleic and linolenic acids, all containing 16 and 18 carbon atoms, saturated, mono, di- and tri-unsaturated carboxylic acids. Other important fatty acids in nature are ricinoleic acid from castor oil, which presents a hydroxyl group along its aliphatic backbone, and α-eleoestearic acid from tung oil that bears an epoxy group. Table 7.1 summarizes the structure of these fatty acids, and in Table 7.2, the main vegetable oil sources of these acids are shown.

Table 7.1 Structures of some of the most important fatty acids [27].

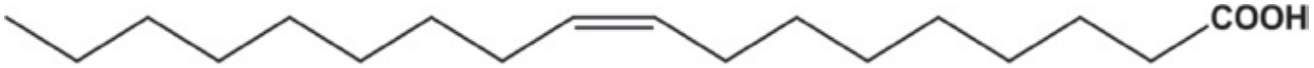
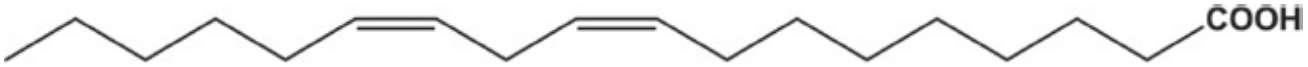
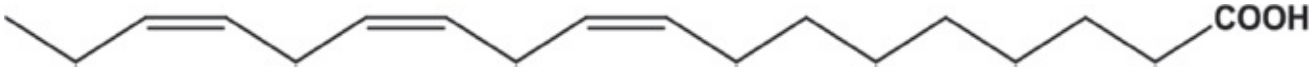
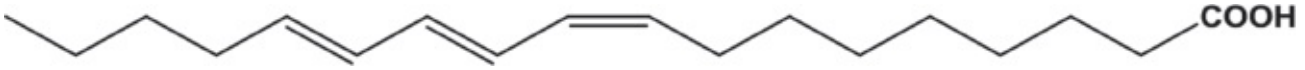
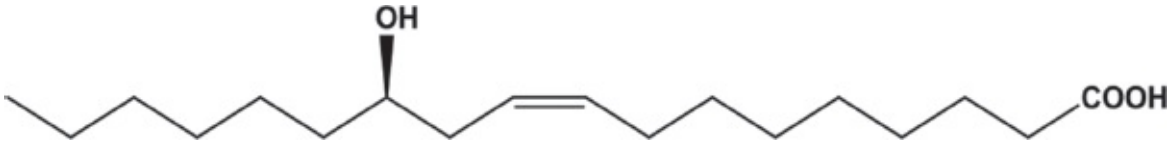
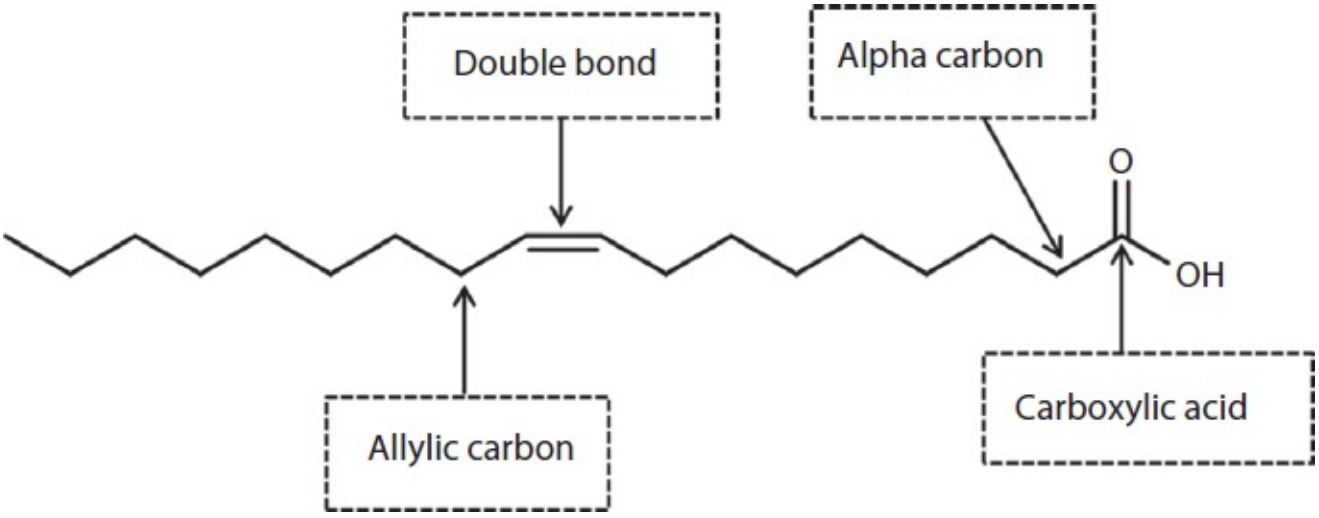
Fatty acid	Structure
Palmitic	
Palmitoleic	
Stearic	
Oleic	
Linoleic	
Linolenic	
α-Eleoestearic	
Ricinoleic	

Table 7.2 The average annual production and compositions of some commodity oils [10].

Natural oil	Average annual production (10^6 tons)	Palmitic	Stearic	Oleic	Linoleic	Linolenic
Soybean	43.41	11.0	7.8	7.8	7.8	7.8
Palm	53.33	40.5	40.5	40.5	10.1	–
Rapeseed	23.52	4/4.1	2/1.8	56/60.9	26/21.0	10/8.8
Sunflower	13.81	5.2	2.7	37.2	53.8	1.0
Olive	3.39	13.7	2.5	71.1	10.0	0.6
Linseed	0.83	5.5	3.5	19.1	15.3	56.6

Figure 7.2 Reactive sites in the fatty acid molecule (e.g. oleic acid) for the incorporation of functional groups.



7.2.1 Chemical Modification of Fatty Acids for Free Radical Polymerization

Fatty acids bearing non-conjugated double bonds are not sufficiently reactive to undergo effective free radical polymerization. The variety of active sites in their structure allows the selective functionalization or chemical modification through a wide number of chemical transformations [12, 23, 57, 58] making possible the design of a broad range of chemically modified fatty acids [59].

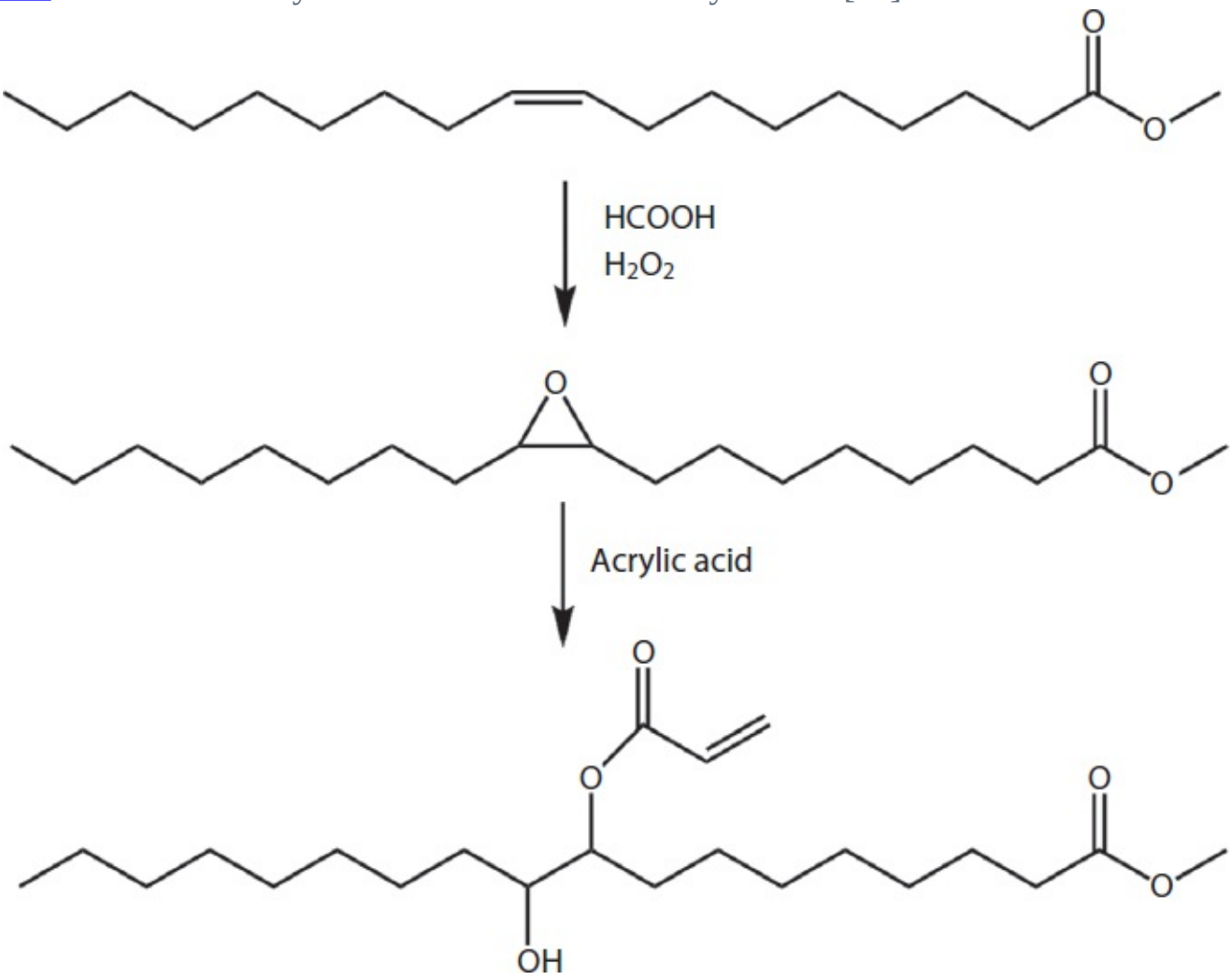
A huge number of chemical routes have been already implemented to prepare vegetable oil derivatives useful in the preparation of polymers and composites [58], which can be extrapolated to the modification of fatty acids. There are four main sites in the fatty acid molecule that can be chemically modified with the aim of incorporating a polymerizable molecule afterwards: (1) the allylic carbon and the carbon alpha to the carboxylic group, (2) the double bonds and (3) the carboxylic acid (Figure 7.2).

1. *Chemical modification through the allylic carbon and the α-carbon.* The C–H bonds of unsaturated fatty acids are activated carbons by an adjacent double bond (allylic carbon) or a carbonyl group (α-carbon), which can be oxidized relatively easy with different oxidizing agents. For instance, the allylic methyl oleate has been oxidized to give allyl alcohols [12]. The allylic position of high-oleic sunflower oil triglyceride was also used to get α,β-unsaturated ketones that were further reduced to the corresponding hydroxylic compounds to be eventually acrylated with

acryloyl chloride [60].

2. *Chemical modification through the fatty acid double bonds*. The chemical modification through the fatty acid unsaturation has been the most common approach to incorporate a molecule containing allyl or vinyl functionalities active in free radical polymerization. Some potential modification is the attachment of maleates [61] or the direct dihydroxylation with Osmium or Ruthenium catalysts [62]. Epoxidation of alkenes with peracids is however, the widest applied method in industry for the epoxidation of fatty acids [63–65]. Thus, the epoxidation of the oleic acid unsaturation double bonds followed by the addition of acrylic acid was reported by Bunker et al. as an interesting synthesis pathway to obtain acrylated fatty acids [66, 67] (Figure 7.3). Jensen et al. [68] synthesized also acrylated methyl oleate (AMO) using a different pathway. They performed a three-step reaction: (1) esterification of oleic acid with methanol, (2) epoxidation of the OA double bond and (3) acrylation of the epoxidized methyl oleate with acrylic acid.

Figure 7.3 Scheme of the synthesis of AMO from methyl oleate [66].

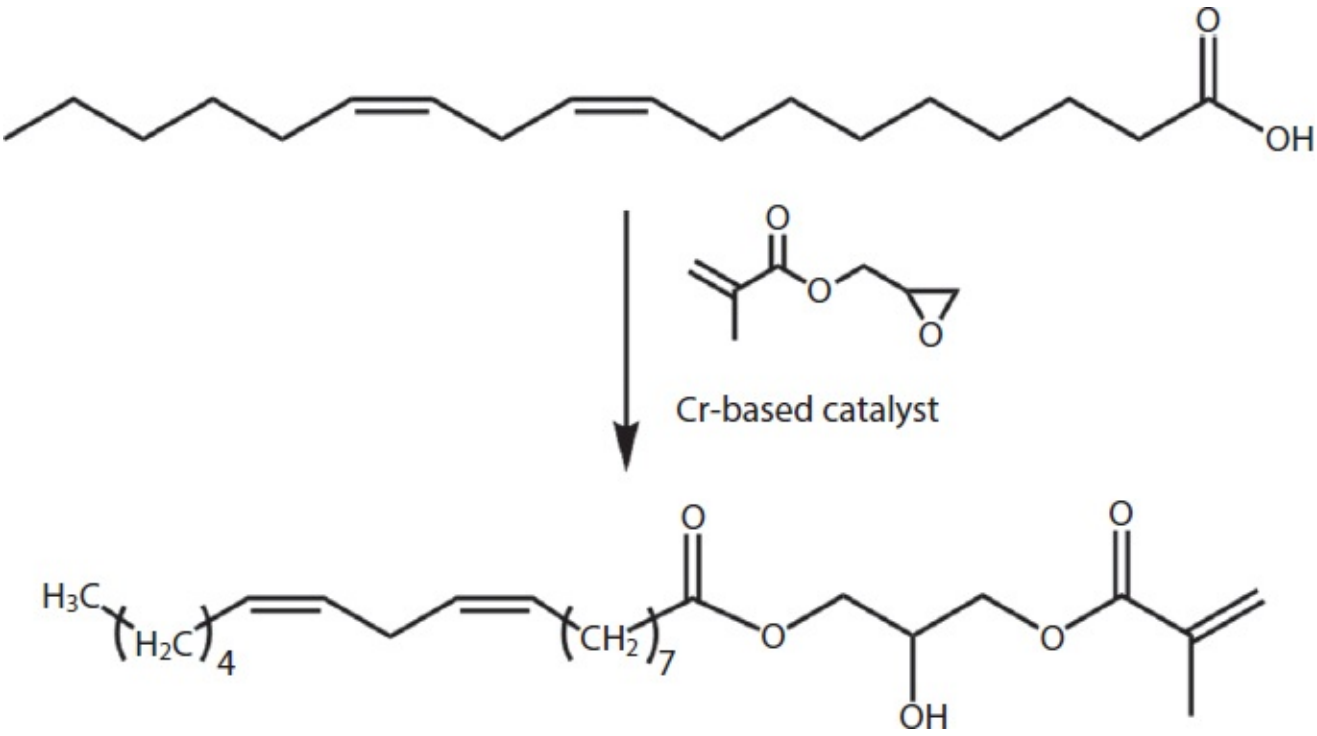


All these synthetic pathways result in the consumption of the fatty acids double bonds, precluding therefore their auto-oxidative capability. This represents an important drawback since the potential to improve the mechanical properties and the chemical resistance of the final polymer during the post curing is limited. Therefore, for these polymers to be used in coating applications, the incorporation of a more reactive polymerizable functional group through the carboxylic acid appears as a clever approach to synthesize free radically active fatty acid while preserving the alkyl chain double bonds.

3. *Chemical modification through the carboxylic group*. In this line, different strategies for the

chemical functionalization through the carboxylic group have been reported. Thus, La Scala *et al.* [69] directly converted fatty acids into a meth(acrylate) functionality in a one-step metal-catalyzed reaction with glycidyl methacrylate (GMA) (see Figure 7.4). This idea was employed afterwards by Moreno *et al.* [70, 71], who synthesized methacrylated derivative oleic (MOA) and linoleic acid (MLA). In these works, no solvents were used neither purification of the monomers was required.

Figure 7.4 Functionalization of linoleic acid with GMA [71].



Vilela *et al.* [72] synthesized fatty acid vinyl esters via transition-metal-catalyzed transvinylation reaction between vinyl acetate and oleic or linoleic acid (schematic synthesis in Figure 7.5). The resulting monomers were purified to achieve optimum yields. Chen and Bufkin [73] synthesized fatty acrylate monomers from various fatty alcohols (linolenyl, linoleyl, oleyl and lauryl alcohol) and acryloyl chloride. Barbosa *et al.* [74] prepared acrylic fatty acid derivative (AcFAD) and allyl fatty acid derivative (AFAD) monomer. The former was obtained from the esterification of a mixture of conjugated fatty acids with ethylene glycol followed by esterification with acryloyl chloride and the latter by indirect esterification of a conjugated fatty acids mixture with allylic alcohol. In both cases, purification steps were necessary to achieve an optimum yield. All these monomers were further polymerized by free radical polymerization. The structure of the above mentioned compounds is shown in Table 7.3.

Figure 7.5 Transition-metal-catalyzed transvinylation reaction of oleic acid with vinyl acetate [72].

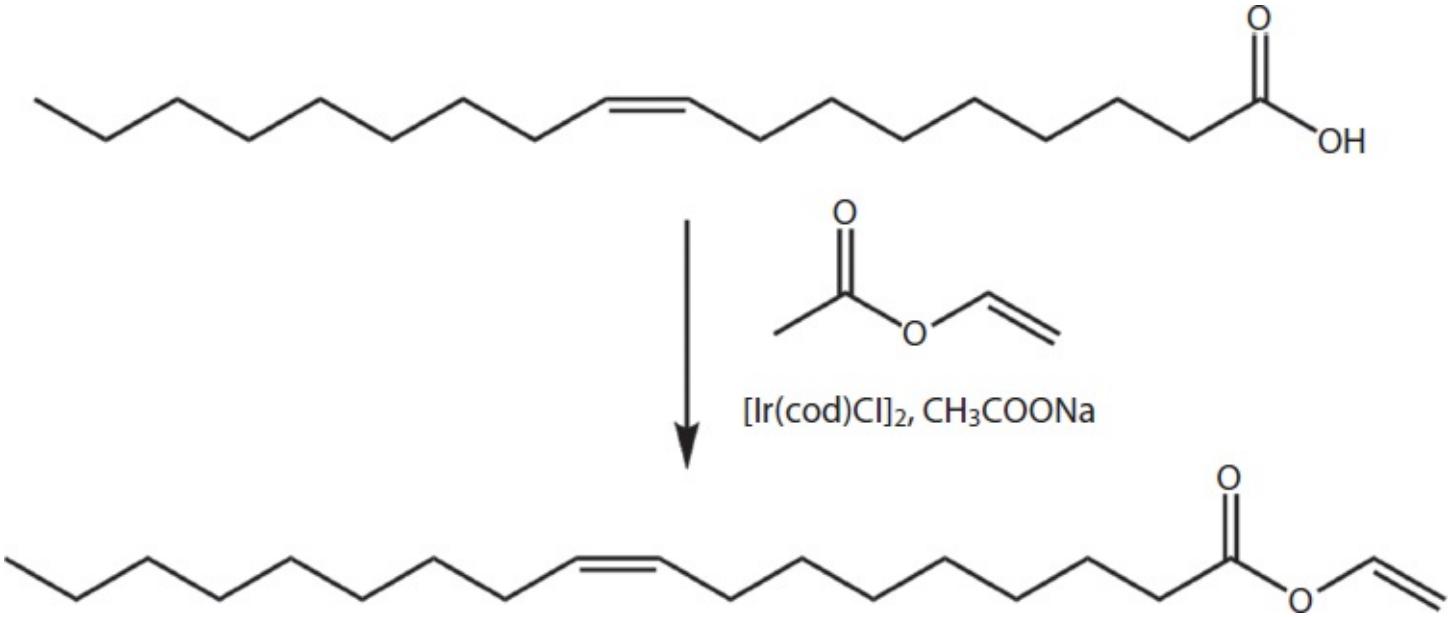
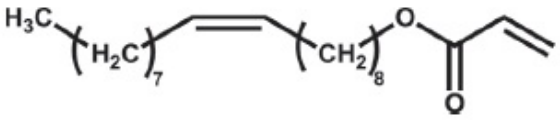
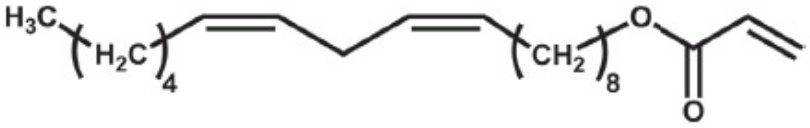
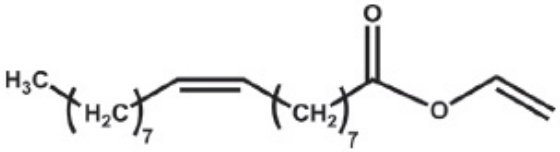
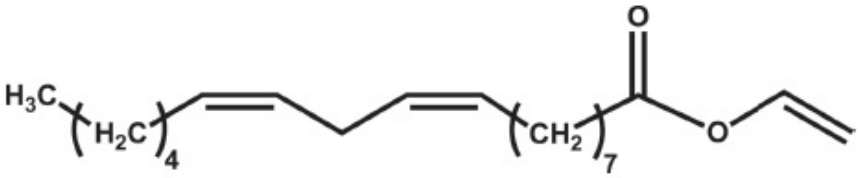
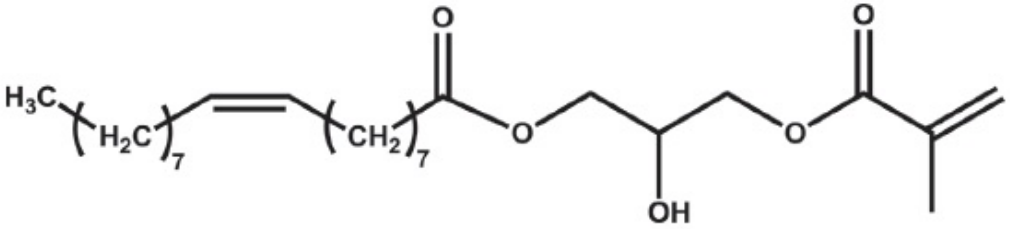
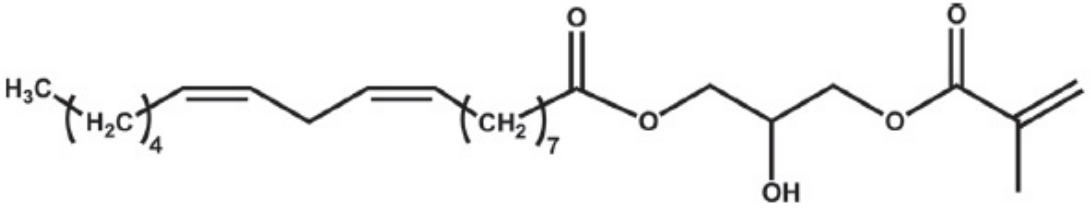
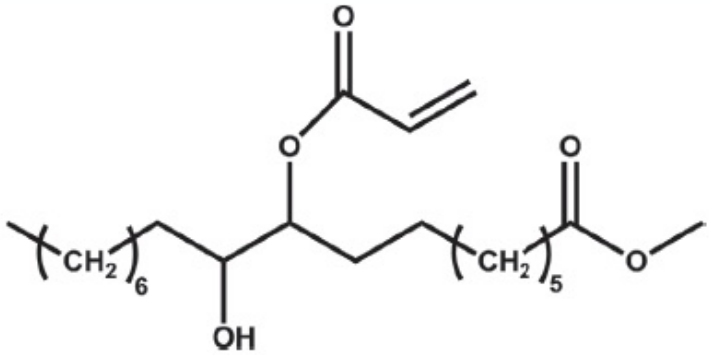
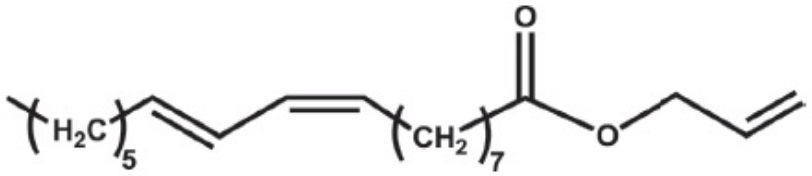
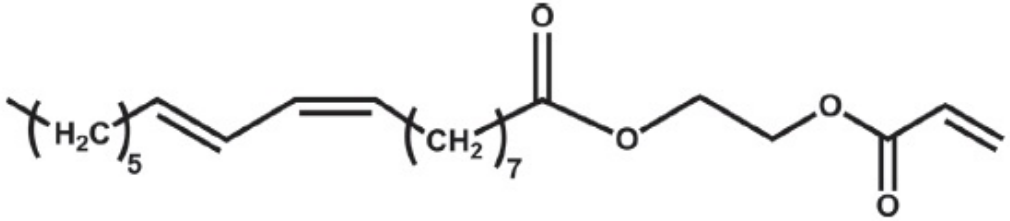


Table 7.3 Summary of the fatty acid-based monomers prone to free radical polymerization.

Fatty acid-based monomer	Structure	Polymerization technique	Authors
Oleyl acrylate (OA)		Emulsion	Chen *et al.* [39]
Linoleyl acrylate (LA)		Emulsion	Chen *et al.* [39]
Vinyl oleate (VO)		Solution	Vilela *et al.* [72]
Vinyl linoleate (VL)		Solution	Vilela *et al.* [72]
Methacrylated oleic acid (MOA)		Emulsion	Moreno *et al.* [70]

Methacrylated linoleic acid (MLA)		Emulsion	Moreno *et al.* [71]
AMO		Emulsion	Bunker *et al.* [66], Jensen *et al.* [75]
Allyl fatty acid derivative (AFAD)		Solution and emulsion	Barbosa *et al.* [76, 77]
AcFAD		Solution and emulsion	Barbosa *et al.* [76, 77]

7.3 Polymerization of Fatty Acid-Based Monomers in Aqueous Media

Fatty acid-derived monomers such as vinyl and allyl esters of fatty acids have been already polymerized and copolymerized by free radical polymerization either in bulk, solution and dispersion. Thus, vinyl esters of stearic, oleic and linoleic acids were polymerized by Harrison and Wheeler [78] by free radical polymerization in bulk. However, the problem of heat transfer and mixing due to the rise in viscosity represents serious drawbacks of these techniques. The VO and VL monomers synthesized by Vilela *et al.* [72] were polymerized in toluene solution resulting in polymers of low molecular weight (Mn 1000–3000 $gmol^{-1}$). However, the replacement of organic solvents is strongly advisable to meet the current environmental regulations. Hence, polymerization in water as dispersed media appears as a benign process that provides an added value to both, the polymerization method and the final product [79]. Moreover, emulsion polymerization allows an easy heat removal due to the excellent capacity of the water to dissipate heat.

7.3.1 Emulsion Polymerization

Most of the works devoted to the preparation of waterborne polymers from fatty acid derivatives involve only the partial replacement of the petroleum-derived acrylic formulations. Chen and Bufkin [39] were pioneers in polymerizing fatty acid-based monomers in emulsion polymerization. They prepared high conversion emulsion cross-linkable polymers by adding small amounts (up to 8 wt.%) of acrylate-based fatty acids to conventional formulations of ethyl acrylate and methyl methacrylate (MMA). The effect of the amount of FA on the molecular weight was also evaluated observing a decrease in the molecular weight as long as the FA concentration increased. The AFAD and AcFAD (up to 10%) synthesized by Barbosa *et al.* [76, 77] were incorporated and copolymerized by solution and emulsion copolymerization with the acrylic resins MMA/butyl acrylate/acrylic acid (MMA/BA/AA) commonly used for coating formulations. It was shown that a high number of unsaturations were maintained for later auto-oxidative cross-linking when emulsion was used instead of solution polymerization. It was demonstrated that the incorporation of these self-cross-linking monomers improved the performance of the acrylic resin while avoiding the use of volatile coalescing agents. AMO monomer synthesized by Jensen *et al.* [68] was copolymerized with styrene in emulsion polymerization. Reactions exhibited high monomer conversion when AMO content was below 15%. Above %20 reaction kinetic exhibited a long induction period and conversions were lower than 70%. The low water solubility of AMO monomer affected particle nucleation. To increase the AMO content in the copolymer, the water-soluble initiator amount was increased to amounts above 6.6 g L^{-1}.

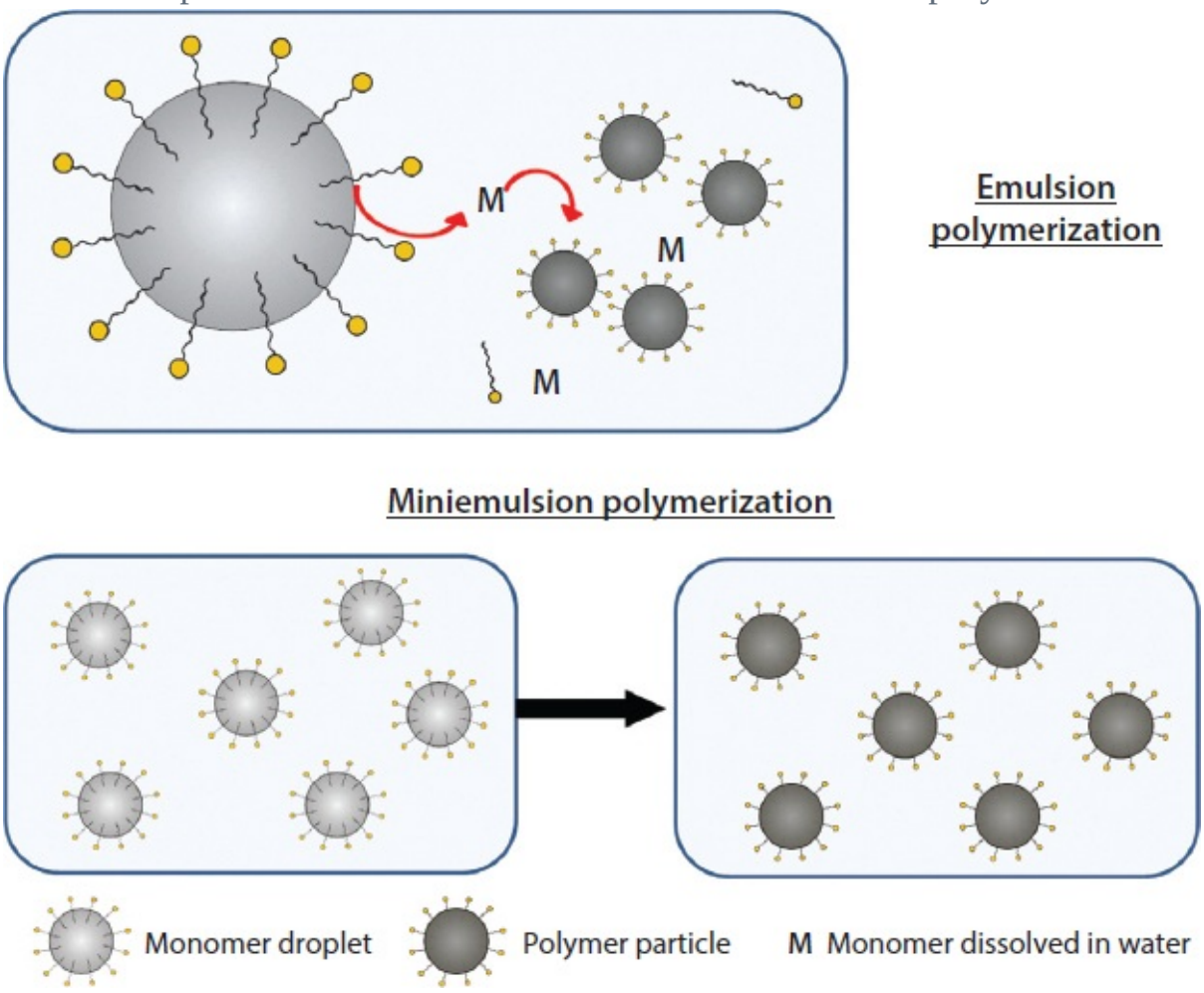
7.3.2 Miniemulsion Polymerization

Bunker *et al.* [66, 80] homopolymerized AMO using both emulsion and miniemulsion polymerization. The resulting polymers presented glass transition temperatures well below room temperature (RT), typical for PSA applications. They observed that the emulsion polymerization

required excessive amount of surfactant and long reaction time as a consequence of the low monomer water solubility. All these limitations were overcome by using sonication to perform miniemulsion polymerization. The reaction time decreased from 18 to 1 h, in addition to the surfactant concentration being reduced from 15 to 2 wt.%.

The monomer transport through the aqueous phase from the big monomer droplets to the polymer particles, where the polymerization takes place, is a crucial requirement in conventional emulsion polymerization. Thus, a minimum water solubility of the monomer is required. This represents a severe limitation in the case of hydrophobic monomers, such as the fatty acid derivatives. In miniemulsion, however, polymerization occurs mainly in the small monomer droplets if they are small enough to have high surface area and favour their nucleation, so transport of monomer through the aqueous phase to the polymerization loci is greatly diminished [81–84]. The miniemulsification process requires then, high energy input to obtain submicron sizes as well as the presence of a co-stabilizer (which in many cases are considered as VOCs) and an efficient surfactant to protect against diffusional degradation and coalescence respectively. A schematic representation of both processes is shown in Figure 7.6.

Figure 7.6 Schematic representation of the emulsion and miniemulsion polymerization techniques.



Spagnola *et al.* [85] successfully used miniemulsion polymerization to polymerize oleyl methacrylate and a mixture of linoleyl and oleyl methacrylate. These fatty acid-derived monomers were copolymerized with 2-ethylhexyl acrylate and MMA at different ratios up to 28% mol in monomer using sonication and hexadecane (which is considered a VOC) as co-stabilizer to perform the miniemulsification process. They observed a decrease in conversion as the amount of fatty acid-derived monomer increased and used redox initiators to improve conversion.

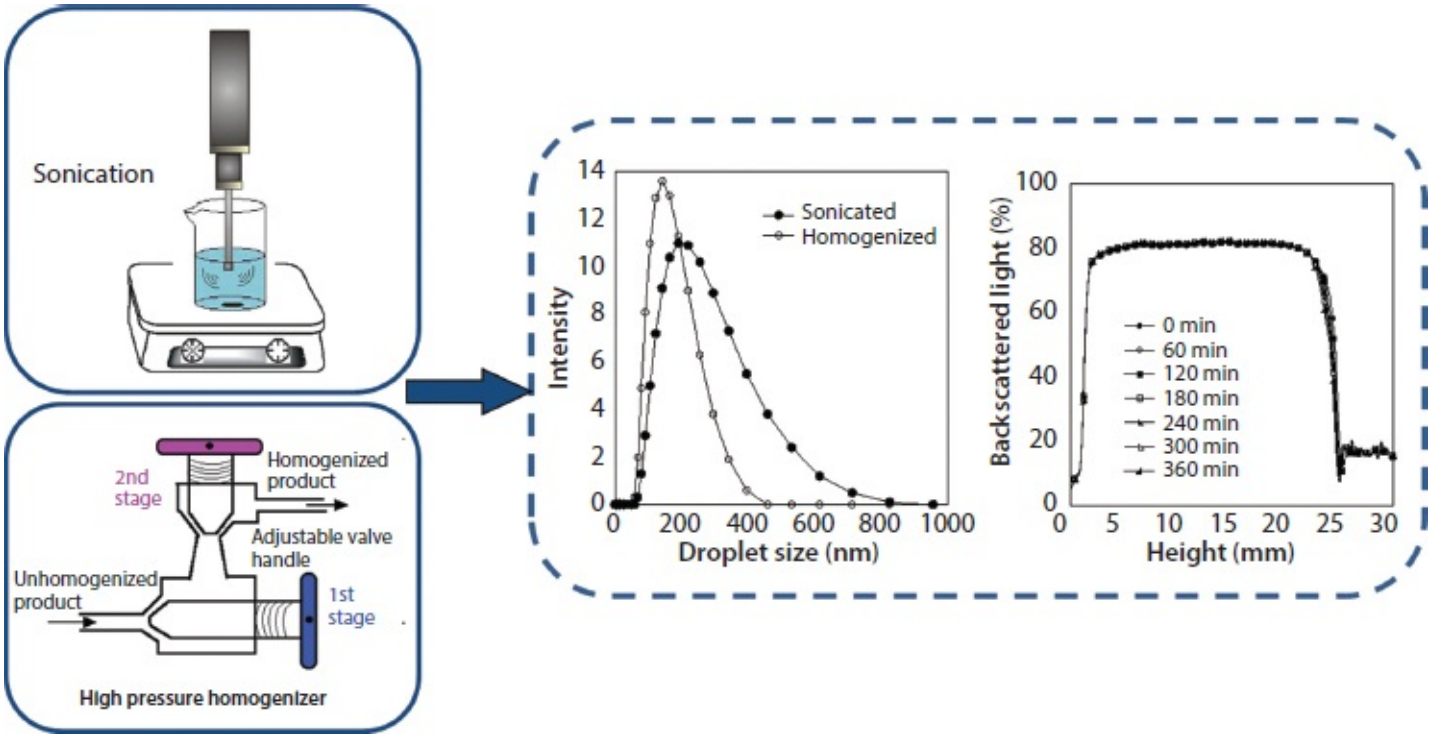
The use of miniemulsion polymerization allowed an important step forward in order to obtain sustainable polymers for coating applications based on fatty acid derivatives. Moreno *et al.* [70] produced polymers entirely made of fatty acid-based monomers MOA and MLA by miniemulsion polymerization. The general formulation of a 45% solids content dispersion contained 1 wbm% initiator [either thermal as potassium persulfate (KPS) or redox as *tert*-butyl hydroperoxide/ascorbic acid (TBHP/AsA)], 2 wbm% of Dowfax 2A1 as emulsifier and sodium bicarbonate to diminish electrostatic interactions between droplets that helps to control the viscosity of the miniemulsion (Table 7.4).

Table 7.4 Formulation recipe for 45% solids content polymers.

Amount (g)				
Fatty acid-based monomer	Dowfax 2A1	$NaHCO_3$	Water	Initiator
218	9.73	0.97	269	2.19

Moreno *et al.* used a two-step miniemulsification process, namely, sonication followed by high pressure homogenization. They observed by measurements of the back-scattered light evolution (TurbiscanLAB^{expert}) that 45 solids contents % MOA and MLA miniemulsifications were stable in spite of no adding additional co-stabilizer. It was observed that the monomer itself, due to its low water solubility, was able to stabilize the miniemulsion. The combination of sonication and high-pressure homogenization allowed obtaining smaller droplets with low polydispersity, which is beneficial for the resulting latex particle size and stability. Figure 7.7 shows the procedure as well as some results illustrating the benefits of combining sonication and high pressure homogenization on the droplet size distribution and the final stability of the miniemulsion.

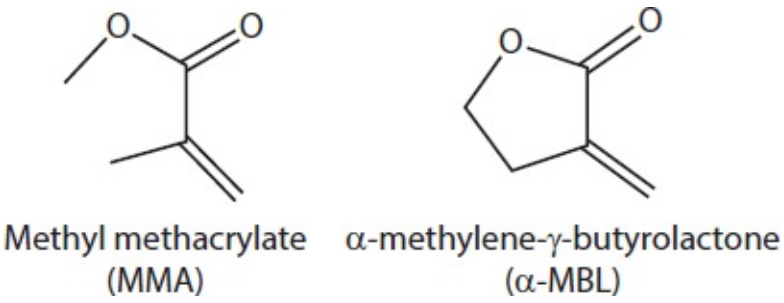
Figure 7.7 Miniemulsification strategy.



With the aim of broadening the portfolio of novel fatty acid-based polymer latexes, Moreno *et al.* [86] used as comonomer a high glass transition temperature renewable resource monomer, alpha-methylene gamma-butyrolactone (α-MBL). This compound, also known as Tulipalin-A, is the simplest member of a family of naturally occurring gamma-lactones, and it is isolated from several

plants such as Artabotrysodoratissimus and tulips [87–89]. The main interest in this biobased monomer relies on its structure, because it is the cyclic analogous of MMA (see Figure 7.8), as well as on its improved solvent resistance and a high glass transition temperature (195 °C) compared to most petroleum sourced acrylic monomers. Copolymers at different ratio of MOA to α-MBL as well as MLA to α-MBL were synthesized by miniemulsion polymerization, achieving polymeric materials in a broad range of glass transition temperatures, going from soft to hard polymers.

Figure 7.8 Chemical structure of MMA and α-MBL.



7.3.3 Effect of Preserving Alkyl Double Bonds

7.3.3.1 Kinetics and Microstructural Properties

Moreno *et al*. thoroughly studied the kinetics using both thermal (KPS) and redox (TBHP/AsA) initiators, and polymer microstructure of the polymers synthesized with the homopolymers MOA and MLA. Table 7.5 shows a summary of the main characteristics of the synthesized MOA and MLA polymers in terms of conversion, molecular weight of the polymer solubilized in THF ($M_{w,sol}$), the non-solubilized fraction (given as gel content), the swelling capability, which is an indication of the degree of cross-linking, and the fraction of reacted double bonds (RDB).

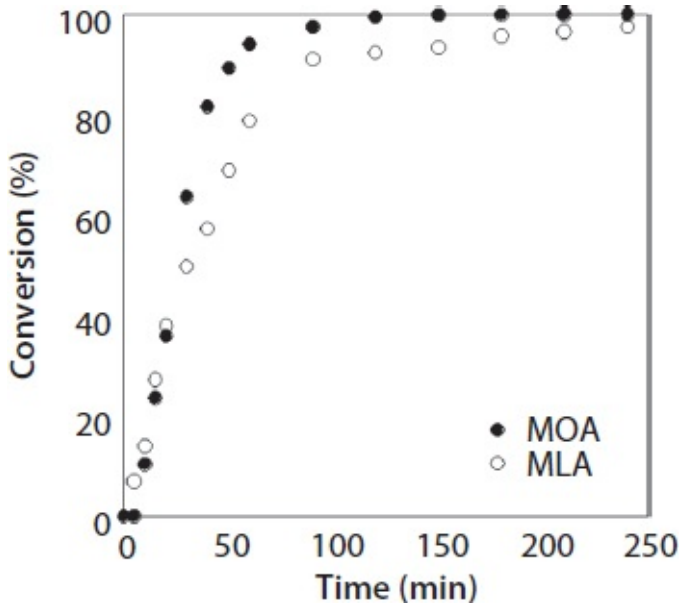
Table 7.5 Summary of the main properties of MOA and MLA polymers.

	Conversion (%)	$M_{w,sol}$ (g/mol)	Gel content (wt.%)	Swelling (%)	RDB (%)
MOA	97–100	27100–110000	56–68	17.0 ± 3.0[a] 4.1 ± 0.0[b]	25–35
MLA	94–98	15900–44900	0–71	6.4 ± 0.8[a] 3.8 ± 0.9[a]	20–35

[a] Before cross-linking.
[b] After cross-linking.

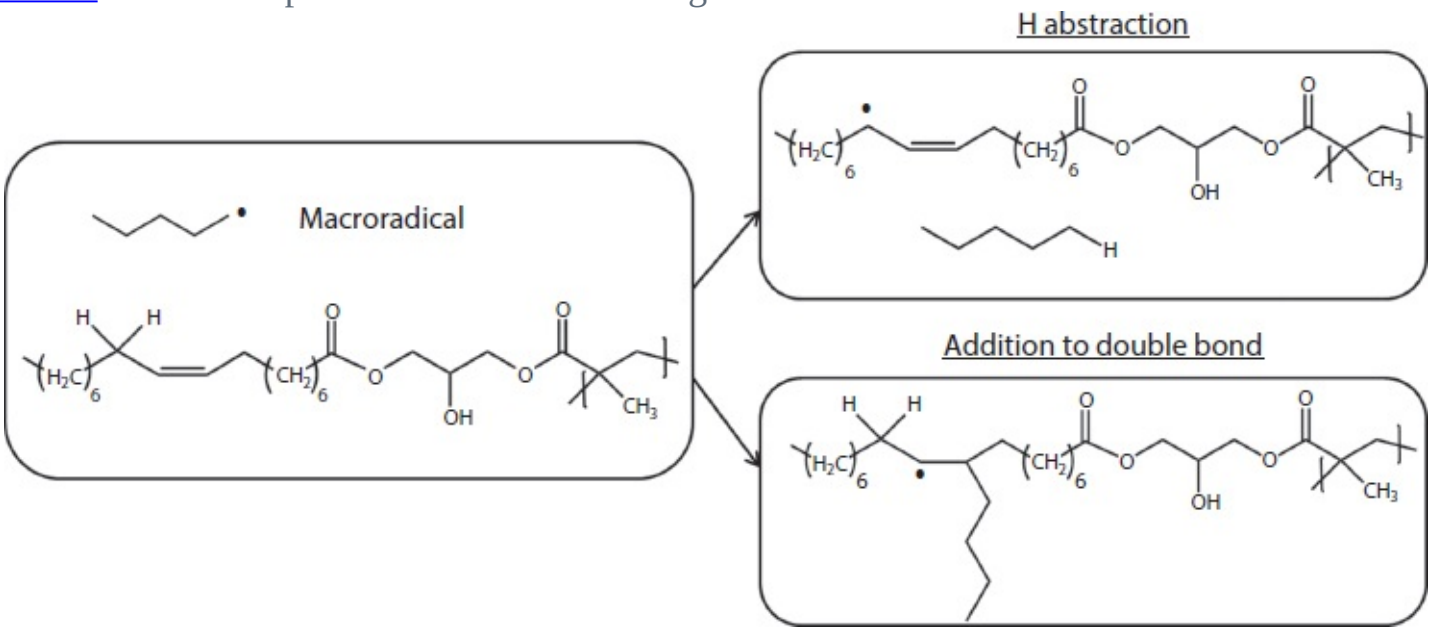
From this data, it is clear that oleic and linoleic acid-derived monomers behaved in a different way under free radical polymerization. Figure 7.9 revealed that polymerization rate was slower when linoleic acid-based monomer was used, even if large amount of initiator was used (KPS, 1.5 wbm%).

Figure 7.9 Polymerization kinetics of MOA and MLA synthesized with 1.5% initiator (KPS).



The gel content for MOA polymers was always high irrespective of the type of initiation used and therefore, low $M_{w,sol}$ were achieved, because the higher molecular weight species were forming the gel. However, gel content varied enormously for MLA polymers depending on the initiator type used, being almost negligible with KPS and up to 71 with TBHP/AsA, while sol M_w remained always lower than for MOA polymers even for low gel contents. Gel polymer can be formed by two mechanisms (see Figure 7.10): chain transfer to polymer through abstraction of the allylic hydrogen followed by termination by combination of branched chains; or/and, by propagation to the double bond of the fatty acid moiety. The likelihood of these mechanisms is enhanced at high polymer concentration, when the free monomer concentration is very low.

Figure 7.10 Scheme of possible mechanisms for gel formation.

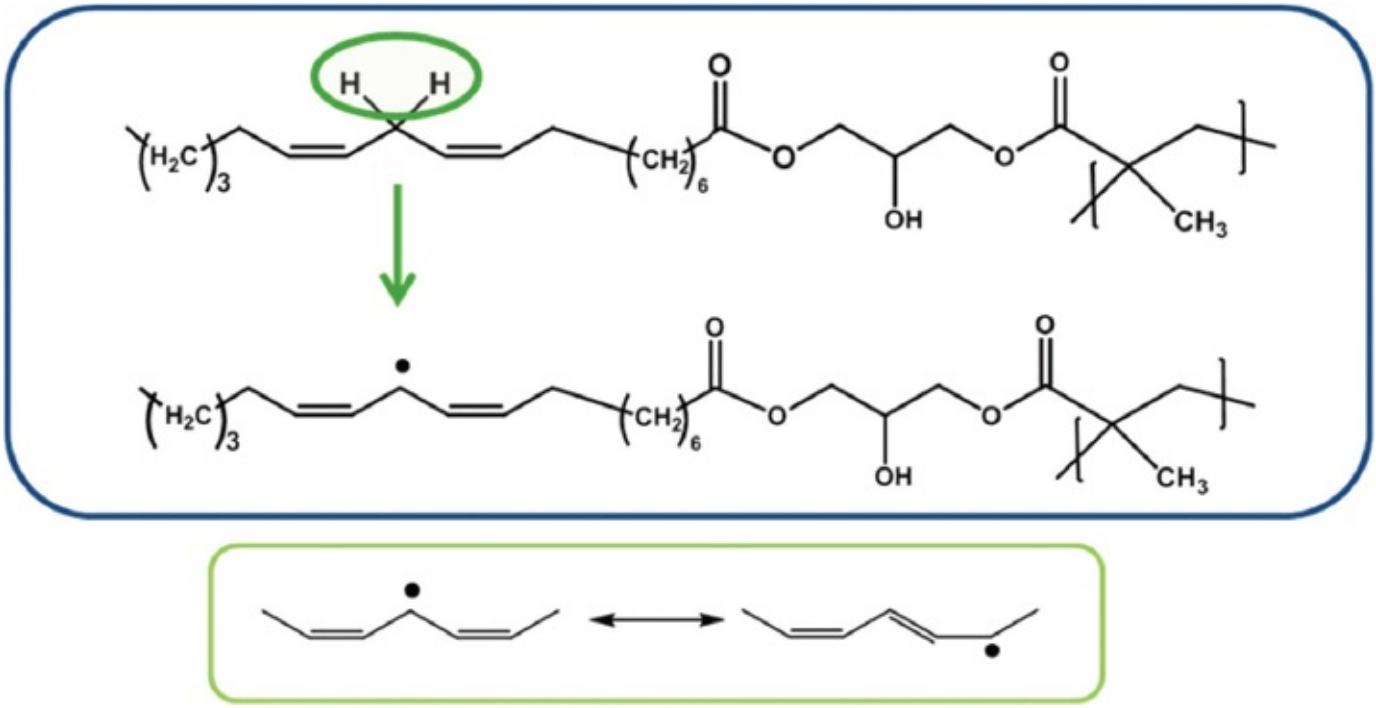


On the one hand, it is well known that a macroradical with methacrylate end is more likely to graft via hydrogen abstraction of the alpha-hydrogen on the fatty acid chain rather than directly react with the alkyl double bond due to the sterically hindered methyl group adjacent to the vinyl bond [90]. On the other hand, the hydrogen atoms of the methylene group that separates the two double bonds of the linoleic acid moiety are very labile and therefore, much more prone to undergo abstraction than the allylic hydrogen of the MOA chain. In fact, hydrogen abstraction mechanism was very important in the case of MLA mainly when redox initiation was used, so very low M_w were expected. In spite of

this, gel was formed. Thus, having gel does not necessarily imply that a very high-molecular-weight polymer is obtained. The swelling capability was lower for MLA polymers, which indicates that shorter although more densely cross-linked chains were formed for MLA.

Additionally, the resultant linoleic acid-derived radical from hydrogen abstraction is stabilized by conjugation with the adjacent double bonds (Figure 7.11), so propagation is inhibited and instead, termination with another radical is favoured, causing reduction in the polymerization rate of MLA compared to MOA, as well as a decrease in the final sol molecular weight of MLA.

Figure 7.11 Mechanism of hydrogen abstraction in the MLA and radical stabilized structures.



7.3.3.2 Auto-Oxidative Curing and Mechanical Properties

Figure 7.10 shows that the hydrogen abstraction does not consume double bonds, whereas the addition to double bond mechanism does. The preservation of these double bonds is of paramount importance in order to keep the auto-oxidative capacity of these coatings once the film is formed. It is worth emphasizing that even though around 30% of the fatty acid double bonds were consumed during polymerization (see Table 7.5), there was still a large fraction retained for later curing reactions during and after film formation.

Auto-oxidation is defined as the direct reaction of molecular oxygen with organic compounds under relatively mild conditions [91]. The curing of vegetable oils containing unsaturated fatty acids such as linoleic and linolenic has been extensively studied [92, 93]. The oxidation of linoleic acid under natural conditions involves as a first step the abstraction of one of the bis-allylic hydrogen atoms on a methylene group in the unsaturated fatty acid chain that results in the formation of a radical species, which is stabilized by delocalization. Molecular oxygen reacts very fast with this radical species to form a peroxy radical (Figure 7.12). Curing proceeds faster as the temperature is higher. Table 7.5 shows a decrease in swelling when films were dried at 120 °C, which indicates that cross-linking was enhanced by heating. This effect is also seen in Figure 7.13. When the film is annealed at 120 °C there is a notorious increase in stiffness and tensile strength because of the cross-linking induced by the auto-oxidative curing of the acid double bonds.

Figure 7.12 Auto-oxidation mechanism of linoleic acid.

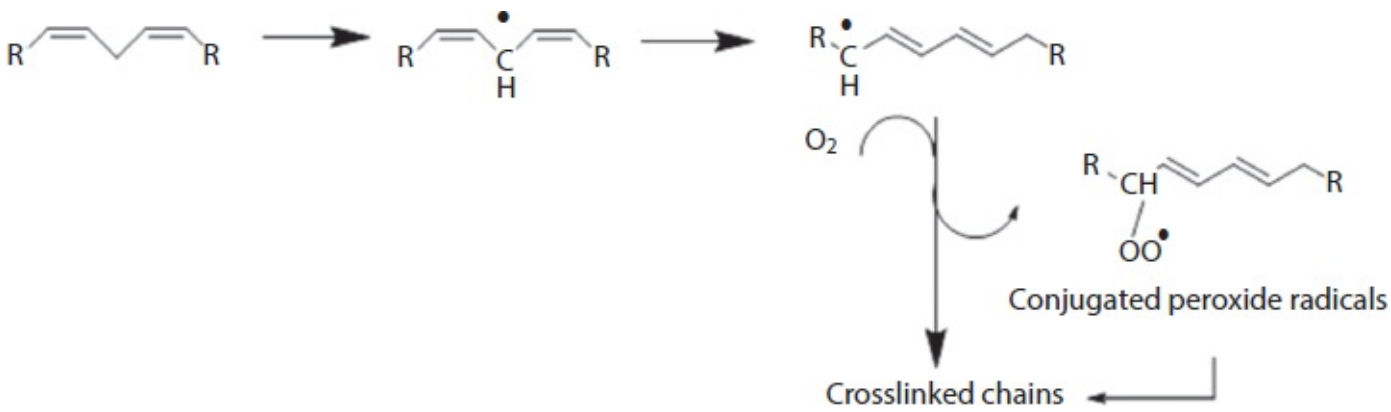
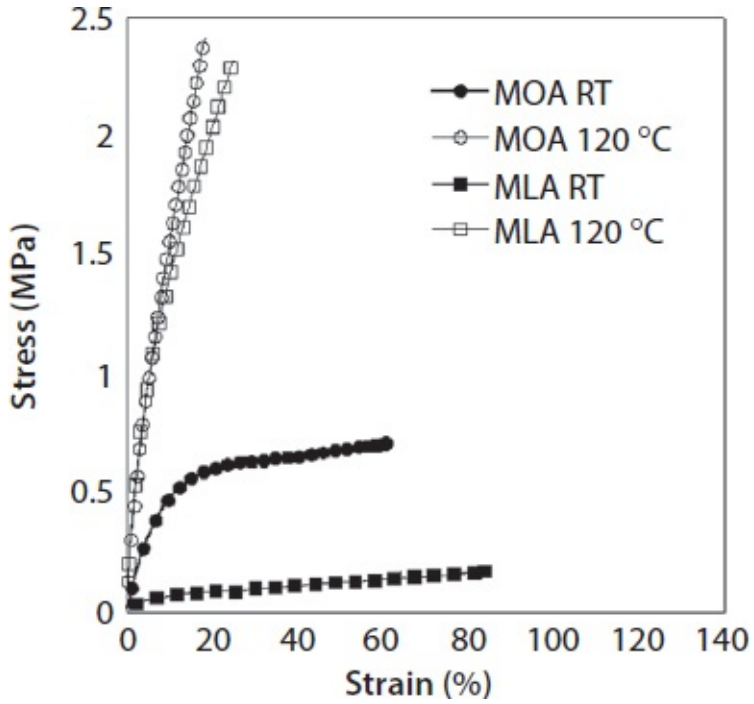


Figure 7.13 Stress strain curves for MOA and MLA polymers. Films were annealed at RT and at 120 °C.

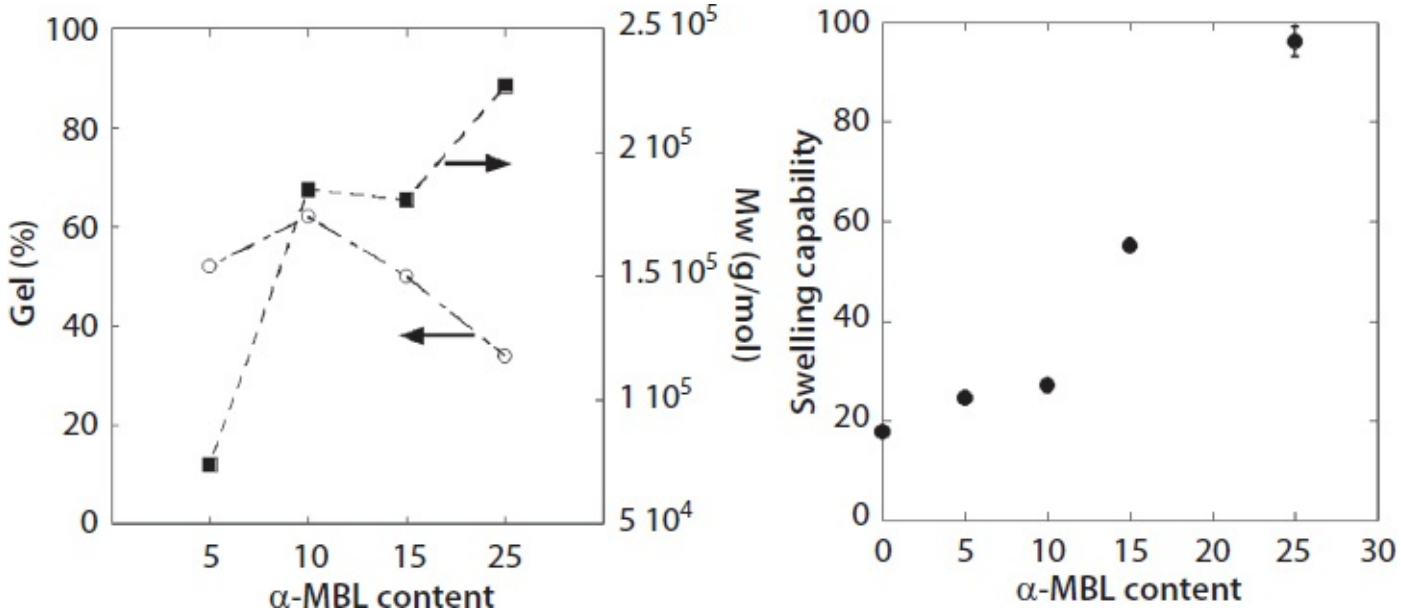


Moreover, Figure 7.13 shows that after curing, both polymers present similar mechanical properties, despite the lower molecular weight of the MLA. The conjugated double bonds of linoleic are more reactive to oxygen than oleic acid ones, and so, the auto-oxidative cross-linking is greater which counterbalances the effect of the lower M_W.

7.3.3.3 Effect of Incorporating α-MBL as Comonomer

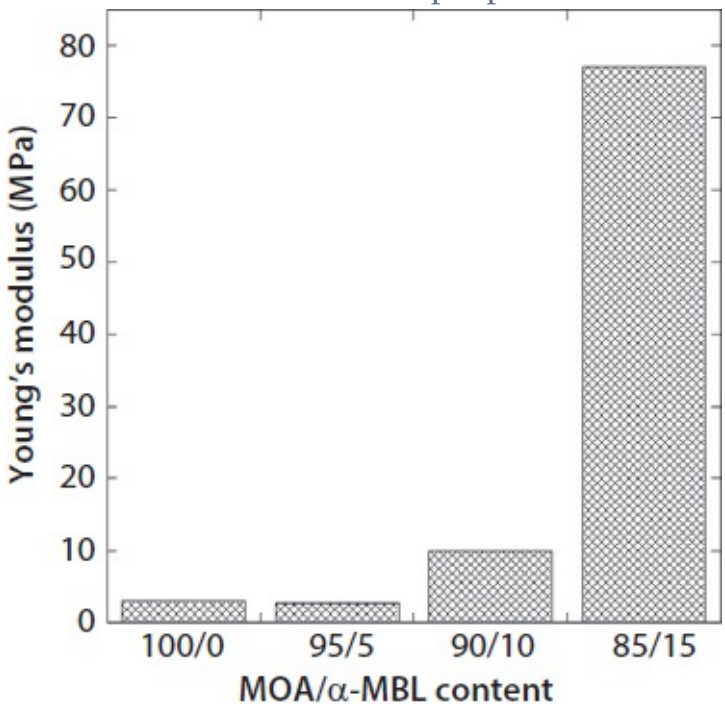
The main microstructural features of the MOA/α-MBL copolymers are summarized in Figure 7.14. The gel content decreased as α-MBL increased, while the sol molecular weight increased because there are less long chains incorporated to the cross-linked networks. α-MBL is a molecule that has no abstractable hydrogens that could lead to cross-linking points. Thus, the formation of gel should occur mainly through the oleic acid molecule. The larger the amount of oleic acid in the polymer, the greater the possibility of producing cross-linking reactions. This fact was corroborated by the swelling capability measurements, which are represented in Figure 7.14b. Shorter and less densely cross-linked networks were formed as the α-MBL content increased.

Figure 7.14 Effect of comonomer ratio on (a) gel and sol M_w and (b) on swelling capacity.



Mechanical properties are strongly influenced not only by microstructural properties, but also by glass transition temperature (T_g). Accordingly, significant differences were expected while increasing the amount of high T_g monomer. In fact, the renewable resource monomer α-MBL substantially improved the mechanical properties of the homopolymers. As example, Figure 7.15 shows that Young's modulus increased due to the incorporation of the high α-MBL, that is, the force needed to elongate the polymer increased. In the MOA homopolymer, the presence of free oleic acid provided with greater molecular mobility to the polymeric network, increasing flexibility of the chains that can elongate more before breaking. When incorporating the lactone, the loss of plasticizing effect (less MOA in the final copolymer) together with the increase in T_g, accounted for the restriction of polymer chains mobility and consequently, caused a decrease in strain at break and an increase in Young's modulus.

Figure 7.15 Effect of comonomer ratio on mechanical properties.



7.4 Incorporation of Fatty Acid Derivatives in Waterborne Coatings

Important properties of fatty acid-derivative polymers to be used as binders in paints are the minimum film forming temperature (MFFT) and glass transition temperature (T_g). The T_g must be low enough to permit coalescence of the latexes at the lowest anticipated temperature, yet high enough to assure adequate film hardness and toughness. MFFT must be below the temperature at which the coating undergoes drying, namely a transition from opaque to clear that is an indication of complete particle coalescence. The targeted T_g and MFFT are usually attained by copolymerizing monomers whose homopolymers have much higher and much lower T_g than the target ones. However, in some applications coalescing agents are employed to lower the MFFT. These compounds are plasticizers with low molecular weights that soften polymer particles favouring the formation of a homogeneous and continuous film [94]. Traditionally organic compounds such as glycol ethers or alcohols that release VOC to the atmosphere when evaporating have been used, breaking the current environmental regulations.

The use of reactive fatty acids as coalescing agents represents an excellent alternative because they are non-volatile and since they remain after film formation, can undergo cross-linking when drying forming hard and non-tacky films with better mechanical properties. Barbosa *et al*. [76] observed the reduction in the MFFT of a MMA/BA/AA (47.5/47.5/5 wt.%) coating formulation latex when adding either an allylic fatty acid derivative (AFAD) as reactive coalescing agent and an AcFAD as comonomer in acrylic waterborne coatings. In this last case, the plasticization was associated to the presence of long aliphatic chains from AcFAD in the polymer, which originated higher segment mobility through increased intermolecular distance. Moreover, they found reductions in through drying-time and increase in scrub resistance, which was more evident for AcFAD, indicating that self-cross-linking occurred through the conjugated double bond in the fatty acid derivatives. Other paint properties such as whiteness and yellowness were similar to the reference paint. However, gloss decrease was noticeable in the paint containing AcFAD. This was attributed to the competitive effect of film formation and oxidative curing. The higher cross-linking degree caused the paint to harden at a faster rate, impairing coalescence. As a consequence, a less smooth film surface with lower gloss was formed.

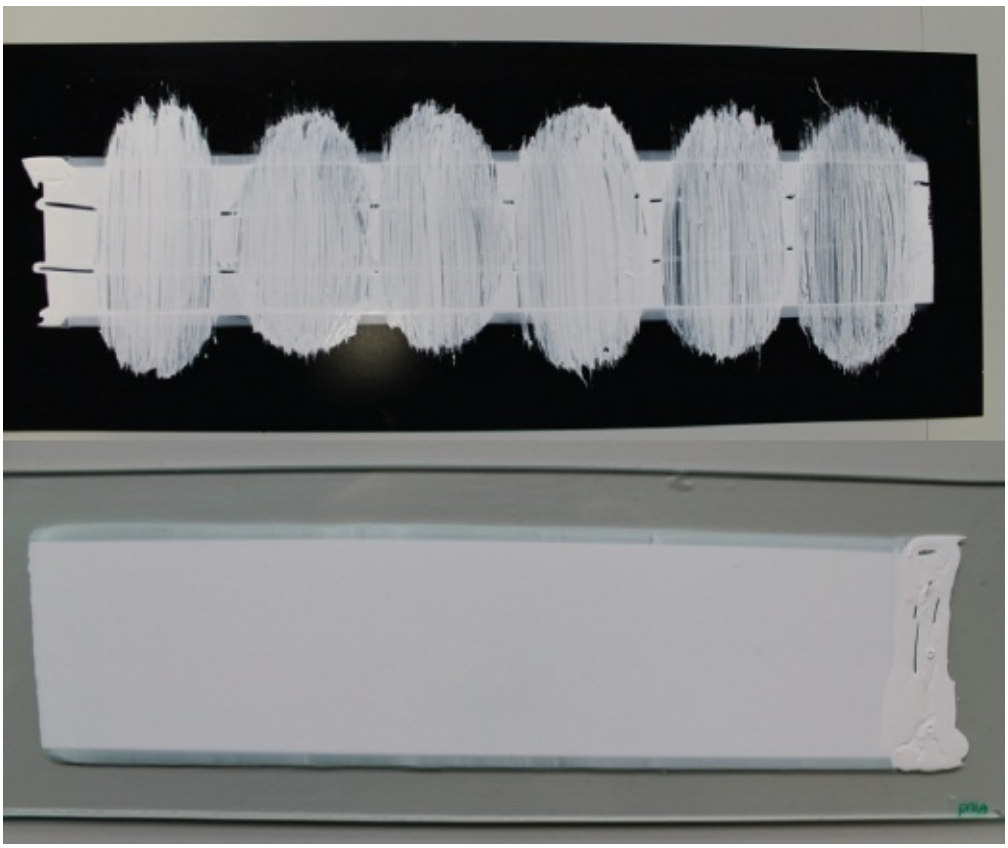
Successful examples of the incorporation of fully renewable fatty acid-based polymers as binders in waterborne paints can be found in the recent work of Moreno *et al*. [95]. They first evaluated the potential performance as binders of the MOA and MLA homopolymer latexes as well as their copolymers synthesized with the renewable resource monomer α-MBL. The reasonable low T_g (ranging from about 0 °C up to 40 °C as it can be seen in Table 7.6) and low MFFT (below 0 °C for all the polymers, likely because of the plasticizing effect of free fatty acid), made those latexes suitable for their use in the production of waterborne coatings. Moreover, they also observed how the T_g of MOA and MLA homo and copolymers increased after film formation due to the cross-linking of the oleic acid derivative, and in major extent, of the linoleic acid derivative. This increase in T_g gave rise to an increase in polymer stiffness as demonstrated by an increase in Young's modulus.

Table 7.6 Glass transition temperatures of MOA and MLA homo and copolymers before and after cross-linking.

	MOA–MBL				MLA–MBL	
Monomer ratio	100	95/5	90/10	85/15	100	85/15
T_g (°C) before cross-linking	–2	1	11	35	–17	1
T_g (°C) after cross-linking	5	8	17	39	3	33

The next step was the incorporation of these fatty acid-derivative latexes as binders into paint formulations. In this case, formulation for decorative paints was used, and a dispersant, pigment, thickener and a drier were added. High-volume solids paints were formulated, up to 40.6 volume solids %. The properties such a gloss and open times were in most cases comparable with commercial waterborne paints, even though the new paints were formulated using a standard formulation without any additional effort to improve paint properties. For instance, open times around 10 min were measured for all the paints. Moreover, gloss values at 20° were in the range of 60–65°, quite close to the 70° of the commercial paint. With respect to hardness, particularly MLA-based paints presented similar hardness than the commercial paint. However, while MLA homopolymer paint exhibited the maximum hardness very quickly, because the unreacted double bonds of the alkyl chain undergo cross-linking very fast, MLA–copolymer hardening process was much slower, likely because the presence of the α-MBL hindered the cross-linking. Moreover, films with good appearance and without cracking were obtained when the paints were applied onto glass panels (Figure 7.16).

Figure 7.16 High-volume solids MOA paint applied onto rubber substrate for open time test and onto glass panel.



7.5 Conclusion

In this chapter, the use of fatty acids as renewable resources to produce new coatings with lower

environmental impact was evaluated. Though fatty acids are not sufficiently reactive to undergo effective free radical polymerization, they possess a genuine chemical structure that allows the functionalization and further incorporation of a more reactive allyl or vinyl moiety. Among the different functional sites, the strategy of modifying the fatty acid through the carboxylic group allows the preservation of the alkyl chain double bonds, which may play an important role during polymerization, broadening the range of polymer properties as well as can undergo auto-oxidative cross-linking during after film formation, improving the application properties.

The progress towards sustainability achieved by the use of renewable feedstocks such as fatty acids was greatly improved by the use of a solvent-free environmentally friendly technology: emulsion polymerization. Several (meth)acrylated fatty acids have been polymerized in (mini)emulsion. Some of these polymers have been incorporated as binders in waterborne coatings and the resulting paints were very promising for the coating industry.

References

1. A look at EPA Accomplishments: 25 Years of Protecting Public Health and the Environment, http://www.epa.gov/history/topics/epa/25b.html, 1995.

2. European Commission: The Paints Directive 2004/42/EC, http://ec.europa.eu/environment/air/pollutants/stationary/paints/paints_legis.htm, 2012.

3. A. Overbeek, F. Bückmann, E. Martin, P. Steenwinkel, and T. Annable, *Progress in Organic Coatings*, Vol. 48, p. 125–139, 2003.

4. A. Goldsmith and H.-J. Streitberger, *Basf Handbook on Basics of Coating Technology*, Hannover, Vincentz Network, 2007.

5. D. Stoye and W. Freitag, Paints, Coatings and Solvents, in D. Stoye and W. Freitags, eds., Wiley-VCH, 1998.

6. E.S. Stevens, *Green Plastics. An introduction to the New Science of Biodegradable Plastics*, Princeton University Press, 2002.

7. S. Fakirov and D. Bhattacharyya, *Handbook of Engineering Biopolymers: Homopolymers, Blends and Composites*, Munich, Hanser Publishers, 2007.

8. R.P. Wool and X.S. Sun, *Bio-Based Polymers and Composites*, Elsevier, 2005.

9. J. Dewulf and H. Van Langenhove, *Renewable-Based Technology. Sustainable Assessment*, John Wiley & Sons Ltd., 2006.

10. A. Gandini and M.N. Belgacem, *Monomers, Polymers and Composites from Renewable Resources*, Amsterdam, Elsevier, 2008.

11. U. Biermann, U. Bornscheuer, M.A.R. Meier, J.O. Metzger, and H.J. Schäfer, *Angewandte Chemie International Edition*, Vol. 50, p. 3854–3871, 2011.

12. U. Biermann, W. Friedt, S. Lang, W. Lühs, G. Machmüller, J.O. Metzger, M. Rüsch gen. Klaas, H.J. Schäfer, and M.P. Schneider, *Angewandte Chemie International Edition*, Vol. 39, p. 2206–2224, 2000.

13. H. Mutlu and M.A.R. Meier, *European Journal of Lipid Science and Technology*, Vol. 112, p. 10–30, 2010.

14. A. Gandini, *Macromolecules*, Vol. 41, p. 9491–9504, 2008.

15. C.K. Williams and M.A. Hillmyer, *Polymer Reviews,* Vol. 48, p. 1–10, 2008.

16. A. Gandini, *Green Chemistry,* Vol. 13, p. 1061–1083, 2011.

17. L. Yu, K. Dean, and L. Li, *Progress in Polymer Science,* Vol. 31, p. 576–602, 2006.

18. L. Yu, S. Petinakis, K. Dean, A. Bilyk, and D. Wu, *Macromolecular Symposia,* Vol. 249–250, p. 535–539, 2007.

19. V. Sharma and P.P. Kundu, *Progress in Polymer Science,* Vol. 31, p. 983–1008, 2006.

20. V. Sharma and P.P. Kundu, *Progress in Polymer Science,* Vol. 33, p. 1199–1215, 2008.

21. Y. Xia and R.C. Larock, *Green Chemistry,* Vol. 12, p. 1893–1909, 2010.

22. F.W. Lichtenthaler and S. Peters, *Comptes Rendus Chimie,* Vol. 7, p. 65–90, 2004.

23. J.C. Ronda, G. Lligadas, M. Galià, and V. Cádiz, *European Journal of Lipid Science and Technology,* Vol. 113, p. 46–58, 2011.

24. M.J.L. Tschan, E. Brule, P. Haquette, and C.M. Thomas, *Polymer Chemistry,* Vol. 3, p. 836–851, 2012.

25. A.L. Holmberg, K.H. Reno, R.P. Wool, and I.I.I.T.H. Epps, *Soft Matter,* Vol. 10, p. 7405–7424, 2014.

26. J.C.R. Gerard Lligadas, Marina Galià, Virginia Cádiz *Materials Today,* Vol. 16, p. 337–343, 2013.

27. F. Seniha Güner, Y. Yağcı, and A. Tuncer Erciyes, *Progress in Polymer Science,* Vol. 31, p. 633–670, 2006.

28. M.R. Infante, L. Pérez, M.C. Morán, R. Pons, M. Mitjans, M.P. Vinardell, M.T. Garcia, and A. Pinazo, *European Journal of Lipid Science and Technology,* Vol. 112, p. 110–121, 2010.

29. H. Wagner, R. Luther, and T. Mang, *Applied Catalysis A: General,* Vol. 221, p. 429–442, 2001.

30. A. Li and K. Li, *RSC Advances,* Vol. 4, p. 21521–21530, 2014.

31. R.G. Verhe, "Industrial products from lipids and proteins", in C.V. Stevens and R.G. Verhés, eds., *Renewable Bioresources:Scopee and Modification for Non-Food Applications,* John Wiley & Sons, Ltd, pp. 208–250, 2004.

32. F.N. Jones, "Alkyd Resins", *Ullmann's Encyclopedia of Industrial Chemistry,* Wiley-VCH Verlag GmbH & Co. KGaA, 2000.

33. J.A. Melero, J. Iglesias, and G. Morales, *Green Chemistry,* Vol. 11, p. 1285–1308, 2009.

34. S. Lestari, P. Mäki-Arvela, J. Beltramini, G.Q.M. Lu, and D.Y. Murzin, *ChemSusChem,* Vol. 2, p. 1109–1119, 2009.

35. *Oilseeds World Markets and Trade*. 2015, USDA: United States Department of Agriculture.

36. M.N. Belgacem and A. Gandini, *Monomers, Polymers and Composites from Renewable Resources,* Elsevier: Amsterdam, 2011.

37. J.W. Gooch, G.C. Wildman, and B.G. Bufkin, *Journal of Coatings Technology,* Vol. 56, 1984.

38. J.G. Tsavalas, J.W. Gooch, and F.J. Schork, *Journal of Applied Polymer Science,* Vol. 75, p. 916–927, 2000.

39. F.-B. Chen and B.G. Bufkin, *Journal of Applied Polymer Science,* Vol. 30, p. 4551–4570, 1985.

40. D.D. Andjelkovic, M. Valverde, P. Henna, F. Li, and R.C. Larock, *Polymer,* Vol. 46, p. 9674–9685, 2005.

41. M.A.R. Meier, J.O. Metzger, and U.S. Schubert, *Chemical Society Reviews,* Vol. 36, p. 1788–1802,

2007.

42. Y. Lu and R.C. Larock, *ChemSusChem*, Vol. 2, p. 136–147, 2009.

43. V. Athawale and R. Nimbalkar, *Journal of the American Oil Chemists' Society*, Vol. 88, p. 159–185, 2011.

44. J.W. Gooch, *Emulsification and Polymerization of Alkyd Resins*, New York, Plenum, 2002.

45. J. Beetsma, *Pigment and Resin Technology*, Vol. 27, p. 12–19, 1998.

46. E.M.S. Van Hamersveld, J.J.G.S. Van Es, A.L. German, F.P. Cuperus, P. Weissenborn, and A.C. Hellgren, *Progress in Organic Coatings*, Vol. 35, p. 235–246, 1999.

47. J. Guo and F.J. Schork, *Macromolecular Reaction Engineering*, Vol. 2, p. 265–276, 2008.

48. P.J.J. Kivit, E. Aramendia, A.A. Cabrera, and L.M. Ríos, *Macromolecular Symposia*, Vol. 283–284, p. 290–299, 2009.

49. Y. Nakayama, *Progress in Organic Coatings*, Vol. 33, p. 108–116, 1998.

50. J.W. Gooch, H. Dong, and F.J. Schork, *Journal of Applied Polymer Science*, Vol. 76, p. 105–114, 2000.

51. A. Hofland, *Progress in Organic Coatings*, Vol. 73, p. 274–282, 2012.

52. D.W. Foster, *The Journal of Clinical Investigation*, Vol. 122, p. 1958–1959, 2012.

53. S. Ooi and H. Pee, *Journal of the American Oil Chemists' Society*, Vol. 62, p. 348–351, 1985.

54. N. Sonntag, *Journal of the American Oil Chemists' Society*, Vol. 61, p. 229–232, 1984.

55. H. Khor, N. Tan, and C. Chua, *Journal of the American Oil Chemists' Society*, Vol. 63, p. 538–540, 1986.

56. A. Coteron, M. Martinez, and J. Aracil, *Journal of the American Chemical Oil's Society*, Vol. 75, p. 657–660, 1998.

57. A. Köckritz and A. Martin, *European Journal of Lipid Science and Technology*, Vol. 110, p. 812–824, 2008.

58. S.N. Khot, J.J. Lascala, E. Can, S.S. Morye, G.I. Williams, G.R. Palmese, S.H. Kusefoglu, and R.P. Wool, *Journal of Applied Polymer Science*, Vol. 82, p. 703–723, 2001.

59. M.A. Oakley, S. Woodward, K. Coupland, D. Parker, and C. Temple-Heald, *Journal of Molecular Catalysis A: Chemical*, Vol. 150, p. 105–111, 1999.

60. L.M. de Espinosa, J.C. Ronda, M. Galià, and V. Cádiz, *Journal of Polymer Science Part A: Polymer Chemistry*, Vol. 47, p. 1159–1167, 2009.

61. G.W. Bussel, *Maleinized fatty acid esters of 9-oxatetracyclo-4.4.1.2,5O1,6O8,10 undecan-4-ol*. 1974.

62. K.S. Yonehara, Y. 2005.

63. A. Overeem, G.J.H. Buisman, J.T.P. Derksen, F.P. Cuperus, L. Molhoek, W. Grisnich, and C. Goemans, *Industrial Crops and Products*, Vol. 10, p. 157–165, 1999.

64. J. La Scala and R. Wool, *Journal of the American Oil Chemists' Society*, Vol. 79, p. 59–63, 2002.

65. D.A.A. Dantas T. N. C., Santos R. A., *Inf Tecnol*, Vol. 10, p. 73–81, 1999.

66. S.P Bunker and R.P. Wool, *Journal of Polymer Science Part A: Polymer Chemistry*, Vol. 40, p. 451–458, 2002.

67. J. Lu, S. Khot, and R.P. Wool, *Polymer,* Vol. 46, p. 71–80, 2005.

68. A.T. Jensen, C. Sayer, P.H.H. Araújo, and F. Machado, *European Journal of Lipid Science and Technology,* Vol. 116, p. 37–43, 2014.

69. J.J. La Scala, J.M. Sands, J.A. Orlicki, E.J. Robinette, and G.R. Palmese, *Polymer,* Vol. 45, p. 7729–7737, 2004.

70. M. Moreno, M. Goikoetxea, and M.J. Barandiaran, *Journal of Polymer Science Part A: Polymer Chemistry,* Vol. 55, p. 4628–4637, 2012.

71. M. Moreno, J.I. Miranda, M. Goikoetxea, and M.J. Barandiaran, *Progress in Organic Coatings*, Vol. 77, p. 1709–1714, 2014.

72. C. Vilela, R. Rua, A.J.D. Silvestre, and A. Gandini, *Industrial Crops and Products,* Vol. 32, p. 97–104, 2010.

73. F.-B. Chen and B.G. Bufkin, *Journal of Applied Polymer Science,* Vol. 30, p. 4571–4582, 1985.

74. J.V. Barbosa, E. Veludo, J. Moniz, F.D. Magalhães, and M.M.S.M. Bastos, *European Journal of Lipid Science and Technology,* Vol. 114, p. 1175–1182, 2012.

75. A.T. Jensen, C. Sayer, P.H.H. Araújo, and F. Machado, *European Journal of Lipid Science and Technology,* Vol. 116, p. 37–43, 2013.

76. J.V. Barbosa, E. Veludo, J. Moniz, A. Mendes, F.D. Magalhães, and M.M.S.M. Bastos, *Progress in Organic Coatings*, Vol. 76, p. 1691–1696, 2013.

77. J. Barbosa, J. Moniz, A. Mendes, F. Magalhães, and M.S.M. Bastos, *Journal of Coatings Technology and Research,* Vol. 11, p. 765–773, 2014.

78. S.A. Harrison and D.H. Wheeler, *Journal of the American Chemical Society*, Vol. 73, p. 839–842, 1951.

79. J.M. Asua, *Journal of Polymer Science Part A: Polymer Chemistry*, Vol. 42, p. 1025–1041, 2004.

80. S. Bunker, C. Staller, N. Willenbacher, and R. Wool, *International Journal of Adhesion and Adhesives*, Vol. 23, p. 29–38, 2003.

81. J. Ugelstad, M.S. El-aasser, and J.W. Vanderhoff, *J PolymSciLett Ed,* Vol. 11, p. 503–513, 1973.

82. K. Landfester, *Macromolecular Rapid Communications,* Vol. 22, p. 896–936, 2001.

83. J.M. Asua, *Progress in Polymer Science*, Vol. 27, p. 1283–1346, 2002.

84. S.F. Thames, J.W. Rawlins, and S.K. Mendon, "Miniemulsion Polymerization of Vegetable Oil Macromonomers", *Miniemulsion Polymerization Technology,* John Wiley & Sons, Inc., pp. 139–171, 2010.

85. L. Spagnola, E.S. Daniels, V.L. Dimonie, M.S. El-Aasser, and A. Klein, *Polymeric Materials: Science and Engineering*, Vol. 99, p. 80–81, 2008.

86. M. Moreno, M. Goikoetxea, J.C. de la Cal, and M.J. Barandiaran, *Journal of Polymer Science Part A: Polymer Chemistry,* Vol. 52, p. 3543–3549, 2014.

87. H.F. Wong and G.D. Brown, *Phytochemistry,* Vol. 59, p. 529–536, 2002.

88. M.W.P.C.V. Rossum, M. Alberda, and L.H.W.V.D. Plas, *Phytochemistry,* Vol. 49, p. 723–729, 1998.

89. A. Trendafilova, M. Todorova, B. Mikhova, A. Vitkova, and H. Duddeck, *Phytochemistry,* Vol. 67, p. 764–770, 2006.

90. J.G. Tsavalas, Y. Luo, and F.J. Schork, *Journal of Applied Polymer Science,* Vol. 87, p. 1825–1836,

2003.

91. E.N. Frankel, *Journal of the Science of Food and Agriculture*, Vol. 54, p. 495–511, 1991.

92. J. Mallégol, J. Lemaire, and J.-L. Gardette, *Progress in Organic Coatings*, Vol. 39, p. 107–113, 2000.

93. S. Boyatzis, E. Ioakimoglou, and P. Argitis, *Journal of Applied Polymer Science*, Vol. 84, p. 936–949, 2002.

94. T. Raja, A. Brouwer, T. Nabuurs, and R. Tennebroek, *Colloid and Polymer Science*, Vol. 290, p. 541–552, 2012.

95. M. Moreno, C. Lampard, N. Williams, E. Lago, S. Emmett, M. Goikoetxea, and M.J. Barandiaran, *Progress in Organic Coatings*, Vol. 81, p. 101–106, 2015.

Chapter 8

Environmentally Friendly Coatings

Xiaofeng Ren, Lei Meng, and Mark Soucek*

Department of Polymer Engineering, The University of Akron, Akron, OH, USA

**Corresponding author:* chris.uakron@gmail.com

Abstract

The utilization of clean and renewable resources for coating applications is receiving increasing attentions in both industrial and academic areas due to concerns regarding environmental sustainability. Nowadays, most commercially available coatings are derived from non-renewable resources. Coatings from petrochemicals typically contain significant amounts of volatile organic compounds, which pose threat to the environmental health. There is an urgent need to develop coatings from clean and renewable resources. During the past decades, the use of environmentally friendly waterborne coatings in the preparation of various industrial coatings has become popular, and the application of natural seed oil-based coatings has been revitalized because of the environmental concerns. This chapter covers the introduction and development of waterborne coatings and seed oils-based coatings. The development of seed oil-based UV-curable epoxy coating, urethane coating, thiol-ene chemistry, hybrid coating, as well as alkyd coating as specific examples are also discussed.

Keywords: Volatile organic compound, waterborne, emulsion, seed oil, reactive diluent, epoxy, polyurethane, UV-curable coatings, alkyd

8.1 Waterborne Coatings

8.1.1 Introduction of Waterborne Coatings

Waterborne coatings are commonly defined as coatings that primarily use water as the solvent, which have low to zero volatile organic compounds (VOCs) and hazardous air pollutants (HAP) emissions. The small amounts of organic solvents, such as glycol ether, are usually limited to less than 3.5 pounds per gallon water by most regulations [1, 2], which make waterborne coatings eco-friendly.

Waterborne coatings bear plenty of advantages not only for trade sales but also for industrial applications. The easy application (brushing or rolling), minimal odor when painting at home and easy cleanup with water render waterborne coatings popular in daily living usage. As a result, waterborne coatings occupy more than 80% for the interior coatings markets and more than half for exterior coatings [2]. The exterior house coatings are usually the alkyd paints with good durability,

adhesion and weathering properties. The guideline for waterborne coatings in exterior application is to improve adhesion and durability to be competitive with alkyd paints. With more attention paid to personal health and the government regulations of limited amount of volatile solvent, waterborne coatings are the only paints that can be used in some strict areas [1]. Waterborne coatings are also very attractive in the industrial applications, which are mostly high-performance finishes. This can be due to the advantages such as low flammability, reduced toxicity and environmental pollution, which increase not only the labor safety but also compliance with environmental legislation. Moreover, waterborne coatings can be produced by using conventional finishing lines, which save a huge cost of the change of the production line. Fire hazard and emission of organic solvents are the most important concerns in the industrial finish lines, which are seriously restricted by the government regulations. In this way, a significant growth of waterborne coatings is expected in the trade sales market and in the industrial products with continued improvement of properties. However, the use of water may cause some issues that need to be concerned during formulation and application. Detailed information about advantages and disadvantages of waterborne coatings is listed in Table 8.1.

Table 8.1 Lists of advantages and disadvantages of waterborne coatings.

Advantages	**Disadvantages**
Reduced VOC and HAP emissions	Higher cost per gallon on an equivalent solids basis compared with conventional coating
Reduced toxicity and odor, resulting in improved worker safety and comfort	Require longer drying times or increased oven temperatures
Easy to clean up	Require good temperature/humidity control
Conventional application processes available	Require clean surface for high quality application; surface must be free of oil and dust
Minimized or eliminated disposal of hazardous waste	
Excellent appearance, high-gloss retention and non-yellowing film	

8.1.2 History of Waterborne Coatings

The history of waterborne coatings can be traced back to the very beginning of human history. At that time, water was the only available solvent. The simple paints, the mixture of eggs, milk, and other materials were used to decorate the living environment by the caveman. Although the mixture could be defined as the earliest paints that are produced and used, it has been a long road for waterborne coatings to be widely used. The important milestones of the development of waterborne coatings are listed in Table 8.2.

Table 8.2 Historical development of waterborne coatings [3].

~1600	Earliest waterborne paints: whitewash to casein paints
1865	The first U.S. waterborne paint patent (U.S. 50068) issued to Darwin P. Flinn
1912	A patent (German patents 254 and 255) about dispersion polymerization of isoprene issued to Germany Kurt Gottlob in Germany
1932	A patent (U.S. patent 1,864,078) about a method for making a SBR latex material issued to Luther and Hück working for I. G. Farbenindustrie in Germany
1941	The first widely sold commercial water based paint-Kemtone® sold by Sherwin-Williams
~1940	The era of synthetic latex paint
1943	Styrene–butadiene synthetic rubber latex developed and the production started in the USA
1944	Germans use waterborne paint similar to PVA, for Tiger tanks

1946	Styrene–butadiene latex commercialized for paper coatings
1948	First use of styrene–butadiene latexes in architectural paints
~1950	Interior wall paints based on styrene–butadiene latex put on market
1951	Acrylic polymers for emulsion paints under development
~1952	Waterborne alkyd introduced for industrial applications
1953	First all-acrylic latex introduced commercially-Rhoplex® AC-33 in USA and PrimalTM AC-33 in Europe
1955	Water soluble/dispersible thermosetting resins introduced, e.g. alkyds and acrylics
1956–1960	Cross-linking latexes are introduced
1957	Exterior house paints based on acrylic latexes put on market
1962	Electrodeposition of waterborne paint developed for industrial applications
1964	Texanol® registered as trademark by Eastman Chemicals used as a coalescing additive for latex paints to make the application of latex paints possible over a much broader range of environmental conditions
1967	Polyurethane dispersions in water put on the market
1968	Semigloss latex paints introduced
1982	Epoxy waterborne dispersions introduced

In the past decades, more and more high-tech paints and coatings are formulated. The range of the resins available for waterborne coatings has been significantly increased, which has provided paint manufactures with more opportunities to design coatings that can exceed solventborne coatings. High-performance resins can be formulated into waterborne coatings with many available waterborne polymers, such as unmodified and modified acrylics, polyurethanes, epoxy, polyester and silicones [4]. Nowadays, coatings have more functional properties than only protection and decoration: they can be thermal/electrical insulator as well as the conductor; they can be light absorber and also a light reflector; they can also be deposited especially for printed electronics and solar energy applications. Everything in the whole world is covered actually by paints and coatings and therefore paints and coatings are of significance to the modern world [4].

As is indicated in the recent report “Waterborne Coatings Market by Resin, by Application-Global Forecast to 2019” [4], the global waterborne coatings market are divided based on resin type, application, and region. The global market value of waterborne coatings is estimated to grow at a CAGR (Compound annual growth rate) of about 5.92% within 5 years based on the global demand for waterborne coatings. The increasing growth of waterborne coatings application has been demanded for both decorative market and industrial coatings.

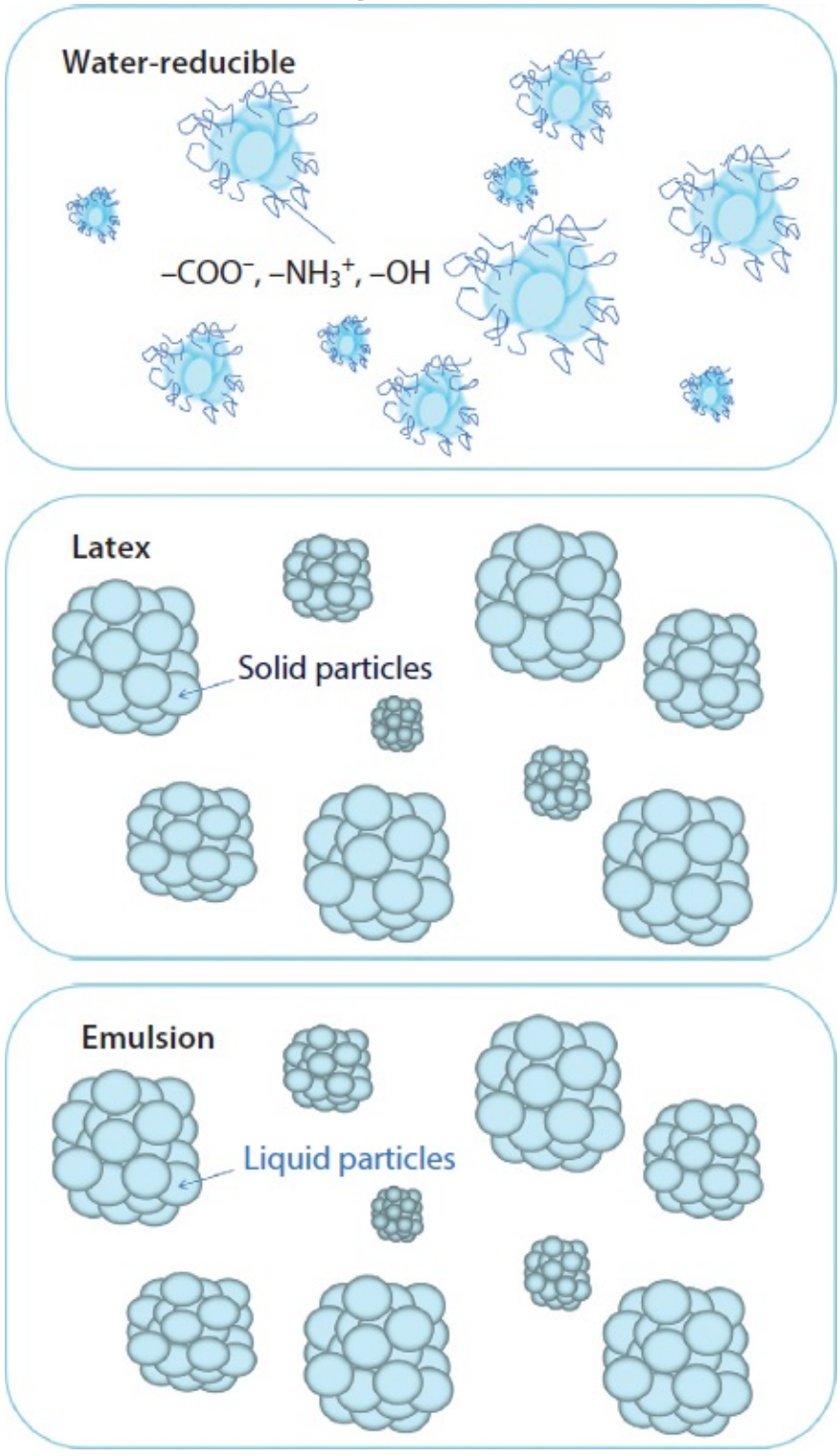
8.1.3 Category of Waterborne Coatings

With the increasing popularity of waterborne coatings, different types of waterborne coatings appear with quite similar and shared terminology. Almost each resin that is available in the solventborne systems can be accessible in the waterborne coatings, such as acrylics, polyurethane, polyester, epoxy, and carboxyl-terminated alkyds.

The category of waterborne is mostly mixed, and terminology is nonuniform and confusing. A proper method is to classify waterborne coatings based on the fluidized state of resin as is shown in Figure 8.1. Therefore, three main types of waterborne coatings are water-reducible, latex and emulsion coatings. Water-reducible coatings are generally produced as high-solids solutions in water-miscible solvents and water is post added. In practice, the emulsion and latex coatings are not clearly differentiated. Some authors call all dispersion coatings as emulsion coatings or latex

coatings or dispersions. Actually, both emulsion and latex are small particles of binder dispersed in water phase. Latex, which is usually prepared by emulsion polymerization, is solid polymer dispersed in water. This should not be confused with real emulsion coatings, which are liquid dispersed in water. The mixture of these waterborne coatings is growing up. Detailed information of these three types of coatings can be found in the following sections.

Figure 8.1 Classification of waterborne coatings based on the fluidized state of resins.



8.1.3.1 Water-Reducible Coatings

Water-reducible coatings are coatings that have the ability to be diluted with water or a water/co-solvent mixture. Many researchers still would like to call water-reducible as water-soluble coatings although the resin is not soluble in water. In water-reducible coatings, water is post added. The

general preparation of water-reducible coatings can be described in three steps. First, the resins are generally synthesized via polycondensation or polymerization reactions in a water-miscible organic medium. As a result, water-reducible coatings usually contain organic co-solvents (glycol ethers, alcohols) that are soluble or miscible with water but the content is less than 15%. The resin should bear some water-soluble groups (–OH groups) or ionic groups (–COOH or $–NH_2$). Then the ionic groups are neutralized with small molecule counter ions (amine–acid pair). In the end, water is added. Based on the types of resins used, water-reducible coatings can be mainly divided into three groups listed in Table 8.3.

Table 8.3 Three groups of water-reducible coatings.

	Functional groups	**Neutralizing or cross-linking agent**
Nonionic water reducible	–OH	Cross-linked with aldehyde groups
Anionic water reducible	–COOH	Neutralized with amines, ammonium, sodium or other hydroxide
Cationic water reducible	$–NH_2$	Neutralized with hydrochloric or acetic acid

Because of viscosity anomalies, waterborne coatings made with water-reducible binders such as alkyds, polyesters, polyacrylates, epoxies, and epoxy esters have only about 30–40% solids content by weight. Despite their sensitivity to water, water-reducible coatings have a high gloss and a high level of corrosion protection, along with good pigment, wetting, and stabilization.

8.1.3.2 Latex Coatings

Latex coatings commonly known as colloidal systems are coatings that have small clusters of insoluble polymer particles that are suspended in water. Generally, the acrylic and vinyl latexes are produced by traditional emulsion polymerization process shown in Figure 8.2 or micro/mini-emulsion polymerization in the presence of an external surfactant or colloidal stabilizer [5]. Small amounts of organic solvents, which are usually less than 5% by weight, are commonly used as coalescing agents that evaporate during film formation process. Polyurethane dispersions also fall into this category. Compared to the preparation of acrylic latex in Figure 8.2, different methods and processes are used to synthesize polyurethane latex [6]. Acetone process is the earliest method to prepare the polyurethane dispersions, as shown in Figure 8.3a. Some new processes are proposed without using the acetone, as shown in Figure 8.3b. The first step involves preparation of low molecular weights isocyanate endcapped ionomers in a solvent. This prepolymer is usually prepared from the reaction of a diol and an excess of diisocyanate. Then the ionomers are dispersed in water followed by the chain extension with reaction of isocyanate functional groups with water or the resulted amine.

Figure 8.2 Emulsion polymerization process.

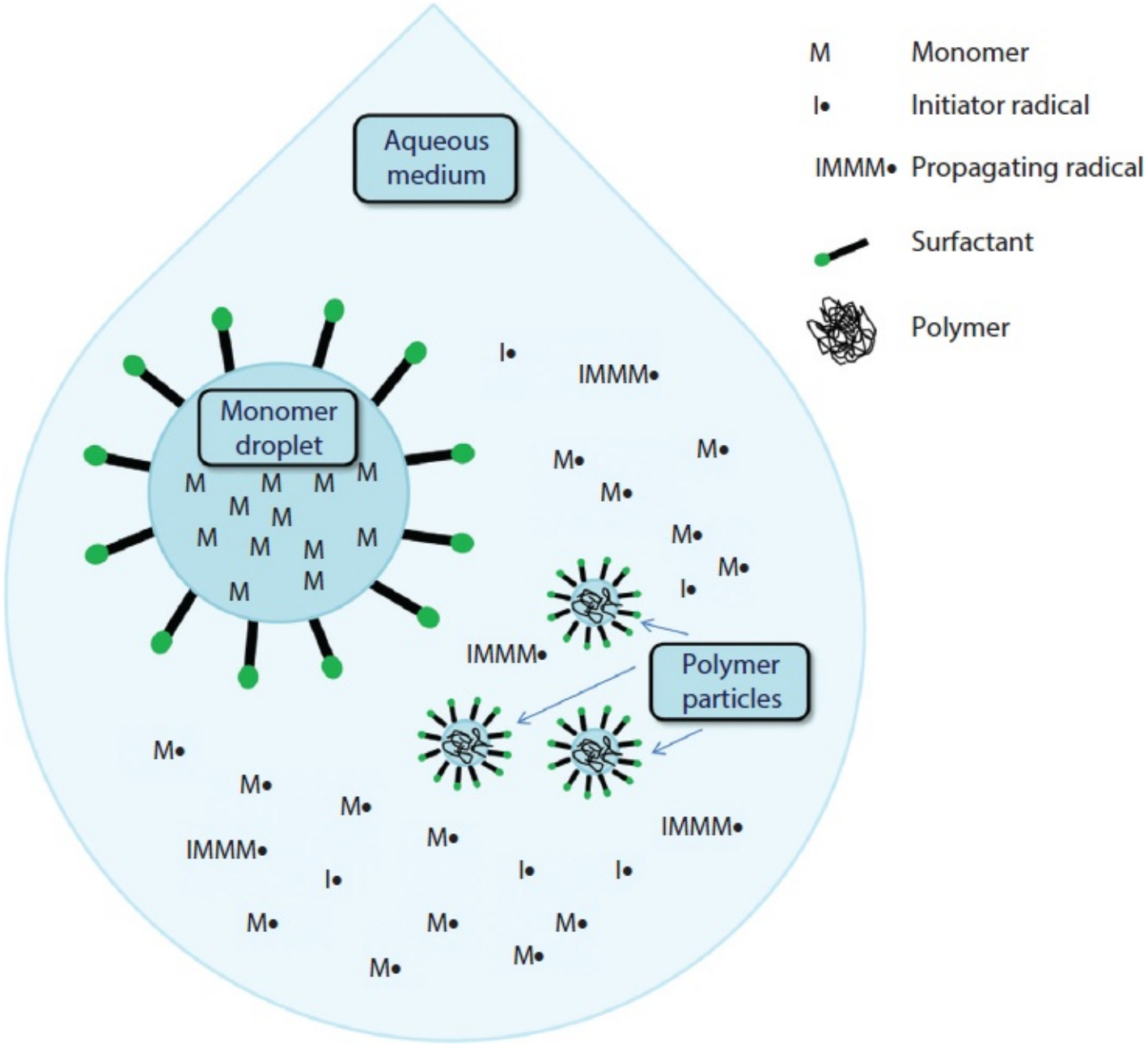
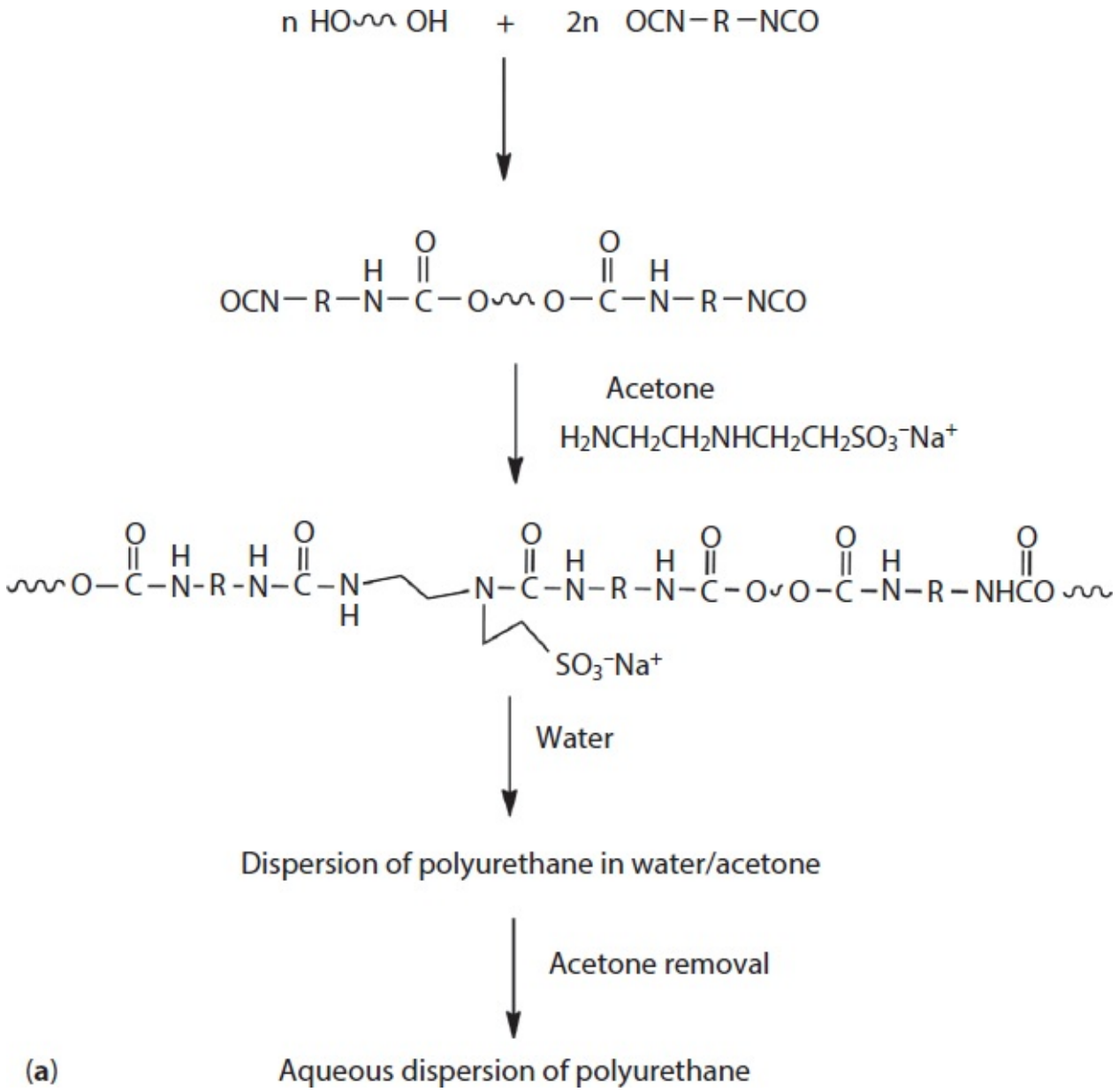
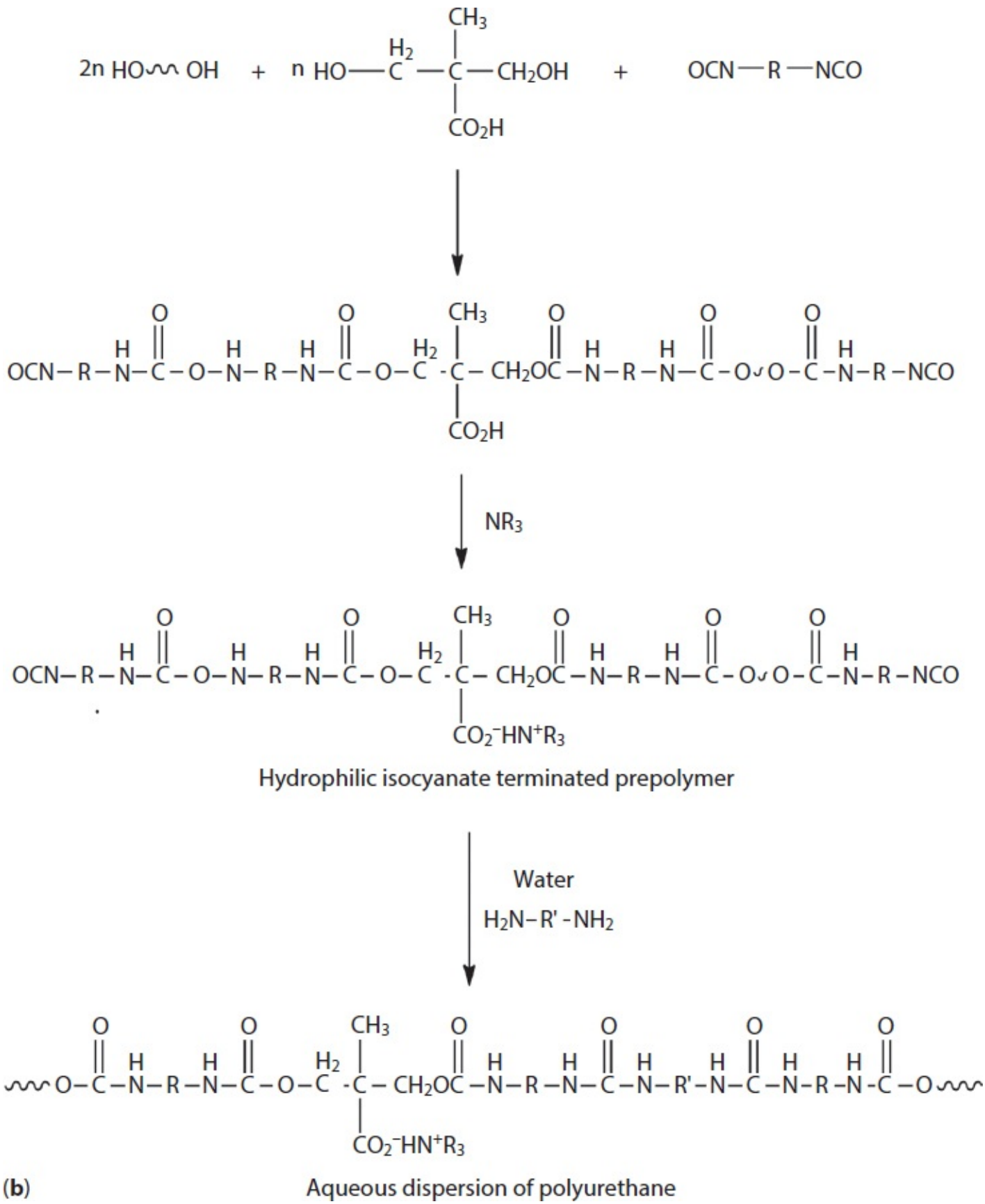


Figure 8.3 Preparation of polyurethane dispersions: (a) acetone process and (b) prepolymer mixture process. (*Continued*)


n HO OH + 2n OCN–R–NCO
Acetone
$H_2NCH_2CH_2NHCH_2CH_2SO_3^-Na^+$
$SO_3^-Na^+$
Water
Dispersion of polyurethane in water/acetone
Acetone removal
Aqueous dispersion of polyurethane

(**a**)



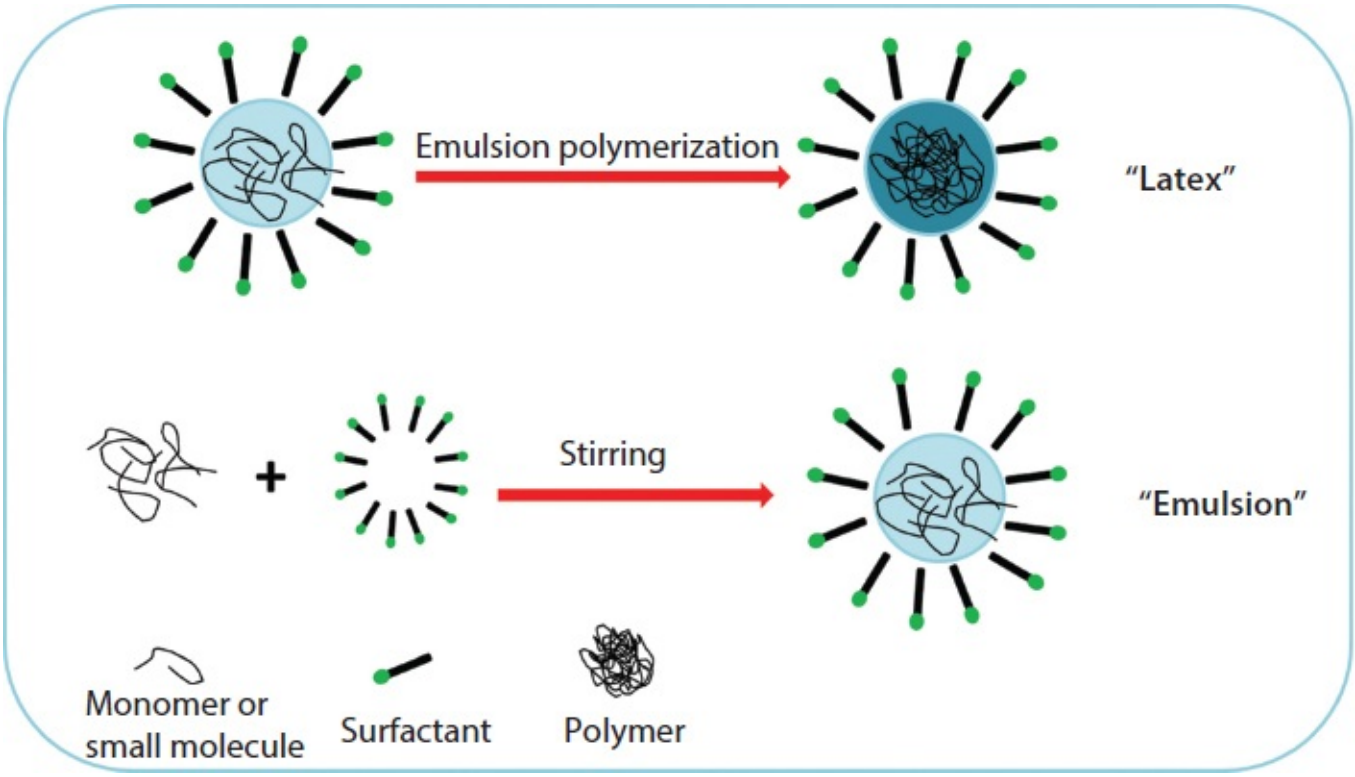
(**b**)

Latex paints are widely used in the architectural coatings. A variety of resins are available for manufacturing latex paints, including styrene–butadiene copolymers, polyvinyl acetate, acrylics, alkyds, polyurethane, and polystyrene. Latex paints have been the major vehicle for those architectural coatings because latex coatings bear even more advantages over many solventborne paints if formulated properly. The blistering or peeling failure is reduced with the increased permeability of latex films to water vapors.

8.1.3.3 Emulsion Coatings

Emulsion coatings are different from latex coatings, although in most cases manufacturer and even scientists use the two words “emulsion” and “latex” [7] as no difference. Based on the dispersing state shown in Figure 8.4, emulsion is defined as a liquid dispersed in a liquid, while latex is a solid dispersed in a liquid. Emulsion paints are not so widely used as the water-reducible or latex paints. However, emulsion paints do have advantages in some specific applications.

Figure 8.4 Comparison of latex and emulsion paints.

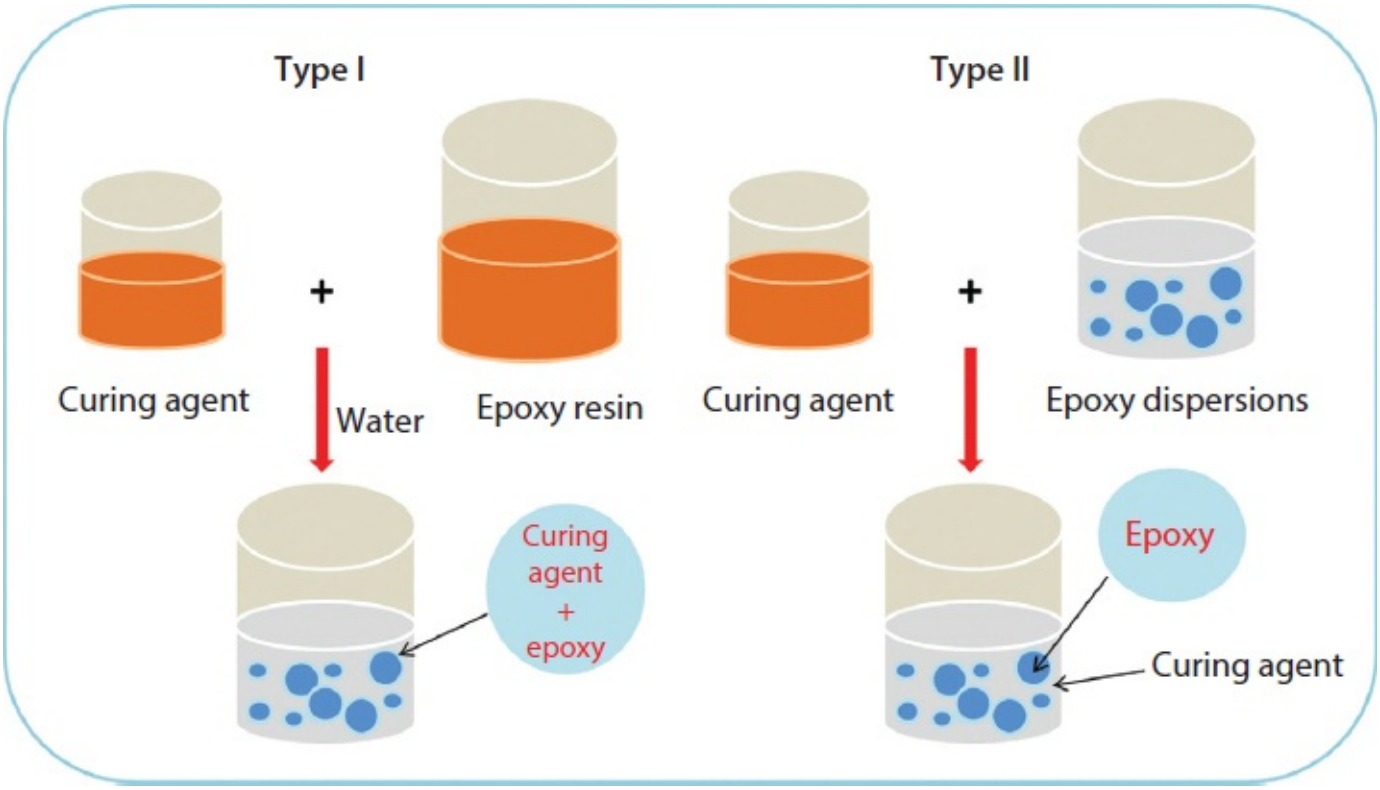


Alkyd emulsion is one way to convert traditional solventborne alkyd into the low VOC waterborne alkyds. In principle, alkyd emulsion is prepared by dispersing alkyd in water and stabilizing it with an external surfactant. Two different techniques [8, 9] are generally used, i.e. direct emulsion and emulsion through inversion. Direct emulsion is a method in which the alkyd is directly dispersed into water with the high shear stirring. For example, the emulsification of traditional long oil alkyd can be achieved by high shear stirring of alkyd in water with the conventional surfactants. In this method, the intensity of the stirring and the properties contributed from the surfactant determine the final droplet size, to a large extent. With the proper stirring speed and selection of surfactant, the emulsion with droplet size less than 0.5 um can be obtained. The other one is the inversion emulsion, in which the first formed water-in-oil (W/O) emulsion is inverted into an oil-in-water (O/W) emulsion. This inversion can happen by changing temperature or the water content. In addition, the choice of surfactant can determine which emulsion is formed. Although the solventborne alkyd has been used for long time due to combination of low cost and good performance, the development of alkyd emulsion is stimulated largely due to the regulation of the organic solvents used in the solventborne coatings and the recognition of the hazardous VOC effect on the environments, paint workers, and users [1].

Another common emulsion coating is the 2K epoxy emulsion coating [10]. Similar to the solventborne 2k epoxy coatings, the two packages are the BPA epoxy resin solution and the modified amine as the cross-linking agent. Two types of waterborne epoxy systems are developed based on the molecular weight range of epoxy resin. Type I systems are based on low molecular weight epoxy

resins, which are widely used as the liquid bisphenol A/F epoxy resins. Type II are based on the high molecular weight epoxy resins, which form the solid epoxy dispersions (Type II should be actually categorized into latex according to the definition in this chapter, but they are put here for comparison between the two types). Unlike the 2K solventborne epoxy coating, the emulsion epoxy systems do not show any change in viscosity. For the early generations, such kind epoxy emulsion can only be used for wall coatings due to the inferior film properties. For the high-performance applications, the epoxy emulsions suffer from the presence of surfactant after film drying. The general preparation procedure is simple shown in Figure 8.5. First, the amine package containing external surfactant is diluted with water. Then, under the strong stirring, the epoxy solution is added. For the liquid type I epoxy, the pot life is very short since epoxy and amine present in the same particles. In addition, the short and rigid backbone results in the good hardness but poor flexibility and toughness. Due to the brittleness of coating formed from the liquid epoxy, type II based on higher molecular weight solid epoxy resins are developed. In this type system, high molecular weight epoxy is pre-dispersed in water as shown in Figure 8.5. The aminecuring agent is then added. Compared with type I, pot life of type II is extended. This can be explained with the lower concentration of epoxide groups as well as the retarded diffusion of curing agent. Unlike type I system, where coalescence happens easily and forms the uniform film morphology, the amine will react with epoxy at the surface of particles, which retards the flow of amine into the epoxy core. Generally, the resulted films bear inferior chemical resistance compared with the solventborne 2K epoxy.

Figure 8.5 Two types of water-based epoxy systems.



8.1.4 Development and Prospect of Waterborne Coatings

Without discussion about the environmentally safe technologies, the trace of the rise of waterborne paints can hardly be described. Since 1865 when the first U.S. waterborne paint patent was issued, the rise of the waterborne paint technology had been gradually increased in the following one hundred years [3]. Until 1967, EPA Rule 66(5) that regulated the use of potentially harmful solvents in industrial coatings was invoked in Los Angeles County [3]. To meet this strict restriction of solvent,

high-solids coatings, which mean 60% solids by weight or higher are highly demanded. Since then, the world of coatings has been changed in the USA. Traditional solventborne coatings are generally dissolved in 40–60% organic solvents. Then, these organic solvents will evaporate during the process of not only the formulation, but also mainly the film formation of the coatings. The release of organic solvents noticeably contaminates the working and environment, which is the most undesirable for the sustainable development. The use of waterborne materials with very low or zero VOC allows coatings industry to decrease the pollution of the environment up to almost 100%. In the modern society, the government of the developed countries proposed a lot of national legislations on the coating industry. This is definitely the main stimulus of the stable tendency of the development of waterborne systems and their industry applications.

In addition, the first place is definitely occupied by the waterborne systems among environmentally safe products. The use of water as a solvent in the coating shows evident advantages. Many types of other environmentally friendly coating systems are also mainly used in the industry but they are not as universal as waterborne coatings. Water is odorless, fire resistant, nontoxic, inexpensive and easily accessible. The use of radiation and UV curing still contains some volatile and toxic components during the formulation and film formation. High-solid coating systems have at least 60% solid content and therefore can generate important technological problems in rheology. Moreover, waterborne systems can be formulated based on all known polymeric products, produced by using the traditional production line and applied to all kinds of surfaces by using various available procedures. However, the powder coating systems require special and quite complicated equipment for their application and great amounts of energy for the formation of coatings. Dating back to 1996, the statistical data has shown the leading role played by waterborne systems, especially in most of the developed countries [11].

8.1.4.1 Development of Resins Used in Waterborne Systems

As more and more attention paid to the health and environments, the development of high-quality coatings with zero or low VOC is significant and difficult for coating industries today. Researches on waterborne coatings have been stimulated by both economic and ecological concerns. These coatings using the evaporation of water, if designed properly, can outperform solventborne coatings and perform better than expectations in various severe environments. A lot of attempts have been made from scientific and technological viewpoints.

Polyacrylate has been one of the most common resins for the preparation of latex. The properties of latex can be easily tailored by emulsion polymerization of acrylic monomers and different functional groups can also be incorporated into the side chain as the cross-linking sites. In most cases, latexes are typically used for thermosetting coatings [12]. 2-Hydroxyetyl methacrylate (HEMA) has been used as a functional monomer with hydroxyl groups. The incorporation of hydroxyl functional groups in the polymer chains behaves as the reaction sites for reactions with isocyanate functionalized or melamine–formaldehyde curing agents [5, 12, 13]. At the same time, many researches have been done regarding the effect of HEMA on the final particles. Soucek and coworkers [14] made extensive research on the effect of introduction mode of hydroxyl functionality on morphology and film properties of cycloaliphatic diepoxide cross-linkable core–shell latex. The same amount of hydroxyl functional monomer was used in the three series of core–shell hydroxyl-functionalized latexes. The HEMA functionality in different locations provided respective properties. According to their results, the higher hardness and tensile modulus was found with hydroxyl

functionality in the core, while the highest cross-linking density was observed with hydroxyl functionality in the shell. The homogeneous distribution of the hydroxyl functionality, however, showed a significant increase in elongation at break. The concentration of HEMA in the three series of hydroxyl-functionalized latexes system is around 16.4 mol%. It was also reported that a bimodal particle size distribution was observed for high concentrations of functional monomers, which was explained by homogeneous secondary nucleation mechanism [15].

In the past few decades, epoxy coatings have been evolved from high VOC systems to more environmentally friendly technologies. The waterborne epoxy curing agent technology has been advanced greatly accordingly. Zhou *et al.* [16] synthesized a new silane modified waterborne epoxy curing agent (Figure 8.6). The cross-linking density, hardness, adhesive property as well as the water resistance were improved as expected due to the presence of silane part. The reason for poor film properties is that the presence of emulsification of curing agent on epoxy rarely incorporated into the curing process. A new type of curing agent bearing good emulsifying behavior was synthesized (Figure 8.7) [17]. The reacted epoxide groups help improve the compatibility between the curing agent and epoxy resin and the presence of the hydroxyl groups ensures the hydrophilicity. The emulsification and curing processes are therefore combined at the same time with the new curing agent. Good properties were obtained from the cured film prepared by the emulsion-type curing agents and epoxy resins. With the development of new types of waterborne curing agents, waterborne coatings are expected in applications where high performance is required.

Figure 8.6 Waterborne epoxy curing agent modified by silane.

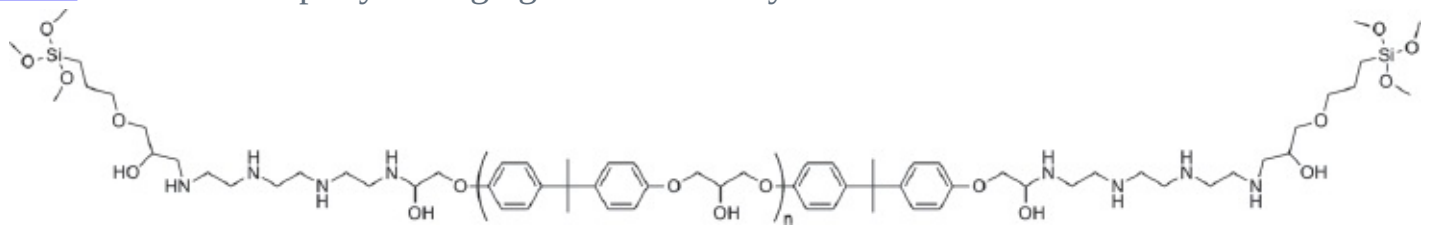
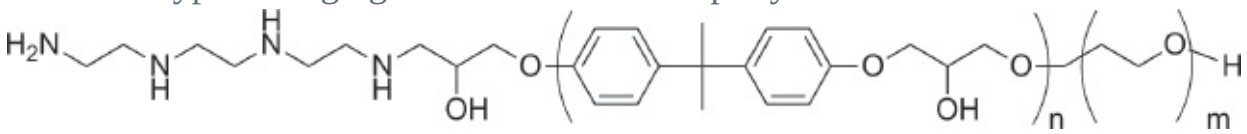


Figure 8.7 Emulsion-type curing agent for waterborne epoxy.

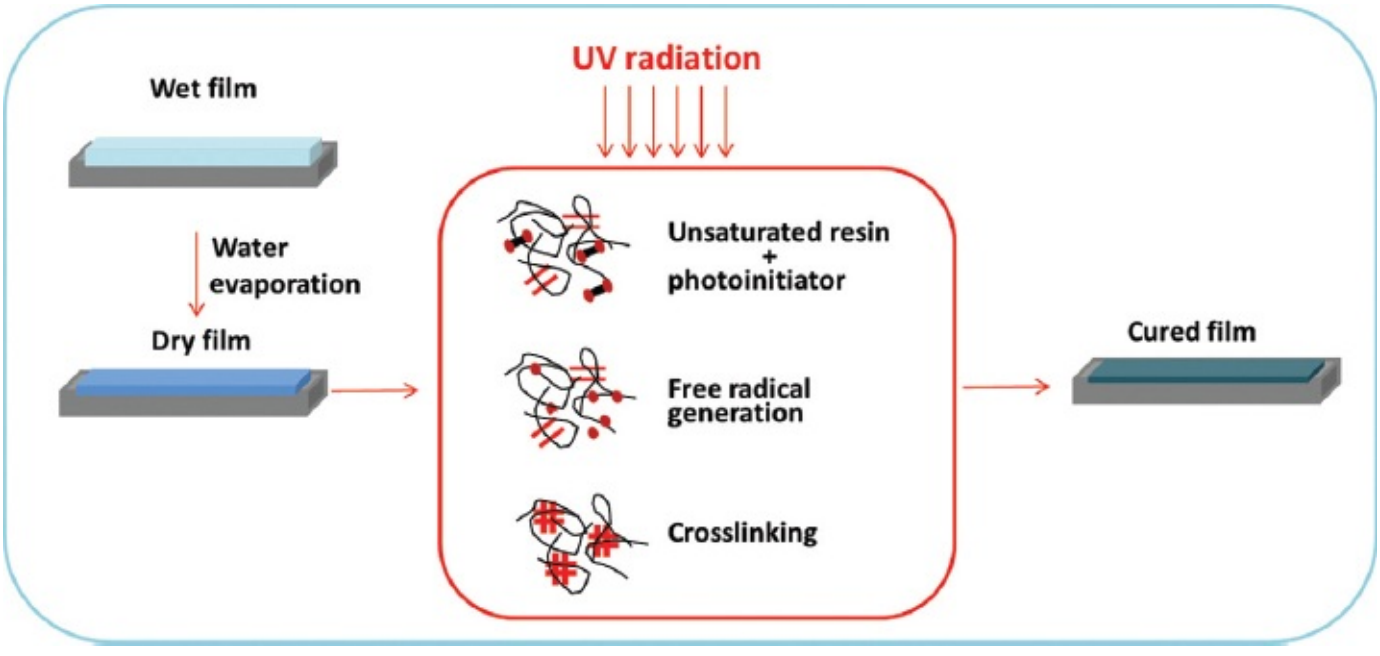


Alkyd emulsions, last but not the least, offer almost zero VOC. It has also been recognized that the alkyd emulsions are very promising to be the real green resin since the raw material comes from the seed oil, such as the most commonly used soybean oil, linseed oil, and tung oil. This promotes the biodegradability of the resulting coating films. The alkyd emulsion itself, can offer superior properties with low costs, such as good penetration to the porous substrates, adhesion to metal, good gloss, and so on. In addition, the alkyd backbone can be modified by other chemical materials to further improve the performance. For example, acrylic addition can improve the durability of the coating and urethane incorporation will enhance the elasticity, abrasion resistance, hardness, and chemical resistance. The application of alkyd emulsion is enlarged and developed significantly due to the improvement resulted from these chemical modifications as well as the maintained good properties of alkyd. Long oil alkyd emulsions of droplet diameter less than 500 nm was achieved using polymerizable emulsifiers [18]. Modifications of alkyds for coating application are described in Section 8.2.7 of this chapter. The drying and washability resistance of alkyd emulsions were enhanced since the polymerizable surfactants become the integral part of alkyd. At the same time, the mechanical, electrolytic and freeze-thaw stability were also improved.

8.1.4.2 Combination of Waterborne with Other Techniques

Not only resins are developed for application in the field of waterborne coatings, but also waterborne coatings have been combined with other environmental techniques. The waterborne UV curable coatings have drawn significant attention in the markets of paper coatings, wood furniture and wood floor coatings. First of all, low VOC emission is ensured by the waterborne coatings and the high production efficiency at the same time by the UV cure. In addition, the production line can be shared with the traditional solventborne coatings and the cure can be done by adding a UV source at the end of the production line. The process of UV curable waterborne acrylic coatings are described in Figure 8.8. The photochemical process is achieved through a free-radical mechanism to form the cross-linking networks. First, free radicals are generated from photoinitiators split by the ultraviolet (UV) radiation. Then the resulted free radicals react with the double bonds of acrylic resin and generate more free radicals. Finally termination is achieved and the cross-linking network is formed. In these UV waterborne coatings formulations, the resins have higher molecular weight than the traditional UV coating formulation. This is due to the presence of water, which is very efficient in viscosity control and therefore allows the higher molecular weight to lead to higher performance. Therefore, the UV curable waterborne coatings occupy the increasing share of the coating market. The development of UV waterborne resin technology has advanced largely in the past decades. The kinetic study of the UV curing process was conducted by Infrared spectroscopy [19]. The critical factors of the polymerization rate and cure extent, such as the type of photoinitiators and the chemical structures of the acrylate functionalized oligomers, have been investigated. A faster curing was obtained from emulsion coatings than dispersion coatings due to the greater molecular mobility. Good resistance of accelerated weathering was shown in the UV cured waterborne polyurethane–acrylates coatings containing adequate light stabilizers. Recently, a novel proprietary emulsion technology [20] was proposed in order to extend the application field of waterborne UV curable products. This technological opportunity allows the high extent of curing of pigmented polyurethane dispersions and therefore the combination of film properties, such as chemical resistance, mechanical and adhesive properties. UV waterborne systems are expected to be an excellent candidate for high-performance applications [20].

Figure 8.8 Film formation process of UV waterborne coatings.



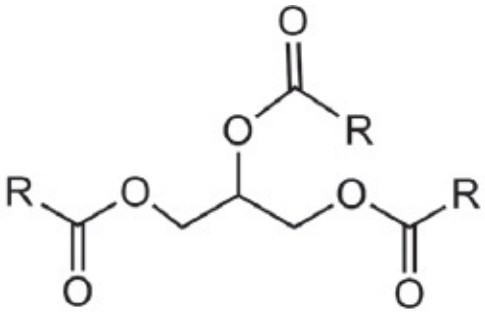
8.2 Seed Oil-Based Coatings

8.2.1 Seed Oils

Seed oils are extracted from the seeds of a variety of annual plants, mostly for human consumption. Seed oils have been used for centuries in the coating industry [21, 22], and seed oils have been modified for the synthesis of various polymeric resins such as alkyds, epoxy, and polyurethanes for coating applications. Seed oils have the advantages of being low-cost, readily available, and renewable with high annual production around the globe.

The chemical composition of seed oils arises from the esterification of glycerol with three fatty acid molecules, as shown in Figure 8.9. A given seed oil is always made up of a mixture of triglycerides bearing different fatty acid residues. Soybean, tung, linseed, and castor oils are the most common seed oils. The typical fatty acid composition of some commonly used seed oils is given in Table 8.4. Some fatty acids are saturated and some of them are unsaturated. Saturated fatty acids have no C=C double bonds, while unsaturated fatty acids have one or more than one C=C double bond. If the C=C double bonds in the carbon chains are separated by at least two carbon atoms, double bonds are called isolated. If single and double bonds alternate between certain carbon atoms, double bonds are called conjugated. Besides, some fatty acids have different structures, such as hydroxyl and epoxy groups in the fatty acid chains. The physical and chemical properties of seed oils depend on their fatty acid distribution. The numbers of C=C double bonds, as well as their positions within the aliphatic chain, affect strongly the oil properties [23, 24]. The average degree of unsaturation is measured by the iodine value, which corresponds to the amount of iodine (g) which reacts with the double bonds in 100 g of the oil under investigation. Seed oils are divided into three groups depending on their iodine values. The oils are classified as “drying” if their iodine value is above 140, “semi-drying” if this parameter ranges from 125 to 140, and “non-drying” when it is below 125 [25].

Figure 8.9 General structures of triglyceride and some common fatty acids.



Triglyceride generic structure

(R = fatty acid chain)

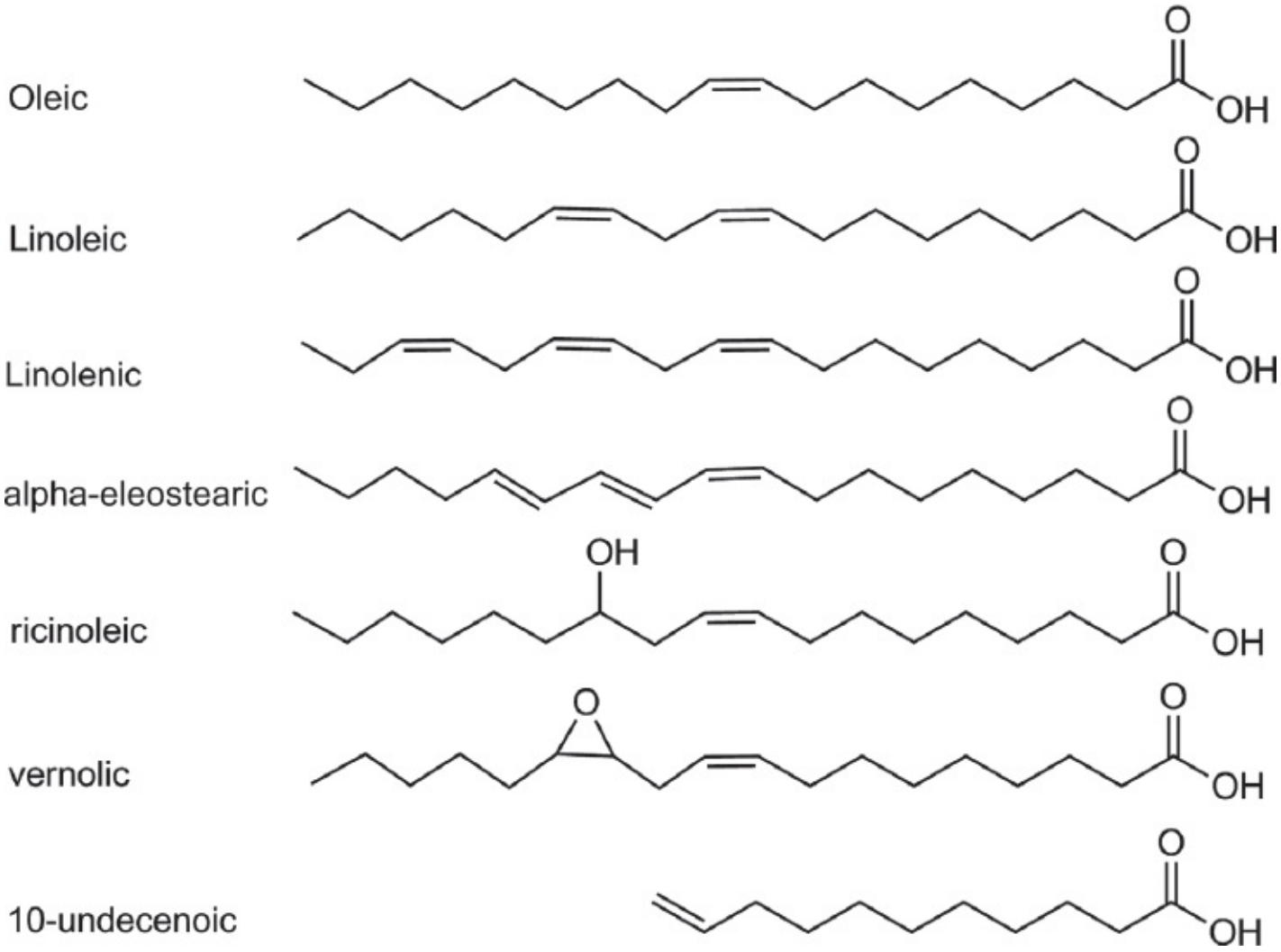
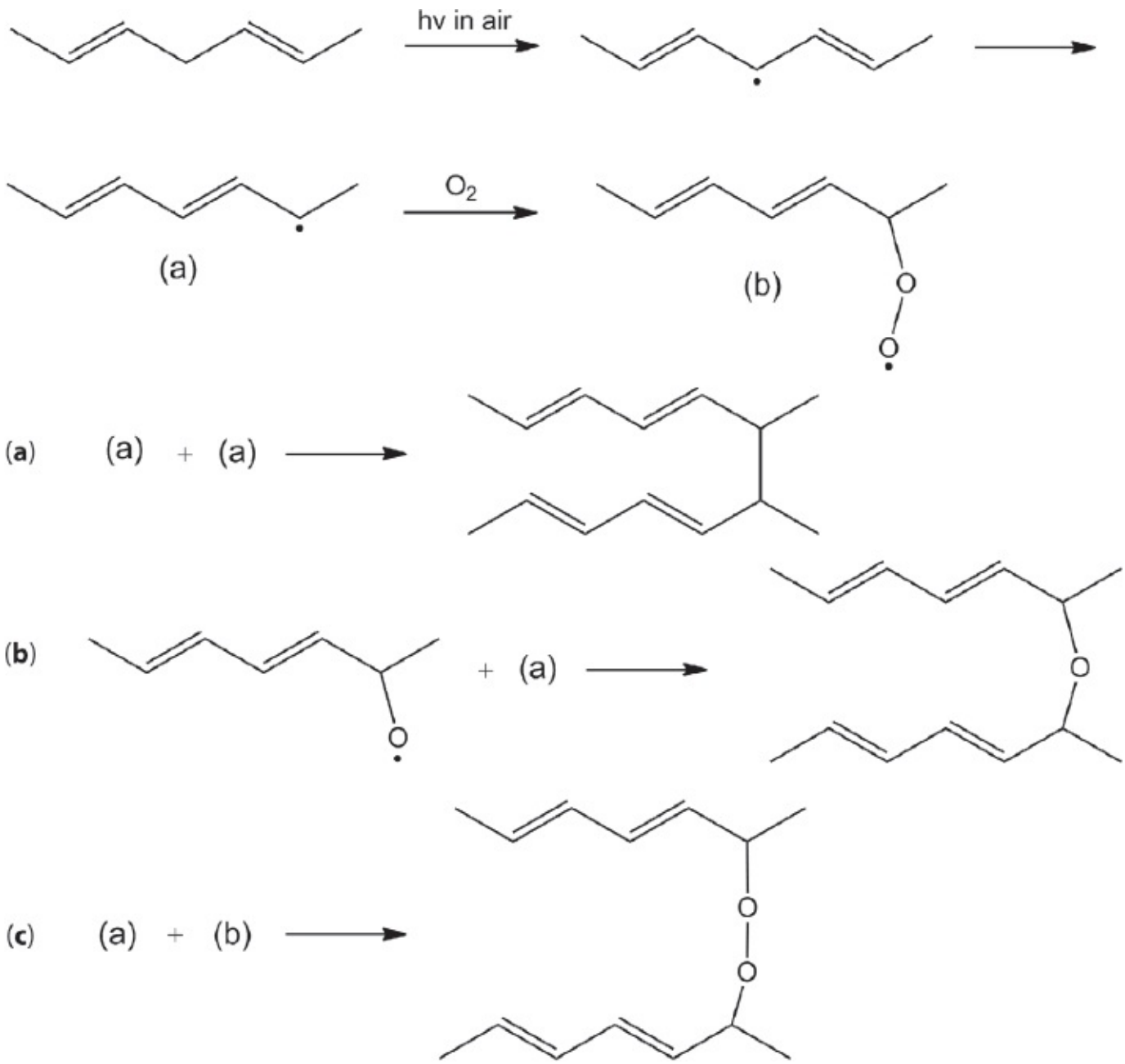


Table 8.4 Typical fatty acid composition of some seed oils [23].

	Soybean oil	Linseed oil	Tung oil	Castor oil
Oleic acid	24	22	4	5
Linoleic acid	53	17	8.5	4
Linolenic acid	7	52	–	0.5
α-Eleostearic acid	–	–	82	–
Ricinoleic acid	–	–	–	87.5
Other	16	9	7.5	3

The C=C double bonds in seed oils can be polymerized by free-radical polymerization. Seed oils can undergo autoxidation with the help of an oxygen atmosphere to form peroxides which undergo cross-linking through radical recombination to form highly branched or cross-linked polymeric materials. Oxidation of the drying oil begins when molecular oxygen attacks an active center on a fatty acid chain, followed by the hemolytic cleavage of the peroxide to produce free radicals. Hydrogen is abstracted from the methylene group between C=C double bonds followed by isomerization in a double bond position to form a conjugated structure. Termination results in C–C (reaction A), ether (reaction B), and peroxy linkages (reaction C) which create an interlocking network [22, 23] (Figure 8.10).

Figure 8.10 Autoxidation of seed oils [22, 23].



Because of the low reactivity of the double bonds within the seed oils molecule and the flexibility of the triglyceride fatty acid structure, seed oils are usually chemically modified to be useful for applications in industrial products. Various chemical pathways for functionalization of these triglycerides have been studied. A lot of efforts have been made to chemically modify seed oils in order to enhance their reactivity and improve the final coating properties over the last few decades [22, 26–29].

8.2.2 Seed Oil-Based Coatings from Copolymerization with Vinyl Monomers

One of the oldest methods for the modification of seed oils is the copolymerization of drying and semi-drying oils with vinyl monomers like styrene, alpha-methylstyrene or cyclopentadiene [22, 30–32]. Since the products have improved film properties, they can be used in the formulation of surface-coating materials.

Styrene is the most important monomer for this purpose. Linseed, tung, soybean, sunflower and oiticica oils and dehydrated castor oil are widely used in the preparation of styrenated-seed oil

products. As a reactive diluent for seed oil-based polymer systems, styrene works well and is relatively low cost. However, styrene is a VOC and HAP. The US Department of Health and Human Services added styrene to its report on carcinogens (ROC), a science-based document that identifies chemicals and biological agents that may put people at increased risk for cancer on June 14, 2011. The National Toxicological Program's (NTP) 12th Report on Carcinogens classifies styrene as "reasonably anticipated to be a human carcinogen" [33]. Therefore, the market of styrene as a reactive diluent is shrinking.

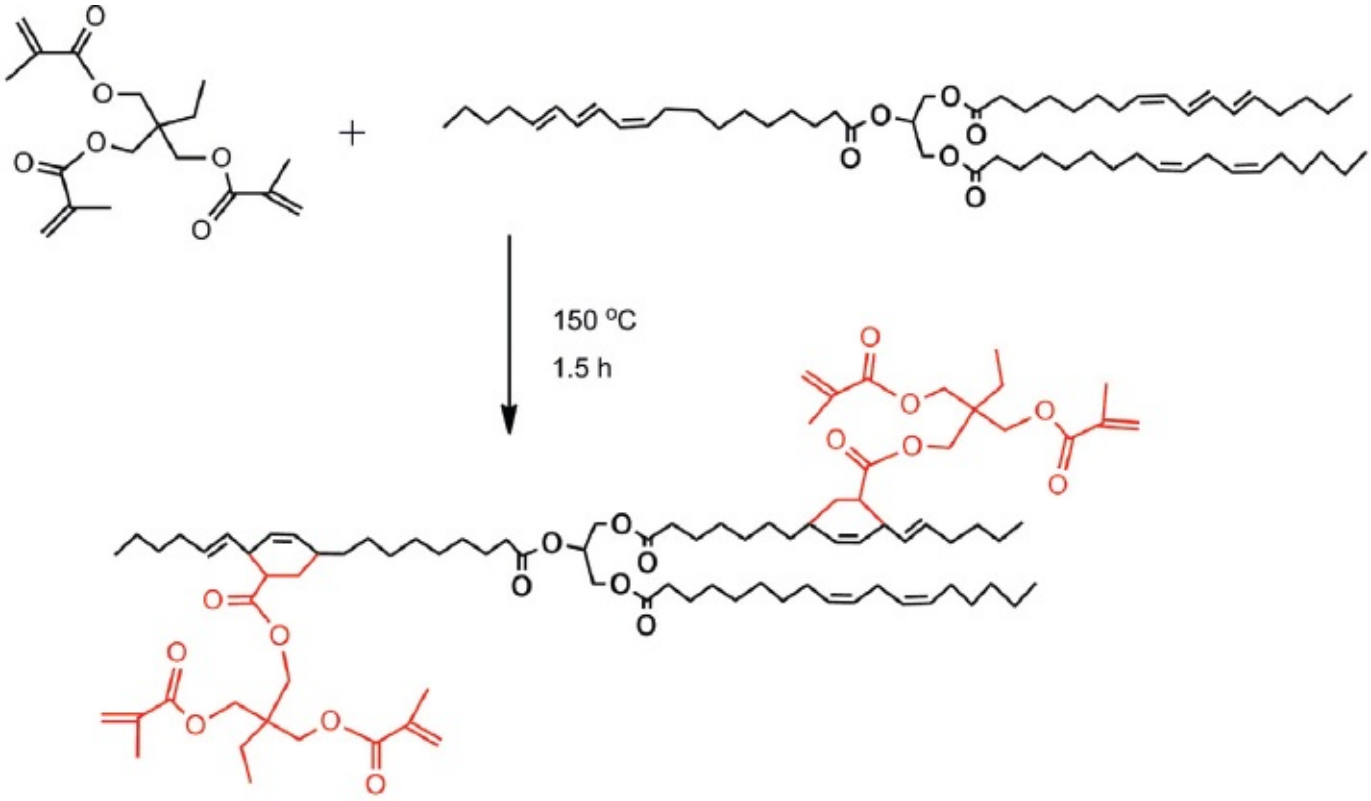
8.2.2.1 Seed Oil-Based Reactive Diluents for Coating Applications

The researchers at Cargill corporation modified linseed oil by reacting with cyclopentadiene at high temperature to form a partially norbornylized commercial product Dilulin, which is a mixture of norbornenyl-functionalized linseed oil and dicyclopentadiene (DCPD) oligomers in a weight ratio of 95:5 [34]. Researchers found that Dilulin possesses an average of approximately one bicyclic moiety per triglyceride. Soucek and coworkers improved the percentage of norbornyl groups of norbornyl linseed oils [35, 36].

Tung oil is advantageous as a raw material for coatings in that it has conjugated C=C structure, imparting the resulting products with faster drying times, higher water resistance, and higher hardness compared to unconjugated drying oils such as linseed or soybean oils [37–40]. In addition, it can more easily be chemically modified to achieve desirable properties. The high content of α-eleosterate (80 wt.%) of tung oil triglyceride is considered as major source of conjugated diene, while the acrylate molecules is a good dienophile. The carbonyl group on acrylates serves as an electron withdrawing group, which plays an important role by lowering the activated energy of the reaction [40]. Thus tung oils have been modified by acrylates for the production of various polymers. Tung oil polymers possess very good dynamic mechanical properties as well as thermal stability at room temperature.

Soucek and coworkers have made extensive research on UV-curable tung oils (UVTOs) and relevant derivatives [37, 41]. They developed UVTO based on acrylate photoinitiated free radical curing via a Diels–Alder cycloaddition (Figure 8.11). The tung oil was bodied with a phenolic resin and then reacted with trimethylolpropane trimethacrylate (TMPTMA) as a reactive diluent.

Figure 8.11 Reaction scheme of UVTO [37].



It is desirable for the coating industry to produce coatings with low solvent amount. However, conventional solventborne coatings typically contain 30–60 wt.% volatile materials which pose threat to the environment and human health. Development of environmentally friendly coatings requires coatings to bear the properties with low VOCs [41]. Varieties of coating techniques such as powder coatings, waterborne coatings, UV radiation curable coatings, and high-solid coatings have been used to reduce VOCs. The last decade has witnessed extensive investigations on high-solid coatings. High-solid coatings have several advantages such as environmental compliance, performance, and economic benefits [41–45]. However, the development of high-solid coatings has the difficulty in achieving an appropriate viscosity for application as well as the difficulty in achieving a curing rate that is not significantly lower than that of conventional coatings. Those difficulties created several technological challenges for high-solid coatings [46].

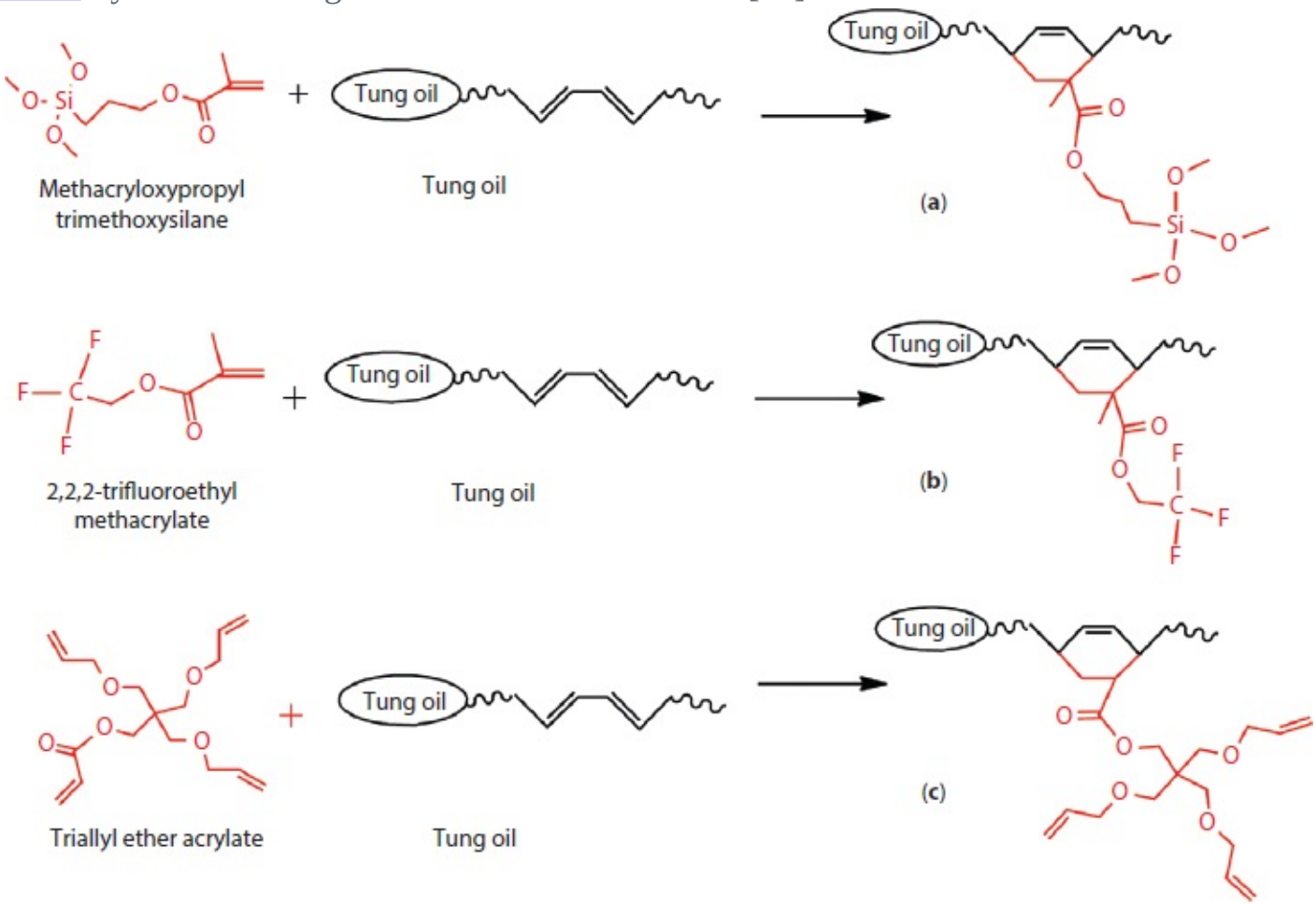
There are several other ways to reduce the VOC. It is commonly accepted that decreasing the viscosity of the polymer reduces the amount of organic solvents. Preparation of a low-viscosity coating requires the use of polymers having either a low molecular weight or a narrowed molecular weight distribution [41]. For this purpose, various novel methods for preparation of low-viscosity resins have been proposed. The use of reactive diluents is one of the most effective means of achieving high-solid alkyd formulation.

A reactive diluent not only serves as a solvent, but participates in the film formation by taking part in the curing process. A good reactive diluent is required to have properties such as low viscosity, low volatility, good compatibility with the binder, and ability to polymerize either by homopolymerization or copolymerization with alkyd under the cure conditions. The reactive diluent would provide additional environmental benefits if it can be derived from renewable sources like seed oils which could reduce the VOC and provide biodegradable properties to the final film [41, 44, 45, 47].

Low viscosity and the ability to undergo autoxidation make seed oils an attractive choice for use as reactive diluents [38–40, 47]. Soucek and coworker prepared three tung oil-based reactive diluents by functionalizing tung oil with three different functional groups of acrylate monomers including

alkylsiloxane, triallyl ether, and fluorinated alkyl, via a Diels–Alder reaction [38, 40] (Figure 8.12). The reactive diluents were formulated with a soya-based alkyd to evaluate viscosity reduction and drying time.

Figure 8.12 Synthesis of tung oil-based reactive diluents [40].



The siloxane functionalized material (Figure 8.12a) shows the lowest viscosity reduction, followed by the fluorine modified product (Figure 8.12b) and the triallyl-ether-functionalized tung oil (Figure 8.12c). These differences are attributed to the varying levels of cycloaddition at the conjugation sites of tung oil that is achieved in each modification reaction. These results signify the use of these new materials in small quantities to reach application viscosities of alkyd resins, eliminating the need for some or all of the organic solvents in alkyd-based coatings.

The siloxane and fluorine functionalized material dried by a different mechanistic pathway from the triallyl-ether-functionalized material. The siloxane functionalized material was slower than the triallyl-ether-functionalized material; however, it was in line with what would be expected with a moisture curing alkoxysilane process. The siloxane functionalized material would be expected to dry slower than the allyl ether, since some of the active autoxidative sites have been removed by virtue of forming the proposed Diels–Alder adduct.

The viscosity of alkyd was reduced up to 70% using the reactive diluents. The drying time for the autoxidative reactive diluents with alkyds was 1.8–1.7 times faster than alkyd alone [40]. However, tung oil is expensive, and its films discolor rapidly due to the presence of the three conjugated double bonds [41]. These shortcomings were the driving force to synthesize conjugated soybean oils for modification with acrylate monomers. Compared with tung oil, soybean oil remains a dominant renewable feedstock and is a more attractive choice for use as a reactive diluent due to its readily availability and low cost.

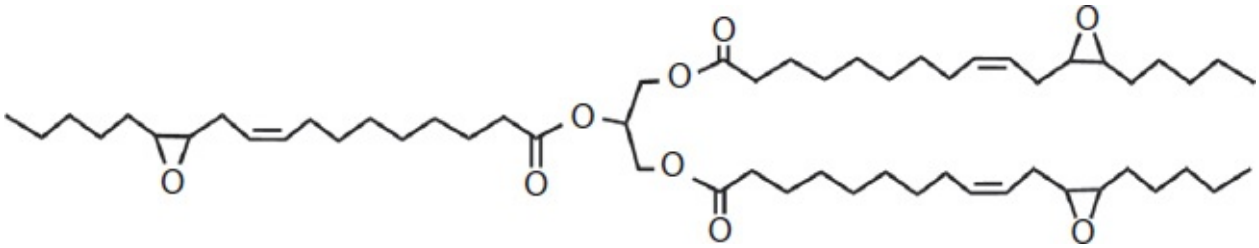
Conjugated soybean oil has been shown to be obtained from a rhodium-mediated isomerization. This conjugated soybean oil was then modified via a Diels–Alder reaction with the same three acrylate monomers that were used for tung oil modifications. The resulting functionalized soybean oils acted as reactive diluents by reducing the viscosity of the alkyd formulation by up to 86% [47]. Triallyl-ether-functionalized conjugated soybean oil resulted in the highest reduction in the viscosity of the alkyd formulations. Alkoxysilane and allyl ether functionalities take part in the film formation via condensation and autoxidative curing, respectively. These two reactive diluents improved the tensile strength, tensile modulus, cross-link density and glass transition temperature. While fluorinated alkyl functionality does not take part in film formation, it affects the properties of the final film, including surface energy, thermal stability, hydrophobicity and solvent resistance [40, 47]. The elimination or reduction of VOCs in coatings processing by using those reactive diluents derived from renewable and cost-effective seed oils should be an important advancement in the mitigation of the environmental impact of VOCs.

8.2.3 Seed Oil-Based Epoxy for UV-Curable Coatings

UV-curable coatings are typically VOC-free systems, and offer advantages such as fast cure, high-energy efficiency, and low volatile contents. Compared to free-radical UV curing, cationic-initiated UV curing has the advantage of insensitivity to oxygen and lower film shrinkage. The cationic-initiated UV curable coatings find specialized applications in paper coatings, wood coatings, plastic substrate coatings, screen printing inks and decorative metal varnishes. Epoxides are one of the most important and widely used coatings for cationic UV-curable applications. Polymers obtained from multifunctional epoxide monomers offer advantages such as excellent adhesion, low shrinkage, and superior chemical resistance.

The presence of the epoxy group as a natural constituent of certain seed oils has been known for a long time. It is reported that there are more than 60 species of plants that produce epoxy groups in their main chains [48]. Of all the epoxy-bearing seed oils, vernonia oil has attracted the attention of many researchers. Vernonia oil (Figure 8.13) represents the most promising of these epoxidized oils due to its ease of production, seed oil content, and concentration of epoxidized triglyceride in oil. There is about 75–80% vernolic acid in the triglyceride [49]. Vernonia oil has been used as reactive diluent. However, the limited availability and higher cost of vernonia oil limits its use. Muturi *et al.* studied the performance of vernonia oil and found it to be comparable to that of epoxidized soybean oil (ESO) and epoxidized linseed oil [50].

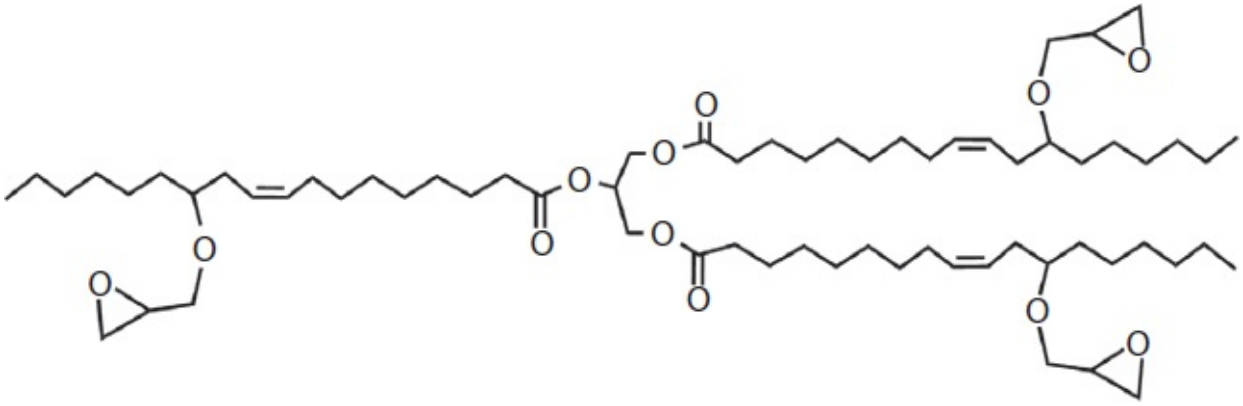
Figure 8.13 Structure of vernonia oil.



Castor oil has been modified for the production of epoxy. Modification of castor oil, containing about 90% hydroxyl-containing fatty esters, with glycidyl ether functionality has provided a promising product for cationic UV-curable coating applications. Coatings formulated from castor oil glycidyl ether (COGE) (Figure 8.14), epoxy resin, and photoinitiator produced smooth coatings with excellent gloss and good flexibility, adhesion, gloss retention, and water resistance. Formulations

containing up to 50% COGE afforded promising coating performance attributes. Cationic UV-curable coatings were developed containing up to 60% COGE concentrations [51].

Figure 8.14 Structure of COGE.



It has been shown that the synthesis of epoxidized castor oil (ECO) as an interesting and inexpensive biorenewable monomer could be achieved by an efficient and low cost epoxidation process [52]. The photoinitiated cationic polymerization of ECO was studied using diaryliodonium salt photoinitiators. The photopolymerization rate of ECO is highest for diaryliodonium salts containing the SbF_6- counter ion and may be accelerated through the use of photosensitizers such as anthracene and 2-isopropylthioxanthone. ECO displays excellent reactivity in photoinitiated cationic polymerization compared to other epoxidized seed oils due to the presence of the hydroxyl groups in the molecule. ECO has been used for the preparation of interpenetrating polymer networks (IPN), and these were characterized for their dynamic mechanical behavior [53]. It was observed that the cross-linked IPNs from the epoxidized oil and adducts of tung oil with maleic anhydride had very good compatibility. The hydroxyl groups of ECO form hydrogen bonds with the carbonyl groups in tung oil. These hydroxyls are more reactive toward tung oil adducts than epoxidized cottonseed oil.

ESOs have been widely utilized to synthesize oil-based coating resins. However, ESO-based coatings suffer from lower T_g value and a higher coefficient of thermal expansion, which was attributed to a lower degree of epoxidation compared to some other epoxidized oils, i.e. linseed oil and castor oil [55, 56]. The epoxidation reaction of sucrose soyate resin to produce epoxidized sucrose soyate (ESS) (Figure 8.15) has shown to be an extremely promising route to overcome the drawbacks of ESO-based coatings and create high-performance, bio-based thermoset resins [54–58]. ESSs have been used as resins for cationic UV-curable coatings. The epoxy anhydride curing of ESSs has been studied, and it demonstrated that ESS-based thermosets have exceptional performance [54–57]. Cross-linking reactions involving epoxy homopolymerization of 100% biobased ESSs were studied. ESSs were found to have superior coating properties, compared to ESO and the petrochemical-based soybean esters, which might be due to a higher T_g and a higher modulus of ESSs. ESSs were cross-linked with a liquid cycloaliphatic anhydride to prepare polyester thermosets. Compared with ESO, the ESSs-based thermosets have high modulus and are hard and ductile, high-performance thermoset materials while maintaining a high bio-based content. A novel 100% bio-based thermosetting coating system was developed from ESS with bio-based dicarboxylic acids. The resulting coating systems have good adhesion to metal substrates and perform well under chemical and physical stress.

Figure 8.15 Sucrose soyate-based epoxy for thermoset applications [58].

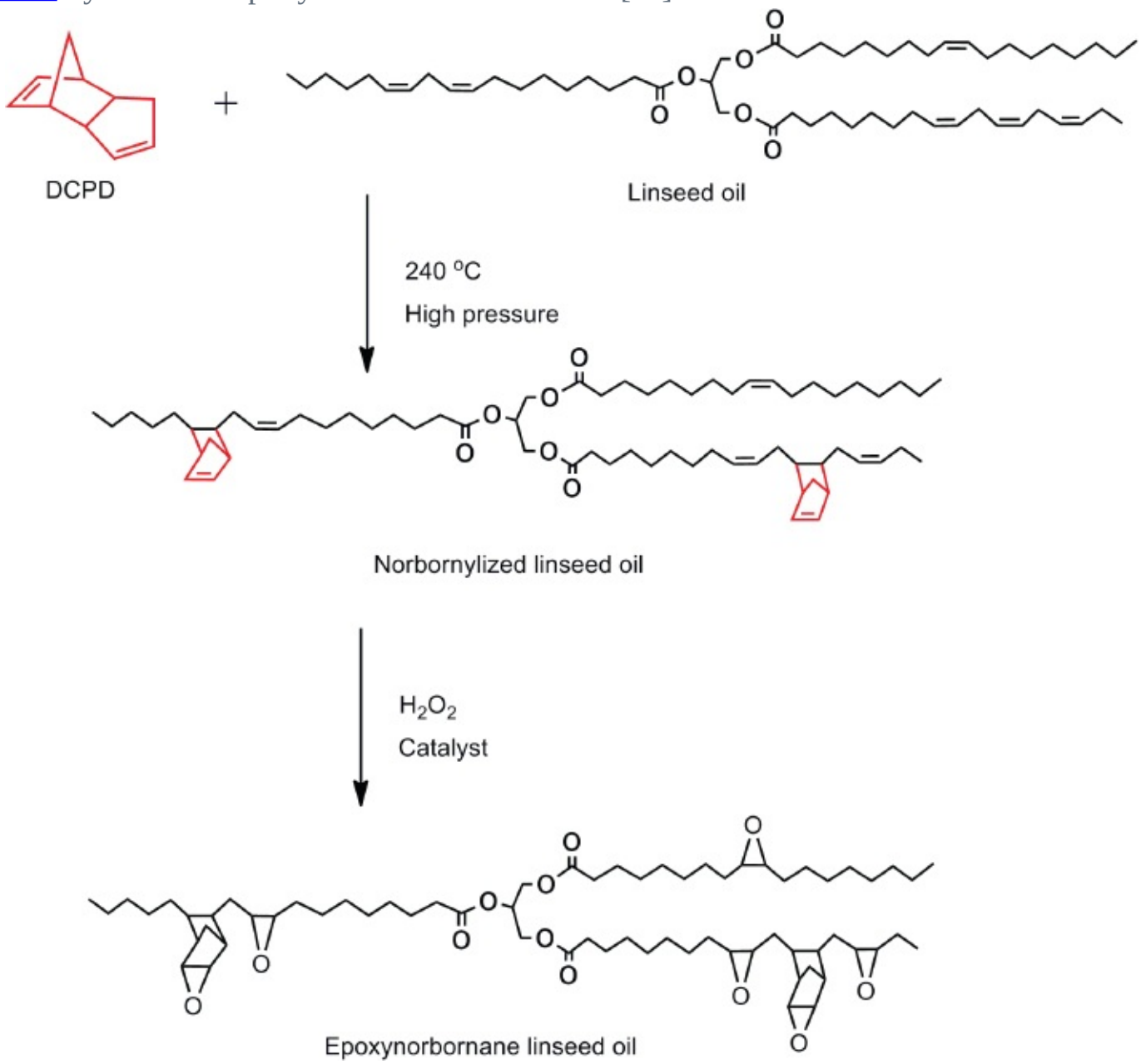


The relative reactivity during cationic ring-opening polymerization of different epoxy monomers is highly dependent on the structure of the monomers. Researchers concluded that glycidyl esters were less reactive than glycidyl ethers, which were, in turn, less reactive than epoxidized α-olefins [36, 59, 60]. The most reactive monomers were cycloaliphatic epoxy monomers bearing the epoxycyclohexane moiety.

There are many possible parameters that affect the reactivity of epoxides in cationic polymerization. One factor that may contribute to the reactivity of an epoxy monomer is the ring strain. However, the epoxide group in ESOs has a relative low reactivity compared to cycloaliphatic epoxides. Research has been performed to improve the reactivity of epoxidized linseed oil by introducing a cycloaliphatic epoxy functionality onto the backbone of linseed oil. The preparation of norbornylized linseed oil epoxynorbornane linseed oil is detailed in Figure 8.16. Soucek and coworkers characterized the cationic polymerization of linseed oils with and without

epoxynorbornene group [35], and they attributed the faster curing of epoxynorbornene linseed oils to the higher ring strain of the norbornene ring system. They determined the reactivity of those monomers via the decreases in the epoxide absorption bands in the 850 cm^{-1} region with the real-time FTIR. The ring strain in the cyclohexene ring system is higher as compared to their linear aliphatic or glycidyl ether counterparts.

Figure 8.16 Synthesis of epoxynorbornane linseed oil [35].



The cyclohexene derivitized linseed oil (CLO) was synthesized by Diels-Alder cycloaddition with 1,3-butadiene [60]. Then, the epoxidized cycloaliphatic linseed oil (ECLO) was prepared via oxidation with hydrogen peroxide/quaternary ammonium tetrakis-(diperoxotungsto) phosphate. The ECLO was photopolymerized using UV-light, and the kinetics of the photocuring reactions was evaluated by real-time FT-IR and photo-DSC. The kinetics study by real-time FT-IR and photo-DSC revealed that the cationic photopolymerization rate of ECLO was slightly faster than that of epoxidized linseed oil. The faster curing speed of cycloaliphtic epoxide was attributed to ring strains of ECLO. It was also very interesting to find that ECLO did have a faster curing speed than epoxidized linseed oil even with only 10–15% cycloaliphatic functionalities.

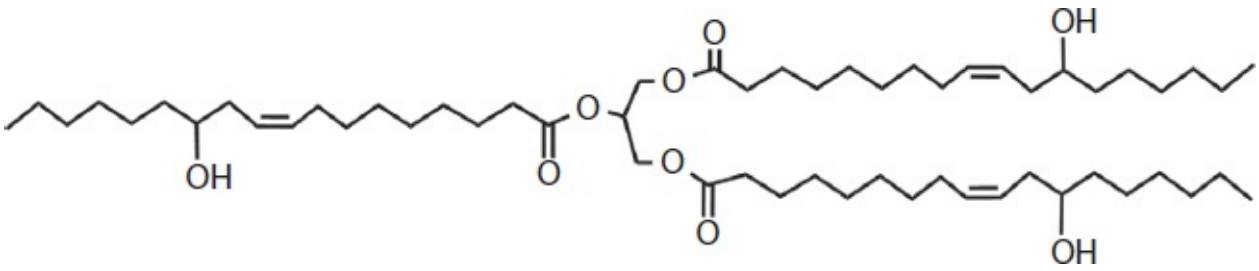
Besides ring strain, viscosity is another factor which has effect on the reactivity of the epoxy

monomers. In previous work, it was reported that without the addition of reactive diluent, the monomers with higher viscosity exhibited an intrinsically slower relative reactivity. A series of epoxynorbornane linseed oils were prepared as a function of the norbornane content [36]. The cationic photopolymerization of epoxynorbornane linseed oil and epoxidized linseed oil was studied by various methods of characterization. The addition of reactive or non-reactive diluents reduced the viscosity of the formulations and was found to have significant effect on epoxy conversion and the rate of polymerization of epoxynorbornane linseed oil. It was reported that the photopolymerization of epoxides was accelerated due to the presence of vinyl ether [36]. This was attributed to the generation of a large number of propagating cationic species via a redox reaction between the vinyl ether and the photoinitiator diaryliodonium salt.

8.2.4 Seed Oil-Based Polyurethanes

The unsaturated C=C double bonds in seed oils make possible various reactions for productions of various bio-based polyols, which react with diisocyanates to get polyurethanes. Among seed oils, castor oil (Figure 8.17) represents a promising raw material due to advantages such as low cost, low toxicity, and availability as a renewable agricultural resource. More importantly, its major constituent recinoleic acid is a hydroxyl containing fatty acid. Castor oil is the only commercially available natural oil polyol that is produced directly by nature, and can be used directly as a raw material for the preparation of polyurethanes without any future modification.

Figure 8.17 Structure of castor oil.



Castor oil was reported to be directly utilized for the production of rigid polyurethanes, and the resulting polyurethanes had the advantages of good water resistance and flexibility [61, 62]. However, some disadvantages limited the wide application of castor-based polyurethanes, such as low functionality and low reactivity which lead to semi-flexible and semi-rigid materials.

Several researches have been done in terms of millable polyurethane elastomers based on the castor oil and toluene diisocyanate (TDI) dimer as the cross-linking agent. Investigation of the polyurethane properties showed that the elastomers could be tailored in order to fulfill industrial needs [63]. Comparison of physical and mechanical properties of the prepared elastomers with one of the commercially available polyester urethane samples showed that these elastomers exhibited comparable tensile strength, compression set, resilience and a little inferior abrasion resistance and elongation at break properties.

With the exception of castor oil, nearly all seed oils do not naturally have the hydroxyl groups for polyurethanes production. However, the carbon–carbon double bonds present in triglycerides allow for the introduction of hydroxyl groups. Seed oils with higher unsaturation should give polyols with higher functionality. The glass transition of these polymers, irrespective of their chemical structure, was almost linearly dependent of the polyols OH number, and thus, cross-linking density of polyurethanes [64].

Epoxidation and ring opening reaction with haloacids or alcohols, ozonolysis and hydration are some of the common methods for functionalization of unsaturated seed oils. The introduction of hydroxyl groups can be achieved by direct oxidation of double bonds. However, this process has the disadvantages of bad control and selectivity, which lead to a number of by-products and oxidation species such as peroxides, aldehydes, and ketones. Some other conventional methods for preparing polyols from seed oil either do not produce polyols having a significant content of hydroxyl groups, or do not produce products having a desirable viscosity. Moreover, the presence of high unsaturation has been another issue with these polyols which makes the resulting products susceptible to oxidation, and color and property change with time [65, 66]. Better control of oxidation is achieved by epoxidation where epoxy groups are inserted exactly at the position of double bonds. This process is well established and has been commercially applied. Ring opening of epoxy groups can be achieved with alcohols or water in the presence of acid catalysts, with organic acids, inorganic acids, and by hydrogenation [65].

Many factors affect the properties of polyurethanes prepared from epoxidized seed oils, such as the fatty acid composition and the nature of the starting oil, the extent of epoxidization, the number and location of the hydroxyl groups and residual C=C double bonds in the final polyurethane as well as the presence of long dangling chains. Epoxidized linseed oils were used for the synthesis of anticorrosive coatings. It was found that the synthesized resin showed good performance in various corrosion tests. The resulting resin obtained with 10% loading of TDI gives the best physico-mechanical and anticorrosive performance. These studies seem suggest that polyurethanes from linseed oils hold promise for commercial application as anticorrosive coating material [67]. Canola oil has been used for the production of polyurethanes for comparison with soybean oil-based polyurethanes. It was found that the properties of the resulting products were strongly dependent on processing, such as the cross-link density and the molar ratio of polyols to isocyanate component. The glass transition temperatures (T_g) of the elastomers were found to increase as the OH/NCO molar ratio decreased from 1:0.8 to 1:1.2. With the same OH/NCO molar ratio, T_g of canola-oil-based polyurethanes was higher than that of soybean-oil-based polyurethanes. With the same OH/NCO molar ratio, the elastomers made from canola-oil-based polyol showed slightly higher Young's modulus and tensile strength [68].

The use of bio-based polyols for the manufacture of polyurethanes is a real positive point for the environmental impact of polymers. It is interesting to use biobased polyols in polyurethanes synthesis since polyols represent the major part of polyurethanes.

8.2.5 Seed Oil-Based Thiol-ene Chemistry in UV-Curable Coatings

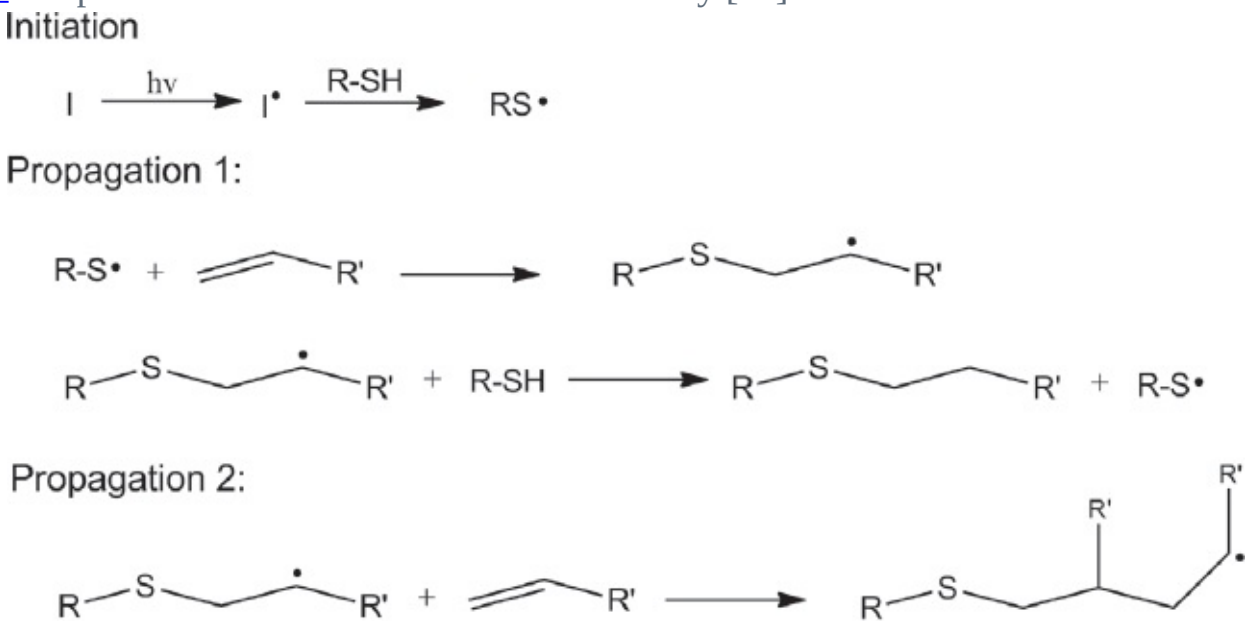
Despite the advantages, most UV-curable coatings have limitations such as poor threedimensional curing, curing limits with pigmented systems, and sensitivity to oxygen (free-radical mechanism). Cationic UV systems are insensitive to oxygen and have been used as replacement of free-radical UV systems in certain specialty applications. However, cationic curing has the disadvantages such as extreme sensitivity to moisture and water, limited monomer variety, and required longer UV exposure times [69, 70].

The thiol-ene chemistry is a well-established reaction that is known for more than 100 years. Currently, it is undergoing resurgence in many areas of chemistry. Thiol-ene UV cure occurs through

a step-growth reaction mechanism that offers many advantages such as delayed gel points, uniform structures, low polymerization shrinkage and reduced stress, which render thiol-ene polymers high-performance materials, especially in UV-curable coatings [71, 72]. Hence, thiol-ene system can be expected to enhance the UV-curing speed of seed oil due to oxygen inhibition and provide benefits such as renewable resource utilization and low VOC emissions. Due to those merits, thiol-ene chemistry has attracted extensive research interest in recent years.

Figure 8.18 shows the proposed radical step growth mechanism for the photoinitiated thiol-ene polymerization [73]. The primary radicals produced in the photolysis of the photoinitiator can abstract the hydrogen atom of the thiol group and produce a thiyl radical. This thiyl radical would react with the C=C double bond of the unsaturated monomer to generate a secondary free radical, which in turn could abstract the hydrogen atom of a second molecule of the thiol, generating a new thiyl radical to repeat the cycle.

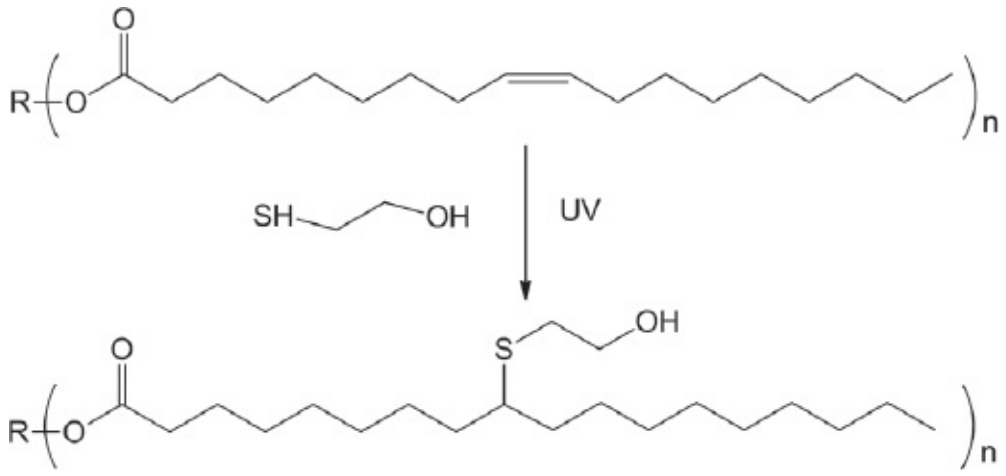
Figure 8.18 Proposed mechanism of thiol-ene chemistry [73].



Various thiol-ene chemistries based on various seed oils have been used for UV-curable coatings. Aluminum substrates were shown functionalized via mercaptosilanes, and the resulting thiol groups were reacted with linseed oil under UV radiation to yield thin films that exhibited reduced surface friction under high loads [74]. The reactivity of canola and corn oils as enes toward butanethiol under UV irradiation was investigated. The results revealed that it was possible to obtain up to 97% of double bond conversion [75]. Castor oil was utilized in a thiol-ene UV curable coating formulation [69]. Allyl, acrylate, and vinyl ether derivatives of castor oil were blended with multifunctional thiols to yield films with about 40% seed oil content without VOCs. It was demonstrated that each bio-based monomer exhibited excellent thin film performance, high solvent, resistance and hardness with adhesion and flexibility regardless of functionality. Testing on films immediately upon cure and a week after UV exposure indicated increased cross-linking and improved physical properties upon aging. It was shown that 2-mercaptoethanol could be photochemically grafted onto vinyl groups of rapeseed oil by thiol-ene addition to yield bio-based polyols (Figure 8.19) [76]. Finally, the functionalized rapeseed oil was used to synthesize polyurethanes with HDI and MDI. The thermal properties of elastomeric products were found to be similar to those from a commercial polyol. This study confirmed that thiol-ene photoreaction could be performed under mild conditions, requiring neither solvent nor photoinitiator, and the crude product could be purified by an easy procedure. This one-step route to produce fatty polyols represents a significant advance compared to the traditional

epoxidation approach (that occurs in two steps) and further evidence of the synthetic usefulness of thiol addition in materials chemistry.

Figure 8.19 2-Mercaptoethanol photoaddition onto fatty compounds bearing one double bond per chain [76].

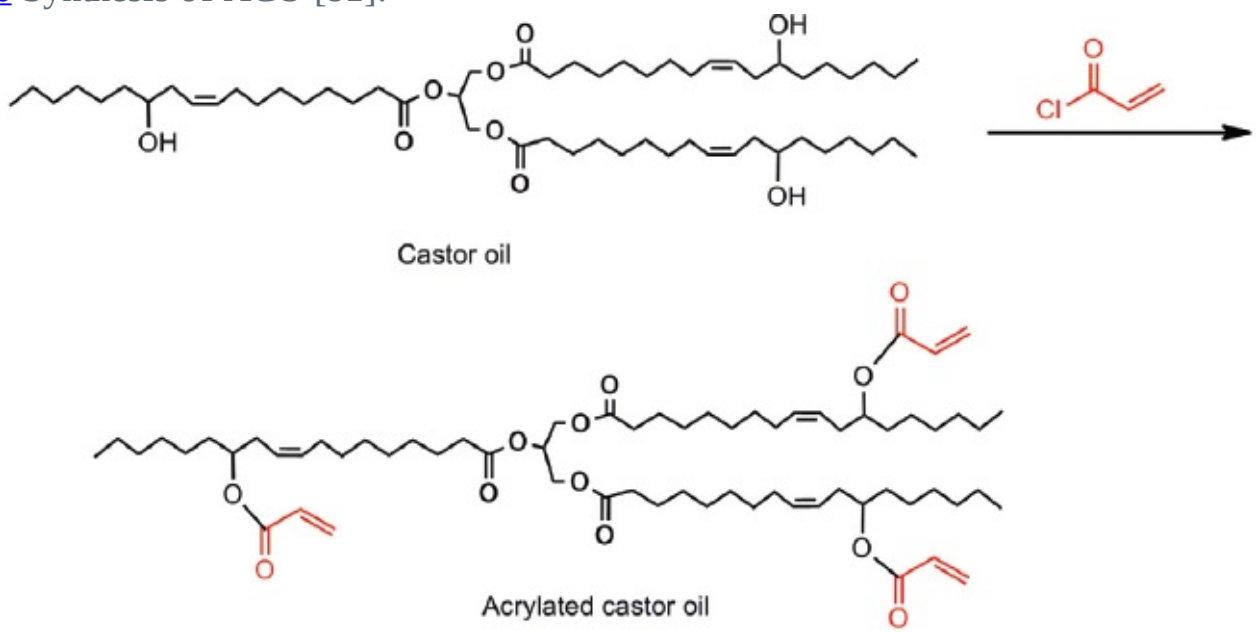


In contrast to the above work which used commercial thiol compounds to cure functionalized triglycerides, Webster and co-workers synthesized novel soya-based thiols and enes via BF_3-catalyzed ring opening reaction of ESO by appropriate thiols and alcohols, respectively [77]. The soya-based thiols and enes were formulated with petrochemical based enes and thiols, respectively, to make thiol-ene UV-curable coatings. It has been shown that soya-based thiols and enes with higher functionality can be UV-cured in combination with petrochemical-based enes or thiols even without the presence of free-radical photoinitiators. It was also shown that better coating material properties could be obtained by the addition of multifunctional, hyperbranched acrylates which could improve the T_g and tack-free of the coating formulation. Biobased thiols were also synthesized via the thermal thiol-ene reactions between sucrose soya and multifunctional thiols [78]. Thermoset thiourethane coatings were prepared from these thiol oligomers and polyisocyanate trimer resins. Generally, all the coatings showed good adhesion to aluminum panels, and had high gloss. Coatings based on more rigid isophorone diisocyanate (IPDI)-based polyisocyanate showed higher T_g, hardness and direct impact resistance compared with the HDI based polyisocyanate counterparts. ESS-based, thiol-functionalized oligomers were prepared from ESS and bio-[mercaptanized soybean oil (MSO) and di-pentene dimercaptan (DD)] or petro-based multifunctional thiols via a thermally initiated thiol-ene reactions. Thermoset thiourethane coatings were then formulated from these thiol oligomers and HDI trimer and IPDI trimmers. MSO-based coatings showed higher thermal stability than DD-based ones, which indicate that the higher functionality and more branched structure had a great impact on the thermal stability of these coatings [78].

Modified seed oils with thiol siloxane colloid showed higher reactivity than conventional seed oils in thiol-ene UV cure. Norbornylized linseed oil (NLO) could be photopolymerized and used in UV-curable coatings and inks. However, the NLO suffers from a sluggish reaction rate without reactive diluent. Soucek and coworkers developed a novel functional oligomer thiol siloxane colloid that could enhance the polymerization rate of seed oil derivatives [79, 80]. Multifunctional thiol siloxane oligomer was prepared by the sol-gel method from mercaptopropyltrimethoxysilane (MPTS). The formation of MPTS/NLO hybrid film involves the simultaneous polymerization either by thiyl radical with norbornylized linseed oil or directly by reaction between the reactive -SH groups in thiol siloxane oligomer with cyclic-olefin bonds in norbornylized linseed oil. There is a large fraction of -

SH reactive groups in the MPTS oligomer that could increase the rate of UV-curing polymerization and the cross-link density. These -SH reactive groups are distributed throughout the inorganic particles and could bond inorganic particles to the organic phase. Therefore, it is anticipated that the MPTS colloids will function as a hyperbranched cross-linker. With thiol siloxane MPTS colloid loading, high photocuring rate, high cure content and high cross-link density were achieved compared with the pure NLO systems. MPTS thiol siloxane oligomer could be used in an extensive range of UV-curable, organic-inorganic hybrid systems [79, 80]. It was demonstrated that hybrid materials based on thiol-contained polyhedral oligomeric silsesquioxane (POSS-OA/SH) and acrylated caster oil (ACO) (Figure 8.20) could be photocured through “thiol-ene” reaction. Compared with the pure ACO, the hybrid component of POSS-OA/SH and ACO exhibited much faster photocured speed upon the exposure of UV light. The obtained hybrid materials were transparent to visible light and no obvious phase separation was observed. AFM and SEM demonstrated that POSS nanoparticles were well-dispersed in the ACO matrix without obvious aggregation even if the content of POSS is higher than 60%. The introduction of POSS can decrease the surface energy of the obtained hybrid materials. The thermal stability of the obtained hybrid materials increased with the increase of POSS content. These characteristics gave the obtained hybrid material potential application in coatings [81].

Figure 8.20 Synthesis of ACO [81].



8.2.6 Seed Oil-Based Organic–Inorganic Coatings

Organic–inorganic hybrid coatings have become a hot research topic during the past 20 years. In general, the organic matrix is the continuous phase in creamer materials and the inorganic matrix is the discontinuous phase. Organic materials exhibit great processing and mechanical properties, while inorganic materials have excellent thermal stability, solvent resistance and adhesion to metal substrates. The resulting hybrid materials provide a combination of physical properties found in both ceramic and polymeric materials by producing a homogenous material with both organic and inorganic characteristics at low cure temperatures. Organic-inorganic coatings provide advantages such as improved abrasion resistance, chemical resistance, adhesion, and mechanical properties [82–87].

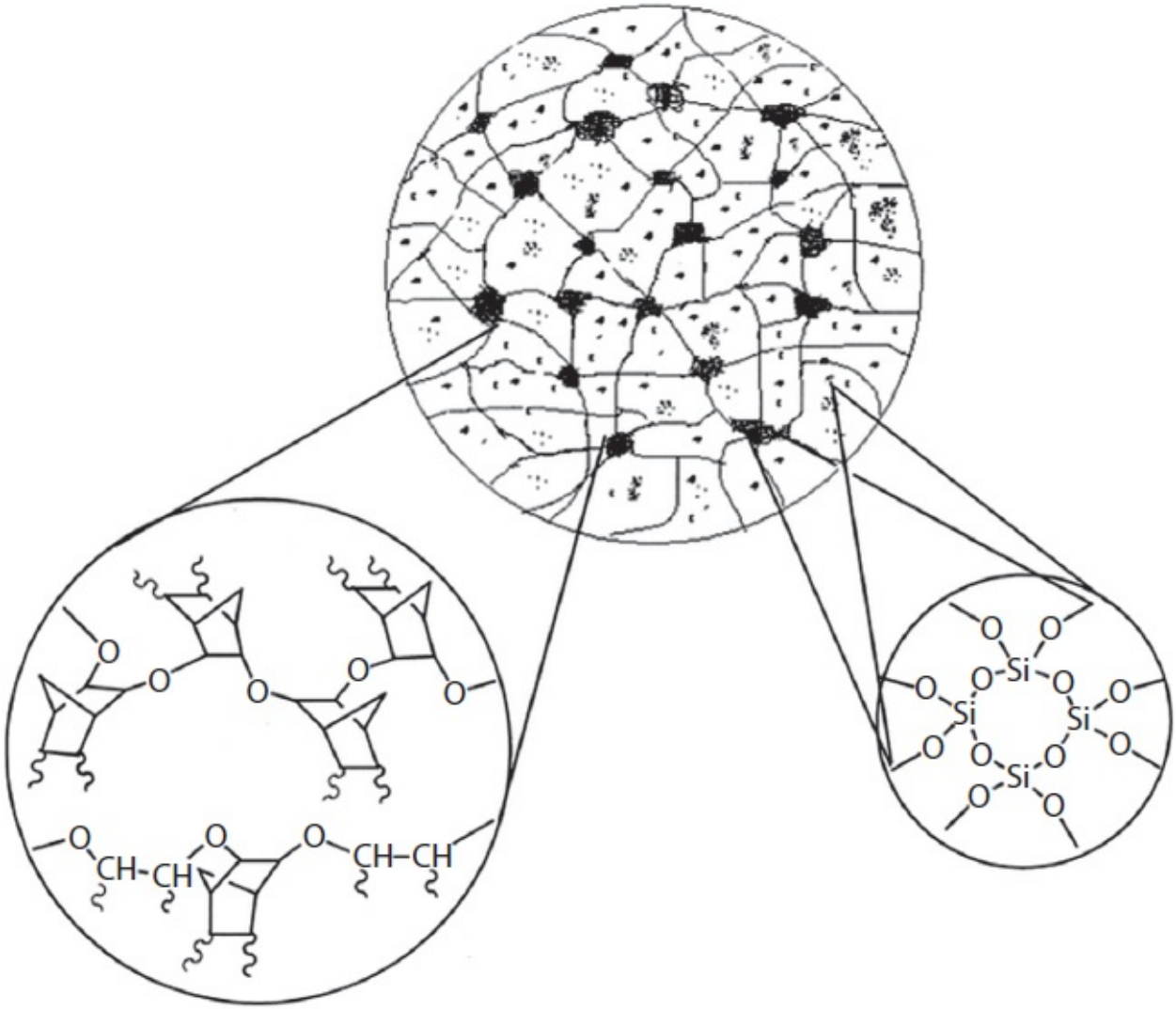
The sol-gel technique of alkoxysilanes is one of the useful methods to prepare organic-inorganic

hybrid materials. A wide variety of organic-inorganic systems contain either tetramethyl orthosilicate (TMOS) or tetraethyl orthosilicate (TEOS) as the inorganic precursors. The hybrid materials are formed by co-condensation of functionalized oligomers with sol-gel precursors in which a covalent bond is established between the two phases. The advantage of the sol–gel technique is that the reaction proceeds at ambient temperature to form hybrid materials compared to the traditional methods at high temperature. It has been reported that the hybrid coatings display improved hardness, tensile strength, tensile modulus and anticorrosive protective properties.

Organic-inorganic coatings based on seed oils as the organic phase and metal alkoxides as the inorganic phase have been developed in Soucek's lab [83–87]. The primary interest in the development of these coatings was to reintroduce seed oils as a renewable resource for coating applications. A variety of seed oils such as linseed, soybean, safflower, and sunflower oil have been used in organic-inorganic formulations. The metal alkoxides used in these formulations include $Ti(Oi\text{-}Pr)_4$, $Ti(Oi\text{-}Pr)_2(ACAC)_2$, $Zr(On\text{-}Pr)_4$, and $Zn(Ac)_2 \cdot 2H_2O$. The incorporation of metal alkoxides in seed oil coatings significantly increased the mechanical and physical properties relative to the parent seed oil coatings.

Soucek and coworkers studied the properties of UV-curable organic–inorganic hybrid films derived from epoxynorbornane linseed oil [85, 86]. Different levels of epoxynorbornane linseed oil and tetraethylorthosilane (TEOS) were used in the study. The organic-inorganic hybrid films are formed either from the inorganic phase formation within the organic film or a simultaneous polymerization of both organic and inorganic reactive groups (Figure 8.21). It was also observed that the incorporation of TEOS oligomers improved the performance of films and enhanced tensile strength, fracture toughness, thermal stability and general coating properties of epoxynorbornane linseed oil. Organic-inorganic hybrid films based on epoxidized cyclohexene derivatized linseed oil (ECLO) and tetraethylorthosilicate (TEOS) oligomers were prepared via a UV-curing process [83]. The kinetics of the hybrid materials were studied by photodifferential scanning calorimetry (DSC). The hybrid films exhibited higher hardness, tensile strength, and tensile modulus, fracture toughness, cross-link density, thermal stability, and abrasion resistance compared to the ECLO organic film. However, they exhibited lower reverse impact compared to the ECLO organic film. The improvement in physical properties was attributed to the distribution and connectivity of the silicon oxide phase prepared in situ within the organic phase. An optimum balance of tensile properties, fracture toughness, hardness, adhesion, abrasion resistance and reverse impact was achieved at 15 wt.% TEOS oligomer. It was postulated that the TEOS oligomers were reactive diluents. The photo-DSC data suggested that the TEOS oligomer increased the curing rate of the organic phase and functioned as a reactive diluent.

Figure 8.21 A theoretical structural model depicting the interaction between the inorganic and organic phases [86].



The metal carboxylates have the capacity of forming covalent bonds between the organic and inorganic phases to form a homogenous network. The proposed interaction between the organic and inorganic phases occurs in situ cross-linking between the seed oils and the unsaturated metal carboxylates.

8.2.7 Seed Oil-Based Alkyd Coatings

8.2.7.1 Introduction of Alkyds

Seed oils were one of the important ingredients in coatings prior to the 1920s. A revolution in the coating industry kicked off when Kienle discovered a new class of alkyds in 1927 [88]. It was reported that the alkyd resin prepared from phthalic anhydride, glycerol, and an unsaturated fatty acid showed more flexibility and toughness than the resin derived from polyhydric alcohol and polybasic acid alone. This discovery made the alkyd resin be extensively applied in several applications, such as coatings, plasticizer, adhesives, printing inks, and molding. Full-scale commercial production of alkyd resins began in 1933 at General Electric [89]. Alkyds grew to dominate the coatings industry by the 1940s. However, the further development of alkyd coatings has largely stalled during the last 50 years because of a focus on synthetic technology: acrylic resins, polyurethanes, epoxy systems, and latex coatings. These petrochemical derivatives are economical and readily available, and they have provided many new curing technologies that have led to extraordinary coating properties [89, 90]. The last decade witnessed a resurgence of alkyds due to the tight environmental regulations for low

VOC coatings, as well as the requirement for coatings from a renewable, reusable, and low cost source. Thus, alkyd resins continue to be produced in large quantities today. Alkyd has several merits, which might account for its recent resurgence.

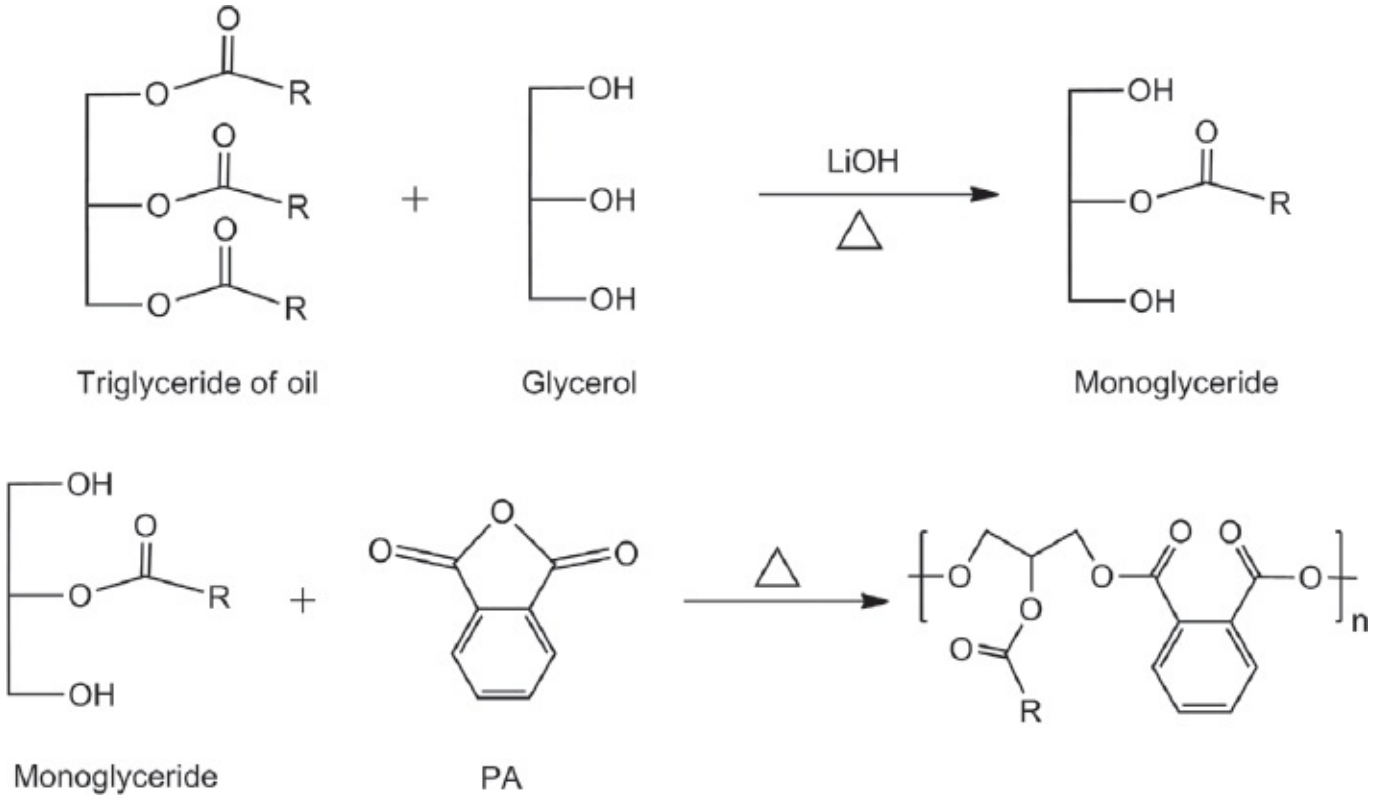
Alkyds have the advantage of renewability. A large portion of starting materials for alkyds synthesis, such as seed oil (or a specific fatty acid) and glycerol, is based on readily available and renewable natural sources. This makes alkyds very interesting coating components from an ecological point of view [90–93]. Glycerol is usually used as the polyol for alkyd synthesis. As a by-product of biodiesel production, glycerol is an important starting material when considering the sustainability of soy materials derived chemicals. The production of fatty acids and esters (biodiesel) from triglycerides gives about 10 wt.% of glycerol and is becoming increasingly abundant [94, 95]. Therefore, glycerol is currently discussed as a platform chemical of a future bio-based chemical industry.

Alkyds are low cost. The seed oils, glycerol, and PA for alkyd synthesis are cost-effective materials. The increased price on fossil oil has affected the raw material prices for fossil based resins more compared to renewable resources such as seed oils. The prices of seed oils and glycerol are relative stable compared to those of the fossil oil.

Alkyds are very versatile polymers due to their compatibility with many polymers such as nitrocellulose, phenolic resins, epoxy resins, amino resins, silicone resins, chlorinated rubber, cyclized rubber, hydrocarbon resins, and acrylic resins. This versatility, along with the extremely wide formulating latitude, made alkyds suitable for the production of a very broad range of coating materials.

There are two primary methods for alkyd synthesis: monoglyceride process and fatty acid process. In the monoglyceride process (Figure 8.22), seed oil is used and reacted with polyol to generate a monoglyceride product via a transesterification reaction. Then a polybasic acid is added to the monoglyceride to form an alkyd resin via an esterification reaction. In the fatty acid process, fatty acid, polyol and acid are reacted all in one step. The monoglyceride has the advantage of low cost, while the fatty acid process has the advantage of more process control [25].

Figure 8.22 Monoglyceride process for alkyd synthesis.



Alkyd resins are classified according to their oil length referring to the oil weight percentage of an alkyd. When the oil length is above 60%, the resin is a long oil alkyd. When the oil length is below 40%, the resin is called a short oil alkyd. When oil amounts ranges between 40% and 60%, it is called medium oil alkyd. Oil length plays an important role in affecting the properties of the final product. Long oil alkyds are typically used in brushing enamels, while short oil alkyds are most used for baked finishes on automobiles, refrigerators, stoves, and washing machines [25].

8.2.7.2 Modified Alkyds for Coatings

In spite of the advantages, alkyds have the disadvantages such as lack of hardness, low hydrolytic stability, poor alkali resistance, and poor exterior weatherability which limited the wide application of alkyd [96]. Thus modifications of alkyds are desired. Some of the main issues for current systems based on alkyd technology range from hybrid alkyd/acrylate systems, alkyd emulsions, modified oils, to UV-curable oil based coatings.

8.2.7.2.1 Acrylate-Modified Alkyds

Over the last half century, varieties of modifications have been developed for alkyd resins. The first modification was done with styrene [25, 97]. Styrene modified alkyds have the advantages of lower cost, faster drying, and reduced viscosity systems. However, the end-use applications for styrene modified alkyds are virtually limited to primers. Moreover, styrene has been recognized as a carcinogen [33]. As stricter environmental regulations on coating formulations continue to be enforced, new modification methods for alkyds with low VOC and with precise control over molecular structures are desirable.

When waterborne acrylic coatings are gaining popularity, the research of an acrylic-alkyd hybrid through mini-emulsion polymerization was reported. Several research groups have investigated the development of acrylic-alkyd hybrid systems using a mini-emulsion process. It has been shown that the hydrolytic stability of the acrylic-alkyd emulsion system can be obtained and adjusted by careful

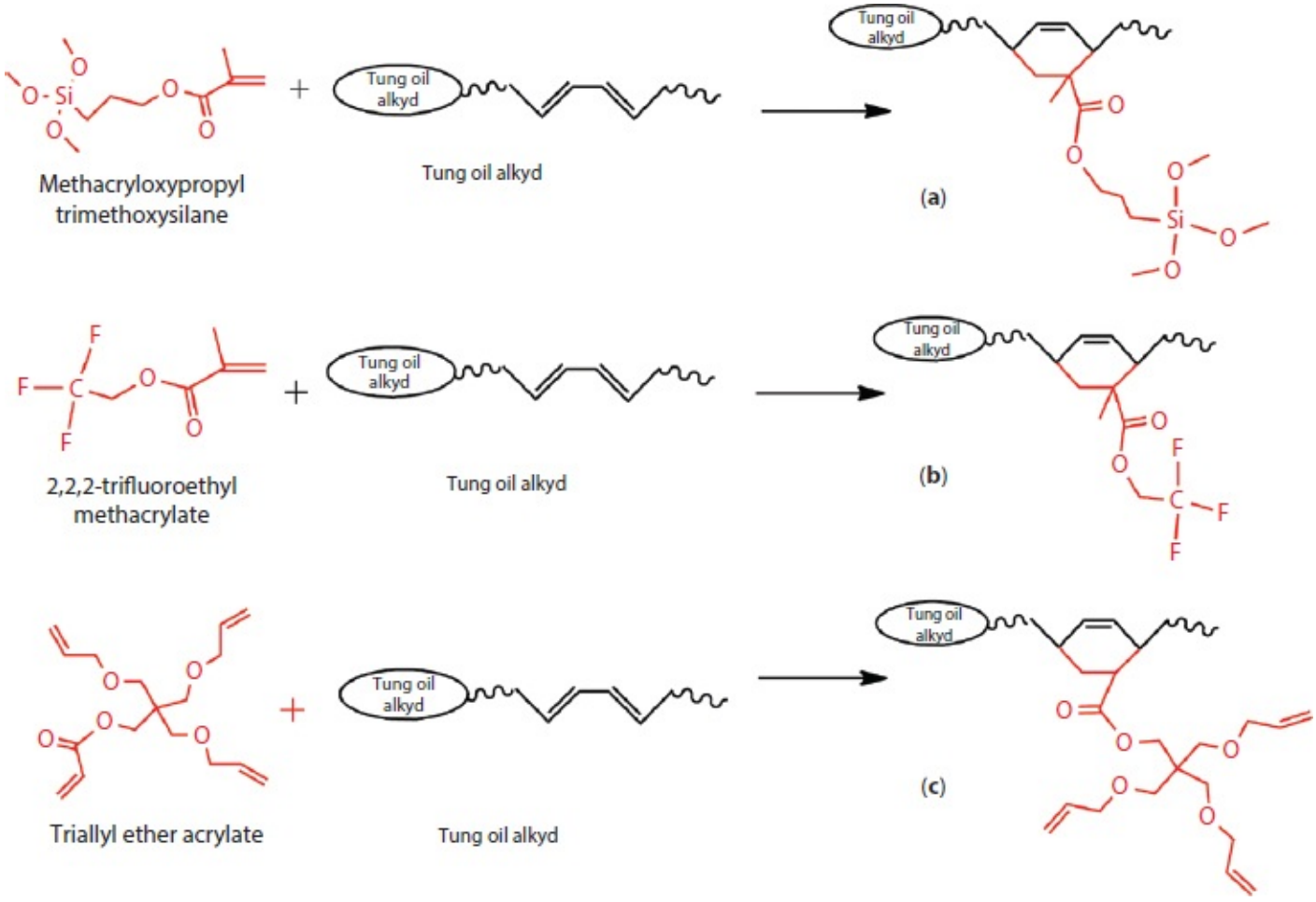
selection of monomers used in the acrylic portion of the formula [98]. Soucek and coworkers have investigated the acrylic-alkyd system prepared by free-radical polymerization. A water-reducible acrylic-alkyd hybrid resin was made from alkyd resins with varying oil lengths. Long, medium, and short oil alkyds were prepared using seed oil, glycerol, PA, and tetrahydrophthalic anhydride (THPA) as the alkyd phase. Acrylic co-monomer formulas containing methyl methacrylate, butyl acrylate, methacrylic acid, and vinyl trimethoxysilane were polymerized in the presence of the different alkyds. Acrylic monomers were introduced to alkyd resins with different levels of unsaturation in the backbone, different ratios of acrylic to alkyd, and different oil lengths of the alkyd resins under monomer starved reaction conditions [98]. It was found that the oil length of the alkyd and acrylic to alkyd ratio are two of the most important factors for final coating properties of the resins. The researchers concluded that the hydrolytic stability of the resulting acrylic-alkyd was dependent on the acrylic to alkyd ratio.

Controlled free-radical polymerization (CFRP) processes have been used for alkyd synthesis. Reversible-addition fragmentation chain transfer (RAFT) polymerization is one of the most important CFRP. RAFT polymerization has the advantages of diversity in monomer choices, versatility in fabricating complex materials with controlled molecular weights, controlled block locations, and narrow molecular weight distributions [99]. It has been shown that the RAFT-mediated reaction imparted a more controlled free-radical process for the synthesis of acrylic-alkyd materials. Use of the alkyd macro-RAFT agent provided a novel pathway to acrylic-alkyds that imparted a more controlled way to tailor specific material properties [100]. For commercial acrylic-alkyd resins that are achieved by free-radical chemistry process, side reactions are expected including radical-radical termination, reaction at pendant fatty acids, and homo-polymerization. By employing a RAFT-mediated mechanism, better control of acrylic location is expected; all the side reactions are expected to be limited with the RAFT process. The demonstration of constructing acrylic-alkyd materials using RAFT polymerization techniques has established a novel pathway to achieve acrylic-alkyd resins with precise control for use in coatings [100].

Besides the above mentioned acrylic-alkyd hybrids, acrylates have been used to modify tung oil alkyds via Diels–Alder reactions. Unlike most seed oils, tung oil is conjugated. Conjugated double bonds such as α-eleostearate of the tung oil triglyceride, which are dienes, can be reacted with dienophiles. Acrylates are good dienophiles [37, 39].

The α-eleosterate pendent fatty acid of a tung oil based alkyd was functionalized via a Diels–Alder reaction with three different acrylate monomers including alkylsiloxane, triallyl ether, and fluorinated alkyl, via a Diels–Alder reaction. The monomers were selected to have different effects on the film properties of the alkyd. The alkoxysilane group was selected for its reaction with water, thus, a dual-cure system of autoxidative and moisture cure was possible. A fluorine–acrylate was selected for improved chemical stability and low surface energy. A triallyl ether group was selected to assist the autoxidative cure rate by increasing the functionality of the alkyd. The viscoelastic and drying time results show that the alkyd modified with siloxane and triallyl group affords a faster drying time, higher cross-link density and higher glass transition temperature compared to the unmodified alkyd, whereas the fluorinated alkyd possesses surface active properties, but suffers in terms of drying and crosslinking density [39].

Figure 8.23 Synthesis of tung oil-based alkyds. (a) reaction of siloxane functionalized tung oil-based alkyd; (b) reaction of fluorine functionalized tung oil-based alkyd; (c) reaction of triallyl ether functionalized tung oil-based alkyd.



8.2.7.2.2 Alkyd from Recycled PET

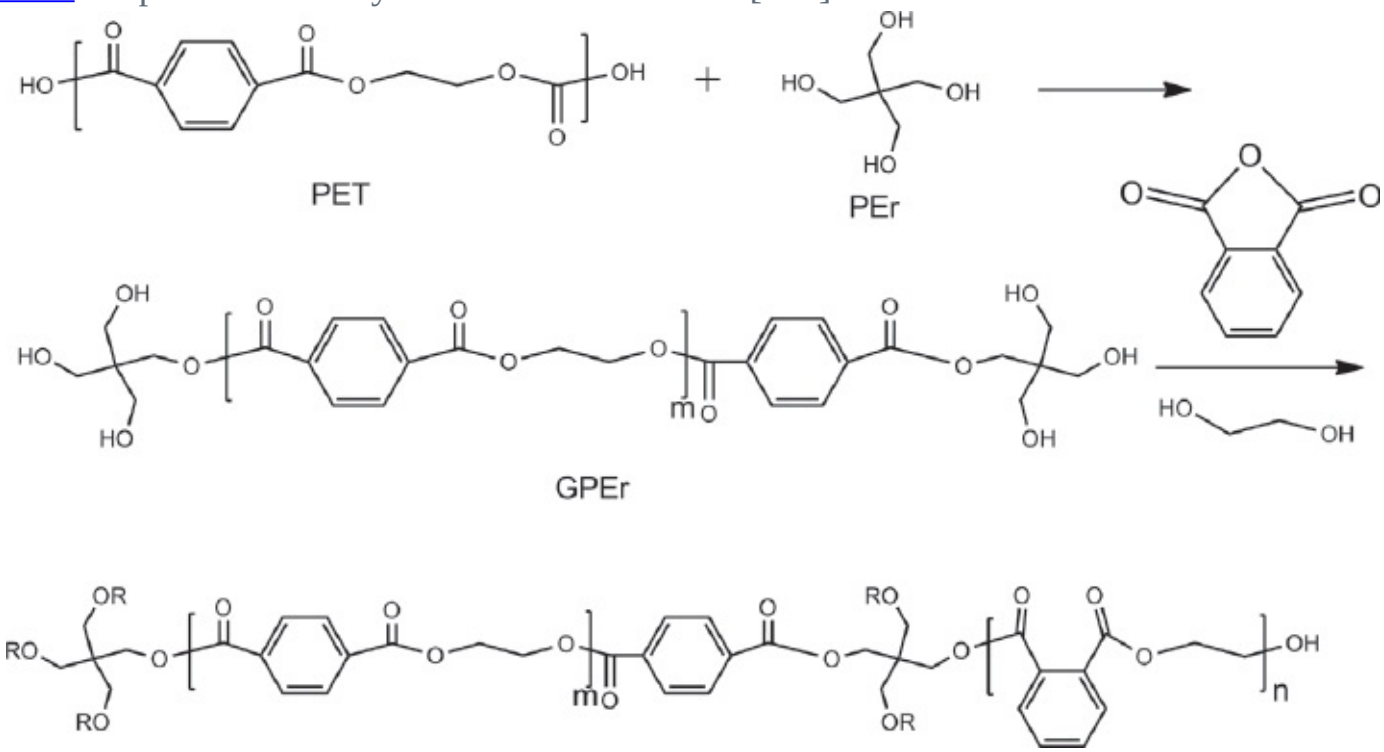
Poly(ethylene terephthalate) (PET) is the most recycled plastic due to its widespread use particularly in the beverage industry. PET wastes cannot decompose in the nature easily and they can cause significant visual pollution to the environment [101, 102]. The post-consumer PET recycling represents one of the most successful and widespread examples of polymer recycling. The main motivation for the recycling of post-consumer PET is its widespread use, particularly in the beverage industry. The recycling of PET not only serves as a partial solution to the solid waste problem but also contributes to the conservation of raw petrochemical products and energy. Chemical recycling processes can result in total depolymerization to the monomers or partial depolymerization to the oligomers.

The last decade has witnessed an increasing interest in the hydrolysis of waste PET for chemical recycling, and the use of hydrolysis products of waste PET in alkyd resin synthesis have been investigated [103]. PET was used due to their high ratio of OH group that could function as polyols in the preparation of alkyd resins, so as to reduce the cost and to modify their adhesion properties as modified organic coats to protect carbon steel from different corrosive environments [104]. The results showed that hydrolysis products of waste PET improved the physical and chemical film properties of alkyd resins. Drying time, hardness, alkaline resistance, and thermal oxidative degradation resistance of the PET-based alkyd resins are better than these properties of reference resin. It was concluded that the hydrolysis products are suitable for manufacturing of alkyd resins [103].

Long oil alkyd resins were prepared from depolymerization products of the waste PET, glycerin, sunflower oil fatty acids and glycol (Figure 8.24). The alkyd resins based on sunflower oil and GPEr possess good mechanical properties due to the higher ratios of cross-link density. The cured alkyd

resins based on GPEr have excellent chemical resistances as organic coatings among other cured resins. The high alkaline and acidic resistance can be attributed to high cross-link density of networks. PET-based alkyds have been shown to offer corrosion resistance to protect carbon steels [104].

Figure 8.24 Preparation of alkyd resins based on PET [104].

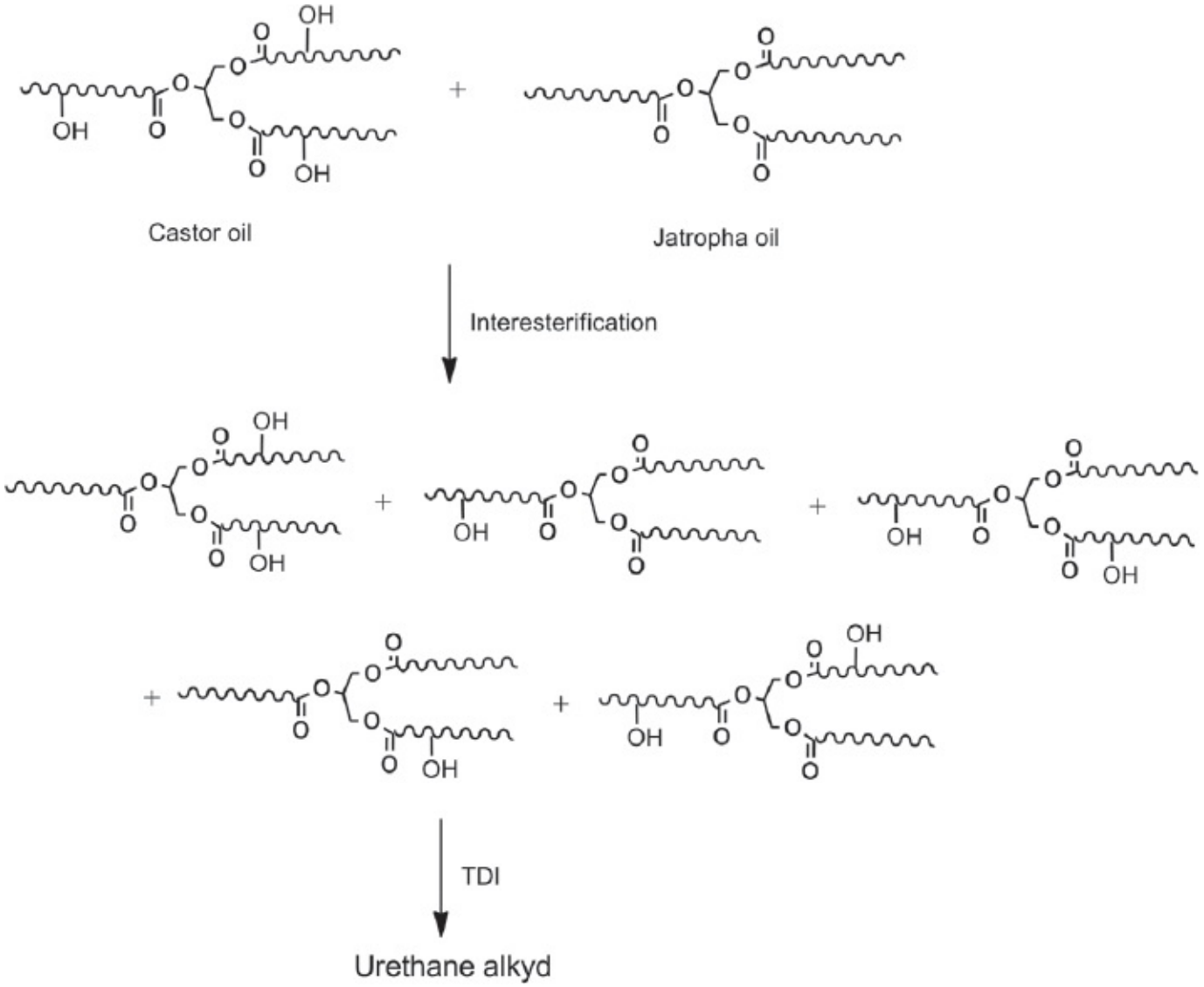


8.2.7.2.3 Urethane-Modified Alkyd

Urethane modified alkyds (uralkyds) are oil-modified polyurethane coatings that are typically produced by the reaction between a diisocyanate with a mixture of mono- and diglycerides obtained from the alcoholysis between oils and polyol [99]. The properties of urethane alkyds depend on the type and amount of oil, polyol, and isocyanate used in their preparation. Urethane alkyd is generally prepared by a two-step procedure. In the first step, triglyceride oil is reacted with a polyol until the reaction mixture is completely soluble in alcohol. In the second step, a diisocyanate is added to the reaction mixture and the remaining hydroxyl groups react with isocyanate groups to form the urethane linkages. Glycerol as a polyol, along with seed oils, is the most widely used components in urethane alkyd preparation [97].

Urethane alkyd has been obtained from the interesterification of castor oil with jatropha oil followed by subsequent reaction with TDI (Figure 8.25). Castor oil has been used to replace the glycerol and pentaerythritol as polyols. Jatropha oil is extracted from the seeds of the physic nut or jatropha, a non-edible crop that is widely cultivated in Thailand for biodiesel production. The seed-oil consists of 78.4% unsaturated fatty acids, mainly oleic acid (42.4%) and linoleic acid (35.2%) [105]. Jatropha oil is classified as a semi-drying oil that could be a potential raw material for the coating industry. Alkyd resins prepared from jatropha oil have been found to be closely comparable with the commercial standards in their performances [99, 106].

Figure 8.25 Scheme for synthesis of urethane alkyd from interesterified castor oil/jatropha oil [99].



Urethane alkyd prepared from a castor oil/jatropha oil mixture exhibited properties that are broadly comparable with the conventional and commercial products. They share similar film properties such as excellent flexibility, adhesion and high impact resistance. In addition, they also exhibited excellent resistance to water and acids [99]. However, the alkali resistance of the castor oil/jatropha oil-based urethane alkyd film was the lowest whereas the commercial one the highest. The lower alkali resistance of the castor oil/jatropha oil-based urethane alkyd film is due to the high amount of oil in this prepared resin, which leads to the poorest alkali resistance because of the high content of ester groups that are hydrolyzed under alkaline conditions. The use of castor oil with jatropha oil as alternative raw materials for urethane alkyd preparation is possible for applications where alkali resistance or extreme hardness is not required.

8.2.7.2.4 Siloxane-Alkyd Hybrid

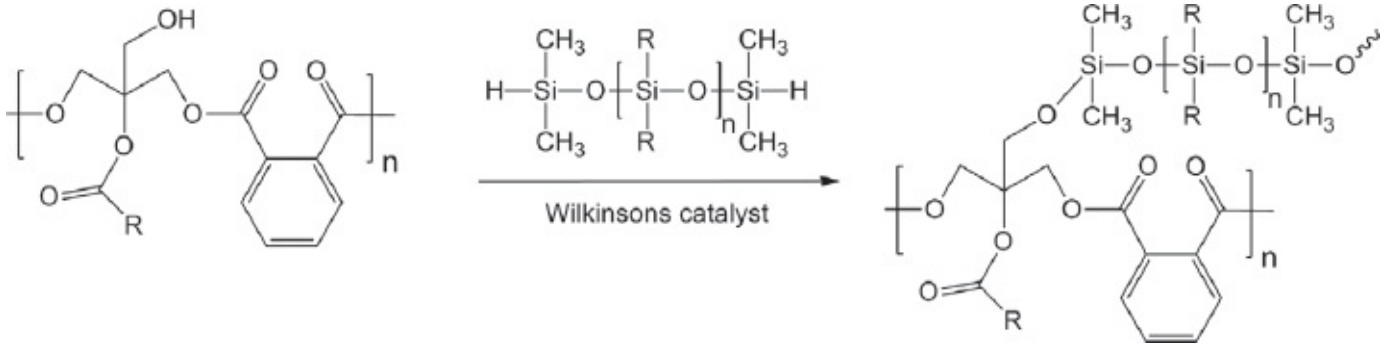
Siloxanes have advantages of excellent resistance to heat, oxidation and chemical inertness. Siloxanes also have excellent moisture and UV-degradation resistance. The siloxane modified alkyd may benefit from the synergistic properties of the two components, which impart the resultant copolymer to have higher temperature resistance and better exterior durability [107]. The properties of copolymer could be substantially improved compared with the alkyd resins. Moreover, the mechanical properties of the siliconized alkyds could be enhanced in terms of the glass transition temperature, imparting the hybrid with superior performances to siloxanes [108–110].

Soucek and coworkers first reported in literature the preparation of a siliconized alkyd via a

dehydrocoupling reaction [111]. The dehydrocoupling reaction has the advantages in that it gives more control of the grafting reaction and limits side reactions compared with random siloxane condensation reactions. They posed the presumption that the siloxane condensation and grafting approach could result in more self-condensation of the siloxane than actual grafting, and that there should be enough grafting to compatibilize the alkyd with the ungrafted siloxane polymer resulting in a system with reasonable miscibility. Another advantage of reacting organically modified silicones with alkyds is that the linkage will be Si–C–C rather than Si–O–C. Si–C–C linkage has much higher resistance than Si–O–C bond [111].

The properties of siliconized-alkyd hybrids are a function of oil length and polyester backbone. Thus, the effect of oil length of alkyds and substitution of siloxane backbone has been studied for alkyd-siloxane hybrids. Nine different siloxane-alkyd hybrids were prepared using a dehydrocoupling reaction from linseed oil based alkyds of three different oil lengths and three siloxanes with different backbone substitutions. Three linseed oil-based alkyds with either a long, medium, or short oil length were grafted with three hydride-terminated siloxanes substituted with methyl, cyclopentyl, or cyclohexyl groups. A hydrocoupling reaction was used to couple the telechelic siloxane with the hydroxyl functionality of the alkyds [111].

Figure 8.26 Reaction pathway for dehydrocoupling reaction [111].



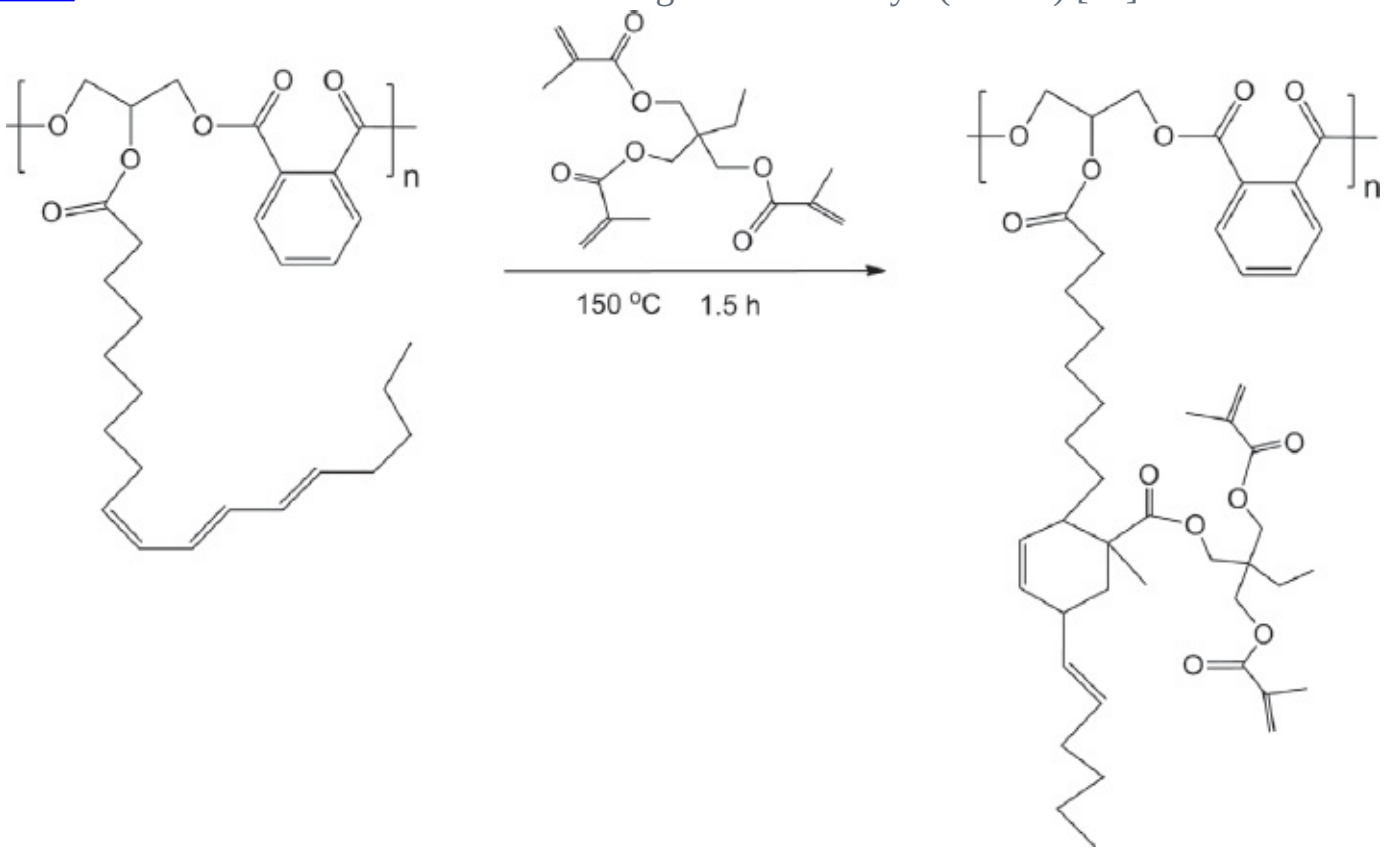
The mechanical properties of the resulting coatings were found to be complex functions of oil length and siloxane backbone substitutions. Cross-link density, flexibility, and reverse impact resistance were found to be directly proportional to oil length. Tensile modulus, elongation-at-break, glass transition temperature, through dry time, and fracture toughness were inversely proportional to oil length. The larger-sized cyclopentyl and cyclohexyl groups resulted in better mechanical and rheological properties than the methyl-containing siloxanes. The cycloaliphatic substituents on the siloxane backbone enhanced all the mechanical and coating properties of the hybrids while decreasing the cross-link density. The drying time and the overall coating properties were similar to commercially prepared siliconized alkyds. The hardness of the siloxanes is close to phenyl-substituted siloxanes without the drawback of the poor photo-oxidative stability. In the hybrid resin systems involving siloxane polymers, intermediate properties within the extremities of polydimethylsiloxane and polydiphenylsiloxanes can be obtained by using these cycloaliphatic-substituted siloxanes [111].

8.2.7.2.5 UV-Curable Alkyd

In coating applications, VOCs are a major environmental and toxic issue worldwide. Free-radical-based UV curing, especially acrylate or methacrylate monomers, has advantages of fast cure along with industrial acceptance. Soucek and coworkers developed UV-curable tung oil alkyds (UVTA) by free-radical photopolymerization [37]. A synthetic scheme for UVTA is shown in Figure 8.27. UVTA

was prepared by reacting trimethylolpropane trimethacrylate (TMPTMA) onto the α-eleosterate of a tung oil alkyd molecule via a Diels-Alder reaction. The reactions were conducted at elevated temperature and atmospheric pressure. The UVTA was formulated with a free-radical reactive diluent, tripropylene glycol diacrylate (TPGDA), and photoinitiator. It is hoped that the concept of UV-curable alkyd will have great potential for widespread use in the field of coatings.

Figure 8.27 Chemical structures: UV-curable tung oil-based alkyd (UVTA) [37].



Alkyds have the advantage of self-disperse all pigments, thus they are used in both clear and pigmented coatings [41]. However, formulation of pigmented UV-curing alkyd coatings has been a major challenge, due to the reflection and absorption characteristics of pigment particles. Pigments prevent sufficient penetration of UV energy to efficiently activate the photoinitiated cross-linking systems, resulting in the amplification of the cure gradient in the film, which is responsible for the creation of wrinkles on the film surface [41].

The photocuring of a pigmented UVTA was investigated by Soucek and coworkers. A mixture of yellow iron oxide, red iron oxide, titanium dioxide and lamp black pigments were applied to obtain an observed yellow color. The pigment mixture, UV-curable alkyd and a reactive diluent were formulated together and photocured via a free-radical mechanism [41].

The coating tests showed that the use of long chain linear structure diluents, such as isodecyl methacrylate, provided UV-curable paint films with better impact resistance, flexibility, and adhesion over other reactive diluents. Though cure limited the maximum pigment level in formulations to 14 wt%, high quality pigment dispersions were obtained. A mono-functional monomer, isodecyl methacrylate (IDMA), was found to impart excellent flexibility, impact resistance and adhesion to the metal substrate [41].

8.3 Conclusion

Coatings from petrochemicals typically contain significant amounts of VOC which pose threat to the environmental health. Environmentally-friendly coatings are gaining popularity and may have a bright future for development and application as more and more attention is being paid to environmental health. It is highly desired that the coatings developed today have zero or low VOC. Waterborne coatings, via the evaporation of water, can out-perform solventborne coatings and perform better than expectations in various severe environments if designed properly. The application of natural seed oil-based coatings has been revitalized due to their advantages such as being cost-effective, good performances, easy for modification, and more importantly, environmentally-friendly. The seed oils have been successfully used for the development of UV-curable epoxy coating, urethane coating, thiol-ene chemistry, hybrid coating, as well as alkyd coating. The market shares of waterborne and seed oil-based coatings are supposed to increase attributed to the advantages of those coatings.

References

1. H. Jotischky, *Surface Coatings International Part B: Coatings Transactions*, Vol. 84, pp. 11–20, 2001.

2. Volatile Organic Compounds Indoor Air US Environmental Protection Agency. Epa.gov. http://www.epa.gov/iaq/voc.html, 2010-11-17.

3. C. Stuart, History of Paint Science and Technology, http://www.ndsu.edu/fileadmin/croll/HistoryofPaintSGC.pdf, 2009.

4. Coating Resins Market by Type (Acrylic, Alkyd, Vinyl, PU, Epoxy, Amino, UPR, SPR & Others), by Technology (Waterborne, Powder, High Solvents, High Solids, UV Cure), by Application (Architectural, Automotive, Wood, & Others)-Global Forecast to 2019, http://www.marketsandmarkets.com/Market-Reports/coating-resins-market-72316133.html, 2014.

5. P.A. Lovell and M.S. El-Aasser, *Emulsion Polymerization and Emulsion polymers*, Wiley, 1997.

6. B.K. Kim, *Colloid and Polymer Science*, Vol. 274, pp. 599–611, 1996.

7. S. Slomkowski, J.V. Alemán, R.G. Gilbert, M. Hess, K. Horie, R.G. Jones, and R.F. Stepto, *Pure and Applied Chemistry*, Vol. 83, pp. 2229–2259, 2011.

8. D.R. Karsa and W.D. Davies, *Waterborne Coatings and Additives*, Springer, 1995.

9. G. Östberg, B. Bergenstähl, and M. Huldén, *Colloids and Surfaces A: Physicochemical and Engineering Aspects*, Vol. 94, pp. 161–171, 1995.

10. M. Rufo, D. Shah, W. Raymond, F.H. Walker, M. Lohe, A. Klippstein, and M. Cook, 2K Waterborne Epoxy Systems: Technology Overview and New Developments, http://www.airproducts.nl/~/media/Files/PDF/industries/paints-coatings-2k-waterborne-epoxy-systems-technology-overview.pdf, 2005.

11. S.I. Omel'chenko, S.O. Tryhub, and N.M. Laskovenko, *Materials Science*. Vol. 37, pp. 790–801, 2001.

12. S. Bas and M.D. Soucek, *Reactive and Functional Polymers*, Vol. 73, pp. 291–302, 2013.

13. M.D. Soucek and E. Pedraza, *Journal of Coatings Technology and Research*, Vol. 6, pp. 27–36, 2009.

14. G. Teng and M.D. Soucek, *Journal of Polymer Science Part A: Polymer Chemistry.* Vol. 40, pp. 4256–4265, 2002.

15. E.P. Pedraza and M.D. Soucek, *Polymer.* Vol. 46, pp. 11174–11185, 2005.

16. G. Lu, J. Sun, and Q. Zhou, *Chinese Journal of Chemical Engineering,* Vol. 15, pp. 899–905, 2007.

17. H. Sun, W. Ni, B. Yuan, T. Wang, P. Li, Y. Liu, and L. Wang, *Journal of Applied Polymer Science*, Vol. 130, pp. 2652–2659, 2013.

18. R.M. Shah and N.M. Padave, *Paintindia*, Vol. 59, pp. 69–82, 2009.

19. C. Decker and I. Lorinczova, *JCT Research,* Vol. 1, pp. 247–256, 2004.

20. M. Tielemans, P. Roose, P. De Groote, X. Deruyttere, C. Moulaert, *CoatingsTech.,* Vol. 10, pp. 36, 2013.

21. F. Seniha Güner, Y. Yağcı, and A. Tuncer Erciyes, *Progress in Polymer Science*, Vol. 31, pp. 633–670, 2006.

22. V. Sharma and P.P. Kundu, *Progress in Polymer Science,* Vol. 31, pp. 983–1008, 2006.

23. Y. Xia and R.C. Larock, *Green Chemistry,* Vol. 12, pp. 1893–1909, 2010.

24. L. Montero de Espinosa and M.A. Meier, *European Polymer Journal*, Vol. 47, pp. 837–852, 2011.

25. Z.W. Wicks Jr, F.N. Jones, S.P. Pappas, and D.A. Wicks, *Organic Coatings: Science and Technology,* John Wiley & Sons. 2007.

26. S.B. David, K. Sathiyalekshmi, and G.A.G. Raj, *Journal of Materials Science: Materials in Medicine,* Vol. 20, pp. 61–70, 2009.

27. S.N. Khot, J.J. Lascala, E. Can, S.S. Morye, G.I. Williams, G.R. Palmese, and R.P. Wool, *Journal of Applied Polymer Science*, Vol. 82, pp. 703–723, 2001.

28. M. Desroches, M. Escouvois, R. Auvergne, S. Caillol, and B. Boutevin, *Polymer Reviews,* Vol. 52, pp. 38–79, 2012.

29. X. Ren and K. Li, *Journal of Applied Polymer Science*, Vol. 128, pp. 1101–1109, 2013.

30. F. Li, M.V. Hanson, and R.C. Larock, *Polymer.* Vol. 42, pp. 1567–1579, 2001.

31. F. Li, A. Perrenoud, and R.C. Larock, *Polymer.* Vol. 42, pp. 10133–10145, 2001.

32. F. Li and R.C. Larock, *Journal of Polymer Science Part B: Polymer Physics*, Vol. 39(1), pp. 60–77, 2001.

33. Styrene, 12th Report on Carcinogens, National Institute of Environmental Health Science, http://www8.nationalacademies.org/onpinews/newsitem.aspx?RecordID=18725, 2011.

34. P.H. Henna, M.R. Kessler, and R.C. Larock, *Macromolecular Materials and Engineering*, Vol. 293, pp. 979–990, 2008.

35. J. Chen, M.D. Soucek, W.J. Simonsick, and R.W. Celikay, *Polymer,* Vol. 43, pp. 5379–5389, 2002.

36. Z. Zong, M.D. Soucek, Y. Liu, and J. Hu, *Journal of Polymer Science Part A: Polymer Chemistry,* Vol. 41, pp. 3440–3456, 2003.

37. N. Thanamongkollit, K.R. Miller, and M.D. Soucek, *Progress in Organic Coatings,* Vol. 73, pp. 425–434, 2012.

38. K. Wutticharoenwong, J. Dziczkowski, and M.D. Soucek, *Progress in Organic Coatings,* Vol. 73, pp. 283–290, 2012.

39. N. Thanamongkollit and M.D. Soucek, *Progress in Organic Coatings*, Vol. 73, pp. 382–391, 2012.

40. K. Wutticharoenwong and M.D. Soucek, *Macromolecular Materials and Engineering*, Vol. 295, pp. 1097–1106, 2010.

41. P. Chittavanich, K. Miller, and M.D. Soucek, *Progress in Organic Coatings*, Vol. 73, pp. 392–400, 2012.

42. J. Lindeboom, *Progress in Organic Coatings*, Vol. 34, pp. 147–151, 1997.

43. K.D. Weiss, *Progress in Polymer Science*, Vol. 22, pp. 203–245, 1997.

44. K.H. Zabel, R.P. Klaasen, W.J. Muizebelt, B.P. Gracey, C. Hallett, and C.D. Brooks, *Progress in Organic Coatings*, Vol. 35, pp. 255–264, 1999.

45. W.J. Muizebelt, J.C. Hubert, M.W.F. Nielen, R.P. Klaasen, and K.H. Zabel, *Progress in Organic Coatings*, Vol. 40, pp. 121–130, 2000.

46. H. Hintze-Brüning, *Industrial Crops and Products*, Vol. 1, pp. 89–99, 1992.

47. P.P. Nalawade, B. Mehta, C. Pugh, and M.D. Soucek, *Journal of Polymer Science Part A: Polymer Chemistry*, Vol. 52, pp. 3045–3059, 2014.

48. F.R. Earle, *Journal of the American Oil Chemists Society*, Vol. 47, pp. 510–513, 1970.

49. C.K. Mambo, P.M. Gitu, B.M. Bhatt, J. Chweya, S. Grinberg, and D. Mills, *Bulletin of the Chemical Society of Ethiopia*, Vol. 12, pp. 121–128, 1998.

50. P. Muturi, D. Wang, and S. Dirlikov, *Progress in organic coatings*, Vol. 25, pp. 85–94, 1994.

51. S.F. Thames, H. Yu, and R. Subramanian, *Journal of Applied Polymer Science*, Vol. 77, pp. 8–13, 2000.

52. S. Chakrapani and J.V. Crivello†, *Journal of Macromolecular Science, Part A: Pure and Applied Chemistry*, Vol. 35, pp. 691–710, 1998.

53. R. Wang and T.P. Schuman, *Express Polymer Letters*, Vol. 7, pp. 272–292, 2013.

54. X. Pan, P. Sengupta, and D.C. Webster, *Biomacromolecules*, Vol. 12, pp. 2416–2428, 2011.

55. X. Pan and D.C. Webster, *Macromolecular Rapid Communications*, Vol. 32, pp. 1324–1330, 2011.

56. T.J. Nelson, T.P. Galhenage, and D.C. Webster, *Journal of Coatings Technology and Research*, Vol. 10, pp. 589–600, 2013.

57. X. Pan, P. Sengupta, and D.C. Webster, *Green Chemistry*, Vol. 13, pp. 965–975, 2011.

58. T.J. Nelson, B. Masaki, Z. Morseth and D.C. Webster, *Journal of Coatings Technology and Research*, Vol. 10, pp. 757–767, 2013.

59. J.V. Crivello and R. Narayan, *Macromolecules*, Vol. 29, pp. 433–438, 1996.

60. K. Zou and M.D. Soucek, *Macromolecular Chemistry and Physics*, Vol. 206, pp. 967–975, 2005.

61. C.K. Lyon, V.H. Garrett, and E.N. Frankel, *Journal of the American Oil Chemists Society*, Vol. 51, pp. 331–334, 1974.

62. M. Van der Steen and C.V. Stevens, *ChemSusChem*, Vol. 2, pp. 692–713, 2009.

63. H. Yeganeh and M.R. Mehdizadeh, *European Polymer Journal*, Vol. 40, pp. 1233–1238, 2004.

64. I. Javni, Z.S. Petrović, A. Guo, and R. Fuller, *Journal of Applied Polymer Science*, Vol. 77, pp. 1723–1734, 2000.

65. Z.S. Petrović, *Polymer Reviews*, Vol. 48, pp. 109–155, 2008.

66. G.L. Wilkes and T.W. Pechar, Structure-Property Studies of Polyurethane Networks that

Incorporate Soy-Based Polyols, in United Soybean Board, Technical Advisory Panel (TAP) Meeting, Detroit, Vol. 40, pp. 12–13, 2005 April.

67. S. Ahmad, S.M. Ashraf, E. Sharmin, F. Zafar, and A. Hasnat, *Progress in Crystal Growth and Characterization of Materials*, Vol. 45, pp. 83–88, 2002.

68. S.S. Narine, X. Kong, L. Bouzidi, and P. Sporns, *Journal of the American Oil Chemists' Society*, Vol. 84, pp. 55–63, 2007.

69. M. Black and J.W. Rawlins, *European Polymer Journal*, Vol. 45, pp. 1433–1441, 2009.

70. S.F. Thames and H. Yu, *Surface and Coatings Technology*, Vol. 115, pp. 208–214, 1999.

71. J.A. Carioscia, J.W. Stansbury, and C.N. Bowman, *Polymer*, Vol. 48, pp. 1526–1532, 2007.

72. J.P. Phillips, N.M. Mackey, B.S. Confait, D.T. Heaps, X. Deng, M.L. Todd, and C.E. Hoyle, *Chemistry of Materials*, Vol. 20, pp. 5240–5245, 2008.

73. R.A. Ortiz, B. A. P. Urbina, R.G. Santos, L.B. Duarte, A.E.G. Valdez, and M.D. Soucek, *Macromolecular Materials and Engineering*, Vol. 293, pp. 731–739, 2008.

74. U. Bexell, M. Olsson, M. Johansson, J. Samuelsson, and P.E. Sundell, Surface and Coatings Technology, Vol. 166, pp. 141–152, 2003.

75. G.B. Bantchev, J.A. Kenar, G. Biresaw, and M.G. Han, *Journal of Agricultural and Food Chemistry*, Vol. 57, pp. 1282–1290, 2009.

76. M. Desroches, S. Caillol, V. Lapinte, R. Auvergne, and B. Boutevin, *Macromolecules*, Vol. 44, pp. 2489–2500, 2011.

77. Z. Chen, B.J. Chisholm, R. Patani, J.F. Wu, S. Fernando, K. Jogodzinski, and D.C. Webster, *Journal of Coatings Technology and Research*, Vol. 7, pp. 603–613, 2010.

78. J. Yan, S. Ariyasivam, D. Weerasinghe, J. He, B. Chisholm, Z. Chen, and D. Webster, Polymer International, Vol. 61, pp. 602–608, 2012.

79. M.J. He, K.M. Wollyung, and C. Wesdemiotis, *Basics and Applications of Photopolymerization Reactions*, Vol. 2, pp. 133, 2010.

80. M.D. Soucek, J. Wu, N. Thanamongkollit, P. Chittavanich, Z. Zong, and J. Chen, *Radtech Report*, pp. 37–42, June 2013.

81. A. Luo, X. Jiang, H. Lin, and J. Yin, *Journal of Materials Chemistry*, Vol. 21, pp. 12753–12760, 2011.

82. R.L. Ballard, J.P. Williams, J.M. Njus, B.R. Kiland, and M.D. Soucek, *European Polymer Journal*, Vol. 37, pp. 381–398, 2001.

83. K. Zou and M.D. Soucek, *Macromolecular Chemistry and Physics*, Vol. 205, pp. 2032–2039, 2004.

84. R.L. Ballard, S.J. Tuman, D.J. Fouquette, W. Stegmiller, and M.D. Soucek, *Chemistry of Materials*, Vol. 11, pp. 726–735, 1999.

85. Z. Zong, J. He, and M.D. Soucek, *Progress in Organic Coatings*, Vol. 53, pp. 83–90, 2005.

86. Z. Zong, M.D. Soucek, and C. Xue, *Journal of Polymer Science Part A: Polymer Chemistry*, Vol. 43, pp. 1607–1623, 2005.

87. G. Teng, J.R. Wegner, G.J. Hurtt, and M.D. Soucek, *Progress in Organic Coatings*, Vol. 42, pp. 29–37, 2001.

88. R.H. Kienle and C.S. Ferguson, *Industrial & Engineering Chemistry*, Vol. 21, pp. 349–352, 1929.

89. A. Hofland, *Progress in Organic Coatings,* Vol. 73, pp. 274–282, 2012.

90. W.M. Kraft, *Journal of the American Oil Chemists' Society,* Vol. 39, pp. 501–502, 1962.

91. R.H. Kienle and C.S. Ferguson, Industrial & Engineering Chemistry Research, Vol. 21, pp. 349–352, 1929.

92. M.D. Soucek and M.K. Johansson, *Progress in Organic Coatings,* Vol. 73, pp. 273, 2012.

93. D.T.C. Ang and S.N. Gan, *Progress in Organic Coatings,* Vol. 73, pp. 409–414, 2012.

94. C.H.C. Zhou, J.N. Beltramini, Y.X. Fan, and G.M. Lu, *Chemical Society Reviews,* Vol. 37, pp. 527–549, 2008.

95. M. McCoy, *Chemical & Engineering News,* Vol. 84, pp. 7–8, 2006.

96. S.M. Cakić, I.S. Ristić, V.M. Jašo, R.Ž. Radičević, O.Z. Ilić, and J.K. Simendić, *Progress in Organic Coatings.* Vol. 73, pp. 415–424, 2012.

97. D. A. Wicks and Jr, Z.W. Wicks, *Progress in Organic Coatings,* Vol. 54, pp. 141–149, 2005.

98. J. Dziczkowski and M.D. Soucek, *Progress in Organic Coatings,* Vol. 73, pp. 330–343, 2012.

99. O. Saravari and S. Praditvatanakit, *Progress in Organic Coatings,* Vol. 76, pp. 698–704, 2013.

100. J. Dziczkowski, U. Chatterjee, and M.D. Soucek, *Progress in Organic Coatings,* Vol. 73, pp. 355–365, 2012.

101. D.E. Nikles, and M.S. Farahat, *Macromolecular Materials and Engineering,* Vol. 290, pp. 13–30, 2005.

102. G.P. Karayannidis, A.K. Nikolaidis, I.D. Sideridou, D.N. Bikiaris, and D.S. Achilias, *Macromolecular Materials and Engineering,* Vol. 291, pp. 1338–1347, 2006.

103. Ö. Tuna, A. Bal, and G. Güçlü, *Polymer Engineering & Science,* Vol. 53, pp. 176–182, 2013.

104. A.M. Atta, A. Rasha, and A.M. El-Saeed, *International Journal of Electrochemical Science,* Vol. 8, pp. 5136–5152, 2013.

105. P. Chatakanonda, K. Sriroth, L. Vaysse, and S. Liangprayoon, Fatty acid composition and properties of Jatropha seed oil and its methyl ester, in Proceedings of 43rd Kasetsart University Annual Conference, Thailand, pp. 641–648, 2005.

106. F. Seniha Güner, Y. Yağcı, and A. Tuncer Erciyes, *Progress in Polymer Science,* Vol. 31, pp. 633–670, 2006.

107. A.A. Karim, B. Golding, and R.A. Morgen, *Journal of Chemical and Engineering Data,* Vol. 5, pp. 117–125, 1960.

108. M.J. Hunter and L.A. Rauner, Condensation of an organo silane with a polyhydric alcohol and thereafter with a polycarboxylic acid and product, US Patent 2584351, assigned to Dow Corning, February 5, 1952.

109. M. Alagar, A. Ashok Kumar, K. P.O. Mahesh, and K. Dinakaran, *European Polymer Journal*, Vol. 36, pp. 2449–2454, 2000.

110. J. Beetsma, *Pigment & resin technology,* Vol. 27, pp. 12–19, 1998.

111. R. Chakraborty, M. Thatte, and M.D. Soucek, *Journal of Coatings Technology and Research,* Vol. 6, pp. 471–481, 2009.

Chapter 9

Low-Temperature Aqueous Coatings for Solar Thermal Absorber Applications

Saleh Khamlich*, Mokhotjwa Dhlamini, Bakang Mothudi, and Malik Maaza

UNESCO-UNISA Africa Chair in Nanosciences–Nanotechnology, College of Graduate Studies, University of South Africa, Pretoria, South Africa

Nanosciences African Network (NANOAFNET), iThemba LABS-National Research Foundation, Western Cape Province, South Africa

Department of Physics, College of Science, Engineering and Technology, University of South Africa, Johannesburg, South Africa

**Corresponding author*: skhamlich@gmail.com

Abstract

There has been interest in monodisperse particles in the micro-nano range, and various applications are benefiting from strides in development of such particles. This chapter concentrated on the coating of α-Cr_2O_3 monodispersed meso-spherical particles for solar thermal absorbers applications. These particles are grown on a metallic substrate by an inorganic condensation of hydrated metal ions complexes method, the so-called aqueous chemical growth (ACG) method, specifically with spherical morphology. Furthermore, this method is based on a low-temperature approach that is only weakly influenced by the substrate and allows for the growth of α-Cr_2O_3 monodispersed particles on various substrates. The ACG method is an efficient way to generate wafer scale and densely packed arrays of α-Cr_2O_3 even on polymer materials. Furthermore, structural and optical characterisations confirmed that samples where the deposited particles were aged for longer time yielded a high chromium percentage on the surface, high absorptivity and emissivity. This can be reduced by a suitable heating mirror and samples deposited for less aging time, which gave high absorptivity and low emissivity. These results indicate that this type of nano-coatings onto Cu or stainless steel rough substrates is good candidates for solar absorbers at temperature lower than 500 °C.

Keywords: Chromium(III) oxide, ACG, solar absorbers, surface coating

9.1 Introduction

Monodispersed spherical particles of α-Cr_2O_3 are defined as particles that are highly uniform in size

and shape. The major significance of α-Cr_2O_3 monodispersed particles is attributed to the uniformity in physico-chemical properties of individual particles in a dispersed system, which allows direct correlation of properties of a whole system with those of each particle and facilitates theoretical approaches. However, to meet so many scientific and practical demands, great effort has to be devoted to the preparation of well-defined α-Cr_2O_3 micro to nanoparticles with controlled particle size, shape and composition [1, 2]. The α-Cr_2O_3 meso-spherical particles are also very useful as models for fundamental studies since many properties of the dispersed matter are affected by particle size and shape [3].

Chromium(III) oxide has been widely studied due to its useful physico-chemical properties required in industrial applications. It is an important refractory material due to its high melting temperature of about (~2435 °C) [4]. It has high corrosion and oxidation resistance [5], hardness and antiferromagnetic properties [6]. These enable its use as a coating material for thermal protection [7], as intermediate layers in corrosion-resistant applications on semi-conductors and metals [8], as an active tunnelling barrier or pinning system for spintronic applications [9], as a pigment powder with high Near-Infrared (NIR) reflectance [10], and it is widely used for solar absorbers applications as Cr/Cr_2O_3 cermet [11]. Furthermore, α-Cr_2O_3 micro to nanoparticles can be deposited using various techniques including the thermal decomposition of a Cr(III) nitrate solution [12], the sol–gel process [13], urea-assisted homogeneous precipitation [14], laser induced pyrolysis [15], a microwave plasma [16], hydrothermal reduction [17] and gas condensation [18]. However, these methods still have limitations when considered in an industrial context, which demand synthesis of α-Cr_2O_3 mesoparticles at low cost, high yield and high performance.

While the fundamental and practical importance of monodispersed systems is generally accepted, it is not easy to attain them for individual purposes, because many factors have influences on the monodispersity and other relevant characteristics. A large number of monodispersed particles have been prepared by trial and error or by optimisation of preparation conditions. It is rare to find studies which shed light on the fundamental formation mechanisms, leading to general principles, or design synthetic systems on the basis of reasonable guidelines. Nevertheless, underlying mechanisms for the formation of monodispersed particles have continued to be investigated, so that the formation processes are gradually being clarified. Such studies will finally lead to reasonable and more precise control of α-Cr_2O_3 monodispersed spherical particles.

In response to the persistent demand for the industrial use of α-Cr_2O_3 monodispersed particles and other metal oxides of potential benefits, the so-called “aqueous chemical growth” (ACG) technique was developed to resolve the essential problems of the high-cost production and pollutant emissions. This method is based on using water as a dispersion liquid because of its ability to dissolve mineral salts. It is safe, chemically stable and remains liquid over a wide temperature range. It is the solvent of choice for metallic cations because it is the most convenient reaction medium, in the laboratory as well as in industry. The ability of water to dissolve ionic and ion covalent solids stems from two main characteristics: the high polarity of the water molecule (μ = 1.84 Debye) and high dielectric constant (ε = 78.5 at 25 °C). The ACG technique is a challenge to conventional physical chemistry of metal oxide systems, on which existing α-Cr_2O_3 monodispersed particles have been synthesised. This technique has been applied to the synthesis of a wide range of nanoparticulate materials due to its ease of implementation and high degree of flexibility. The main difficulty with this method is that it is depended on size and size distribution of the generated particles. Parameters of the reaction are not

fully understood and, therefore, the optimal reaction conditions are determined in an empirical manner [19]. The synthesis of α-Cr_2O_3 spherical particles using ACG is a cost-efficient technique. This route gives high yield and relatively low cost. Little effort has been made to study the various aspects of the resultant properties of α-Cr_2O_3 particles synthesised using the ACG technique, in particular the effect of ageing on the growth mechanism of α-Cr_2O_3 monodispersed spherical particles. Furthermore, ageing may take place over a long time scale, from hours to days, allowing the system to tend towards, or reach stability. This may be the reason why ageing is often associated with the modification of some chemical or physical characteristics of the particle, such as the change in crystal type, increase in particles size or changes in morphology [20]. In view of these considerations, a comprehensive study on the preparation, characterisation, and technological applications of α-Cr_2O_3 is indicated. This would be useful for the understanding of the underlying principles of general monodispersed systems and mechanisms of individual practical cases, as well as for creating novel systems.

Black chromium–chromium(III) oxide cermet (Cr-Cr_2O_3) also shows potential for use in solar absorber applications. It exhibits attractive solar absorption characteristics with a high solar absorption, a, and low emissivity, ε, over a large temperature ranges [21]. It is used widely as a selective solar heat thermal collector nanocoating for temperatures ≤400 °C in concentrated solar photothermal (CSP) devices. The black chromium-selective solar absorbers have been, and are, produced by various high-vacuum technologies, such as reactive sputtering [22], pulsed sputtering [23], e-beam and evaporation techniques [24], or by electroplating of black chrome. This latter employs Cr–Cr_2O_3 cermet material and results in the most widely used solar absorber [25, 26]. Based on the survey of Kennedy [27], electrodeposited black chromium cermet on Ni, Fe, Cu, stainless steel substrates, has an α/ε (100 °C) = 0.97/0.09 for temperatures <300 °C [28–35]. Black chrome is commercially produced by MTI on Ni-plated Cu in the United States, by Chrome Coat of Denmark on copper, and on stainless steel by Energie Solaire in Switzerland [36, 37]. Researchers have found that a layer of Ni between the substrate and black chrome coating enhances the thermal stability up to 400 °C [38]. Oxidation of the metallic Cr crystallite and densification of the crystallites is a primary cause of degradation of this selective coating [39]. At high temperatures, Ni diffusion from the substrate contributes to optical degradation [40]. When Cr^{3+} concentrations in the standard black chrome baths were reduced, laboratory samples were produced that were stable in air for 3908 and 670 h at 350 °C and 400 °C [41], respectively. The reflectance after exposure at 350 °C in air is approximately equivalent to that after exposure at 400 °C in vacuum [42]. Heat treatments have established that black chrome fails optically between 500 °C and 600 °C after 1 h in both air and under vacuum, in addition to the mechanical peeling after 600 °C in air [43]. It was demonstrated that improvements in performance can be achieved by addition of an anti-reflection (AR) top coating. Or if metallic layer is used at the interface, to act as the infrared reflective (IR) layer, instead of the Cu or Al substrates. Diffusion of Cu and Al from the substrate at higher CSP operating temperatures becomes significant. Also, black chrome solar selective films can be improved by admixing molybdenum, up to a limit of about 20% of the chromium content [44].

The aim of this research/study is to demonstrate the possibility of preparing large surface coatings of monodispersed meso-spherical particles of chromium(III) oxide by using the ACG method for solar absorber application. Specific objectives include

- To synthesis, characterise and investigate the nature of the growth mechanism of the

monodispersed meso-spherical particles of chromium(III) oxide, α-Cr_2O_3, which might have direct relationship with diffusion-controlled growth;
- To investigate the possible application of α-Cr_2O_3 monodispersed meso-spherical particles in solar thermal absorbers.

9.2 Samples Preparation

Monodispersed spherical particles of hydrated Cr_2O_3 can be obtained by prolonged heating at ~75 °C of diluted solutions of $KCr(SO_4)_2.12H_2O$, although hydrated Cr_2O_3 could be easily converted into crystalline α-Cr_2O_3 by heating at 500 °C for 1 h. Therefore, the synthesis is based on the deprotonation of the blue–grey hexaaqua chromium(III) ions, $[Cr(H_2O)_6]^{3+}$. The potential precursors are the zero-charge complexes $[Cr(OH)_3(H_2O)_3]^0$ and $[Cr_2(OH)_6(H_2O)_4]^0$ that condense by olation (the reaction that leads to the formation of a hydroxo bridge). The growth of the nuclei takes place in a uniform and isotropic manner and results in the formation of monodisperse, meso-spherical particles of hydrated chromium oxide onto the substrates, by heteronucleation at mild temperatures. At the final stage, annealing results in its thermodynamically stable green sesquioxide corundum phase, α-Cr_2O_3.

The growth of the monodispersed meso-spherical particles of hydrated Cr_2O_3 was conducted according to the literature [45, 46]. The synthesis was performed with reagent-grade chemicals. An aqueous solution (MilliQ, 18.2 MΩ cm) of 1 mM of chromium potassium sulphate dodecahydrate, $KCr(SO_4)_2.12H_2O$, at pH 6.5, mixed in a glass bottle with autoclavable screw cap (Duran laboratory) containing a rough copper substrates, was heated in a laboratory oven at a constant temperature of 75 °C with different aging times. Subsequently, the durable and scratch resistant thin films were thoroughly washed with water to remove any residual salts. The particulate coatings were then heat treated in a flowing H_2 gas at 500 °C, based on thermal analysis data, for 1 h, to obtain α-Cr_2O_3 monodispersed and meso-spherically shaped core–shell particles.

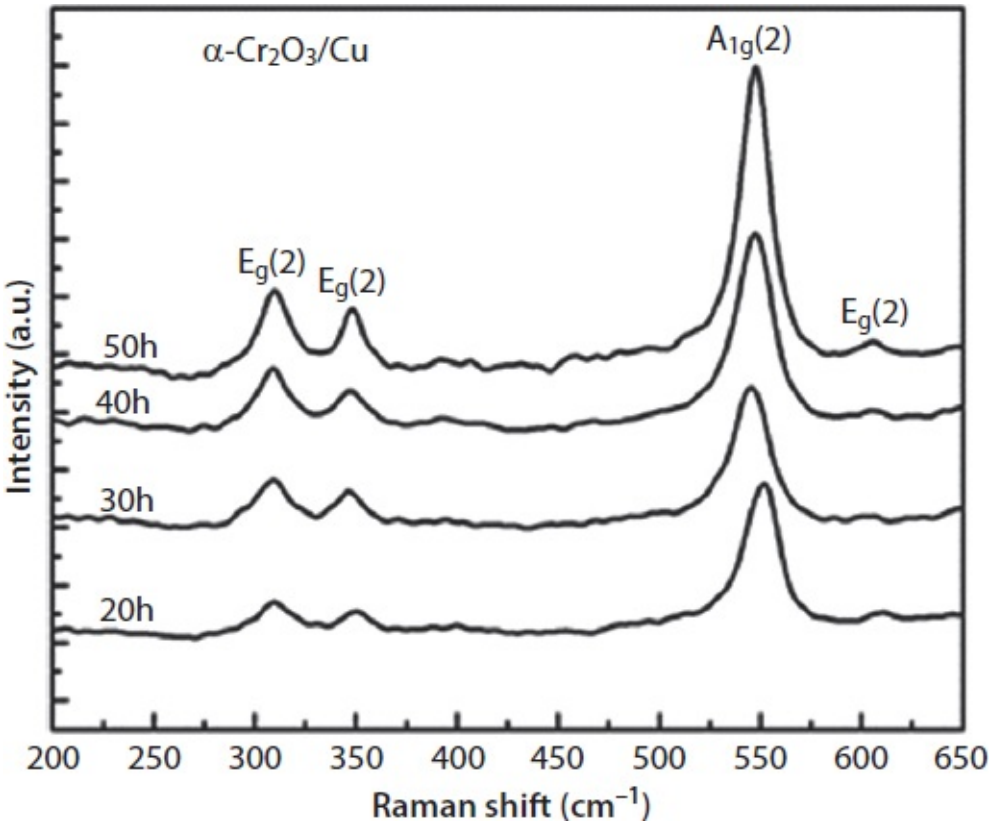
9.3 Structural and Morphological Investigations of α-Cr_2O_3 Monodispersed Meso-spherical Particles

9.3.1 Raman Spectroscopic Study

The Raman spectra of α-Cr_2O_3 monodispersed meso-spherical particles are depicted in Figure 9.1. However, all the peaks that occurred showed only three E_g and one A_{1g} modes of chromium(III) oxide. Moreover, chromium(III) oxide has a corundum structure that belongs to the D^6_{3d} space group and consists of a hexagonal close packed array of oxide anions with 2/3 of the octahedral holes occupied by chromium. The site symmetry for the Cr atoms is C_3, whereas the O atoms are on sites

having C_2 symmetry. The irreducible representations for the optical modes in the crystal are $2A_{1g}$, $2A_{1u}$, $3A_{2g}$, $2A_{2u}$, $5E_g$ and $4E_u$ vibrations, however, only two A_{1g} and five E_g vibrations are Raman active [47]. Hart *et al.* [48], in their Raman measurements on a Cr_2O_3 single crystal, observed seven Raman bands. In this present work, it was found that all peaks belonging to samples aged for 20, 30, 40 and 50 h showed only three E_g and one A_{1g} modes of chromium(III) oxide (see Figure 9.1). The observation of only four modes in the samples is possibly due to the polycrystallinity of α-Cr_2O_3 meso-spherical particles. On other hand, it is evident from Figure 9.1 that Raman intensity was increased with increase of ageing time and became nearly constant after 50 h. These results indicate that the size and amount of particles are almost stable after 50 h. This was also confirmed by scanning electron microscopy (SEM) results in a previous study on the growth kinetics of α-Cr_2O_3 spherical particles [49].

Figure 9.1 The Raman spectra of α-Cr_2O_3 monodispersed meso-spherical particles.

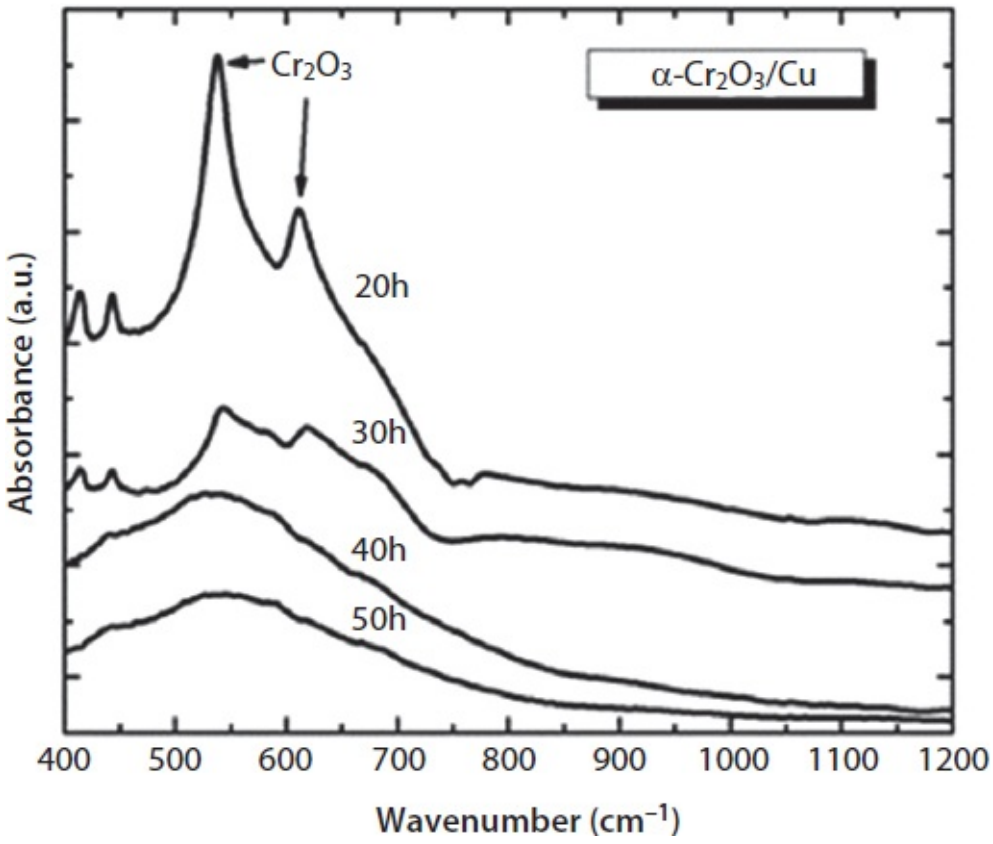


9.3.2 Attenuated Total Reflection Study

The attenuated total reflection (ATR) spectra for α-Cr_2O_3 monodispersed meso-spherical particles deposited on copper at different aging time, and heated at 500 °C in a flowing H_2 gas, can be found in Figure 9.2. The gradual disappearance of Cr–O and O–O bands with increasing aging time is observed. This may be due to the black thin layer of chromium metal coated on the surface of the particles due to the surface reduction of Cr_2O_3 during the heating process of the samples in a flowing H_2 gas at 500 °C. Furthermore, samples aged for 20 and 30 h reveal two strong bands, centred at 539 and 611 cm^{-1}. These values fall well within the range reported in the literature for samples having the exact α-Cr_2O_3 stoichiometry [50]. Both bands are associated with Cr–O stretching modes (symmetrical stretching and anti-symmetrical stretching) in α-Cr_2O_3 and are due to various

combinations of O^{2-} and Cr^{3+} displacements in the lattice. The pair of sharp bands, at 442 and 411 cm^{-1}, correspond to two specific O^{2-} displacements in the lattice. From the ATR and Raman results, it can be concluded that the coating consisted of pure α-Cr_2O_3. Moreover, since chromium metal does not give any peaks in the Raman/ATR spectra in the wave number range studied, suggests the use of an electron energy-dispersive spectroscopy technique to investigate the existence of Cr layer on the surface of α-Cr_2O_3 monodispersed meso-spherical particles.

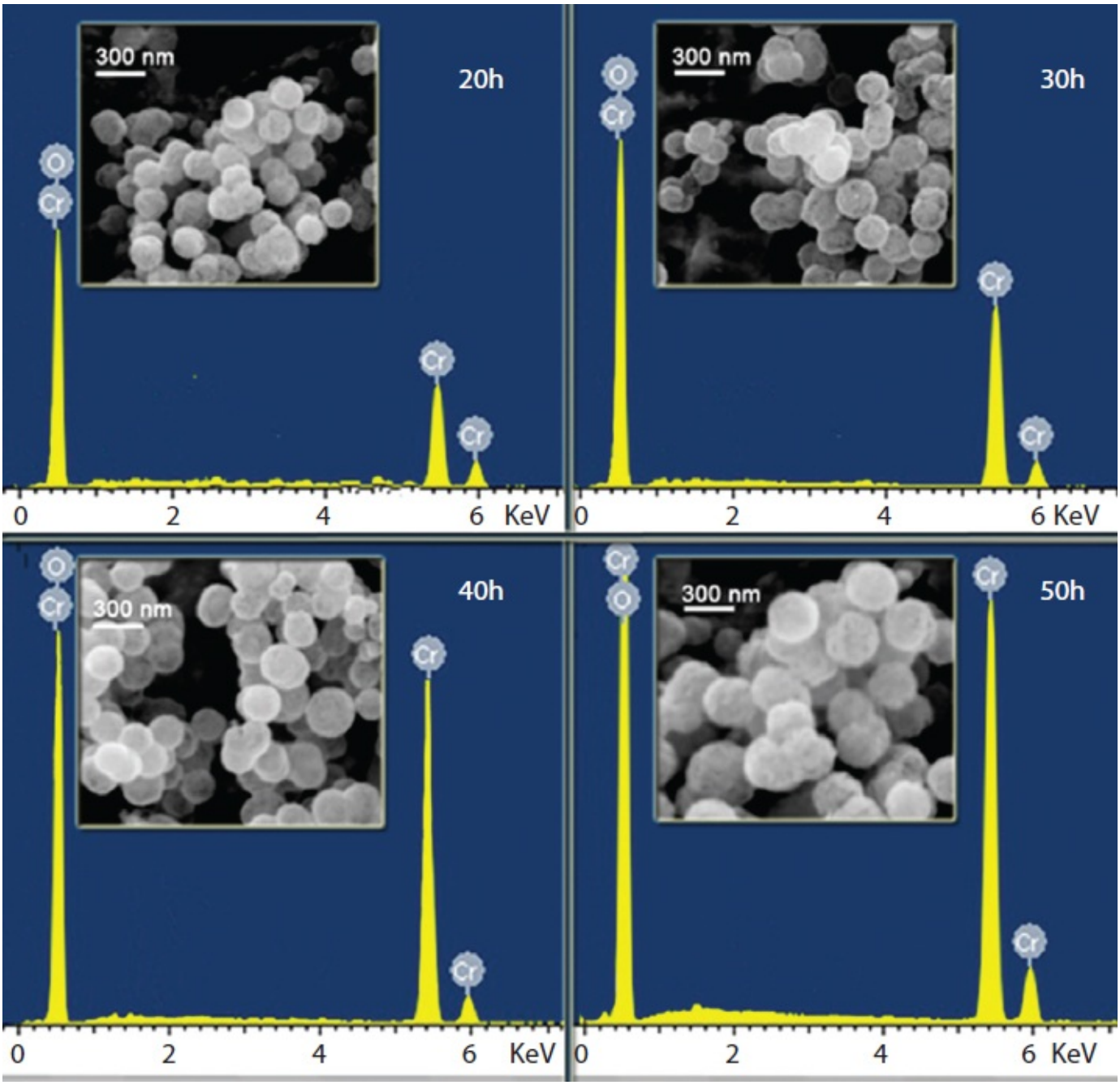
Figure 9.2 The Attenuated Total Reflection spectra for α-Cr_2O_3 monodispersed meso-spherical particles.



9.3.3 Field-Emission Scanning Electron Microscopy (FESEM) and Energy-Dispersive X-Ray Analysis (EDX)

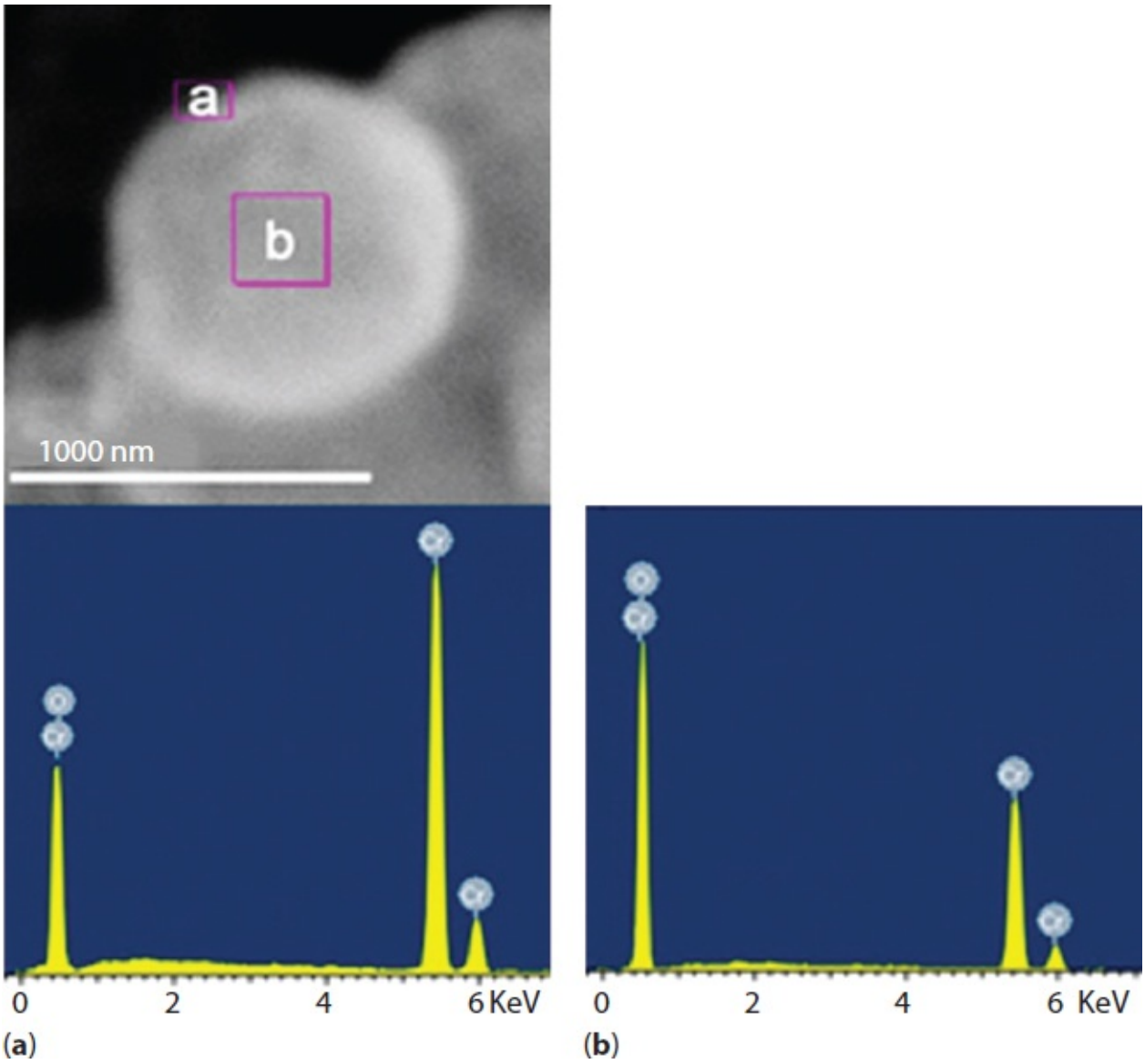
FESEM micrographs in the inset of Figure 9.3 revealed that the α-Cr_2O_3 coatings consisted of meso-spherical particles, with an average size of about 498, 990, 1010 and 1185 nm, respectively. This result demonstrated that α-Cr_2O_3 can be produced with well-defined surface morphology, narrow size distribution and excellent shape control, not only when placed onto standard amorphous substrates but also on metallic substrates.

Figure 9.3 SEM/EDS of α-Cr_2O_3 monodispersed meso-spherical particles.



The analysis of the chemical composition of the α-Cr_2O_3 monodispersed meso-spherical particles by EDX indicated that the coatings contained black chromium (see Figure 9.3). No chromium in metallic form was found by Raman/ATR measurements, but EDX results confirmed that the film contains chromium. Further, EDX analysis confirmed that the percentage of chromium increased with increasing aging. In order to discriminate between the shell of Cr and the core of α-Cr_2O_3, a fine electron probe beam of 3 nm in the EDX system was used. Thereafter, EDX spectra were acquired by positioning at different parts of the large-size particles. In Figure 9.4a and b, the results of the EDX spectra acquired by positioning the electron probe through only the shell and through the core and shell can be seen. It is apparent that the shell was dominated by Cr, while the core is rich in α-Cr_2O_3, suggesting that the shell of the large-size particle was Cr.

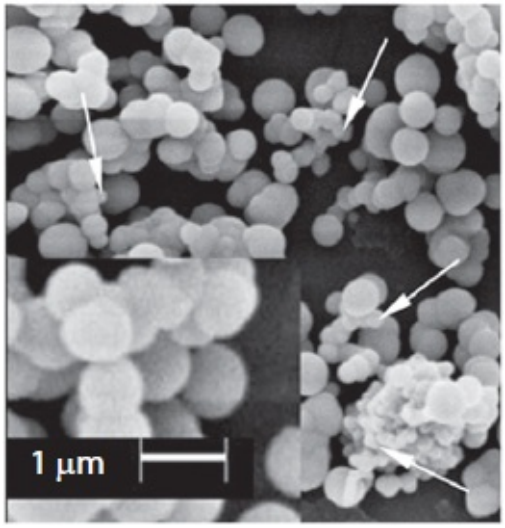
Figure 9.4 Investigation of shell and core of one α-Cr_2O_3 monodispersed meso-particle.



9.4 Growth Mechanism

The study of the influence of ageing on the average diameter of α-Cr_2O_3 spherical particles was investigated in our previous study [49]. We confirmed that the growth rate of the particles between ageing times of 8 and 40 h was very fast. On the other hand, after 40 h, the particles started approaching stability in terms of growth. Also, the average size of the final particles depended on the number of nuclei and the amount of matter available during synthesis, but the width of the particle size distribution was linked to the mechanism of nuclei growth. This phenomenon can be explained by the unstable nature of critical-size nuclei formed during the nucleation stage (before the growth stage) that leads to growth through incorporation of precursor molecules, which continue to be generated after nucleation [51]. The existence of small nano-particles with α-Cr_2O_3 particles is indicated by white arrows in Figure 9.5. The presence of small nanoparticles along with the α-Cr_2O_3 particles after a sufficiently long period of ageing (44 h), suggested that the diffusion-limited Ostwald ripening may be operative, in which large particles grow at the cost of smaller ones. At the early stage of the growth, the monomer concentration was sufficiently high for the hydrated Cr_2O_3 particles to grow, and the growth process was fast. After longer times, the monomer concentration was depleted below a certain critical level, resulting in the smaller nanoparticles being dissolved.

Figure 9.5 FESEM image of α-Cr_2O_3 particles obtained after 48 h of reaction. Arrows indicate the existence of small nanocrystals along with the monodispersed particles of α-Cr_2O_3.



9.4.1 Development of a Mathematical Model [Lifshitz–Slyozov–Wagner (LSW) Model]

The growth of nanocrystals in solution involves two important processes, the nucleation followed by the growth of the nanocrystals [52].

9.4.1.1 Basic Assumptions

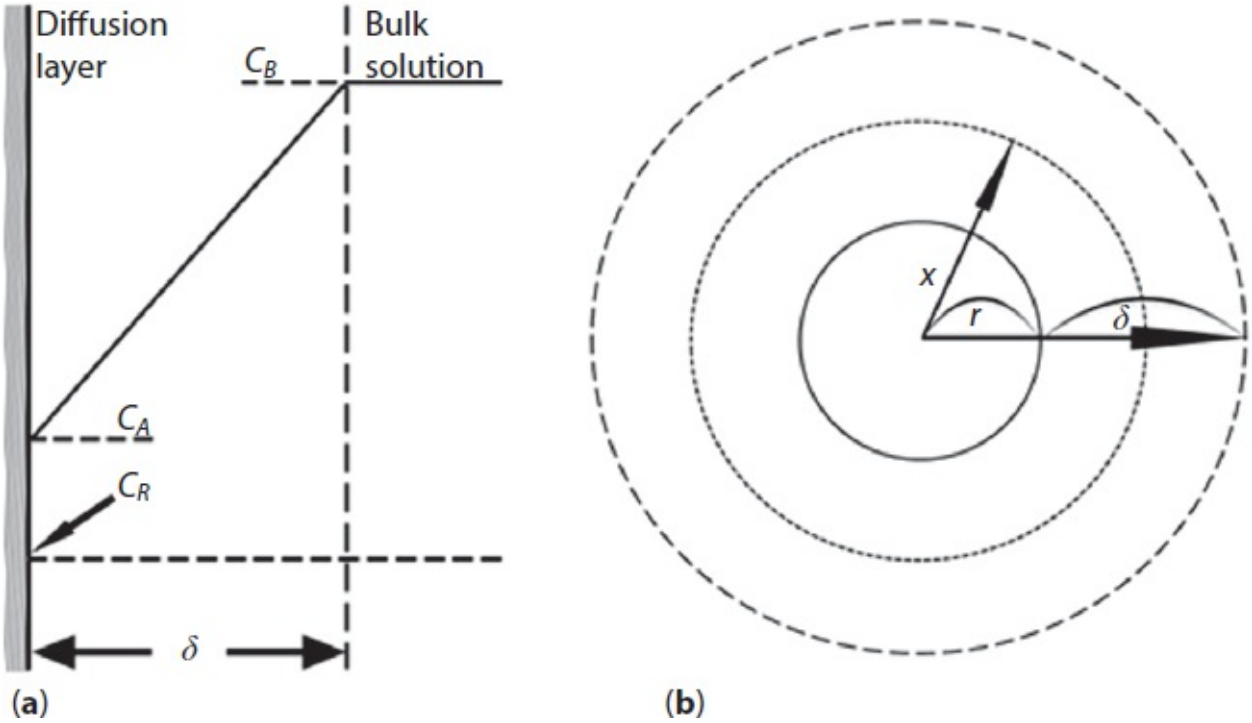
The assumptions are made according to the LSW theory [53, 54]:

- particles are assumed to be spherical in a supersaturated medium;
- the total mass of the solute is conserved;
- assumptions of the particle being spherical are characterised only by the radius distribution;
- processes such as nucleation and aggregation that introduce new particles are negligible.

9.4.1.2 Mathematical Formulation

Attempts have been made [52–55] to obtain information regarding the growth mechanisms of α-Cr_2O_3 based on the time evolution of the average diameter of the spherical particles Figure 9.6. If the diffusion-limited Ostwald ripening according to the LSW theory were to be the only contributor of the growth mechanism, then the rate law would be given by solving Fick's first law of diffusion.

Figure 9.6 (a) The profile of solute concentration in a diffusion layer. (b) The diffusion layer around a spherical particle [56].



C_A = Concentration at the interface

C_B = Concentration at the bulk phase

C_R = Solubility of the particle with radius, r

x = Radius at any time

δ = Thickness of the diffusion layer

By using Fick's first law, the flux passing through a spherical surface with radius x within the diffusion layer is

$$J = D \times 4\pi x^2 \times \frac{dc}{dx} \quad (9.1)$$

where J is the flux, D the coefficient of diffusion and dc/dx the concentration gradient.

At steady state, J is constant over the diffusion layer x. Here, diffusion of the molecules from interface to the bulk phase takes place. Then, solving Equation 9.1 and integrating with proper limits:

$$J \times \int_{r}^{r+\delta} \frac{dx}{x^2} = 4\pi D \int_{C_A}^{C_B} dc \quad (9.2)$$

$$J\left[\frac{-1}{x}\right]_{r}^{r+\delta} = 4\pi D\int_{C_A}^{C_B} dc$$

$$J\left[\frac{-1}{r+\delta}+\frac{1}{r}\right] = 4\pi D\left[C_B - C_A\right]$$

$$J\left[\frac{1}{r}-\frac{1}{r+\delta}\right] = 4\pi D\left[C_B - C_A\right]$$

$$J\left[\frac{r+\delta-r}{r\left(r+\delta\right)}\right] = 4\pi D\left[C_B - C_A\right]$$

$$J\left[\frac{\delta}{r\left(r+\delta\right)}\right] = 4\pi D\left[C_B - C_A\right]$$

$$J = \frac{4\pi D\left(C_B - C_A\right)r\left(r+\delta\right)}{\delta} \quad (9.3)$$

The above flux is due to diffusion.

Another flux is due to the first order reaction at the surface. This flux can be equated to the consumption rate of the monomer species at the surface of the particles [52]. So, the flux due to the reaction is

$$J = 4\pi r^2 \times K_d\left(C_A - C_R\right) \quad (9.4)$$

where K_d is the first-order decomposition rate constant.

At a steady state, the two fluxes (flux due to diffusion and reaction at the surface) are same.

Then,

$$\frac{C_A - C_R}{C_B - C_A} = \frac{D}{rK_d}\left(\frac{r+\delta}{\delta}\right)$$

$$\frac{C_A - C_R}{C_B - C_A} = \frac{D}{rK_d}\left(1+\frac{r}{\delta}\right) \quad (9.5)$$

$$\text{with atoms in a crystal} = \frac{4\pi r^3}{3V_m} \quad (9.6)$$

and the rate of species entering, $J = \frac{d}{dt}\left(\frac{4\pi r^3}{3V_m}\right)$

$$J = \frac{4\pi r^2}{V_m} \times \frac{dr}{dt} \quad (9.7)$$

$$\frac{dr}{dt} = \frac{JV_m}{4\pi r^2} \quad (9.8)$$

where dr/dt is the growth rate and V_m the molar volume.

In solution, it is very difficult to measure C_A, so we have to eliminate C_A from the two Equations 9.3 and 9.4:

$$J = 4\pi r^2 \times K_d\left(C_A - C_R\right)$$

$$C_A - C_R = \frac{J}{4\pi r^2 K_d}$$

$$C_A = \frac{J}{4\pi r^2 K_d} + C_R \quad (9.9)$$

Substituting the value of C_A in Equation 9.3:

$$J = 4\pi Dr\left(1+\frac{r}{\delta}\right)(C_B - C_A)$$

$$J = 4\pi Dr\left(1+\frac{r}{\delta}\right)\left(C_B - \frac{J}{4\pi r^2 K_d} - C_R\right)$$

$$J\left(4\pi Dr \times \frac{J}{4\pi r^2 K_d}\right)\left(1+\frac{r}{\delta}\right) = 4\pi Dr\left(1+\frac{r}{\delta}\right)(C_B - C_R)$$

$$J\left(1+\frac{D}{rK_d}\left(1+\frac{r}{\delta}\right)\right) = 4\pi Dr\left(1+\frac{r}{\delta}\right)(C_B - C_R)$$

$$J = \frac{4\pi Dr\left(1+\frac{r}{\delta}\right)(C_B - C_R)}{\left(1+\frac{D}{rK_d}\left(1+\frac{r}{\delta}\right)\right)} \quad (9.10)$$

Substituting the value of J in Equation 9.10:

$$\frac{dr}{dt} = \frac{4\pi Dr\left(1+\frac{r}{\delta}\right)(C_B - C_R)V_m}{\left(1+\frac{D}{rK_d}\left(1+\frac{r}{\delta}\right)\right)4\pi r^2}$$

$$\frac{dr}{dt} = \frac{D\left(1+\frac{r}{\delta}\right)(C_B - C_R)V_m}{r\left(1+\frac{D}{rK_d}\left(1+\frac{r}{\delta}\right)\right)} \quad (9.11)$$

According to Gibbs–Thompson equation,

$$C_R = C_\infty e^{\left(\frac{2V_m\sigma}{rRT}\right)} \quad (9.12)$$

where C_∞ is the equilibrium concentration at the flat surface (bulk solubility), σ the interfacial energy, R the universal gas constant and T the temperature.

Assuming that $\frac{2V_m\sigma}{rRT}$ is very small, so neglecting the higher order terms in the series expansion,

then

$$C_R = C_\infty \left(1 + \frac{2V_m\sigma}{rRT}\right) \quad (9.13)$$

Similarly C_B can be written as

$$C_B = C_\infty \left(1 + \frac{2V_m\sigma}{r_B RT}\right) \quad (9.14)$$

Substituting the values of C_B and C_R in Equation 9.11:

$$\frac{dr}{dt} = \frac{2V_m^2\sigma C_\infty \left(1 + \frac{r}{\delta}\right)\left(\frac{1}{r_B} - \frac{1}{r}\right)}{rRT\left[\frac{1}{D} + \frac{1}{rK_d}\left(1 + \frac{r}{\delta}\right)\right]} \quad (9.15)$$

Mainly diffusion layer thicknesses are of the order of microns. So, in case of nanocrystal we assume, $r \ll \delta$.

So for $r \ll \delta$, Equation 9.15 becomes

$$\frac{dr}{dt} = \frac{2V_m^2\sigma C_\infty \left(\frac{1}{r_B} - \frac{1}{r}\right)}{rRT\left[\frac{1}{D} + \frac{1}{rK_d}\right]} \quad (9.16)$$

This is a diffusion limited growth mechanism. In this case, diffusion is the slowest step and also the rate controlling step and the particle growth is mainly controlled by the diffusion of the monomers to the surface [53, 54].

For $D \ll rK_d$

Then Equation 9.16 reduces to

$$\frac{dr}{dt} = \frac{2V_m^2 D\sigma C_\infty \left(\frac{1}{r_B} - \frac{1}{r}\right)}{rRT}$$

$$\frac{dr}{dt} = \frac{2V_m^2 D\sigma C_\infty \left(\frac{r}{r_B} - 1\right)}{r^2 RT}$$

$$\frac{dr}{dt} = K_D \times \frac{\left(\frac{r}{r_B} - 1\right)}{r^2} \quad (9.17)$$

$$\text{where, } K_D = \frac{2V_m^2 D\sigma C_\infty}{RT} \text{ (Constant).} \quad (9.18)$$

If the total mass of the system is kept conserved, the LSW theory showed that the ratio r/r_B is constant. So, then assuming r/r_B as constant, Equation 9.17 reduces to

$$\frac{dr}{dt} = \frac{K_D \times Const}{r^2}$$

$$\frac{dr}{dt} = \frac{K_C}{r^2}$$

$$\int_{r_0}^{r} r^2 dr = K_C \int_0^t dt$$

$$\frac{1}{3}\left(r^3 - r_0^3\right) = K_C t$$

$$r^3 - r_0^3 = Kt \quad (9.19)$$

Since the diameter $d = r \times 2$

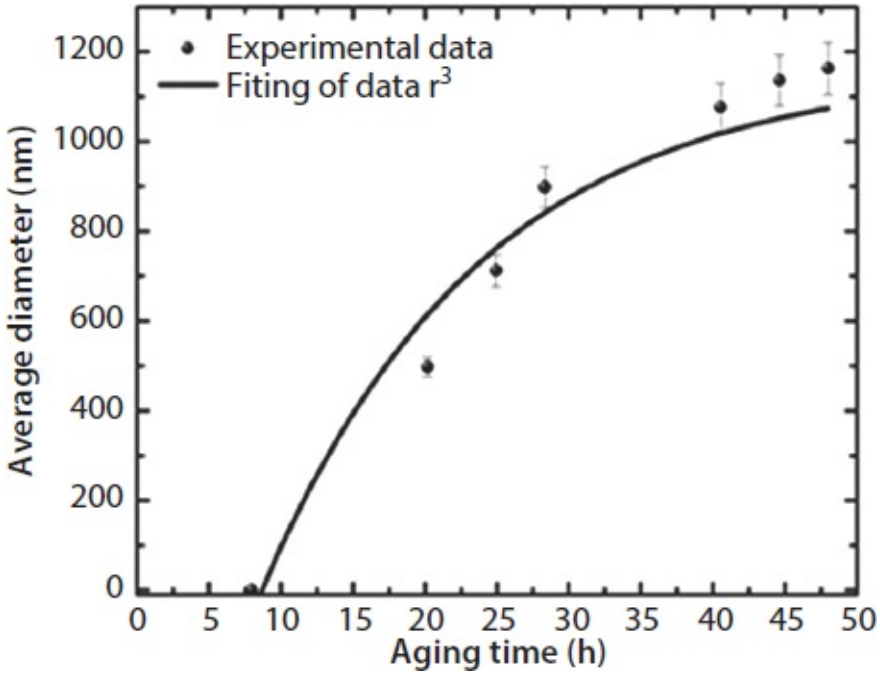
then:

$$d^3 - d_0^3 = 8Kt \quad (9.20)$$

where d is the average diameter at time t and d_0 is average initial diameter of α-Cr_2O_3 spherical particles. The rate constant, K, is given by $K = 8\gamma D V_m^2 C_\infty / 9RT$, where $D = k_B T/6\pi\eta a$ is the diffusion coefficient at temperature T = 348.15 K, the molar volume of chromium(III) oxide is V_m = 0.0292 m^3 k mol^{-1} [57], γ = 3 J m^{-2} is the surface energy [58], and C_∞ = 0.1 mM is the chromium potassium sulphate concentration, R = 8.3143 J K^{-1} mol^{-1} is the universal gas constant, k_B is Boltzmann constant, η~0.398 × 10^{-3} kg $m^{-1}s^{-1}$ is the viscosity of water at 348.15 K and a is the mean hydrodynamic radius

of Cr_2O_3 particles in the range of 30 nm. When fitting the d(t) data obtained from SEM to the Ostwald ripening model (Equation 9.20), a reasonably good fit for the spherical particles of α-Cr_2O_3 was found, as can be seen from Figure 9.7.

Figure 9.7 Effect of aging times on the average diameter of the α-Cr_2O_3 spherical particles.



From the average particle diameter measurements against ageing time, Figure 9.7, for syntheses carried out at ~75 °C, a non-negligible growth can be noticed in the particles size, even when transformation was complete. Moreover, the growth rate of the particles increased between time 8 and 40 h, and slightly after 40 h. The standard deviation increased with increase of ageing time (Table 9.1). Furthermore, the growth of the particles (Figure 9.7) was not completely arrested, even when the transformation was complete. This would indicate an Ostwald ripening process related to dissolution of the smallest particles and coarsening of the largest was taking place. In these cases, the ripening process lead to the disappearance of entire classes of particles and the appearance of new classes. As a result, it can be seen that the size of α-Cr_2O_3 particles increased with increasing ageing time and the growth mechanism was based on the diffusion-limited Ostwald ripening process on the basis of the LSW theory.

Table 9.1 Particles average diameter, versus aging time of α-Cr_2O_3 monodispersed particles.

Aging time (h)	Particles average diameter (nm)	Standard deviation of particles average diameter (nm)
20	498	210
24	645	311
28	991	358
40	1010	447
44	1140	518
45	1183	622

9.5 Potential Applications in Solar Absorbers

Efficient thermal solar collectors, which convert incident solar radiation into useful heat, for

applications such as heating of water, drying and cooking, make use a spectrally selective surface that maximise absorption of solar radiation and minimise thermal radiation [59]. There are currently high-performing selective surfaces available, but there are difficulties with many of these, including long-term durability, moisture resistance, adhesion, scratch resistance and costly technically advanced production techniques [27]. The most commonly used design is based on a selective solar-absorbing and infrared transparent layer on top of a substrate that has high infrared reflectance. The base material of solar absorbers (substrate) is often a metal with high thermal conductivity, such as copper [60]. This metal fulfils the requirement of having high infrared reflectance and can, therefore, also act as the infrared reflector. They are not, however, resistant to the microclimatic conditions in a solar collector [61] if the absorbing coating on top is not also functioning as a protection layer. In order to make thermal solar collectors more accepted and widespread, the price per unit has to be reduced. The most costly component of a thermal solar collector is the spectrally selective surface. The cost has to decrease in order to make thermal solar devices more commercially interesting, where solar thermal energy still has a very low impact on the energy market. The advantages of the solution-chemical technique are that it is simple and easy to control, the coating can be manufactured under ambient pressure and temperature conditions, the chemicals involved are environmentally friendly and it is low in material consumption. Furthermore, electroplated black chromium, which employs a $Cr\text{-}Cr_2O_3$ cermet material, is currently the most widely used solar absorber [62], but preparation of a black chromium solar coating using an electroplating technique is not suitable due to environmental pollution.

9.5.1 Diffuse Reflectance and the Infrared Emissivity (ε) Study of α-Cr_2O_3 Meso-spherical Particles

The total diffuse reflectance, specular and non-specular reflectivity, of different samples over the UV–VIS–NIR range, is represented in Figure 9.8. In general, very low reflectance spectra were obtained with samples aged for more than 40 h. Furthermore, it is observed that the spectral reflectance of the materials decreased with increasing aging time. A quantitative comparison of the total solar absorbance calculated by numerical integration using the measured total diffuse reflectance spectrum in Figure 9.8 in the solar radiation region of 300–2500 nm and the solar irradiance at Air Mass 1.5 (AM1.5) and the measured infrared emissivity of all the samples are presented in Table 9.2. The absorptivity and emissivity of sample aged for high aging times, $t \sim 50$ h, is high, but its emissivity can be reduced by a suitable heat mirror, such as SnO_2:F. For samples aged at lower aging times, $t \sim 20$ h, the absorptivity was relatively high and the emissivity low, hence such nanocoatings are potentially competitive for solar absorbers application. However, this difference in the optical properties is strongly dependent on the aging time of the samples and can be attributed to many factors, including the film microstructure, surface composition and morphology.

Figure 9.8 The total diffuse reflectance of different samples over the UV-VIS-NIR range.

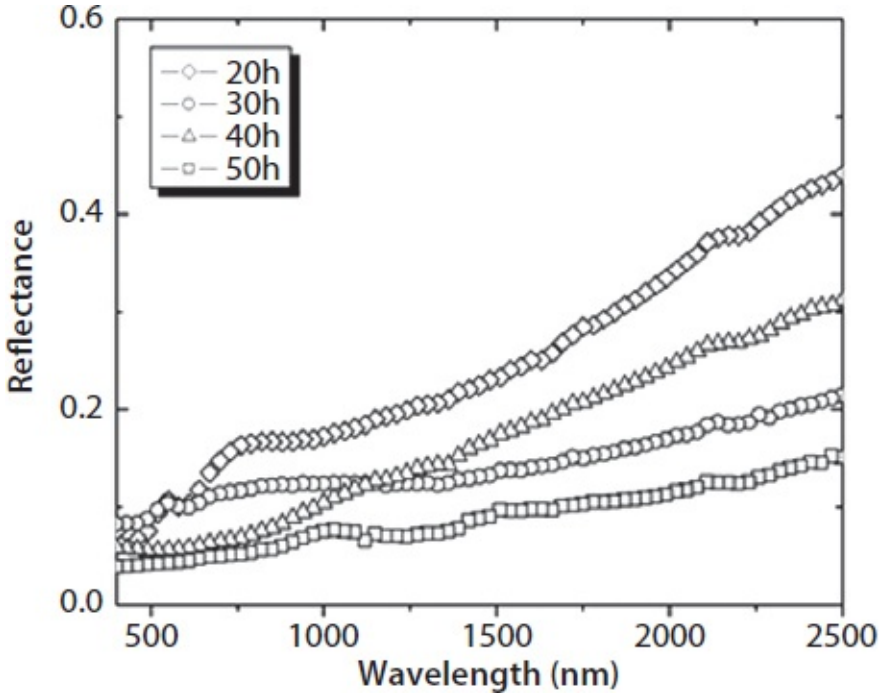


Table 9.2 The solar selectivity of Cr/α-Cr_2O_3 monodispersed spherical core-shell particles coated on Copper substrates.

	Aging time (h)	Absorbance (α)	Emittance (ε)
Sample 1	20	0.84	0.49
Sample 2	30	0.88	0.77
Sample 3	40	0.90	0.60
Sample 4	50	0.94	0.80

9.6 Conclusions

The controlled growth of uniform fine meso-spherical particles of α-Cr_2O_3 at a low temperature with a soft chemistry preparative technique (so-called ACG method) was achieved. The kinetics of the growth of monodispersed spherical particles of chromium(III) oxide, α-Cr_2O_3 in aqueous solution were studied as a function of ageing time. The observation of small fine spherical particles together with the α-Cr_2O_3 particles in SEM images, lends support to a growth mechanism based on the diffusion-limited Ostwald ripening process on the basis of the LSW theory. The experimental data were analysed in the frame of existing coarsening and particle growth mechanisms, i.e. Ostwald ripening. The good peaks fits of the *d(t)* data of α-Cr_2O_3 particles with d^3 model confirmed the growth mechanism to be mainly diffusion-controlled. Furthermore, This ACG technique has demonstrated that it is a potential method to produce reproducible high quality-low cost coatings. Samples deposited for longer aging time exhibited high chromium percentage on the surface of the particles, high absorptivity and emissivity, but this could be reduced by a suitable heating mirror. Samples deposited for lower aging time exhibited high absorptivity and low emissivity. As conclusion, these preliminary results indicate that this type of nano-coatings on Cu rough substrates, are good candidates for solar absorbers applications at temperature lower than 500 °C.

Acknowledgements

This work was sponsored within the framework of the UNESCO UNISA Africa Chair in Nanosciences & Nanotechnology and the Nanosciences African Network (NANOAFNET) by the National Research Foundation of South Africa, the African Laser Centre (ALC), the University of South Arica (UNISA) in collaboration with the Vice-Chancellor of the University of Pretoria, the National Research Foundation (NRF) of South Africa, iThemba LABS and the Abdus Salam ICTP-Trieste, Italy.

References

1. L. Vayssieres, A. Manthiram, *Journal of Physical Chemistry,* Vol. 107, pp. 2623–2625, 2003.

2. C.H. Lin, P. Shen, and S.Y. Chen, *Applied Physics B: Lasers and Optics,* Vol. 98, pp. 443–450, 2010.

3. B.P. Farrell, I.V. Sevonkaev, and D.V. Goia, *Platinum Metals Review,* Vol. 57, pp. 161–168, 2013.

4. *P.* Gibot and *L. Vidal*, *Journal of the European Ceramic Society,* Vol. 30, pp. 911–915, 2010.

5. D.C. Dube, D. Agrawal, and S. Agrawal, R. Roy, *Applied Physics Letters,* Vol. 90, pp. 124–105, 2007.

6. D.W. Kim, S. Seung-II, J.D. Lee, and S.G. Oh, *Materials Letters,* Vol. 58, pp. 1894–1898, 2004.

7. P. Berdahl, *Journal of Heat Transfer,* Vol. 117, pp. 355–358, 1995.

8. G. Carta, M. Natali, G. Rossetto, P. Zanella, G. Salmaso, S. Restello, V. Rigato, S. Kaciulis, and A. Mezzi, *Chemical Vapor Deposition,* Vol. 11, pp. 375–38, 2005.

9. S. Sahoo and Ch. Binek, *Philosophical Magazine Letters*, Vol. 87, pp. 259–268, 2007.

10. T. Thongkanluang, T. Kittiauchawal, and P. Limsuwan, *Ceramics International,* Vol. 37, pp. 543–548, 2011.

11. S. Khamlich, R. McCrindle, Z.Y. Nuru, N. Cingo, and M. Maaza, *Applied Surface Science,* Vol. 265, pp. 745–749, 2013.

12. B. Hou, X. Ji, Y. Xie, J. Li, B. Shen, and Y. Qian, *Nanostructured Materials,* Vol. 5, pp. 599–605, 1995.

13. A. Kawabata, M. Yoshinaka, K. Hirota, and O. Yamaguchi, *Journal of the American Ceramic Society,* Vol. 78, pp. 2273–2273, 1995.

14. M. Ocaña, *Journal of the European Ceramic Society,* Vol. 21, pp. 931–939, 2001.

15. G. Peters, K. Jerg, and B. Schramm, *Materials Chemistry and Physics,* Vol. 55, pp. 197–201, 1998.

16. D. Vollath, D.V. Szabo, and J.O. Willis, *Materials Letters,* Vol. 29, pp. 271–279, 1996.

17. Z. Pei, H. Xu, and Y. Chang, *Journal of Alloys and Compounds,* Vol. 468, pp. L5–L8, 2008.

18. U. Balachandran, R.W. Siegel, Y.X. Liao, and T.R. Askew, *Nanostructured Materials,* Vol. 5, pp. 505–512, 1995.

19. G. Schmid, *Clusters and Colloids: From Theory to Applications,* 1st ed., Wiley-VCH, New York, 1994.

20. D.M. Kaz, R. McGorty, M. Mani, M.P. Brenner, and V.N. Manoharan, *Nature Materials,* Vol. 11, pp. 138–142, 2012.

21. P.H. Holloway, K. Shanker, G.A. Alexander, and Li. De. Sedas, *Thin Solid Films,* Vol. 177, pp. 95–105, 1989.

22. V. Teixeira, E. Sousa, M.F. Costa, C. Nunes, L. Rosa, E. Roman, and J. Gago, *Thin Solid Films,* Vol. 392, pp. 320–326, 2001.

23. H.C. Barshilia, N. Selvakumar, K.S. Rajam, and A. Biswas, *Journal of Applied Physics,* Vol. 103, pp. 023507–023511, 2008.

24. C.G. Granqvist, Spectrally selective surfaces for heating and cooling applications. SPIE Publications, Washington, 1989.

25. Q. Zang and D. Mills, *Solar Energy Materials and Solar Cells,* Vol. 27, pp. 273–290, 1992.

26. M.F.M. Costa, V. Teixeira, and C.M. Nunes, *Solar Optical Materials XVI,* Vol. 3789, pp. 140–148, 1999.

27. C.N. Kennedy, Review of Mid- to High-Temperature Solar Selective Absorber Materials. *National Renewable Energy Laboratory Report,* NREL/TP-520-31267, 2002.

28. G.E. Mcdonald, *Solar Energy,* Vol. 17, pp. 119–122, 1975.

29. A. Ignatiev, P. O'neill, and G. Zajac, *Solar Energy Materials,* Vol. 1, pp. 69–79, 1979.

30. P.H. Holloway, K. Shanker, R.B. Pettit, and R.R. Sowell, *Oxidation of electrodeposited black chrome selective solar absorber films,* International conference on metallurgical coatings, San Diego, CA, USA. 1980

31. C.M. Lampert, *A chemical, structural, and optical characterization of a black chrome solar selective absorber.* Ph.D. Thesis, Berkeley, CA: Lawrence Berkeley Laboratory, 1980a.

32. P.M. Driver, *Solar Energy Materials,* Vol. 14, pp. 179–202, 1981.

33. W.F. Bogaerts, and C.M. Lampert, *Journal of Materials Science,* Vol. 18, pp. 2847–2975, 1983.

34. J.N. Sweet, R.B. Pettit, and M.B. Chamberlain, *Solar Energy Materials,* 10, 251–286, 1984.

35. G.B. Smith, R.C. Mcphedran, and G.H. Derrick, *Applied Physics A: Materials Science & Processing,* Vol. 36, pp. 193–204, 1985.

36. S. Brunold, U. Frei, B. Carlsson, K. Möller, and M. Köhl, *Solar Energy,* 68, 313–323, 2000

37. S.P. Sukhatme, J.K. Nayak, *Principles of thermal collection and storage.* Tata McGraw-Hill publishing, New Delhi, India, 2008.

38. A. Muehlratzer, G.P. Goerler, E. Erben, and H. Zeilinger, *Solar Energy,* Vol. 27, pp. 115–120, 1981.

39. G. Zajac, G.B. Smith, and A. Ignatiev, *Journal of Applied Physics,* Vol. 51, pp. 5544–5554, 1980.

40. K.D. Lee, W.C. Jung, and J.H. Kim, *Solar Energy Materials and Solar Cells,* Vol. 63, pp. 125–137, 2000.

41. R.B. Pettit and R.R. Sowell, *Black chrome solar selective coating.* Report Number: SAND-80-1480. Albuquerque, NM: Sandia National Laboratory, 1980.

42. C.M. Lampert, *Thin Solid Films,* Vol. 72, pp. 73–82, 1980b.

43. C.M. Lampert and J. Washburn, *J. Microstructure and optical properties of black chrome before and after exposure to high temperatures.* Second Annual Conference on Absorber Surfaces for Solar Receivers, Gounder, CO, pp. 24–25, 1979.

44. G.B. Smith and A. Ignatiev, *Solar Energy Materials,* Vol. 4, pp. 119–133, 1981.

45. L. Vayssieres and A. Manthiram, *Journal of Physical Chemistry,* Vol. 107, pp. 2623–2625, 2003.

46. S. Khamlich, O. Nemraoui, N. Mongwaketsi, R. Mccrindle, N. Cingo, and M. Maaza, *Physica B: Condensed Matter Journal*, Vol. 407, pp. 1509–1512, 2012.

47. J. Mougin, T. Le Bihan, and G. Lucazeau, *Journal of Physics and Chemistry of Solids,* Vol. 62, pp. 553–563, 2001.

48. T.R. Hart, R.L. Aggarwal, and B. Lax, *Light Scattering in Solids.* Proc. Int. Conf. on, Paris, pp. 174–179, 1971.

49. S. Khamlich, E. Manikandan, B.D. Ngom, J. Sithole, O. Nemraoui, I. Zorkani, R. Mccrindle, N. Cingo, and M. Maaza, *Journal of Physics and Chemistry of Solids*, Vol. 72, pp. 714–718, 2011.

50. M. Tabbal, S. Kahwaji, T.C. Christidis, B. Nsouli, and K. Zahraman, *Thin Solid Films,* Vol. 515, pp. 1976–1984, 2006.

51. A.E. Nielsen, *Kinetics of precipitation.* Pergamon Press, Oxford, UK, 1964.

52. C.N.R Rao, A. Müller, and A.K. Cheetham, *Nanomaterials chemistry: recent developments and new directions.* 1st *ed,* Wiley-VCH, Weinheim, 2007.

53. I.M. Lifshitz and V.V. Slyozov, *Journal of Physics and Chemistry of Solids, Vol.* 19, pp. 35–50, 1961.

54. C. Wagner, Theorie der Alterung von Niederschlägen durch Umlösen Ostwald–Reifung. *Z. Elektrochem*, Vol. 65, pp. 581, 1961.

55. S. Panigrahi, *Studies on growth kinetics of nanoparticles Formation in bulk solution. Roll No. 10600028, Department Of Chemical Engineering, National Institute of Technology, Rourkela, India*, 2010.

56. T. Sugimoto, *Advances in Colloid and Interface Science,* Vol. 28, pp. 65–108, 1987.

57. M. Bojinov, A. Galtayries, P. Kinnunen, A. Machet, and P. Marcus, *Electrochimica Acta,* Vol. 52, pp. 7475–7483, 2007.

58. W. Xiao, K. Xie, Q. Guo, and E.G. Wang, Growth and electronic structure of Cu on Cr_2O_3(0001). *Journal of Physics: Condensed Matter,* 15, 1155–1163, 2003.

59. M. Farooq, A.A. Green, and M.G. Hutchins, *Solar Energy Materials and Solar Cells,* Vol. 54, pp. 67–73, 1998.

60. K. Gelin, T. Boström, and E. Wäckelgård, *Thin Solid Films* 437, 25–33, 2003.

61. M. Kohl, B.O. Carlsson, S.E. Jorgensen, and A.W. Czanderna, *Performance and Durability Assessment: Optical Materials for Solar Thermal Systems.* 1st *ed,* Elsevier Science Publisher, New York, 2004.

62. O.P. Agnihotri and P.K. Gupta, *Solar Selective Surfaces.* 1st *ed,* Wiley-Interscience Publication, New York, 1981.

Chapter 10

Eco-Friendly Recycled Pharmaceutical Inhibitor/Waste Particle Containing Hybrid Coatings for Corrosion Protection

Victoria Bustos[1], Liseth Concha[1], Carmina Menchaca-Campos[1]*, Jorge Uruchurtu[1], Mario A. Romero[2], Marcos Esparza[3], Alba Covelo[4], Miguel Hernandez[4] and Estela Sarmiento[5]

[1]*Centro de Investigación en Ingeniería y Ciencias Aplicadas, Universidad Autónoma del Estado de Morelos, Cuernavaca, Morelos, México*

[2]*Universidad Autónoma Metropolitana, Azcapotzalco, Cd. México, México*

[3]*Universidad Autónoma Metropolitana, Iztapalapa, Cd. México, México*

[4]*Universidad Nacional Autónoma Mexico, Cd. México, México*

[5]*Universidad Tecnológica Emiliano Zapata, Temixco, Morelos, México*

**Corresponding author*: cmenchaca@uaem.mx

Abstract

Eco-friendly coatings are a step forward to protect the environment and recycled expired medicines and waste mesoporous particles used as containers combined with waterborne organic coating schemes, seem a good idea to protect the environment. This chapter outlines such schemes, giving examples of them. Discarded fluconazole and lansoprazol medicines are used to obtain the inhibitors, combining with waste silica or kaolinite particles as *containers* being part of a waterborne alkyd organic coating. The hybrid coating system efficiency is evaluated for steel corrosion, in simulated corrosive environment, using electrochemical impedance and polarization techniques. Good corrosion protection performance is obtained for the coating system for extended periods of immersion. The results demonstrate the good barrier properties of the hybrid coatings, showing the particles task to store and liberate the corrosion inhibitor, when it is needed.

Keywords: Eco-friendly recycled pharmaceutical inhibitor, waste particle container, hybrid coatings, steel, chloride media

10.1 Introduction

Most of the infrastructure and operating machinery are made of steel, exposed to the atmosphere, and as stated by the Mexican Chamber of Steel Industries, around 25% of steel production is dedicated to replace damaged structures due to atmospheric corrosion. In exposed structures to the atmosphere, corrosion rates are determined mainly by the time of wetness and atmospheric pollution. A wide variety of corrosion protection possibilities are available and with adequate application allow extension of the structure's useful life. Most protection schemes are metallic and/or organic coatings, and the success will depend on the knowledge of the actual atmospheric corrosiveness of the area and the proper selection of the coating [1, 2].

On the other hand, some chemical substances with atoms such as phosphor, sulphur, nitrogen and oxygen with π bonds in their molecules known as inhibitors are effective to control metallic corrosion [3, 4]. These characteristics allow them to be adsorbed over the metal surface and consequently improve the inhibition efficiency. Other inhibitors include inorganic compounds such as chromates, dichromates, nitrates and others very efficient but very harmful to the environment are now starting to be substituted by natural products, non-toxic to the environment with corrosion inhibition properties.

Nevertheless, inhibitor efficiencies depend not only on the metal structure, but also from the parameters concerned, for atmospheric corrosion environmental parameters such as relative humidity, time of exposure and the type and concentration of pollutants: deposited particles, sulphur dioxide and/or sodium chloride.

10.1.1 Recycled Pharmaceutical Inhibitors

Recently, some pharmaceutical drugs such as antibiotics, painkillers, gastric treatment drug, and so on derived chemicals synthesized [5–16] were tried as possible corrosion inhibitors for different metals. Most researches were made for steel in acid solutions, due to the interest in process industrial applications. Also, the inhibition activity of anti-fungal drugs based on azole compounds has been tried for aluminium or steel in acid corrosion, but little or no work in near neutral or neutral solutions [17–20]. The azole compounds (heterocyclic compounds derived from pirrole and tiophene obtained by the substitution of one of the =CH– groups from the ring by a nitrogen atom) form a pharmaceutical heterogeneous family sharing the presence of an azole ring, therefore the antifungal action mechanism, consists in the inhibition of the ergosterol synthesis [21]. They have a special characteristic, being stable to temperature. 2-(2,4-Difluorophenyl)-1,3-bis(1H-1,2,4-triazol-1-yl)propan-2-ol(fluconazole) [3, 4] is an antifungal drug structurally composed of two rings of type 1,2,4 triazole, a benzene ring ortho and para-difluorine and tertiary alcohol. Obot and Obi-Egbedi [17–20] suggest that in acid solutions (pH1), the fluconazole has excellent properties as corrosion inhibitor on aluminium and its alloys. Recently, Jebakumar and Sethuraman [21] found that fluconazole has inhibitory activity on mild steel corrosion in an acid media. Other gastric treatment pharmaceutical drugs are based on imidazole compounds, which is a known corrosion inhibitor substance.

Lansoprazol is a compound comprising the basic structure of 2-mercaptobenzoimidazole in its oxidized form, being an efficient proton pump inhibitor, since it suppresses the gastric acid segregation. It can be considered as a green corrosion inhibitor, primarily being a medicament for ulcers caused by gastro-esophageal reflux disease. The compound contains π electrons and hetero-atoms such as nitrogen, sulphur, oxygen and fluorine. For acid corrosion conditions over mild steel, it had proved efficient corrosion inhibition. A further possible application is under neutral or near-

neutral solutions in the presence of chloride ions, since localized pitting corrosion involves the production of HCl within pits.

10.1.2 Hybrid Coatings

In the 1990s, the use of water-based paint coatings became extensive due to environmental reasons, substituting the harmful solvent-based coatings, rendering less polluting. In addition, the constant environmental changes in urban and industrial areas lead to the research for a new generation of corrosion coatings that control or slow down the action of aggressive environmental agents on the metallic substrate. In this context, an '*intelligent'* system using ferric nitrate ($Fe(NO_3)_3$) as a corrosion inhibitor, for steel in a sulphate chloride solution simulating an aggressive urban environment, was proposed [22, 23]. It was found that this system reduces the corrosion rate of mild steel, two orders of magnitude. As Menchaca and coworkers [22] state that polymeric materials efficiency as corrosion protection coatings for metals increase when polymeric ligands are modified using corrosion inhibitors. Nanocontainers with storage properties, liberating inhibitors in a controlled way, can be used to manufacture a new family of hybrid coatings that respond to changes within the coating environment or its integrity. Liberation of encapsulated inhibitors within nanocontainers is activated by the corrosion process itself, preventing spontaneous leaking out of the inhibitor from the coating. With this restriction, it is possible to reach the double goal of corrosion protection by a barrier and inhibitor mechanism of metallic elements. The research and use of nano or mesoporous particles such as carbon fibres, graphene, silica, modified nylon fibres, and so on as inhibitor storage containers, are becoming common [22–37].

Therefore bearing in mind the former premises, development of recycled outdated pharmaceutical discarded by millions, with combined mesoporous particles waste residues; a hybrid water-based corrosion protection coating formed seems a good solution for the environment.

10.2 Hybrid Coating Preparation

10.2.1 Recycled Pharmaceutical Inhibitors

Expired medicines can be tested as corrosion inhibitors, since the active component only degrades slightly. An important study by the Food and Drug Administration (FDA) in 1985 demonstrated that 90% of pharmaceutical drugs maintain stability long after outdated date.

Outdated discarded medicine capsules for gastric treatment, 2-[[[3-Methyl-4-(2,2,2-trifluoroethoxy)-2-pyridyl]-methyl]sulfinyl]benzimidazole [*103577-45-3*] (lansoprazol), with benzimidazole active component accounting for 25 mg in total weight were used in dissolution. Two solutions were prepared: the first one contains 100 ml methanol and the second with 50 ml acetone and 50 ml methanol. Another example is a pharmaceutical drug extracted from an antifungal (afungil) to obtain the active component fluconazole. The content of two capsules (130 mg of fluconzole) were poured into 50 ml of methanol as a solvent, agitating for 20 min, filtrating the solution afterwards and after evaporation a white crystal like powder (fluconazole) was obtained and dried at 60 °C for 24 h.

10.2.2 Mesoporous Particles

As mesoporous particles, kaolinite waste residue particles from the ceramic industry were used for inhibitor storage. In a porcelain capsule, 5 mg kaolinite particles sample was thermally treated for 24 h at different temperatures, finding the best condition at 400 °C, better particle dispersion and interlaminar distance of 7.16 Å. After thermal treatment, kaolinite particles were successively washed with oxygen peroxide solution, acetone, methanol and dried at 120 °C, for 1 h [44].

Afterwards, loading of the inhibitor into the kaolinite container particles was performed; kaolinite particles were added into the stirring solution containing the different inhibitor concentrations and mixed. Then, the solution was removed and particles were left to dry at room temperature, and the distribution was kaolinite 86.8% and lansoprazol 13.2%. As an example, Table 10.1 shows the EDX characterization: kaolinite, lansoprazol and the inhibitor loaded particles in percent composition, suggesting the loading was achieved.

Table 10.1 EDX weight % of lansoprazol loaded particles and components.

Elements	Kaolinite	Lansoprazol	Loaded particles
Carbon	7.63	39.54	21.95
Nitrogen	–	2.2	1.79
Oxygen	56.33	39.81	47.54
Fluorine	–	–	0.71
Sulphur	–	0.01	0.03
Silica	30.96	10.13	18.71
Aluminium	5.09	1.72	2.42

Similar approach was performed for fluconazole loading but using silica particles as reported in the literature [22].

10.2.3 Hybrid Coating

Hybrid coating consists of a mixture of an inorganic part (kaolinite or silica inhibitor loaded with sufficient inhibitor to obtain desired concentration) and the organic part (commercial waterborne acrylic). After being prepared, a hybrid coating layer was applied to the mild steel abraded surface, by hand brush. After drying for 24 h at room temperature, a second layer was applied and left to dry for 48 h obtaining a film thickness of 111 μm, ready for electrochemical evaluation.

10.2.3.1 Characterization

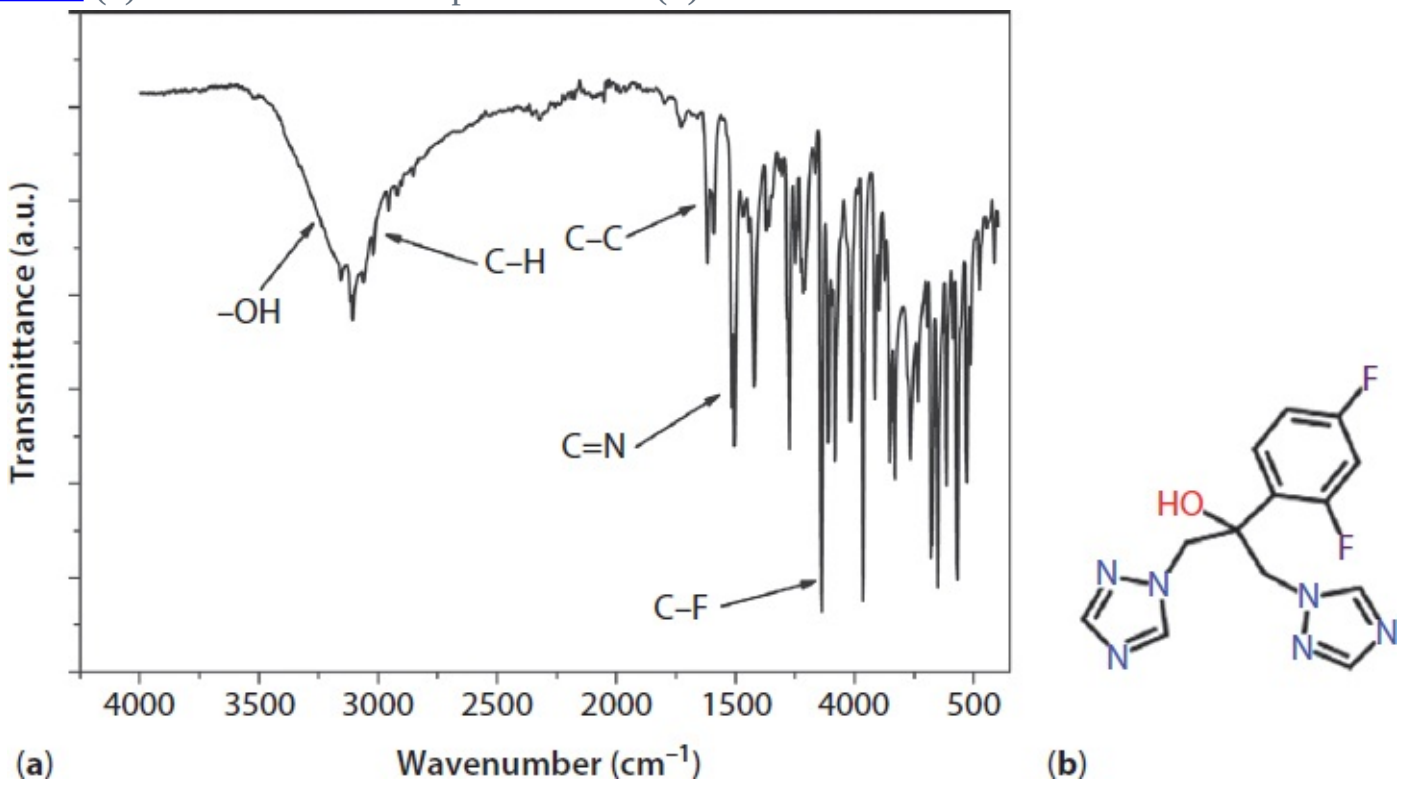
Hybrid coating and particle components characterization was performed using scanning electron microscopy (SEM), X-ray diffraction (XRD) and particle size laser measurement system. The active powder can be characterized by Fourier Transformed Infrared Spectroscopy (FTIR) with Attenuated Total Reflectance (ATR) being extremely reliable and recognized fingerprint characterization methods [22].

10.3 Hybrid Coatings Performance

10.3.1 Materials Characterization

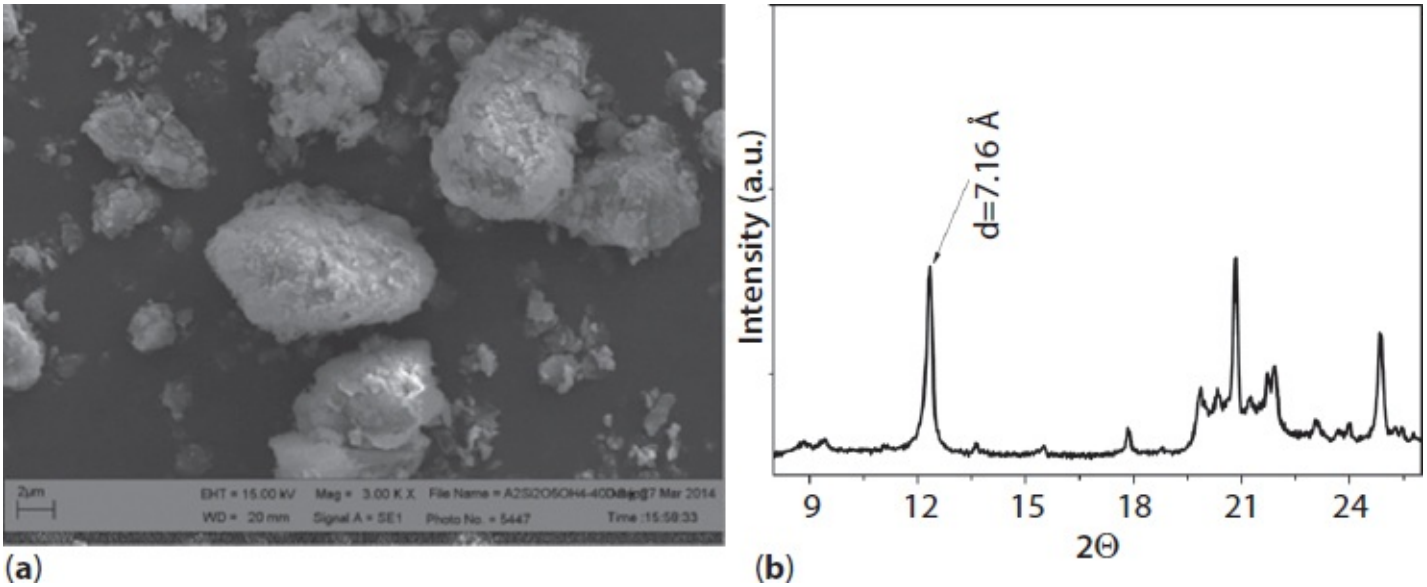
Figure 10.1(a) depicts the IR absorption spectrum. The characteristic absorption bands of fluconazole appear at 1135 cm^{-1} for the C–F bond, in the benzene ring; in 1500 cm^{-1} C=N; C–C bond of the aromatic ring absorbs in 1520–1623 cm^{-1}; and finally, the bands for the C–H and –OH bonds appear around 3100 cm^{-1}. Figure 10.1(b) presents the chemical structure.

Figure 10.1 (a) FTIR fluconazole spectrum and (b) chemical structure.



After kaolinite treatment preparation, particle size is in the range of 2–16 μm (Figure 10.2(a) SEM micrograph), as well as the characteristic peak is present at 2Θ angle in the XRD spectrum (Figure 10.2(b)), as reported in the literature (44).

Figure 10.2 Kaolinite particles after treatment (a) SEM micrograph and (b) XRD spectrum.



10.3.2 Electrochemical Inhibitor Evaluation

To evaluate the corrosion performance, electrochemical methods were performed in mild steel (C: 0.16%, Mn: 0.51% and Fe: 99.33% wt.% composition) samples. As a reference, a second group of coupons were used for inhibitor performance (optimal concentration) and efficiency and third group for coating evaluation. The electrolytic medium was Na_2SO_4 0.1 M + 3% wt. NaCl, presenting highly corrosive properties, simulating an aggressive urban marine atmosphere. All electrochemical evaluations performed include corrosion potential, electrochemical impedance spectroscopy and potentiodynamic polarization, the details being reported elsewhere [40–43].

The measurements were made at room temperature by immersing the working electrode in the electrolyte solution in the absence and presence of different inhibitor concentrations and for coating evaluation and performance. Polarization resistance curves (Tafel plots) were obtained, and the Tafel slopes in the anodic and cathodic curves were extrapolated to the corrosion potential to obtain the corrosion current density (i_{corr}) and the corrosion potential (E_{corr}).

The corrosion inhibition efficiency (IE %) was calculated from the corrosion current density (i_{corr}) using the following relation:

$$IE(\%) = \left[\frac{i_{corrI} - i_{corr}}{i_{corrI}}\right] \times 100, \quad (10.1)$$

where i_{corr} is the corrosion current density without inhibitor and i_{corr} is the corrosion current density with inhibitor.

Alternatively, from EIS measurements in an AC frequency range of 10 KHz to 0.1 Hz, with a 20 mV amplitude, and Nyquist and Bode plots the charge transfer resistance (R_{ct}) values were used to calculate the inhibition efficiency as in:

$$IE(\%) = \left[\frac{R_{ct}(I) - R_{ct}}{R_{ct}(I)}\right] \times 100 \quad (10.2)$$

where $R_{ct}(I)$ is the charge transfer resistance with inhibitor and R_{ct} is the charge transfer resistance without inhibitor. Also, for the coating evaluation impedance measurements allow to obtain the total, charge and coating impedance, as well as coating and double layer capacitance.

10.3.2.1 Potentiodynamic Polarization

Figure 10.3 shows the potentiodynamic polarization curves of mild steel in the sulphate–sodium chloride solution, at room temperature, for both inhibitors (fluconazole and lansoprazol). It could be observed that the cathodic and anodic reactions were modified, resulting in the decrease of the corrosion current and ennoblement of the corrosion potential. These results are shown in Table 10.2. This is due to the adsorption of inhibitor molecules on the mild steel surface retarding the corrosion reaction. The displacement of both E_{corr} and i_{corr} suggests that they act as mixed inhibitors (both reactions, anodic and cathodic).

Figure 10.3 Polarization curves for mild steel with different inhibitors concentrations of: (a) fluconazole and (b) lansoprazol.

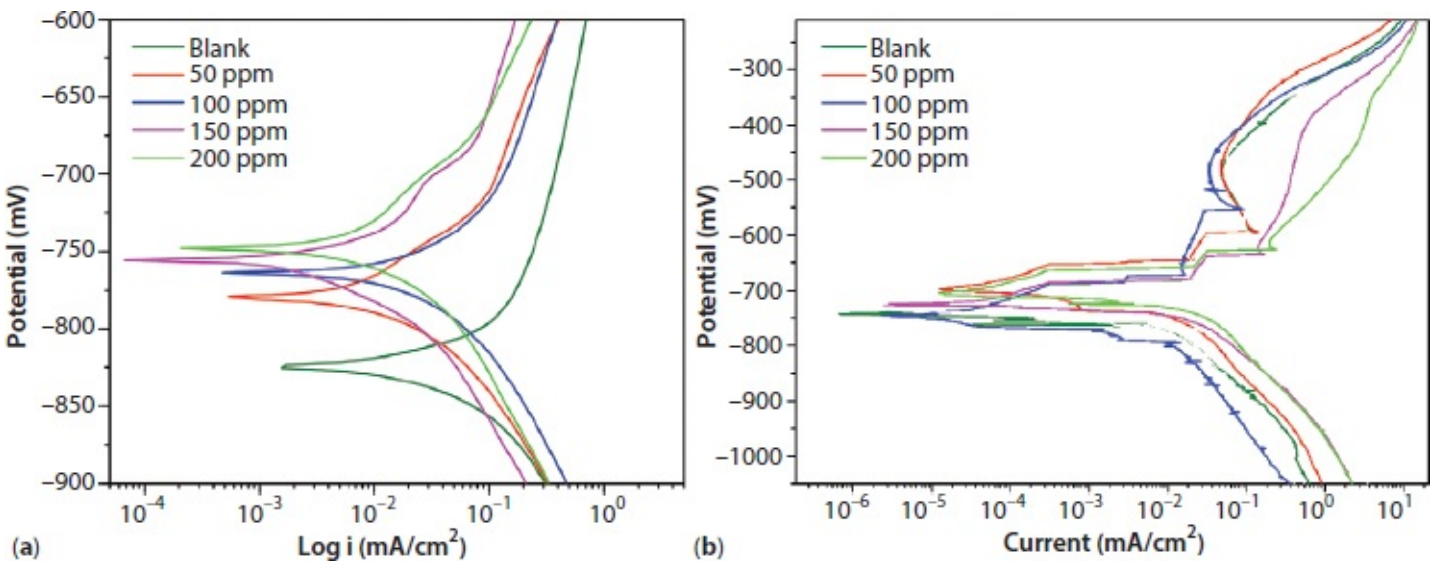


Table 10.2 Polarization parameters for mild steel with different concentrations of inhibitors.

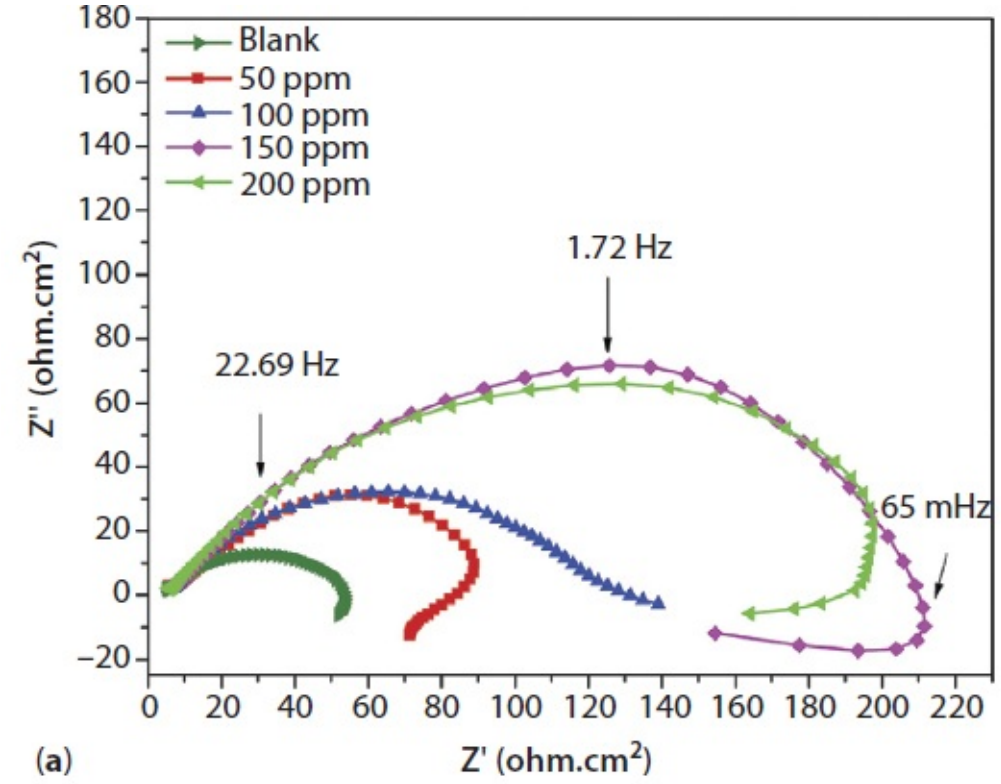
Conc. (ppm)	Fluconzole E_{corr} (mV)	Lanzoprasol E_{corr} (mV)	Fluconzole i_{corr} (μA/cm²)	Lanzoprasol i_{corr} (μA/cm²)	Fluconazole IE (%)	Lansoprazol IE (%)
Blank	−828	−745	3140	3100	–	–
50	−758	−697	2690	300	74	90
100	−755	−749	2590	150	75	95
150	−748	−725	1630	250	84	91
200	−758	−700	2580	750	73	75

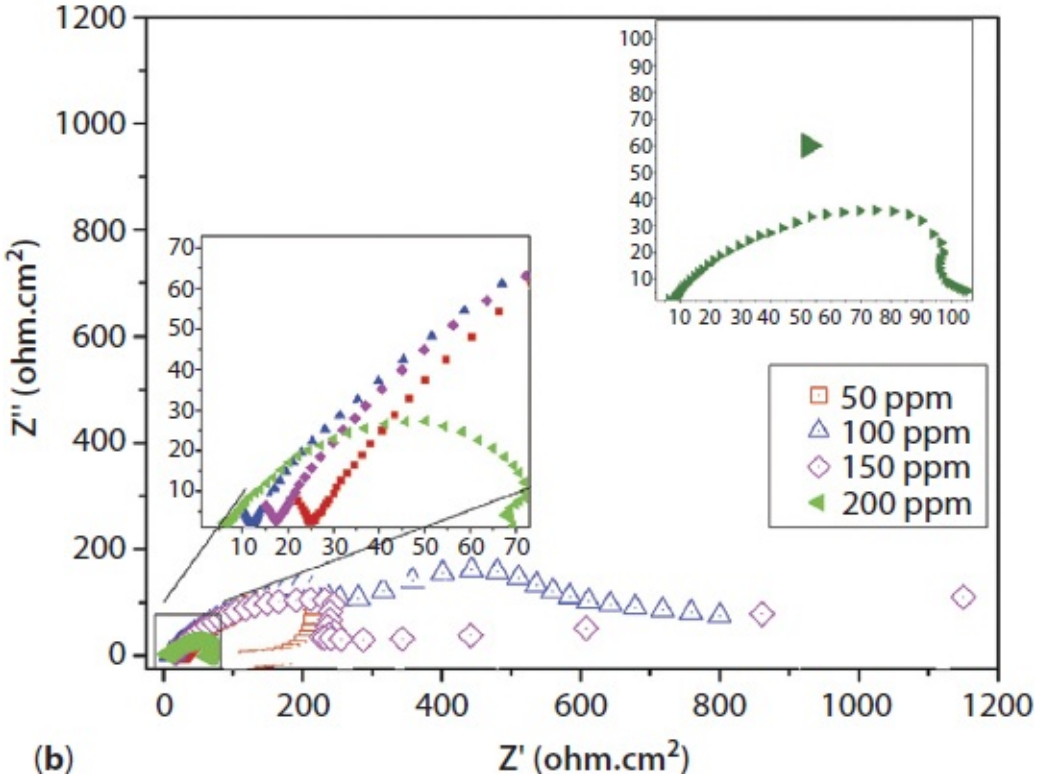
The inhibition efficiency increases with the increase in concentration of the inhibitor as well. For the inhibitors, the best concentration was 150 ppm, with 84% efficiency for fluconazole, and 100 ppm with 95% for lansoprazol, respectively.

10.3.2.2 Electrochemical Impedance

Electrochemical impedance was recorded for mild steel corrosion in the sulphate chloride solution in the absence and presence of different inhibitor concentrations, for inhibitor performance (see Figure 10.4). For the blank uninhibited solution, Nyquist plot described a single, depressed capacitive-like semicircle at all frequencies with its centre in the real axis, indicating that the corrosion process is under charge transfer control from the metal to the electrolyte through the electrochemical double layer. The charge transfer resistance (R_{ct}) value is a measure of electron transfer across the metal surface and is inversely proportional to the corrosion rate.

Figure 10.4 Nyquist impedance plots of mild steel corrosion with different inhibitor concentrations of: (a) fluconazole and (b) lansoprazol.





In the presence of inhibitors, capacitive depressed semicircles at high and intermediate frequencies are registered, and a second, inductive loop or a '*tail-like*', is present at lower frequencies. This behaviour indicates the corrosion process is now under adsorption–desorption control of an intermediate species [45]. As inhibitors concentration increase, the capacitive semicircles diameter increased, reaching its highest values.

Sometimes, inhibitors react with the environment forming insoluble, external, protective films, which protects the metal diminishing corrosion. It is generally accepted that the first step during the adsorption of an organic inhibitor on a metal surface, usually involves replacement of water molecules absorbed on the metal surface [46]:

(10.3) $Inh_{sol} + xH_2O_{ads} => Inh_{ads} + xH_2O_{sol}$

The inhibitor may then combine with freshly generated Fe^{2+} ions on the steel surface, forming metal-inhibitor complexes [47, 48]:

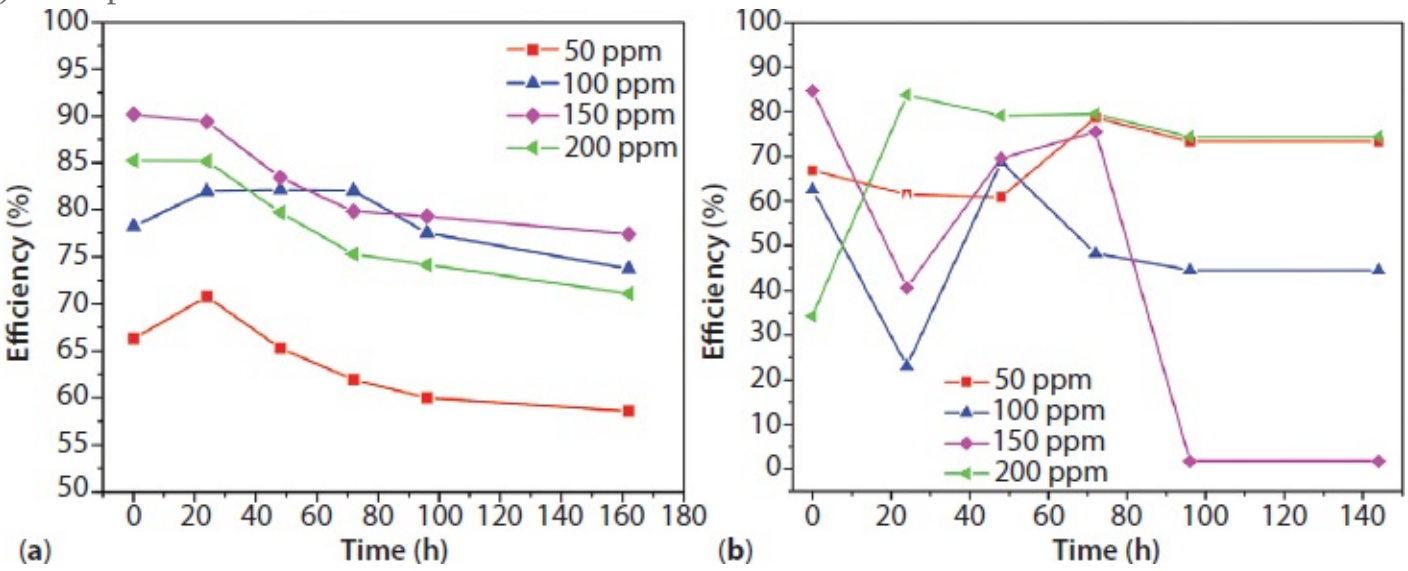
(10.4) $Fe => Fe^{2+} + 2e^-$

(10.5) $Fe^{2+} + Inh_{ads} => [Fe\text{-}Inh]_{ads}^{2+}$

The resulting complex, depending on its relative solubility, can either inhibit or catalyze further metal dissolution or increase its corrosion rate. At low concentrations, the amount of inhibitor is insufficient to form a compact complex with the metal ions, so resulting adsorbed intermediate may be readily soluble in the environment. But at relatively higher concentrations, more molecules become available for complex formation, which subsequently diminishes the solubility of the surface layer, leading to improve the inhibition of metal corrosion [46].

Figure 10.5 shows the efficiency, as function of time of immersion. The inhibitor efficiency increases in the beginning, as the fluconazole concentration increases (Figure 10.5a). The behaviour of all systems follows the same trend, the inhibitor continues protecting the metal after 168 h of testing but with lower efficiency. At the end of the tests, the 150 ppm of fluconazole was the best concentration for the corrosion inhibition of the mild steel in the referred solution, with efficiency around 80%. In the case of the lansoprazol inhibitor, the first few days the 200 ppm concentration condition steel sample presents the best behaviour. Afterwards, after 50 days of immersion, the sample in the 50 ppm lansoprazol concentration improves the efficiency remaining till the end of the experiment, with 75% efficiency. The behaviour observed (Figure 10.5) may be due to desorption of the inhibitor (200 ppm) from the steel surface, while protective film may be formed for the lower concentration (50 ppm).

Figure 10.5 Inhibitor efficiency for different concentrations as function of time for: (a) fluconazole and (b) lansoprazol.



10.3.3 Electrochemical Hybrid Coating Evaluation

Electrochemical impedance was recorded to evaluate the hybrid coating performance for mild steel corrosion in the sulphate/chloride solution in the absence and presence of the hybrid coatings, for different periods of immersion. Some samples surfaces were scribed in order to stimulate the inhibitor action [22, 41]. Figure 10.6(a) shows the total impedance for the hybrid fluconazole/silica

particles and waterborne alkyd coating, for samples prepared for different inhibitor concentrations and compared with the steel sample (blank). Similar trends were observed, but the 100 and 150 ppm maintained its total impedance above and around 100,000 Ω cm^2.

Figure 10.6 Total impedance as function of time for hybrid waterborne alkyd coating containing: (a) fluconazole/silica particles prepared for different inhibitor concentrations and (b) lansoprazol/kaolinite particles for blank, scribed and fully coated surface.

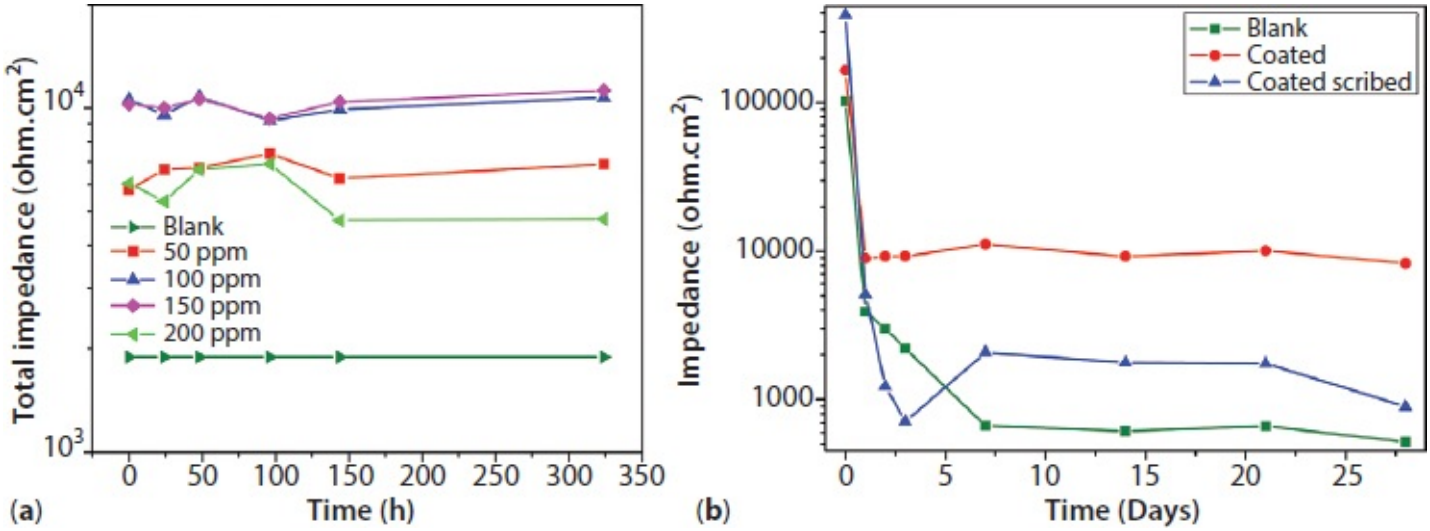
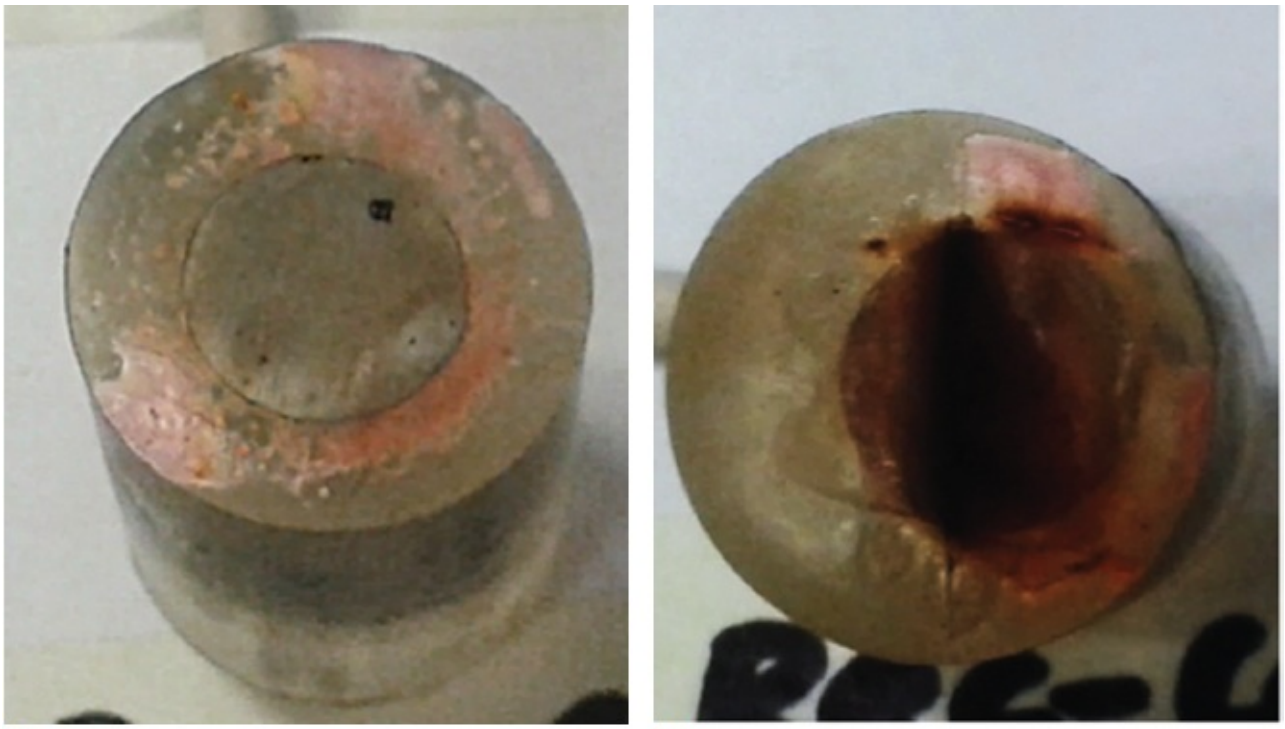


Figure 10.6(b) presents the total impedance as a function of time of immersion, for the lansoprazol/kaolinite/waterborne alkyd coating. A comparison among blank scribed and fully coated samples are presented. The total impedance increased, under these different surface conditions, and the inhibitor action may be responsible for the higher impedance value obtained with respect to the blank sample.

As an example, Figure 10.7 presents photographs showing the steel surface condition in the presence of the hybrid coating after immersion as a function of time test, without and with a scribe across the coating surface. Corrosion products are visible in the scribed sample promoted by the lansoprazol inhibitor.

Figure 10.7 Mild steel samples after 28 days of immersion (a) coated and (b) scribed coating surface.



(a) (b)

These inhibitors also promote the corrosion protection of damaged defect coating sites, by stimulating the formation of protecting films over the exposed metal surface. This may be due to the growth of insoluble complex oxide compounds over the damaged area. On the other hand, this could in turn promote disbondment of the coating from the metal surface [41].

10.4 Conclusions

The inhibitors obtained from discarded pharmaceuticals present good inhibitory activity over mild steel, in the sulphate–chloride solution, as shown. The best inhibitor concentrations were 150 ppm for fluconazole and 100 ppm for lansoprazol, maintaining its effect but at lower efficiencies, even after 8 days. Waste particles such as kaolinite acted as inhibitor containers and part of the coating schemes proposed. For aggressive immersion conditions tested, both coatings present good performance that will reflect favourably under atmospheric exposure.

Recycled hybrid coatings appear as a good proposition to develop eco-friendlier corrosion protection coatings.

Acknowledgment

The authors gratefully acknowledge to CONACyT for the financial support.

References

1. M. Morcillo, E. Almeida, M. Marrocos, and J. Uruchurtu, *Corrosión y Protección de Metales en las Atmósferas de Iberoamérica, parte 1. Mapas de Iberoamerica de Corrosividad Atmosferica,* Eds. CYTED, Madrid, 1999.

2. M. Morcillo, E. Almeida, F, Fragata, and Z. Panossian, *Corrosión y Protección de Metales en las*

Atmósferas de Iberoamérica, parte II. Proteccion Anticorrosiva de Metales en las Atmosferas de Iberoamerica. Eds. CYTED, Madrid, 2002.

3. Y.S. Kara, Seda G. Sagdin, and A. Esme, *Protection of Metals and Physical Chemistry of Surfaces*, Vol. 48, pp. 710–721, 2012.

4. U. Ergun and K.C. Emregul, *Journal of Materials Engineering and Performance,* Vol. 23, pp. 213–221, 2014.

5. G. Gece, *Corrosion Science,* Vol. 53, pp.3873–3898, 2011.

6. S. Ramesh and S. Rajeswari, *ElectrochimicaActa,* Vol. 49, pp. 811–820, 2004.

7. B.P. Markhali, R. Naderi and M. Sayebani, *Anti-Corrosion Methods and Materials,* Vol. 61, pp. 300–306, 2013.

8. E. Sayed. E. Ashry, A.E. Nemr, S.A. Esawy and S. Ragab, *ElectrochimicaActa,* Vol. 51, pp. 3957–3968, 2006.

9. A. Popova, M. Christov and A. Zwetanova, *Corrosion Science,* Vol. 49, pp. 2131–2141, 2007.

10. F. Bentiss, M. Traisnel, H. Vezin and M. Lagreneé, Industrial Engineering Chemical Research, Vol. 39, pp. 3732–3736, 2000.

11. W. Li, Q. He, C. Pei, and B. Hou, *ElectrochimicaActa*, Vol. 52, pp. 6386–6394, 2007.

12. W. Li, Q. He, S. Zhang, C. Pei, and B.Hou, *Journal of Applied Electrochemistry,* Vol. 38, pp. 289–295, 2008.

13. H.B. Ouici, O.Benali, Y. Harek, and L. Larabi, *Research. Chemical Intermediates,* Vol. 39, pp. 2777–2793, 2013.

14. D. Gopi, K.M. Govindaraju, and L. Kavitha, *Journal of Applied Electrochemistry,* Vol. 40, pp. 1349–13567, 2010.

15. A. Espinoza-Vazquez, G.E. Negrón-Silva, R. Gonzalez-Olvera, D. Angeles-Beltrán, H. Herrera-Hernández, M. Romero-Romo, and M. Palomar-Pardavé, *Materials Chemistry and Physics,* Vol. 145, pp. 407–417, 2014.

16. A.Y. Musa, A.A.H. Kadhum, A.B. Mohamad, M.S. Takriff, A.R. Daud, and S.K. Kamarudin, *Corrosion Science,* Vol. 52, pp. 526–53, 2010.

17. I.B. Obot, *Portugaliae. Electrochimica Acta,* Vol. 27, pp. 539–553, 2009.

18. I.B. Obot, N.O. Obi-Egbedi, S.A. Umoren, and E.E. Ebenso, *Chemical Engineering Communication,* Vol. 198, pp. 711–725, 2011.

19. I.B. Obot, and N.O. Obi-Egbedi, *Corrosion Science,* Vol. 52, pp. 198–204, 2010.

20. I.B. Obot, and N.O. Obi-Egbedi, *Colloid Surface A: Physicochemical Engineering Aspects,* Vol. 330, pp. 207–212, 2008.

21. T. Jebatumar and M.G. Sethuraman, *Electrochemistry,* Article ID256086, 2013.

22. J. Uruchurtu, C. Avila, R. Cruz, C. Menchaca, and G. Sepúlveda, *Journal of Nanotechnology,* Article ID461313, 2011.

23. C. Menchaca, S. Hernández, A. Tejeda, E. Sarmiento, J. Uruchurtu, and M.A. Sánchez, *Adsorption Science and Technology,* Vol. 29, pp. 507–517, 2011.

24. A.N. Khramov, N.N. Voevodin, V.N. Balbyshev, and M.S. Donley, *Thin Solid Films,* Vol. 447–448, pp. 549–557, 2004.

25. M.L. Zheludkevich, R. Serra, M.F. Montemor, K.A. Yasakau, I.M.M. Salvado, and M.G.S. Ferreira, *Electrochimica Acta,* Vol. 51, pp. 208–217, 2005.

26. R.G. Buchheit, S.B. Mamidipally, P. Schmutz, and H. Guan, *Corrosion,* Vol. 58, pp. 3–14, 2002.

27. R.B. Leggat, S. R. Taylor, W. Zhang, and R.G. Buchheit, *Corrosion,* Vol. 58, pp. 283–291, 2002.

28. W. Meier, *Chemical Society Reviews,* Vol. 29, pp. 295–303, 2000.

29. C.S. Peyratout, H. Möhwald, and L. Dähne, *Advanced Materials,* Vol. 15, pp. 1722–1726, 2003.

30. S. Förster and T. Plantenberg, *AngewandteChemie International Edition,* Vol. 41, pp. 689–714, 2002.

31. A. Manna, T. Imae, K. Aoi, M. Okada, and T. Yogo, *Chemistry of Materials,* Vol. 13, pp. 1674–1681, 2001.

32. A. Sunder, M. Krämer, R. Hanselmann, R. Mülhaupt, and H. Frey, *AngewandteChemie International Edition,* Vol. 38, pp. 3552–3555, 1999.

33. X. Lu and Z. Xin, *Colloid and Polymer Science,* Vol. 284, pp. 1062–1066, 2006.

34. C.I. Zoldesi, C.A. Van Walree, and A. Imhof, *Langmuir,* Vol. 22, pp. 4343–4352, 2006.

35. G. Schneider and G. Decher, *Nano Letters,* Vol. 4, pp. 1833–1839, 2004.

36. E. Abdullayev, R. Price, D. Shchukin, and Y. Lvov, *Interfaces,* Vol. 1, pp. 1437–1443, 2009.

37. D.V. Andreeva and D.G. Shchukin, *Materials Today,* Vol. 11, pp. 24–30, 2008.

38. N. Vaszilcsin, V. Ordodi, and A. Borza, *International Journal of Pharmaceutics,* Vol. 431, pp. 241–244, 2012.

39. S. Kugler, K. Kowalczyk, and T. Spychaj, *Progress in Organic Coatings,* Vol. 85, pp. 1–7, 2015.

40. J. Uruchurtu-Chavarin and J.M. Malo, *Trends in Corrosion Research,* Vol. 2, pp. 49–58, 1997.

41. C. Menchaca, I.E. Castañeda, A. Soto-Quintero, R. Guardián, R. Cruz, M.A. García-Sánchez, and J. Uruchurtu, Characterization of a “Smart” Hybrid Varnish Electrospun Nylon Benzotriazole Copper Corrosion Protection Coating, International *Journal of Corrosion*, Vol. 2012, Article ID 925958, 2012.

42. M. Hernández, J. Genescá, J. Uruchurtu, and J. Barba, *Corrosion Science,* Vol. 51, pp. 499–510, 2009.

43. L. Mariaca-Rodríguez, J. Genescá-Llongueras, J. Uruchurtu-Chavarín, and L.S. Hernández, *Corrosividad Atmosférica (MICAT-México),* Plaza y Valdes, México, 1999.

44. É. Makó, J. Kristóf, E. Horváth, and V. Vágvölgyi, *Applied Clay Science,* Vol. 83–84, pp. 24–31, 2013.

45. M.A. Ameer and A.M. Fekry, *International Journal of Hydrogen Energy,* Vol. 35 pp. 7641–7651, 2010.

46. A. Rodríguez-Torres, M.G. Valladares-Cisneros, and J.G. Gonzalez-Rodríguez, *International Journal of Electrochemical Science,* Vol. 10, pp. 4053–4067, 2015.

47. B.P. Markhali, R. Naderi, and M. Mahdavian, *Journal of Electroanalytical Chemistry,* Vol. 56, pp. 714–729, 2014.

48. B. Ramezanzadeh, S.Y. Arman, M. Mehdipour, and B.P. Markhali, *Applied Surface Science,* Vol. 289, pp.129–140, 2014.

Chapter 11

Chemical Interaction of Modified Zinc–Phosphate Green Pigment on Waterborne Coatings in Steel

Miguel Hernandez[1]*, Carmina Menchaca[2], Jorge Uruchurtu[2], and Alba Covelo[1]

[1]*Facultad de Ingeniería, CENISA-DIMEI, Universidad Nacional Autónoma de México, México D.F., Méxic*

[2]*Centro de Investigación en Ingeniería y Ciencias Aplicadas, IICBA, Universidad Autónoma del Estado de Morelos, Cuernavaca, Morelos, México*

**Corresponding author.* mahdz2010@comunidad.unam.mx

Abstract

The use and incorporation of non-toxic, environmental green pigments in coatings binders have become of great importance because environmental regulations has forbidden the use of chromate or lead compounds. However, the efficiency of the green pigments is lower than that obtained by the classical compounds. For this reason, during the past decades, a new class of green pigments based on zinc phosphate composition has been develop in order to protect the steel substrate. This ecological alternative offers a good inhibitive effect in alkaline media depending on the cationic nature of the zinc phosphate pigment. The specific case of the zinc– aluminium–phosphate (ZAP) has evidenced higher protection properties because the coating failure has been notably reduced at cathodic delamination conditions, due to the formation of a zinc–phosphate layer (α-hopeite). The purpose of this chapter is to explain the protection mechanism against corrosion and the chemical interaction between the ZAP pigment and the steel substrate.

Keywords: Coating, steel, zinc–phosphate pigments, green pigment, protection properties

11.1 Introduction

In the mid-nineteenth century, the use of zinc as part of pigments in coatings became of great interest in the automotive industry. Zinc-rich paints resulted in new formulations to protect steel in chlorinated media. However, an intense study of protection mechanisms of these new formulations started in 1940 [1], where a galvanic action between zinc and steel as primary protection stage was first identified. Afterwards, a second protection stage consisted of zinc salts precipitates covering the metal substrate slowing down the metal oxidation by inhibiting effects was proposed [1, 2]. Factors such as oxygen permeability through the coatings, barrier pigments (chromates and molybdates) and

polymeric binders enhance notably the barrier properties of the coatings. However, detailed information about the contribution of each constituent into the polymeric matrix has not been completely understood.

Zinc–phosphate-derived pigments on iron have led to numerous researches concerning both mechanical and electrochemical properties because their inhibiting action has less toxicity and environmental problems that those who formed passive film layer on the steel surface [3]. Zinc–phosphates that contain low solubility are thought to be a reservoir of phosphate anions that are released during the formation of a protective oxide layer in alkaline media [4]. It has been also proposed that the inhibiting mechanisms of modified phosphates coatings is due to low solubility in water and a neutralizing interaction of the vehicles and corrosive agents; the passivating or inhibiting process occurs by dissolution of ionic species from the pigment [5]. This latter explanation becomes more efficient when additional pigments are added to the binder. In a previous publication [6], it was evidenced that phosphate anion showed a typical pH buffering response at about 7.2 that corresponds to the nominal second ionization pK_a for phosphoric acid (PO_4^-), indicating that phosphates act as pH-dependent inhibitors. If pH raises the PO_4^{2-} species predominate; on the other hand, if an acid media prevails the PO_4^{3-} species is found. It should be borne in mind that zinc–phosphate has the ability to form adhesion and inhibitor complexes that according to particle structure and particle size distribution; the steel shall be phosphated mainly in anodic areas [7].

Modified zinc–phosphate pigments such as zinc–aluminium–phosphate (ZAP) pigment has higher solubility allowing the released of major phosphate anions in alkaline pH conditions [6]. However, it must be taken into account that increasing the pigment solubility may lead to major delaminated and blister propagation area due to the dissolution of the oxide layer because its bond with the metal substrate is destroyed [7]; this latter consideration is proposed as the major mechanism of delamination process [8]. On the other hand, when neutral pH range prevails the ZAP pigment exhibits a positive role in reducing the cathodic delamination advancement in waterborne coatings [6].

The protective properties given by ZAP, where PO_4^-, PO_4^{2-} and PO_4^{3-} anions are involved, could be explained by the interaction of ZAP hydrate molecules with the binder-carboxyl groups and the metal substrate [7]. However, the ZAP pigment, which can be considered as green inhibitor pigment, not only shows this interaction with metallic substrate. Pigments such as iron zinc–phosphate, lithium zinc phosphate or potassium zinc–phosphate cationically modified also show anticorrosion properties [8–12]. All pigments, regardless the nature of their binder, are considered to be protective due to the formation of a protective layer on the metallic substrate, which act as a buffering pH control.

11.2 Cathodic Delamination of Coatings

It is generally accepted that adhesive failure on coatings is induced by accelerated electrochemical reactions occurring at the metal-coating interface of cathodic reactions mainly. The magnitude of the acceleration depends of the overvoltage applied to the system; however, in general terms any external perturbation in voltage and/or current promotes deterioration of the coating known as cathodic debonding or cathodic delamination. When cathodic reactions prevail the formation of OH anions and intermediate OH radicals weakens by hydrolysis and saponification the adhesive strength between the coating and the metallic substrate [13, 14]. These OH anions are considered as the main driven

force of coating debonding produced by the action of the oxygen reduction, where the local pH is increased at the cathodic sites (defects). The oxygen reduction can be described as follows:

$$\frac{1}{2}O_2 + H_2O + 2e \rightarrow 2OH^-.$$

Therefore, taken into account the above features, the cathodic delamination can be defined as follows: *Cathodic delamination is the failure of the coating caused by the production of local OH anions at the polymer/metal interface via oxygen reduction reactions that occur on cathodically polarized metal sites.*

Although delamination may result from blistering phenomenon, it is necessary to point out that the latter can be produced by a poor adhesion as well as a bad surface preparation prior to deposition procedure of the paint. The increment of the pH carried out at the cathodic delamination front depends on the following factors [14]: (a) *cathodic reduction rate*, (b) *shape or morphology of the delamination front*, (c) *OH anions diffusion rate from the delamination front and* (d) *buffering reactions surrounding the delamination front.* The interfacial ion mobility is rate-determining step in the delamination kinetic, which usually shows a linear progress of delamination with square root of time [15]. For this reason, several researches have extensively studied the influence of the cation mobility [13, 14, 16], dissolved oxygen concentration [17, 18], electrolyte concentration [16, 18], temperature solution [16], the effect of the cathodic polarization magnitude [16] and thickness and type of coating binders [16, 19].

Therefore, the cathodic delamination mechanism is a very complex phenomenon, which is not completely understood. Different researches propose that the OH anions solubilised the oxide layer of the metal-coating interface previously formed during the curing process of the coating. The oxide dissolution breaks the iron–oxygen–polymer bond leading a raising in pH, which provokes localized attack, and as a consequence the beginning of the delamination process [14]. Wroblowa [20] found out that during the oxygen reduction process different intermediate radicals of short length, peroxides mostly, may turn to be more destructive that the OH anions, which means that the delamination kinetic becomes faster when these radicals prevail at the delamination front.

$$O_2 + e^- \rightarrow O_2^-$$
$$O_2^- + H^+ \rightarrow O_2H^*$$
$$O_2H^* + e^- \rightarrow O_2H^-$$
$$O_2H^- + H^+ \rightarrow H_2O_2$$
$$H_2O_2 + e^- \rightarrow OH^* + OH^-$$
$$OH^* + e^- \rightarrow OH^-$$

11.3 Modified Zinc–Phosphate Pigment

The whole explanation given above becomes necessary in order to understand the effect of the inhibitive pigments described in the first section in order to slow down the formation of the above species. As already described, the nature of the pigment is considered to be determining step for the cathodic delamination delay; however, the morphology and size of the pigment play a main role for

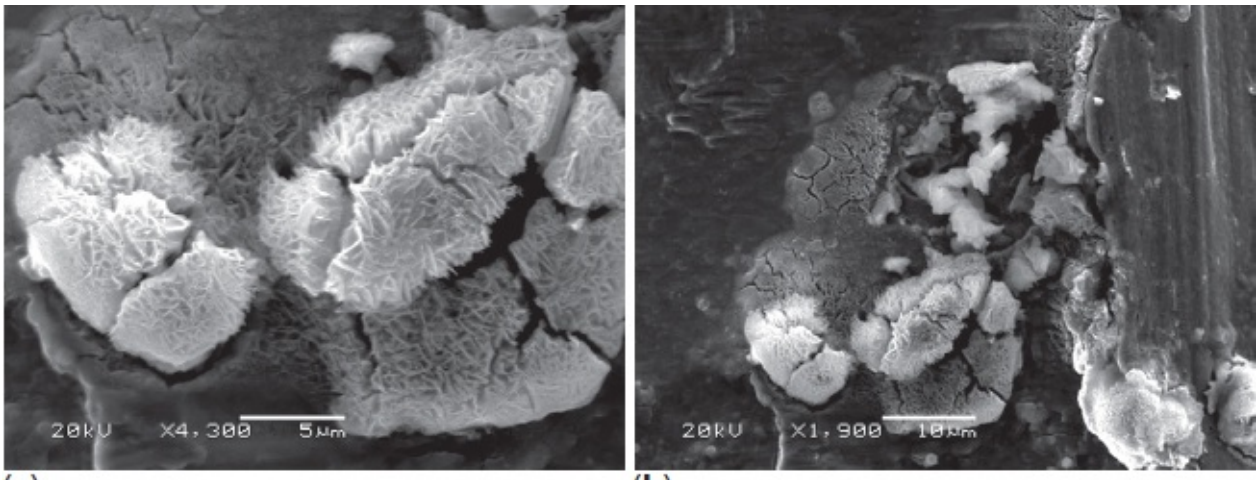
reducing the delamination rate. Acicular, flake-shaped or rounded morphology determines the efficiency of the protection action of the substrate against aggressive species. In terms of lower permeability, the flake-shaped pigments have shown good results in reducing the delamination front [21]. Although some attempts of improving the delamination resistance of paints with loaded nanocontainers within coatings have been made [22], it should be borne in mind that the incorporation of clays, nanoparticles, nanotubes, fibbers or any entrapped component may turn as a result in thicker films due to dense particulates or larger agglomerates formed during the curing time of the coating.

So, the smart release of inhibitor in coatings is essentially designed when aggressive species modify the interface condition (pH and corrosion potential) leading to possible restoration of electrochemical equilibrium. The inhibitor entrapped within these fillers may vary in nature including both inorganic and organic ionic species. Whether it is the coating formulation modified during synthesis or if the coating is loaded with nanoparticles, the main aim of the corrosion inhibitors is to guarantee that the inhibitors could diffuse to a defect site of the delamination front in order to trigger or stabilize the pH.

Taking over the modified zinc–phosphate pigment loaded on coatings deposited on steel, important results have come out [2, 6, 22–24]. The ZAP pigment can be considered as an excellent environmentally friendly profile (or green inhibitor) due to the replacement of carcinogenic compounds of commercial chromate compounds by zinc-free pigment in accordance to European Community (directive 76/464 EEC, codified as 2006/11/EEC). The modified zinc–phosphate with calcium, strontium and aluminium has become of great importance during the last decade. The case of ZAP pigment incorporated in epoxy and acrylic coatings has shown that this compound is a function of the pigment damping capacity to neutralize the local production of OH^- at local defects such as a delamination front. Within this defect, the water accumulates forming an anodic site. As the chemical interaction amongst cathodic (water and oxygen) and anodic (metal) species increases, a complex phosphated film [2] is being developed slowing down the oxygen reduction reaction rate. It has been established that this phosphated film formation is favoured by the phosphate ions liberation once the pigment solubility is increased [6].

Different stages of the phosphated film formation that originates a decrement of the delaminated area as well as the blister propagation have been proposed. It has been found that during the curing stage between the water base coating and the metal, a film mainly constituted by Zn and Na compounds is generated. However, when this film is in contact with brine solution under delamination cathodic conditions (–1.1 V, SCE) seems to be an interaction with the liberated phosphate ions coming from ZAP that modifies the film composition. Thus, it is considered that the phosphate film polarizes the oxygen cathodic reaction diminishing the delamination kinetics allowing a significant increment in the coating performance. According to research performed with Raman spectroscopy, the composition film was identified as α-hopeite, $\alpha\text{-}Zn_3(PO_4)_2 \cdot H_2O$ [2]. The morphology of the α-hopeite is shown in Figure 11.1 where porous acicular needles embedded in thicker plates of corrosion products were formed.

Figure 11.1 Morphology of the α-hopeite.



The chemical mapping carried out by SEM revealed that within the delamination area (Figure 11.2), a homogeneous distribution of Zn, P, O and Na is detected. The aluminium distribution was scarce and localized in specific regions, indicating that this element did not have a relevant participation in the phosphate film composition. The iron mapping revealed an even distribution along the surface; nevertheless, a lower presence of the element in the areas of the oxide film (dark areas) was detected. The case of the chemical mapping in a non-delaminated area, Figure 11.3, reveals that the presence of Fe followed by C, O, Mn, Al and P traces were detected. No zinc presence was evident, but Mn distribution was revealed probably ascribed to iron composition, because the SEM detection limit depth was 1 µm. These results evidence that the release of the phosphate anions from the coating to the metal-coating interface is carried out when cathodic conditions prevail or when a physical damage (defect) is formed.

Figure 11.2 Chemical mapping within the delamination area.

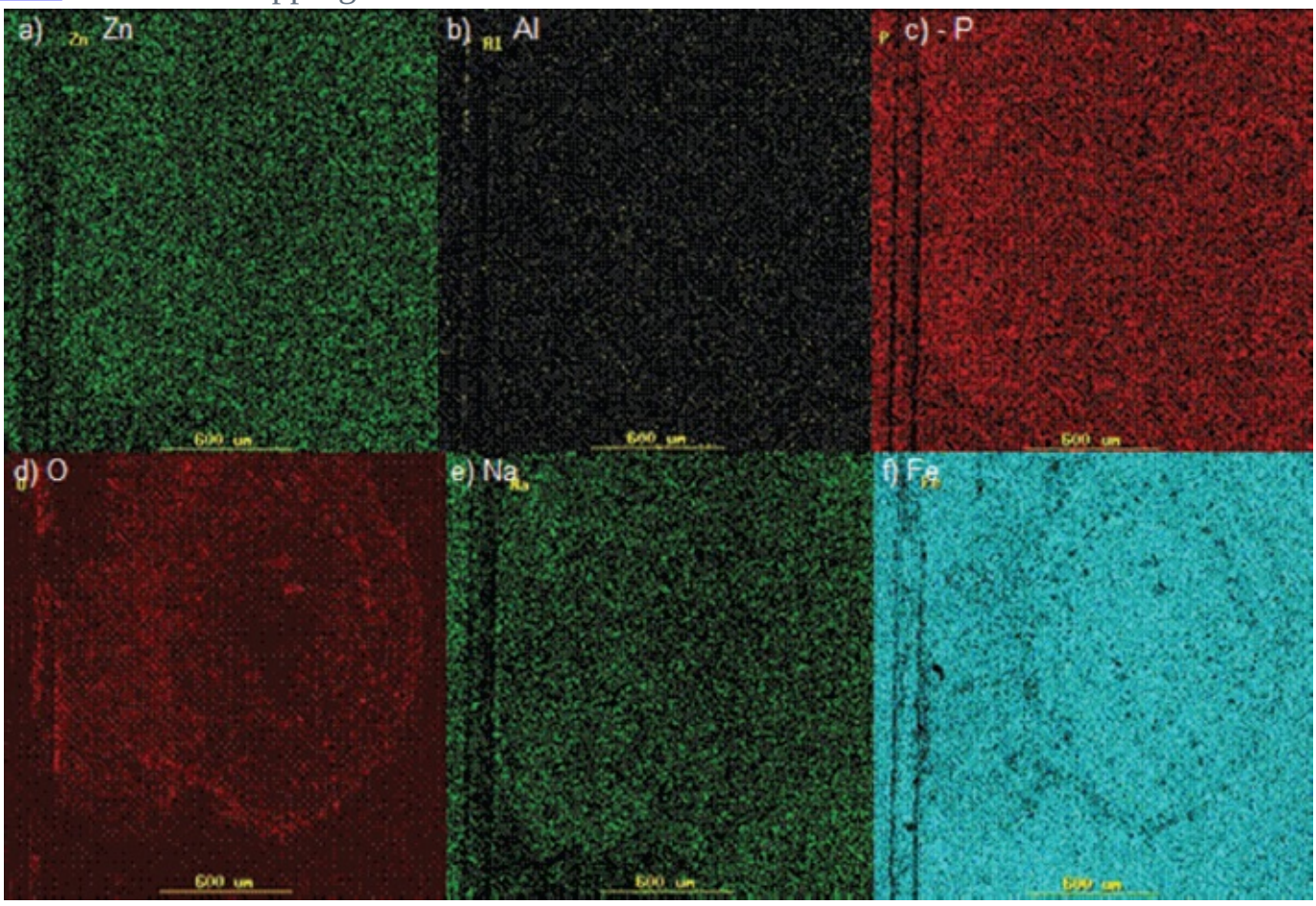
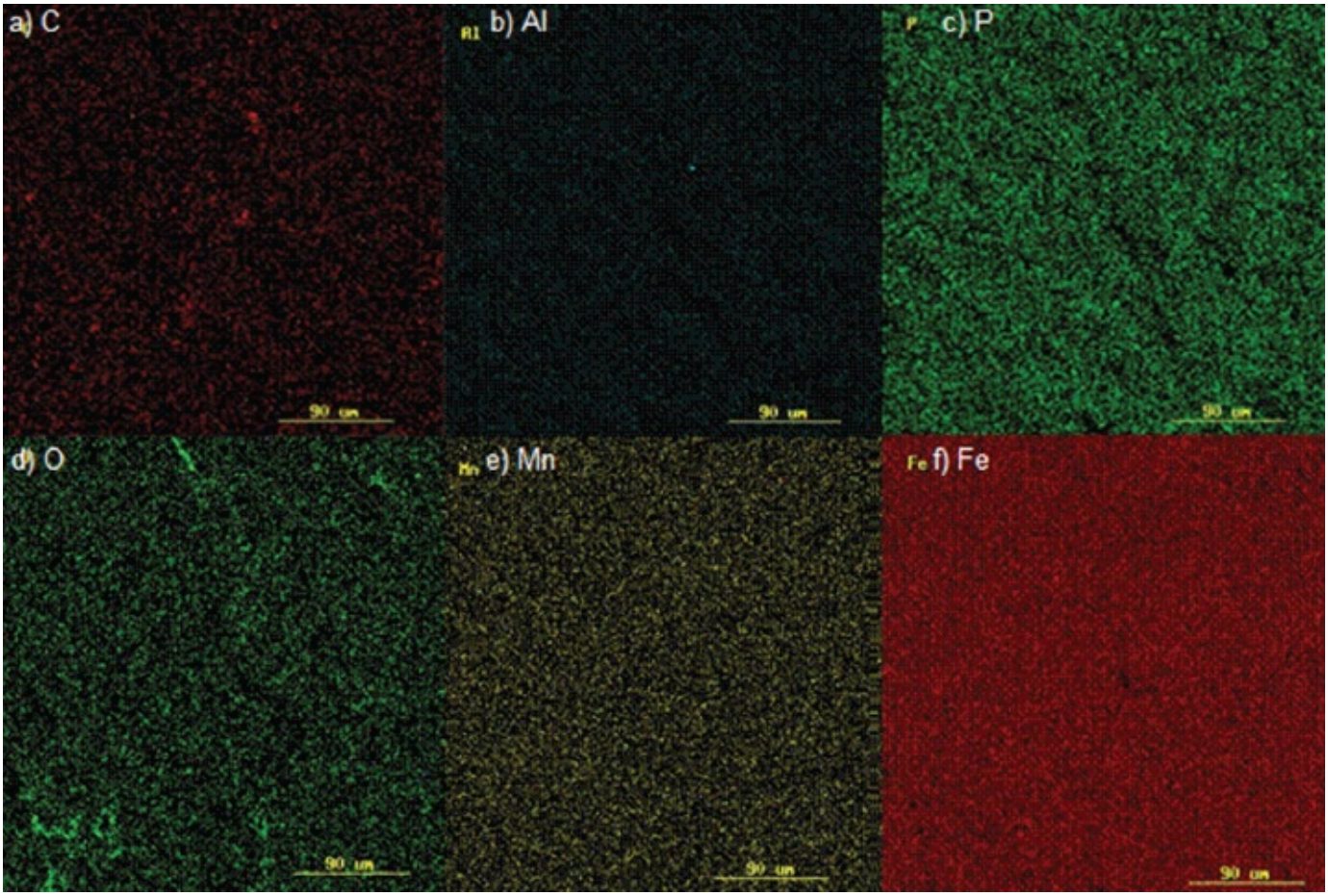


Figure 11.3 Chemical mapping in a non-delaminated area.



In order to understand the chemical interaction of ZAP pigment with steel substrate and taking into account previous results on the literature, the following reactions for the α-hopeite formation are elucidated.

Reduction:

$$O_2 + 2H_2O + 4e^- \rightarrow 4OH^-$$

Oxidation:

$$Fe^{2+} + 2e^- \rightarrow Fe$$

According to De Pauli *et al.* [25, 26], the Zn oxide film formation in a PO_4 media could be associated to a dissolution precipitation mechanism amongst different phosphate species. So, the Zn in combination with PO_4 (from ZAP) in solution forms Zn^{2+} and PO_4^{3-} ions; thus, the PO_4^{3-} ions promote continuous releasing of Zn in aqueous media [25, 26]. The releasing of Zn may be explained in terms of the damping capacity (buffering) of PO_4^{3-} to regulate the OH^- concentration at the metal-coating interface, i.e., at alkaline conditions the following reaction takes place.

$$PO_4^{3-} + H_2O \Leftrightarrow HPO_4^{2-} + OH^-$$

This reaction occurs between values of pH among 11.5–13.5 [26]. The HPO_4^{2-} originates a Zn corrosion potential between –0.65 and –0.85 V (SCE) [27, 28], which is consistent with results obtained with electrochemical noise assessment [29]. In a latter publication [6], it was concluded that the maximum buffering response of phosphate anion is found at a centre value of 7.2, which corresponds to the nominal second ionization for phosphoric acid in the form of PO_4^{2-}. In agreement with this, it is feasible that Zn^{2+}, PO_4^{2-} and PO_4^{2-}, interact at the metal-coating promoting a dissolution mechanism given by:

$$Zn^{2+} + 2H_2PO_4^- \rightarrow Zn(H_2PO_4)_2$$

According to the metal-coating interface conditions, the dissolution reaction is accompanied by a precipitation mechanism.

$$3Zn(H_2PO_4)_2 \rightarrow Zn_3(PO_4)_2 \cdot 4H_2O + 4H_3PO_4$$

where the $Zn_3(PO_4)_2 \cdot H_2O$ compound is known as α-hopeite. This film formed and deposited on the metal-coating interface acts as a barrier layer between the metal substrate and the aggressive species coming from solution.

11.4 Conclusions

The green zinc–phosphate inhibitive pigments show a promise route to protect the steel substrate against corrosion phenomenon when these compounds are incorporated into coating binders. The efficiency of these pigments depends on the morphology and size as well as the cationic species incorporated into the pigment formulation. The ZAP pigment acts as a protective inhibitor when alkaline conditions prevail at local defects such as pores or delamination front. The release of the PO_4^{3-} specie from the ZAP pigment induces consecutive reactions (dissolution and precipitation) that lead the formation of hydrated zinc–phosphate layer known as α-hopeite. This oxide layer is formed during cathodic delamination conditions within the local defects slowing down the blistering and the coating failure due to barrier effects.

In summary, the use of new waterborne coating schemes, including the use of mesoporous or nanoporous particles as inhibitor carriers, and pigments such as ZAP considered as green inhibitor is becoming more efficient in terms of corrosion protection and becoming extensively used in industry and more friendlier to the environment.

Acknowledgement

Authors acknowledges Proyectos de Colaboración Conjunta, Fondo de Colaboración del Instituto de Ingeniería y la Facultad de Ingeniería, UNAM, 2015–2016. Jorge Uruchurtu acknowledges the Estancia Sabática Nacional 2016 (N° 265526) from CONACYT program. This research has been supported by the CONACYT project 167856.

References

1. S.E. Faidi, J.D. Scantlebury, P. Bullivant, N.Y. Whittle, and R. Savin, *Corr. Sci.,* Vol. 35(5–8), p. 1319, 1993.

2. M. Hernandez, J. Genesca, J. Uruchurtu, F. Galliano, D. Landolt, *Prog. Org. Coat.,* Vol. 56(2–3), p. 199, 2006.

3. R. Romagnoli, V.F. Vetere, *Corr. Sci.,* Vol. 51(2), p. 116, 1995.

4. J. Barraclough, J.B. Harrison, *J. of Oil Colour Chem. Assoc.,* Vol. 48, p. 341, 1965.

5. A. Bittner, *J. Coat. Tech.,* Vol. 61(777), p. 111, 1989.

6. M. Hernández, F. Galliano, D. Landolt, *Corr. Sci.*, Vol. 46(9), p. 2281, 2004.

7. G. Adrian, A. Bittner, *J. Coat. Tech.*, Vol. 58(740), p. 59, 1986.

8. M.J. Gimeno, S. Chamorro, R. March, E. Oró, P. Pérez, J. Gracenea, J. Suay, *Prog. Org. Coat.*, Vol. 77(12 A), p. 2024, 2014.

9. M. Bethencourt, F.J. Botana, M. Marcos, R.M. Osuna, J.M. Sanchez-Amaya, *Prog. Org. Coat.*, Vol. 46(4), p. 280, 2003.

10. E. Alibakhshi, E. Ghasemi, M. Mahdavian, *Corros. Sci.*, Vol. 77, p. 222, 2013.

11. R. Naderi, M.M. Attar, *Corros. Sci.*, Vol. 51(8), p. 1671, 2009.

12. R. Naderi, M.M. Attar, *Prog. Org. Coat.*, Vol. 69(4), p. 392, 2010.

13. A. Leng, H. Streckel, M. Stratmann, *Corr. Sci.*, Vol. 41, p. 579, 1999.

14. H. Leidheiser Jr, W. Wang, L. Igetoft, *Prog. Org. Coat.*, Vol. 11, p. 19, 1983.

15. J. Wielant, R. Posner, R. Hausbrand, G. Grundmeier, H. Terryn, *Corros. Sci.*, Vol. 51, p. 1664, 2009.

16. U. Steinsmo, I. Skar, *Corrosion*, Vol. 50(12), p. 934, 1994.

17. W.J. Muizebelt, W.J.M. Heuvelsland Thomas, Polymeric Materials for Corrosion Control, ACS Symposium Series 322, American Chemical Society, Washington, DC, p. 110, 1986.

18. Leng, H. Streckel, K. Hoffmann, M. Stratmann, *Corr. Sci.*, Vol. 41, p. 599, 1999.

19. J.L. Luo, C.J. Lin, Q. Yang, S.W. Guan, *Prog. Org. Coat.*, Vol. 31, p. 289, 1997.

20. H.S. Wroblowa, *J. Electr. Chem.*, Vol. 339, p. 31, 1992.

21. P.A. Sorensen, K. Dam-Johansen, C.E. Weinell, S. Kiil, *Prog. Org. Coat.*, Vol. 68, p. 283, 2010.

22. M. Mahdavian, R. Naderi, M. Peighambari, M. Hamdipour, S.A. Haddadi, *J. Ind. Eng. Chem.*, Vol. 21, p. 1167, 2015.

23. R. Naderi, M.M. Attar, *Prog. Org. Coat.*, Vol. 77, p. 830, 2014.

24. F. Askari, E. Ghasemi, B. Ramezanzadeh, M. Mahdavian, Dyes and Pigments, Vol. 109, p. 189, 2014.

25. C.P. De Pauli, M.C. Giordano, H.T. Mishima, *J. Electroanal. Chem.*, Vol. 103, p. 95, 1979.

26. C.P. De Pauli, O.A.H. Derosa, M.C. Giordano, *J. Electroanal. Chem.*, Vol. 86, p. 335, 1978.

27. V.K. Gouda, M.G.A. Khedr, A.M. Shams El Din, *Corr. Sci.*, Vol. 7, p. 221, 1967.

28. Xiaoge Gregory Zhang, Corrosion and Electrochemistry of Zinc. Plenum Press, New York and London, 1996.

29. M. Hernandez, J. Genesca, J. Uruchurtu, A. Barba, *Corr. Sci.*, Vol. 51, p. 499, 2009.

Chapter 12

Development of Soybean Oil-Based Polyols and Their Applications in Urethane and Melamine-Cured Thermoset Coatings

Senthilkumar Rengasamy* and Vijay Mannari

Coating Research Institute, Eastern Michigan University, Ypsilanti, MI, USA

**Corresponding author*: senthilkumar_27@yahoo.com

Abstract

Polyols are versatile and increasingly important resins for thermoset coatings, adhesives, sealants and foam applications. Bio-based polyols have emerged as an environmentally friendly and sustainable alternative to petrochemical-based ones due to their renewability, lower carbon footprint and often lower cost. Novel family of vegetable oil-based polyols has been derived from epoxidized soybean oil (ESO) with a broad range of chemical structures and hydroxyl contents. This research focuses on design of unique polyol architectures and use of novel synthetic approaches for deriving these polyols and demonstration of their potential application in polyurethane and melamine-cured thermoset coatings. The chemical structure of these polyols and their functionality primarily dictate performance properties and their end-use applications. The successfully synthesized polyols have been characterized with nuclear magnetic resonance and Fourier transform infrared spectra for qualitative confirmation of functional groups. ESO has also been characterized and compared with other polyols.

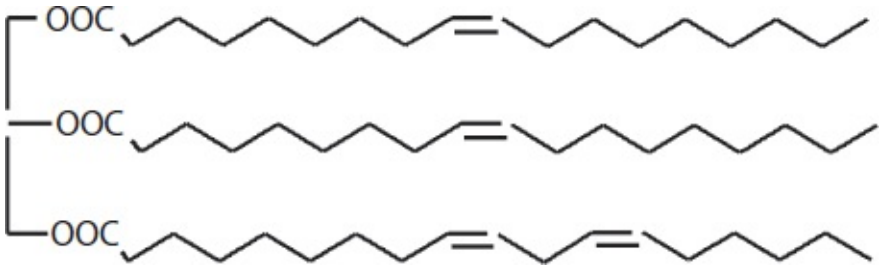
Keywords: Soy bean-polyol, ring opening polymerization, green coatings, green polyols, soy-based polyurethane, polyester polyol.

12.1 Introduction

Polyols are indispensable components of polyurethanes that are finding increasingly important applications in such diverse products as plastics, foams, coatings, composites, and adhesives, among others. Most of the commercially available conventional polyols are petrochemical-based and are available in wide range of chemistries, morphologies, functionalities viscosities, and cost. Due to their dependence on petroleum, these polyols are not very sustainable. Bio-based materials are increasingly used in meeting the present-day demands of developing sustainable products and processes. Vegetable oils are excellent agro-based resources for development of polyols for aforementioned applications. Vegetable oils are composed of fatty acid triglycerides of variety of

types as shown in Figure 12.1. Depending upon their end-use applications, polyols are required to meet such demanding requirements as functionality, reactivity, compatibility, hydrolytic stability, surface tension, rheology, to name a few. The unique combination of chemical structure, functionality and reactivity combined with low toxicity and inherent biodegradability makes vegetable oils an excellent resource for deriving sustainable polymers [1–14].

Figure 12.1 Triglyceride molecule of natural oil.



A variety of soybean oil derived polyols, frequently referred in literature as soy-polyols, prepared from different synthetic routes, have been reported in the literature [15–31]. Polyurethanes prepared from these soy-polyols, replacing petro-based polyols show interesting performance properties besides their high bio-renewable contents [15–31]. Soy-polyols for use in polyurethane dispersions (PUD) require unique set of properties and hydroxyl functionality. Except castor oil and lesquerella oil with naturally occurring hydroxyl groups all other natural oils need to be chemically modified to introduce hydroxyl groups at their unsaturated sites [32]. This can be accomplished by hydroformylation, followed by hydrogenation [33]; epoxidation, followed by oxirane opening [1]; ozonolysis, followed by hydrogenation [4, 22, 34] and microbial conversion [35].

Epoxidized soybean oil (ESO), a commercial bio-based product has been used for decades as plasticizer and stabilizer for polyvinyl chloride (PVC), a commodity plastic. ESO offers unique chemical structure and functionality that allows design and development of a wide range of polyols. This paper presents our research efforts on development of a range of polyols useful for coatings and allied applications. In the present work, ESO and their derivatives have been used as starting materials in polyol synthesis. Synthetic routes to derive a range of polyols with controlled chemical structures, types and number of functional groups, hydroxyl equivalent weight, viscosity and their potential applications are studied.

12.2 Experimental

12.2.1 Raw Materials

Vikoflex 7170 – ESO was procured from Arkema, Inc., USA and used without purification. Phosphoric acid, calcium oxide (CaO), phthalic acid and tertiary butanol, dibutyl tindilaurate (DBTDL) was obtained from Sigma Aldrich, USA and used as received. Hexamethylene diisocyanates (Desmodur N75BA/X) was procured from Bayer MaterialScience, LLC, USA and used without purification. Hexamethoxymethylmelamine (Cymel 303) was obtained from Cytec Industries, Inc., USA and used as received.

12.2.2 Standard Testing Methods

Successfully developed polyols have been characterized for oxirane oxygen content (ASTM D – 1652-97), acid number (ASTM D – 1639-96), and hydroxyl number (ASTM D – 4274-05). Viscosity of the epoxidized vegetable oil-based polyols was determined at 25 °C using Brookfiled viscometer. Proton NMR spectra of polyols were recorded on a Bruker NMR spectrometer in $CDCl_3$ at room temperature. A 45° pulse width, 400 MHz field strength, 2.18 s acquisition time and 5 s pulse delay were used in the spectrum analysis. Functional group characterization of Soy-polyol was done recording Fourier transform infrared (FTIR) spectra with Bruker Tensor 27 FTIR analyzer in the range of 400–4000 cm^{-1} at room temperature. The urethane cured and melamine-cured coatings' film properties were characterized using ASTM standards such as pencil hardness (ASTM D – 3363), impact resistance (ASTM D – 2794-99), adhesion (cross-cut) test (ASTM D – 3359-02), and MEK double rub test (ASTM D – 4752-98). BYK film thickness gauge instrument was used to check the dry film thickness.

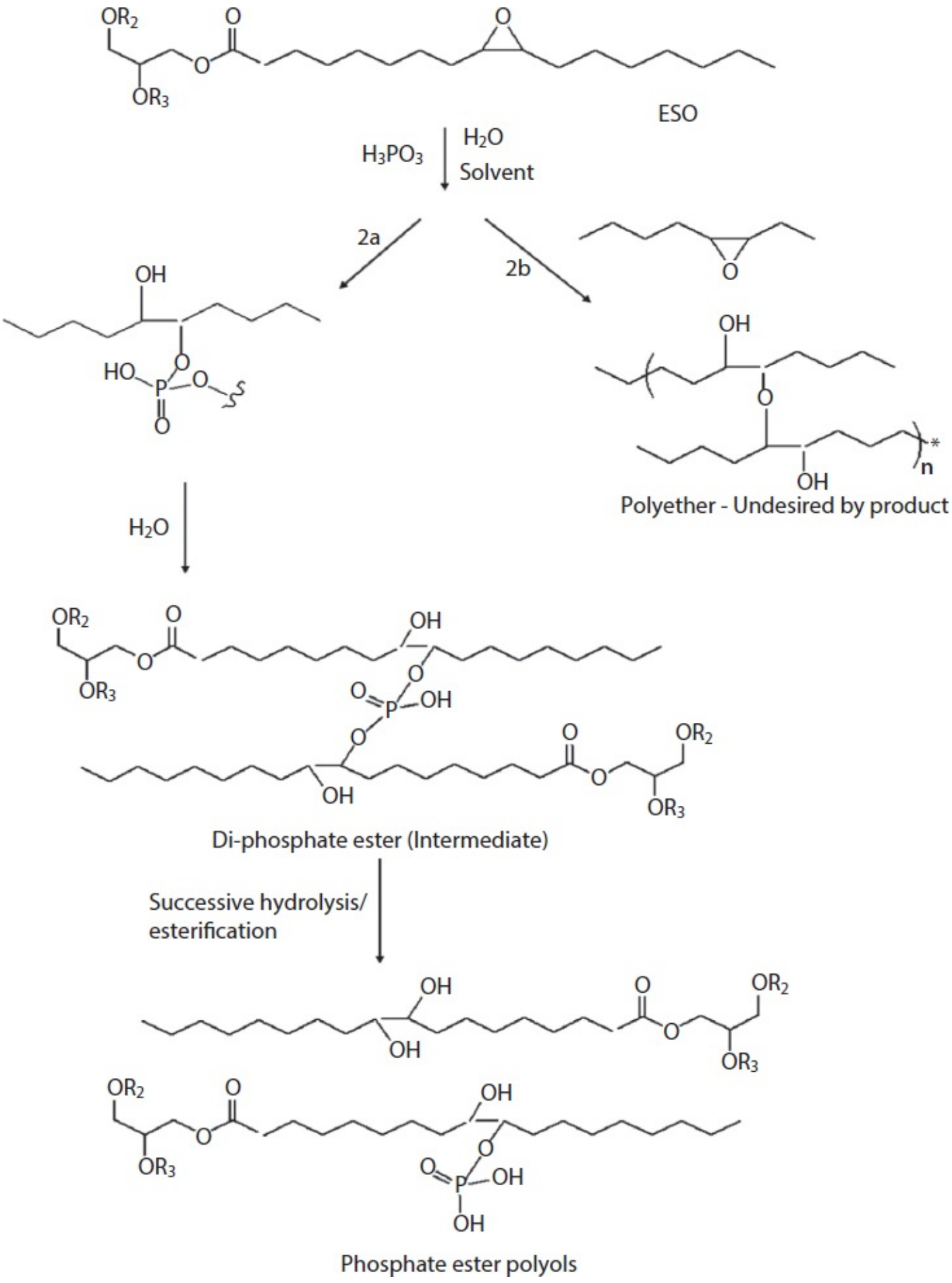
12.2.3 Coating Composition and Sample Preparation

To study the potential application of developed polyols, urethane-based and melamine-based coating formulations were prepared by cross-linking the polyols with Hexamethylene diisocyanates (Desmodur N75BA/X) and Hexamethoxymethylmelamine (Cymel 303), respectively. The coating compositions are shown in Tables 12.3 and 12.4. Coatings were applied on cold-rolled steel panels (6"× 4" × 0.032") to ~50 micron wet film thickness and cured under 80 °C for 4 h before testing for their film properties.

12.2.4 Synthesis of ESO-Based Phosphate Ester Polyol (ESO–Polyol)

ESO (100.0 g/0.1 mole) and tertiary butanol (90.0 g) was added in a three-neck flask equipped with mechanical stirrer, temperature controller, heating mantle, additional funnel and water condenser. Acid solution was prepared by mixing phosphoric acid (4.5 g/0.0459 mole) with 10 g of tertiary butanol and 10.0 g of Deionized water. The prepared acid solution was slowly added from an additional funnel into the three neck flask maintained at 80 °C for about 45 min. The progress of reaction was monitored by %oxirane oxygen content (%OOC) and acid value of the reaction mixture at a regular interval. Reaction was continued until the %OOC of ESO dropped from 7% to less than 0.3%. Rotary vacuum evaporator was used to remove solvent and other volatiles. The final product was stored in glass bottle in a desiccator. Figure 12.2a shows simplified reaction scheme for synthesis of phosphate-ester polyol from ESO. Figure 12.2b shows the reaction of oxirane oxygen groups with another oxirane oxygen group.

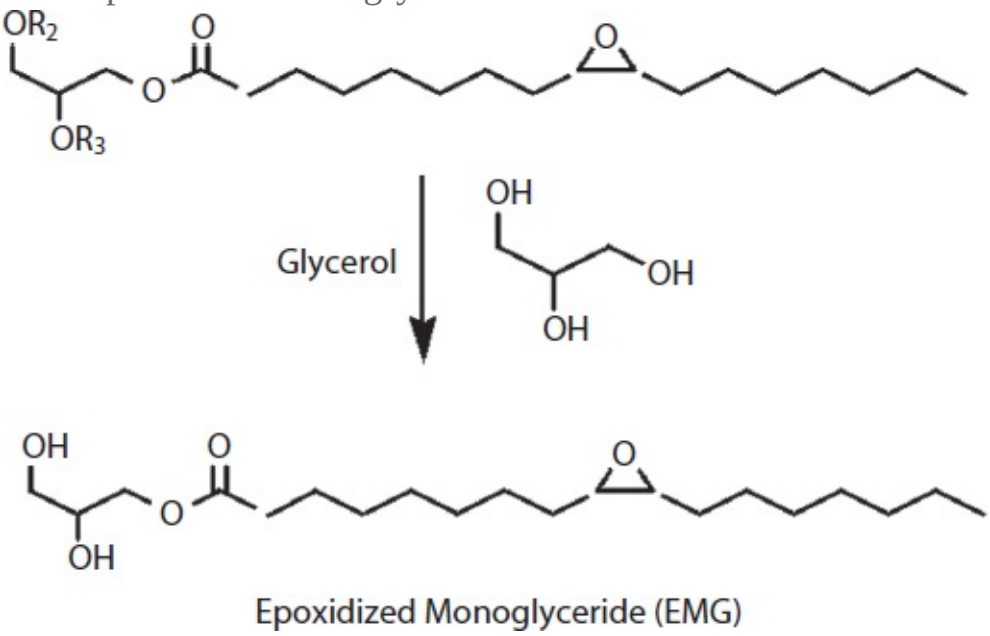
Figure 12.2 Reaction scheme for synthesis of phosphate ester polyol based on ESO.



12.2.5 Synthesis of Epoxidized Soybean Oil Monoglyceride (EMG)

One mole of ESO (1000.0 g) was taken in three-neck flask equipped with addition funnel, mechanical stirrer, and temperature controller. Reaction was carried out at 145 °C in presence of nitrogen gas and at this temperature 1.9 mole (174.8 g) glycerol was slowly added from an addition funnel within 5 min. The CaO (0.2% based on ESO weight) was used as catalyst. The reaction was continued at 145 °C for 3 h and then the %OOC was determined to study the loss of oxirane oxygen content during reaction. The unreacted excess glycerol was removed by centrifuge method. A waxy like final product (EMG) was obtained which was characterized for %OOC, hydroxyl number and viscosity. Figure 12.3 shows the schematic representation of synthesis of EMG.

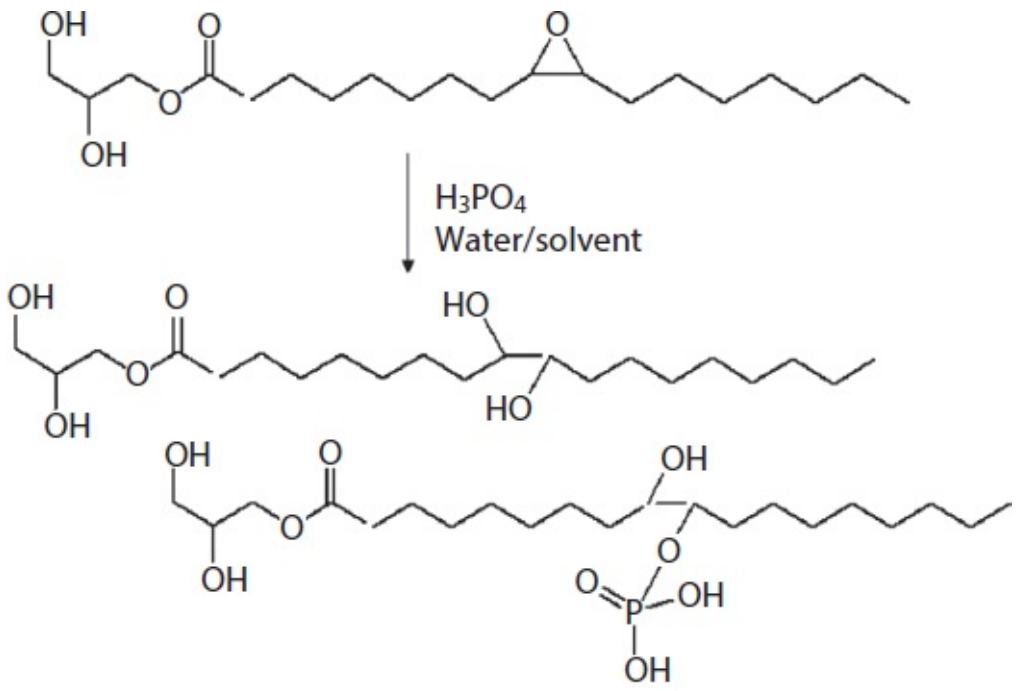
Figure 12.3 Synthesis of epoxidized monoglyceride.



12.2.6 Synthesis of EMG-Based Phosphate Ester Polyol (EMG Polyol)

EMG (100 g/0.2649 mole) and tertiary butanol (90 g) was taken in three-neck flask connected to mechanical stirrer, temperature controller, heating mantle, additional funnel and a water condenser. Phosphoric acid (3.9984 g/0.0408 mole) was placed in a beaker and mixed with DI water (10 g) and tertiary butanol (10 g). Similar to ESO polyol synthesis, in this reaction also EMG and tertiary butanol was taken as 1:1 weight ratio. About 90% of tertiary butanol was added in to the three-neck flask and rest of the amount was used to prepare acid solution. The prepared solution in the beaker was placed into an addition funnel and added slowly into the three neck flask at 80 °C for about 30–45 min. Reaction was continued until %OOC of ESO dropped from 7.0% to less than 0.3%, which took about 3 h. Rotary vacuum evaporator was used to remove solvent and other volatiles from the product. The final phosphate ester polyol was characterized for its %OCC, viscosity and hydroxyl numbers. Figure 12.4 shows the schematic representation of EMG-based phosphate ester polyol.

Figure 12.4 Synthesis phosphate ester polyol from epoxidized monoglyceride.

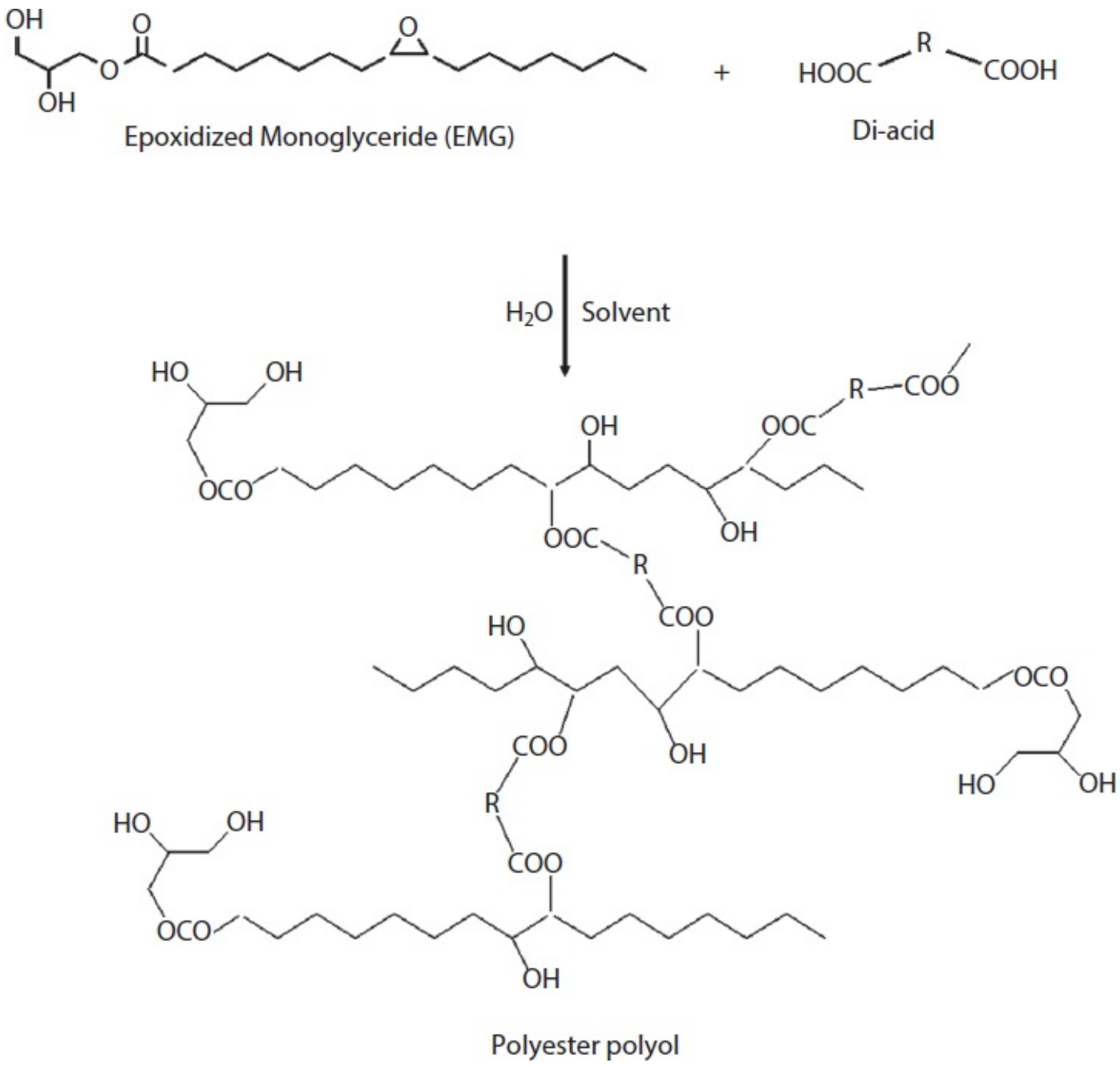


EMG based phosphate ester polyol

12.2.7 Synthesis of EMG-Based Phthalic Acid Ester Polyol (EMG–PEP)

The phthalic acid ester-based polyol was successfully synthesized from EMG and phthalic acid in the presence of tertiary butanol. In the three neck flask, EMG (100 g/0.2649 mole) and 50 g of tertiary butanol was added and the reaction kettle was connected with water condenser, temperature controller, heating mantle and nitrogen inlet/outlet. The reaction mixtures were heated to 80 °C and at this temperature the addition of phthalic acid was started. The phthalic acid (18 g/0.1084 mole) was divided as three equal parts and added one part at a time as 15-min interval. The part-by-part addition of phthalic acid was followed to control the exothermic reaction and maintain the reaction temperature with in 80 °C. After the addition of acid, the reaction was carried out at this temperature until desired %OOC values (less than 0.3%) was achieved. Once the desired %OOC value was achieved, the solvent was removed from the final product using rotary vacuum evaporator. The final product was characterized for its viscosity and hydroxyl numbers. Figure 12.5 shows the schematic representation of phthalic ester-based polyol.

Figure 12.5 Schematic representation of synthesis of phthalic acid based polyester polyol.



12.3 Results and Discussion

12.3.1 Characterization of Polyols

Acid-catalyzed addition of nucleophile to oxirane group has been extensively studied and reported in the literature [18]. Under the conditions of reaction two competing reactions are known to take place, (a) esterification by addition of phosphoric acid to the oxirane group to form phosphate ester product, and (b) reaction of oxirane group with another oxirane (carbocation) to form an ether linkage. As shown in Figure 12.2a, phosphoric acid reacts with oxirane oxygen groups of ESO and protonate them. The protonated epoxides form electrophilic site, which will be attacked by available nucleophilic compound phosphoric acid to produce diphosphate ester intermediate. The nucleus-seeking agent further attacks carbon of carbonyl groups of diphosphate ester and results in the final product phosphate ester polyol. S_N2 mechanism is also possible if one alcohol chain act as nucleophile and protonated alcohol chain acts as substrate. As shown in Figure 12.2b, the protonated

oxirane oxygen groups might react with each other and also forms oligomeric ethers. Similar kind of reaction can also be observed in epoxidized monoglyceride-based phosphate ester polyol and phthalic ester polyol.

Table 12.1 represents the characterization of the bio-polyols. The table proves that nucleophilic attack on electrophilic site results in newly formed hydroxyl groups.

Table 12.1 Bio-Polyol Characteristics.

Bio-Polyol Types	%OOC	Acid Value (mgs KOH/g)	Viscosity @ 25 °C	Hydroxyl Value (mgs KOH/g)
ESO Polyol	0.2	0.3	1100	165
EMG Polyol	0.12	0.1	1385	373
EMG - PEP	0.3	0.4	1200	389

12.3.2 Proton NMR Characterization

Spectroscopic characterization of ESO, EMG, and EMG–PEP polyols has been carried out using ^{1}H NMR and their characteristic peaks are summarized in Table 12.2. For every hydroxyl groups appearing at epoxy moieties, the corresponding peak appears at 3.6–3.76 ppm. It can be viewed from the Table 12.2 that both ESO-polyol and EMG-polyol derived almost identical proton NMR peaks. This may be due to the types of reagents used to synthesis the aforementioned polyols. Both the polyols were derived from ESO and in both cases phosphoric acid was used to open the oxirane oxygen ring of ESO and its derivative EMG. The difference between EMG – PEP polyol with ESO and EMG polyols can be observed from the peaks obtained at 7.0 to 7.6 ppm. These peaks represent the aromatic protons of phthalic ester fragment of polyester of EMG– PEP polyol.

Table 12.2 ^{1}H NMR Characteristics peaks of developed polyols.

^{1}H NMR Spectra (Signal Peak – PPM)	**ESO Polyol**
0.9	CH_3 (terminal group)
1.20–1.40	CH_2 (aliphatic backbone)
2.25–2.35	CH_2–C=O
3.68–3.76	CH–OH (low field region)
3.98–4.30	Triglycerols (or) glyceryl carbons
^{1}H NMR Spectra (Signal Peak – PPM)	**EMG – Polyol**
0.9	CH_3 (terminal group)
1.20–1.40	CH_2 (aliphatic backbone)
1.44–1.66	CH_2 (aliphatic backbone)
2.28–2.38	CH_2–C=O
3.60–3.70	OH groups
3.90–4.22	Triglycerols/glyceryl carbons
^{1}H NMR Spectra (Signal Peak – PPM)	**Phthalic Acid base Polyester Polyol**
0.88	CH_3 (terminal group)
1.20–1.60	CH_2 (aliphatic backbone)

2.25–2.50	Methyl group at phenyl ring
3.60–3.72	CH–OH (low field region)
4.20–4.32	CH_2–C=O (low field region)
7.0–7.60	Low field region contains aromatic protons or phthalic ester fragment of polyester

12.3.3 FTIR Characterization

Typical FTIR spectra of ESO and its corresponding hydroxylated derivatives are shown in Figures 12.6–12.8. The oxirane (C–O–C) groups in ESO and EMG can be clearly observed from the absorption peaks at 824 and 844 cm^{-1}. The oxirane groups and enhancement of peak at 3421 cm^{-1} corresponding to OH groups from EMG proves that not only the epoxy groups are surviving during synthesis but also glycerides are attached to end of the polymer chain. The disappearance of oxirane groups from ESO polyol, EMG polyol, and polyester polyol proves that newly formed hydroxyl groups at 3400 cm^{-1} are result of ring opening of oxirane groups. The FTIR analysis corroborates very well with chemical characteristics of the products determined (epoxy value, hydroxyl number). This also concludes that the epoxide groups are reacted with acid in the presence of nucleophilic agent, resulting in the formation of an ether group and –OH group, as proposed in the above reaction schemes.

Figure 12.6 FT-IR Characteristics of ESO polyol.

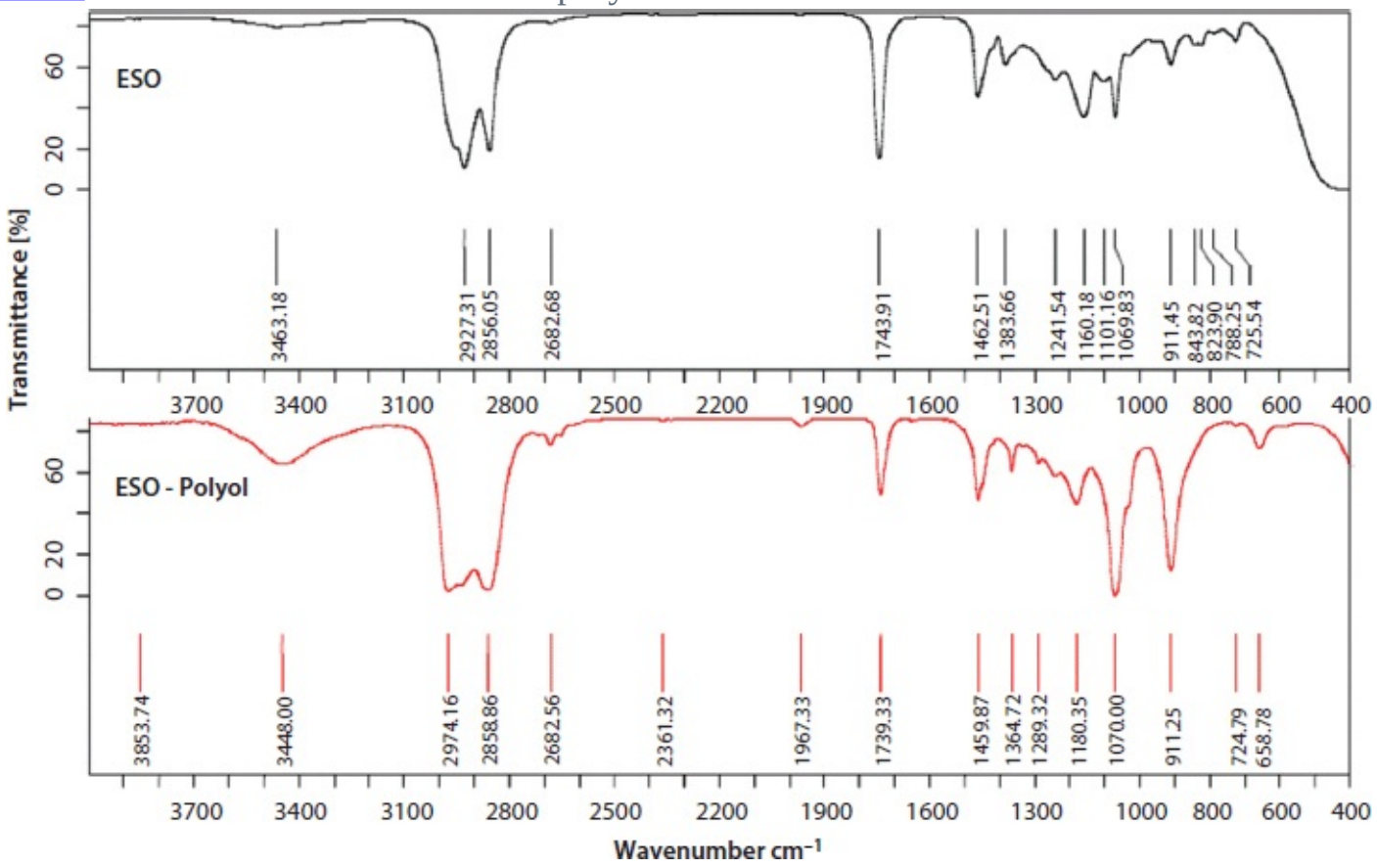


Figure 12.7 FT-IR Characteristics of EMG Polyol.

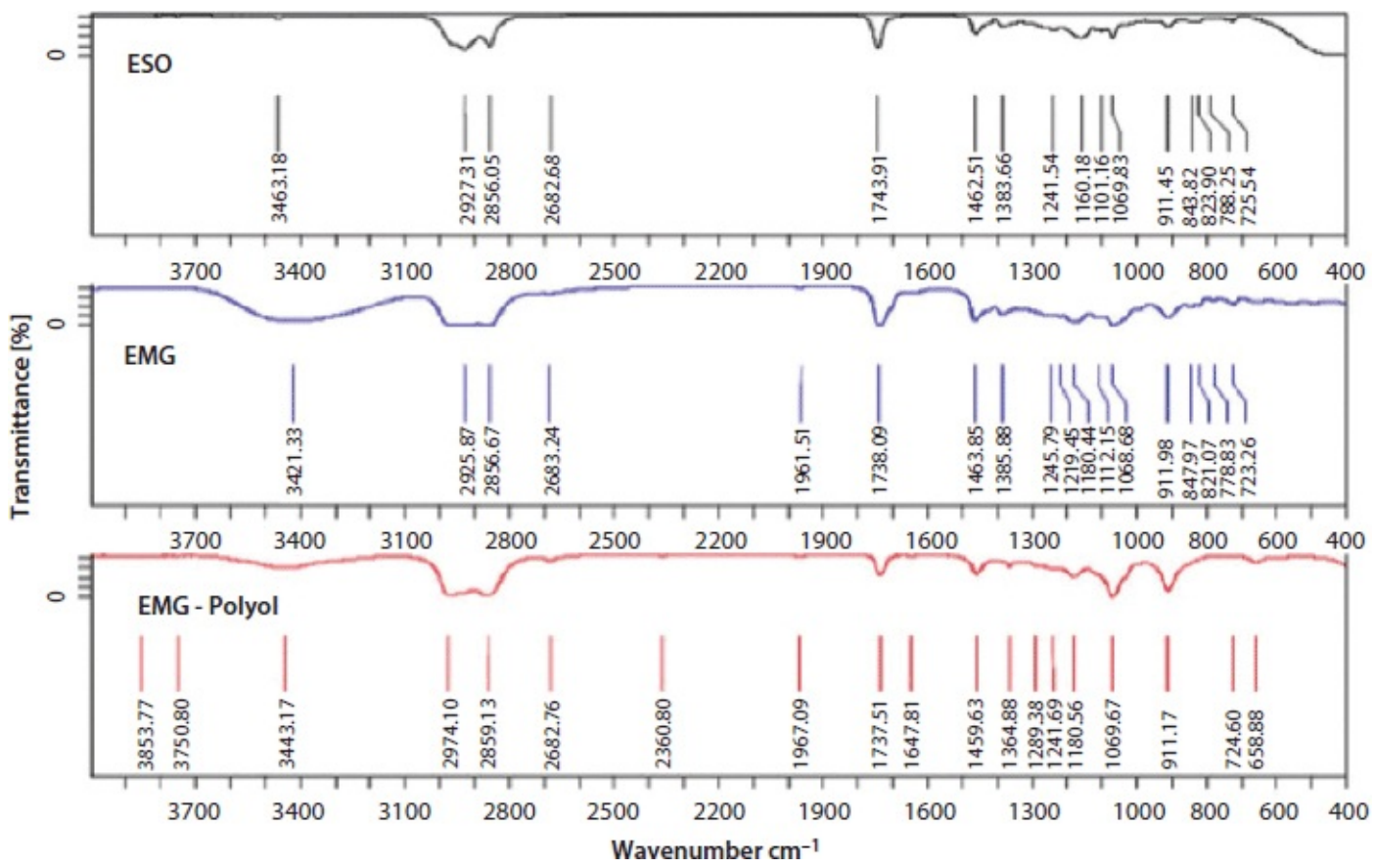
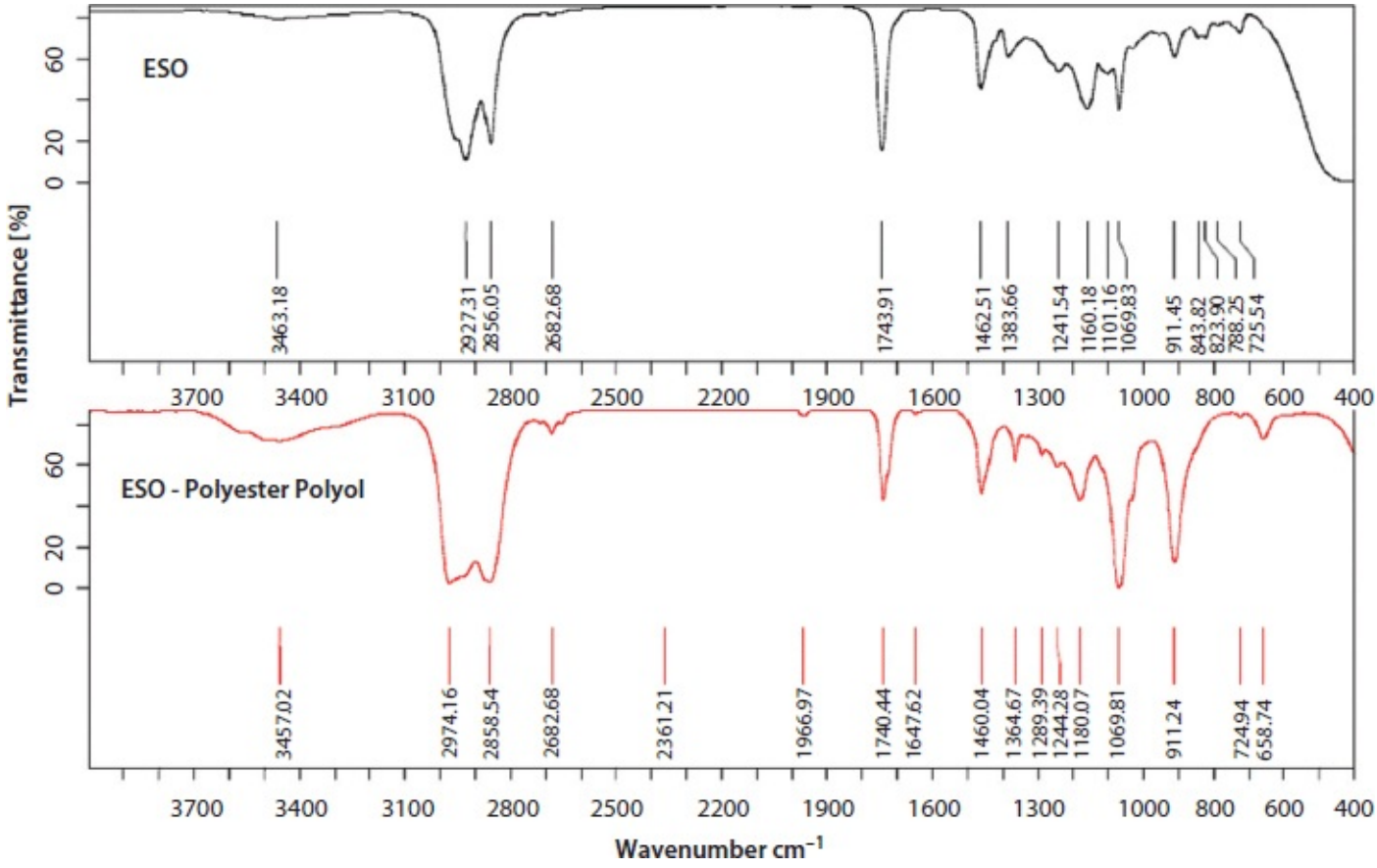


Figure 12.8 FT-IR characteristics of phthalic acid based polyester polyol.



12.3.4 Urethane and Melamine-Cured Film Properties

Polyol and hexamethylene diisocyanate (Desmodur N75BA/X) was thoroughly mixed with 0.01% of DBTDL and applied on the steel panels using automatic applicator. After curing at 80 °C for 4 h, the urethane coating panels were tested for basic film properties. All the polyurethane films derived from

the developed polyols resulted in moderate film properties. The significant difference can be observed from the impact resistance and solvent resistance (MEK double rub) of the polyurethane films. Generally, solvent resistance depends on polarity of polymer backbones such as hydroxyl groups and urethane groups from the aforementioned urethane coatings. Interestingly, the ESO-polyol with low hydroxyl numbers resulted in poor solvent resistance property. This may be due to the additional urethane linkages obtained in the ESO-polyol-based coatings. When the polyols were reacted with the isocyanate in 1:1 equivalent weight ratio, the ESO-polyol demanded more isocyanate functional groups due to the low hydroxyl number. This also increased the cross-link density of the ESO-polyol-based urethane coatings. The effect of cross-link densities can be seen from the pencil hardness and koenig hardness of the developed films. Like polar groups, cross-link densities of polymer networks are also directly related to its solvent resistance properties. Based on the obtained solvent resistance values, one can understand that polarity and hydrogen bond network of the polymers dominate the cross-link density effect on the solvent resistance properties of developed coatings. Though the hydroxyl groups and cross-link density of the urethane networks in EMG-polyol and EMG-PEP polyols are similar, the excellent solvent resistance property of the EMG-PEP polyol might be the result of aromatic groups from the phthalic ester backbone of the EMG-PEP polyol. These bulky pendant groups can also increase the molecular mobility of the polymeric chain. Because of this increased mobility, the flexibility of the urethane coatings increased which can be seen from the excellent reverse impact resistance of EMG-PEP coating films.

As shown in Table 12.4, by changing the hydroxyl groups of polyols to melamine weight ratio from 90:10 to 60:40 various coating formulations were prepared. These coatings were applied on the steel panels using automatic applicator and cured at 80 °C for 4 h, before testing for basic film properties. It can be seen from Table 12.4, the pencil hardness, koenig hardness and the solvent resistance of the coating films were increased as the melamine content increased in all three types of formulations. Increasing the melamine content in the formulation increased the cross-link network between hydroxyl groups polyol to amine groups of melamine. These cross-linked networks were responsible for the excellent hardness and solvent resistance of the polymeric film. Unfortunately, the restriction in the free volume density adversely affected the impact resistance and adhesion properties of the coating films.

Table 12.3 Cured Film Properties: (Urethane)

Composition		ESO –Polyol	EMG - Polyol	EMG - PEP
Polyol		10.00 g	10.00 g	10.00 g
Desmodur N75BA		15.46 g	6.84 g	6.56 g
Desmodur N75BA used as 1: 1 equivalent weight ratio to OH groups				
Film Properties				
Pencil Hardness		2H	HB	HB
Koenig Hardness		73	42	29
Impact Resistance lbs.inches	Direct	160	160	160
	Reverse	100	140	160
MEK double rub		50	105	225
Cross-cut adhesion		5B	5B	5B
Dry Film Thickness		1.5 mil	1.5 mil	1.5 mil

Table 12.4 Melamine (Cymel 303) Cured Film Properties.

Formulation OH/ Melamine weight ratio	Pencil Hardness	Koenig Hardness (Seconds)	Impact Resistance (Direct/ Reverse lbs. inches	MEK Double Rub	Cross–Cut Adhesion	Dry Film Thickness (mil)
ESO - Polyol						
60/40	3H	143	28/4	75	2B	1.5
70/30	3H	126	40/4	25	3B	1.5
80/20	2H	84	40/12	25	4B	1.5
90/10	H	28	60/20	25	5B	1.5
EMG - Polyol						
60/40	4H	205	10/0	250	2B	1.5
70/30	4H	191	40/0	350	3B	1.5
80/20	HB	32	120/20	200	5B	1.5
90/10	HB	15	140/30	75	5B	1.5
EMG - PEP						
60/40	3H	186	30/0	600	2B	1.5
70/30	3H	174	30/0	500	3B	1.5
80/20	2H	156	70/6	25	3B	1.5
90/10	HB	104	140/10	25	5B	1.5

12.4 Conclusion

A range of polyols has been synthesized from soybean oil derivative – ESO. The results of our investigation showed that it is possible to prepare polyols from oxirane derivatives of soybean oil under controlled reaction conditions. However, due to competing oxirane-oxirane reactions under acid-catalyzed conditions, some of the oxirane groups do not yield –OH groups but form polyether derivatives. While this is undesirable, it is difficult to control and suppress this reaction and hence the resulting polyols almost always have polyether structure present.

Further, it has been demonstrated that it is possible to carry out transesterification reaction of ESO with glycerol without affecting oxirane groups. This allows incorporation of additional hydroxyl groups and related modifications before ring-opening reaction. The polyols prepared by transesterification followed ring-opening esterification/etherification have been characterized for various properties. The study also demonstrates usefulness of these polyols as components of thermoset coatings. Two series of coatings – polyurethane and melamine-cured thermosets have been prepared and their properties indicate their usefulness for a variety of end-use coating applications.

Acknowledgements

The research work is part of the PhD thesis belongs to Senthilkumar Rengasamy. The authors sincerely acknowledge USDA for financial support under Cooperative State Research Education, and extension Services (CSREES) through Grant Award No. 2009–38303-05085. We would also like to express the deepest appreciation to Arkema, Inc. & Bayer Material Science for providing raw materials, respectively, ESO & Desmodur 75BA/X.

References

1. A. Guo, Y. Cho, and Z.S. Petrovic, *Journal of Polymer Science, Part A: Polymer Chemistry,* Vol. 38, p. 3900, 2000.

2. Z.S. Petrovic, A. Guo, and W. Zhang, *Journal of Polymer Science, Part A: Polymer Chemistry,* Vol. 38, p. 4062, 2000.

3. G. Lligadas, *Biomacromolecules,* Vol. 8, p. 686, 2007.

4. X.H. Kong and S.S. Narine, *Biomacromolecules,* Vol. 8, p. 2203, 2007.

5. A. Zlatanic, Z.S. Petrovic, and K. Dusek, *Biomacromolecules,* Vol. 3, p. 1048, 2002.

6. A. Zlatanic, C. Lava, W. Zhang, and Z.S. Petrovic, *Journal of Polymer Science, Part B: Polymer Physics,* Vol. 42, p. 809, 2004.

7. Z.S. Petrovic, M.J. Cevallos, I. Javni, D.W. Schaefer, and R. Justice, *Journal of Polymer Science, Part B: Polymer Physics,* Vol. 43, p. 3178, 2005.

8. I. Javni, W. Zhang, and Z.S. Petrovic, *Journal of Applied Polymer Science,* Vol. 88, p. 2912, 2003.

9. I. Javni, Z.S. Petrovic, A. Guo, and R. Fuller, *Journal of Applied Polymer Science,* Vol. 77, p. 1723, 2000.

10. I. Javni, Z.S. Petrovic, W. Zhang, and A. Guo, *58th Annual technical conference–society of plastics engineers,* Vol. 3, p. 3732, 2000.

11. A. Guo, W. Zhang, and Z.S. Petrovic, *Journal of Materials Science,* Vol. 41, p. 4914, 2006.

12. A. Guo, I. Javni, and Z. Petrovic, *Journal of Applied Polymer Science,* Vol. 77, p. 467, 2000.

13. A. Guo, D. Demydov, W. Zhang, and Z.S. Petrovic, *Journal of Polymers and the Environment,* Vol. 10, p. 49, 2002.

14. Z.S. Petrovic, W. Zhang, and I. Javni, *Biomacromolecules,* Vol. 6, p. 713, 2005.

15. G. Lligadas, J.C. Ronda, M. Galia, U. Biermann, and J.O. Metzger, *J. Polym. Sci., Part A: Poly. Chem.,* Vol. 44, p. 634, 2006.

16. L. Hojabri, X. Kong, and S.S. Narine, *Biomacromolecules,* Vol. 10, p. 884, 2009.

17. M.J. Dumont, X. Kong, and S.S. Narine, *J. App. Polym. Sci.,* Vol. 117, p. 3196, 2010.

18. Y. Guo, J.H. Hardesty, V. Mannari, and J.L. Massingill. *J. Am. Oil. Chem. Soc.,* Vol. 84, p. 929, 2007.

19. G. Lligadas, J.C. Ronda, M. Galia, and V. Cadiz, *Biomacromolecules,* Vol. 8, p. 686, 2007.

20. G. Lligadas, J.C. Ronda, M. Galia, and V. Cadiz, *Biomacromolecules,* Vol. 8, p. 1858, 2007.

21. Y. Lu, and R.C. Larock, *Biomacromolecules,* Vol. 8, p. 3108, 2007.

22. Y. Lu and R.C. Larock, *J. Appl. Polym. Sci.,* Vol. 9, p. 3332, 2008.

23. S.N. Khot, J.J. Lascala, E. Can, S. Shantaram, G.I. Williams, G.R. Palmese, S.H. Kusefoglu, and R.P. Wool, *J. App. Polym. Sci.,* Vol. 82, p. 703, 2001.
24. E. Sharmin, S.M. Ashraf, and S. Ahmad, *Eur. J. Lipid. Sci. Technol.,* Vol. 109, p. 134, 2007.
25. Z.S. Petrovic, A. Guo, I. Javni, I. Cvetkovic, and D.P. Hong, *Polym. Int.,* Vol. 57, p. 275, 2008.
26. I. Javni, W. Zhang, and Z.S. Petrovic, *J. Appl. Polym. Sci.,* Vol. 88, p. 2913, 2003.
27. J. Patel, S. Rengasamy, and V. Mannari, *Eur. Coat. J.,* Vol. 4, p. 125, 2011.
28. S. Rengasamy and V. Mannari, *J. Appl. Polym. Sci.,* Vol. 130, p. 3874, 2013.
29. S. Rengasamy and V. Mannari, *Prog. Org. Coat.,* Vol. 77, p. 557, 2014.
30. S. Rengasamy and V. Mannari, *Prog. Org. Coat.,* Vol. 76, p. 78, 2013.
31. S. Rengasam, and V. Mannari, *Eur. Coat., J.* Vol. 3, p. 80, 2013.
32. Y. Lu and R.C. Larock, *Prog. Org. Coat.,* Vol. 69, p. 31, 2010.
33. Z.S. Guo, A., I. Javni, I. Cvetkovic, and D.P. Hong. *Polym. Int.,* Vol. 57, p. 275, 2008.
34. Z.S. Petrovic, W. Zhang, and I. Javni, *Biomacromolecules,* Vol. 6, p. 713, 2005.
35. C.T. Huo, *Adv. Appl. Microbiol.,* Vol. 41, p. 1, 1995.

Chapter 13

Powder Coatings from Recycled Polymers and Renewable Resources

Martino Colonna[1]*, Claudio Gioia[1], Annamaria Celli[1], and Alessandro Minesso[2]

[1]*Department of Civil, Chemical, Environmental and Materials Engineering, Alma Mater Studiorum, University of Bologna, Bologna, Italy*

[2]*Allnex Italy S.r.l., Romano d'Ezzelino (VI), Bologna, Italy*

**Corresponding author*: martino.colonna@unibo.it

Abstract

Powder coating constitutes a very interesting class of eco-friendly green coatings since the production process is solvent-free, and therefore the problems associated with the emission of volatile organic compounds are completely absent. Moreover, the polyesters that constitute the main component of powder coatings can be produced using monomers derived from renewable resources and/or recycled polymers. In this chapter, we report the recent advances in the field of eco-friendly green powder coatings, focussing in particular on the use of monomers derived from renewable resources such as isosorbide, succinic acid and glycerol together with the use of recycled polymers such as poly(ethylene terephthalate).

Keywords: Powder coatings, chemical recycle, isosorbide, poly(ethylene terephthalate)

13.1 Introduction

Technical reports [1] predict that, if the present consumption will continue at a constant rate, the fossil oil feedstocks will finish before the end of the century. Therefore, the era of a chemical industry based on fossil resources will probably come to an end before that time. The Kyoto protocol along with the desire to reduce the dependence on fossil oil has directed the attention of academia and industrial companies toward the use of biomass as source of energy and commodity chemicals [2–4].

From an industrial point of view, the increased prices for most chemicals obtained from crude oil have made more attractive not only the use of renewable resources to produce polymers, but also the recycling of plastic wastes [5]. Indeed, the recycling of polymers is an important route for the reduction of the carbon footprint of such materials since it reduces the use of feedstocks obtained from non-renewable resources. The recycling of plastics can be performed by a chemical approach through a depolymerization process [6]. This strategy can be in principle performed also using

reagents obtained from renewable resources, making this approach even more interesting from an environmental point of view.

Coating producers are trying to find alternative sources for the chemical ingredients derived from petroleum or other fossil sources. The increased need for environmentally friendly and sustainable technologies has made the use of renewable feedstocks in the paint and coating area more and more important [7, 8]. Among coating techniques, powder coating has already been widely accepted in the industrial market because of its numerous advantages [9]. Since it does not employ solvents and the material can be fully recovered, this technique represents a green alternative to other less environmental-friendly industrial procedures.

Therefore, the aim of the present chapter is to report the progress in the field of environmental-friendly coatings prepared by powder coating techniques. In particular, the use of monomers derived from renewable resources and the use of recycled polymers will be discussed and the properties of the coatings obtained with these new routes will be compared with commercially available coatings made from non-renewable resources.

13.2 Powder Coating as a Green Approach to Coatings

Although already available since more than 50 years, powder coating is still considered as an advanced, fast growing technology widely recognized by the market for its durability, gloss retention, weatherability, possibility of application at high thickness films and for its unlimited range of colours, finishes, glosses and textures.

The first thermosetting powder coating appeared on the market in the late 1950s [10–12], with the development of a process where the part to be coated was heated in an oven at a temperature above the melting point of the powder and dipped into a fluidized bed. Using this process, only coatings with thickness over 250 μm were obtained, differently from film coatings thinner than 100 μm that were achievable with conventional paint-like liquid coatings.

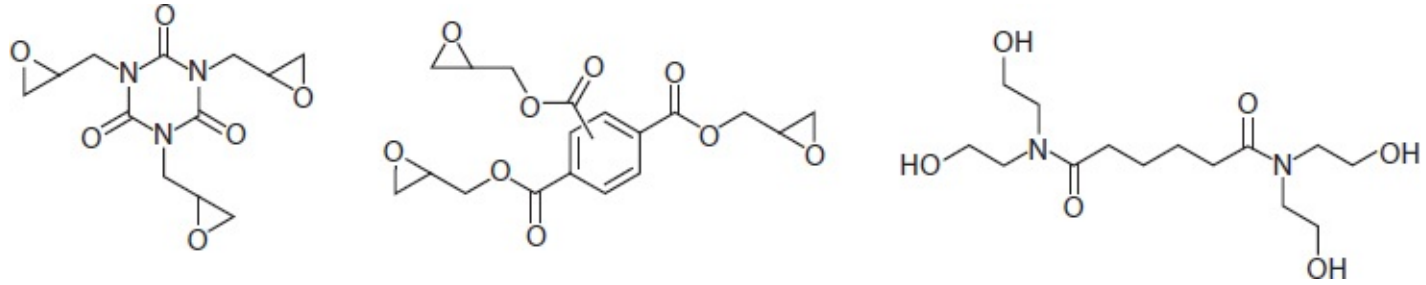
A step beyond was made with the electrostatic spray process, developed in the early 1960s allowing the application of coatings with thinner layer thicknesses [10]. With this technique, the coating powder is dispersed in an air stream and passed through a corona discharge field where the particles acquire an electrostatic charge. The coated object, usually metallic and at room temperature, is then placed in an oven where the powder melts and forms the coating as a result of a curing chemical reaction. Since the production of the powder paint takes place mainly in melt processes, extrusion is the preferred method in order to mix the different ingredients. The extruded product is then solidified passing through a roller and a cooling belt forming plates which are then crushed, grinded and sieved to powder with an average particle sizes between 18 and 80 μm. In order to avoid the fusion of the powder paint during the production process, particularly during the milling step, high softening temperature for the powder components are required. The selection of resins for powder coatings is consequently restricted to polymers having glass transition temperature higher than 45–50 °C. Therefore, powder coating films are relatively hard and brittle compared with liquid coatings, which are soft and tacky after evaporation of solvent and become hard and non-tacky only after curing.

Effective cross-linking of powder coatings is a critical step in order to increase the toughness of the film and balance hardness and flexibility to optimum levels [12]. Popular thermo-set powders include

epoxy, polyesters, polyester urethane and acrylic resins. Polyester resins are the most important in the powder coating market. In fact, the possibility to select the type and the amount of functional groups, together with the broad availability of different polycarboxylic acids and polyfunctional alcohols to be used as monomers for direct polycondensation, make thermosetting powder coating particularly versatile and flexible. Furthermore, the possibility of combining the polymer resins with numerous different types of cross-linking agents allows to cover different market applications and different film effects with the best balance of applicative properties.

Hybrid systems of epoxy resins and polyester resins are the most common powder coating system for indoor applications. The properties of these coatings are similar to pure epoxy systems but with relative lower hardness and resistance to chemicals and solvents and better yellowing resistance and outdoor durability. Powder coatings for exterior applications cannot contain bisphenol A epoxy resins because of their poor resistance to UV light. Triglycidylisocyanurate (TGIC) has been considered the most important hardener for properly designed acid functionalized, saturated polyester resins to be used for outdoor applications. However, since the end of 1990s TGIC has been subsequently replaced, mainly in Europe, by less- or non-toxic alternatives, like glycidyl esters of aromatic polycarboxilic acids (e.g. Araldite® PT 910 from Huntsman) or β-hydroxyalkylamides (Primid® XL 552 from EMS-Chemie) (Figure 13.1) [10–13].

Figure 13.1 Triglycidylisocyanurate, Araldite® PT 910 and Primid® XL 552.



The main difference when powder is compared with liquid coating is that no solvents are used. Therefore, virtually no volatile organic compounds (VOCs) are emitted during manufacturing and final application. Powder coating reduces the costs of compliance to environmental regulations and remains the process of choice where VOCs must be reduced to the lowest possible values, as for example in many Original Equipment Manufacturer (OEM) and automotive coating operations. The environmental-friendly character of powder compared to liquid coatings is also reinforced by the fact that oversprayed powder can be completely recovered and then recycled, resulting in higher material utilization and waste (paint sludge) minimization. Powder coating has also higher transfer efficiency if compared with other paint applications, resulting more sustainable and efficient. In addition, the powder coating process uses less transportation energy than liquid coatings, which generally show higher packaging and shipping costs. In summary, the combination of the higher efficiency and lower costs with the environmental advantages and minor regulatory compliance issues, has contributed to the growth of powder coating technology in areas where the conventional liquid paints have been traditionally used [12, 14]. The powder coating market has been driven by several opportunities to replace liquid coatings, resulting in a double digits annual growth rate over the past decades until the early 1990s [16]. Due to the economic contraction and financial crisis, the growth rate as decreased in the recent years mainly in the European and North American markets, while the demand remains higher in the Asian market. According to the available marketing data [16–18], the global powder coatings market production in 2013 was about 2000 ktons with a value in terms of earned revenue of about USD 7.7 billion, growing at a compounded annual growth rate

(CAGR) between 6% and 7% over the period 2014–2018. The trend is supported by the increasing demand for powder coatings in emerging markets such as China, India, Brazil and Russia. Asia-Pacific represents the largest regional market with a share of more than 50% [17], and it is expected to continue its growth in the next future, mainly driven by the Chinese and Indian markets. The major market segments for powder coating applications are appliances, furniture, automotive, general industry, architectural and construction. The market share for the different segments can change in a significant extent due to the big variation in the different geographic areas and the fragmentation of the market structure, with a very high number of small and medium sized industry participants [13]. Specifically, appliances sector is considered having the major market share with about 23% in terms of volume in 2013, according to Markets and Markets [18], while it was counting for the 14% of the market share in 2007, according to BCC Research [14]. Automotive and architecture coatings are the second and third largest end uses for the powder coating market, accounting for another 30–35% of the market share. Automotive market is mainly related to primer applications, a coating protecting the electrocoat primer and providing a smooth surface for the basecoat. Moreover, automotive clear topcoats are usually based on epoxy functional acrylic resins and dodecandicarboxylic acid or its (poly)anhydride as cross-linkers. The architectural market for powder coatings has grown rapidly in Western Europe; to date, US market has been low, but it is expected to increase at a higher rate than any other end-use sector. Powder coating of architectural aluminium is also well established in the Middle East, Brazil, South Africa and Australia, and growing rapidly in Southeast Asia. Powder can be applied to windows, doors, column covers and many other aluminium building and construction elements. Total annual global powder consumption for architectural aluminium was about 200 ktons in 2013. Total market potential is estimated at 500 ktons, with a market share of about 40%.

In recent years, development trends in powder coating have been oriented towards improving the quality of binders, specifically the polyester resins which have been object of affordable modifications in order to achieve new applicative performances and access new market segments. Different key technologies have recently seen significant improvement and can drive the growth in the next future [15]. Low cure temperature powder and UV-cured systems have been more and more developed in order to be able to use powder coating techniques for applications onto heat sensitive substrates, as for example plastics with low glass transition temperature, wood substrates including medium density fibreboards (MDF) and some special alloys. In-mould powder coatings have been developed in order to provide a simpler coating process compared to the use of powder paint on post-coated components, because the powder is sprayed onto a hot mould before pressing and moulding.

Although powder coating technology is a totally solvent-free finishing and almost 100% recyclable process, regulations and opinion leaders are requiring further improvements in environmental impact of powder coating producers and end-users, including the process and materials used in the different pre-treatment steps of the metal substrates. Current surface pre-treatment methods employed to ensure adequate corrosion protection on metal surfaces for ACE applications (e.g., zinc or iron phosphate on steel surfaces and yellow chromate on aluminium) still poses environmental challenges, while the introduction in the market of pre-treatments with a more environmental-friendly character is requiring better corrosion resistant coatings to balance the lower protecting efficiency of these novel pre-treatments. Furthermore, renewable polymers and plastics have been developed in the recent years to replace petrochemical products in several applications. Recent developments have investigated new synthesis processes of sustainable and cost-efficient polyester resins for powder coating, combining the chemical recycle of polymers recovered from post-consumer waste streams

with the use of bio-based monomers as building blocks for the polymerization. These new environmental-friendly approaches will be described in detail in the following paragraphs.

13.3 The Use of Materials from Renewable Resources in Powder Coating Applications

Bio-based polymers used for the production of powder coatings can be classified in two main groups, according to the chemical characteristics of the monomers:

1. Polymers derived from bio-based monomers, which are identical to the currently used petro-derived monomers. Therefore, the polymers and the resulting coatings behave in an identical manner to the currently used coatings;

2. Polymers derived from new bio-based monomers, which are used to produce polymers with novel chemical structures and, therefore, properties and performances. For this reason, a process development is necessary in order to achieve optimal properties of the final coating.

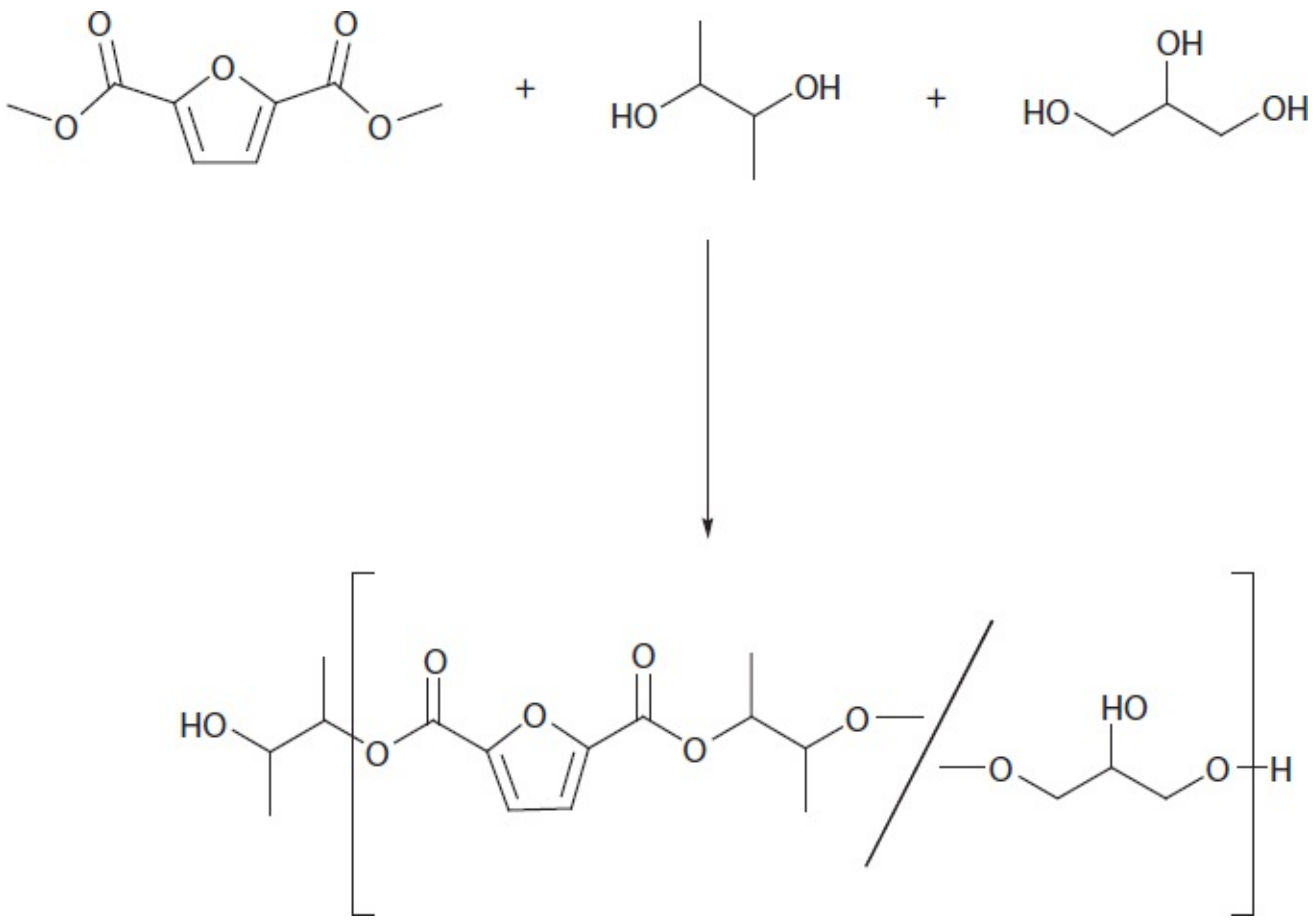
Today, the commercial availability of bio-based monomers is relatively restricted and prices are significantly higher with respect to petro-derived chemicals, even if it is probable that in a next future this trend will change and bio-based chemicals will become commercially viable at advantageous prices. For example, from Group 1, terephthalic acid (TPA), which is one of the most used monomers to prepare polyesters for powder coating, can now be obtained from bio-based resources. However, these processes are not yet industrially and economically feasible [1, 19, 20]. Therefore, established that in both groups of bio-based monomers, the commercial availability is yet limited, the attention will be here focused on the second class, i.e. on new biomass sourced monomers, that represent the new frontiers of research.

From a powder coating perspective, polyesters are the most important class of bioresins. Therefore, we here summarize the most recent results described in the literature for the preparation of bio-based coatings based on these polymers.

Polyesters for powder coating are characterized by specific properties, in particular by an amorphous and rigid architecture able to provide T_g values higher than 45–50 °C. Indeed, traditional polyester resins for powder coating are based on aromatic diacids, such as TPA or isophthalic acid (IPA) (which provide rigid chains) and an aliphatic diol which is used to give a certain degree of chain flexibility.

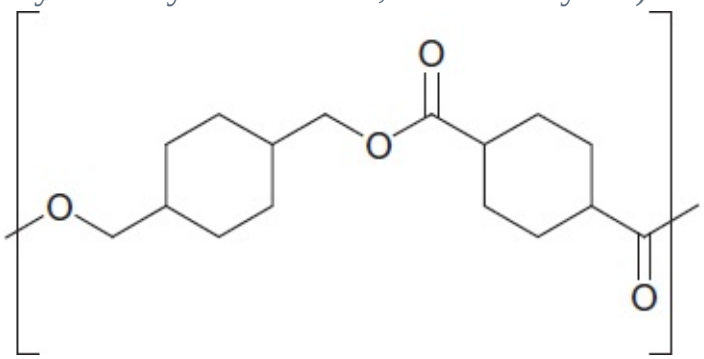
The most promising candidate to replace TPA is 2,5-furandicarboxylic acid (FDCA), which is readily accessible from sugars. Recently, polyesters based on FDCA and 2,3-butanediol have been tested for powder coating applications [21–23]. In this way, amorphous resins, with suitable molecular weights and predominantly hydroxyl endcapped, have been successfully prepared (Figure 13.2). The T_g values, resulting in the range of 70–90 °C, then exceeding the required minimum values of 45 °C, indicate that the furan-based materials possess very rigid structures. This means that the final (co) polyesters present high storage stability. Various linear and branched resins based on FDCA, suitable for powder coating applications, have been prepared. However, they are characterized by brittleness and low impact resistance.

Figure 13.2 Polyesters for powder coatings based on 2,5-furandicarboxylic acid.



Other aromatic monomers available in nature have been exploited in order to build new macromolecular structures: for example, ferulic acid and vanillic acid [24–26]. However, specific tests for powder coating applications have not yet been reported. On the other hand, T_g values of 45–50 °C are difficult to be obtained with most aliphatic systems, especially with the low number average molecular weights (Mn) (3000–10,000) used in powder coating applications. For example, also the presence of aliphatic cycles in poly(1,4-cyclohexylidenecyclohexane-1,4-dicarboxylate) (PCCD) oligomers (Figure 13.3) is not sufficient to achieve high T_g values and alternative strategies must be found to increase the polymer performances, for example through the formation of anhydride linkages [27].

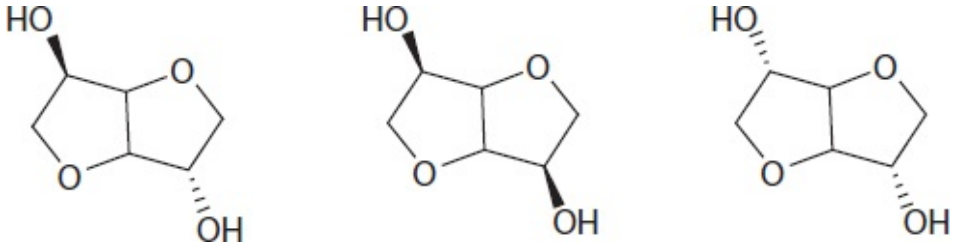
Figure 13.3 Poly(1,4-cyclohexylidenecyclohexane-1,4-dicarboxylate).



Therefore, due to the availability of a range of aliphatic bio-based diacids, such as succinic acid, the strategy to prepare bio-polyesters for powder coating requires a rethinking in order to build macromolecular structures with the requested properties, mainly in terms of macromolecular rigidity. For example, flexible diacids must be coupled with rigid diols, such as anhydro-alditols (isosorbide, isoidide, isomannide) (Figure 13.4). Linear and branched co- and terpolyesters based on succinic acid and isosorbide, in combination also with other renewable monomers, 2,3-butanediol,

1,3-propanediol, and citric acid (CA), have been prepared [8, 28]. Upon incorporation of 60–80% of isosorbide, the resulting T_g is high enough to ensure a good processing and storage stability of the polyester resin. It was also found that the incorporation of other diols has a beneficial effect on the colour of the resin. The novel polyesters resulted to be suitable for powder coating applications. In particular, coatings made using branched polyesters show significantly improved mechanical and chemical resistances compared to those of coatings made using linear polymers. Isosorbide can also be substituted with isoiodide [29], which is slightly more reactive in polycondensation reactions due to the *exo*-orientation of its hydroxyl groups. Furthermore, it is also thermally stable. However, isoiodide is not yet commercially available.

Figure 13.4 Isosorbide, Isomannide and Isoidide.



CA, which is commercially produced by fermentation, has been also studied as a polyfunctional modifier to transform polyesters, having hydroxyl end-groups of moderate reactivity, derived for example from isosorbide, into novel, slightly branched polymers with high acid functionalities [30]. It was observed that CA forms a reactive anhydride intermediate above its melting temperature (i.e., between 150 and 160 °C), which reacts rapidly with OH groups to form ester linkages. CA-modified polyesters have been applied as coatings, using conventional cross-linking agents, showing rapid curing that produced chemically and mechanically stable coatings. Therefore, CA can be seen as a cheap, aliphatic and bio-based alternative to trimellitic anhydride. The new renewable macromolecular structures, however, do not exhibit specific UV resistance, that, instead, is one of the current main objectives in the preparation of coating from petrochemical sources. For example, isosorbide-based coating systems appear to have similar weathering resistance as conventional TPA-based poly(ester urethane) coatings [30].

Isosorbide, isoiodide and isomannide have also been exploited in order to obtain OH-functional bio-based polycarbonates for coating applications [31]. Different synthetic routes have been investigated and curing of the various bio-based linear and branched aliphatic (co)polycarbonates using conventional polyisocyanate cross-linkers yielded colourless to pale yellow, transparent, glossy coatings, having excellent chemical and mechanical resistances.

Finally, by considering other classes of resins for powder coating, bio-epoxy resins can be obtained by epichlorohydrin prepared from bio-based glycerol. Acrylic-based systems, which are relatively less significant for powder coating applications, could be probably more easily obtained due to the availability of bio-based acrylic monomers [32].

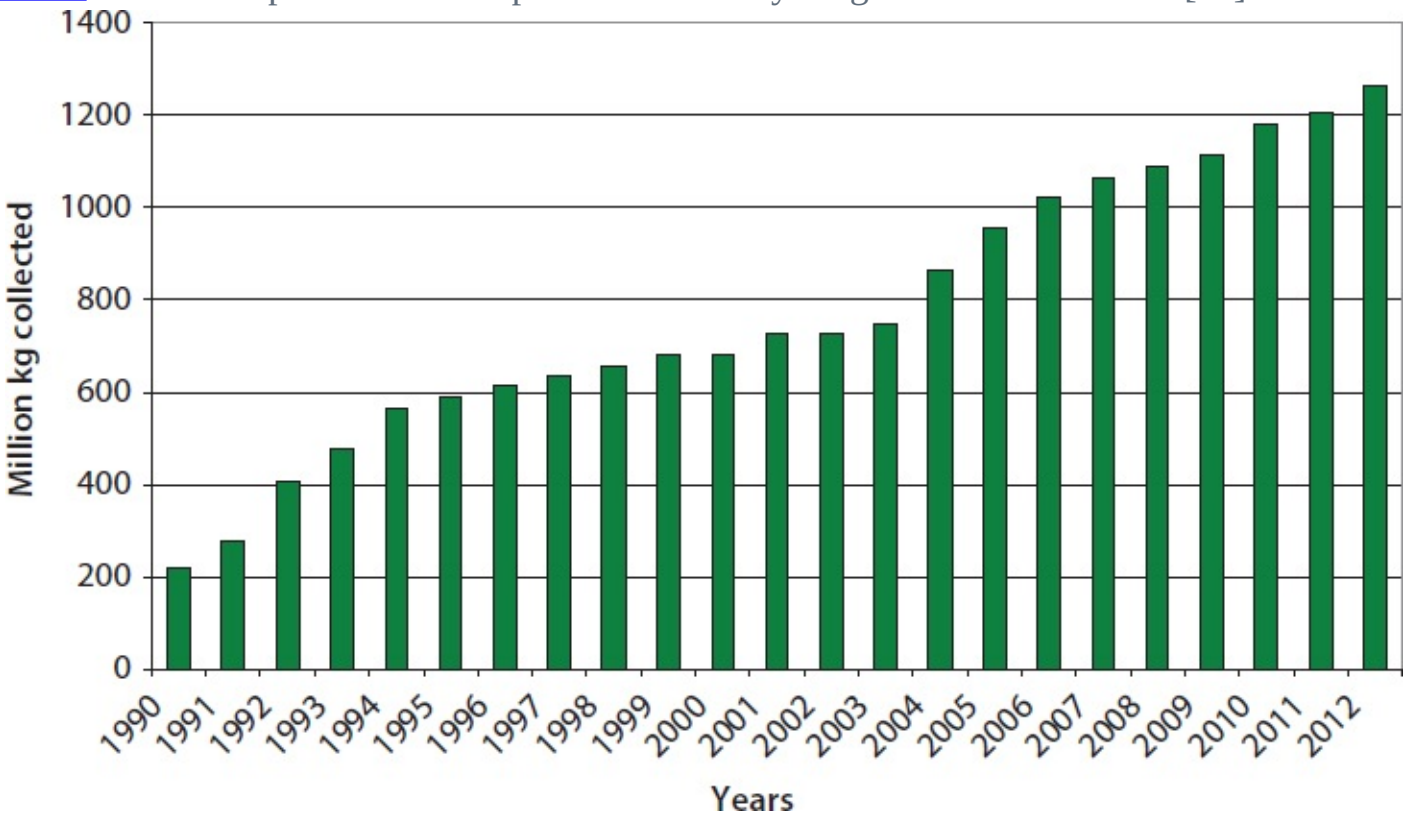
13.4 The Use of Recycled Polymers for the Preparation of Coatings

Recycled plastics can be considered nowadays a very promising feedstock for the production of value-added materials. Governmental initiatives and a more spread social awareness toward

environmental issues are producing a constant increase in the recovery of post-consumer waste all over the world. Indeed, in 2009 almost 25 million tons of waste have been collected only in Europe. About 90% of such amount consists of thermoplastic materials such as poly(ethylene terephthalate) (PET), high- and low-density polyethylene (HDPE, LDPE), polypropylene (PP), polyvinyl chloride (PVC) and polystyrene (PS) [33].

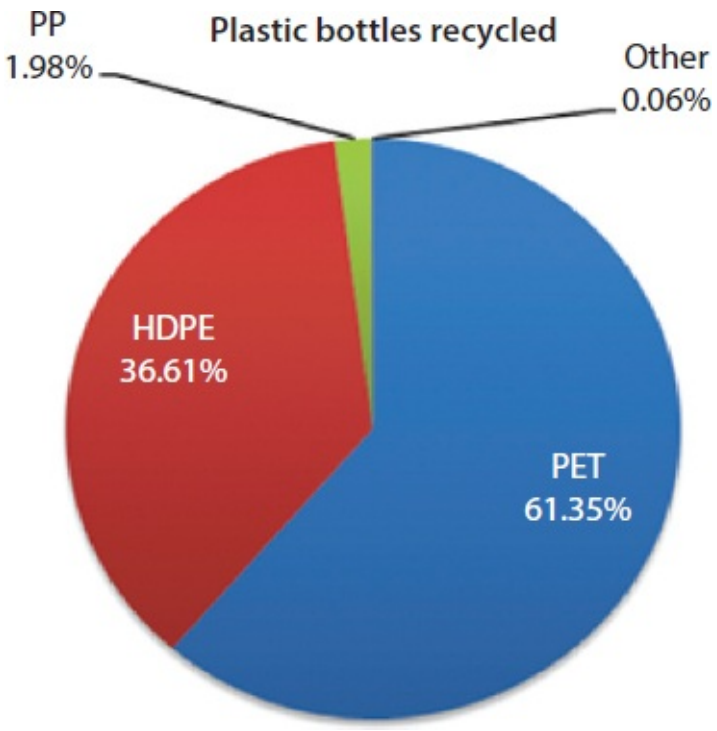
PET is one of the most important recycled polymers due to its high reactivity that permits to perform several different chemical recycling processes [34]. The most important source for recycled PET consists of post-consumer packaging and in particular of plastic bottles. According to the US national post-consumer plastics bottle recycling report [35], in 2012 the amount of plastic bottles recycled in the US reached the record of about 1.26 million tons (Figure 13.5) with an annual increase 6.2% and a collection rate of 30.5%.

Figure 13.5 Growth in post-consumer plastic bottle recycling from 1990 to 2012 [35].



Post-consumer plastic bottle recycled wastes contains mainly PET (62%), HDPE (37%), PP (2%) and other materials (0.059%) (Figure 13.6). Therefore, the amount of PET deriving from bottles recycle has increased from 2011 of 51.5 million kg, reaching a total amount of 780 million kg.

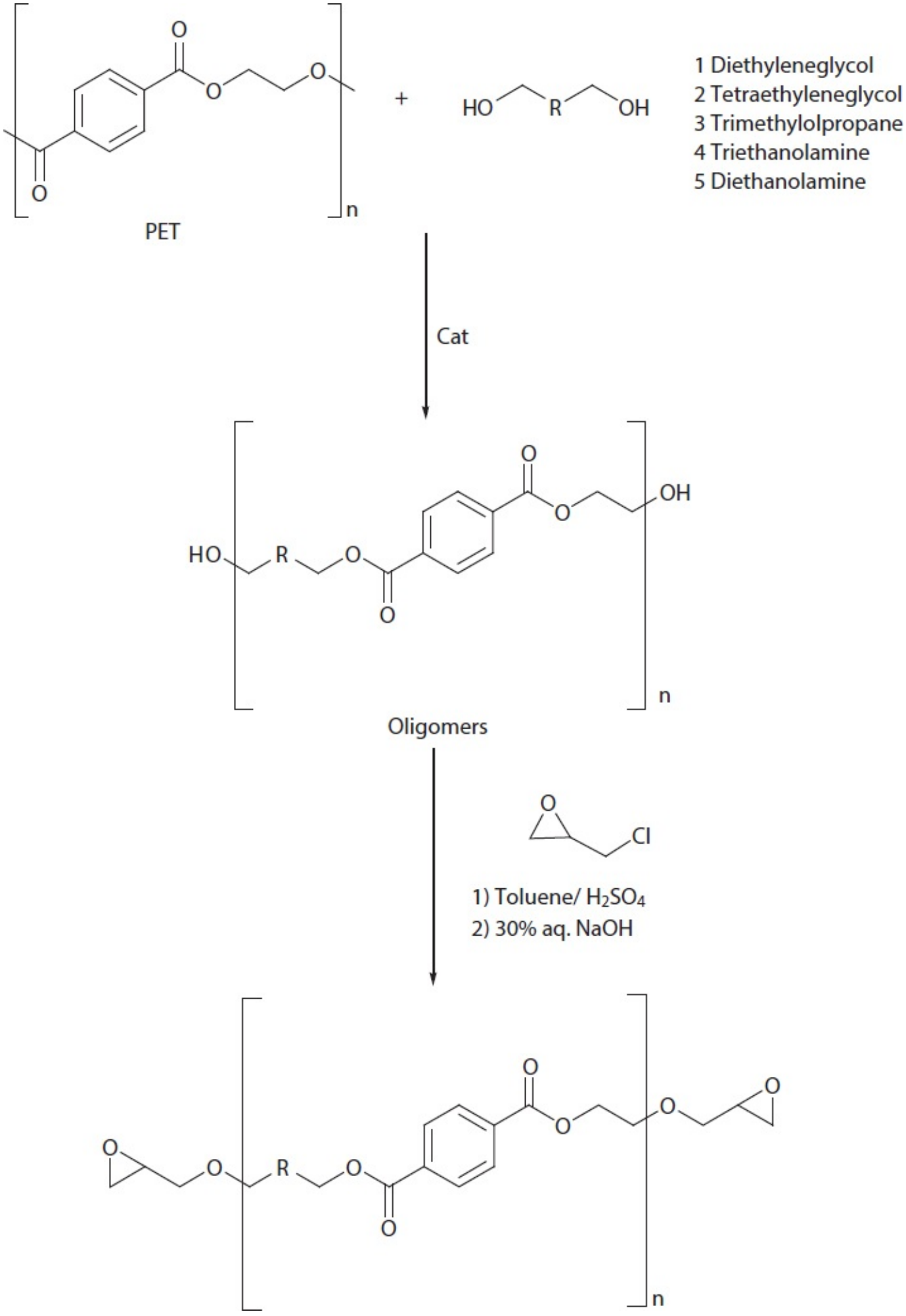
Figure 13.6 Composition of recycled bottles in 2012 [35].



Chemical recycling consists in the selective depolymerization of macromolecules in order to obtain low molecular weight molecules that can be used for the preparation of new polymeric materials. The purification of low molecular monomers from impurities can be performed more easily compared to the purification/separation of impure polymer mixtures and for this reason high purity monomers and oligomers can be prepared.

Chemical recycling of PET can be performed by different processes (e.g. hydrolysis, acidolysis, aminolysis), but glycolysis can be considered the most widespread method for the production of monomers or oligomers. These substances can be subsequently repolymerized in order to obtain new materials for different applications (e.g. coatings). Atta and Czub [36–38], for example, have studied and optimized the synthesis of epoxy resins from PET oligomers (Figure 13.7). In the first step, they have performed a controlled glycolysis of PET with diethylene glycol, tetraethylene glycol, trimethylol propane, triethanolamine and diethanolamine. The oligomers obtained were further modified with epichlorohydrine for the synthesis of the epoxy resin.

Figure 13.7 Chemical recycle of PET with various glycols.

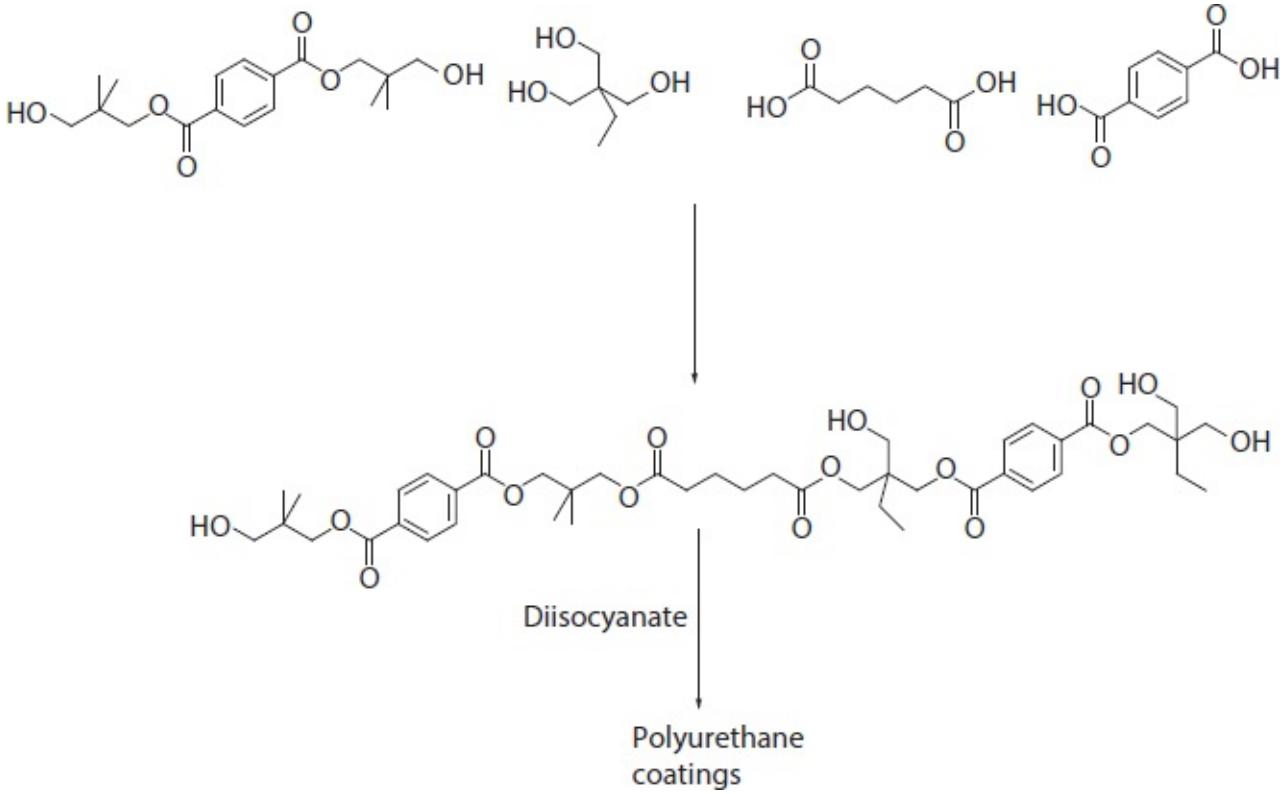


The epoxy resin obtained were cured with different hardeners; the properties observed for the

obtained coatings demonstrated to be tuneable according to the type of glycol used in the first step. Furthermore, the coatings showed enhanced properties of adhesion with steel and high chemical resistance. In addition, oligomers presenting epoxy groups could be employed as hardeners for polyester resins for powder coating; nevertheless such application has not been investigated yet.

Another approach for the preparation of coatings from recycled plastic wastes consists in the isolation of bis(hydroxyalkyl)terephthalate obtained from extensive glycolysis of PET. Sabnis *et al.*, have isolated and purified the bis(hydroxyalkyl)terephthalate obtained by chemical recycling PET with neopentyl glycol. They have used this monomer for the synthesis of a polyester that was then used for the preparation of polyurethane coatings (Figure 13.8) [39]. The purpose of their work was to demonstrate the possibility to use new compounds derived from recycled PET in order to substitute or partially replace virgin petrol based reagents in the synthesis of polyurethane coatings.

Figure 13.8 Chemical recycle of PET by glycolysis with neopentyl glycol.



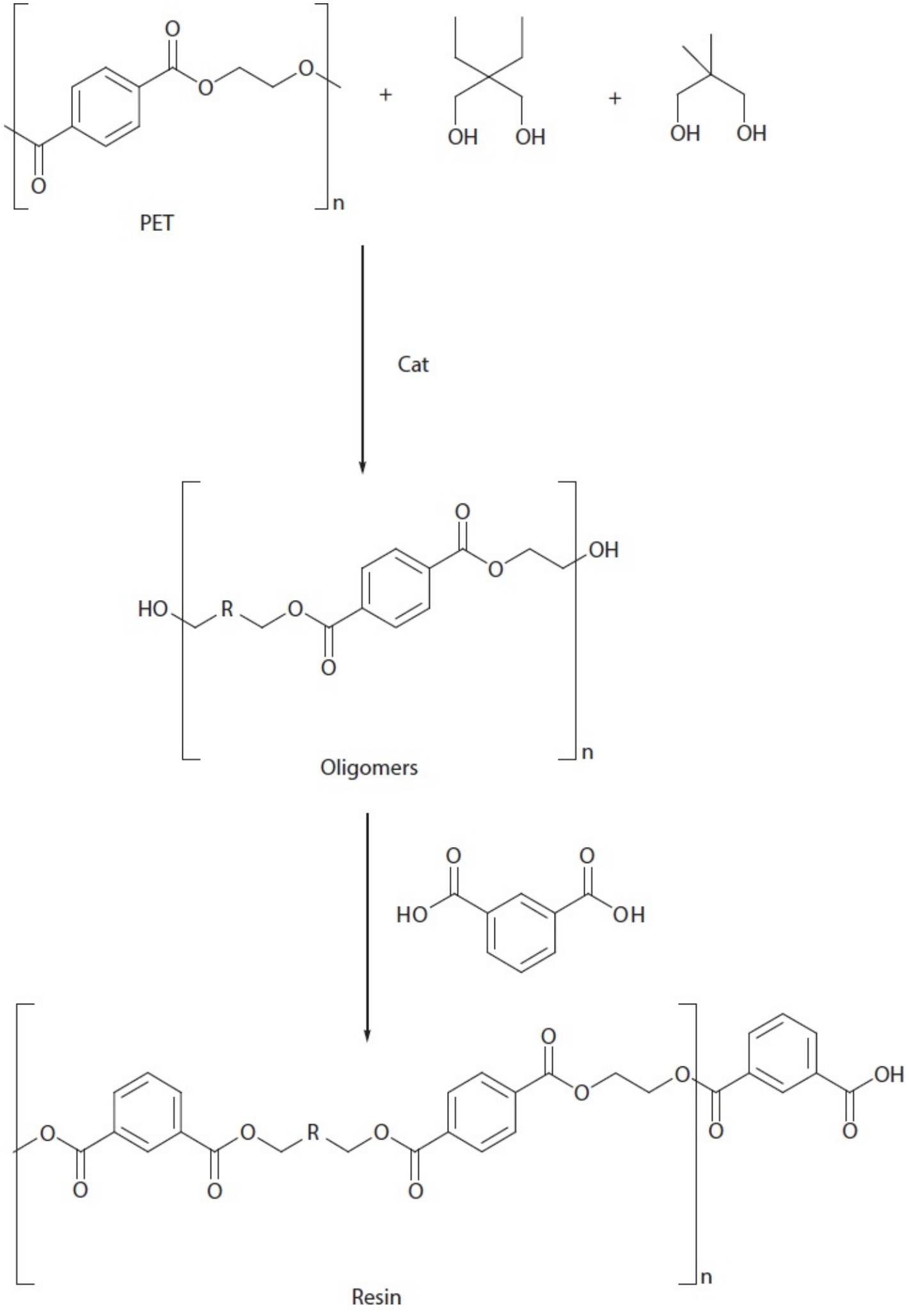
This concept was more extensively applied to the preparation of alkyd resins. These coatings, in fact, involve the use of many natural oils and fatty acids, but require aromatic compounds in order to obtain suitable mechanical properties. The substitution of virgin petrol based compounds with recycled feedstocks from PET therefore result in an increased sustainability of the product. Guclu [40], Einloft [41] and Kawamura [42] have studied the glycolysis of PET and the consequent combination of such oligomers with natural fatty acid in order to partially replace phthalic anhydride. The results obtained demonstrate that oligomers deriving from PET could be easily combined with polyols and fatty acids in order to reduce or in some case avoid the use of petrol based aromatic compounds. The properties of such coatings, in fact, were completely comparable or in some case superior to the reference commercial coatings.

Although the previously reported results clearly demonstrate the feasibility of the employment of recycled PET for the preparation of coatings, very few attempts have been performed in the field of powder coatings.

Kawamura *et al.* [42] have developed a process for the synthesis of oligomers suitable for powder coatings. Their procedure involves, in the first step, the use of neopentyl glycol and trimethylol

propane as depolymerizing agents for PET. The obtained oligomers were then reacted, in the second step, with isophthalic acid in order to obtain a new (co)polyester presenting the desired acid terminal groups suitable for powder coatings (Figure 13.9).

Figure 13.9 Depolymerization of PET with neopenthyl glycol and trimethylol propane.


PET
Cat
Oligomers
Resin

The aim of the paper was clearly to demonstrate the value of recycled PET as an alternative feedstock with respect to fresh petrol based TPA. Also in this case the properties and the composition of the new resin for powder coating were completely comparable with the properties of the reference material.

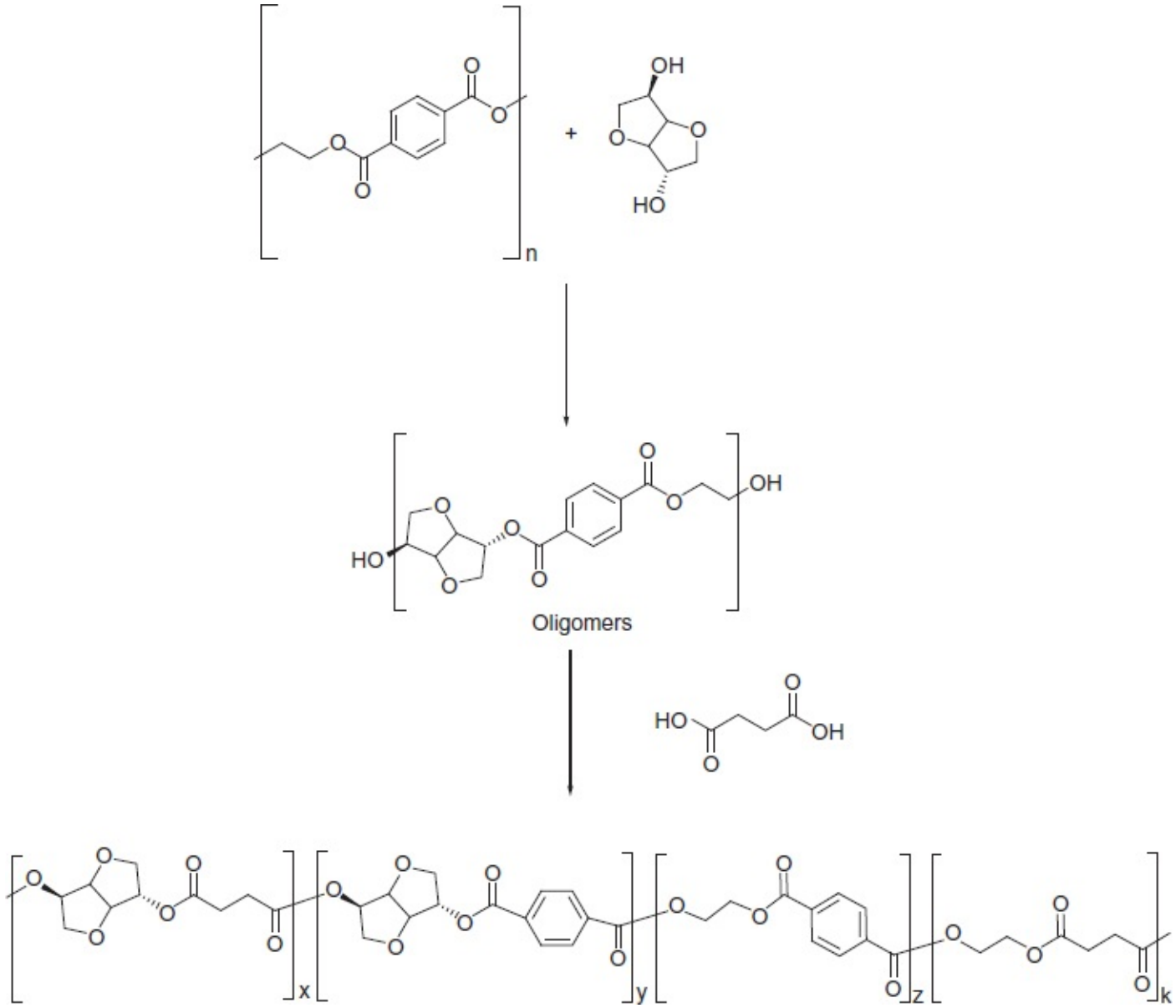
13.5 Powder Coatings from the Combined Chemical Recycle of Polymers and the Use of Renewable Resources

As reported in the previous paragraphs, both the use of recycled polymers and of renewable resources provide environmental-friendly routes for the preparation of coatings. Therefore, it is clear that the combination of these two processes permits to further decrease the carbon footprint of the coating.

As previously described, PET is widely available from the recycle of plastic bottles [43]. This polymer is suitable for chemical recycling due to the presence of ester groups that can react with aliphatic diols to produce oligomers or low molecular weight polymers. Moreover, TPA is often used for the preparation of polyesters for powder coating since permits to obtain polymers with high stability to ageing and with the correct glass transition temperature needed for the preparation of powder coatings [21]. Indeed, a well-determined set of chemical and physical parameters are necessary in order to obtain powder coatings with properties suitable for industrial applications. In particular, the glass transition temperature, the molecular weight and the type of end-groups are of fundamental importance for the cross-linking and application process of the coating [21]. Therefore, the diols to be used in the depolymerization process needs to produce a polymer with the proper glass transition temperature (with a minimum value of 45 °C). For this reason, linear aliphatic diols (e.g. ethylene glycol, 1,4-butanediol, etc.) commonly used for the depolymerization of PET cannot be used for this purpose. Therefore, rigid diols, such as isosorbide [44], must be preferred in order to obtain polyester with a T_g and a molecular weight suitable for powder coating applications. Moreover, the polymers prepared by depolymerization must present a high stability to ageing and mechanical properties able to guarantee a wide range of commercial applications.

On the basis of these considerations, Allnex (formerly Cytec) together with University of Bologna has started in the past few years the development of an industrial process to produce powder coatings combining the use of renewable resources with the chemical recycle by depolymerization of poly(ethylene terephthalate) (Figure 13.10) [45–47].

Figure 13.10 Approach for the development of powder coatings from renewable resources and recycled polymers.



In the following paragraphs we report a detailed study of this process that combines chemical recycling with the use of renewable resources. The aim is to show the characteristics that a polyester for powder coating application should have and the properties of the coatings obtained with this new environmental-friendly process. These data can be useful in the development of new processes that uses renewable resources and/or recycled polymers.

13.5.1 Depolymerization of PET with Isosorbide

13.5.1.1 Catalysts Used for the Depolymerization of PET with Isosorbide

Trans-esterification reactions proceed with very slow rate if no catalytic system is added during the reaction and for this reason Lewis acids are used as catalysts for the PET depolymerization process [48]. Isosorbide presents a lower reactivity with respect to primary alcohols such as ethylene glycol or butanediol, generally used for the depolymerization of PET [28]. The use of an active catalyst permits to reduce the reaction time and therefore discoloration, since it is well known that isosorbide suffers of discoloration [49] if maintained for long times at temperatures exceeding 230 °C.

The results reported in Table 13.1 show that several catalytic systems (Sb_2O_3, GeO_2, $Zn(CH_3CO_2)_2$,

$Mn(CH_3CO_2)_2$) are not effective in these reaction conditions while monobutyltin oxide (MBTO) and titanium tetrabutoxide (TBT) present good catalytic activities.

Table 13.1 Conversion with different catalysts at 230 °C for 60 minutes.

Catalyst	Conversion
Sb_2O_3	<5%
GeO_2	<5%
$Zn(CH_3CO_2)_2$	<5%
$Mn(CH_3CO_2)_2$	<5%
MBTO	62%
TBT	63%

13.5.1.2 Depolymerization Process

An important aspect to be considered in the development of a polyester for coating applications is the discoloration that occurs during the polymerization process, in particular when a monomer such as isosorbide, is used. Model reactions indicate that MTBO give rise to less discoloration with respect to titanium based catalysts.

The amount of isosorbide necessary to obtain the depolymerization of PET and to produce a homogenous molten reaction mixture at 230 °C is 65% by mol (with respect to PET repeating unit) of isosorbide since with lower isosorbide contents no homogenous reaction mixture can be obtained even for reaction times up to 5 hours at 230 °C.

Two phases are present during the depolymerization process: a molten phase and a solid phase. After 15 min of reaction the molten phase has a Mw lower than 2000 indicating a strong molecular weight decrement of the original PET by reaction with isosorbide. The glycolysis of PET is complete after 60 min since the molecular weight and polydispersity index (PDI) of the overall reaction mixture reach those of the liquid phase, with a PDI value typical of a homogenous polycondensation polymers (2.1). The ^{1}H-NMR analysis of the reaction mixture after the depolymerization step shows that part of ethylene glycol present in the starting PET has been removed from the polymer after the glycolysis with isosorbide and that no isosorbide is lost in the depolymerization step. The different reactivity of OH groups can be determined by ^{1}H-NMR analysis, showing that the exo/endo ratio of esterified OH groups is 63/37 (by mol) indicating that the exo-group is more reactive compared to the endo-group.

13.5.1.3 Polycondensation after Glycolysis with Isosorbide

Succinic acid should be added in the polymerization step in order to generate the carboxylic end-groups which are necessary to obtain the cross-linking of the polyester with the hardener after the application of the powder coating on the substrate. The amount of succinic acid to be added can be determined on the basis of the OH groups present in the reaction mixture after the depolymerization step. Using 65% by mol (with respect to PET repeating unit) of isosorbide, the minimum amount of succinic acid necessary to react with OH end-groups is 49% by mol with respect to the repeating unit of the starting PET. Succinic acid can also react with the polymer backbone by acidolysis reaction, and therefore a larger amount with respect to the minimum content reported above (49%), should be used in order to obtain polymers mainly terminated with COOH end-groups. Indeed, the results of the

tests conducted with different amounts of succinic acid have shown that with a succinic acid content below 80% by mol (with respect to the PET repeating unit), the amount of carboxylic end-groups is lower with respect to OH end-groups, while the use of a succinic acid content of 80% gives rise to a polymer mainly terminated by COOH end-groups. On the contrary, if a larger succinic acid content is used, polymers with a molecular weight too low for powder coating applications are obtained due to the cleavage, by acidolysis reaction, of the polyester chain.

Glycerol (5% by mol with respect to PET repeating unit), that is derived from triglycerides, can be also added at the beginning of the depolymerization step in order to obtain a melt viscosity suitable to powder coating applications. Indeed, the addition of tri-functional monomers is often used in the industrial production of polyesters for powder coatings in order to increase the melt viscosity and improve the application process [10].

Dynamic vacuum must be applied in the last part of the polymerization process in order to help the removal of the reaction by-products and increase molecular weight. A long reaction time (10 h) is necessary in order to reach a molecular weight sufficient for powder coating applications. This slow polycondensation rate can be ascribed to the very low reactivity of isosorbide.

The ratio between succinic and terephthalate groups does not significantly change during the reaction (77% by mol, 3% by mol less with respect to the monomer feed). Three resins have been prepared in order to assess the effect of molecular weight and end-groups on the properties of the coating (Table 13.2).

The sustainable polyesters prepared form renewable resources and recycled PET present properties similar to those of a commercial polyester for powder coating applications (Crylcoat® 1771-3).

Table 13.2 Properties of the polyesters prepared by chemical recycling of PET compared with those of a commercial polyester for powder coating.

Polyester	COOH end-groups content (meq/g of resin)	OH end-groups content (meq/g of resin)	Melt Viscosity at 200 °C (mPa.s)	T_g (°C)
Resin 1	0.58	0.14	5500	59
Resin 2	0.89	0.09	1700	54
Resin 3	0.45	0.14	8500	58
Crylcoat® 1771-3	0.59	0.09	4900	56

13.5.2 Coatings Application Tests

Epoxy resin cross-linker is generally used to cross-link polyesters in powder coating applications. The ratio between the polyester and the epoxy resin (Table 13.3) must be determined according to the carboxylic groups and OH groups contents of the polyesters and to the amount of epoxy groups in the epoxy resins. The preparation of the coatings using the polyesters from renewable resources and recycled PET can be performed using a standard industrial procedure for the preparation of powder coatings.

Table 13.3 Properties of the coatings.

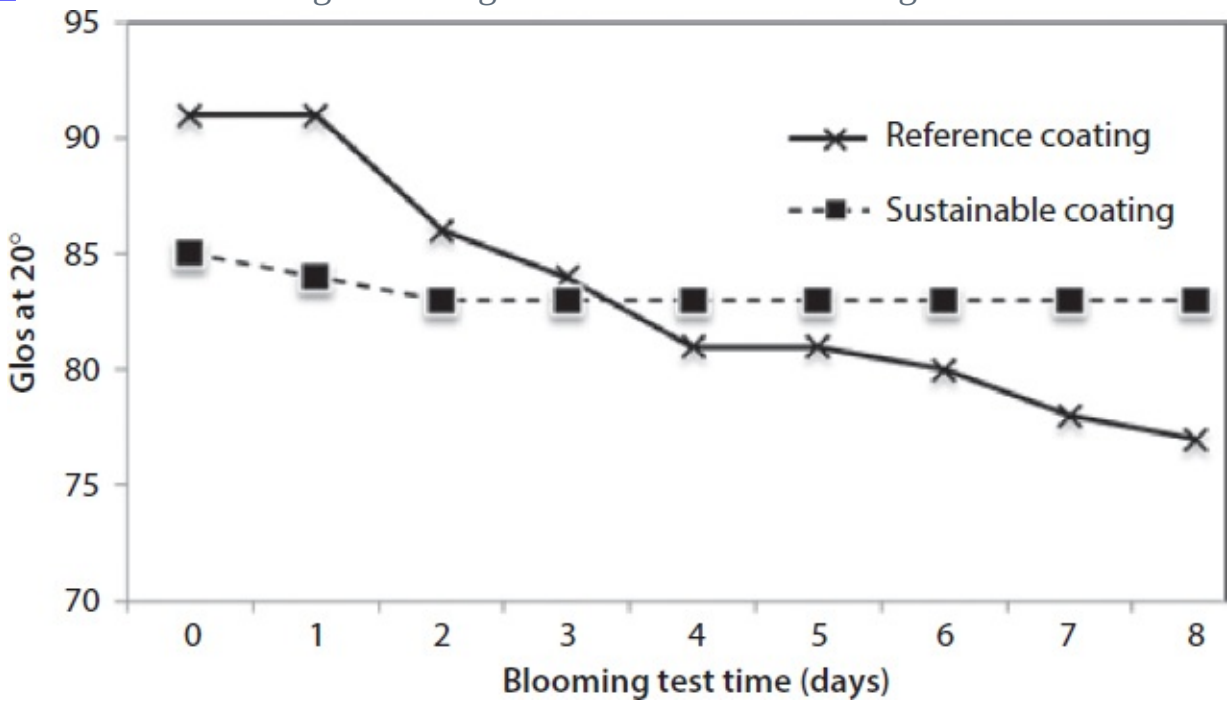
Formulation	Gloss, 20°/60°	D.I./R.I. (kg.cm)	T-bend	Erichsen (mm)	Pencil hardness	Adhesion
Coating 1	89/98	160/160	0-T	9.5	F-HB	GT0
Coating 2	95/99	160/160	0-T	9.5	F-HB	GT0
Coating 3	91/101	160/160	0-T	9.1	F-HB	GT0
Reference coating	92/98	160/160	0-T	9.5	F-HB	GT0

The analysis of the properties of the coatings (Table 13.3) shows that the materials obtained using the new approach, based on the chemical recycling of PET and on the use of isosorbide and succinic acid, have properties that are comparable with those of a commercial coating prepared using non-renewable resources. The chemical composition (amount of succinic acid) and the end-groups content do not have a significant effect on coating performances that are always suitable for industrial applications and comparable with the reference coating made of TPA and neopentyl glycol. It is therefore possible to assume that the increased mobility due to the presence of linear aliphatic chains (derived from succinic acid and from ethylene glycol) is counter-balanced by the stiffness of the repeating unit derived from isosorbide.

13.5.2.1 Blooming Resistance

Blooming is a haze on the surface of a coated film that appears as a white patina on the surface, causing a progressive decrease of the gloss. The blooming effect becomes evident when a standard powder coated panel is kept for a sufficient length of time at a temperature above the glass transition temperature. The blooming resistance tests analyse the behaviour (by measuring the gloss at 20°) of the coating at 120 °C. The results of the tests (Figure 13.11) show a significant improvement in performances of the coating based on the sustainable polyester resin compared to the standard product.

Figure 13.11 Gloss at 20° during blooming test on sustainable coating and reference coating.



The almost constant gloss retention of the powder coating after blooming test could bring to the

possibility of a blooming-free generation of polyester for powder coating, which is of great importance for “low cure” applications that have an expanding commercial market. The “low cure” applications for powder coatings are performed using curing temperatures 20 °C lower than the standard curing temperature for a specific powder coating system (that is around 140 °C for polyester/epoxy systems).

13.5.2.2 Effect of Overbaking

Most coatings are designed for a specific baking time and temperature. For several reasons (oven overheating, line stoppages, rerouting back through ovens, etc.) the prescribed time and/or temperature of the bake is often exceeded. The effect of overbaking can be evaluated taking into account the b index that represents the sample position on the blue/yellow axis in CIELAB colour space, blue being in the negative direction and yellow being in the positive direction.

The colorimetric data reported in Table 13.4 show that both the starting yellowing index and the overbaking resistance of the powder coating based on renewable resources and recycled PET are significant worse than the reference coating. The comparison could be not completely significant because the polyester used in the reference coating contains a phenolic antioxidant while the sustainable coating does not contain any antioxidant. Therefore, it is clear that antioxidants must be used in order to obtain coatings with no overbaking issues.

Table 13.4 Effect of overbaking on color index.

	b initial[a]	Δb1[b]	Δb2[c]
Sustainable coating	2.60	0.25	2.43
Reference coating	0.57	0.11	1.17

[a] Standard curing, 10 minutes at 180 °C.
[b] First overbake, 10 minutes at 180 °C.
[c] Second overbake, 30 minutes at 220 °C.

13.5.2.3 Effect of Ageing

Powder coatings must retain properties after ageing in order to be used for commercial applications. The tests performed after 6 months of ageing show that the powder coating based on renewable resources and recycled PET still presents an outstanding flexibility, while a decrease of the properties has been observed for the reference coating (Table 13.5). These results indicates the positive effect on long term stability of the isosorbide and succinic acid groups with respect to the neopentyl glycol used for the reference coating. The reason of the higher stability can be ascribed to the rigidity of the isosorbide group that confers a higher stiffness to the polymeric chain and therefore higher impact properties also after ageing.

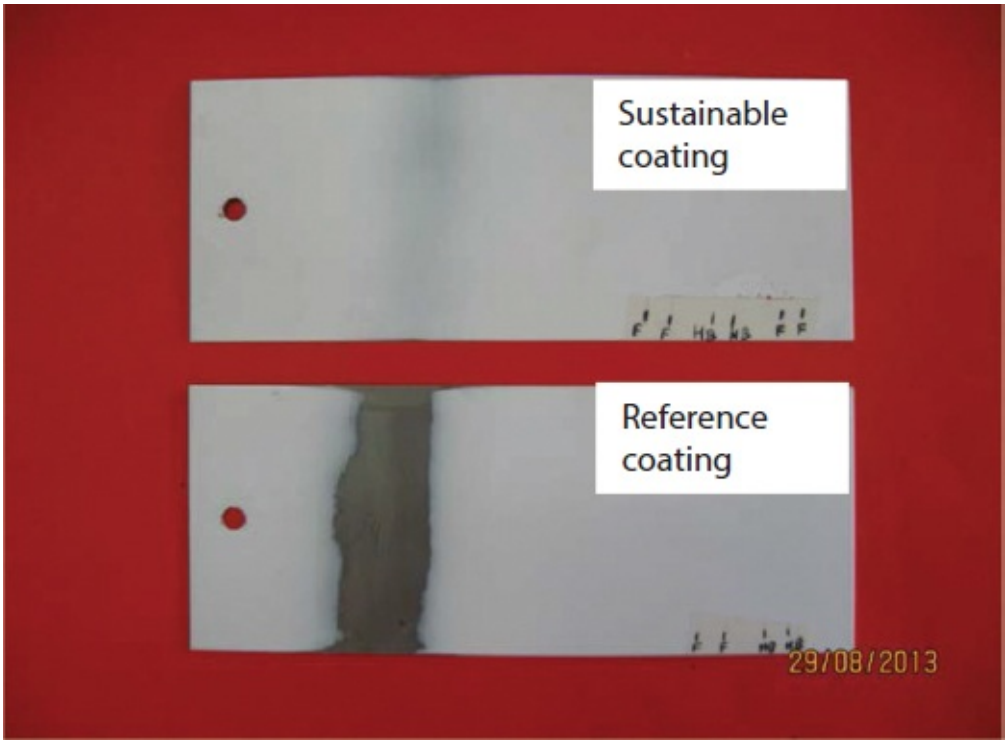
Table 13.5 Coating properties after 6 months of ageing at room temperature.

	DI/RI	T-bend	Gloss
Sustainable coating	140/140	1-T	86/97
Reference coating	80/10	4-T	87/97

13.5.2.4 Solvent Resistance

Powder coatings should reach specific levels of solvent resistance in order to be used in industrial applications. The level of solvent resistance depends on the type of coating and application. In particular, for indoor powder coating systems (with applications like appliances, furniture, etc.) the solvent resistance is an application property of fundamental importance. Solvent resistance measured according to ASTM D5402-93 with a solvent rub technique using methyl ethyl ketone (MEK) is reported in Figure 13.12.

Figure 13.12 Solvent resistance test on sustainable coating and reference coating (adapted from ref 47).



The results of solvent resistance tests show an improved resistance for the coating based on the sustainable polyester resin compared to the standard product. This increased solvent resistance can be ascribed to the increased stiffness of the polymeric chain due to the presence of isosorbide or to a more efficient cross-link of the sustainable polyester that also contains aliphatic carboxylic acid end-groups.

13.5.3.5 Boiling Water Resistance Tests

The stability to hydrolysis is another important factor to be taken into account in industrial applications. The tests are performed immersing the coatings into boiling water for 2 h. The analysis permits the detection of blisters, the variation of brightness, the adhesion and changes in mechanical properties.

The sustainable coating present an excellent resistance to boiling water since no blisters can be detected and the adhesion properties are not compromised (Figure 13.13). The results of gloss and adhesion tests, reported in Table 13.6, indicate a higher gloss and adhesion retention after boiling water tests for the coating from renewable resources with respect to the reference coating.

Figure 13.13 Boiling water resistance test on sustainable and reference coatings (adapted from ref 47).

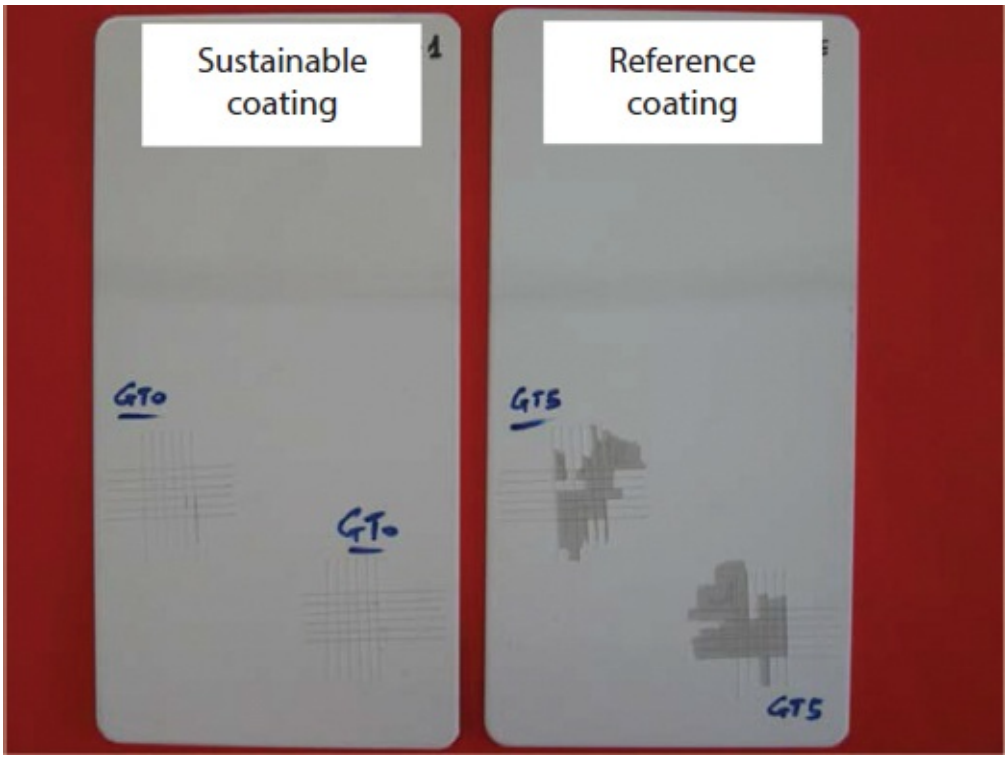


Table 13.6 Gloss and adhesion before and after boiling water tests.

Formulation	Gloss at 20°/60°	Gloss at 20°/60° after boiling water tests	Adhesion	Adhesion after boiling water tests
Sustainable coating	89/98	2.0/10.5	GT0	GT0
Reference coating	92/98	1.8/7.0	GT0	GT5

The higher stability to water boiling can be ascribed to the lower reactivity of isosorbide toward esterification, trans-esterification and hydrolysis reactions due to the sterical hindrance of the hydroxylic groups.

13.6 Conclusions

Powder coating constitutes a very important class of eco-friendly coatings due to several features that makes process and materials environmental friendly. First of all, the production process is solvent-free and therefore the problems associated with volatile organic emissions are completely absent. In addition, the powders are used without any loss since only the material in direct contact with the substrate is retained on the article and the excess of powder almost entirely recovered and reused. Moreover, powder coatings give the possibility to use monomers from renewable resources. In particular, isosorbide, succinic acid and glycerol (that are mainly obtained at low costs from renewable resources) can be used for the synthesis of polyesters employed for the preparation of powder coatings. Using those monomers it is possible to obtain polyesters with end-groups compositions and with chemical–physical characteristics (e.g. molecular weight and glass transition temperature) suitable for the preparation for powder coatings. In addition, recycled polymers can be also used for the preparation of the polyesters that are the main component of the coatings. For example, poly(ethylene terephthalate) that is one of the most recycled polymers, can be depolymerized for the production of polyesters for powder coatings. The carbon footprint of the coatings can be further decreased performing the chemical recycling of polymers with molecules

derived from renewable resources. The coatings obtained using these environmental-friendly procedures have similar, and in some cases superior, applicative properties with respect to commercial coatings obtained from non-renewable resources.

The future development in this field should include a wider range of starting eco-friendly materials. In particular, other molecules from renewable resources should be tested for powder coating application both as monomers for polyesters and as depolymerizing agents for the chemical recycle of polymers. Moreover, other polymers should be tested for the chemical-recycling approach. Finally, more efforts should be made in the development of eco-friendly starting materials to be used in cross-linking systems and additives for the preparation of powder coatings.

References

1. C. Okkerse and H. van Bekkum, *Green Chemistry,* Vol. 1, p. 107, 1999.

2. A. Corma, S. Iborra, and A. Velty, *Chemical Reviews,* Vol. 107, p. 2411, 2007.

3. A. Gandini, *Green Chemistry,* Vol. 13, p. 1061, 2011.

4. N. Belgacem and A. Gandini, *Monomers, Polymers and Composites from Renewable Resources,* Oxford, Elselvier, 2008.

5. C. Berti, M. Colonna, M. Fiorini, C. Lorenzetti, and P. Marchese, *Macromolecular Materials and Engineering,* Vol. 289, p. 49, 2004.

6. V. Sinha, M.R. Patel, and J.V. Patel, *Journal of Polymers and the Environment,* Vol. 18, p. 8, 2010.

7. J.P.T. Derksen, F.P. Cuperus, and P. Kolster, *Progress in Organic Coatings,* Vol. 27, p. 45, 1996.

8. J. Haveren, E.A. Oostveen, F. Miccichè, B.A.J. Noordover, C.E. Koning, R.A.T.M. Benthem, E. Frissen, and J.G.J. Weijnen, *Journal of Coating Technology and Research,* Vol. 4, p. 177, 2007.

9. T.A. Misev, *Powder Coatings: Chemistry Technology, 1st Ed.*, New York, John Wiley and Sons, 1991.

10. E. Spyrou, *Powder Coatings: Chemistry and Technology,* Hanover, Vincentz Network, 2012.

11. B. Müller and U. Poth, *Coatings Formulation,* Hanover, Vincentz Network, 2006.

12. Kirk-Othmer, *Encyclopedia of Chemical Technology,* John Wiley & Sons, Inc.

13. E. Linak, T. Kälin, A. Kishi, and J. Liu, *Specialty Chemicals Update Program: Thermosetting Powder Coatings*, IHS Chemical, 2014.

14. B. Moran, *Market Research Report: Powder Coatings: Materials, Coatings, Technologies*, Wellesley, BCC Research, 2009.

15. T. Herrmann, *New Technologies and Trends in Powder Coating, PCI Magazine*, November 2014.

16. Specialty Chemicals Overview, SRI Consulting, 2008.

17. D. Gagro, *European Coatings Journal*, Vol. 12, p. 10, 2014.

18. R. Salgarkar, *Powder Coatings Market by Resin Type and by End-User Industries – Global Forecast to 2019*, Markets and Markets 2012.

19. M. Colonna, C. Berti, M. Fiorini, E. Binassi, M. Mazzacurati, M. Vannini, and S. Karanam, *Green Chemistry,* Vol. 13, p. 2543, 2011.

20. S. Tavener, *Green Chemistry*, Vol. 5, p. 46, 2003.

21. E. Gubbels, J.P. Drijfhout, C. Posthuma-van Tent, L. Jasinska-Walc, B.A.J. Noordover, and C.E. Koning, *Progress in Organic Coating*, Vol. 77, p. 277, 2014.

22. E. Gubbels, L. Jasinska-Walc, B.A.J. Noordover, and C.E. Koning, *European Polymer Journal*, Vol. 49, p. 3188, 2013.

23. E. Gubbels, L. Jasinska-Walc, and C.E. Koning, *Journal of Polymer Science part A: Polymer Chemistry*, Vol. 51, p. 890, 2013.

24. I. Barbara, A.L. Flourat, and F. Allais, *European Polymer Journal*, Vol. 62, p. 236, 2015.

25. F. Pion, P.H. Ducrot and F. Allais, *Macromolecular Chemistry and Physics*, Vol. 215, p. 431, 2014.

26. C.H.R.M. Wilsens, B.A.J. Noordover, and S. Rastogi, *Polymer*, Vol. 55, p. 2432, 2014.

27. E. Dogan and A.E. Acar, *Progress in Organic Coatings*, Vol. 76, p. 513, 2013.

28. B.A.J. Noordover, V.G. van Staalduinen, R. Duchateau, C.E. Koning, R.A.T.M. van Benthem, M. Mak, A. Heise, A.E. Frissen, and J. van Haveren, *Biomacromolecules*, Vol. 7, p. 3406, 2006.

29. B.A.J. Noordover, A. Heise, P. Malanowksi, D. Senatore, M. Mak, L. Molhoek, R. Duchateau C.E. Koning, and R.A.T.M. van Benthem, *Progress in Organic Coatings*, Vol. 65, p. 187, 2009.

30. B.A.J. Noordover, R, Duchateau, R.A.T.M. van Benthem, W. Ming, and C.E. Koning, *Biomacromolecules*, Vol. 8, p. 3860, 2007.

31. B.A.J. Noordover, D.I. Haveman, R. Duchateau, R.A.T.M. van Benthem, and C.E. Koning, *Journal of Applied Polymer Science*, Vol. 121, p. 1450, 2011.

32. G. Crapper, *Polymer Science part A*, Vol. 10, p. 541, 2012.

33. I.A. Ignatyev, W. Thielemans, and B. Vander Beke, *ChemSusChem*, Vol. 7, p. 1579, 2014.

34. D.E. Nikles and M.S. Farahat, *Macromolecular Materials and Engineering*, Vol. 290, p. 13, 2005.

35. 2012 United States National Post-Consumer Plastics Bottle Recycling Report, American Chemistry Council, Association of Postconsumer Plastic Recyclers, 2012.

36. A.M. Atta, A.F. El-Kafrawy, M.H. Aly, and A.A. Abdel-Azim, *Progress in Organic Coatings*, Vol. 58, p. 13, 2007.

37. A.M. Atta, M.E. Abdel-Raouf, S.M. Elsaeed, and A.A. Abdel-Azim, *Progress in Organic Coatings*, Vol 55, p. 50, 2006.

38. P. Czub, *Polymers for Advanced Technologies*, Vol. 20, p. 183, 2009.

39. M. Kathalewar, N. Dhopatkar, B. Pacharane, A. Sabnis, P. Raut and V. Bhave, *Progress in Organic Coatings*, Vol. 76, p. 147, 2013.

40. G. Güçlü and M. Orbay, *Progress in Organic Coatings*, Vol. 65, p. 362, 2009.

41. J. Dullius, C. Ruecker, V. Oliveira, R. Ligabue, and S. Einloft, *Progress in Organic Coatings*, Vol. 57, p. 123, 2006.

42. C. Kawamura, K. Ito, R. Nishida, I. Yoshihara, and N. Numa, *Progress in Organic Coatings*, Vol. 45, p. 185, 2002.

43. D. Paszun and T. Spychaj, *Industrial Engineering Chemical Research*, Vol. 36, p. 1373, 1997.

44. C. Lavilla and S. Muñoz-Guerra, *Green Chemistry*, Vol. 15, p. 144, 2013.

45. L. Moens, Polyesters for coatings, Assigned to Cytec, Patent application WO 2011/058130, 2011.

46. C. Gioia, M. Vannini, P. Marchese, A. Minesso, R. Cavalieri, M. Colonna, and A. Celli, *Green Chemistry*, Vol. 16, p. 1807, 2014.

47. A. Minesso, R. Cavalieri, C. Gioia, P. Marchese, A. Celli, and M. Colonna, *Journal of Coatings Technology and Research,* in press.

48. T.E. Banach, C. Berti, M. Colonna, M. Fiorini, E. Marianucci, M. Messori, F. Pilati, and M. Toselli, *Polymer,* Vol. 42, p. 7511, 2001.

49. F. Fenouillot, A. Rousseau, G. Colomines, R. Saint-Loup, and J.-P. Pascault, *Progress in Polymer Science,* Vol. 35, p. 578, 2010.

Chapter 14

The Synthesis and Applications of Non-isocyanate Based Polyurethanes as Environmentally Friendly "Green" Coatings

Peter Zarras, Paul A. Goodman, Alfred J. Baca, Joshua E. Baca, and Shelley Vang

NAWCWD, Polymer Science & Engineering Branch (Code 4F0000D), China Lake, CA, USA

**Corresponding author*: peter.zarras@navy.mil

Abstract

Polyurethanes (PUs) are used as components and coatings for numerous everyday products and materials, which make them ubiquitous in our lives. Industrial production of polyurethanes currently requires the use of isocyanates. Not only are isocyanates toxic, but the production of isocyanates commonly employs phosgene, a highly toxic substance, as a reagent. These facts have a direct impact on the health and safety of scientists, engineers and the public. This review will discuss the current methods used to produce isocyanates and polyurethanes, as well as alternative synthetic methods using benign, environmentally friendly, strategies that replace isocyanates with cyclic carbonates. Polycondensation and polyaddition reactions using cyclic carbonates to prepare non-isocyanate polyurethanes (NIPU) will be thoroughly discussed. Additionally, miscellaneous non-isocyanate based polymerization reactions, such as cationicring opening polymerization (ROP) and copolymerization of substituted aziridines with carbon dioxide, will also be discussed. Finally, a brief summary of several current applications using NIPUs will be presented.

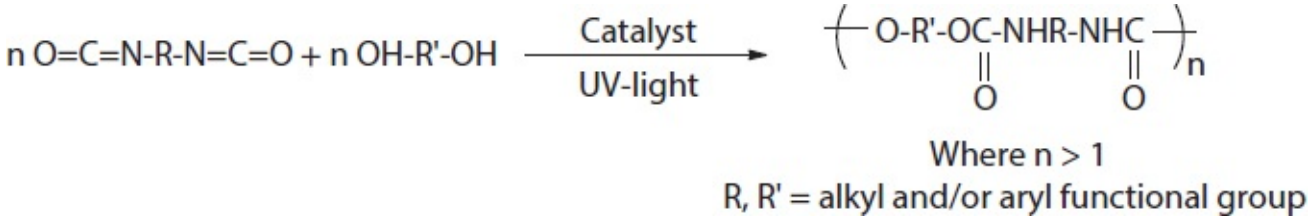
Keywords: Polyurethanes, isocyanates, phosgene, toxicological properties, non-isocyanate polyurethane, carbon dioxide, oxiranes, cycloaddition, cyclic carbonates, polycondensation, polyaddition

14.1 Introduction to Isocyanate-based Polyurethane Chemistry

Polyurethanes, commonly abbreviated as PU, are polymers that are composed of repeating organic units with carbamate (urethane) linkages. Polyurethanes are typically formed by combining molecules with two or more isocyanate functional groups with a polyol containing two or more reactive hydroxyl groups (Figure 14.1) [1–4].The formation of the PU is initiated via a catalyst or

with ultraviolet light.

Figure 14.1 Polyurethane synthesis based on isocyanate chemistry.



Polyurethanes were first synthesized in 1937 at the IG Farben chemical company located in Leverkusen, Germany [5].These PUs were limited to fibers and flexible foams, and were applied on a small scale for use as aircraft coatings during World War II [6]. During the 1950's DuPont began using polyether polyols to make PUs, and by the 1960's over 45,000 metric tons of flexible PU foams were produced in the United States [6]. In the 1980's and 90's polyurethane flexible foams were used for many applications, such as automotive panels and air filters. They also found widespread use as coatings on both civilian and military aircraft [7]. Currently, the commercial market for polyurethanes is $43.3 billion USD, as reported in 2013 by Grand View Research, with projections of up to $73.6 billion USD by 2020 [8]. Due to their unique physical and mechanical properties (e.g., physical toughness, durability, elasticity and abrasive resistance) polyurethanes rank 6th among the most widely used commodity polymers worldwide [8–10].

Polyurethanes are used in a diverse array of commercial and industrial applications. In fact, their use is so widespread that one probably encounters at least one polyurethane product every day. Some of these applications include nonflexible, high-resilience foam seating, rigid foam insulation panels, gaskets, surface coatings, high-performance adhesives, surface sealants, synthetic fibers, elastomeric wheels and tires, hard-plastic parts for electronics, and biomedical materials. Because of the relatively straightforward chemistry used to produce them, PU properties can be tailored according to specific industrial needs. Simply changing the types of isocyanates and/or polyols used during production will change the properties of the resulting product [11, 12]. Polyols that contain long, flexible segments can produce soft elastomeric polymers, whereas the use of a high degree of crosslinking agents (i.e., more alcohol functionality) can produce PUs that are tough and rigid. In addition to the choice of reagents, one can influence the properties of the PU through manipulation of the processing technique, like modification of stirring speeds, which makes them well suited for a tremendously diverse set of applications [13].

14.2 Synthesis of Isocyanates

Isocyanates are reactive materials containing the functional group R-N=C=O. They are strong electrophiles that readily react with a variety of nucleophiles, like alcohols, amines and water. When an isocyanate reacts with an alcohol a urethane linkage is formed. Diisocyanates, those compounds containing two isocyanate functional groups, are typically used in PU synthesis. The diisocyanates most commonly used for PU synthesis include methylene diphenyl diisocyanate (MDI), toluene diisocyanate (TDI), hexamethylene diisocyanate (HDI) and isophorone diisocyanate (IPDI) [14–20]. Typically, isocyanates are produced by treating amines with phosgene ($COCl_2$). For example, methyl isocyanate (MIC) is produced by reacting monomethylamine with phosgene, producing the N-methylcarbamoyl chloride (MCC) intermediate, which is then reacted with a tertiary amine and

purified via distillation to obtain the MIC (see Figure 14.2) [21–25]. A similar method is used for making diisocyanates, for instance, MDI is produced by reacting aniline and formaldehyde using HCl as a catalyst, which produces a diamine precursor. The precursor is further reacted with phosgene to produce the MDI, which is purified via distillation or fractionation to obtain the desired isomer (see Figure 14.3) [26, 27]. In each of these procedures, and in many other preparations of isocyanates, the common factor is the utilization of phosgene as an active reagent.

Figure 14.2 Synthesis of Methyl Isocyanate.

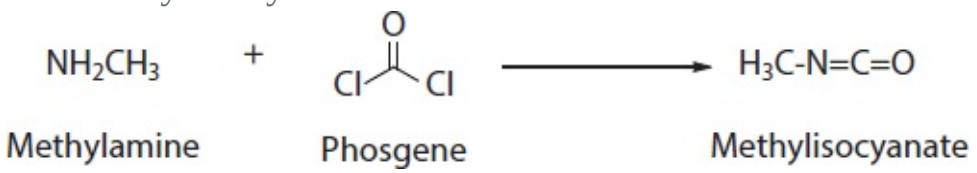
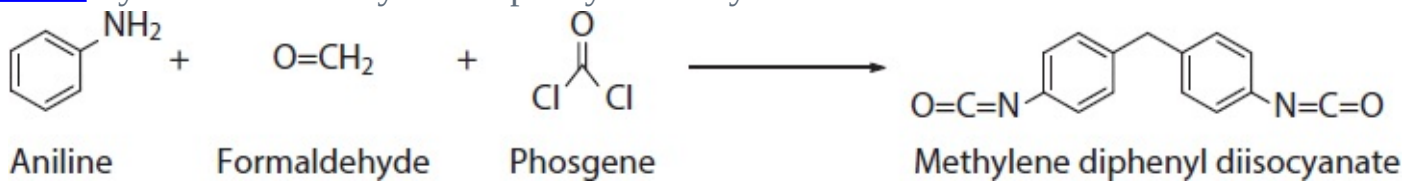


Figure 14.3 Synthesis of Methylene Diphenyl Diisocyanate.



Phosgene is an insidious poison; the musty hay-like odor may not be noticed at low concentrations and symptoms do not appear immediately. Table 14.1 summarizes the LC_{50} for various mammalian species when exposed to phosgene [28–31]. In all cases, phosgene can produce acute lung injury, even during limited exposure times. The odor threshold for phosgene is 0.4 ppm which is well above the United States National Institute of Occupational Safety and Health (NIOSH), permissible exposure limit (PEL) of 0.1 ppm. Phosgene causes proteins in the pulmonary alveoli to crosslink through their amine functionality, preventing gas exchange across the blood-air barrier, which ultimately results in suffocation [32–35]. Eliminating its use is highly desirable.

Table 14.1 Lethal Exposure Dose for Phosgene.

Lethal Concentration	Mammalian Species
LC_{50}	Humans (500 ppm/minute)
LC_{50}	Dog (1022 ppm/20 minutes)
LC_{50}	Rat (340 ppm/30 minutes)
LC_{50}	Mouse (438 ppm/30 minutes)

14.3 Toxicological Properties of Isocyanates

Isocyanates are low molecular weight, highly reactive chemicals that are ubiquitous for both industrial and commercial applications. Due to their widespread use there has been increased scrutiny over their deleterious health effects. Isocyanates are irritants to the mucous membranes of the eyes, gastrointestinal and respiratory tracts that pose a significant health risk [36, 37]. Direct skin contact can cause inflammation and isocyanates can sensitize workers. Repeated dermal or respiratory exposure to isocyanates can cause isocyanate-induced asthma, a form of work-related asthma (WRA) [38, 39]. The mechanism by which isocyanates cause WRA is still a matter of investigation [40, 41]. Even at low concentrations, isocyanates can act as sensitizing agents. Several studies have found that isocyanates can induce functional and inflammatory changes of the eyes, airways and pulmonary

passages at concentrations as low 1 ppb [42–44]. At higher concentrations isocyanates can permanently damage mucous membranes [45].

In order to limit the effects of isocyanate exposure resulting in WRA and other diseases, the United States government, through the NIOSH agency, has issued permissible exposure limits (PEL) for various isocyanates (see Table 14.2) [46, 47]. These recommendations represent a critical step in reducing the health hazard of isocyanate exposure. Further recommendations such as closed systems and ventilation including appropriate personal protective equipment to minimize dermal exposure are also required to reduce isocyanate exposure.

Table 14.2 NIOSH Federal Exposure Limits for Isocyanates in Air Workers Breathing Zone.

Isocyanate Compound	PEL ppm for 8hr TWA*
TDI	0.005
MDI	0.005
HDI	0.005
IPDI	0.005
MIC	0.02

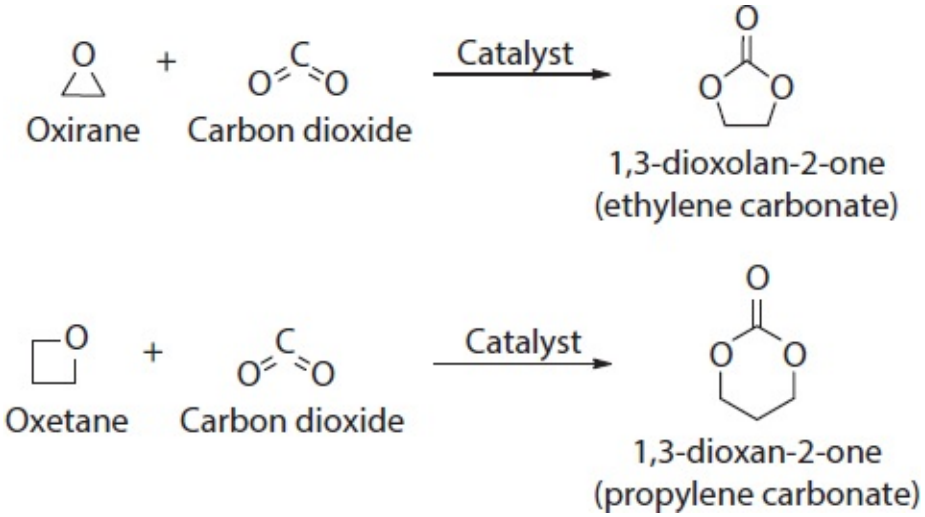
*TWA = Time weighted average

14.4 Synthesis of Phosgene-free Precursors

Since the synthesis of isocyanates and diisocyanates requires the reaction of amines or diamines with phosgene ($COCl_2$), an alternative synthetic procedure that eliminates the use of this lethal reagent is highly desirable. Phosgene-based isocyanates have been investigated and commercialized for over 70 years, so a certain amount of resistance to change is reasonable [48–50]. The use of cyclic carbonates as the starting materials for non-isocyanate polyurethane (NIPU) chemistry, which eliminates the use of isocyanates and therefore phosgene altogether, has sparked both academic and industrial interest [51, 52].

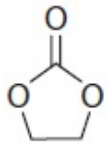
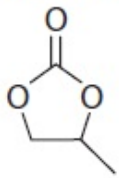
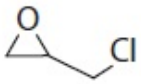
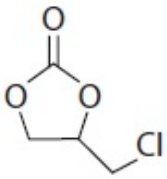
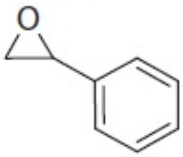
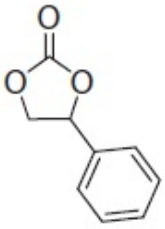
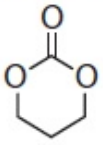
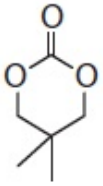
The first reported synthesis of cyclic carbonates was carried out by Carothers in the 1930's [53] The synthesis involved the depolymerization of oligocarbonates at high temperature using catalyst such as Sn(II), Mn(II), Fe(II) or Mg(II) [54]. Currently cyclic carbonates, such as ethylene carbonate and propylene carbonate, are produced on an industrial scale via cycloaddition reaction using the appropriate oxirane (epoxide) and carbon dioxide (CO_2) with either a Lewis acid or Lewis base catalyst under high pressure and temperature [55–58]. The use of CO_2 as an active reagent in the generation of cyclic carbonates represents a viable replacement for the use of isocyanates that require phosgene. This process is not only environmentally friendly, but CO_2 is readily abundant, nontoxic, nonflammable, and is considered a renewable carbon resource [59]. Five membered cyclic carbonates (ethylene carbonate) are produced from oxiranes and CO_2 (Figure 14.4 top), whereas, oxetanes and CO_2 produce six-membered rings (propylene carbonate) (Figure 14.4 bottom) [54, 60–62].

Figure 14.4 Cycloaddition Reaction of CO_2 with Oxirane (top) or Oxetane (bottom).



This approach is beneficial not only to the environment, because it reduces CO_2 emissions from fossil fuel combustion, but also allows for a cleaner and safer industrial process [63]. The cycloaddition reaction does suffer from several drawbacks including the inherent stability of CO_2 and kinetic inertness [64]. Numerous studies have been conducted over several decades to investigate various catalyst systems that can improve yields, allow mild reaction conditions, increase recovery and reuse of the catalyst, and accomplish asymmetric reactions [65]. Several novel catalyst systems that have been employed for this reaction include amines [66, 67], phosphines [68, 69], alkali metal halides [70, 71], onium salts [72, 73], organometallic compounds [74], transition metal complexes [75, 76], metal salen complexes [77, 78], metal porphyrins [79] and ionic liquids [80, 81]. There are numerous oxiranes and oxetanes that can undergo a cycloaddition reaction with CO_2 using various catalysts to produce a variety of cyclic carbonates. Table 14.3 provides a representative selection of various oxiranes and oxetanes that have been used to produce cyclic carbonate products. Due to the diversity of oxiranes and oxetanes that can be reacted with CO_2 to produce cyclic carbonates, many products like polar aprotic solvents, electrolytic components for lithium secondary batteries, precursors for polycarbonate formation, intermediates for pharmaceuticals, fine chemicals, and agricultural chemicals, produced by this method have been commercialized [82, 83].

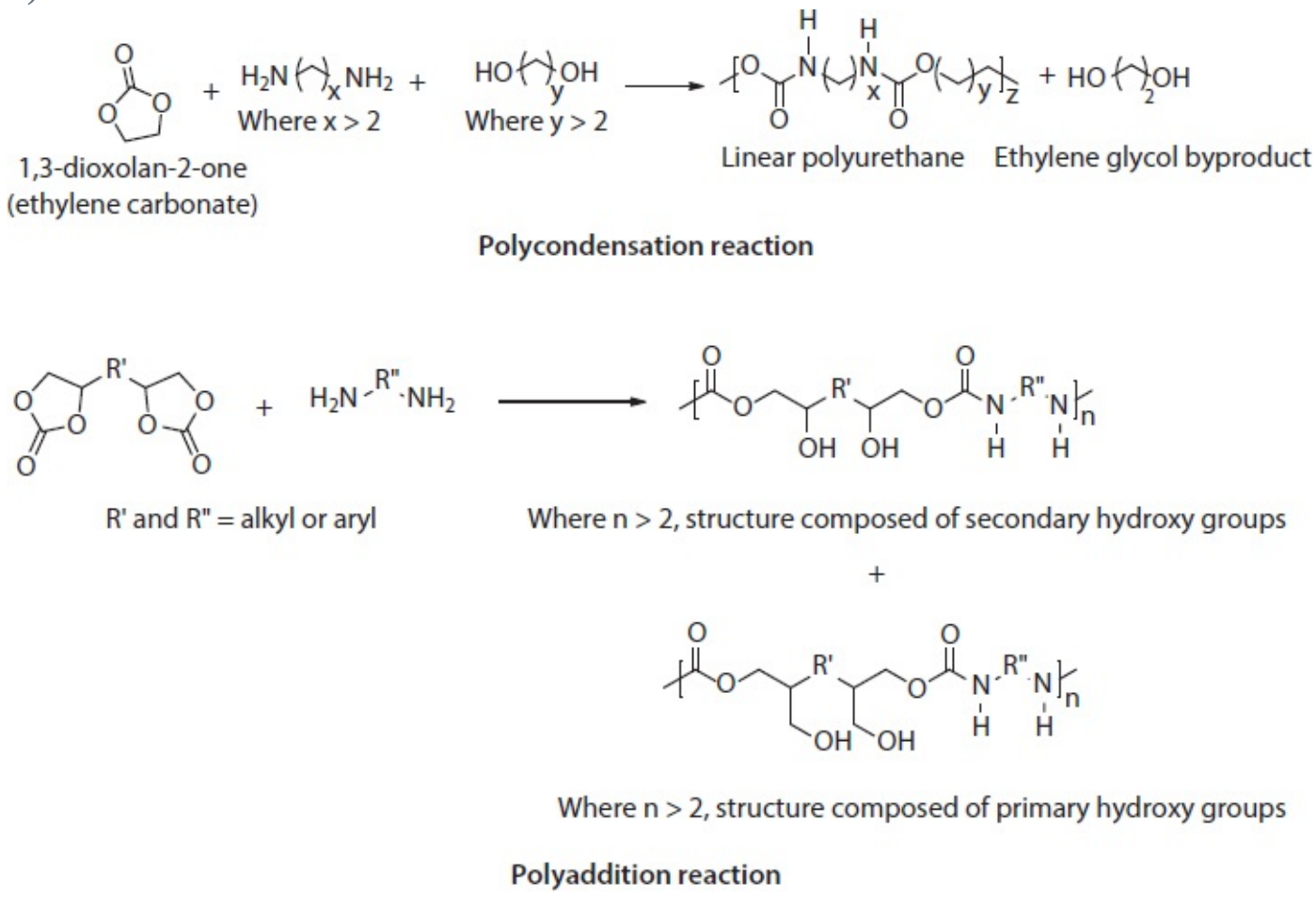
Table 14.3 Cycloaddition reaction of various oxiranes and/or oxetanes with CO_2 and the resulting cycloaddition product(s).

Oxirane or oxetane	Cycloaddition product	Catalyst used	Reference
Oxirane 	1,3-dioxolan-2-one 	Homogeneous dual-ligand zinc complex	[84]
2-methyloxirane 	4-methyl-1,3-dioxolan-2-one 	Imidazolium salt-modified porous polymers	[85]
2-(chloromethyl)-oxirane 	4-(chloromethyl)-1,3-dioxolan-2-one 	Phosphorus-based bifunctional organocatalyst	[86]
2-phenyloxirane 	4-phenyl-1,3-dioxolan-2-one 	Silanediol catalyst	[87]
Oxetane 	1,3-dioxan-2-one 	Tetraphenylstibonium iodide catalyst	[62]
3,3-dimethyl-oxetane 	5,5-dimethyl-1,3-dioxan-2-one 	Aluminum complex catalyst	[88]

14.5 Non-isocyanate-based Polyurethanes (NIPU)

There are several routes available for the preparation of NIPUs. These routes are green and environmentally friendly alternatives to the isocyanate and diisocyanate routes developed over many decades. Several synthetic procedures are used to produce NIPUs. Polycondensation reactions of 1,3-dioxolan-2-one (ethylene carbonate) with diamines and diols, and polyaddition reaction of bifunctional cyclic carbonates with diamines (see Figure 14.5 for schematic representation) will be covered in detail here. Additional miscellaneous reactions leading to NIPU can be accomplished via cationic ring-opening polymerization of cyclic urethanes and copolymerization of substituted aziridines with CO_2 [89].

Figure 14.5 Synthesis of NIPU via Polycondensation Reaction (Top), and Polyaddition Reaction (Bottom).

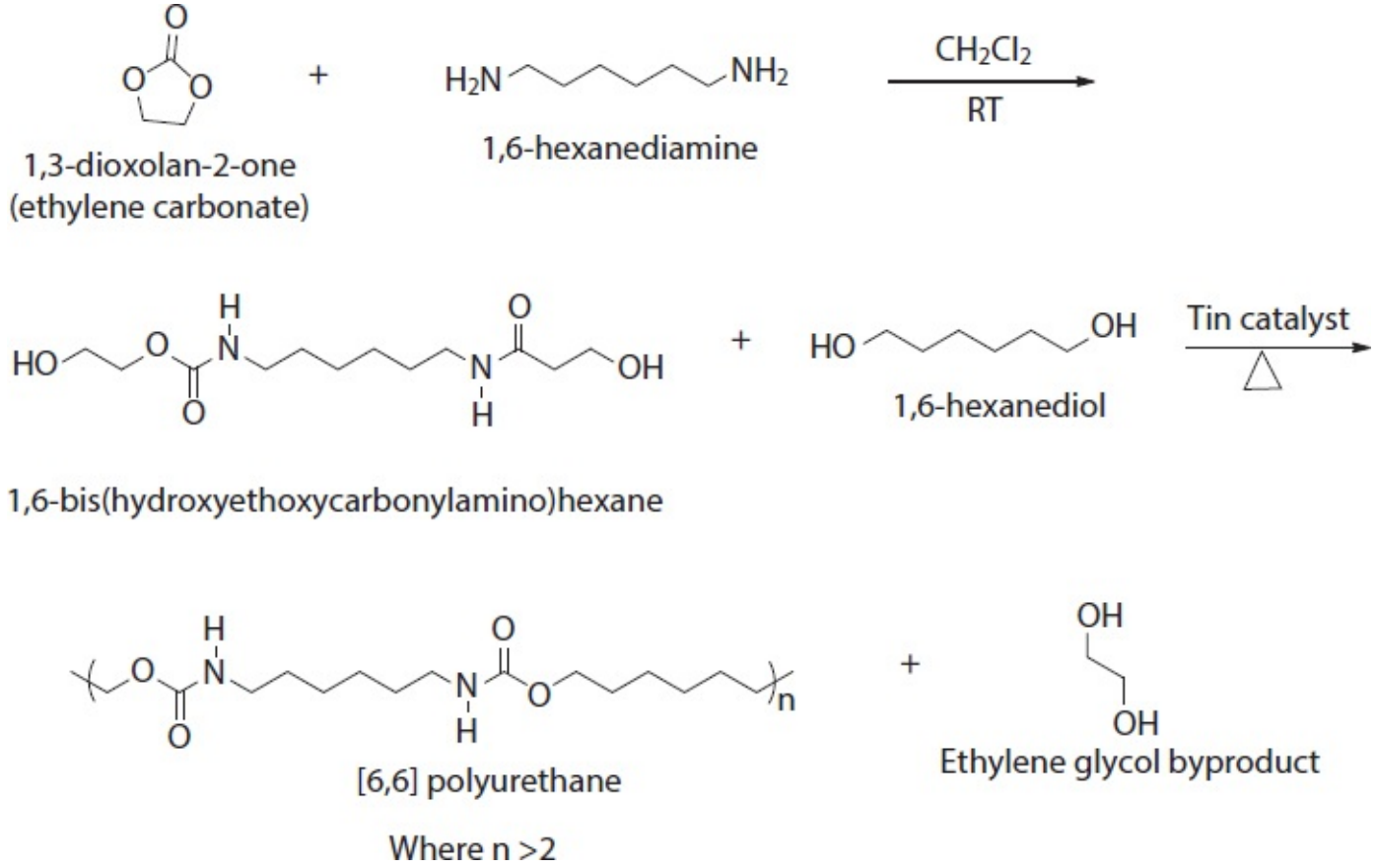


14.5.1 Polycondensation Reaction

Generally, the polycondensation method consists of the reaction of ethylene carbonate (1,3-dioxolan-2-one), or a similar derivative, with diamines and diols resulting in the formation of linear PUs. This produces a non-isocyanate, phosgene-free PU, but low molecular weight byproducts are also produced during this reaction [90]. As an example of this type of reaction, Rokicki *et al.*, reacted ethylene carbonate and 1,6-hexanediamine without any catalyst under ambient conditions to give the resulting 1,6-bis (hydroxyethoxycarbonylamino)hexane in quantitative yield, and further reaction with 1,6-hexanediol and tin coordination catalyst under moderate heating gave the [6,6] polyurethane

and ethylene glycol as a byproduct (see Figure 14.6) [91].

Figure 14.6 Synthesis of [6,6]polyurethane.



The proposed mechanism of this polycondensation is a back-biting reaction of the hydroxyl group in the hydroxyethyloxycarbonylamine prepolymer. The amine can further react with another hydroxyethyloxycarbonate functional group to produce urea linkages in the polymer backbone with subsequent loss of the ethylene glycol byproduct [91].

14.5.2 Polyaddition Reaction

The polyaddition reaction is also an isocyanate-free method to obtain PUs. This route has been reviewed by both Keul *et al.*, [92] and Ochiai [93]. The formation of the poly(hydroxyurethane) linkages is via a step-growth polyaddition reaction of the bifunctional cyclic carbonates and diamines (see Figure 14.5 bottom). Unlike the polycondensation method, this reaction produces no byproducts. The reaction mechanism has been investigated by Zabalov *et al.*, using DFT methods. Their investigations revealed that the ring opening of the cyclic carbonate can be both first and second order with respect to the amine. In addition, their calculations showed that the second amine molecule can act as a catalyst for the NIPU formation with a concurrent decrease in the activation energy of the overall reaction [94].

The synthesis of the bifunctional cyclic carbonates uses green chemistry methods that rely on the insertion of CO_2 into bis(epoxides). As an example, 2,2-bis[4-(1,3-dioxolane-2-one-4ylmethoxy)-phenyl]propane was synthesized from the corresponding bis(epoxy) compound (bisphenol A diglycidyl ether) using an ammonium iodide salt (dicyclohexylamine hydroiodide) and CO_2 to give the target bifunctional cyclic carbonate in quantitative yield (see Figure 14.7) [95]. This is a metal-free catalytic synthesis using mild reaction conditions that is environmentally benign. The synthesis of NIPU's resulting from these reactions produces polyurethanes containing pendant hydroxyl units

(primary and secondary) which are formed at the β-carbon atom of the urethane group. An example of the polyaddition reaction resulting in the formation of poly(hydroxyurethane) is the reaction of 2,2-bis[4-(1,3-dioxolane-2-one-4ylmethoxy)-phenyl]propane and 1,6-hexanediamine in aprotic polar solvents with heating to 100 °C for 24 hours (see Figure 14.8). The poly(hydroxyurethanes) that are obtained from this reaction have molecular weights in the range of 20–30kDa [96]. The hydroxyl groups promote intra-and inter-molecular hydrogen bonding between the polymer chains increasing their adhesion properties. These NIPU's have no unstable biurets or allophanates present in their backbone, which improves their thermal and chemical stability to non-polar solvents [97].

Figure 14.7 Synthesis of 2,2-Bis[4-(1,3-dioxolane-2-one-4ylmethoxy)-phenyl]propane, [Bifunctional Cyclic Carbonate].

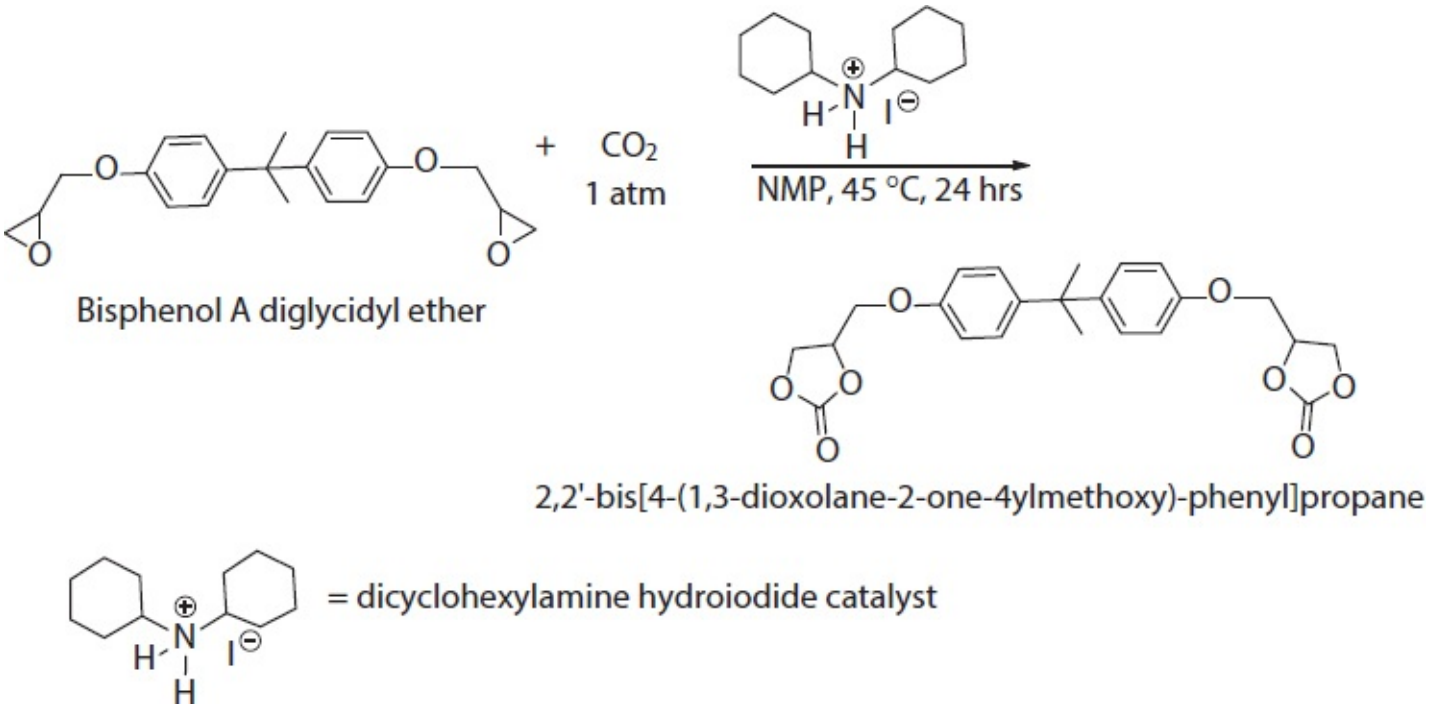
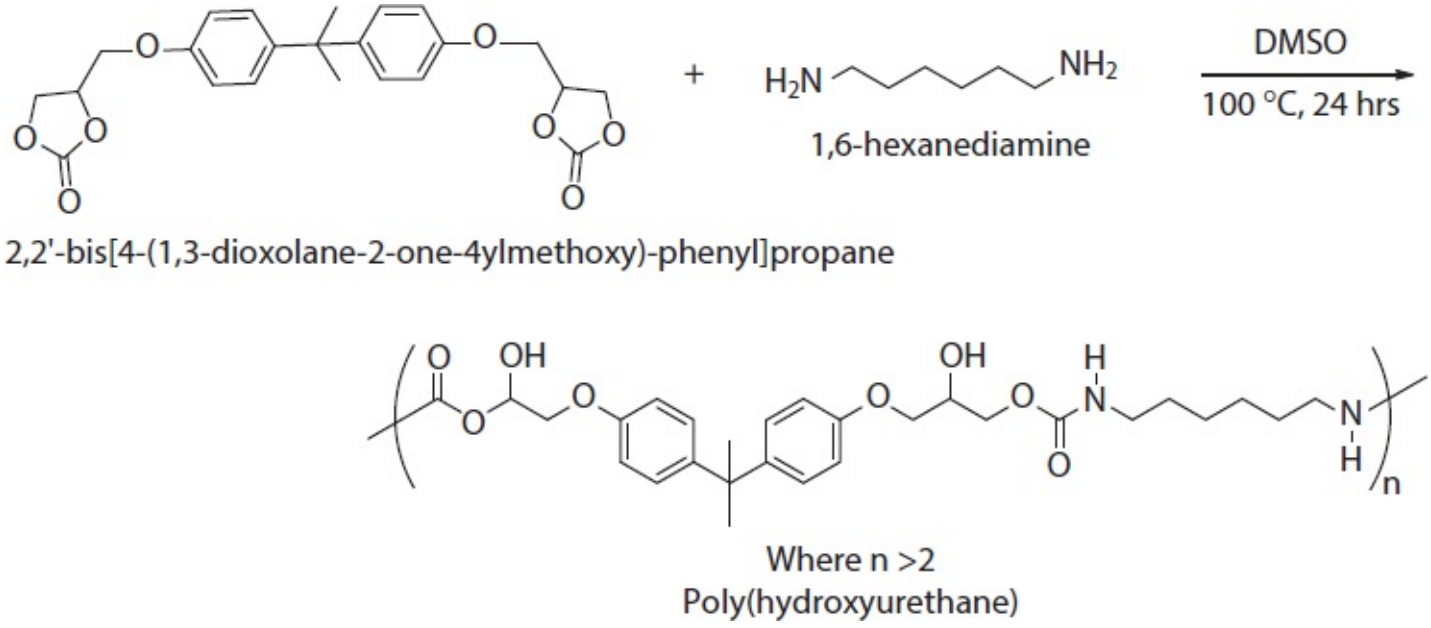


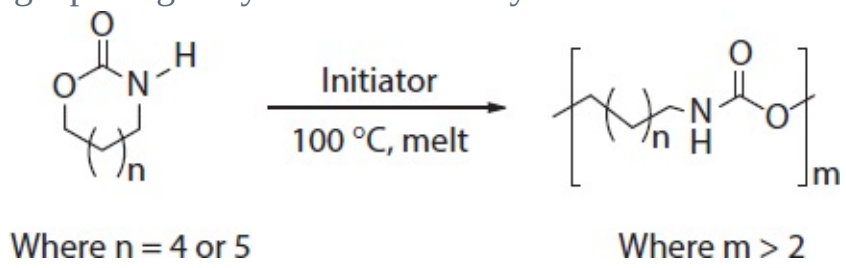
Figure 14.8 Synthesis of Poly(hydroxyurethane) from the Polyaddition Reaction of 2,2-Bis[4-(1,3-dioxolane-2-one-4ylmethoxy)-phenyl]propane and 1,6-Hexanediamine.



14.5.3 Additional Polymerization Reactions Leading to Non-isocyanate Polyurethanes (NIPU)

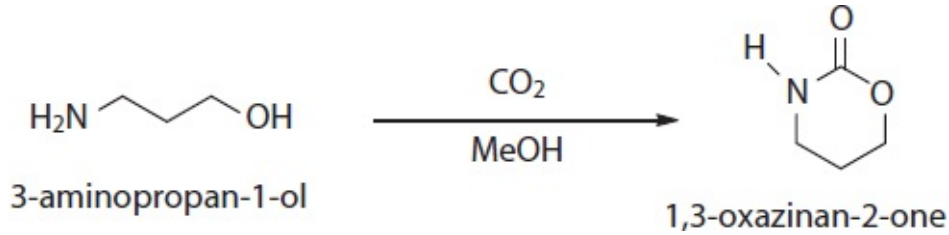
The ring-opening polymerization (ROP) of aliphatic cyclic urethanes is an alternative method for obtaining NIPUs (see Figure 14.9). This method employs cationic initiators such as Bronsted or Lewis acids which catalyze the ring opening of the cyclic urethane. The formation of [n]-polyurethanes with uniform microstructures are obtained via this method [98]. The proposed mechanism by Hoecker *et al*. using NMR spectroscopy revealed that the polymerization occurs via an active chain end mechanism [99].

Figure 14.9 Cationic Ring-opening Polymerization of Cyclic Urethanes.



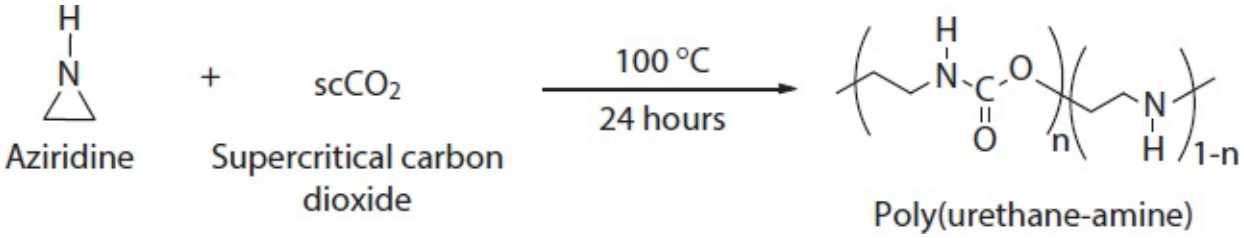
The synthesis of the starting aliphatic cyclic urethanes can be accomplished via methods that are both phosgene and isocyanate-free using amino alcohols with pressurized CO_2. No catalyst is required. As an example, 1,3-oxazinan-2-one was synthesized via the reaction of 3-aminopropan-1-ol in methanol with pressurized CO_2 (0.5–6 MPa) to give a white solid (see Figure 14.10) [100]. The main drawback in using this procedure to produce NIPU is that many of the cyclic urethanes are not easy to synthesize. The cyclic urethanes that are easy to produce are thermodynamically stable and do not polymerize. Thus, the [4] and [5]-polyurethanes can be obtained via ROP but [3]-polyurethanes cannot be obtained via this method. [101]

Figure 14.10 Synthesis of 1,3-oxazinan-2-one.



Finally, another alternative method used to prepare NIPU is the reaction of aziridines and substituted aziridines with supercritical (sc) CO_2 to give polyurethanes (see Figure 14.11) [89]. The ratio of amine and urethane linkages can be controlled via reaction conditions, like temperature, pressure, and co-solvents. The ROP mechanism of the aziridine molecule is initiated by nucleophilic attack of the aziridine or carbamate anion on the carbon atom of the aziridinium cation. This cation provides ring-opening intermediates that can further react, leading to a polymer. By producing ammonium carbamate under high pressure CO_2, urethane linkages in the copolymerization of aziridines are favored [102, 103].

Figure 14.11 Synthesis of NIPU from the Copolymerization of Aziridines and CO_2.



14.6 Applications of Non-isocyanate Polyurethanes (NIPU)

Isocyanate-based PU's have several limitations, like toxicity concerns, moisture-sensitivity and issues with hydrolytic stability [104]. NIPU's have several improvements in their properties, such as environmentally benign production methods, moisture insensitivity, excellent adhesion, greater hydrolytic stability, improved abrasion and chemical resistance [105]. As with traditional PU coatings, NIPU's are of significant interest to the coatings industry. NIPU coatings represent a sizeable research area for both academic and industrial entities, because NIPUs can offer improvements where traditional PUs exhibit shortcomings in their properties, safety and performance. NIPUs have found applications in diverse systems like diluents for UV-curable coatings [106], chemical resistance coatings [107], UV- and thermally stable coatings [108], flame-retardant/resistant coatings [109], and water-borne dispersive coatings [110]. Recently, a NIPU floor covering has been commercialized under the trade name Green Polyurethane™ [111]. This NIPU is a hybrid polyurethane/epoxy high performance coating that uses no isocyanates during manufacture. This product has shown superior performance over traditional poly/epoxy floor coverings.

14.7 Conclusions

The toxic effects of phosgene and isocyanates in polyurethane chemistry can be mitigated through innovative synthetic strategies that eliminate the use of these compounds. NIPUs represent a significant area of research that has combined CO_2 fixation into innovative chemical synthetic methods. The chemical industry can use these strategies to produce environmentally benign and safe processes, materials and commercial PUs via CO_2 fixation methods. Multiple pathways have been reviewed which produce starting materials that are phosgene-free and can be utilized for the production of NIPU polymers. Numerous coating applications have been presented for these innovative NIPU's and it remains an active area of research for both academic and industrial scientists.

Acknowledgements

The authors gratefully acknowledge financial support from the NAWCWD 219 Program.

References

1. M.F. Sonnenschein and W. Koonce, “Polyurethanes,” in H. F. Mark, ed., *Encyclopedia of Polymer Science and Technology (4th Edition)*, John Wiley & Sons, Chapter 11, pp. 204–266, 2014.

2. Y. Berezkin, and M. Urick, *ACS Symposium Series*, 1148(Polymers for Personal Care and Cosmetics), pp.65–81, 2013.

3. H-W. Engels, H-G. Pirkl, R. Albers, R. W. Albacjh, J. Krause, A. Hoffmann, H. Casselmann, and J. Dormish, *Angewandte Chemie, International Edition*, Vol. 52(36), p. 9422, 2013.

4. Y. He, D. Xie and X. Zhang, *Journal of Materials Science*, Vol. 49(21), p. 7339, 2014.

5. O. Bayer, *Angewandte Chemie*, Vol. 59, p. 257, 1947.

6. R. B. Seymour, Popular Plastics, Vol. 30(5), p. 14, 1985.

7. P. Jacobs, K. Best, M. Dvorchak, M. Shaffer, W. Myron, T. Wyat, and P. Yu, in J. E. Kresta, E. W. Eldred ed., 60 Years of Polyurethanes[International Symposium and Exhibition], Detroit, January 15–16, 1998, pp. 204–223.

8. Global Polyurethane (PU) Market by Product (Rigid Foam, Flexible Foam, Coatings, Adhesives & Sealants, Elastomers), End-use (Furniture and Interiors, Construction, Electronics & Appliances, Automotive) Is expected to Reach USD 73.6 Billion By 2020: New Report By Grand View Research, Inc., *Grand View Research* October 24, 2014, http://www.prnewswire.com/news-releases/polyurethanes-market-worth-736-billion-by-2020-grand-view-research-inc-288524621.html

9. R. B. Seymour, and G. B. Kauffman, *Journal of Chemical Education*, Vol. 69, p. 909, 1992.

10. M. Furukawa, *Kobunshi Kako*, Vol. 48(11), p. 506, 1999.

11. M. Furukawa, and T. Yokoyama, *Nippon Setchaku Gakkaishi*, Vol. 28(12), p. 501, 1992.

12. Y. Liu, Y. Wang, Jiang, X., and X. Zhang, *Polymer Bulletin (Heidelberg, Germany)*, Vol. 72(8), p. 2105, 2015.

13. C. Li, X. Cai, F. Shen, and H. Xu, *Journal of Macromolecular Science, Part B: Physics*, Vol. 55(1), p. 1, 2016.

14. F. Ji, Q. Wang, G. Li, W. Tu, Q. Liu, Y. Xie, and P. Huang, *Guandong Huagong*, Vol. 40(23), p. 42, 2013.

15. M. Shinohata, and N. Miyake, Separation method and method for producing isocyanate from thermally decomposed carbamic acid ester mixture, PCT Int.Appl.20120467, assigned to Asahi Kasei Chemicals Corporation, Japan April 12, 2012.

16. N. Perret, and D. Revelant, Use of a piston reactor to implement phosgenation process, PCT Int. Appl. April 2010076515, assigned to Perstorp France, Fr., July 8, 2010.

17. J. Ma, H. Feng, X. Pei, J. Guo, and Y. Wei, *Yingyong Huagong*, Vol. 38(3), p. 429, 2009.

18. D. Peng, and X-H. Zhang, *Huazxue Yu Nianhe*, Vol. 30(5), p. 61, 2008.

19. H. Ulrich, *The Chemistry and Technology of Isocyanates*, John Wiley & Sons, New York, 2001.

20. H. Takayanagi, “Materials for Polyurethane” in K. Matsunaga ed., *Kinosei Poriuretan no Kiso to Oyo*, pp. 1–11, 2000.

21. Z. Li, Z. Xu, C. Weng, and J. Gen, *Faming Zhuanli Shenqing*, CN 104557441 A, 2015.

22. Q. Ai., H. Luo, F. Yuan, L. Wang, K. You, P. Liu, R. Huang, Process for continuous preparation of 1,5-naphthalene diisocyanate, CN 103214397A, assigned to Xiangtan University, Peoples Republic of China, July 31, 2013.

23. B. Wu, X. Wang, H. Su, Q. Zheng, and F. Shi, *Faming Zhuanli Gongkai Shuomingshu*, CN 86100286 A, 1986.

24. H. J. Twitchett, *Chemical Society Reviews*, Vol. 3(2), p. 209, 1974.

25. R. J. Slocombe, E. E. Hardy, J. H. Saunders, and R. L. Jenkins, *Journal of the American Chemical Society*, Vol. 72, p. 1888, 1950.

26. H. Kiso, Manufacture of polyurethanes with low volatile content, JP 2012131837A, assigned to Tosoh Corporation, December 17, 2010.

27. R. Boehling, S. Kueber, S. Maixner, E. Stoefer, J. Henkelmann, G. Krug, and W. Bolz, Process for preparing isocyanates by reaction of phosgene with amine in parallel chambers of liquid phase split-recombine reactor, WO 2008049783 A1, assigned to BASF Se, Germany, May 2, 2008

28. G. D. Leikauf, V. J. Concel, K. Bein, P. Liu, A. Berndt, T. M. Martin, K. Ganguly, A. S. Jang, K. A. Brant, and R. A. Dopico, Jr., *American Journal of Respiratory Cell and Molecular Biology*, Vol. 49(3), p. 368, 2013.

29. S. M. Duniho, J. Martin, J. S. Foster, M. B. Cascio, T. S. Moran, L. B. Carpin, and A. M. Sciuto, *Toxicology Pathology*, Vol. 30(3), p. 339, 2002.

30. A. M. Scuito, R. B. Lee, J. S. Forster, M. B. Cascio, D. L. Clapp, and T. S. Moran, *Inhalation Toxicology*, Vol. 14(5), p. 487, 2002.

31. D. Massaro, and G. D. Massaro, *American Journal of Physiology*, Vol. 282(3, Pt. 1), p. L345, 2002.

32. G. D. Massaro, and D. Massaro, *Annual Review of Physiology*, p. 5873, 1996.

33. J. Pauluhn, A. Carson, D. L. Costa, T. Gordon, U. Kodavanti, J. A. Last, M. A. Matthay, K. E. Pinkerton, and A. M. Sciuto, *Inhalation Toxicity*, Vol. 19(10), p. 789, 2007.

34. S. C. Lim, J. Y. Yang, A. S. Jang, Y. U. Park, Y. C. Kim, I. S. Choi and K. O. Park, *The Korean Journal of Internal Medicine*, Vol. 11(1), p. 87, 1996.

35. J. Pauluhn, *Inhalation Toxicology*, Vol. 18(9), p. 609, 2006.

36. J. Pauluhn, *Journal of Applied Toxicology*, Vol. 24(3), p. 231, 2004.

37. V. Castranova, D. G. Frazer, L. K. Manley, and R. D. Dey, *International Immunopharmacology*, Vol. 2(2–3), p. 163, 2002.

38. D. Leftowitz, E. Pechter, E. K. Fitzsimmons, M. Lumia, A. C. Stephens, L. Davis, J. Flattery, J. Weinberg, R. J. Harrison, M. J. Reilly, M. S. Filios G. E. White, and K. D. Rosenman, *American Journal of Internal Medicine*, Vol. 58(11), p. 1138, 2015.

39. A. Fisseler-Eckhoff, H. Bartsch, R. Zinsky, and J. Schirren, *International Journal of Environmental Research and Public Health*, Vol. 8, p. 3672, 2011.

40. A. V. Wusenwski, and M. Jones, *Clinical and Experimental Allery: Journal of the British Society for Allergy and Clinical Immunology*, Vol. 40(8), p. 1155, 2010.

41. C. E. Mapp, A. A. Fryer, N. DeMarzo, V. Pozzato, M. Padoan, P. Boschetto, R. C. Strange, A. Hemmingsen, and M. A. Spiteri, *The Journal of Allergy and Clinical Immunology*, Vol. 109(5), p. 867, 2002.

42. C. Lemiere, P. Romeo, S. Chaboillez, C. Tremblay, and J-L. Malo, *Journal of Allergy and Clinical Immunology*, Vol. 110(4), p. 641, 2002.

43. L. Svensson-Elfsmark, B. L. Koch, A.Gustafsson, and A. Bucht, *International Archives of Allergy and Immunology*, Vol. 153(3), p. 229, 2009.

44. M. Littorin, A. Axmon, K. Broberg, C-J., Sennbro, and H. Tinnerberg, *Scandinavian Journal of Work, Environment & Health*, Vol. 33(4), p. 280, 2007.

45. P. K. Mishra, R. M. Samart, N. Pathak, S. K. Jain, S. Banerjee, and K. K. Mudar, *International Journal of Occupational Medicine and Environmental Health*, Vol. 22(3), p. 193, 2009.

46. Centers for Disease Control and Prevention, Isocyanates, NIOSH Workplace Safety and Health Tips, *NIOSH Publication No. 2008-109*, January 2008, http://www.cdc.gov/niosh/topics/isocyanates/

47. Fact Sheet Hazard Evaluation System & Information Service, Isocyanates: Working Safely, *California Department of Public Health-California Department of Industrial Relations*, May 2014, http://www.cdph.ca.gov/programs/ohb

48. M. Praw, *CoatingsTech*, Vol. 8(7), p. 24, 2011.

49. R. Bi, L. Ma, and S. Zheng, *Huagong Jinzhan*, Vol. 25(7), p. 796, 2006.

50. D. J. Sparrow, and I. G. Walton, *Macromolecular Chemistry(London)*, Vol. 3, p. 93, 184.

51. G. L. Gregory, M. Ulmann, and A. Buchard, *RSC Advances*, Vol. 5(49), p. 39404, 2015.

52. J. A. Castro-Osma, and M. North, *Current Green Chemistry*, Vol. 1(3), p. 257, 2014.

53. J. W. Hill, and W. H. Carothers, *Journal of the American Chemical Society*, Vol. 55, 5039, 1933.

54. J. W. Hill, and W. H. Carothers, *Journal of the American Chemical Society*, Vol. 55, p. 5031, 1933.

55. S. Fukuoka, H. Miyaji, H. Hironori, and K. Matsuzaki, Process for production of dialkyl carbonate and diol on an industrial scale, WO 2007072728 A1, assigned to Asahi Kasei Chemicals Corporation, Japan, June 28, 2007.

56. J-L. Wang, C-X. Miao, X-Y, Dou, J. Gao, and L-N. He, *Current Organic Chemistry*, Vol. 15(5), p. 621, 2011.

57. Z. Li, K. M. Zhao, J. Wei, Q. Li, X. Wang, and H. Xiang, *Jingxi Huagong*, Vol. 25(5), p. 511, 2008.

58. O. Malay, E. Gulsen, N. K. Apohan, A. Gungor, Y. Z. Menceloglu, ACS *PMSE Preprints*, Vol. 98, p. 860, 2008.

59. Y-N. Li, L-H. He, Z-F. Diao, and Z-Z. Yang, "Carbon Capture with Simultaneous Activation and its Subsequent Transformation," in *Advances in Inorganic Chemistry CO_2 Chemistry*, Vol. 66, Elsevier Inc., Chapter 9, pp. 289–340 2014.

60. M. Taherimehr, J. P. C. C. Serta, A. W. Kleij, C. J. Whiteoak, and P. P. Pescarmona, *ChemSusChem.*, Vol. 8(6), p. 1034, 2015.

61. M. Fujiwara, A. Baba, and H. Matsuda, *Journal of Heterocyclic Chemistry*, Vol. 26(6), p. 1659, 1989.

62. A. Baba, H. Kashiwagi, and H. Matsuda, *Tetrahedron Letters*, Vol. 26(10), 1323, 1985.

63. A-H. Liu, Y-N. Li, and L-N. He, *Pure and Applied Chemistry*, Vol. 84(3), p. 581, 2012.

64. G. Rokicki, P. G. Parauchowski, and M. Mazurek, *Polymers for Advanced Technologies*, Vol. 26, p. 707, 2015.

65. L-N. He, Z-Z. Yang, A-H. Liu, and J. Gao, "CO_2 chemistry at Nankai group: catalytic conversion of CO2 into value-added chemicals," in Y. H. Hu ed., *Advances in CO_2 Conversion and Utilization*, ACS Symposium Series Vol. 1056, American Chemical Society, USA, pp. 77–101, 2010.

66. S. Darbha, R. Srivastava, and P. Ratnasamy, Catalytic cycloaddition process for preparing cyclic carbonates from epoxides and carbon dioxide, U.S Patent 20060094893 A1, assigned Council of

Scientific and Industrial Research, India, May 4, 2006.

67. Y. Taguchi, K. Yanagiya, I. Shibuya and Y. Suhara, *Bulletin of the Chemical Society of Japan*, Vol. 61(3), p. 921, 1988.

68. X. Chen, H. Zhou, Y. Ma, B. Liu, and S. Wang, Method for the preparation of methyl 3-hydroxypropanoate using supercritical carbon dioxide and homogeneous catalyst systems, Faming Zhuanli Shenqing CN 102050736 A, assigned to Guangdong University of Petrochemical Technology, Peoples Republic of China, May 11, 2011.

69. Z. Tang, Y. Chen, Z. Qu, Q. Zheng and Z. Jin, *Shiyou Huagong*, Vol. 25(6), p. 409, 1996.

70. L. Li, S. Shi, L. Song, L. Guo, Y. Wang, H. Ma, J. Hou, and H. Wang, *Journal of Organometallic Chemistry*, Vol. 794, p. 231, 2015.

71. Y. Urano, and Y. Kadono, Method for the production of 1,3-dioxolanes, European Patent Application, EP 413558 A2, assigned to Nippon Shokubai Kagaku Kogyo Co., Ltd., Japan, February 20, 1991.

72. A. Sibaouih, P. Ryan, M. Leskelae, B. Rieger, and T. Repo, *Applied Catalysis A: General*, Vol. 365(2), p. 194, 2009.

73. T. Bok, E.K. Noh, and B. Y. Lee, *Bulletin of the Korean Chemical Society*, Vol. 27(8), p. 1171, 2006.

74. S. Yin, R. Qiu, Z. Meng, X. Song, Y. Qiu, K. Yu, S. Luo, X. Xu, and Y. Zhou, Solvent-free catalytic method for synthesizing cyclic carbonate esters, Faming Zhuanli Shenqing, CN 102775378 A, assigned to Hunan University, Peoples Republic of China, November 14, 2012.

75. X. Liu, C. Cao, Y. Li, P. Guan, L. Yang, and Y. Shi, *Synlett*, Vol. 23(9), p. 1343, 2012.

76. M. Aresta, A. Dibenedetto, C. Dileo, I. Tommasi, E. Amodio, *Journal of Supercritical Fluids*, Vol. 25(2), p. 177, 2003.

77. S. Duan, X. Jing, D. Li, and H. Jing, *Journal of Molecular Catalysis A: Chemical*, Vol. 411, p. 34, 2016.

78. Y. Wang, Y. Qin, X. Wang, and F. Wang, *Catalysis Science & Technology*, Vol. 4(11), p. 3964, 2014.

79. D. Bai, Z. Zhang, G. Wang, and F. Ma., *Applied Organometallic Chemistry*, Vol. 29(4), p. 240, 2015.

80. M. Feng, G. Zhao, H. Gao, and S. Zhang, *Australian Journal of Chemistry*, Vol. 68(10), p. 1513, 2015.

81. X. Zhang, and D. Wang, *Advanced Material Research (Durnten-Zurich, Switzerland)*, Vol. 989–994(Materials Science, Computer and Information Technology), p. 676, 2014.

82. M. V. Bidevkina, N. G. Ivanov, E. B. Guglya, Z. I. Zholdakova, E. A. Tul'skaya, and O. A. Leont'eva, *Toksikologicheski Vestnik*, Vol. 5, p. 55, 2010.

83. L. Cheng, J. Zhou, D. Wu, and Z. Zhang, *Jingxi Shiyou Huagong Jinzhan*, Vol. 9(12), p. 44, 2008.

84. T-L. Shi, P. Zhang, D-H. Liu, P-F. Zhou, and L-B. Sun, *Catalysis Letters*, Vol. 145(9), p. 1673, 2015.

85. J. Wang, W. Sng, G. Yi, and Y. Zhang, *Chemical Communications (Cambridge, United Kingdom)*, Vol. 51(60), p. 12076, 2015

86. T. Werner and H. Buettner, *ChemSusChem.*, Vol. 7(12), p. 3268, 2014.

87. A. M. Hardman-Baldwin, and A. E. Mattson, *ChemSusChem*, Vol. 7(12), p. 3275, 2014.

88. C. J. Whiteoak, N. Kielland, V. Laserna, E. C. Escudero-Adan, E. Martin, and A. W. Kleij, *Journal of the American Chemical Society*, Vol. 135(4), p. 1228, 2013.

89. O. Kreye, H. Mutlu, and A. A. R. Meier, *Green Chemistry,* Vol. 15, p. 1431, 2013.

90. A. Piotrowska, and G. Rokicki, *Zeszyty Naukowe Politechniki Slaskiej, Chemie,* Vol. 146, p. 87, 2001.

91. G. Rokicki, and A. Piotrowska, *Polymer,* Vol. 43, p. 2927, 2002.

92. C. Hahn, H. Keul, and M. Moller, *Polymer International,* Vol. 61, p. 1048, 2012.

93. B. Ochiai, *Kobunshi Ronbunshu,* Vol. 63(8), p. 519, 2006.

94. M. V. Zabalov, R. P. Tiger, and A. A. Berlin, *Russian Chemical Bulletin, International Edition,* Vol. 61(3), p. 518, 2012.

95. N. Aoyagi, Y. Furusho, and T. Endo, *Journal of Polymer Science, Part A: Polymer Chemistry,* Vol. 51, p. 1230, 2013.

96. N. Kihara, and T. Endo, *Journal of Polymer Science: Part A: Polymer Chemistry,* Vol. 31, p. 2765, 1993.

97. O. Figovsky, L. Shapovalov, A. Leykin, O. Birukova, and R. Potashnikova, *PU Magazine,* Vol. 10(4), p. 2, 2013.

98. S. Neffgen, H. Keul, and H. Hoecker, *Macromolecular Rapid Communications,* Vol. 17(6), p. 373, 1996.

99. S. Neffgen, H. Keul, and H. Hoecker, *Macromolecules,* Vol. 30, p. 1289, 1997.

100. B. M. Bhanage, S-I. Fujita, Y. Ikushima, and M. Arai, *Green Chemistry,* Vol. 5, 340, 2003.

101. S. Neffgen, J. Kusan, T. Fey, H. Keul, and H. Hoecker, *Macromolecular Chemistry and Physics,* Vol. 201(16), p. 2108, 2000.

102. O. Ihata, and Y. Kayaki, *Macromolecules,* Vol. 38, p. 6429, 2005.

103. W. Kuran, A. Rokicki, and D. Romanowska, *Journal of Polymer Science: Polymer Chemistry Edition,* Vol. 17, p. 2003, 1979.

104. B. Ji, Y. Xu, and X. Zhai, *Juanzhi Gongye,* Vol. 23(6), p. 39, 2008.

105. R. Pathak, M. Kathalewar, K. Wazarkar, and A. Sabnis, *Progress in Organic Coatings,* Vol. 89, p. 160, 2015.

106. X. Wang, and M. D. Soucek, *Progress in Organic Coatings,* Vol. 76(7–8), p. 1057, 2013.

107. J. Guan, Y. Song, Y. Lin, X. Yin, M. Zuo, Y. Zhao, X. Tao, and Q. Zheng, *Industrial & Engineering Chemistry Research,* Vol. 50(11), p. 6517, 2011.

108. O.L. Figovsky, L. D. Shapovalov, and F. Buslov, *FATIPEC Congress,* Vol. 27(1), p. 247, 2004.

109. O. L. Figovsky, L. Shapovov, and O. Axenov, *Surface Coatings International, Part B: Coatings Transactions,* Vol. 87(B2), p. 83, 2004.

110. V. J. Tramontano, M. E. Thomas and R. D. Coughlin, Synthesis and coating properties of novel waterborne polyurethane dispersions in ACS Symposium Series Vol. 663(Technology for Waterborne Coatings), American Chemical Society, Washington DC, pp. 164–182, 1997.

111. https://www.gogreenworldproducts.com/Green-Polyurethane-Paints-(non-socyinate).html

Index

2-(Vinyloxy)ethyl soyate
AA2024
AA7075
Absorptivity
Acid - catalyze
Acrylated methyl oleate (AMO)
Acrylic
Acrylic fatty acid derivative (AcFAD)
Acrylic modified Alkyds
Adsorption–desorption
Aggregation
Aircraft
Alginate
Alkoxysilane
  3-Aminopropyltriethoxysilane (APTES)
  3-Glycidoxypropyltrimethoxysilane (GPTMS)
  Tetraethoxysilane (TEOS)
  Vinyl trimethoxysilane (VTMS)
Alkyd
Allyl fatty acid derivative (AFAD)
Aluminium
Aluminium alloys
a-methylene gamma-butyrolactone (a-MBL)
Anacardic acid
Anodic reaction
Anti-corrosion
Anticorrosive
  effect
  pigment
Antiferromagnetic
Anti-fingerprint
Anti-fog
Antifouling
Anti-microbial
Anti-mist
Antioxidant
Anti-reflective
Anti-static

Anti-stick
Aqueous Chemical Growth (ACG)
Aqueous coatings
Ascorbic acid
Aspiration dust
Atmospheric corrosion
Attenuated Total Reflection (ATR)
Auto-oxidative curing
Autoxidation
Azole

Bacteria
Benzoic acid
Binder
Bio-based Polyols
Bisphenol A (BPA)
Blister
Browning

Carbocation
Carbocationic polymerization
Carbon dioxide
Carbonate
  calcium
  magnesium
carboxy methyl cellulose (CMC)
Cardanol
Cardanol ethyl vinyl ether
Carrageenan
Cashew nut liquid
Castor oil (CO)
Cathodic reaction
  effect, mechanism
  inhibition
CeCC
Centrifuge method
Cerium compounds
Cerium corrosion inhibitors
Charge transfer
Chemical recycling
Chemical vapor deposition
Chitosan
Coarsening

Coating
anticorrosive organic
barrier properties
composition
ferrite-filled alkyd
film
formulation
matrix
multifunctional
Coating application tests
blooming resistance
boiling water resistance test
effect of ageing
effect of overbaking
solvent resistance
Coatings
Compound
Controlled atmosphere (CA)
Conversion coatings
Copolymerization
Corn zein
Corrosion
Corrosion inhibition efficiency
Corrosion inhibitors
Corrosion protection
ability
efficiency
inhibition
performance
stability of steel
steel
Corrosion rate
Corrosion test
Corrosivity
Corundum
Crayamid® 115 (C115)
Crevice
Cross-link densities
Cyclic carbonates
Cycloaddition
Cyclohexyl vinyl ether

Defect
Delamination
Densification
Depolymerization process
Deposition
  electrodeposition
  spontaneous
  spray
Dielectric
Diffusion-limited
Diglycidyl ether of bisphenol A (DGEBA)
Diglycidyl ether of bisphenol-A
Dip-coating
Discoloration
Dissolution

Electrochemical
  cell
  corrosion
  deposition
  impedance
  interaction
  measurement
  method
  process
  reaction
  synthesis
  technology
Electrode
  counter
  reference
  working
Electrophilic site
Electroplating
Electrostatic spray process
Emissivity
Emulsifiers
Emulsion polymerization
Environmental restrictions
Environmentally compliant
Environmentally friendly
Epoxide water based

Epoxidized linseed oil (ELO)
Epoxidized Monoglyceride (EMG)
Epoxidized Soybean Oil (ESO)
Epoxy
Esterification
Ethylene glycol monostearate
Eugenol
Eugenol ethyl vinyl ether

Fatty acid
  average annual production
  chemical modification
  raw material
  reactive site
  structure
Fatty acid-based monomer
Fatty acid-based polymer
Fatty acids
Ferrite
  anticorrosive effect
  calcium
  composition
  copper
  core-shell
  double-cation
  formula
  high temperature resistance
  kernel
  magnesium
  micaceous
  multi-cation
  nanodimensional
  nickel
  PANI-modified
  passivating effect
  pH valuie of aqueous extract
  physicochemical chartacteristics
  pigment
  platelet-shaped
  single
  strontium
  structure

synthesis
triple-cation
zinc
zinc-nickel
Film Properties
cross-cut adhesion
impact resistance
koenig hardness
mek-double rub
pencil hardness
Fluconazole
chemical structure
formula
FTIR
Fresh-cut
Galvanic sludge
Gellan
Generally regarded as safe (GRAS)
Glycerol
Glycerol monostearate
Graphene
Green
Growth mechanism
Heteronucleation
Hexaaqua chromium (III)
Hexamethylenediamine (HMDA)
Hybrid coatings
Hydrocolloids
Hydrodynamic
Hydrolysis
Hydrophilic
Hydrophobic
Hydroxo
Hydroxy propyl cellulose (HPC)
Hydroxy propyl methyl cellulose (HPMC)
Hydroxyl
Ice-phobic
Infrared Reflective (IR)
Infrared spectroscopy (FTIR)
Inhibition efficiency

Inhibitor
Inhibitor efficiency
Inhibitors reactions
Inorganic condensation
Inorganic-organic hybrid coatings
Intermetallics
Iron
  oxidation process
  pourbaix diagram
Isocyanates
Isophthalic acid (IPA)
Isotropic

Lansoprazol
  definition
  formula
Lanthanides
Latex
Lecithin
Lifshitz–Slyozov–Wagner (LSW)
Linoleic acid
Linoleyl (meth) acrylate
Linseed oil
Linseed oil (LO)
Lipids
Living polymerization
Localized corrosion

Mechanical properties
Medicine
Melamine
Menthol
Menthol vinyl ether
Methacrylated linoleic acid (MLA)
Methacrylated oleic acid (MOA)
Methyl cellulose (MC)
Methyl soyate
Methyl triethoxysilane (MTES)
Microbially Induced Corrosion
Microcapsules
Microorganisms-95
Miniemulsion polymerization
Mixed inhibitors

Modified atmosphere packaging (MAP)
Monodispersed particles
monoglycerides
Monomer
Morphology

N,N'-bis-(1-methylheptyl)-1,4-phenylenediamine (BMPDA)
N,N'-bis-(2-(phenyl-henyl-hydrazono)-ethylidene)-benzene-1,4-diamine (BPPDA)
Nanocoatings
Nanocomposite
Nanoparticles
Nanoparticles (NPs)
Nanotechnology
Nanotubes (NTs)
Nanowires (NWs)
Non-isocyanate polyurethane
Nuclear magnetic resonance (NMR)
Nucleation
Nucleus-seeking agent
Nuclopephilic

Olation
Oleic acid
Oleophobic
Oleyl methacrylate
Organic inhibitors
Organically modified silica (ORMOSIL)
Organicaly modified ceramic (ORMOCER)
Organic-inorganic coatings
Organosilica
Ostwald ripening
Oxidation
Oxirane Oxygen Content (OOC)
Oxiranes
Ozone

Paints
Palm oil
Pentaethylene glycol ethyl vinyl ether
Peroxyacetic acid
PET alkyd
pH conditions
Phosgene

Phosphate Ester Polyol
Phosphated film formation
Photothermal
Phthalic Acid
Pigment
  anticorrosive
  chromate
  toxic
  volume comcentration
Pitting
Plasticizers
Polarization
Pollutant
Poly(ethylene terephthalate) (PET)
Polyaddition
Polycondensation
Polycondensation after glicolysis
Polydimethysiloxane
Polyethylene glycol
Polyethylenglycol (PEG)
Polyhexamethylene biguanide (PHMB)
Polylactic acid (PLA)
Polymer coatings
Polysaccharides
Polysorbates
Polyurethane (PU) thermoplastic polyurethane (TPU)
Polyurethane dispersions
Polyurethanes
Postharvest
Potassium sorbate
Pourbaix diagrams
p-Phenylenediamine (PDA)
Precipitation
Primid
Propylene glycol
Protective
  ability
  coatings
  film
  layers
  properties

Proteins
Protonate
Pyrolysis
Radiation
  electromagnetic
  microwave
Rare Earth
Reduction
Renewable resources
  2,5-furandicarboxylic acid (FDCA)
  citric acid (CA)
  glycerol
  isosorbide
  succinic acid
Respiration
Ring opening
Scanning electron microscope (SEM)
Scratch resistant
Seed base reactive diluents
Seed oil coatings
Self Assembled
  barrier layers
  Monolayers
Self-healing
Self-healing coating
Sesquioxide corundum
Shelf life
Silica
Silicon alkoxide
Smart release
SN2 Mechanism
Sodium benzoate
Solar absorber
Sol-gel
  coatings
  process
Solubility
Sorbitan monostearate
Sorbitol
Soybean oil
Soybean oil (SO)

Specie
Spectroscopic Characterization
  FT-IR
  NMR
Spin-coating
Spraying
Standard deviation
Steel
Steels
Stoichiometry
Structure
  spinel
Sucrose
Sucrose ester
Superhydrophilic
Swelling

Technique
  autocatalytic combustion
  ceramic
  mechanochemical
  microwave-assisted hydrothermal
  non-ceramic
  self-propagating combustion
  sol-gel
  using industrial wastes
Terephthalic acid (TPA)
Tetraethoxysilane (TEOS)
Thermal analyses
  differential scanning calorimetry (DSC)
  thermogravimetric analysis (TGA)
Thermosets
  thermosetting
Thiol-ene seed oil
Toxic/toxicity
Transesterification
Transparent coatings
Triglycerides
Ttoxicological properties

Urethane
Urethane modified alkyd
UV protective

UV-curable alkyd
UV-curable seed oil coatings
UV-curable waterborne coatings

Vegetable oils (VOs)
Vinyl ether monomer
Vitamin
Volatile organic compound (VOC)
Volatile organic compounds (VOC)
Volatile organic compounds (VOCs)

Water contact angle (WCA)
Waterborne coatings
Waterborne paint
Water-reducibe Coatings
Waxes
Wettability

Xanthan gum

Zinc-aluminium–phosphate (ZAP)
Zinc–phosphate pigments
α-hopeite

Also of Interest

Check out these published and forthcoming books in the Materials Degradation and Failure series

Lifetimes and Compatibility of Synthetic Polymers

Edited by James P. Lewicki and George Overturf
Forthcoming 2016. ISBN 978-1-119-03852-8

Fruits and Vegetables: Degradation and Preservation

By Anjali Bishnoi and Sandeep Rai
Forthcoming 2016. ISBN 978-1-118-92584-3

Biobased and Environmentally Benign Coatings

Edited by Atul Tiwari, Anthony Galanis and Mark D. Soucek
Published 2016. ISBN 978-1-119-18492-8

Materials and Failures in MEMS and NEMS

Edited by Atul Tiwari and Baldev Raj
Published 2015. ISBN 9781119083603

Reactions and Mechanisms in Thermal Analysis of Advanced Materials

Edited by Atul Tiwari and Baldev Raj
Published 2015. ISBN 9781119117575

Other Scrivener books edited by Atul Tiwari

Concise Encyclopedia of High Performance Silicones

Edited by Atul Tiwari and Mark D. Soucek
Published 2014. ISBN 978-1-118-46965-1

Nanomaterials in Drug Delivery, Imaging, and Tissue Engineering

Edited by Ashutosh Tiwari and Atul Tiwari
Published 2013. ISBN 978-1-118-29032-3

Materials Degradation and Failures Series

Biobased and Environmentally Benign Coatings

Edited by **Atul Tiwari, Anthony Galanis, and Mark D. Soucek**



Scrivener Publishing

WILEY